



HAL
open science

Tannin and carbohydrates based non-isocyanate polyurethane for foams, surface finishes and adhesives

Xinyi Chen

► **To cite this version:**

Xinyi Chen. Tannin and carbohydrates based non-isocyanate polyurethane for foams, surface finishes and adhesives. Chemical Sciences. Université de Lorraine, 2021. English. NNT : 2021LORR0286 . tel-03702716

HAL Id: tel-03702716

<https://hal.univ-lorraine.fr/tel-03702716>

Submitted on 23 Jun 2022

HAL is a multi-disciplinary open access archive for the deposit and dissemination of scientific research documents, whether they are published or not. The documents may come from teaching and research institutions in France or abroad, or from public or private research centers.

L'archive ouverte pluridisciplinaire **HAL**, est destinée au dépôt et à la diffusion de documents scientifiques de niveau recherche, publiés ou non, émanant des établissements d'enseignement et de recherche français ou étrangers, des laboratoires publics ou privés.



AVERTISSEMENT

Ce document est le fruit d'un long travail approuvé par le jury de soutenance et mis à disposition de l'ensemble de la communauté universitaire élargie.

Il est soumis à la propriété intellectuelle de l'auteur. Ceci implique une obligation de citation et de référencement lors de l'utilisation de ce document.

D'autre part, toute contrefaçon, plagiat, reproduction illicite encourt une poursuite pénale.

Contact : ddoc-theses-contact@univ-lorraine.fr

LIENS

Code de la Propriété Intellectuelle. articles L 122. 4

Code de la Propriété Intellectuelle. articles L 335.2- L 335.10

http://www.cfcopies.com/V2/leg/leg_droi.php

<http://www.culture.gouv.fr/culture/infos-pratiques/droits/protection.htm>

THÈSE

Polyuréthanes à base de tannins et de glucides sans isocyanate (NIPU)
pour adhésifs, mousses et finitions

Présentée devant l'Université de Lorraine
pour l'obtention du titre de

DOCTEUR DE L'UNIVERSITE DE LORRAINE,

Spécialité : Sciences du Bois et des Fibres

Par:

Xinyi CHEN

Directeurs de thèse: Prof. Christine GERARDIN et Dr. Emmanuel FREDON

Soutenance le 15 Décembre 2021

Composition du jury

Rapporteurs: M. Bertrand CHARRIER, Professeur, Université de Pau et des
Pays de l'Adour (PREM), France
Mme. Sophie THIEBAUD-ROUX, Professeur, Directrice du
Laboratoire de Chimie Agro-industrielle, Toulouse, France

Examineurs: Mme. Sandra TAPIN LINGUA, Chef de projet, FCBA, Grenoble
Mme. Christine GERARDIN, Professeur, Directrice de l'Ecole
Doctorale SIMPPÉ, Université de Lorraine
M. Emmanuel FREDON, Maître de conférences, LERMaB,
Université de Lorraine

Invité: M. Antonio PIZZI, Professeur, LERMaB, Université de Lorraine

REMERCIEMENTS

Thanks are due to the China Scholarship Council (CSC, grand No. 201808530468), for providing the funding to support my research work. Thanks are also due for the great China-France friendship for giving me the chance to experience the unforgettably enjoyable life in France.

I have had an unforgettably wonderful time in the LERMAB at the Université de Lorraine, Épinal, France, but unfortunately passed so quickly. It has also been a hard but hopeful time, for both the research work for my Ph.D. thesis and for daily life, especially during the COVID-19 world pandemic. It has anyhow been still a progressive time for not only my personal experience but also for my professional skills, for the chance that to widen my horizons to see the development of the whole world, for the opportunity to study my professional knowledge further, and for the occasion to give back to my country. Thus, there are many kind people that I would like to thank for helping me to fulfill successfully my research and my life.

I would like to thank my supervisors Prof. Christine Gerardin and Dr. Emmanuel Fredon, for providing me with their patient guidance throughout my thesis research. I could not have completed this research work in its entirety without their full help. I'd also like to express my gratitude to Dr. Emmanuel Fredon for teaching me the use of a variety of testing equipment, for searching for the relative raw materials of my experiments, and for coordinating the resolution of the laboratory problems besetting the ENSTIB.

I would like to express my deep gratitude to Prof. Antonio Pizzi, for giving me the chance to do the Ph.D. degree, helping me to apply for the scholarship from the Chinese government, and providing the patient guidance for each experiment and for the paper's publications.

Special thanks to all the staff in the laboratory of the LERMAB and of the ENSTIB. Thanks to them to help me with the laboratory maintenance, for chemical purchasing, and for their guidance with the use of the testing machines.

I am very glad to have gained the friendship of so many nice people, such as Sarah Troilo, Adele Chabert, Eyinga Jean Jalin, Linda Bosserr, Matthieu Debal, Siham Amirou, and Tuan-anh Bui.

Thanks to Dr. Xuedong Xi for giving me all his help when I arrived in France, discussing the research plan, and helping me to do my thesis experiments. Thanks to Mr. Dongxia Wu, Xiaoyu Ma, and Bengang Zhang: we have had a good time together enjoying the views in Europe, including Switzerland, Germany, Austria, Luxembourg, and France. Special thanks for his wonderful driving skill to Mr. Xiaoyu Ma, making us have a trip both enjoyable and in

Remerciements

safety. Thanks also to Dr. Jingjing Liao for giving me help to register at the university. Many thanks to Dr. Junmei Qi, I would never forget the time which you brought many kinds of food to me during my quarantine time in Nancy. I would never forget those memorable moments spent with you.

I am extremely thankful to my parents, my wife's parents, my wonderful wife, and my pretty daughter, for their understanding, support, tolerance, and dedication.

Special thanks to my teacher Prof. Guanben Du, Xiaojian Zhou, Hong Lei, for giving me a lot of help in my research work and sample testing as well as funding for my works. Special thanks to my dear friends in China, including Chao Luo, Yuhong Rong, Jinxing Li, and others.

Thanks to you all!

Xinyi CHEN

25/07/2021, in Épinal, France

Sommaire

REMERCIEMENTS.....	i
Sommaire.....	iii
Résumé	I
Abstract.....	IV
Présentation des publications	VII
General Introduction.....	1
1 STATE OF ART.....	5
1.1 Generalities of wood adhesives.....	5
1.1.1 Phenol-formaldehyde (PF) resin	5
1.1.2 Urea-formaldehyde (UF) resin.....	6
1.1.3 Melamine-urea-formaldehyde (MUF) resin.....	7
1.1.4 Other resins for wood panels.....	7
1.2 The properties of biomass resources and its applications in wood adhesives	8
1.2.1 Lignin resources and Lignin-based wood adhesives	8
1.2.2 Tannin resources and tannin-based wood adhesives.....	23
1.2.3 Plant protein resources and protein-based wood adhesives.....	52
1.2.4 Humins material and its applications	64
1.2.5 Other wood adhesives	65
1.2.6 Perspectives	67
1.3 Tannin resource as the starting materials for green foam fabrication	68
1.3.1 Tannin-furanic based foam preparation and its modification	69
1.3.2 Tannin-isocyanate foams preparation.....	74
1.3.3 Mechanically Blown tannin-based foams	75
1.3.4 Tannin-based polyurethane foams.....	76
1.3.5 Other researches	78

1.3.6 Prospective	80
2 REFERENCES.....	80
3 PRESENTATION DES PUBLICATIONS.....	106
3.1 Adhésifs pour bois thermodurcissables au polyuréthane sans isocyanate à base d'humines non furaniques (NIPU).....	106
3.2 Isolat de protéine de soja Non-isocyanates Polyuréthanes (NIPU) Adhésifs pour bois	121
3.3 Préparation et propriétés d'un nouveau type de colle à bois à base de tanin	135
3.4 Les tanins naturels comme nouveaux matériaux de réticulation pour les adhésifs à base de soja.....	154
3.5 Lignine déméthylée oxydée comme adhésif biosourcé pour le collage du bois	171
3.6 Panneau de particules bio-adhésif par lignine glyoxalée et amidon dialdéhyde oxydé réticulé par l'urée.....	190
3.7 Adhésifs pour bois en polyuréthane sans isocyanate à base de tanin (NIPU) à température de durcissement inférieure : préparation et évaluation des propriétés	220
3.8 Bio-mousses NIPU condensées à base et tanin-glucose de résistance au feu améliorée	233
3.9 Préparation et caractérisation des mousses rigides de polyuréthane non isocyanate condensé (NIPU) par soufflage à température ambiante	246
3.10 Biomousses Tannin-Humins auto-gonflantes à température ambiante.....	267
3.11 Mousses tannin-furaniques modifiées par l'isolat de protéine de soja (SPI) et l'addition de formaldéhyde de substitution de lignine industrielle	294
4 CONCLUSIONS GENERALES.....	307

Résumé

Les travaux de recherche présentés ont été menés à partir de bioressources, notamment de tanins, de lignine, de protéines de soja, des humines, pour préparer des colles et mousses de bois biosourcées. Par conséquent, ce travail se concentre sur quatre parties, la préparation de deux principaux types de colles à bois en utilisant des bio-ressources, les colles à bois NIPU et les colles à bois biosourcées (tanin, SPI et lignine), pour contribuer à des produits collés n'émettant pas de formaldéhyde; deux types de formulations pour les produits de mousse isolantes de tanin, c'est-à-dire une mousse de tanin-furanique typique et des mousses de type polyuréthane sans isocyanate.

(1) Des humines commerciales l'isolat de protéines de soja (SPI), et tanin mimosa ont été utilisés pour préparer des adhésifs pour bois, sur la base de la formulation de polyuréthanes non isocyanates (NIPU). Concernant les humines, elles sont principalement composées d'acide fulvique et de ses dérivés, et d'acide humique, mais présentant également des structures polyfuraniques et lignanes dans leur mélange. Les propriétés de base des adhésifs ainsi préparés ont été déterminées. Des techniques telles que MALDI-ToF et FTIR ont été utilisées pour caractériser les produits obtenus et pour analyser les mécanismes réactionnels impliqués. Une analyse thermomécanique (TMA) a été utilisée pour étudier le comportement thermique des adhésifs. Enfin, les panneaux de laboratoire tels que le contreplaqué ou les panneaux de particules ont été préparés et leurs performances adhésives évaluées selon les exigences normatives. Les résultats ont indiqué que les bio-ressources utilisées contenaient un grand nombre de groupes -OH dans leurs structures moléculaires, mais à un niveau inférieur dans l'isolat de protéine de soja (SPI). Le contreplaqué ou les panneaux de particules collés avec ces adhésifs présentent une performance acceptable à l'exception des formulation SPI. La température de pressage des adhésifs SPI, normalement supérieure à 200°C, et leur émission chimique, sont le principal inconvénient de leur application industrielle. Par conséquent, de petites quantités d'un époxy partiellement biosourcé, à savoir l'éther diglycidyle de glycérol (GDE), ont été utilisées pour les améliorer. Le GDE introduit a diminué la température de durcissement, mais a également amélioré l'adhésion du contreplaqué.

De plus, la réticulation directe du tanin et de l'isolat de protéine de soja a été prouvée par spectrométrie MALDI-ToF et FTIR, indiquant que ce type d'adhésif biosourcé pouvait être appliqué pour coller du bois.

(2) Un nouvel adhésif pour bois à base de biomasse a été préparé avec de l'extrait de tanin de Mimosa commercial et de l'éther diglycidyle de glycérol (GDE) sous agitation par

mélange mécanique. Le GDE a servi d'agent de réticulation du tanin sans aucune addition d'aldéhyde, produisant des réseaux tridimensionnels durcis. Différents rapports pondéraux tanin/GDE ont été étudiés par un certain nombre de techniques pour déterminer leur influence sur les propriétés finales. Les résultats ont montré qu'une liaison éther non hydrolysable peut se former entre les groupes époxy du GDE et les groupes hydroxyle du tanin, ce qui est le facteur critique pour la bonne résistance à l'eau obtenue avec les colles à bois ainsi préparées. De plus, la résistance au cisaillement sec et humide a montré une corrélation positive avec la proportion de GDE ajouté. Même à une proportion relativement faible de GDE (33 % du poids de tanin sec), les résistances au cisaillement à sec et à l'eau froide de 24 h du contreplaqué collé satisfaisaient aux exigences d'une norme pertinente (GB/T 9846-2015, $\geq 0,7$ MPa). La stabilité thermique de la colle à bois à base de tanin ainsi préparée est progressivement améliorée avec l'augmentation de la proportion de GDE. De plus, la réticulation directe du tanin et de l'isolat de protéine de soja a été prouvée par spectrométrie MALDI-ToF et FTIR, indiquant que ce type d'adhésif biosourcé pouvait être appliqué au collage des contreplaqués.

Un nouvel adhésif à base de lignine a été préparé en utilisant de la lignine modifiée au glyoxal et de l'amidon dialdéhyde réticulé par de l'urée. Les espèces moléculaires formées et le mécanisme réactionnel impliqué ont été déterminés par FT-IR, RMN ^{13}C et spectrométrie de masse MALDI-ToF. L'urée semble réagir à la fois avec la lignine glyoxalée et l'amidon dialdéhyde. Les adhésifs préparés sur cette réaction ont été testés pour le collage de panneaux de particules, par calorimétrie différentielle à balayage (DSC) et analyse thermomécanique (TMA). Les résultats de résistance de liaison interne (IB) obtenus avec ce système adhésif étaient acceptables pour la préparation de panneaux de particules conformément à la norme européenne pertinente. L'utilisation de 5% massique de résine d'éther glycidique de glycérol partiellement bio-sourcé (GDE) améliore la force de liaison des résines ainsi formées par une réaction de réticulation supplémentaire dont les principaux sites ont également été déterminés. De plus, la lignine a été modifiée avec succès pour préparer un adhésif pour le bois en seulement deux étapes de synthèse: la déméthylation et l'oxydation au périodate. La spectroscopie infrarouge à transformée de Fourier (FTIR), la spectrométrie de masse à temps de vol d'ionisation par désorption laser assistée par matrice (MALDI-ToF) et l'analyse thermomécanique (TMA) ont été combinées pour caractériser les adhésifs obtenus. De plus, les performances mécaniques de cet adhésif biosourcé à base de lignine ont été déterminées en testant la résistance à la traction par cisaillement des joints collés.

(3) Sur la base de la formulation d'un système de polyuréthane sans isocyanate, le tanin a été utilisé comme source de -OH pour préparer des mousse polyuréthanes sans isocyanate

(NIPU). Une mousse rigide de polyuréthane non-isocyanate (NIPU) à base de tanin de mimosa auto-moussante à température ambiante a été préparée. Un mélange d'acide citrique et de glutaraldéhyde a servi d'agent gonflant utilisé pour fournir de l'énergie moussante et réticuler la résine. Des séries de mousses NIPU à base de tanin contenant une proportion différente d'acide citrique et de glutaraldéhyde ont été préparées. Le mécanisme de réaction des mousses NIPU à base de tanin a été étudié par spectrométrie de masse Fourier Transform InfraRed (FT-IR), Matrix Assisted Laser Desorption Ionization (MALDI-TOF) et ^{13}C Nuclear Magnetic Resonance (^{13}C RMN). De plus, le tanin a également montré son intérêt pour améliorer les propriétés finales des mousses, pour ses propriétés ignifuges et la résistance à la compression.

(4) Les mousses tanin-furanique-formaldéhyde ont suscité l'intérêt des chercheurs car elles sont non seulement basées sur une ressource renouvelable mais aussi en raison de leur préparation auto-soufflante à température ambiante/modérée et de leurs performances comparables aux mousses PF commerciales. Cependant, le formaldéhyde normalement utilisé comme agent de réticulation pour maintenir la densité de la mousse peut être maintenu. La réticulation limitée entre le tanin et le formaldéhyde fournit des propriétés mécaniques limitées des mousses typiques à base de tanin. Par conséquent, la recherche d'un agent de réticulation biosourcé alternatif pour remplacer le formaldéhyde était intéressante, et particulièrement fructueuse si elle entraînait également des propriétés mécaniques améliorées et une résistance au feu améliorée. Pour cela, un déchet de bioraffinerie, des humines, et un isolat de protéine de soja (SPI) ont été sélectionnés comme réticulants biosourcés de substitution du formaldéhyde pour deux types de formulations de mousses à base de tanin. Comme attendu, les propriétés ont été améliorées en utilisant ces réticulants biosourcés. Les propriétés de base des mousses de tanin en série ont été étudiées. Les caractéristiques de morphologie et de structure ont été observées par microscopie électronique à balayage (MEB). De plus, les mécanismes de réaction de réticulation entre le tanin avec les deux réticulants biosourcés, à savoir les humines et le SPI, ont été déterminés par spectrométrie MALDI-ToF et FTIR. Enfin, la stabilité thermique, les propriétés mécaniques, le caractère ignifuge et l'émission de formaldéhyde ont été évalués par les techniques appropriées.

Mots clés:

Tanin de mimosa; lignine; Isolat de protéines de soja (SPI); Humines; Polyuréthane sans isocyanate (NIPU); colle à bois; mousse de biomasse.

Abstract

The research work presented was carried out based on bioresources, including tannin, lignin, soybean protein, humins, to prepare bio-based wood adhesives and foams. Therefore, there are four parts on which this work is focused, the preparation of two main kinds of wood adhesives by using bio-resources, bio-sourced NIPU wood adhesives and bio-based (tannin, SPI, and lignin) wood adhesives, for contributing to bonded products not emitting formaldehyde; two kinds of formulations to tannin foam products, i.e., typical tannin-furanic foam and non-isocyanate polyurethane foams.

(1) Commercial humins predominantly composed of fulvic acid and its derivatives, and of humic acid, but also presenting some polyfuranic and lignan structures in their mix, soybean protein isolation (SPI), and mimosa tannin have been utilized to prepare wood adhesives, based on the formulation of non-isocyanate polyurethanes (NIPU). The basic properties of the adhesives so prepared were determined. Techniques such as MALDI-ToF and FTIR were used to detect the products obtained and for analyzing the reaction mechanisms involved. Thermomechanical analysis (TMA) was utilized to investigate the thermal behavior of the adhesives. Finally, the laboratory plywood or particleboard was prepared and their bonding performances were evaluated according to the relative standard requirements. The results indicated that the bio-resources used contained many -OH groups in their molecular structures, but at a lower level in soy protein isolate (SPI). The plywood or particleboard bonded with these adhesives does present an acceptable performance, except for SPI. Nevertheless, these adhesives press temperature, normally over 200°C, and their chemical emission, are the main drawbacks for their industrial application. In tannin-based NIPU adhesive, small amounts of a partially bio-sourced epoxy, namely glycerol diglycidyl ether (GDE), were used to improve them. The GDE was introduced not only to decrease the curing temperature, but also to improve plywood bonding.

(2) A novel biomass-based wood adhesive was prepared with commercial mimosa tannin extract and glycerol diglycidyl ether (GDE) by convenient mechanical mixing. GDE served as the crosslinker of the tannin without any aldehyde addition yielding hardened three-dimensional networks. Different weight ratios of tannin/GDE were investigated by several techniques to determine their influence on final properties. The results showed that a non-hydrolyzable ether bond can be formed between the epoxy groups of GDE and hydroxyl groups of tannin, this being the critical factor for the good water resistance obtained with the wood adhesives so prepared. Moreover, the dry and wet shear strength showed a positive correlation with the

proportion of the GDE added. Even at a relatively small proportion of GDE (33% of the weight of dry tannin), the dry and 24 h cold water shear strengths of the bonded plywood satisfied the requirements of a relevant standard (GB/T 9846-2015, ≥ 0.7 MPa). The thermal stability of the tannin-based wood adhesive so prepared progressively improved with the increasing proportion of GDE. Moreover, direct crosslinking of tannin and soybean protein isolate was shown to occur by MALDI-ToF and FTIR spectrometry, indicating that this kind of bio-based adhesive could be applied to bond wood.

A novel lignin-based adhesive was prepared by using glyoxal modified lignin and dialdehyde starch cross-linked by urea. The molecular species formed and the reactions' mechanism involved were determined by FT-IR, ^{13}C NMR and MALDI-ToF mass spectrometry. Urea appears to react with both glyoxalated lignin and dialdehyde starch. The adhesives based on this reaction were tested by bonding laboratory particleboard, by differential scanning calorimetry (DSC), and thermomechanical analysis (TMA). The internal bond (IB) strength results obtained with this adhesive system were acceptable for preparing particleboard according to the relevant European Norm. Additional chemical cross-linking using 5% on resin solids of partial bio-sourced glycerol glycidyl ether (GDE) improves the bonding strength of the resins so formed through an additional cross-linking reaction the main sites of which were also determined. In addition, Lignin was successfully modified to prepare a bio-based wood adhesive by just two synthesis steps: demethylation and periodate oxidation. Fourier Transform Infrared Spectroscopy (FTIR), Matrix Assisted Laser Desorption Ionization Time of Flight (MALDI-ToF) Mass Spectrometry and Thermomechanical Analysis (TMA) were combined to characterize the bio-based adhesives obtained. Furthermore, the adhesion performance of this bio-based lignin adhesive was determined by testing the tensile shear strength of the bonded joints.

(3) An ambient temperature self-blowing mimosa tannin-based non-isocyanate polyurethane (NIPU) rigid foam was prepared, based on a formulation of a tannin-based non-isocyanate polyurethane (NIPU) resin. A citric acid and glutaraldehyde mixture served as a blowing agent used to provide foaming energy and cross-link the tannin-based resin to prepare the NIPU foams. Series of tannin-based NIPU foams containing a different proportion of citric acid and glutaraldehyde were prepared. The reaction mechanism of the tannin-based NIPU foams were investigated by Fourier Transform InfraRed (FT-IR), Matrix Assisted Laser Desorption Ionization (MALDI-TOF) mass spectrometry, and ^{13}C Nuclear Magnetic Resonance (^{13}C NMR). Additionally, tannin was also used as a natural fire-retardant to improve the final properties of glucose-based NIPU foams, including fire retardancy and compression strength.

(4) Tannin-furanic-formaldehyde foams have attracted the researcher's interest as they are not only based on a renewable resource but also because of their self-blowing preparation under ambient/moderate temperature, and their comparable performance with commercial PF foams. However, the formaldehyde is normally used as a crosslinker to keep the foam density can be maintained. The limited crosslinking between tannin and formaldehyde provides limited mechanical properties of typical tannin-based foams. Therefore, the search for an alternative biobased crosslinker to replace formaldehyde was of interest, and particularly fruitful if it also resulted in enhanced mechanical properties and improved fire retardancy. A biorefinery waste, humins, and soybean protein isolate (SPI) were selected as formaldehyde substitute bio-sourced crosslinkers for two kinds of tannin-based foam formulations. As expected, the properties were improved by using these bio-sourced crosslinkers. The basic properties of series tannin foams were investigated. The morphology and structure characteristics were observed by scanning electron microscopy (SEM). Additionally, the crosslinking reaction mechanisms between tannin with the two bio-sourced crosslinkers, i.e., humins and SPI, were determined by MALDE-ToF and FTIR spectrometry. Finally, the thermal stability, mechanical properties, fire retardancy and formaldehyde emission were evaluated by the relevant techniques.

Key words:

Mimosa tannin; Lignin; Soybean protein isolation (SPI); Humins; Non-isocyanate polyurethane (NIPU); wood adhesive; biomass foam.

Présentation des publications

I Préparation de colles pour bois à base du système de résine polyuréthane non isocyanate (NIPU).

1. **Chen, X.**, Pizzi, A., Essawy, H., Fredon, E., Gerardin, C., Guigo, N., & Sbirrazzuoli, N. (2021). Non-Furanic Humins-Based Non-Isocyanate Polyurethane (NIPU) Thermoset Wood Adhesives. *Polymers*, 13(3), 372.
2. **Chen, X.**, Pizzi, A., Xi, X., Zhou, X., Fredon, E. et al. (2021). Soy Protein Isolate Non-Isocyanates Polyurethanes (NIPU) Wood Adhesives. *Journal of Renewable Materials*, 9(6), 1045-1057.
3. **X.CHEN**, A.PIZZI, E.FREDON, C.GERARDIN, X.ZHOU,B.ZHANG, G.DU, Lower Curing Temperature Tannin-Based Non-Isocyanate Polyurethane (NIPU) Wood Adhesives: Preparation and Properties Evaluation, *Int.J.Adhesion Adhesives*, *accepted* (2021)

II Préparation de colles à bois à base de tanin, de protéine de soja et de lignine.

4. **Chen, X.**, Pizzi, A., Fredon, E., Gerardin, C., Li, J., Zhou, X., & Du, G. (2020). Preparation and properties of a novel type of tannin-based wood adhesive. *The Journal of Adhesion*, 1-18.
5. **Chen, X.**, Xi, X., Pizzi, A., Fredon, E., Du, G., Gerardin, C., & Amirou, S. (2021). Oxidized demethylated lignin as a bio-based adhesive for wood bonding. *The Journal of Adhesion*, 97(9), 873-890.
6. Ghahri, S., **Chen, X.**, Pizzi, A., Hajihassani, R., & Papadopoulos, A. N. (2021). Natural tannins as new cross-linking materials for soy-based adhesives. *Polymers*, 13(4), 595.
7. **X.CHEN**, A.PIZZI, B.ZHANG, X.ZHOU, E.FREDON, C.GERARDIN, G.DU, Particleboard bioadhesive by glyoxalated lignin and oxidized dialdehyde starch cross-linked by urea, *Wood Sci. Technol.*, under review (2021).

III Préparation de mousses à base de tanin à base de système de résine NIPU.

8. **Chen, X.**, Xi, X., Pizzi, A., Fredon, E., Zhou, X., Li, J., ... & Du, G. (2020). Preparation and characterization of condensed tannin non-isocyanate polyurethane (NIPU) rigid foams by ambient temperature blowing. *Polymers*, 12(4), 750.
9. **Chen, X.**, Li, J., Xi, X., Pizzi, A., Zhou, X., Fredon, E., ... & Gerardin, C. (2020). Condensed tannin-glucose-based NIPU bio-foams of improved fire retardancy. *Polymer Degradation and Stability*, 175, 109121.

IV Mousses tanins-furaniques mousses.

10. **Chen, X.**, Guigo, N., Pizzi, A., Sbirrazzuoli, N., Li, B., Fredon, E., & Gerardin, C. (2020). Ambient Temperature Self-Blowing Tannin-Humins Biofoams. *Polymers*, 12(11), 2732.
11. **Chen, X.**, Li, J., Pizzi, A., Fredon, E., Gerardin, C., Zhou, X., & Du, G. (2021). Tannin-furanic foams modified by soybean protein isolate (SPI) and industrial lignin substituting formaldehyde addition. *Industrial Crops and Products*, 168, 113607.

General Introduction

Depletion of petroleum resources and increasingly consideration of eco-friendly conception were making consumers and researchers seek more safe products and resources. Therefore, extensively renewable resources are derived from nature which are utilized in several fields such as, materials science, biological medicine, energy, etc. Thereinto, engineering technology field as a critical part of materials science have been motivated their interesting from traditional fossil-based to intensively investigated topic on high-performance, low cost and eco-friendly bio-derived materials which driven by how to develop biomass engineering technology broadly. Among them, the wood industry was influenced extensively, for instance in wood construction and wood furniture. Then, wood adhesives and energy saving materials as two foundational of wood construction are nowadays also meeting a bottleneck point as their broadly fossil-based and toxicity components application.

Wood adhesives from renewable and non-toxicity resources is nowadays an extensively investigated hot-topic driven by the depletion of petroleum resources together with environmental concerns. The researchers are noticed that some kinds of wastage resources can be obtained from nature and act as the main component for wood adhesive fabrication. Forestry and agricultural residues have attracted more view sights by more researchers as they can provide a broad number of resources for wood adhesives development. And it is proven by the fact that they have huge potential for industrial application. In nature, various biomass resources, including soybean protein, cellulose, hemicellulose, lignin, tannin, starch, oil, etc, have been primarily focused on the wood adhesive manufacturing applications. Even though many successful formulations have been studied and reported, about the forestry and agricultural waste residues value-added wood adhesives applications are still the main topic on that.

Foam, a kind of porous material which possesses more special properties, such as light-weight, low thermal conductivity, strong adsorption, even high mechanical nature, usually acts as exterior-wall of building materials for energy saving or flame retardancy.

And some other applications also have been reported by literature, for instance, synthetic foams were utilized as an electrode or waste-water treatment polluted by heavy-metal or antibiotic or oils after though high temperature or other special modified treatments. But all applications of those foams should base on the properties of the original foams. From those, we can also find some points, such as either fossil-based (like phenol formaldehyde foam, polyurethane foam), toxic raw materials (as phenol, polyurethane, formaldehyde), and high price (polyurethane) or low mechanical properties. Then, there still have more works on how to prepare high performance, environmental-safety, low cost and conveniently biomass foam. Apparently, much works on this concept have been carried out from the last recent decades. One of the most fascinating foams is the tannin-furanic-formaldehyde foam as its light-weight, flame resistance, high porous property, convenient preparation process.

Herein, four main parts including two kinds of wood adhesives and tannin-based foams respectively were reported by using forestry and agricultural residues, such as mimosa tannin, industrial lignin, soybean protein, non-furanic humins, and furanic humins, for wood adhesives and foams preparation.

For the adhesive research part, based on non-isocyanate polyurethane (NIPU) reaction system, natural resources tannin, soybean protein isolate, non-furanic humins were chosen as wood adhesive's main components. Their adhesion properties shown varies based on their raw materials types. For example, our research group studied by Xuedong Xi, he used glucose as the starting material for wood adhesives' preparation, and this kind of system showed excellently bonding properties whatever treated the samples with hot or boiled water. However, SPI was utilized to synthesis SPI-NIPU adhesive system in this research, its properties although can be accepted but shows the strong difference with the glucose system. Therefore, this promoted us to research other biomass resources, like tannin and non-furanic humins, which act as a main part of wood adhesives. As expected, we have got outstanding results from the tannin and non-furanic humins NIPU adhesive systems. In addition, we considered from the industrial application and environmental-friendly aspects, a relatively lower fabrication temperature and low-emission modified formulation was reported based on tannin-

NIPU adhesive system. Obviously, its properties are acceptable and getting close to industrial application target to what we are expected.

Lignin was selected as the biomass resource for wood adhesives production. Two kinds of formulations were reported in this study, even if they showed totally different bonding properties which caused by two main effect pathways. However, these two pathways provide two synthesis concepts for biomass wood adhesives. But one point always keeps going is that non-formaldehyde addition, and retains the biomass resources content as high as possible. In addition, the crosslinking between condensed tannin and soybean protein was reported as well, which indicated that this pathway can satisfy the requirement for formaldehyde-free biomass wood adhesives preparation.

For the foam research part, there are two basic formulations that were reported in this study, i.e., tannin-based NIPU foams and novel tannin-furanic foams without formaldehyde.

For the former one, glucose-based NIPU foam was first reported by our research group, but its high flammability as traditional polyurethane foam therefore, tannin was the modifier to improve their flame retardancy which was then reported in this thesis. Tannin-NIPU has been reported for wood adhesives, then it can be utilized to produce NIPU foam as well. It is proofed by the facts which were shown in this research. For the latter tannin-furanic-based foams were reported by previous researchers as the oldest formulation. And during the last recent decades, many developed formulations were publicized gradually. Those formulations are toward the evolutions on improving their mechanical properties, reducing the toxic raw materials, and increasing their eco-friendly nature, etc. Hence, this work is still based on those development directions. Two main works on biomass resources replacement formaldehyde were carried out and reported here, and those new tannin-based foams were shown a better mechanical property than the traditional tannin-based formaldehyde foams. Furanic-humins which are derived from bio-refining by-product, it was first publicized to produce tannin-furanic foam without any aldehyde addition. This research promoted us to do further research work on biomass replacement formaldehyde formulations, and finally, as we expected that soybean protein isolate (SPI) was utilized to prepare tannin-furanic foam

with improved properties than traditional tannin foam.

1 STATE OF ART

The introduction was summarized from two main parts of research work depending on the specific experiments. The first research is on biomass resources, including tannin, lignin, soybean protein and non-furanic humins, which were selected as raw materials to prepare wood adhesives; Then, the second one is tannin-based foam fabrication without formaldehyde application.

1.1 Generalities of wood adhesives

The advancement of world industry has promoted the vigorous bloom of many fields, wood industry as one of beneficiaries which was keeping a large speed forward, with an undiminished upward trend now for very many decades. Wood adhesives as a crucial part of wood industry undoubtable have got a long-term progress as well. Generally, so-called formaldehyde-containing wood adhesives are normally referred to Phenol-formaldehyde (PF), Urea-formaldehyde (UF), and Melamine-urea-formaldehyde (MUF) resins, using commonly to wood-based panels manufacture. Some other kinds of wood adhesives, such as isocyanate-based, some formaldehyde-containing modified formulations, which were known as synthetic adhesives. Until nowadays, the synthetic wood adhesives do still dominate part in its market[1].

1.1.1 Phenol-formaldehyde (PF) resin

Phenol-formaldehyde (PF) resin was synthesized by reaction of phenol and formaldehyde with difference formulations and conditions. They are fully exterior-class wood adhesives which extensively applied to manufacture particleboard, OSB, and marine plywood as their excellent bonding performance and weather-resistant. PF resins are the second most important wood bonding adhesive (by volume) compared with UF resins, with up to 3 million tons per year being used in worldwide[2]. The main synthesis schematic structure can be described as in Figure 1.

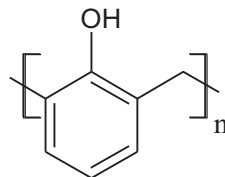


Figure 1 The schematic representation of a PF resin[2].

Even though the PF resins presented such more good performances, there still have some disadvantages substantially. The most striking thing is their highly curing temperature and slowly curing speed. In addition, their starting material chemicals toxically phenol and formaldehyde, in some extent, have attracted by more researchers concern duo to the conception of eco-friendly and economics. Moreover, the instability crude oil price of overworld also influenced the cost of PF resins, thus, in the next future decades, some low-cost non-fossil-based materials alternatively was adopted to substitute phenol for PF preparation.

1.1.2 Urea-formaldehyde (UF) resin

Urea-formaldehyde (UF) resins so far do occupy a master status in synthetic resin market. They were normally used to preparation for interior-grade wood composite panels and then for wood furniture and various of other applications. Approximately 11 million tons per year by volume for industrial utilization of these kinds of wood adhesives in the whole world. Their main synthesis pathway is represented by reaction of urea and formaldehyde according to the simplified Figure 2.

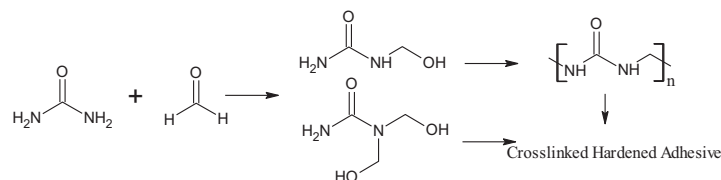


Figure 2 The basis reaction of urea and formaldehyde to prepare UF resin[2].

Compared with PF resin, urea-formaldehyde (UF) resins possess some advantages. The most dominant one is the incomparable price advantage of UF resins. However, some drawbacks such as resistance to exterior weather conditions and emission of formaldehyde remain shown more progress spaces. And, the UF resins presented an excellently bonding properties, their relatively low-cost, and ease of handling natures, which promoted its broadly industrial applications. Therefore, largely number of enhanced modification formulations were reported stimulated by the great potential industry applications and developed new-techs. Moreover, the synthesis technology of UF resins has greatly improved during the past few decades under the pressure of ever more stringent formaldehyde emission regulations and higher bonding performances.

1.1.3 Melamine-urea-formaldehyde (MUF) resin

Melamine-urea-formaldehyde (MUF) resin have been applied extensively to the impregnated paper, particleboard, and plywood as their good thermal stability, well-bonding strength, high-hardness, and transparent film with luster. Nevertheless, the melamine as a part of MUF resins, but its high cost, was utilized as modifier to improve traditional UF resins, commonly with a very small part between 2-5%. And the modified UF resins obtained a lower formaldehyde emission than before. Thus, it was usually considered as a potential pathway to modify UF resins. But, with the increasing addition amount of melamine, with a properly part between 30-40%, the new MUF resins then was applied to prepare wood panels to acceptable properties with exterior- and semi-exterior-grade. Their schematic representation can be shown in Figure 3.

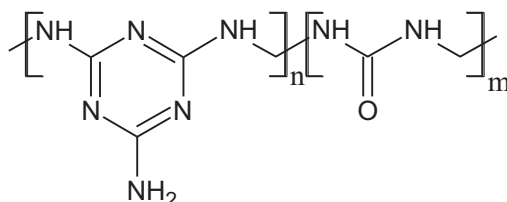


Figure 3 The schematic representation of a MUF resin[2].

Traditionally, the classic formulation of MUF resin usually needs to further develop because of their currently status such as free formaldehyde emission, short spot-life, brittleness, and high cost. A few decades ago, the MUF resins were considered as semi-exterior-grade resins, and their properties still enhancing by the technical progress and the great endeavors from broadly researchers. Fortunately, the progress in their technology has been so considerable that they can compete well in performance with the more classical exterior-grade phenol-formaldehyde (PF) adhesives.

1.1.4 Other resins for wood panels

Even though these parts of adhesives only participation a small portion of application in wood industry, they still do some indispensable contributions to the development of wood adhesives. For instance, isocyanate wood adhesive presented an excellent property as its inherent high activity groups which can easily crosslinking with other groups, such as polyols, forming the strong chemical bonds. And this kind of wood adhesives have attracted by the wood industry due to their non-formaldehyde

emission. In addition, only take a small portion of isocyanate wood adhesive can contribute a good performance which could comparable with tradition formaldehyde-containing wood adhesives. It can be schematically represented as Figure 4.

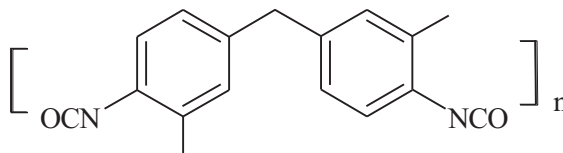


Figure 4 The schematic representation of p-MDI[2].

This adhesive, though, relatively high price than traditional major formaldehyde-based adhesives, causing the enterprises need to consider that the counterbalancing the advantage of the price and bonding performance. Even if it being needed in lower proportions. And simultaneously, its vapor and relative toxicity also bring some pressure to their application due to the strictly environmental regulations. A utilization where it has a particular advantage is in mixing, in smaller proportions, with any of the three formaldehyde-based adhesives to upgrade their performance.

1.2 The properties of biomass resources and its applications in wood adhesives

Wood adhesives severed as a critical role in wood industry, and its properties, including bonding strength, water resistance, cost, and environmental-friendly, determined their specific applications. The reason why traditional formaldehyde-containing wood adhesives occupied much more proportions in wood industry is that not only their competitive outstanding bonding performance but also their acceptable cost. Nevertheless, due to the high pressure from the stringent formaldehyde emission regulations and the instability of starting materials price because of the international oil price, causing and promoting more researchers began to concern that how to prepare novel wood adhesives by using biomass resources. This will be a common theme which the researchers are noteworthy to consider in the whole world nowadays even a long-term in the future. From the literatures in the last few decades, the following involved bioresources have attracted by the researchers and institutions of all the world successfully in wood adhesives field.

1.2.1 Lignin recourses and Lignin-based wood adhesives

1.2.1.1 Lignin resources

Lignin was considered as a ubiquitous biomaterial and an inexhaustible source to its extensively applications in various fields, and matches the worldwide trend for green chemistry and eco-friendly products[3]. It will be the greatest potential feedstock for novel-developed biomaterials because of its biodegradability, easy availability, and renewability nature, attracted much more attention by the researchers from the whole world. As shown in Figure 5, a three-dimensional view of the lignin-carbohydrate complex (LCC) exists in the wood cell wall. About 150 billion tons of nature lignin was biosynthesized by the plants each year, and rendering it as one of the most abundant bio-sources. Its multiple kinds of functional groups, prominently aliphatic and phenolic hydroxyl groups, along with some carbonyl groups leading to that the lignin can be chemical-edited to prepare some target products. And then those resultant-products can be utilized in large number of fields, owing to their complexing, binding, dispersing, and emulsion-stabilizing natures[4, 5]. As expected, that, lignin is not only can play a part in polymer science, being the precursor, but also is the starting materials for sustainable manufacturing small-molecular products, such as ferulic acid, vanillin, and phenol, among others[6]. Moreover, it is reported that there are various kinds of monomers chemicals production techniques which are based on the lignin raw materials but just that they come from natural plant in different classes[7-9]. Even though the lignin renewable source has such potential competitive, its drawbacks, like highly variable complex structure, polydispersity, tendency towards irreversible degradation, etc., limited and will continuing a quite long time its value-added utilization in commercial[3, 10, 11]. Only 5% of native lignin was undergone, nowadays, in low-value either commercial application or incinerated for energy recovery and electricity production[5]. From those abovementioned barriers we can know that it is still a challenge for its isolation, fractionation, modification, and characterization because of the assemblies and complexities of lignin. Hence, more researchers in whole world have done the same effort on this research activities on this hot-topic in the last decades and in future. And they have a same target and dream which is how to efficiency and cleanly utilization of the nature lignin resource.

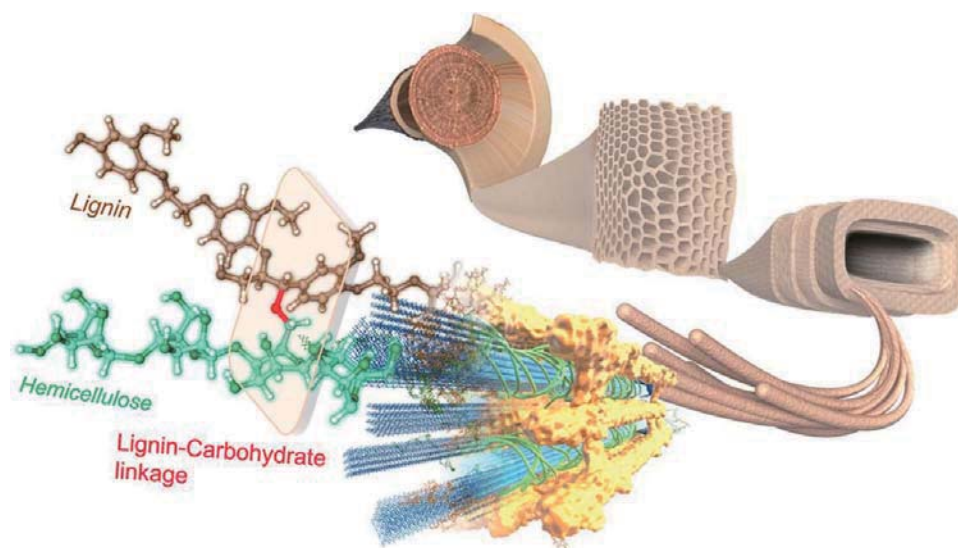


Figure 5 A three-dimensional view of the lignin-carbohydrate complex (LCC) in the wood cell wall[12].

1.2.1.2 Lignin separation and its products

Extraction and separation techniques, determines the products qualities and structures, and have been applied in various bio-sources such as woody origin, agriculture waste, promoting the researchers to know well about the lignin structures, and always keeping improvement[13]. Lignin normally entwined with cellulose and hemicellulose, acted as binder to render them contacting closely each other. As mentioned previously, lignin macromolecular structure will be destroyed by partial cleavage of crosslinking bonds in lignin molecular so that supporting the separation process[14]. Some old functional groups will maintain along with some novels formed, and their chemical activity on certain groups will be improved by losing the barriers of steric hindrance. Indeed, the change of lignin molecular mass could be huge which totally depending on their treatment method. Some potential separation strategies have been reported here, including chemical, physical, mechanical, solvent fractionation and biological pulping processes, and being expected to broadly industrial application[13-15].

The first-time reported method by Bjökman in 1956 to separate lignin with dioxane-water mixture, thereafter several techniques have been developed for lignocellulosic biomass separation with less condensed structure and high purity[5, 16].

The extraction methods are based on the concept of the dissolved or insoluble biomass, so that the lignocellulosic (cellulose, hemicellulose, and lignin) are naturally separated in their different phase (i.e., liquid, and solid phase). Therefore, be represented by Klason and enzymatic mild acidolysis methods are belongs to collect insoluble lignin part but dissolution the carbohydrate fractions mainly including cellulose and hemicellulose products. The other one is that lignin was dissolved into the treatment solutions then separated from the plant sources, leaving the carbohydrate fractions as the insoluble residues. Typically, liginosulfonate process, ionic liquid, and the alkaline wet oxidation pretreatments are categorized to the latter system[17]. According to the literatures, four main kinds of industrial separation techniques were performed currently which are kraft, soda, organosolv, and sulfite processes. They presented several differences not only on their molecular structures but also on the purity, which are shown in Table 1.

Table 1 Chemical composition of different technical lignin[18].

Lignin	Ash content (%)	Sulfur content (%)	Sugar content (%)	Molecular weight (g/mol)	Polydispersity
Kraft	0.5-3.0	1.0-3.0	1.0-2.3	Up to 25000	2.5-3.5
Soda	0.7-2.3	0	1.5-3.0	Up to 15000	2.5-3.5
lignosulfonates	4.8-8.0	2.5-8.0	-	Up to 15000	4.2-7.0
Organosolv	1.7	0	1.0-3.0	Up to 5000	1.5

1.2.1.3 Lignin structure and its chemistry

As we all know one fact is that the three phenylpropane units, i.e., Phydroxyphenyl (H unit), Syringyl (S unit), and Guaicyl (G unit), consisted of the primary chemical structure of native lignin[19-21], as shown in Figure 6. Clearly, the recognition and distinction on them can be performed by the methoxylation degree on the benzene ring[22]. And their relatively percentages are different depending on their diversion of original sources, such as 90-95 wt.% of G units in the total monolignols was biosynthesized to softwood original lignin. For hardwood lignin, the main components of it are both G and S units[17, 23]. But in grass lignin, we can observe all three kinds

of lignin monolignol types[24]. Therefore, the lignin structure and monolignol amounts are difference not only because of their isolation processes, but also due to their origination, for example, the amount of monolignols in softwood and grass will be greatly different[22]. Hence, the ratio of S, G, and H units now are normally utilized to analysis lignin properties during the lignin separation process.

With the lignification during the plant growth, the abovementioned three kinds of monolignols are crosslinked with a randomly way by ether bonds or C-C bonds at the various of locations. So, as shown in Figure 6, this kind of connection randomly way comes from the monolignol interunit linkages then generates several kinds of lignin substructures. The most type is β -O-4' ether linkage which accounts for approximately 50% in the total monolignols interunit linkages[25]. It has been reported in the literatures that this linkage has the most activity during the several activizations, for example, depolymerization process. β -O-4' cleavage always was the significant feature in the modification processes[26]. Therefore, the content variation of β -O-4' linkage was usually considered as a key criterion during the researches on lignin activation and degradation. In addition, some other type of connections including β - β' , β -5', β -1' and 5-5', can be observed in lignin structures as well, however, not as high amounts as β -O-4' linkage[22]. Some studies reported something about that chemical bond in lignin structure, such as probably because of the higher stability and longer lifetime of the sinapyl alcohol radicals making the largely β - β' linkage can be detected in syringyl-rich lignin[27]. Others, coniferyl alcohol through dehydrogenation polymerization promoted β -5' formation and existed in phenylcoumaran substructure[22]. Additionally, the amount of β -5' linkages can further increase during the steam-explosion pretreatment, some evidence indicated that some rearrangement reaction can occur in this process[28, 29]. β -1' type is an acidic instability linkage structure which is mostly in spirodienone substructure[30]. Finally, the linkage 5-5' normally comes from a biphenyl structure, and it is reported that this linkage was considered as a native one usually be found in the milled wood lignin[31].

Various and abundant functional groups have been detected and reported in lignin main structure by researchers, hydroxyl, benzyl, methoxyl, ether, carboxyl, etc.,

typically, so that endowed lignin with amphiphilic features[32]. As we all know, hydroxyl group is the most critical functional groups which also is one of key position for lignin modifications, for example, alkylation, esterification, phenolation, hydroxypropylation, and so on[10, 22, 33, 34]. Moreover, other lignin modifications, such as depolymerization and glyoxalation, are still aim to expose more higher relatively activity hydroxyl groups for the further applications. Two types of hydroxyl groups, aliphatic hydroxyl, and phenolic hydroxyl, respectively, have been found in the lignin structure. Hydroxyl group content was usually as the critical index to measure the etherification and condensation degree of lignin, and it can also influence the activity and solubility of lignin[35]. As report goes, ^{31}P NMR spectroscopy was deemed as one of the most powerful quantification methods to detect the different hydroxyl groups[19]. Two kinds of principal functional groups, benzyl and methoxyl groups are not only make up the monolignol fundamental structure but also have been utilized to distinguishing lignin with other main components in biomass. As described above, methoxyl substitution degree on the aromatic ring was the main differentiating way to identify the monolignol types of lignin. Ether bonds are the commonly existing bonds in lignin structure to connect between monolignols, like the two main types $\beta\text{-O-4'}$ and $\alpha\text{-O-4'}$ linkages. Sometimes, carboxyl group with a relative low concentration also can be observed, but their content can increase largely by modification, such as oxidation[36]. In summary, various of lignin monolignols, chemical bonds, and functional groups presented significantly scientific application values for high-performance materials fabrication.

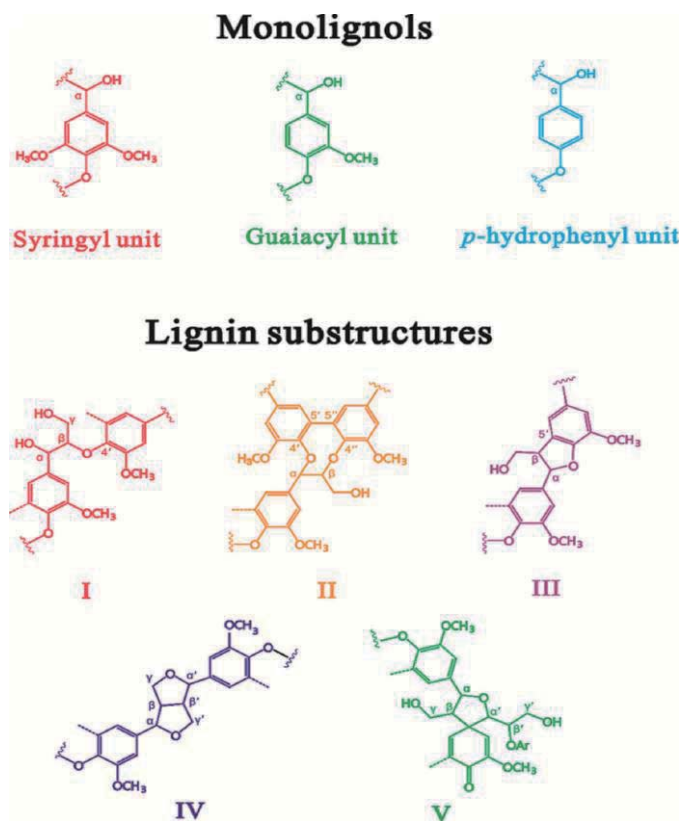


Figure 6 Monolignols (Syringyl; Guaiacyl; p-hydroxyphenyl) and lignin substructures (I: β -O-4' substructure; II: β -O-4', α -O-4' and 5-5' linkage in dibenzodioxocin substructure; III: β -5' linkage in phenylcoumaran substructure; IV: β - β' in resinol substructure; and V: β -1' linkage in spirodienone substructure).

1.2.1.4 Lignin activation and lignin-based wood adhesives

Lignin is a typical macromolecular as similar with the most of plant derived biomass and can be used as binder to adhesive wood pieces. At the same time, lignin-based wood adhesives exhibit highly biomass nature but relatively low bonding performance and the unaccepted water-resistance. Therefore, some targeted modification strategies have been suggested by many researchers, such as demethylation, oxidation, methylolation, phenolation, reduction, and hydrolysis, which are promoted the reactivity of native lignin so that improved the bonding strength undergoing for wood composites[37].

I Lignin activation methods

Demethylated lignin: Demethylation technique is a normal strategy to improve the activation of lignin, and was deemed as the most efficient and potential strategy to

convert the methoxyl groups to phenolic hydroxyl groups. More catechol moieties were obtained in the lignin structure, so that more reactivity points on the lignin phenol ring was released after this process[38]. Typically, four kinds of lignin demethylation strategies were extensively reported by researchers. Some acidic agents, such as hydrogen iodide, hydrogen chloride, and lewis acid, have been utilized to employed remove methoxy groups by cleaving the ether bonds between benzene ring and methyl[39-42]. But in the acidic demethylation lignin process, usually nitrogen protective environment or highly reaction temperature were necessary for ensuring the products inherent characteristic and productivity[43]. Additionally, some mild methods concentrated on the motivate the activity of modified lignin by using fungal (white rot fungi or brown rot fungi) or bacteria (*Pseudomonas* or *Sphingomonas*)[44-46]. And simultaneously, the lignin depolymerization will occur inevitably. Normally, the longer fabrication time consumption than other methods was needed. Therefore, it is still a problem and challenge to solve for the researchers so that can reach the industrial requirement. Some new demethylation agents have been reported, especially nucleophilic reagent, including sulfur-bearing agents (Na_2SO_3 , S, NaSH, n-dodecyl mercaptan), thioalcohol, which are the normally reagents to make demethylated lignin, as shown in Figure 7. And this nucleophilic reagent attacking method can produce the modified lignin under a mild condition, generally low reaction temperature and short preparation time consumption[38, 42]. And the reagent Na_2SO_3 was considered as the most promising and efficient way to produce methylated lignin[38].

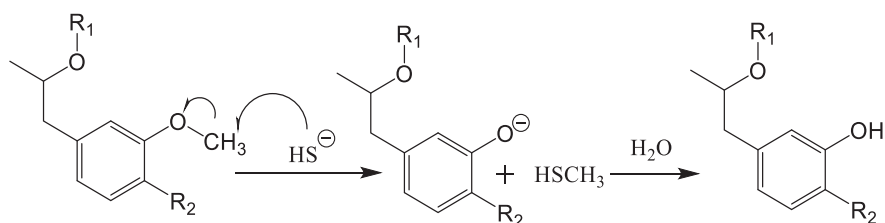


Figure 7 Demethylation of lignin

Methylolation lignin: This method is another way to inspire the lignin activity usually by small molecular aldehyde chemical, such as formaldehyde and glyoxal, so that a side chain was drawn from the benzene ring[37, 47, 48]. And this side-chain can remit the pressure bring from the steric hindrance in some extent, therefore, their

activity was improved. Normally, the methylation of lignin process accompanies with other lignin pretreatment, for example lignin depolymerization. By this process, the small lignin molecular which obtained from depolymerization was connected by using crosslinker, resulting to the products can reach a certain crosslinking degree so that for better lignin-based resin preparation[49]. In addition, like acetic acid lignin (AAL) obtained from phenyl/alcohol refining was sometime used as raw lignin for novel materials preparation. And before the polymerization, lignin reacted with formaldehyde to produce methylation lignin and then obtained an extra activity side chain, as shown in Figure 8. Therefore, a kind of polyurethane-lignin wood adhesive was obtained by using that methylated lignin to react with isocyanate, showing a well bonding strength and water resistance[50].

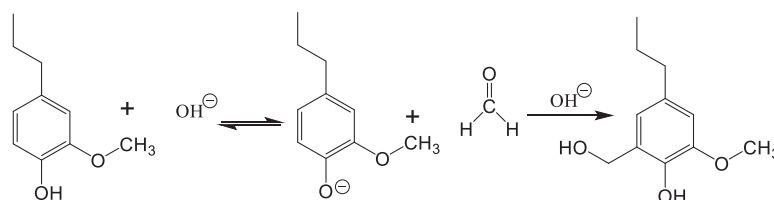


Figure 8 Methylation of lignin under alkaline condition.

Phenolation lignin: The main target of phenolation is to improve the reactivity of lignin, and the meantime to decrease the molecular mass of lignin so that can suitable for various applications[51-55]. The essence of this modification process is based on the reaction between lignin and phenol, as shown in Figure 9[56]. And it was a more potential method for industrial application. However, the phenolation process has selective nature for lignin types. The most problem of this method is its fossil-based toxic phenol raw material. The phenolation modification process can appear on the α position which was an activity center and brought from multi-kinds of functional groups. Thus, there are two basic phenolation modification methods, acidic and alkaline environments, respectively. For example, because of the electron induced effect of the phenol hydroxyl group, the functional groups on the α position, such as hydroxyl group, ether bond, or C=C bond, do occur breakage, then, the phenol hydroxyl group was converted to the methylene quinone structure. The phenol then connected on the lignin structure on the α position by the para-site or ortho-site nucleophilic substitution. It was

reported that as present the alkaline phenolic modification is the one of effective methods for lignin activity[55]. And, this kind of product was great potential for partially substitution fossil-based phenol product for preparation novel phenolic resin adhesives.

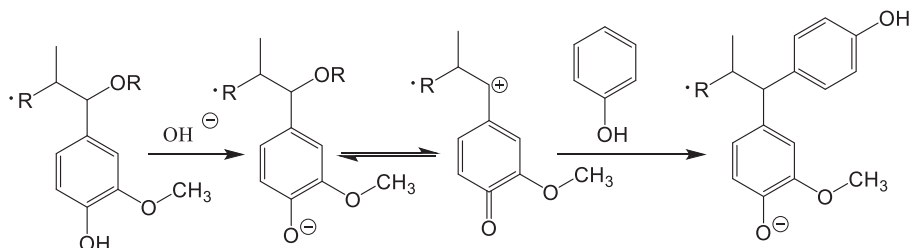


Figure 9 Phenolation of lignin under an alkaline condition.

The phenolation modification also can do fulfil under acidic condition but different with alkaline environment, the α position of lignin macromolecular presents multi-kinds of functional groups breakage, so that forms a carbocation. And then, the phenol then connected to the lignin structure on the α position by the para-site or ortho-site nucleophilic substitution, as shown in Figure 10. Sodium lignosulphonate and kraft lignin were reported to suitable for the acidic condition phenolation process, and can significantly improving lignin activity[51, 53, 56]. Phenolated lignin was normally utilized to prepare lignin-phenol-formaldehyde resins for wood bonding with various technology process. The reduced lignin molecular mass not only decreased its steric hindrance for improving the modified lignin reactivity, but also increased the number of reaction points by introducing phenol on lignin molecular.

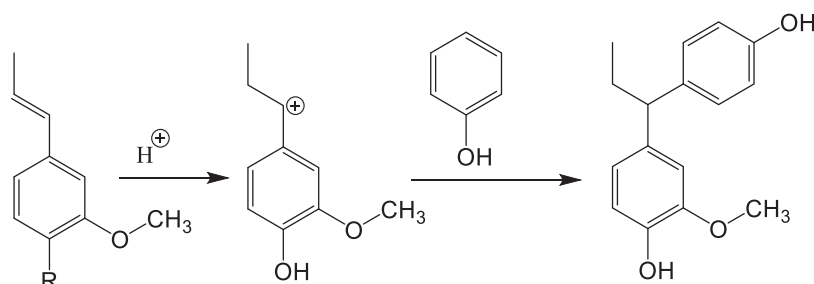


Figure 10 Phenolation of lignin under an acidic condition.

Depolymerization: Lignin depolymerization is an efficiently method to modify lignin by breaking some chemical bonds in lignin structure, but fulfilling this process still a challenge. The lignin reactivity will be extensively improved by depolymerization, this change is coming from not only the decreased steric hindrance,

and some new exposed reaction points after modified. Those depolymerized lignin will promote that it was stripped from the surface of cellulose smoothly, so, enhanced the separation process during lignin recovery from other biomass resources[57]. Furthermore, some energy-related, such as bio-ethanol, bio-diesel, and others, was also the down-stream products of lignin separation, for example, the lignocellulose by pyrolysis converting, leaving the hydrolysis lignin as the residue, so that fulfilled the lignin recycle process[58]. The commonly lignin depolymerization products are related to some commercial chemical products duo to their unique and bio-derived phenol-like monomer structures[57].

II Lignin served as starting materials for wood adhesives preparation

Lignin, as its multi-types of activity groups can used to react with another chemical agents, resulting some complex crosslinked structures thus playing the roles for wood bonding.

A, Aldehyde-containing lignin wood adhesives.

As a nature polyphenol structure biomass source, lignin was commonly utilized as fossil-based phenol chemical substitution mass, for a novel lignin-phenol-formaldehyde (LPF) wood adhesive preparation[55]. According to this strategy, technical lignin was utilized as 10%-70% proportion to substitute non-renewable fossil-based source phenol for LPF manufacturing[59-61]. And, in their reaction system, normally reduced bonding strengths in some extents were obtained comparing with commercial PF resins. But their bonding performance be still accepted for industrial application requirement, even exterior grade. In addition, a critical parameter, formaldehyde emission attracted the researcher's attention as LPF will present a relatively lower emission value than commercial PF resin[59].

As reported abovementioned, the activity of native lignin is quite limited so that it is still a really challenge for industrial preparation[61-63]. Therefore, some modification as mentioned above were commonly utilized to active lignin molecular, and various of modified lignin also usually used for wood adhesives production with a good performance. For example, moroccan sugar cane bagasse lignin was pretreated by alkaline condition, and then the resulted lignin was used to prepare LPF resin with

properly proportions phenol substitution[59]. Biorefinery technical lignin was selected to fabricate LPF resins after phenolation activity pre-treatment under alkaline condition[55].

Although that kind of lignin was considered as a great potential bio-resources to make LPF resins, and those novel lignin-based wood adhesives shown an acceptable performance even more lower formaldehyde emission in some formulations. But the researchers are still working on the topic that how to reduce the hazardous mass release, especially formaldehyde. Alkaline lignin and soda lignin were the raw materials, and glyoxal was utilized to replace formaldehyde to produce lignin-phenol-glyoxal wood adhesives[64]. And the bonding strength is worth to be expected. Series of LPF adhesives studies give all researchers more confidence for this novel products development, but we still have more practice efforts work to realize its industrial applications.

B, Lignin-tannin adhesives.

Lignin and tannin, two native polyphenol sources, their common phenolic structures endow them all served as the candidate for non-renewable phenol chemical substitution to manufacture or modify wood adhesives[2, 65]. Therefore, they have some similar activity groups, for example, benzene ring and its active positions, the phenol hydroxyl groups, thus, there is no exactly reaction between them. That is to say, the crosslinker was necessary to realize the “reaction” between tannin and lignin molecular. But due to their biological compatibility, only need to inflict small amount of crosslinker then can obtain an acceptable crosslinking performance, this strategy still can have more potential for industrial application development.

Between them, some promising crosslinkers have been utilized to make wood adhesives by linking lignin and tannin. In addition, because of the low reactivity of lignin, so, the modified lignin, for example glyoxalated lignin was normally utilized to prepare lignin-tannin wood adhesives[66-69]. Polymeric isocyanate (p-MDI) is a highly reactive substance, can be served as “bridge” to connect tannin and glyoxalated lignin, larging the molecular mass of resulted-products[66]. Furthermore, the p-MDI, and even some synthetic resins were the “fortification” agents to improvement the

bonding performance. Therefore, this kind of formaldehyde and synthetic resin free strategy not only making the harmful aldehyde reaction additive is minimized but also can increasing the proportion of natural sources, environmentally friendly materials are maximized.

Lignin was in considerable proportion, 50%, to modify tannin based non-aldehyde wood adhesives and without any fortification additions such as p-MDI and synthetic resin. Note that an acceptable performance has obtained and can satisfy the interior grade panel application[67, 68]. And, compared with the other crosslinker modified resins, almost 94% of natural parts in these adhesives systems has obtained, and gained the bonding strength more than p-MDI addition. Only the rest 5-6% of the adhesive which are composed of glyoxal, a non-toxic and non-volatile aldehyde and of hexamine, non-formaldehyde-yielding compound, a highly reactive chemical agent with tannin. Additionally, two particleboards and plywood as well, were bonded by using cheaper non-purified organosolv lignin and purified type, and showed the same level with them.

C, Lignin-protein adhesives.

Protein, because of its own various active groups, typically, $-NH_2$, $-COOH$, $-OH$, resulting to a large bunch of materials can crosslink with it, such as lignin, tannin, epoxy, etc. Therefore, in the lignin-protein based adhesives, the final target is that how to improve the crosslinking degree between lignin and protein. Thus, this aim can be achieved by series of strategies[70-76].

Soy protein isolates (SPI) or modified soy protein (MSP) was blended with sorghum lignin (SL) and extruded sorghum lignin (ESL) under natural or alkaline condition directly, respectively, to prepare plywood and obtained excellently dry and wet shear strength along with almost 100% wood failures[70]. The increased lignin proportions can significantly improve the bonding performance due to their molecules could efficiently entrap each other so that can improve water resistance. And extruded sorghum lignin (ESL) has higher promotion efficiency than native sorghum lignin, because of the exposed texture[77]. The adhesives were prepared with lignin and protein under alkaline condition, however, leading to the educement trend on bonding strength than the adhesives obtained under natural.

Low-cost lignin-based resin (LR) with different addition amount proportions was served as modifier to enhance the bonding strength of soybean meal-based wood adhesive in the research[71]. 10% of LR addition was the best incorporation for improving the wet condition shear strength of the resultant plywood. And this adhesive has a good physical property, for example, viscosity, solid content, can suitable for industrial application. The enhanced performance mainly comes from the crosslinker network due to the reaction between LR and the functional groups of soybean meal. In addition, the incorporation of LR can greatly increase the thermal stability of the cured adhesive, forming a crosslinked protein molecule-based structure, and create a smooth surface with fewer holes and cracks to prevent moisture intrusion, which further improved the water resistance of the resultant adhesive. Furthermore, polyamidoamine-epichlorohydrin (PAE) was used to go forward to enhance the bonding strength of LP-soybean meal-based wood adhesives[74]. It is clearly that the highly activity of PAE not only do occur polycondensation so that improved the crosslinking degree of adhesive system, but also PAE do react with LP resin and soybean meal, accompany with a suitable viscosity, spreadability, and permeability.

Lignin through pre-modification before utilized in wood adhesives normally can enhance the bonding performance, due to some groups which originally blocked, will be active by some technique methods, such as lignin ammonification, depolymerization, and oxidation[72, 75, 76]. In the end, those wood adhesives are obtained an acceptable performance and satisfy the relative requirement.

D, Lignin-polyurethane adhesives

Isocyanate-based commercial polymer is an expensive starting material for polyurethane (PU) manufacturing, and its high toxicity synthesis process does not avoid. But, its highly reaction towards to the chemical compounds containing active hydrogen makes it becoming to a crucial chemical raw material, and its resulting products have been applicated in various fields, such as furniture, automobile, aeronautics and astronautics, building, etc. Among them, the most classical synthesis process, polyurethane products were obtained from the reaction of isocyanate and polyols, the resins were finally utilized to prepare PU foams or wood structure applied adhesives.

As for these reasons, isocyanate was commonly used to modify wood adhesives for their performance enhancement[66, 78-80].

Lignin contains -OH on the phenol ring, acts as the functional of polyols to react with isocyanate, thus, this pathway has become a potential method for fossil-based polyols substitution under the extensive consumption and shortage of fossil resources[81-85]. Therefore, lignin firstly was selected as the modifier to improve the bio-content of PU wood adhesives, and there is no significant effect for PU adhesives performance while using a small amount of lignin addition[86, 87].

To fulfil the replacement of polyols using a large proportion, lignin needs to pretreat before polymerization with isocyanate, thus, more reaction activity groups will be exposed by the pretreatment. Hydroxy propylated lignin was utilized to replace 50% of fossil-based polyols for lignin-isocyanate preparation[88]. This kind of material also can obtain an excellent performance. In addition, hydroxymethylated lignin, as abovementioned, can obtain more active -OH amounts by using native lignin pre-reacting with small part of formaldehyde. And then utilized as bio-polyols to react with MDI to produce partially bio-based polyurethane[50, 88]. In the wood adhesive field, this method was a normally utilized as well. And their thermal stability could be enhanced because of the denser urethane crosslinking structure which obtained from the modified lignin and MDI as well as the stiff frame of lignin. Their bonding performance surely have been enhanced by comparing PU wood adhesives modified to native lignin. The main reason on this difference phenomenon is attributed to the -OH groups amount, and this result have been proved by other researchers[89].

However, isocyanate is always the predominant aspect on influencing the price and application fields of PU products. Therefore, some non-isocyanate polyurethane strategies were published. Traditionally, there are several mainly stream methods for preparing non-isocyanate polyurethane, of which biomass sources were the fully bio-polyols, of one method, then by reacting with dimethyl carbonate and diamine. And some kinds of bio-resources, such as tannin, lignin, glucose, sucrose, and SPI, have been utilized to prepare bio-based non-isocyanate polyurethane, and they also have been used to bond wood veneer[90-97].

F, Others

Due to the compatible of lignin, it can be used as wood adhesives not only by cooperating with the previous mentioned materials but also can react with others, for example, polyethyleneimine (PEI), furfuryl-based, for wood adhesive preparation. Lignin can be used to crosslink with PEI, thus, to come true the adhesion functional, however, the pretreatment was necessary, for example demethylation. Normally, two reaction mechanisms have been suggested by researchers between lignin and PEI, i.e., Schiff bases and Michael addition[98]. The crosslinking between them endows an excellently bonding performance along with strong water resistance. As similar as tannin structure, lignin has a phenol-like nature, therefore, lignin was applied to produce wood adhesives following tannin-based formulations. For example, lignin was reported to blinder with furfuryl alcohol resins, the composites bonded by lignin-furfuryl resins can obtain a strong tensile strength similar with PF resin[99, 100].

1.2.2 Tannin resources and tannin-based wood adhesives

1.2.2.1 Tannin resources

The word “tannin” has been viewed at a pronoun of natural phenolic chemical compounds, it contains two different classes of resources: hydrolysable tannins and condensed tannins. The hydrolysable tannin extracts are components of some simple phenols (for example, pyrogallol and ellagic acid), esters of a sugar, principally glucose, and gallic and digallic acids[2]. Its main parts of monomers were shown in Figure 12.

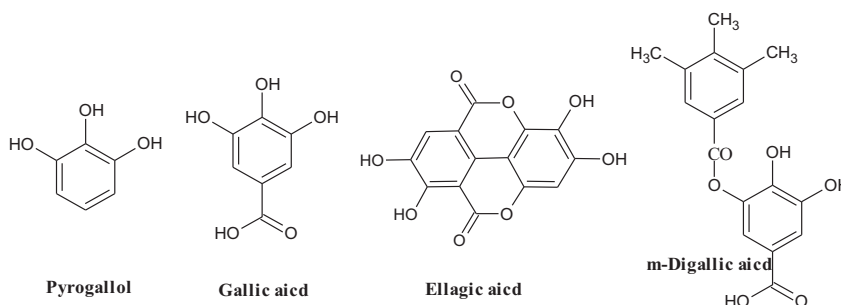


Figure 12 Some monomers of hydrolysable tannin.

From the based structures, their phenol-like monomer making them have been proved that can be utilized to manufacture tannin-phenol-formaldehyde wood adhesives by partially substituting phenol[101, 102], as its chemical behavior to

formaldehyde is analogous to phenol[2]. Nevertheless, the hydrolysable tannin was not taking a large proportion on wood adhesives preparation, because of its lack of macromolecular structure in the natural condition as well as their low nucleophilicity. Moreover, the limited production in worldwide range, results to a higher available price than condensed tannin, preventing their extensively chemical and economical interest. Thus, we did not concern any researches and applications in this thesis based on the hydrolysable tannin resource.

Condensed tannin, whereas, occupied almost 90% of total tannin production within the whole world, which have more potentially applied to produce wood adhesives not only from the chemically aspect but also economically. As well all know, condensed tannins are wide distribution in nature with their elementary flavonoid precursors, especially largely contribution in the wood or bark of various trees[2]. It is broadly reported that condensed tannin resources such as wattle or mimosa bark, quebracho wood, hemlock bark, sumach, and pine extracts have been utilized for various materials preparation (as shown in Figure 13) for example tannin-based foam, wood adhesives, adsorbent, and so on[2, 95, 101, 103-105]. Their commercial application was aroused since the depth fossil-based sources consumption resulting to the increased products price and decreased availability of synthetic phenolic, leading to many researchers to focus on petroleum phenol substitution by natural sources-condensed tannin. For example, the condensed tannin was used to prepare tannin-phenol-formaldehyde wood resins, successfully, and those resultant resin products have been industrial large-scale applied well in south Africa artificial boards industries[2].

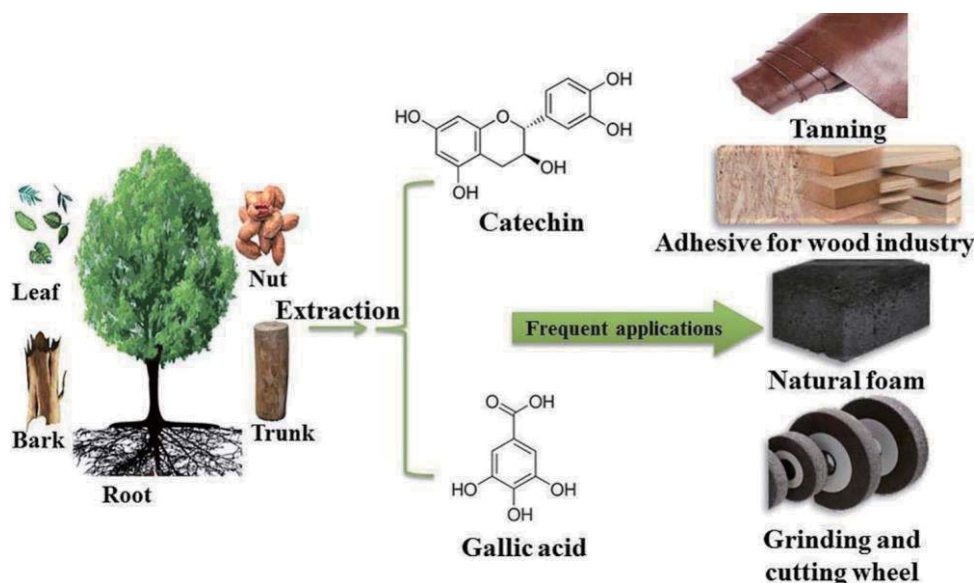


Figure 13 Tannin sources and its potential applications.

1.2.2.2 Tannin separation

Condensed tannin normally exists in plant with a macromolecular which are repeated flavonoid units, by and large, it can be collected by extraction process. The main target of the extraction is done by breaking the relatively unstable bonds between those repeated flavonoid units, and then decreasing the polymerization degree so that can obtain small molecular flavonoid precursors. The extraction process generally does occur in hot water with or without alkaline condition, sometimes along with Na_2SO_3 or NaHSO_3 , and simultaneously tannin oligomers usually accompanied by some impurities, for example, carbohydrates, phenolic monomers, and salts, were both obtained.

The extraction yield and purity were influenced by the plant species as well as the type of solvents used or of the additives added to the solvent. As summarized in Table 2, some different methods for tannin extraction be performed from various plant resources. Traditionally, the solid/liquid extraction was considered as the simplest way from the economy and operability for recovering tannins from plant tissues. Their general operating steps are described in Figure 14. Apart to discover the various high tannin-containing raw materials, such as the barks resources of pine (*Pinus radiata*), oak (*Quercus* sp.) (partially hydrolsable too), mimosa (*Acacia mearnsii*) or the quebracho wood (*Schinopsis balansae* or *lorentzii*)[2, 106-109], and by-product from agricultural

wastes such as tea (from various species) and coffee (*Coffea arabica*)[110-112], and fruit residues such as persimmon (*Diospyros* sp.) hulls, grapes (*Vitis vinifera*) skin, and many others as well[113-116], how to extract tannin oligomers with highly-efficiency and safety ways still occupied a predominant trend from past few year to currently on tannin extraction researches. Therefore, tannin extraction parameters, including temperature, the ratio of solid/liquid, solvent type, extraction time, etc., are also the work points needing to concern carefully[107].

Three main approaches, i.e., maceration, decoction, and soxhlet extraction were performed to perform the tannin separation assignment. But, some health-threatening solvents, such as dichloromethane or hexane, was firstly used to treat the plant sources and to destroy their complete organization, usually chlorophylls and lipids. Thereafter, some more safety solvents have been chosen, stimulating by the healthy requirements, for tannin extraction, typically, water, ethanol, acetone, or methanol[117]. And it was proved by some researchers, a highly tannin yielding was obtained while under some reaction conditions by the solvents of them. Even so, those organic solvents, such as acetone or hexane, have also been utilized in many researches, however, the utilization of them still exist some environmental and human health risks. Thus, water was considered as a desired solvent, for substituting those organic solvents to extract tannin from natural sources[107, 108]. Its water-based extraction system, sometimes accompany with base chemical, normally easy for operating, the residues including solid and liquid obtained do not have the strong negative influence on environment and human healthy. The most importantly is that the tannin extraction yielding is quite elevated, revealing this extraction as an efficient technique, in both economic and environmental terms. However, the highly amount of water required is the main drawback.

Some novel extraction methods are solvent treatment assistant with other techniques, for example microwave, ultrasound-assisted or based on compressed fluids techniques, subcritical water, supercritical fluids, pressurized fluids, or different solvents[95, 117, 118]. Observably, those methods have the relative high requirement on the equipment and the working experience on technicians, representing those

methods are not satisfy the large-scale industrial requirement as well.

Table 2 The part of tannin extraction methods from different natural resources

Species	Extraction methods	Yielding (%)	Ref.
<i>Pinus pinaster</i> Bark	80°C hot water condition	6.4	[119]
	Hot water under alkaline condition	15-30.7	
Silver fir bark (<i>Abies alba</i>)		11.6	
European larch bark (<i>Larix decidua</i>)		20.1	
Norway spruce bark (<i>Picea abies</i>)	60°C hot water condition	10.6	[120]
Douglas fir bark (<i>Pseudotsuga menziesii</i>)		17.3	
Scots pine bark (<i>Pinus sylvestris</i>)		4.8	
Myrcia eximia DC., tree bark	water	27.5	[108]
	3% sodium sulfite solution	35	
Mimosa (bark)		30-33	
Quebracho (wood)	Hot water	26-29	[121]
Pine (bark)		13-15	
Pine (bark)	Sulphite-water (12-15) or sulphite-water-urea (18-25)	12-25	[122]
Coriaria nepalensis bark	NaOH hot water solutions	12.98-	[107]
		16.02	
Spent coffee grounds	NaOH hot water solutions (100°C)	Maximum 21.02	[112]
<i>Pinus pinaster</i> bark	NaOH hot water solutions	13.8-	[123]

STATE OF ART

		22.39	
Grape pomace	Sodium hydroxide (NaOH) at 120°C during 2 h	Around 30	[113]
	NaOH hot water solutions with the concentration 5%-15%	22.6-58.8	
Grape pomace	NaOH (2.5%-7.5) with Na ₂ SO ₃ (2.5%-7.5)	23.2-37	[114]
	NaHCO ₃ (2.5%-7.5) with Na ₂ SO ₃ (2.5%-7.5)	16.7-33.1	
	Na ₂ CO ₃ (2.5%-7.5) with Na ₂ SO ₃ (2.5%-7.5)	22-45.3	
Aleppo pine bark		25-26	
Brown Rhus tripartitum (sumac) bark	Solution of base (NaHCO ₃ 0.5%, NaHSO ₃ 2%)	29-32	
Aumac root bark	water containing 2 % of sodium bisulfite and 0.5 % of sodium bicarbonate	-	[124]

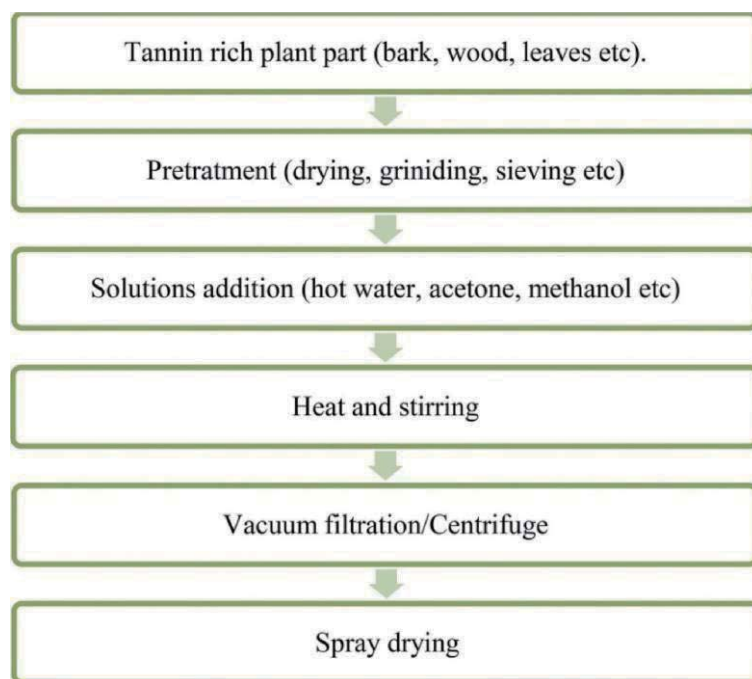


Figure 14 The typical extraction process of condensed tannin.

1.2.2.3 Tannin structure and its chemistry

I Tannin structure

Condensed tannin by definition, it is an integration polymer which consisting of flavonoid units with different condensation degree, and normally crosslinked with flavan-3-ols, flavan-3,4-diols and non-flavonoid ingredients generally some flavonoid analogs, carbohydrates, and traces of amino and imino acids, as reported[2]. Some mono-flavonoids and nitrogen-containing acids also been observed in the extraction products, but usually could not threat the chemical and physical characteristics of extract integration as their low proportion. The simple carbohydrates, normally hexoses, disaccharides, pentoses, and complex glucuronates (often hydrocolloid gums) can influence the viscosity of extraction products solution. An apparently example can prove that the physical performances of the whole natural extracted products would alter while those simple carbohydrates or disaccharides amount reached enough, the most intuitive manifestation of this is viscosity feature.

Condensed tannin monomer is consisting of 3 to 8 flavonoid repetition units by the link position C4–C6 or/and C4–C8 bonds, as shown in Figure 15[125]. The flavan-3,4-diols and flavan-3-ols are mainly the associated precursors to form flavonoid

monomers. From the basic flavonoid monomer structure shown in Figure 15, there are two possible configurations on the phenol rings for A and B, i.e., with or without -OH group on positions 5 and 5'[106]. Basically, four configurations therefore can be generated for condensed tannin polymerization, resulting to different properties for tannin products[126], as shown in Figure 16.

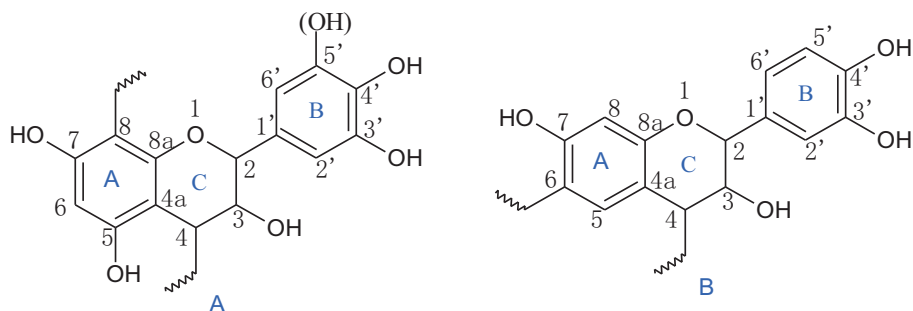


Figure 15 Chemical structure of the C_{15} unit in condensed tannins. $C \rightarrow C$ linkage between C_{15} units: $C4 \rightarrow C8$ (A), and/or $C4 \rightarrow C6$ (B)[125].

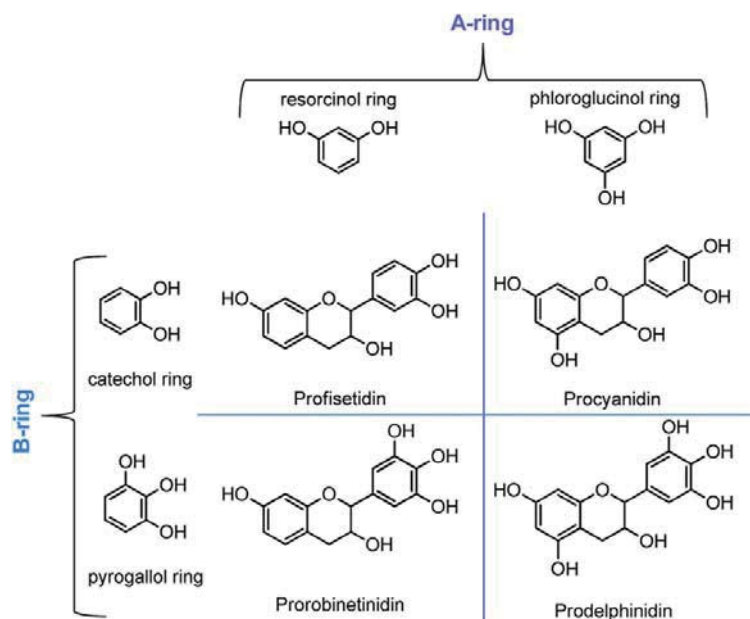


Figure 16 Structures of the four mono-flavonoid building blocks[106].

Due to the relationship of associated precursors (flavan-3-ols and flavan-3,4-diols) of condensed tannin monomers, their each connection is finally based on the nature of the phenol rings. Moreover, the feature of rings is normally related to their number of -OH groups and positions[127]. A resorcinol type A-ring (substitution by an -OH in the meta position) of the flavan-3,4-diol as well as the oxygen in the heterocycle create high nucleophilicity on C6 and C8 positions. Therefore, the tannin monomers are

crosslinked by the C4–C6 or C4–C8 bonds, usually with different condensation degree, as mentioned before. For example, profisetidins and prorobinetidins structures are normally connected by C4–C6 bond but in procyanidins and prodelphinidins structures are broadly found the C4–C8 type connection, as reported by researchers[127].

Generally, the proportion of each mono-flavonoid building blocks can influence the reactive significantly, such as approximate 90% of mono-flavonoid is belong to prorobinetidin, resorcinol A-ring, and pyrogallol B-ring, in mimosa tannin extract[128]. Another, for quebracho tannin contains more than 80% of flavonoid tannin with the type of resorcinol A-ring and catechol B-ring (i.e. profisetinidin flavonoid unit, as shown in Figure16)[129]. However, a more reactive tannin extract from pine bark, so called as pine tannins have a slightly different mono-flavonoid structure with mimosa tannin. This pine is tannin based on the structure of phloroglucinol A-ring and catechol B-ring (i.e. procyanidin flavonoid unit) or/and of phloroglucinol A-ring and a pyrogallol B-ring (i.e. prodelphinidin flavonoid unit)[129]. Consequently, the A-ring of pine tannins usually are far more reactive than the A-rings of mimosa or quebracho-type tannins, in 6-7 times[128, 129].

One of the most intuitive differences is the -OH present on the phenol rings, and that eventually led to huge difference between A-ring and B-ring on the reactive of them. As reported in the many literatures, the nucleophilic centers of the A-ring are usually reactive than B-ring[106, 125, 128, 129]. In addition, this phenomenon also has been proved by their application on wood adhesives. Typically, tannin was usually utilized as nature-phenol structure starting material to replace fossil-based phenol to synthesis tannin-phenol-formaldehyde wood adhesives. During the polymerization process, tannin can easily react with formaldehyde, but this reaction does appear between tannin A-ring and formaldehyde, only for tannin B-ring while the pH presenting a high condition (normally pH=10).

II Physicochemical properties of condensed tannin

Condensed tannins generally are pale yellow-slightly brown solid oligomers/polymers with low-density amorphous non-crystalline features[125]. The stereochemistry of condensed tannins is highly based on their mono-flavonoid structure

and condensation degree. The dried tannin powder exhibits a strong hygroscopic, and represents a highly absorption in the UV-Vis region with several local maxima (λ_{\max} : 250 and 290 nm)[125]. Tannins are mainly soluble in water, short-chain alcohols (methanol, ethanol), and acetone aqueous solutions, and the tannin/water solution usually shows an acid condition, for example, mimosa tannin presenting a pH value around 3.5 when the concentration is 50% in water under a room condition.

Condensed tannins have been exhibited multiple physicochemical properties which are related to their special flavonoid structure and the -OH on the flavonoid rings[130]. The basic physicochemical properties and reactivities of the phenol functional group are shown in Figure 17. For example, phenolic compounds from persimmon pulp have been reported to be a high molecular component, where their large amount of -OH endowed it has a strong hydrogen bond-forming ability[131]. Of course, the antioxidant activity always is their overwhelming superiority[132, 133]. In addition, persimmon condensed tannin was general a candidate to treat pollution water, such as adsorbent for some heavy metal[104]. The phenyl rings and hydroxy substituent of phenol functions result in both hydrophobic and hydrophilic character, which can act either as a hydrogen-bond donor or as an acceptor (Figure 17). Moreover, condensed tannin has been utilized to improve the fire resistance of glucose-based non-isocyanate polyurethane foam and silk because of the ability of oxygen radical extinction[134, 135]. The highly UV protection property also has been reported to be an additive in various materials to enhance their anti-aging performance.

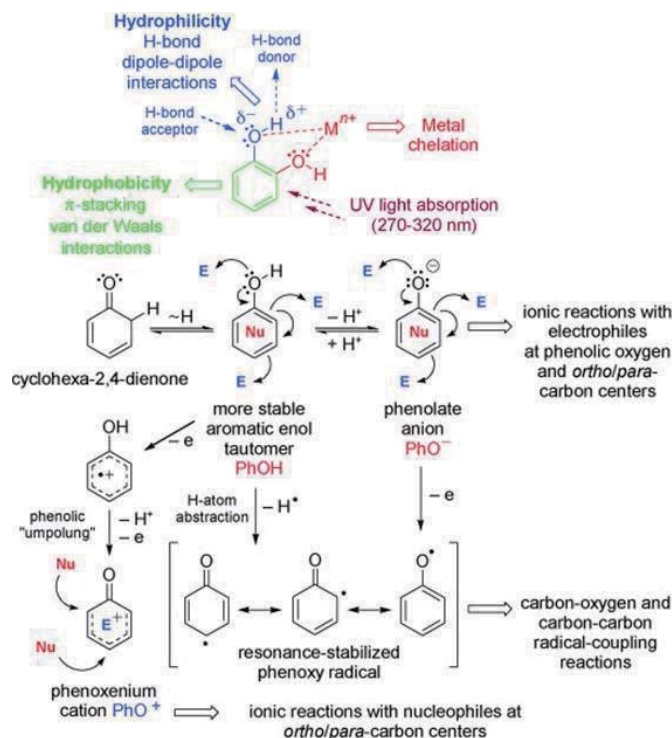


Figure 17 Basic physicochemical properties and reactivities of the phenol functional group. E=Electrophile, Nu=Nucleophile[130].

Oxidative dehydrogenation of catechol- and pyrogallol-type phenols in a certain condition can produce some quinonoid species, as described in Figure 18[130]. This theory does support some research works on the reaction between tannin and plant protein, even some synthesis amine, such as condensed tannin and soybean protein, polyethyleneimine (PEI)[136-140]. These reactive species have been proposed as electrophiles able to react with nucleophilic biomolecules such as proteins[141-143].

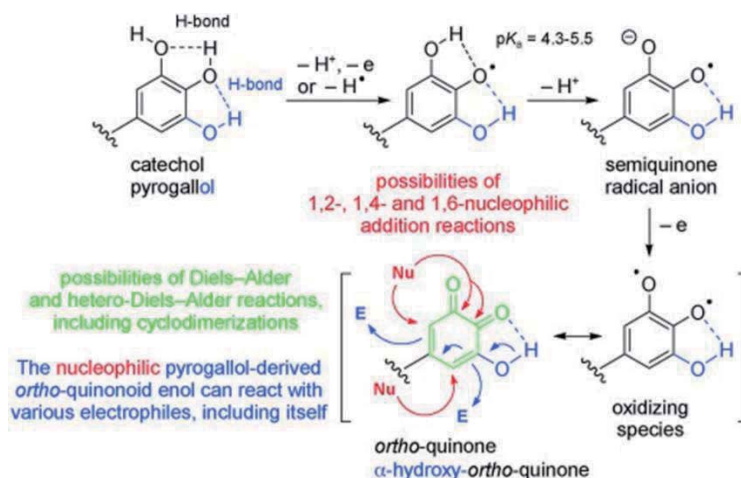


Figure 18 Oxidative dehydrogenation of catechol- and pyrogallol-type phenols into reactive quinonoid species[130].

III Modification and functionalization of condensed tannin

Like the most of natural resources, tannin represents a relatively low chemical reactive when it was utilized in directly for various fields, such as wood adhesive, foam, absorbent, etc., as the raw materials. Even if tannin can be used as the starting materials, especially in tannin-phenol-formaldehyde wood adhesives application, its reactive still was the main drawback needing to enhance. Considering to the structure units of condensed tannin in Figure 16, the phenol ring, heterocycle and its -OH groups are the breakthrough positions for tannin modification and functionalization. In summary, those modification around condensed tannin have the only one target, i.e., improving the activity of tannin, in which can through the following methods. As presented in Figure 19, the main chemical modification can be classified into three main categories.

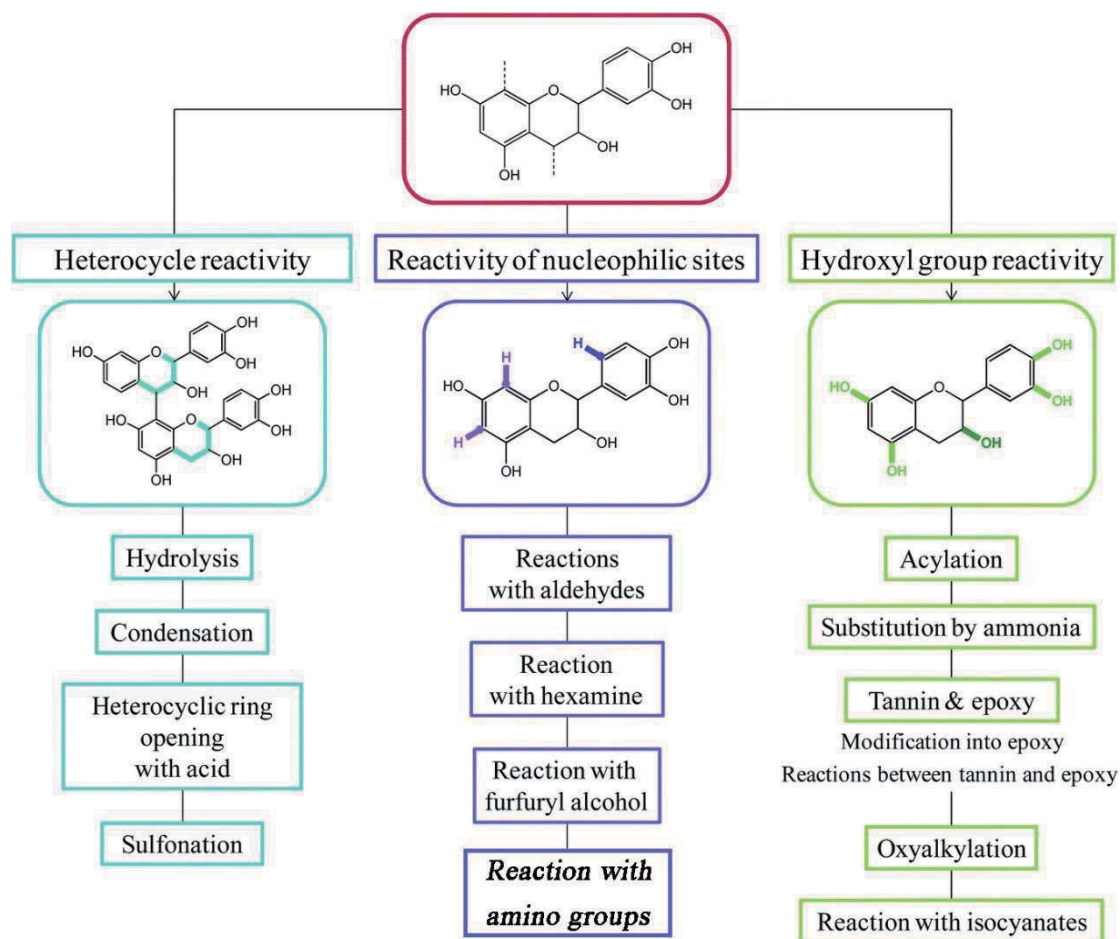


Figure 19 Various types of reactions with catechin, applicable to condensed tannins[106].

A, Heterocycle reactivity

Under both acidic and alkaline conditions, catalyzed rearrangements such as hydrolysis and auto-condensation are common reactions for tannins (Figure 20). The cleavage of the interflavonoid bond can also be acid-catalyzed or induced by a sulfonation reaction.

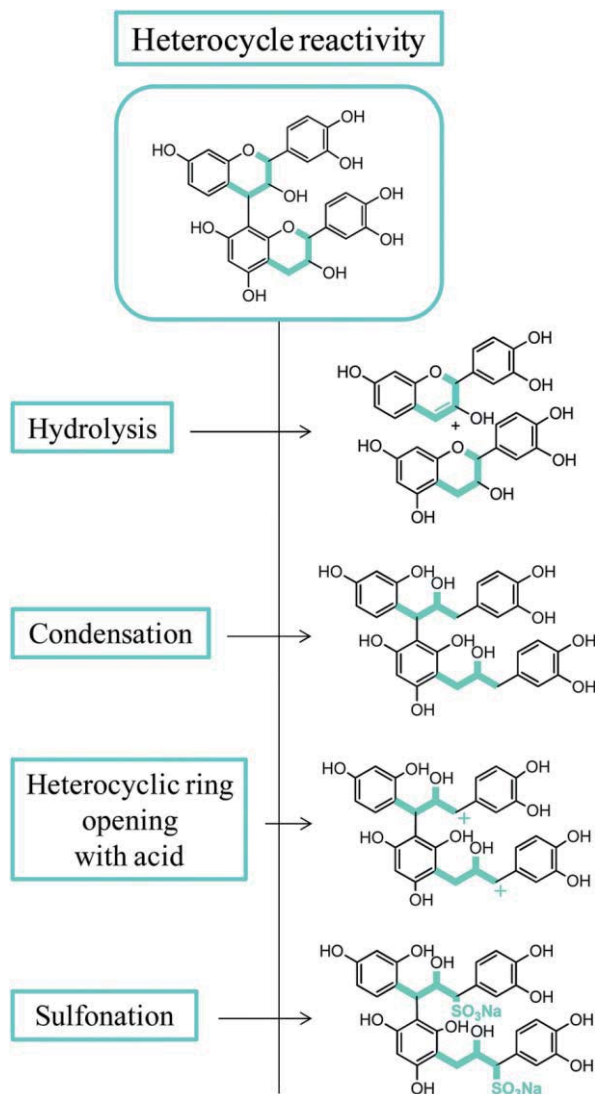


Figure 20 Summary of the chemical reactions from tannin heterocycles[106].

a Hydrolysis and acid/alkaline auto-condensation

Condensed tannin while under a strong acid provided by mineral acids and accompanied with heated, as reported by the researchers, two competing reactions do occur[2, 106]: the first one is tannin degradation so that resulting to anthocyanidins and catechin generation, the typical formation process as presented in Figure 21(a); The second one is the condensation reaction between those products which comes from heterocycle hydrolysis, as described in Figure 21 (b). The condensation is randomly

condition between the p-hydroxybenzylcarbonium ions and nucleophilic centers on other tannin units and then leading to the “phlobaphenes” or “tanners red” generation[2].

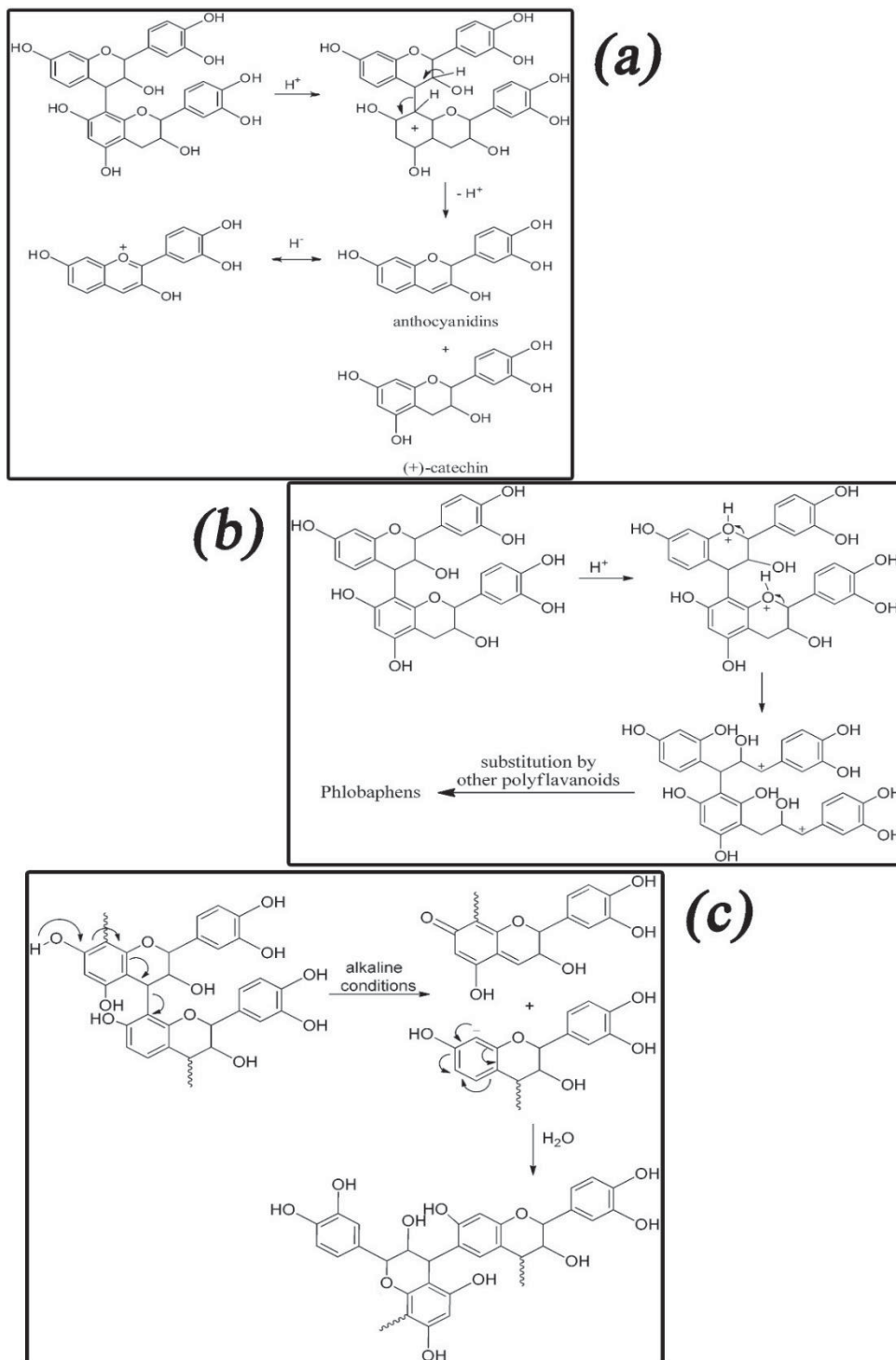


Figure 21 (a) Degradation of tannins in catechins and anthocyanidins; (b) Acid autocondensation by hydrolysis of the heterocycles; (c) Alkaline autocondensation[2, 106].

The partial condensation process could appear while condensed tannin was placed

into a strongly alkaline condition, as shown in Figure 21 (c). This phenomenon can be observed when preparing tannin-water solution at high pHs, showing an apparently viscosity increased, a general example, mimosa tannin-water solution with pH 10, can prove this result greatly. Some researcher described this phenomenon as the rearrangement[106]. From the theoretical level, this rearrangement was thought to be the C4 flavonoids of the lower terminal units crosslinking the C6 or/and C8 flavonoid units of other tannin molecular. This is due to the reactivity of hydroxy-group-carrying C4[2].

b Acid-catalysis heterocyclic ring opening

The heterocyclic ring opening behavior do occur under acid condition, as mentioned before, which is not difficult to fulfill. Generally, the depolymerization condensed tannin could be done at the present of acid and catalyst, this process always along with the tannin heterocyclic ring opening[140]. After the ring opening, a carbocation will be formed as shown in Figure22, which can be captured by a nucleophile, such as phenol, resorcinol, phloroglucinol or the phenolic rings of other flavonoid units[106]. This process can improve the tannin activity and solubility some extent.

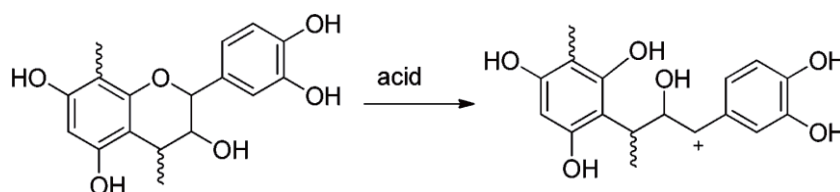


Figure 22 Treatment of mimosa tannin with acid.

c Sulfonation

Tannin sulfonation is an ancient strategy and the most practical reaction during the condensed tannin treatment chemistry, as shown in Figure 23. And it was proven to be a particularly useful technique while tannin sources were utilized for manufacturing tannin-based wood adhesives. This process also does occur in tannin extraction from the plant resources, generally can affords tannin lower viscosity and increased solubility[2, 106]. These results are related to the following reasons:

- The hydrophobic groups, ether cyclic ether group, were destroyed by a large

number, that is the reason that tannin/water mixture is not a true solution but a hydrocolloids suspension.

-The heterocyclic ring was broken and then resulting to hydrophilic groups increased, including the introduced sulfonic group and hydroxyl groups.

-The sulfonation process can significantly reduce the polymer rigidity and steric hindrance, of course, the intermolecular H-bonding formed because of ether cyclic ring opening behavior would decrease as well.

-The hydrocolloid gums were destroyed.

The extensive exist of sodium sulfonate groups make a great potential for tannin phenolics in wood adhesives with a high replacement on fossil-based phenol, mainly because of enhanced solubility, decreased viscosity, and improved reactivity toward to formaldehyde[2]. And the modification process improved the moisture retention by tannin adhesives so that slowed the resin film dry-out leading to a longer assembly time for tannin adhesives applications.

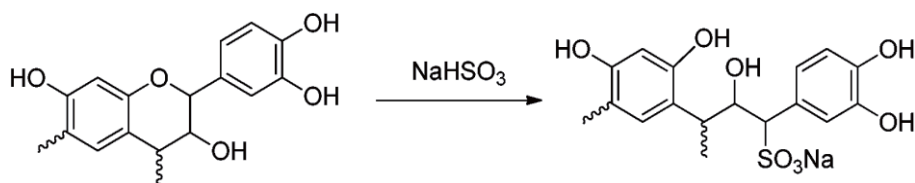


Figure 23 Sulfonation reaction of tannin.

B, Reactivity of nucleophilic sites

The phenol-like structure in tannin molecular endows some nucleophilic sites which can serve as the active positions to fulfill tannin modification and polymerization. These nucleophilic sites are attributed to the phenol groups on the tannin ring, similar with fossil-based phenol structure, electrophilic aromatic substitution's reaction does occur on those sites. Therefore, some nucleophilic substitution reactions as shown in Figure 24 can appear. There are several potential pathways on the nucleophilic substitution reactions for wood adhesives preparation, and have been reported by researchers.

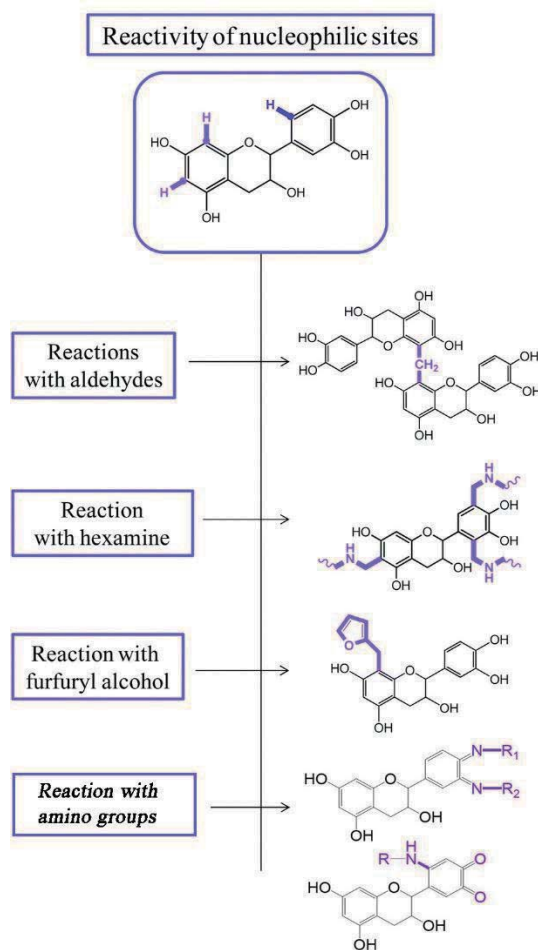


Figure 24 Summary of the chemical reactivity of tannin nucleophilic sites.

a, With aldehyde

Tannin phenol always keeps a high reactivity toward to aldehyde chemicals, making it utilized as natural phenol resources to replace petroleum chemicals in wood industry[2, 106]. The modification and polymerization between tannin and formaldehyde are mainly occurring on the tannin A ring by methylene bridge linkages, probably can linking on the tannin B ring while under a high pH condition (approximately 10) as well[2]. As reported in the previous part, tannin A ring have two nucleophilic sites, i.e., C6 and C8, which can react with formaldehyde though methylene bridge, but their specific location of occurrence mainly depends on tannin resource types. For example, as shown in Figure 25 (left), resorcinol type A rings has an C8 reactive position for polymerization with aldehyde groups. For the phloroglucinol A rings which shown in Figure 25 (right), the reaction cite was on the position C6. It is reported that the C8 position normally presents a higher reactivity than

C6 as its less steric hindrance, thus, phloroglucinol type tannin sources can more reactive towards to formaldehyde[2]. Tannin has been publicized to react with various aldehydes, for example alkyl aldehydes, di-aldehydes, unsaturated carbonyl aldehydes, but formaldehyde still can keep the fastest reactive speed to link tannin molecular as its less steric hindrance, both phloroglucinol and resorcinol type of tannins. One apparently example is the gel phenomenon could be found while mixed tannin with formaldehyde solution under a room condition, as shown in Figure 26, a typical reaction between tannin and formaldehyde.

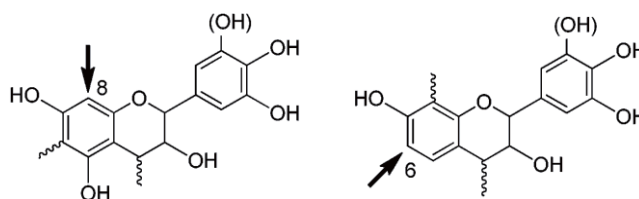


Figure 25 Formaldehyde reactive sites

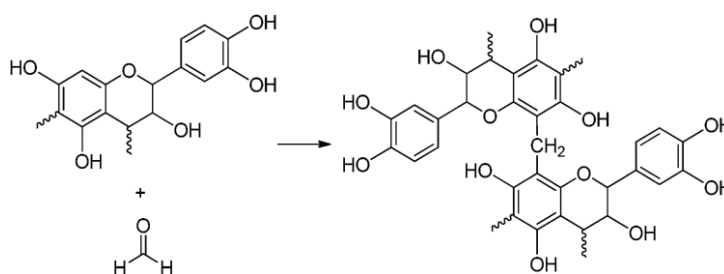


Figure 26 A typical reaction between tannin and formaldehyde.

b, With hexamine

Hexamine has been utilized as an environmental-friendly hardener for a fast-crosslinking species which not through formaldehyde-yielding compound, just only extremely low formaldehyde emission in wood bonding[144]. The decomposition process of hexamine has been confirmed by the researchers, that it does not produce formaldehyde directly but proceeds through reactive intermediates, thus, the crosslinking between tannin and hexamine mainly through reactive imines and imino-amino-methylene bases, normally appearance under alkaline condition[145-147]. And those strong reactive but unstable intermediate fragments exhibit a high reaction speed with tannin, even other analogous activity chemicals, such as melamine, resorcinol, for formulation amino-methylene bridges before yielding formaldehyde. During the whole process, the hexamine could produce the intermediate fragments, and then it was

decomposed firstly thus forming imines followed by their decomposition to imino-methylene bases. Those imino-methylene bases only a single positive charge because of the second methylene group was stabilized by an imine-type bond, as shown in Figure 27[145-147]. The theory indicated that any chemicals or mass with a strong negative charge under alkaline conditions have a strong reactive ability with those intermediate species which are obtained by hexamine decomposition. For example, in the literatures, including condensed tannin, resorcinol or other highly reactive phenol, melamine or other highly reactive amine or amide, or organic or inorganic anion have been reported that they can react with those intermediate components[145-147]. And their reaction ability is far more readily than formaldehyde. That is the reason why only extremely low formaldehyde emission does appear in the wood panels bonded by using the formulation on tannin and hexamine. But if there is no highly reactive species with strong negative charge presenting in the reaction system then those hexamine decomposition species can produce formaldehyde rapidly as reported previously[148].

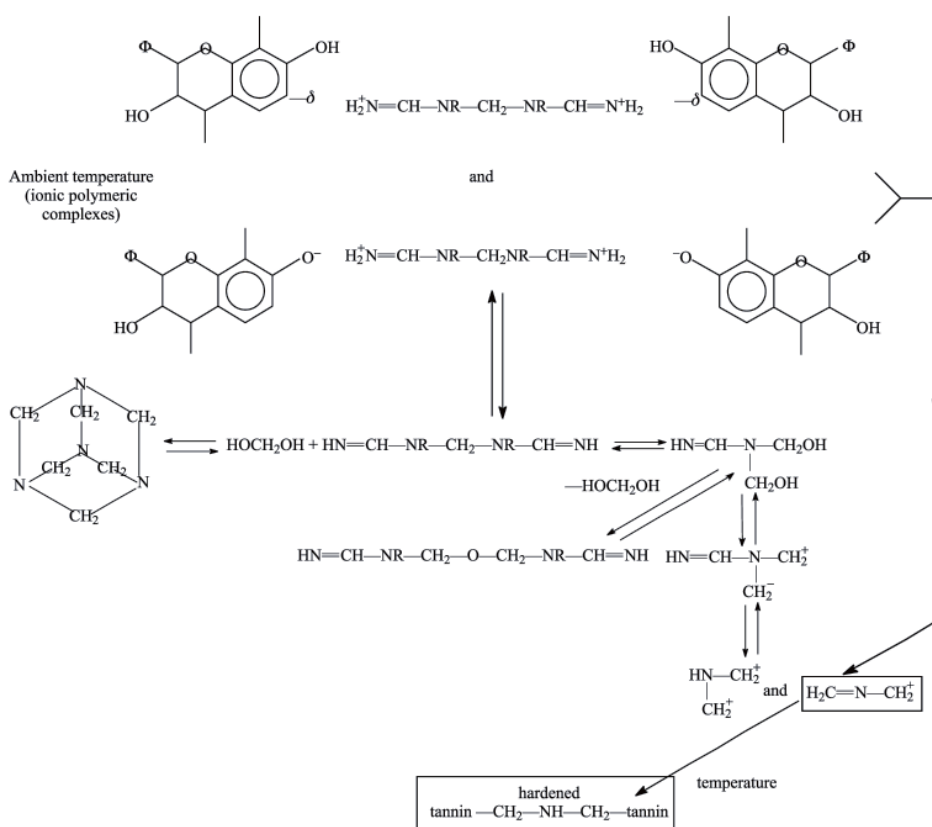


Figure 27 Schematic representation of the decomposition of hexamine to imino amino methylene bases in presence of a reactive species such as tannin to form (i) ionic

polymeric complexes at ambient temperature and (ii) a stable benzylamine covalently bridged network during hardening, at a higher temperature, without producing or releasing any formaldehyde[148].

c, With furfuryl alcohol

Furfuryl alcohol was considered as a green chemical commodity industrially that can obtain by hydrogenation of furfural which prepared through hydrolysis and dehydration of pentosan-rich biomass. It was reported as a green component for wood adhesive production[149]. And during the tannin-based rigid foam formulations, it was a necessary ingredient to provide foaming function under an acid condition[150-152]. As we all know that furfuryl alcohol possess a strong self-condensation activity while under acidic environments, normally resulting to a highly exothermic process.

The previous literatures have reported that the reaction between tannin and furfuryl alcohol can occur under acidic condition, therefore, their crosslinking can form three-dimensional structure so that can provide bonding ability[149, 153, 154]. This reaction was totally exhibited in the acid-based formulations on tannin foam preparation. Furfuryl alcohol do appear self-condensation so that to generate three possible results. Firstly, a classical chain condensation was the dominating reaction, which can happen rapidly once started. Secondly, an ether structure can obtain between two hydroxyl groups. The third one is the rearrangement of the furanic-cycle and will become the source of crosslinking for furfuryl alcohol. But, furfuryl alcohol keeps the reaction ability with tannin molecular by the substitution reaction on the reaction position C6 and C8, as shown in Figure 28.

The reaction between tannin and furfuryl alcohol usually was reported can occur under acidic condition, but the crosslinking between of them can appear under alkaline environment as well. A typical example is the formulation preparation of tannin-furanic foam on the alkaline environment; however, this reaction usually is slow and under an external-thermal condition[155].

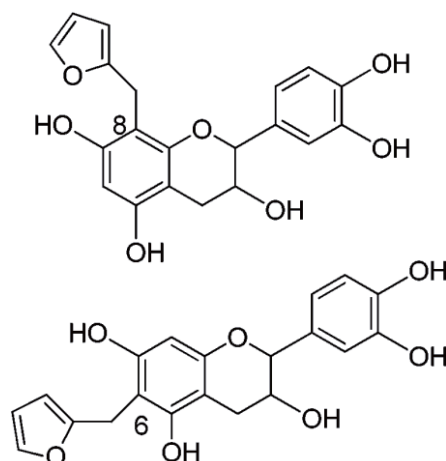


Figure 28 Proposed reaction scheme of a tannin and furfuryl alcohol

d, Reaction with amino groups

The reaction between tannin and amino groups have been reported in several researches, for example soybean protein and polyethylenimine (PEI), for wood adhesives and tannin-based foam preparation[137, 139, 150, 156]. Unfortunately, the exact reaction mechanism between condensed tannin and those are not fully understood. And the researchers are still working on that and give some possible reactions to explain the exactly reaction between them[139, 157]. Therefore, there have some possible reactions are shown in Figure 29. In this reaction, the B-ring structure of condensed tannin is the main reaction position, their catechol moiety is highly susceptible to oxidation resulting in the formation of an ortho-quinone, especially while under an elevated temperature such as the hot-press temperature in the preparation of wood composites. Those ortho-quinone therefore can readily react with amino groups on the chemicals, such as soybean protein and PEI, normally it was called as Schiff bases reaction. Additionally, a reaction called as Michael addition does occur on the ring cites and then can further react with the amino groups by the Schiff Bases reaction. But those reaction similar can be happened under an alkaline system easily, leading to a water-insoluble three-dimensional tannin-amino network.

Moreover, the reaction between tannin and soybean protein under acidic condition was investigated by the researchers with MALDI-ToF mass spectrometry[143, 150]. It is indicated that ionic and covalent bonding between amino acids and tannin constituents are formed and that covalent bonds do predominate at elevated temperature

as present in the hot-pressing of wood panels.

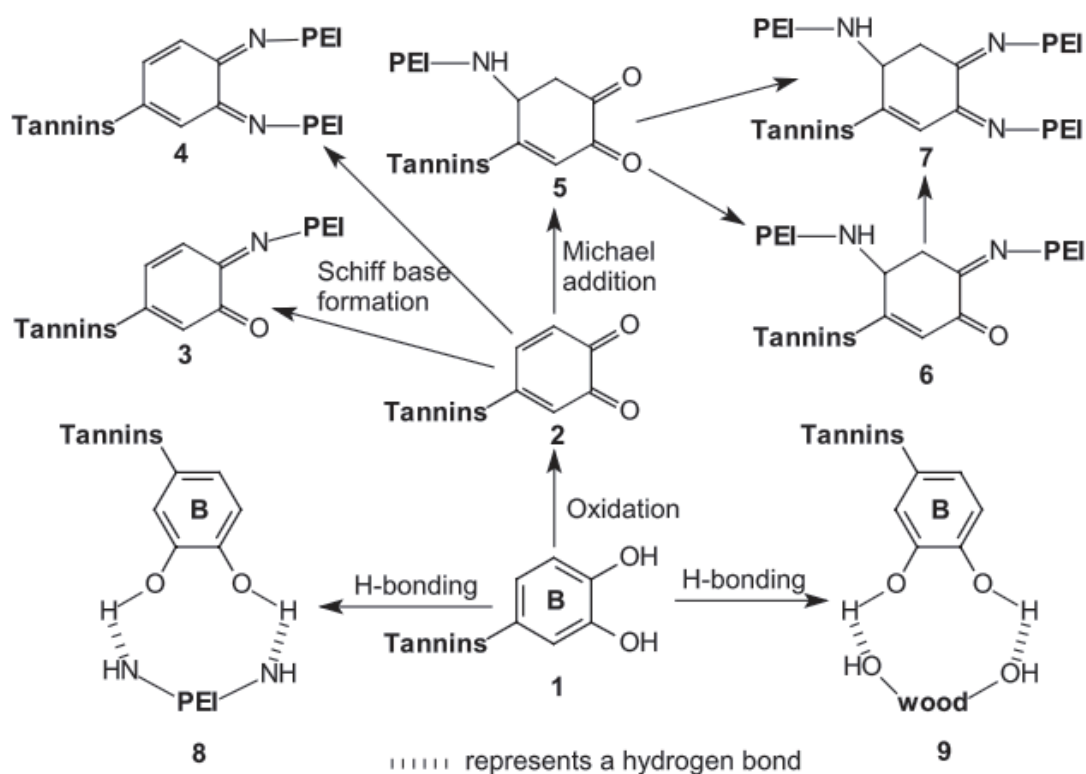


Figure 29 Some possible reactions between condensed tannin and PEI[139].

C, Functionalization of the hydroxyl groups

The phenolic hydroxyl groups (-OH) are the one of reactive sites to allow the tannin modification taking place, then to obtain several tannin derivatives. And those hydroxyl groups on tannin molecular are the dominantly reason to obtain the different solubility. Nevertheless, if those hydroxyl groups cannot participate to the appropriate reaction, allowing much more free -OH still under an activity condition, while utilized in wood adhesives, their water-resistance could be influenced. Considering that situation, tannin modification can be achieved by increasing the -OH chemical reactivity or its solubility in organic solvents, or to improve its processing[106]. Hence, two suggested modification strategies have been reported to get a new building block from tannin, i.e., changing the nature of the reactive sites or (ii) increasing the hydroxyl group reactivity. Different modifications such as acylation, etherification, substitution by ammonia and reactions with epoxy groups or with isocyanates were performed and investigated (Figure 30). Considering the potential industry application, such as operation condition, the chemical utilization, and the preparation process, some

polymerization methods were summarized as following.

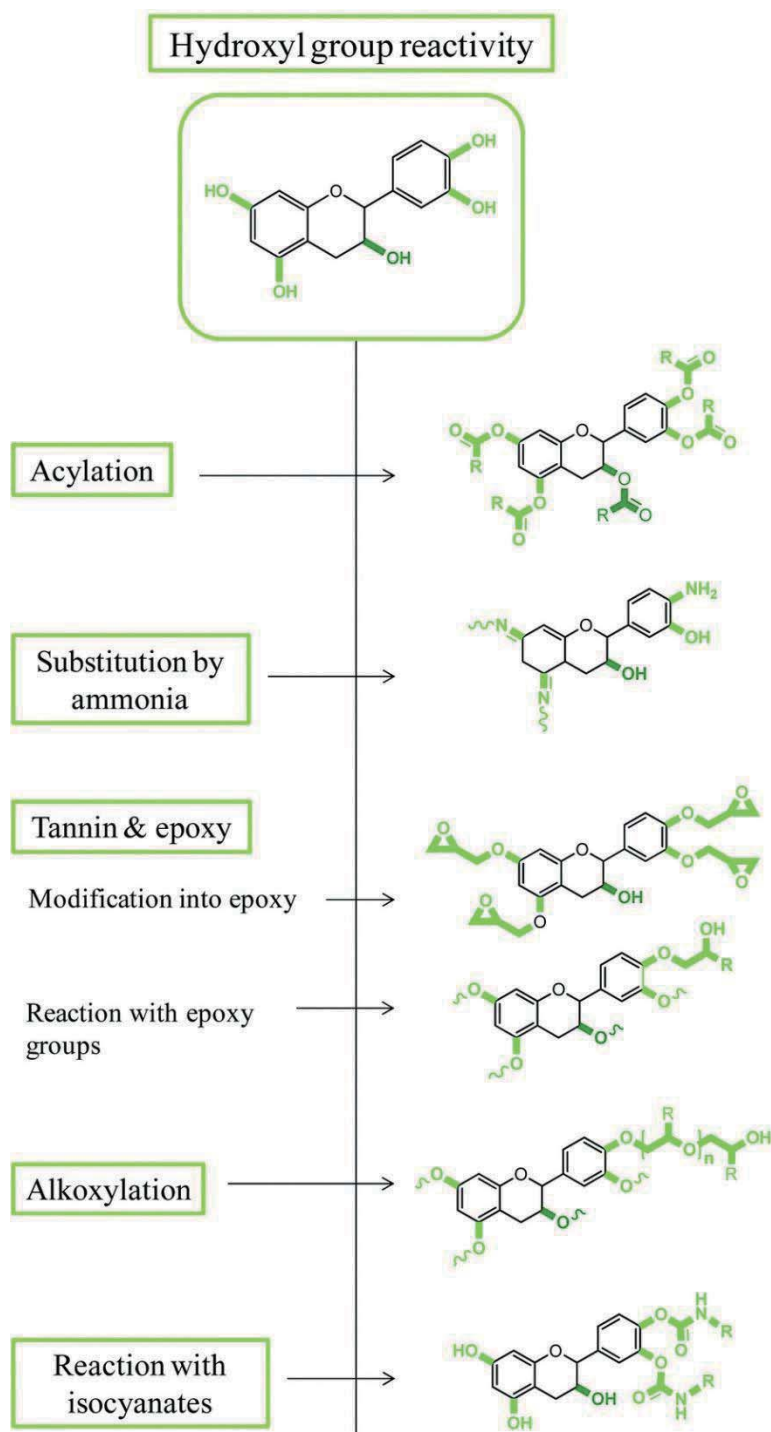


Figure 30 Summary of the chemical reaction with tannin -OH groups[106].

a, Acylation

Tannin acylation process was normally described as pretreatment before tannin characterization, resulting to the as-obtained tannin has various solubility in different solvents[106]. The -OH groups can be subjected to acylation either partially or totally,

thus derivative of tannin loses its water solubility and melts at around 150°C. Acetylated condensed tannins have been introduced as an additive candidate for polylactic acid and its derived-products with an excellent plasticizing affect[158-160].

Usually, acylation agents have been reported that either carboxylic acids or more reactive derivatives, for example, acyl chlorides or acid anhydrides[106]. Some solvents, such as pentanone, acetone, pyridine, and chloroform, have been utilized for better solubility of tannins as well. The scheme of the reaction formulations was summarized in Figure 31.

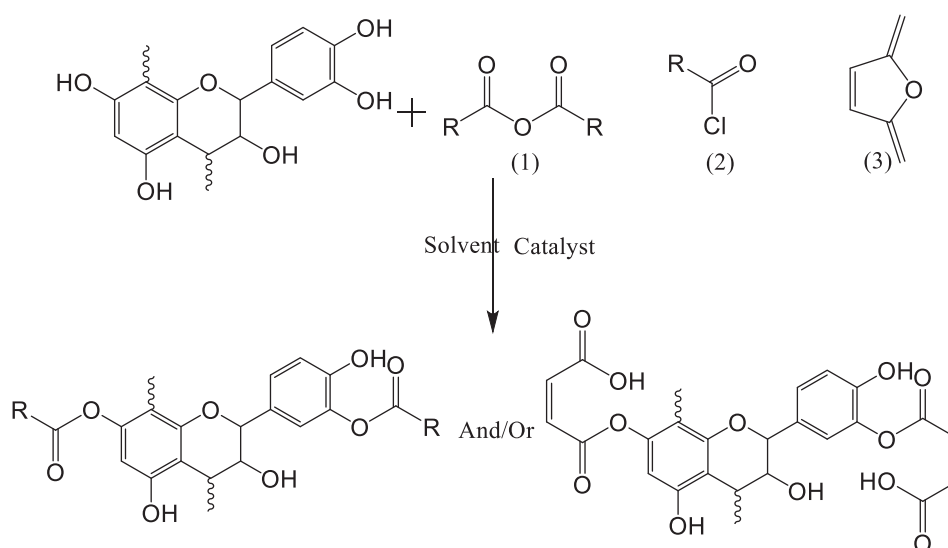


Figure 31 Tannins esterified with (1) anhydrides; (2) acyl chlorides; (3) maleic anhydrides.

b, Substitution by ammonia

Tannin amination reaction can occur between tannin and ammonia (NH_3) which has been reported, their reaction as described in Figure 32[161]. In this process, the phenolic -OH can be substituted by ammonia to realize de-hydroxylation. The reaction between flavonoids and polyflavonoid tannins with ammonia was finally resulting to tannin molecular multi-amination products with different substitution level, but normally with a great proportion of phenolic -OH. And this reaction was considered that can occur both on tannin A- and B-ring[161]. However, some previously theorized also suggested this substitution can only appear on the tannin B-ring. Meanwhile, the oligomerization and cross-linking were confirmed that those are exist in the reaction

system by formation of -N= bridges between flavonoid units. This result explained why the gelation phenomenon can be observed during mixing tannin and ammonia in water.

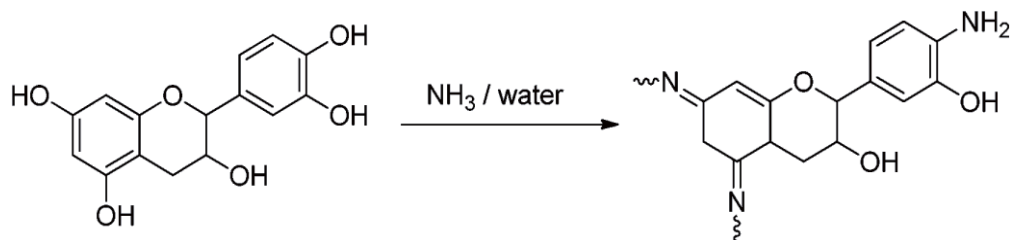


Figure 32 The reaction between tannin and ammonium hydroxide

c, Reactions with epoxy groups

Epoxy resin have been used as the matrix for some advanced composite materials as their excellent properties including outstanding mechanical performance, good chemical resistance, and superior dimensional stability. In wood industry, it was often been utilized to bond structure wood for wood building. Epoxides have activity groups which have been utilized in wood adhesive modification, such as soybean protein based, lignin, starch, of course condensed tannin[162-168]. In tannin wood adhesive system, epoxy groups can react with tannin phenolic -OH groups then resulting to a crosslinked three-dimensional structure, as shown in Figure 33. This method was a potential pathway to reduce the number of tannin phenolic -OH groups.

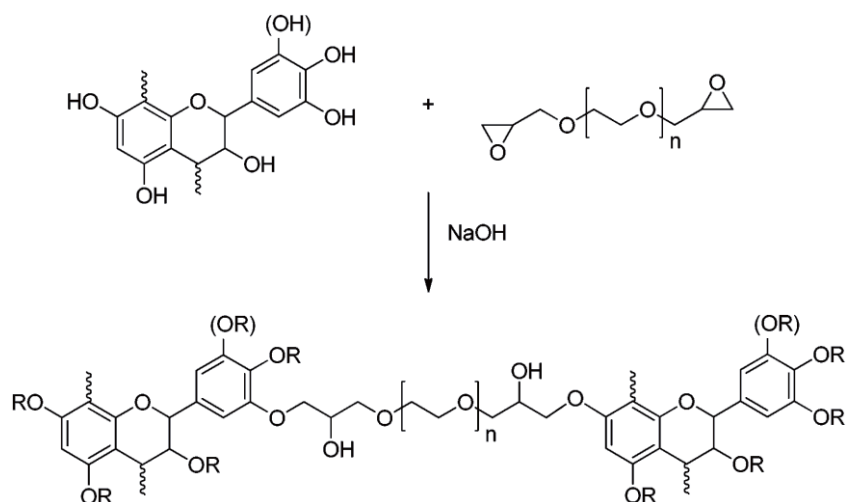


Figure 33 Reaction of pine tannins with ethylene glycol diglycidyl ether.

d, Tannin epoxidation

Tannin epoxidation can be deemed as active pathway to improve the reactivity between condensed tannin and other chemicals. Usually, this method was applied to modify hydrolysable tannin as its solubility in solvents. But condensed tannin also can

be modified by using epichlorohydrin while under a suitable reaction condition, the reaction process as shown in Figure 34[169]. The resultant products containing different amount of epoxy groups have been used to synthesis such as tannin-based bio-foam and to modify soybean protein for wood bonding[170, 171].

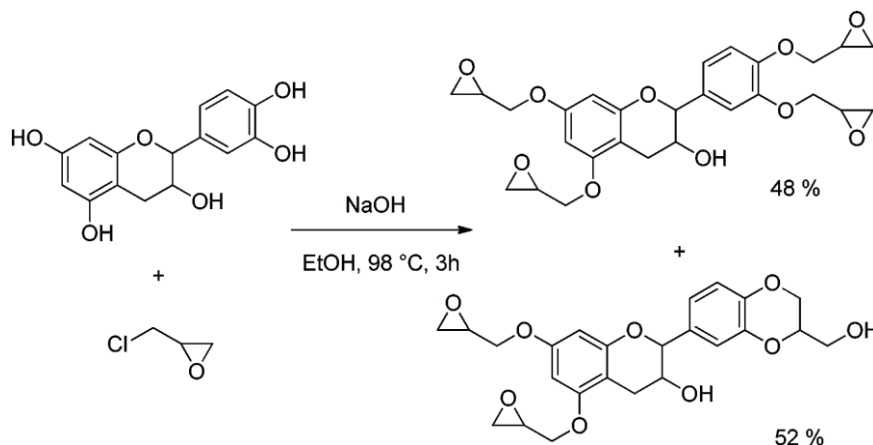


Figure 34 Reaction of catechin glycidylation.

e, Reaction with isocyanates

The research reported that tannin can react with isocyanates to form a well-crosslinked structure, that is why isocyanates can be used as crosslinker to modify tannin-based wood adhesives and foams. For well understanding their exactly reaction process, catechin was selected as the model chemical to perform this research, the urethane structure can obtain after reaction[106]. This reaction was carried out under inert atmosphere at 30°C for 24 h at the present of acetonitrile, exhibiting that the phenol -OH groups on the A-ring are not participate the reaction of isocyanate but only the tannin B-ring, as shown in Figure 35[106]. In addition, the researcher suggested that this phenomenon was caused by the lower electron densities at the oxygen atoms in the A-ring compared to B-ring.

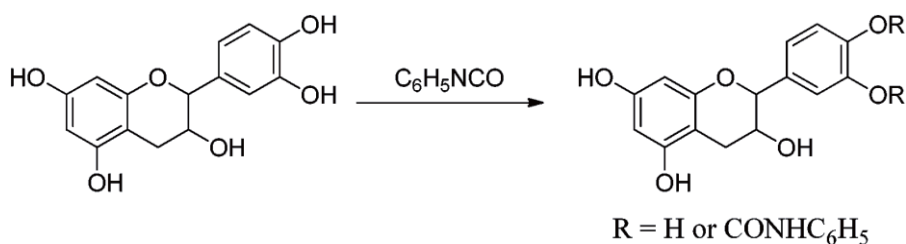


Figure 35 The reaction between tannin and isocyanate[106].

1.2.2.4 Tannin-based wood adhesives

As described as the previous content, accompanying with the extensive consumption of fossil-based resource, tannin due to its natural available property, special phenol-like structure, and activity especially towards to formaldehyde, thus, in the wood industry, it has been broadly utilized to prepare wood adhesives[2]. The scholars always devoted to search a reasonable project to prepare a tannin-formaldehyde wood adhesive with an acceptable performance. Even though the high reaction activity between tannin and formaldehyde, their crosslinker often being thought as a weak level because of the mobility of tannin could be limited with the progressing of the reaction. Hence, the tannin only mixed with formaldehyde usually can obtain a restricted crosslinking degree so that only a limited water resistance[2, 172-177]. In consequence, condensed tannin, usually, has been utilized as the replacement agent to modify traditional phenol-formaldehyde wood adhesive[2, 174, 175, 177]. How to improve the crosslinking degree of tannin-formaldehyde has occupied the main position in the modification of tannin adhesives for quite a long time. It is reported that there are two suggested main modifications with potential industrial strategies. ① Phenolic or urea-formaldehyde resin with middle or high methylene groups bridge was introduced into tannin wood adhesives. Those synthesized resins were considered as curing and reinforcing agents for tannin adhesive properties enhancement[2]. From the past decades, concerning tannin-based wood adhesives have been reported widespread that tannin was used to substitute fossil-based phenol partially for tannin-phenol-formaldehyde adhesives preparation[2, 103, 126, 148, 178]. And an encouraging thing is that this replacement pathway has been applied to industrial-scale application, and the particleboard bonded with tannin-phenol-formaldehyde adhesives reached an outstanding performance for exterior utilization, in south Africa[2, 177]. ② The linear synthesized resins, such as resorcinol-terminated or urea-formaldehyde resins, but not containing methylene groups bridge, have been utilized to crosslink tannin molecular by adding some additional crosslinkers[2]. This linear molecular structure can connect tannin or tannin-formaldehyde reaction products, for improving the overall degree of cross-linking resin as reinforcing agent. In addition, the end-group of this linear molecule (resorcinol or urea formaldehyde resins) reacts

with additional formaldehyde, exposing the active $-\text{CH}_2\text{-OH}$ group at both ends, which can be directly cross-linked with tannin molecules, or through additional cross-linking agents, such as isocyanate[179-181].

Meanwhile, the reaction mechanism of tannin-formaldehyde resin was studied and speculated by professor A. Pizzi and his team. Compared with the phenol-formaldehyde resin, the nucleophilic center of the A-ring is stronger than that of the B-ring, which is due to the nearby hydroxyl substituent group, resulting to the general activation of the B-ring, and has no local effect on the A-ring[175, 182, 183]. As the reaction between tannin and formaldehyde progresses, the molecular weight of the reaction product increases rapidly, and the mobility of flavonoids is greatly limited. And this restriction can further influence the crosslinking by formaldehyde which possibly no even longer participate in the further high cross-linking degree reaction. The crosslinks do occur between tannin and formaldehyde on the site of flavonoid molecules (mainly the A-ring) through methylene bridge bond. For example, the reaction site on tannin A-ring is the position 8 for black wattle tannin as its resorcinol flavonoid unit, but for pine tannin is the position 6 due to its resorcinol flavonoid unit. However, tannin B-ring hardly participates in the reaction towards to formaldehyde but except under a high pH condition (normally greater than or equal to 10). Thus, the concept of metal ion chelating tannin B-ring was put forward for improving the whole reactivity of tannin molecular. It was finally proved by the experiments that the addition of appropriate metal ions can greatly promote the performance of tannin formaldehyde resin[2].

Formaldehyde emission problem is the main issue which was concerned by the consumer as well as the developing in the tannin-based wood adhesives. Therefore, hexamine was chosen as an environmental-friendly hardener to prepare wood adhesive from the past decades[2, 180, 184-186]. In addition, the wood panels bonded with tannin/hexamine adhesives can obtain an acceptable bonding performance and exhibit a great potential industry application. Except that, some low-toxic, nonvolatile aldehydes, including glyoxal, glutaraldehyde, also have been adopted to replace formaldehyde to crosslink tannin[149, 187-191]. And this substitution pathway still is the main research point for the past and the further periods.

Tannin mixed with other bio-sources, including lignin, soybean protein, furfuryl alcohol, starch, etc., with or without addition crosslinker have been attracted by many researchers. Depending on the abovementioned context, those bio-sources can react with tannin either directly or by using additional crosslinker. For example, tannin-lignin mixture wood adhesives with a good property can be obtained but needs additional crosslinker, or pre-modification. Lignin glyoxalation was a usually method to improve lignin activity, and its derived products can be used to prepare various products[192-194]. And then, activated lignin products can also be used to mix tannin for adhesive preparation. Moreover, isocyanate was served as crosslinker to cure tannin/lignin wood adhesive to provide an acceptable performance. And it was proved by many researches and exhibited effectiveness[66, 187].

Some reactiveness sources, including soybean protein, furfuryl alcohol, and other plant extract, comparing with lignin, for tannin-based wood adhesive production, the resultant adhesive can reach almost 100% bio-original, thus, this way can have more potential for industrial application. Tannin-furfuryl alcohol have been reported to prepare tannin-based foam under the acidic agent condition, but their mixture used in the wood bonding fields cannot reach an idea results, normally needs addition crosslinker, for example, epoxy resin[149]. Fortunately, plant protein, especially soybean protein, can react with tannin directly and their bonding performances are ideal, convenient operations, eco-friendly source, and low-cost usually.

Recently, concerning tannin-based wood adhesives still based on their bio-sources and high-performance issues, such as tannin-sugar-based resins. The tannin-sucrose mixed wood adhesive system, like the tannin-soybean protein blend system, has a wide range of industrial application potential, because they can be said to be a completely "green" adhesive system. Sucrose under the condition of acid catalysis, high temperature environment (about 200°C), can be converted to a tannin reaction product -5-hydroxymethylfurfural (5-HMF). Therefore, this adhesive can be used to prepare particleboard. Although their bonding property can be accepted but along with a critical drawback to these adhesive systems, i.e., the extremely lower pH reaction environment, normally in the range of 1-5[195-198].

Searing for tannin hardener from the plant is also a popular way to develop tannin-based wood adhesives. A research team extracted an environmentally-friendly tannin curing agent from the bark of an African tree species and applied it to the preparation of particleboard, which has a high dry binding strength[109].

1.2.3 Plant protein resources and protein-based wood adhesives

1.2.3.1 Plant protein resources

Plant proteins, another natural polymer, belong to a group of been attractive starting materials in wood adhesive fields with the nature of environmental-friendly and sustainable. The extensively utilized plant protein are typical soybean protein[170, 199-210], wheat protein[199, 211-216], cottonseed protein[217-221], as the main protein-sources for wood adhesives preparation, but still conclude some minorities such as camelina protein (a biodiesel residue)[222], alfalfa leaf protein[223], canola protein, potato, and pea protein[208, 224, 225]. Nevertheless, due to their special structures, how to improve their bonding performance endows that can satisfy the related standards of conventional wood adhesives, normally water resistance, still a challenge. Among them, soybean protein has been extensively utilized and been considered as a great potential for industrial-scale application. Soybean protein has been used in wood adhesives by various ratio with synthesized resins, this strategy can improve their biomass content of wood adhesives but would loss a certain of bonding strength[71]. Furthermore, soybean protein can used as wood adhesives lonely but the as-obtained wood panel products always shown a better bonding performance only under dry condition, thus, sometimes, other kinds of proteins, either animal protein like blood protein and casein or plant protein like cottonseed protein, have been utilized to improve their bonding performance[208, 226, 227]. Additionally, some modifications to enhance their properties including physical and chemical methods are carried out by several researchers. Comparing with wheat protein, although soybean protein has attracted interesting on the researchers to prepare wood adhesives, the outputting of soybean is still not lower than it. And concerning wood adhesives based on wheat gluten has been less extensively studied and performed recently[212, 214, 215]. Therefore, this study only focusses on the soybean protein wood adhesives.

Soybeans are the important agricultural products for industry and humans progressing, being the raw materials for plant oil production, and their by-products also being utilized for animal feed. During the oil processed, almost 21 kg of soybean meal can obtain while 5 kg of crude soybean oil yielding, which needs 27 kg of soybeans consumption[228]. Furthermore, the production of soybeans is increasing rapidly on the whole world, about 115 Mt of soybeans yielding in 1993 to 276 Mt in 2013, for the extensively consumption for human and industrial chemicals. The main manufacturing locations are focus on the United States of America, Brazil, Argentina, and China[229]. Most of them are used for animal feedstock and small part of them are utilized for human consumption, in the forms of soy milk, soy flours (SF), soy protein concentrates (SPC) and isolates (SPI), tofu and many retail food products. Therefore, many by-products from soybean-oil production, i.e., soybean meal, which can be deemed as a greatly plant protein original for other applications. Typically, wood adhesives based on soybean protein not only have the abundant coming sources but also have huge potential for industrial application, especially in wood industry.

1.2.3.2 Chemical composition of soy proteins and their properties

Soybean proteins was composed of which 10% of can be water extracted albumins and 90% of can be dilute salt solutions extracted globulins components[230]. And its molecules are complicated macromolecules system. 20 kinds of amino acids have been detected and reported, and each of them with a common backbone and a different side-chain (R), a typical structure is shown in Figure 36[231]. Typically, amino group (-NH₂), α -carbon, and carboxylic group (-COOH) can be found in the backbone of each protein molecular[232]. The neutral form of an amino acid is shown in Figure 37, normally, the amino and carboxylic groups can ionize to specific ionic species, i.e. -NH₃⁺ and -COO⁻, respectively. Each kind of amino acid has their specific characteristic and property which was defined by its side-chain, R, and can provide a unique role during soybean protein industrial application. Three forms of amino acids would be divided by concerning the tendencies of the side-chains to participate in interactions with each other and with water, such as hydrophilic (polar), hydrophobic (non-polar) or amphipathic (residues have both polar and non-polar characteristics), respectively[232].

Furthermore, the amino acids according to the position and characteristics of side-chain, can also be separated into several groups, including aliphatic, cyclic, hydroxylic, acidic, amidic, basic, aromatic, sulphur-containing, and unique amino acids, as summarized in Figure 37.

Soybean protein was commonly deemed as four grade structures. The backbone polypeptide chain consists of amino acids by peptide bonds connecting, acting as the primary structure of proteins and determining the protein folds method so that obtain a higher-level structure[231]. The secondary structure is the local structure which stabilized by hydrogen bonds, main comes from the intra-chain structures by some specific amino sequences formed α -helices and β -sheets (crystallites). Furthermore, the tertiary structure was folded up in an aqueous environment, which comes from some individual protein chains, elements of either α -helix or β -sheet or both, as well as loops and links that have no secondary structures[231]. The tertiary structure stability is always not fulfilled by local interaction. The quaternary structure was formed by some protein molecules (polypeptide chains) interact with one another through inter-chain hydrophobic interactions, salt bridges, covalent disulphide bonds and hydrogen bonds.

The bonding property of protein adhesive was from their side-chain of amino acids but those chain generally hid in the inter of protein. The dense connection does fulfil via different bonds between wood substrate and protein, normally disulphide bridges between thiol groups, hydrogen bonds between polar groups, and salt bridges between acids and bases. Nevertheless, the weak moisture attack ability for protein-based adhesives lead to the bonding failure usually do occur in the adhesive, i.e., the adhesive layer destroyed, while undertaking humid environment, but not between wood and adhesive. Therefore, the first possible step for obtaining a better bonding performance is to expose more functional groups hid inside, such as protein modified/denatured process, so that can enhance the bonding strength to wood and aggregation and cross-linking of protein molecules as well. Various intermolecular and intramolecular bonds for stabilizing the native structure of globular proteins was finally interrupted by the denaturation modification, resulting to re-organization of both secondary and tertiary configuration. Thus, some previously inward-oriented hydrophobic amino acids were

exposure on the surface of protein. The protein subunits, for example quaternary structure of protein, were destroyed by the denaturation as well, causing the aggregation. The aggregation of denatured proteins is usually caused by protein-protein hydrophobic interaction[229]. Thus, the denatured protein products are exits as an aggregated colloid which have a more complicated structure than native proteins[229]. Although the protein already located in a non-native condition, some folded structure kept. Depending on the denaturation degree of protein, various depolymerized structures from native proteins were created by the modification, even if the native protein is a biologically active structure.

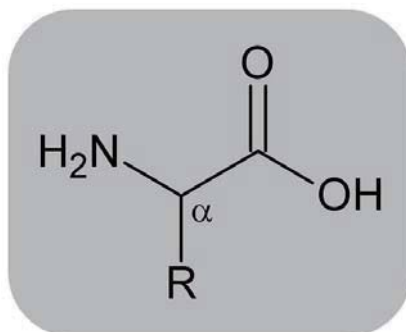


Figure 36. The chemical structure of an amino acid. Backbones are the same for all amino acids, while side-chains (r) are different for each amino acid.

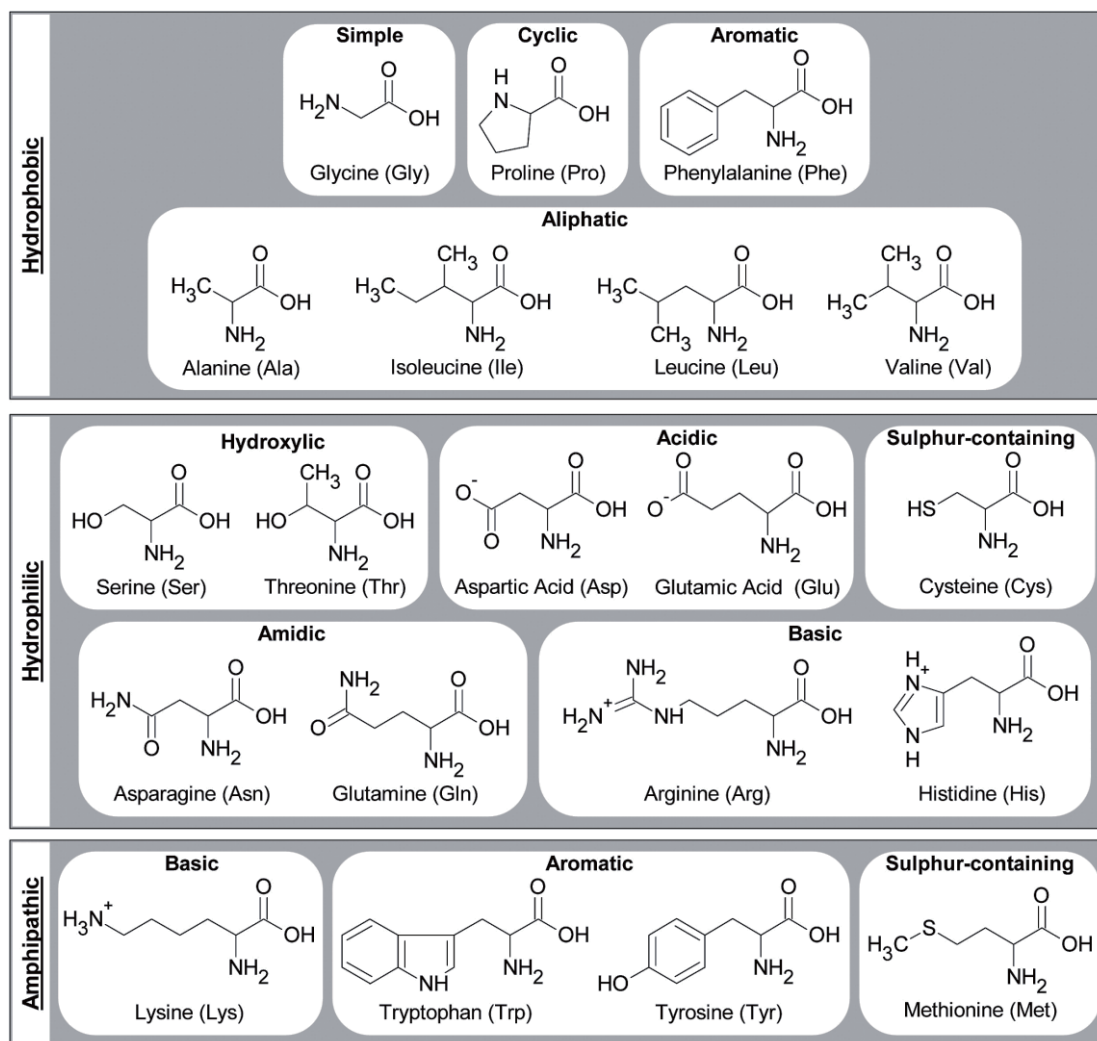


Figure 37. Amino acids grouped as hydrophobic, hydrophilic, and amphipathic, and divided into groups according to the characteristics of the side-chains[232].

1.2.3.3 Soybean protein wood adhesives and its modification

The utilization of soybean protein adhesives in wood industry can be tracked by the 1920s, however, it was replaced by “aldehyde-based” resins in the 1970s because of their weak performance under moisture condition application. Recently, the soybean protein has attracted by the researchers again due to its great source original, low-price, renewable, eco-friendly, and degradable, and shows excellently potential for industry developing, nevertheless, some drawbacks such as low water resistance, high viscosity, slow curing, and easily mildew still limited their industrial application. The bonding strength mainly comes from the mechanical interlocking and the hydrogen bonds between polar groups during the protein thermal denaturation and desiccation of native

soybean protein. Therefore, the three-dimensional structure formed by soybean protein were difference with synthesized resins, for example phenolic resin, urea formaldehyde resin, and can be attacked by the moisture, resulting to weak bonding strength and low water resistance, and slow curing. In addition, its macromolecular structure, and the increased intermolecular frictional force due to the interact force between protein side-chain lead to the high viscosity of soybean protein wood adhesive, thus, it is difficult to obtain the high solid content. The high polysaccharide containing in the raw materials especially soybean meal is the main reason on the mildew drawback. Hence, the majority of researches works have been carried out and achieved a significant progress on their proper application in wood industry by soybean protein wood adhesives. But only 0.1% of soybean protein wood adhesives has been utilized in wood industry. Therefore, there still have some scientific problems need to solve for its large-scale application.

A, Modification by denatured agents

Majority of non-polar groups and partial of polar groups were hidden into the internal of soybean protein molecular quaternary structure so that could not show an acceptable bonding performance while used as wood adhesive, particularly under wet condition. The efficient approach is exposing the hydrophobic non-polar groups by denatured modification, then can obtain an enhanced water resistance for soybean protein wood adhesives. Additionally, the polar groups also be exposed due to the opened fold structure of soybean protein during the modification which can improve the wettability of adhesive so that can increase the reactivity and crosslink degree between protein and crosslinker. There are some approaches reported as following for denatured modification:

a, Acid or base modification

The essence of acid/alkaline modification is destruction the native structure of soybean protein by various pH condition. For instance, the original structures (secondary, tertiary, and quaternary structures) of soybean protein were significantly influenced by the pH condition. The water retardancy was enhanced as exposed more non-polar hydrophobic groups by opening the fold native structures as well as improved

electrostatic repulsion between soybean protein molecular. At the same time, some polar groups also can be exposed, improving the interact environment condition between adhesive and wood. Hydrochloric acid was used to treat soybean protein, and its macromolecular would depolymerize firstly then the protein reorganization do occur to form a hydrophobic structure[164]. The strong acid condition, however, the partial of soybean protein can be hydrolyzed to small molecular which leading to the unstable bonding performance. The alkaline modification was normally used as a pretreatment process, and its products can obtain a fine glue layer while it was utilized as adhesive and then improved the bonding ability. But the viscosity would be increase significantly due to the intermolecular frictional force. Furthermore, the water resistance of wood adhesive prepared by alkaline pretreated (pH=9) soybean protein was improved[233].

b, Surfactant modification

The surfactants have usually been found in the soybean protein wood adhesive system, because of its end of hydrophobic can acting on the hydrophobic groups of protein, and unfolding the native soybean protein structure. Their interaction can form a stable structure and increase the wettability of protein adhesive for improving their bonding performance. But the surfactant modification also can enhance the viscosity of soybean protein wood adhesives. The most commonly utilized surfactant is sodium dodecyl sulfate (SDS)[162, 234].

c, Urea modification

Urea can interrupt the hydrogen bond while it was used to modify soybean protein, leading to its unfolded structure can be opened so that exposing more activity groups. Some researchers have been proved that urea modification can improve the bonding performance of panels bonded by soybean protein adhesives. The opened structure of protein molecular provide more grafting positions for its further modification. But the excessive unfolded structure exposed much more hydrophobic groups which could block the further grafting process.

B, Grafting modification

Grafting strategy is a general way to modify the physical or chemical property of stuff, and was usually utilized in wood adhesive field, for example, soybean protein

grafting is a common way to decrease their hydrophilic nature to enhance their water resistance, especially in starch-based wood adhesives[235-238]. The much more amino groups (-NH₂) are the reaction sites for further modification, and those activity groups can be grafted by other agents to improve the hydrophobicity of protein molecular by using some hydrophobicity chemical agents[238, 239]. Additionally, the soybean protein can be grafted by some reactivity groups for their reactivity improvement, for example, malic acid grafted SPI products can further reacted with PEI, for wood bonding[240]. Polyacrylate emulsion has been utilized to modify soybean protein, the grafted products can obtain a decreased viscosity and an improved wettability[241]. However, the grafting way normally needs a complex process, and it's a high-cost technique, which are limited this process for industrial application.

C, Enzyme modification

Enzymolysis is a typical method for protein treatment, it acts on the amide's bonds of peptide chain, therefore, the primary protein structure was destroyed by the impacting of protease. Thus, the complicated macromolecular was converted to the small pieces of polypeptide chain so that obtained more activity groups, and the apparently expression is the lowered viscosity. The bonding performance of wood panels bonded with soybean protein adhesives has been reduced significantly after enzyme pretreatment due to their small structures. Thus, the addition crosslinker has been used to improve their bonding strength. Enzyme modification has the advantages of safety, pertinence, and less dosage. It is usually used in conjunction with crosslinking agents to reduce the viscosity of adhesives, increase the solid content, improve the coating performance and bonding stability of adhesives[206, 242-244].

D, Crosslinking modification

The multi-functional crosslinking agent can react with the active groups of soybean protein molecules, such as hydroxyl, amino, carboxyl, etc., so that the intermolecular force of soybean protein was converted from hydrogen bond to covalent bond, forming a chemical crosslinking structure, and improving the crosslinking density of the adhesive. At the same time, the crosslinking modification can consume the hydrophilic groups of protein molecules and improve the water resistance of the

prepared adhesive. In addition, the crosslinking modified soybean protein adhesive has simple preparation process and controllable properties, which is the most effective modification method at present. The crosslinking agent of epoxy, emulsion, and synthetic resin to enhance soybean protein adhesive has been applied in industrial production.

a, Epoxide

The epoxy compound has high reactivity with various chemical-groups and only needs a low curing temperature. The epoxy group reacts with the amino group and carboxyl group on the soybean protein to open the epoxy-ring and connect the protein molecules to form a chemical crosslinking structure. Meanwhile, the epoxide can reduce the intermolecular friction force of protein so that the viscosity of the adhesive would decrease. Furthermore, during the curing process, it is conducive to wetting and penetrating the wood surface, forming more mechanical bonds, and improving the water resistance of the adhesive. It is an efficient cross-linking agent of not only soybean protein based but also other biomass-based adhesives[167, 168]. The structure of epoxy crosslinkers is diverse, and their enhancing effects on soybean protein adhesives are different[245-247]. The crosslinking structure of soybean protein adhesives can be regulated by different structure of crosslinkers, so as to realize the bonding performance regulation of adhesives[248].

b, Silane coupling agents

The siloxane group of silane-coupling agent was hydrolyzed into silanol during the wood adhesive bonding which can further react with wood hydroxyl group to form covalent bond. Usually, the silane coupling agent containing one end of epoxy group, such as KH560, can react with protein molecule amino and other active groups to form a crosslinking structure, improving the cohesion of adhesive and the bonding strength of adhesives[249].

c, Isocyanate

Acting as a raw material for typical polyurethane, isocyanate also can commonly use to modify bioresources wood adhesives, and can reach an excellent performance due to its really activity group $-N=C=O$. And in the isocyanate-modified soybean

protein wood adhesive system, the $-N=C=O$ group can react with the active hydrogen on the amino, hydroxyl, and carboxylic acid groups of protein molecules to form a crosslinking network structure, which can improve the crosslinking density and bonding performance of the adhesive, especially water resistance. Furthermore, the isocyanate can also react with the hydroxyl group on the wood surface to form a chemical bond, which can increase the interfacial bonding force between the adhesive and wood, and improve the dry and water-resistant bonding strength of plywood[250-253]. However, the high reactivity of isocyanate, short application life-pot of modified adhesive, and the certain toxicity of isocyanate always limit its industrial application. Importantly, the really high-price of isocyanate is the main reason why various researchers want to search a more renewable strategy.

d, Synthesized resins

The synthesized resins were normally utilized as wood adhesives directly, such as phenol-formaldehyde, urea-formaldehyde, and melamine-urea-formaldehyde. Because of their huge amount of active groups, they have commonly been served as the modifier to improve the bonding performance of other adhesives, especially bioresources-based[253]. According to the weight ratio of synthesized resin and biomass, the modification can be divided into two main targets, the first one is that a certain partial of soybean protein was added into synthesized resins to increase the biomass content within the acceptable bonding performance reduced. This strategy needs to concern an issue which is the controlling crosslinking degree of synthesized resins, otherwise, the bonding strength would be decreased and the formaldehyde emission would be increased[254].

The second target is that, in order to improve the bonding strength of soybean protein wood adhesives, a certain number of synthesized resins were introduced to fulfil this aim. The synthesized resins can improve the crosslinking degree of protein-based adhesive so that can enhance their performance, but still needs to control the addition amounts. Because of the soybean protein adhesives can obtain a glue layer with some defects, usually is some pores, therefore, this phenomenon can be developed by the synthesized resins addition[253, 255].

e, Bio-resources crosslinking agents

The crosslinker has normally been adopted in soybean protein-based wood adhesives for improving their wet condition bonding performance. But the most of crosslinkers for soybean protein adhesives modification are petroleum-based sources and normally with a large addition amount, the weight ratio of crosslinker and soybean protein adhesive always can reach almost 1:2. Therefore, the biomass crosslinker is an attracted research direction for soybean protein wood adhesives. For example, tannin resource, is also a natural polyphenol, can react with soybean protein directly as mentioned in the previous context, the phenol hydroxyl groups of tannin A ring can be substitute by the -NH₂ groups of protein so that enhance the crosslinking degree[137, 142, 143, 150]. In addition, tannin B ring was similar with high adhesion-structure of mussel protein, which can connect to soybean protein and wood surface by strong hydrogen bonds[137]. Furthermore, the pyrocatechol-like tannin B ring can be oxidated and converted to benzoquinone under alkaline condition, and then further react with protein reactivity groups[137]. Another biomass, lignin, also a polyphenol structure natural, but their special structure unlike with tannin, it cannot react with protein directly due to its low reactivity. Therefore, when lignin was used as crosslinker in protein wood adhesives, an additional crosslinker was normally needed to realize the reaction. Sometimes, the activated lignin by phenol-formaldehyde can significantly improve the bonding performance of protein-based wood adhesives[71, 73]. In summary, if lignin was used to modify soybean protein adhesives, the pre-activated process was normally needed to improve the reactivity of lignin, after that to react with protein to realized crosslinking.

f, Polysaccharide modification

Soybean meal is the cheapest original material which usually used as animal feed, containing about 40-50% of protein and 30-40% of soybean polysaccharides. And those polysaccharides are hydrophilic with low reactivity, that it is hard to participate the crosslinking reaction during the hot-press condition. Therefore, those water solubility soybean polysaccharides can eventually interrupt the integrity of glue layer so that decrease their water resistance. Hence, concerning the protein wood adhesives, how to

increase the reactivity of polysaccharides and improve their crosslinking degree are the one of an attractive direction for protein-based wood adhesives. From the literatures, there are two main methods on polysaccharide modification for high-performance wood adhesives application, they are as following:

-Adopting some crosslinker to connect oligosaccharide in soybean meal. For example, sodium hexametaphosphate (SHMP) was chosen as a non-toxic chemical to connect soybean polysaccharide. This method can significantly enhance the crosslinking degree of oligosaccharide, an interpenetrating network structure can be form between modified-oligosaccharide and soybean protein. Thus, their thermal stability and water resistance were obtained an improvement[200].

-The oxidation of saccharides is a mature technique for oligosaccharide modification, for example, cellulose, glucose, and sucrose, etc., after the oxidation, two activity groups, i.e., aldehyde group, can be obtain, and then can take part in the further reaction with other groups. Those aldehyde groups can react with $-NH_2$ groups of protein to form a crosslinked structure. For example, a hyperbranched polyamide containing large number of $-NH_2$ groups was grafted on the oxidated saccharide products can then further crosslink with soybean protein to prepare a high-performance wood adhesive[202]. Furthermore, the researchers studied on different kinds of saccharides influence the bonding performance of soybean protein wood adhesive. And they reported that monosaccharides can improve the water resistance of soybean protein wood adhesives in some extent due to is high reactivity, and the polysaccharides can influence their bonding strength greatly because of their low reactivity[256]. Therefore, some research works on how to convert the soybean meal polysaccharides to small molecular by using acid or plant hydrolase, and then further utilized for wood adhesive preparation[257, 258].

The most effective method is grafting hyperbranched polyamide modified soybean polysaccharide, which can not only improve the crosslinking density of the adhesive system, but also greatly reduce the amount of crosslinking agent and form multiple network structure to increase the toughness of the adhesive layer. In addition, due to the presence of a large number of amino groups, the process performance of the adhesive

has been improved to a certain extent, which is conducive to industrial production and application.

g, Biomimetic modification

It is an important research direction to improve the bonding property of biomimetic soybean protein adhesive by imitating the high adhesion property structure in nature[259]. The performance of the biomimetic soybean protein adhesive has been significantly improved, but the bionic modified process was complex and high-cost starting materials, thus it is difficult for industrial application. Marine mussel foot filament protein has attracted widespread attention as its excellent adhesion properties and water resistance. The dopamine structure in mussel protein (catechol) can produce strong hydrogen bonds and metal chelation with different surfaces to achieve high-performance adhesion. Natural dopamine can be used to improve the interface compatibility between additives and soybean protein adhesives and increase the enhancement effect[137, 260].

h, Nano/micron materials modification

Nano/micron materials have high strength and specific surface area, which can be used to strengthen soybean protein adhesives. It is a new direction for the efficient modification of soybean protein adhesives by modifying the surface of nanomaterials to improve the interface between them and adhesives. For example, nano-cellulose, nano-montmorillonite, and microcrystalline cellulose, etc., have been reported to use as the modifier to improve the bonding performance of soybean wood adhesives[261-263]. Silane coupling agent is often used to improve the compatibility between the interface of nano/micron materials and soybean protein adhesives, and to enhance the water resistance of nano/micron materials to adhesives[264].

1.2.4 Humins material and its applications

Humins are dark and viscous residual products, which was obtained by the acid treatment of polysaccharides[265, 266]. Humins from the acid conversion of fructose or glucose yield polyfuranic materials still bearing fragments of furfuryl alcohol[265-271]. Thus, under very acidic conditions, humins can self-crosslink if heated and the reaction can be accelerated by adding a strong acid initiator, such as p-toluene sulfonic

acid (p-TSA)[271]. The solution of humins in water can be used, for example, to create during a heat treatment a polyfuranic network in the cells of the wood. This so-called “wood humination” follows the same approach as in the furfurylation of wood with aqueous solutions of furfuryl alcohol. However, this approach yields foams of a very limited variety of characteristics and is not usable for wood adhesives. This is due to the limited possibility of formulation of these heterogeneously distributed materials when used alone[272]. It is for this reason that this has opened up the possibility of trying to mix these wastes with other materials, in order to formulate foams and adhesives that are more adaptable to a greater variety of situations.

Mixed furanic/non-furanic but mostly non-furanic humins are produced in abundance by many factories around the world and on several continents. Such humins are material obtained from humic substances, especially rich in humic and fulvic acids. The organic components of the soil can be subdivided into soluble fractions, largely humic acids, and insoluble, humins. Humins make up about 50% of soil organic matter. Humins are also produced during the dehydration of sugars, as occurs during the conversion of lignocellulosic biomass into smaller, more valuable organic compounds such as 5-hydroxymethylfurfural (HMF). These humins can be in the form of viscous liquids or solids depending on the process conditions used. Such humins have a furan-like polymeric structure, with hydroxyl, aldehyde and ketone functionalities. However, their structure depends on the type of raw material (e.g., xylose or glucose) or concentration, reaction time, temperature, catalysts and many other parameters involved in the process. They are used in agriculture to improve the effect and absorption of fertilizers by increasing soil fertility, as foliar fertilizers, in the pharmaceutical-cosmetic field[273], in the preparation of catalytic materials[274] and in applications materials. However, depending on their origin, they seem to contain mainly humic acids, fulvic acid as well as a minority but still significant proportion of furanic materials.

1.2.5 Other wood adhesives

Comparing with the popular bio-resources, such as tannin, lignin, and soybean protein, there still have other resources suitable for wood adhesives preparation,

typically starch, cellulose, and others.

The starch-based wood adhesive researches are not as extensive as other bio-sources due to its weak bonding strength. The most researches on starch adhesives are focused on that how to increase their initial viscosity and reduce the material costs[275, 276]. Starch-based wood adhesive was like other biomass, was firstly used to modify synthesized resins for increasing their biomass contents[277-279]. As expected, that, this pathway can realize the target and this co-mixture wood adhesives normally can obtain an acceptable performance. However, with the concept of environment of consumers, the formaldehyde was generally removed with a partial or totally in wood adhesives. And a typical method on starch-formaldehyde adhesive is using oxidated starch which containing the aldehyde groups, this method can reduce somewhat of formaldehyde so that can decrease the formaldehyde emission[278]. And a simple and convenient acid catalyzed dialdehyde starch preparation method was reported[280]. Because of the -OH groups of starch, therefore, the oxidation and/or grafting strategy is also the modification way to increase the reactivity of native starch[237, 281]. In addition, silane coupling agent (KH570) has been reported to use in starch wood adhesive for bonding performance enhancement[282]. Some high-performance chemicals, such as compound emulsifiers, montmorillonite, nano-TiO₂, and sodium dodecyl sulfate etc., have been utilized to modify starch-based wood adhesives[275, 283-285]. In order to improving the activity of starch, some pre-treatments were carried out, for example, heat pre-treatment, acid hydrolysis denatured[284, 286]. Starch mixed with other biomass especially tannin powder is a normal way to prepare wood adhesives, and from the last decades to nowadays, tannin still can utilize to prepare wood adhesive by mixing another biomass. Some addition crosslinker was used in the past, but with the formulation developing, even totally green biomass starch-containing wood adhesives was reported[287-290].

Polyurethane was normally wood adhesives especially high-performance required structural adhesive as their high bonding performance, formaldehyde-free, and highly water resistance, etc. Isocyanate is the main part of PU adhesives, and it can react not only polyols to form the adhesive network, but also can react with the -OH groups of

wood surface to further strengthen the bonding performance[291]. As because of the highly reactivity of isocyanate, endows it was selected to enhance other wood adhesives, especially biomass-based[292]. And as expected, those modified wood adhesives were usually can obtain a better bonding performance.

With the formulation developing, the fossil-based polyols were gradually replaced by some bio-based resources, such as wood liquefaction products which were utilized to produce so called bio-based polyurethane, of course, wood adhesive is their application field[293, 294]. Recently, some researches focus on the non-isocyanate strategy for polyurethane preparation as the high-price, high activity and toxic natures of isocyanate. Typically, some epoxide groups were needed for the further steps, those groups were converted to five-members cycles which have a unique reactivity for $-NH_2$ groups[295-297]. The conversion process of epoxide groups, however, need a harsh condition, such as high-temperature, high-pressure, catalyst, etc., therefore, this method still need a highly requirement for the either operator or enterprise. Hence, searching for a conveniently method to produce high-performance non-isocyanate polyurethane is still a challenge.

But fortunately, a mild preparation process was reported by the researchers on non-isocyanate polyurethane with biomass resources, for example, tannin, glucose, sucrose, lignin, and their products have been utilized as wood adhesives, and obtained a high-performance[91-93, 96].

Recently, the inorganic wood adhesives were attracted by the researchers as their excellent performance on bonding strength, and another property which other adhesive could not comparable, fire retardant, because of their inorganic elements[207, 298-301]. Their large amount of inorganic network provides a strong water retardancy. Therefore, their products can be utilized for green building application with the excellently fire-retardancy and thermal insulation[302].

1.2.6 Perspectives

During the past decades developing of wood adhesive industry, the formulations can reach the industrial application still are the typical so called “three-aldehydes” based products. And they still dominate the wood adhesive field as their advantages,

such as their acceptable price, better performance, and relatively simple preparation process. But recently, some novel types of wood adhesives have been developed and been utilized in wood industry, such as soybean protein in China, tannin-based wood adhesives in South Africa. But their application still only occupied a small partial in wood industry. Therefore, those successes encouraged the researchers to spend more energy to realize much more large-scale industrial applications by more kinds of bioresources.

Fortunately, biomass-based wood adhesives have been reported by many researchers, those products have an acceptable property either bonding performance or other ones especially formaldehyde-free. Therefore, considering those progress, there are some encouraged measures should be concerned to fulfil large-scale application as following:

- Expanding the bio-sources original for adhesives preparation, using the waste residues which comes from agriculture and forestry.

- Searching some green pathway to use the biomass resources with high utilization. For example, this strategy was adopted to prepare wood adhesive by using a bio-ethanol fermentation residue[303].

- Connecting with new biomass resources closely. There are several kinds of biorefinery residues for example, bio-ethanol, furfuryl alcohol preparation, have the potential for wood adhesive production.

- Realizing the currently biomass wood adhesives large-scale application.

In consequence, even bio-based wood adhesives formulation has been obtained several progresses, if we want to realize the large-scale application, there still have a long way to go and facing more challenges on that.

1.3 Tannin resource as the starting materials for green foam fabrication

Tannin-based bio-foam have been concerning extensively for several years from the first records in 1970s to today as their specific properties[304]. But at that time, the foams still show several problems even many researchers have expended more efforts on their property improvement. In addition, this foam could not be attracted by the industry which dominated by synthetic foams as their relative performance/cost

structure seemed unfavorable at that time, in the public opinion, to totally bio-sourced materials[105]. Fortunately, Meikleham and Pizzi in 1994 was firstly reported an improved formulation that tannin foam exhibited a well performance. This notwithstanding, till to the late years 2000s, the public comes to really focus on these tannin foams[305]. These kinds of foam are phenolic-like foams as the special structure of its starting material, polyphenol tannin. But even so that, their large number of phenol -OH still have attracted by other research groups started from the early 1990s, they obviously do the research on tannin-isocyanate foams in which tannin -OH was described as the polyol[306-308].

Therefore, based on the basic formulation, several developed studies on tannin-furanic phenol-like foams preparation systems were utilized with/without the present of blowing agent. The foaming process was sustained under the impulse of the exotherm generated by either a chemical reaction, typically furfuryl alcohol self-polymerization under acid condition, or exterior heating sources. Furthermore, the mechanical agitation/stirring blowing method is an efficiently way for a novel tannin-based foam production as well, but not the traditional tannin-furanic-based foams. In addition, the researchers keeping work on the tannin-based foams but with some targets: (i) preparing the tannin-based foam with totally or high biomass content bioresources, and avoiding the toxic starting materials utilization; (ii) improving the mechanical properties of tannin-based foams; (iii) realizing its large-scales industrial fabrication and expanding their novel applications. It's encouraging that the researchers have been made some progresses on them.

1.3.1 Tannin-furanic based foam preparation and its modification

From the first time, the tannin-based foam was reported, for the quite a time afterwards, the researchers only focus on the one that formulation by an exothermic reaction produced foam. A dark tannin-based foam was shown in Figure 38, and their basic morphology was studied as well. The early efforts were based on a basic formulation which at the present of diethyl ether as a blowing agent and an exotherm reaction comes from the acid auto-condensation of furfuryl alcohol[309]. But these acid-catalyzed foam exhibits apparent acidic nature when was put into water. Therefore,

the alkaline-catalyzed rigid foams were researched in the early time as well[309]. And either acid or alkaline catalyzed foams all can obtain the comparable properties to synthetic phenolic rigid foams. Compared with commercial synthetic phenolic foams, tannin-based foams were obtained from the tannin-formaldehyde resin that is a partially biomass fluid polymer phase. The expansion (foaming) was a physical process which was brought about by blowing agent heating volatilization, whereas the foam system was reached the desired density, then those dimensional stabilization was achieved through formaldehyde cross-linker. But the blowing agent volatilization heating sources is the self-polymerization of furfuryl alcohol. The crosslinking between tannin and furfuryl alcohol was also contributed to the stability of the expensed system to the desired density[309]. These foams moreover did not give any quantity of toxic gasses on carbonization[310]. After several years efforts on tannin-based foam, some basic foaming formulation work well was reported and then the special features of tannin-based foam were attracted by the researchers again in the late years 2000. And the eco-friendly concept of tannin-based foam was announced, therefore, those potential toxic chemical starting materials were necessary to remove form the foaming system. Hence, the further research works performed by the follow-up researchers are concentrating on the (i) the substitution of diethyl ether with a less dangerous and volatile solvent, and (ii) the elimination of formaldehyde. And their better mechanical properties are the main target as well.

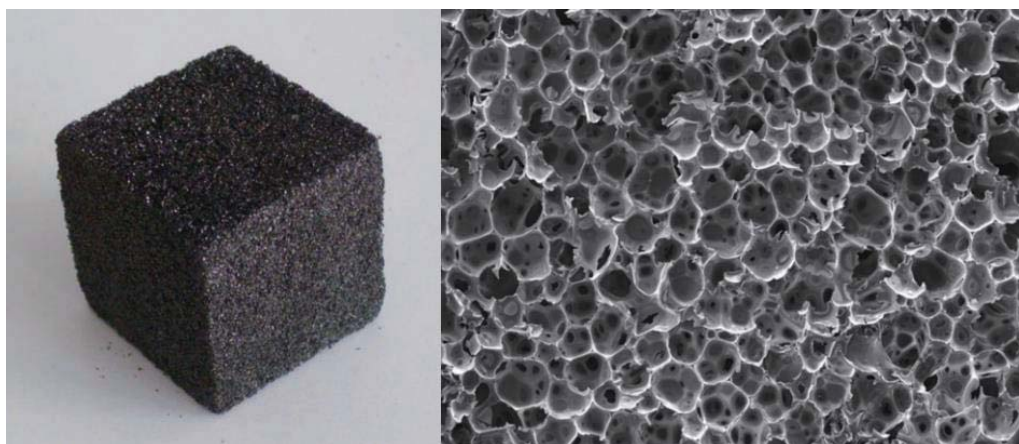


Figure 38 The typical tannin-based foam and its morphology structures observed by SEM.

As their special and excellent properties, such as fire resistance, chemicals stability, absorption of various liquids, permeability, thermal conductivity and mechanical (compressive and tensile) strength, acid catalyzed tannin-based foam have been studied many years. And the applications of these foam were based on their targeted properties[311, 312]. Boric acid and/or phosphoric acid can be used to modify the basic formulation for further improving their fire retardancy[313]. It is reported that the tannin foam underdoing external heat flux, the HRR (Heat release ratio) did not increase with the enhanced heat flux, representing the fire retardancy was retained as the heat flux grows. Therefore, this highly fire safety light-weight materials can be potentially applied to construction decoration only needs they have enough mechanical strength. Beyond that, the foams obtained from the basic formulation still presented other outstanding properties which are (i) highly biomass content, low cost, and easy to preparation. Tannin resources is a natural, non-toxic starting materials, form the aspect of environmental protection point, it was more acceptable for the consumers than the synthetic, more expensive, materials utilized. And their limited using noxious material much lower than synthetic phenol-formaldehyde foam preparation. Pivotaly, the hardening rates of tannin resins were faster than those of synthetic phenol-formaldehyde in 5 to 50 times, which is the crucial point for large-scale industrial production so that consequent financial advantages[313]; (ii) highly resistant to chemicals (strong acids or bases, solvents) and moisture and weathering; (iii) excellently low thermal conductivity[314], which shown their potential for building materials for thermal insulation. And these foams exhibit slightly anisotropic especially on the mechanical properties. In addition, these foams presented a brittle behavior while undergoing loads. X-ray microtomography technique was utilized to examined the basic foams which shown some additional information on physical characteristics, including porosity, fraction of open cells, connectivity, tortuosity, and pore size distribution as a function of the foam's density[315-317].

Because of those reported outstanding properties of tannin-based foams, and their potential applications for the other fields in the future, there are various modification strategies been reported to fulfil their green production, high performance, and largely

applications. Therefore, the first being concerned is the blowing agent in the foaming system, a much safer solvent, namely pentane, was utilized to replace the unacceptable diethyl ether. But the pentane volatile needs a higher foaming temperature, thus, the preparation formulation was adjusted in the new blowing agent foaming system. Their mechanical properties were similar with the typical one while under the same density condition[318]. Finally, the researchers founded a balance formulation between each part of raw materials, and totally removed any blowing agent at presented[319].

Formaldehyde-free tannin-foam formulation was suggested by the researchers at the early years as formaldehyde is an unacceptable chemical for green materials preparation. And some non-formaldehyde tannin-based formulation have been reported in the past several years, those novel tannin foams have a lower thermal conductivity, better compression strength than the basic one[319, 320]. Even if the noxious formaldehyde was totally removed, but other crosslinkers, including glyoxal, glutaraldehyde, p-MDI, and PEG-400, still exist in the modified formulations. And those crosslinker although low-toxicity than formaldehyde whereas they are either high-price or fossil-based or high-toxicity. The functional of crosslinker is nonnegligible as it need to maintaining the desired densities. Therefore, some greener formulations containing almost 90% of renewable starting original materials have been published. A biorefinery byproduct-humins-was firstly reported as the crosslinker, as substitution materials to formaldehyde, due to its some reactivity groups[321]. Those foams with a higher density than basic one, the crosslinking was realized comes from the humins can react with tannin molecular, even higher molecular weight humins species. The most recently, soybean protein isolation (SPI) was been known as a biomass resources normally utilized to prepare wood adhesives[94, 206-210], even acting as a tannin crosslinker to replace formaldehyde for almost totally green tannin foam production[322]. It is noticed that this tannin-SPI foam has great enhanced properties than basic foams. But there still have a shortcoming, the high price of SPI.

The abovementioned foams were prepared by using mimosa and quebracho tannins[323], another more reactive tannin named as pine tannin, was extracted from pine bark, was first reported in pine tannin foam production in 2013[128, 320, 324-326].

Those foams come from a totally adjusted formulations because of the high reactivity of pine tannin in relation to other tannins, therefore developing the foaming system in order to coordinate foam resin hardening, reaction exotherm and solvent blowing allowing the formation of a rigid foam. The formulations with the surfactant polyethylene glycol and castor oil ethoxylate can obtain homogeneous foam cell microstructure. These formulations were permitted clearly the application of the whole class of very reactive procyanidin tannins to obtain typical tannin-furanic foams, not only including the different kinds of pine tannin, but also spruce tannins or others[326-329]. Furthermore, the open cell structure of tannin-furanic foams obtained from pine and mimosa/quebracho tannins have been shown to give good sound absorption/acoustic insulation characteristics at medium and high frequencies (1000-4000 Hz) with coefficient of acoustic absorption of 0.85-0.97[330]. This property of tannin foam was superior to some commercial materials such as polyurethane foams, melamine foams, fiberglass, and mineral wool acoustic insulations during this range. Moreover, at the rang of lower frequencies (250-500 Hz), the tannin foam still shows a good performance, the lower acoustic absorption coefficient between 0.40-0.60. Compared with the commercial synthesized foams, tannin-based open cell foams have the same typical behavior with those commercial light porous materials. The higher open-cell ratio is the tannin foam the better is its sound absorption.

The first elastic flexible tannin foam was reported still based on the basic rigid foam preparation formulation by the addition of an external (non-reacted) plasticizer, namely glycerol[331].

The last problem of this typical tannin-furanic foam is their surface friability, attributing to their weak mechanical property. Therefore, based on the aim of that how to improve their mechanical property but could not loss their other superior properties with a large extent, several enhanced research works have been performed by either adjusting the foaming formulation or adding some additives. Hyperbranched poly (amine-ester) was selected as a modifier to modify tannin foam[332]. This method obtained tannin foam with a better thermal insulation nature and excellent fire resistance, similar with those tradition tannin foams, but the most important is their

mechanical property was enhanced. Oil-grafted flavonoid tannins as the raw materials for foam production, there are two main aspects of improvements, one of them is their enhanced foam surface nature, i.e., the surface friability has been developed. The other one of them is the wettability of foam surface was changed, i.e. less hydrophilic, practically hydrophobic[333]. Moreover, some high-performing sulfur-free tannin foams have been published by removing the traditional sulfur-containing acid catalyst, p-TSA[334]. Their mechanical property has been adjusted. Some sustainable additives, such as cellulose nanofibers (CNF), wood cellulosic fibers were utilized to improve the performance of tannin foams[152, 335]. And the tannin mechanical property all obtained somewhat extent developing. At the same time, the sustainable replacement strategies, for example, humins and SPI, also used to adjust the typical formulation by totally removing the toxic formaldehyde[321, 322]. Those modified tannin foams obtained a better mechanical performance but did not lose their other exceptional properties.

Fortunately, tannin-furanic foams through several years developing can be fulfilled pilot plant up-scaling manufacturing[336]. Tannin foams can be up-scaled to an industrial pilot plant also as lightweight sandwich panels which can be produced without the need of any external adhesive.

1.3.2 Tannin-isocyanate foams preparation

Apart from traditional tannin-furanic foams, the other kinds of tannin-based foams also have been reported by using tannin reacting with some hardeners. It was reported earlier that tannin act as a polyol to react with isocyanate to obtain tannin-PU foams. Those tannin resources can be used directly or by some modifying process to active tannin reactivity. An open cell foams obtained by using condensed tannin reaction with alkoxyated fatty amine and polymeric diphenylmethane isocyanate simultaneous. This foam exhibits a highly flexible/elastic feature[337]. In addition, the presented of tannin endows the modified PU foam obtained some enhanced properties, the most obvious is that some of them can be made flame self-extinguishing and if burning they neither flow nor asperge flaming material around, contrary to what occurs with normal polyurethanes. In addition, isocyanate was used as the modifier to adjust the properties

of tannin-furanic foams, but their products were described to a mixed phenolic-polyurethane-type rigid foam[338]. MALDI-TOF and ^{13}C NMR techniques were utilized to analysis the reaction mechanism of isocyanate modification. It mainly reacts with the flavonoid hydroxyl group at C3, but small part of phenol -OH groups.

Condensed tannin-based polyols are also starting materials for tannin-PU production. But because of the steric hindrance of tannin molecular, not every hydroxyl group of tannin phenol ring can do participate to react with isocyanate, normally their crosslinking does appear on the flavonoid hydroxyl group at C3 position[338]. Thus, the tannin phenol -OH groups show usually lower reactivity in the tannin-isocyanate reaction system. Hydroxypropyl tannin is the method to lengthen the side chain by using chemicals, usually epichlorohydrin, reacting with phenol hydroxyl groups. Therefore, the short chain phenol -OH groups could be lengthened so that breakthrough the steric hindrance resulting to reactive hydroxyl groups[339, 340]. Tannin-based polyols can substitution glycerol-based polyol presented various positive effects on rigid foams preparation and properties[341]. The tannin-polyols modified PU production process can easily be controlled as the less exothermic. In addition, hydroxybutylated condensed tannins as a polyol source in the most recently, do react with isocyanate to prepare polyurethane foams[342]. Those kinds of tannin-based polyurethane foams exhibit a very similar properties, can obtain a better mechanical than fossil-based PU products. Moreover, the aromatic structures of tannin molecular can provide the rigid feature of the resultant foams, promote the char formation, and decrease the flammability. Oxypropylation and hydroxybutylated strategies constitutes an interesting approach to develop tannin-based macro-polyol towards high performance materials, even for foam applications. These bio-based PU foams with advanced properties which can compete with conventional PU foams comes from fossil-based polyols resources, for a large range of applications where high insulation behaviors are required.

1.3.3 Mechanically Blown tannin-based foams

The mechanically blown method is a new method of expansion based on the therapy of fire-fighting or tunneling foams, where a foam concentrate forms a stable

liquid foam (Figure 39). The large number of air bubble was mixed with liquid tannin resin by intense stirring to promote the liquid foam volume expansion. Meanwhile, the liquid foam obtained from the tannin resin and an aqueous solution of surfactant can finally be converted to the solid porous material by heating hardening process[343]. This expanding method was considered as potential way to realize tannin-based foam green preparation, and can efficiently avoids that problem for example shrinkage normally appeared in other formulations where physical or chemical foaming. And their structure can be improved by using some non-ionic surfactants, and the smaller cell structures usually obtained at the same time. Some basic properties including apparent density, mechanical and thermal properties, and morphological appearance of the foams have been characterized and reported[344, 345]. Apart from the mechanical blowing only method, the mixed mechanical-chemical blowing approach has been taken as well. Some reactivity polyamines were adopted to mixed with tannin resin for providing a quacking stiffen speed to avoid the liquid foam volume pours/drips and breaks under the effect of gravity[346].



Figure 39 A tannin rigid foam obtained by mechanically blown.

1.3.4 Tannin-based polyurethane foams

Tannin has been reported to prepare by reacting with a certain amount of dimethyl carbonate and hexanediamide, as shown in Figure 40[96, 97]. This pathway for polyurethane synthesis has been reported that can suit for many bioresources, for example glucose, sucrose, non-polyfuranic humins, tannin, and soybean protein

isolation, and even lignin. Normally, their resultant products have been utilized to apply for either wood particleboard or plywood, and some of them also be used to prepare the non-isocyanate polyurethane foams. Furthermore, the particleboard bonded by the biomass non-isocyanate polyurethane adhesives are not only can obtain their excellently basic properties but also exhibit somewhat boiling water tolerance. For foam preparation, for example, glucose-based products, two potential production ways have been published under high-temperature end even room temperature conditions. Interesting, glucose-based resin foams under high-temperatures obtained a different mechanical property, generally higher than room condition. These foams regardless under which conditions, the flammability is similar with the typical PU foams, showing a lower fire resistance. Therefore, tannin was a natural fire retardance which has been utilized to improve the fire retardancy of glucose-based foam. As expected, the fire retardancy of glucose-based foams have been enhanced accompanying with the improved mechanical property and thermal stability. In addition, tannin-based non-isocyanate polyurethane resins still have the potential for foam preparation, like those small molecular sources (Figure 41). Those tannin-based foam have a totally different properties with tannin furanic foams, such as higher density leading to a better compression strength, and lower fire resistance (Figure 42). But this kind of foam currently has been reported from their reaction mechanism and some basic properties, and still have much more further researches needing to do.

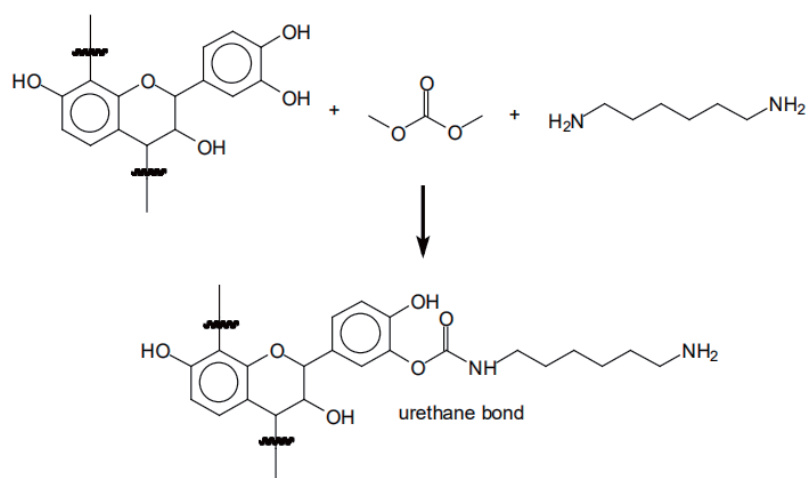


Figure 40 The typical reaction process of tannin NIPU.

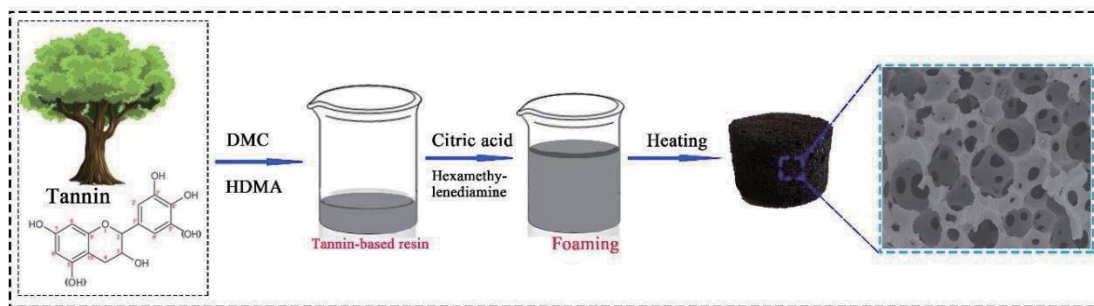


Figure 41 The typical tannin NIPU foam preparation process.

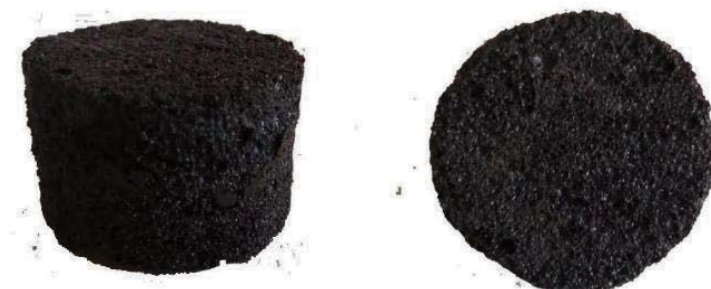


Figure 42 Tannin NIPU foam.

1.3.5 Other researches

From the first reported on tannin-based foams to currently, the researchers remain keeping the concentration on their properties, preparation mechanism, and the exactly preparation process, even their further applications, especially tannin-furanic foams[128, 314, 316, 317, 324, 325, 347, 348]. Furthermore, due to their porous structure, the converted carbon tannin foams have attracted to the researchers[349-355]. Their porous structures have been maintained well even after high temperature carbonation, resulting to their further potential extensively applications, such as thermal insulation for green building, energy storage, and so on. Moreover, tannin-furanic foams still have a great potential for thermal insulation application acting for doors and wall panel[356, 357] and green acoustic absorbers[330]. A lightweight tannin foam/composites sandwich panels based on tannin-furanic foams have been prepared and reported[358]. This sandwich composites are consisting of tannin foam core while covered with the artificial thin panels, leading to lightweight property with better bending strength. And the most important that this composite material obtained a better mechanical property of the brittle rigid tannin/furanic foams.

Tannin foams shown a good nature for heavy mental iron absorption, exhibiting

the ability for adsorbing in waste water solution, up to 12.5% of Cu(II) and 20.1% of Pb(II) with respect to the concentration of these ions[311]. The research on tannin foam formulation optimizing which are acting as absorbent for dye, surfactant and pharmaceutical removal[359]. The different foam properties obtained with various foaming formulations can obtain a different absorption effect on those water contaminants. About other extensive waste water treatment applications have been described in the other studies[312, 360]. In addition, the surface properties of tannin foam also can be changed depending on their applications, such as hydrophobisation modification[361]. Tannin foams obtained the strong water maintaining capacity after formulation adjustment can be utilized to apply in horticultural/hydroponics and floral[362].

On tannin preparation methods, generally, tannin-furanic foam can be obtained under room condition absolutely, or still on the oven condition at the temperature range from 40-80°C[335]. Because of the foaming system can produce enough heating temperature, can reach almost 80-90°C, by the furfuryl alcohol self-condensation under acidic condition release[152]. And this such high temperature can provide enough function to support the blowing agent evaporation. The foaming process based on the typical tannin-furanic foam has been reported by experimental investigation[363]. And a numerical model was created to simulate the foaming process of bio-sourced thermoset foams based on the experimental research[364].

The tannin-based foam resin curing kinetic parameters have been researched and reported with a simulation approach[365]. But tannin foams preparation obtained apart from the basic foaming methods, some assistance approaches have been described as well while with some different formulations, such as microwave, infrared-catalyzed [366, 367]. Apparently, these described tannin-furanic foams have different properties.

The typical tannin-furanic foams compressive strength and impact resistance can improve by a proper percentages of multiwall carbon nanotubes[368]. In addition, various kinds and various amounts of graphite fillers as the modifier to adjust the thermal properties, thermal conductivity, and cell structures of them, which endow some special performance for seasonal storage applications[354]. Moreover, tannin

foams can be used as semi-conductive for primarily building material applications by in-situ polymerization of polyaniline[369].

About the tannin properties investigation, some novel approaches including raman spectroscopic, X-Ray Microtomography have been adopted to help the researchers for discovering some new features which those natures could not investigated and described by the traditional techniques[315, 370].

1.3.6 Prospective

The natural source, condensed tannin, has been reported in several types of research for different tannin-based foam preparation with various formulations. But most presented remain based on typical tannin-furanic-based as their outstanding performance and simple convenient fabricating process. In addition, some practical applications have been speculated and reported based on the current formulations. Nevertheless, the weak mechanical performance and sometimes toxic formaldehyde crosslinker used are still the main two shortages that would limit their wide application. Therefore, the following aspects for tannin-based foam preparation can be considered:

- Modified tannin-furanic-based rigid foams with a well-mechanical property and limited or without toxic crosslinker utilization.
- Tannin-based flexible foams for other applications, such as contaminated water treatment, oil/water separation.
- Novel formulations investigation for tannin-based foam preparation.

2 REFERENCES

- [1] Pizzi, Antonio, Antonios N. Papadopoulos, and Franco Policardi. Wood composites and their polymer binders, *Polymers*, 12 (2020): 1115..
- [2] Pizzi, A. Tannin-based adhesives, *Journal of Macromolecular Science-Reviews in Macromolecular Chemistry*, 18 (1980): 247-315.
- [3] M. Norgren, H. Edlund, Lignin: Recent advances and emerging applications, *Current Opinion in Colloid & Interface Science*, 19 (2014) 409-416.
- [4] R. El Hage, N. Brosse, P. Sannigrahi, A. Ragauskas, Effects of process severity on the chemical structure of Miscanthus ethanol organosolv lignin, *Polymer Degradation and Stability*, 95 (2010) 997-1003.
- [5] J.J. Liao, N.H.A. Latif, D. Trache, N. Brosse, M.H. Hussin, Current advancement on the isolation, characterization and application of lignin, *International journal of*

- biological macromolecules, 162 (2020) 985-1024.
- [6] A. Duval, M. Lawoko, A review on lignin-based polymeric, micro- and nano-structured materials, *Reactive and Functional Polymers*, 85 (2014) 78-96.
- [7] M. Fache, B. Boutevin, S. Caillol, Vanillin Production from Lignin and Its Use as a Renewable Chemical, *ACS Sustainable Chemistry & Engineering*, 4 (2015) 35-46.
- [8] E.A.B.d. Silva, M. Zabkova, J.D. Araújo, C.A. Cateto, M.F. Barreiro, M.N. Belgacem, A.E. Rodrigues, An integrated process to produce vanillin and lignin-based polyurethanes from Kraft lignin, *Chemical Engineering Research and Design*, 87 (2009) 1276-1292.
- [9] P. Upadhyay, A. Lali, Protocatechuic acid production from lignin-associated phenolics, *Preparative Biochemistry & Biotechnology*, 51 (2021) 979-984.
- [10] L.A. Zevallos Torres, A. Lorenci Woiciechowski, V.O. de Andrade Tanobe, S.G. Karp, L.C. Guimarães Lorenci, C. Faulds, C.R. Soccol, Lignin as a potential source of high-added value compounds: A review, *Journal of Cleaner Production*, 263 (2020) 121499.
- [11] B. Jiang, C. Chen, Z. Liang, S. He, Y. Kuang, J. Song, R. Mi, G. Chen, M. Jiao, L. Hu, Lignin as a Wood-Inspired Binder Enabled Strong, Water Stable, and Biodegradable Paper for Plastic Replacement, *Advanced Functional Materials*, 30 (2020) 1906307.
- [12] H. Nishimura, A. Kamiya, T. Nagata, M. Katahira, T. Watanabe, Direct evidence for alpha ether linkage between lignin and carbohydrates in wood cell walls, *Scientific Reports* 8 (2018) 6538.
- [13] S. Iravani, R.S. Varma, Greener synthesis of lignin nanoparticles and their applications, *Green Chemistry*, 22 (2020) 612-636.
- [14] L. Perez-Cantu, A. Schreiber, F. Schutt, B. Saake, C. Kirsch, I. Smirnova, Comparison of pretreatment methods for rye straw in the second generation biorefinery: effect on cellulose, hemicellulose and lignin recovery, *Bioresource technology*, 142 (2013) 428-435.
- [15] Y. Liu, J. Zheng, J. Xiao, X. He, K. Zhang, S. Yuan, Z. Peng, Z. Chen, X. Lin, Enhanced Enzymatic Hydrolysis and Lignin Extraction of Wheat Straw by Triethylbenzyl Ammonium Chloride/Lactic Acid-Based Deep Eutectic Solvent Pretreatment, *ACS Omega*, 4 (2019) 19829-19839.
- [16] C. Crestini, F. Melone, M. Sette, R. Saladino, Milled wood lignin: a linear oligomer, *Biomacromolecules*, 12 (2011) 3928-3935.
- [17] M.P. Pandey, C.S. Kim, Lignin Depolymerization and Conversion: A Review of Thermochemical Methods, *Chemical Engineering & Technology*, 34 (2011) 29-41.
- [18] A. Tribot, G. Amer, M. Abdou Alio, H. de Baynast, C. Delattre, A. Pons, J.-D. Mathias, J.-M. Callois, C. Vial, P. Michaud, C.-G. Dussap, Wood-lignin: Supply, extraction processes and use as bio-based material, *European Polymer Journal*, 112 (2019) 228-240.
- [19] Y. Pu, S. Cao, A.J. Ragauskas, Application of quantitative ³¹P NMR in biomass lignin and biofuel precursors characterization, *Energy & Environmental Science*, 4 (2011) 3154-3166.
- [20] J.L. Espinoza-Acosta, P.I. Torres-Chávez, J.L. Olmedo-Martínez, A. Vega-Rios, S.

- Flores-Gallardo, E.A. Zaragoza-Contreras, Lignin in storage and renewable energy applications: A review, *Journal of energy chemistry*, 27 (2018) 1422-1438.
- [21] G.T. Beckham, C.W. Johnson, E.M. Karp, D. Salvachúa, D.R. Vardon, Opportunities and challenges in biological lignin valorization, *Current opinion in biotechnology*, 42 (2016) 40-53.
- [22] J. Zhu, C. Yan, X. Zhang, C. Yang, M. Jiang, X. Zhang, A sustainable platform of lignin: From bioresources to materials and their applications in rechargeable batteries and supercapacitors, *Progress in Energy and Combustion Science*, 76 (2020) 100788.
- [23] C. Li, X. Zhao, A. Wang, G.W. Huber, T. Zhang, Catalytic transformation of lignin for the production of chemicals and fuels, *Chemical reviews*, 115 (2015) 11559-11624.
- [24] A.U. Buranov, G. Mazza, Lignin in straw of herbaceous crops, *Industrial crops and products*, 28 (2008) 237-259.
- [25] P. Figueiredo, K. Lintinen, J.T. Hirvonen, M.A. Kostianen, H.A. Santos, Properties and chemical modifications of lignin: Towards lignin-based nanomaterials for biomedical applications, *Progress in Materials Science*, 93 (2018) 233-269.
- [26] M.V. Galkin, J.S. Samec, Lignin valorization through catalytic lignocellulose fractionation: a fundamental platform for the future biorefinery, *ChemSusChem*, 9 (2016) 1544-1558.
- [27] J. Zeng, G.L. Helms, X. Gao, S. Chen, Quantification of wheat straw lignin structure by comprehensive NMR analysis, *Journal of agricultural and food chemistry*, 61 (2013) 10848-10857.
- [28] H. Heikkinen, T. Elder, H. Maaheimo, S. Rovio, J. Rahikainen, K. Kruus, T. Tamminen, Impact of steam explosion on the wheat straw lignin structure studied by solution-state nuclear magnetic resonance and density functional methods, *Journal of agricultural and food chemistry*, 62 (2014) 10437-10444.
- [29] T. Auxenfans, D. Crônier, B. Chabbert, G. Paës, Understanding the structural and chemical changes of plant biomass following steam explosion pretreatment, *Biotechnology for biofuels*, 10 (2017) 1-16.
- [30] X. Zhang, J. Zhu, L. Sun, Q. Yuan, G. Cheng, D.S. Argyropoulos, Extraction and characterization of lignin from corncob residue after acid-catalyzed steam explosion pretreatment, *Industrial Crops and Products*, 133 (2019) 241-249.
- [31] K. Radotić, M. MIĆIĆ, M. Jeremić, New insights into the structural organization of the plant polymer lignin, *Annals of the New York academy of sciences*, 1048 (2005) 215-229.
- [32] F. Xiong, Y. Han, S. Wang, G. Li, T. Qin, Y. Chen, F. Chu, Preparation and formation mechanism of size-controlled lignin nanospheres by self-assembly, *Industrial crops and products*, 100 (2017) 146-152.
- [33] H. Liu, T. Xu, K. Liu, M. Zhang, W. Liu, H. Li, H. Du, C. Si, Lignin-based electrodes for energy storage application, *Industrial Crops and Products*, 165 (2021) 113425.
- [34] X. Chen, Z. Li, L. Zhang, H. Wang, C. Qiu, X. Fan, S. Sun, Preparation of a novel lignin-based film with high solid content and its physicochemical characteristics, *Industrial Crops and Products*, 164 (2021) 113396.
- [35] W. Zhao, L.-P. Xiao, G. Song, R.-C. Sun, L. He, S. Singh, B.A. Simmons, G. Cheng,

From lignin subunits to aggregates: insights into lignin solubilization, *Green Chemistry*, 19 (2017) 3272-3281.

[36] P. Mousavioun, W.O. Doherty, Chemical and thermal properties of fractionated bagasse soda lignin, *Industrial Crops and Products*, 31 (2010) 52-58.

[37] A.F. Ang, Z. Ashaari, S.H. Lee, P. Md Tahir, R. Halis, Lignin-based copolymer adhesives for composite wood panels – A review, *International Journal of Adhesion and Adhesives*, 95 (2019) 102408.

[38] J. Li, J. Zhang, S. Zhang, Q. Gao, J. Li, W. Zhang, Fast Curing Bio-Based Phenolic Resins via Lignin Demethylated under Mild Reaction Condition, *Polymers*, 9 (2017) 428.

[39] L. Akim, S. Shevchenko, M.Y. Zarubin, ¹³C NMR studies on lignins depolymerized with dry hydrogen iodide, *Wood science and technology*, 27 (1993) 241-248.

[40] H. Chung, N.R. Washburn, Improved lignin polyurethane properties with lewis acid treatment, *ACS applied materials & interfaces*, 4 (2012) 2840-2846.

[41] K. Sawamura, Y. Tobimatsu, H. Kamitakahara, T. Takano, Lignin Functionalization through Chemical Demethylation: Preparation and Tannin-Like Properties of Demethylated Guaiacyl-Type Synthetic Lignins, *ACS Sustainable Chemistry & Engineering*, 5 (2017) 5424-5431.

[42] J. Li, W. Wang, S. Zhang, Q. Gao, W. Zhang, J. Li, Preparation and characterization of lignin demethylated at atmospheric pressure and its application in fast curing biobased phenolic resins, *RSC Advances*, 6 (2016) 67435-67443.

[43] Y. Song, Z. Wang, N. Yan, R. Zhang, J. Li, Demethylation of Wheat Straw Alkali Lignin for Application in Phenol Formaldehyde Adhesives, *Polymers*, 8 (2016) 209.

[44] L. Zou, B.M. Ross, L.J. Hutchison, L.P. Christopher, R.F.H. Dekker, L. Malek, Fungal demethylation of Kraft lignin, *Enzyme and Microbial Technology*, 73-74 (2015) 44-50.

[45] R. Riley, A.A. Salamov, D.W. Brown, L.G. Nagy, D. Floudas, B.W. Held, A. Levasseur, V. Lombard, E. Morin, R. Otilar, E.A. Lindquist, H. Sun, K.M. LaButti, J. Schmutz, D. Jabbour, H. Luo, S.E. Baker, A.G. Pisabarro, J.D. Walton, R.A. Blanchette, B. Henrissat, F. Martin, D. Cullen, D.S. Hibbett, I.V. Grigoriev, Extensive sampling of basidiomycete genomes demonstrates inadequacy of the white-rot/brown-rot paradigm for wood decay fungi, *Proceedings of the National Academy of Sciences*, 111 (2014) 9923.

[46] Y. Liu, J. Wang, M.P. Wolcott, Multistep process to produce fermentable sugars and lignosulfonates from softwood enzymolysis residues, *ACS Sustainable Chemistry & Engineering*, 4 (2016) 7225-7230.

[47] G. Wang, H. Chen, Carbohydrate elimination of alkaline-extracted lignin liquor by steam explosion and its methylation for substitution of phenolic adhesive, *Industrial Crops and Products*, 53 (2014) 93-101.

[48] S. Feng, T. Shui, H. Wang, X. Ai, T. Kuboki, C.C. Xu, Properties of phenolic adhesives formulated with activated organosolv lignin derived from cornstalk, *Industrial Crops and Products*, 161 (2021) 113225.

[49] H. Paananen, L. Alvila, T.T. Pakkanen, Hydroxymethylation of softwood kraft

- lignin and phenol with paraformaldehyde, *Sustainable Chemistry and Pharmacy*, 20 (2021) 100376.
- [50] Y. Chen, H. Zhang, Z. Zhu, S. Fu, High-value utilization of hydroxymethylated lignin in polyurethane adhesives, *International Journal of Biological Macromolecules*, 152 (2020) 775-785.
- [51] S. Bertella, J.S. Luterbacher, Simultaneous extraction and controlled chemical functionalization of hardwood lignin for improved phenolation, *Green Chemistry*, 23 (2021) 3459-3467.
- [52] H. Younesi-Kordkheili, A. Pizzi, G. Niyatzade, Reduction of Formaldehyde Emission from Particleboard by Phenolated Kraft Lignin, *The Journal of Adhesion*, 92 (2015) 485-497.
- [53] X. Du, J. Li, M.E. Lindström, Modification of industrial softwood kraft lignin using Mannich reaction with and without phenolation pretreatment, *Industrial Crops and Products*, 52 (2014) 729-735.
- [54] J. Podschun, B. Saake, R. Lehnen, Reactivity enhancement of organosolv lignin by phenolation for improved bio-based thermosets, *European Polymer Journal*, 67 (2015) 1-11.
- [55] S. Yang, J.-L. Wen, T.-Q. Yuan, R.-C. Sun, Characterization and phenolation of biorefinery technical lignins for lignin–phenol–formaldehyde resin adhesive synthesis, *RSC Advance.*, 4 (2014) 57996-58004.
- [56] X. Jiang, J. Liu, X. Du, Z. Hu, H.-m. Chang, H. Jameel, Phenolation to Improve Lignin Reactivity toward Thermosets Application, *ACS Sustainable Chemistry & Engineering*, 6 (2018) 5504-5512.
- [57] C. Chio, M. Sain, W. Qin, Lignin utilization: A review of lignin depolymerization from various aspects, *Renewable and Sustainable Energy Reviews*, 107 (2019) 232-249.
- [58] O. Dahlman, A. Jacobs, A. Liljenberg, A.I. Olsson, Analysis of carbohydrates in wood and pulps employing enzymatic hydrolysis and subsequent capillary zone electrophoresis, *Journal of Chromatography A*, 891 (2000) 157-174.
- [59] A. Moubarik, N. Grimi, N. Boussetta, A. Pizzi, Isolation and characterization of lignin from Moroccan sugar cane bagasse: Production of lignin–phenol-formaldehyde wood adhesive, *Industrial Crops and Products*, 45 (2013) 296-302.
- [60] W. Zhang, Y. Ma, C. Wang, S. Li, M. Zhang, F. Chu, Preparation and properties of lignin–phenol–formaldehyde resins based on different biorefinery residues of agricultural biomass, *Industrial Crops and Products*, 43 (2013) 326-333.
- [61] A. Tejado, C. Pena, J. Labidi, J.M. Echeverria, I. Mondragon, Physico-chemical characterization of lignins from different sources for use in phenol-formaldehyde resin synthesis, *Bioresour Technol*, 98 (2007) 1655-1663.
- [62] S. Feng, T. Shui, H. Wang, X. Ai, T. Kuboki, C.C. Xu, Properties of phenolic adhesives formulated with activated organosolv lignin derived from cornstalk, *Industrial Crops and Products*, 161 (2021) 113225.
- [63] W. Yang, M. Rallini, M. Natali, J. Kenny, P. Ma, W. Dong, L. Torre, D. Puglia, Preparation and properties of adhesives based on phenolic resin containing lignin micro and nanoparticles: A comparative study, *Materials & Design*, 161 (2019) 55-63.

- [64] N.A. Aziz, A.F.A. Latip, L.C. Peng, N.H.A. Latif, N. Brosse, R. Hashim, M.H. Hussin, Reinforced lignin-phenol-glyoxal (LPG) wood adhesives from coconut husk, *International Journal of Biological Macromolecules*, 141 (2019) 185-196.
- [65] A. Moubarik, A. Pizzi, A. Allal, F. Charrier, B. Charrier, Cornstarch and tannin in phenol-formaldehyde resins for plywood production, *Industrial Crops and Products*, 30 (2009) 188-193.
- [66] H. Lei, A. Pizzi, G. Du, Environmentally friendly mixed tannin/lignin wood resins, *Journal of Applied Polymer Science*, 107 (2008) 203-209.
- [67] H.R. Mansouri, P. Navarrete, A. Pizzi, S. Tapin-Lingua, B. Benjelloun-Mlayah, H. Pasch, S. Rigolet, Synthetic-resin-free wood panel adhesives from mixed low molecular mass lignin and tannin, *European Journal of Wood and Wood Products*, 69 (2010) 221-229.
- [68] P. Navarrete, H.R. Mansouri, A. Pizzi, S. Tapin-Lingua, B. Benjelloun-Mlayah, H. Pasch, S. Rigolet, Wood Panel Adhesives from Low Molecular Mass Lignin and Tannin without Synthetic Resins, *Journal of Adhesion Science and Technology*, 24 (2010) 1597-1610.
- [69] P. Navarrete, A. Pizzi, H. Pasch, L. Delmotte, Study on Lignin-Glyoxal Reaction by MALDI-TOF and CP-MAS ¹³C-NMR, *Journal of Adhesion Science and Technology*, 26 (2012) 1069-1082.
- [70] Z. Xiao, Y. Li, X. Wu, G. Qi, N. Li, K. Zhang, D. Wang, X.S. Sun, Utilization of sorghum lignin to improve adhesion strength of soy protein adhesives on wood veneer, *Industrial Crops and Products*, 50 (2013) 501-509.
- [71] J. Luo, J. Luo, C. Yuan, W. Zhang, J. Li, Q. Gao, H. Chen, An eco-friendly wood adhesive from soy protein and lignin: performance properties, *RSC advances*, 5 (2015) 100849-100855.
- [72] J. Xin, P. Zhang, M.P. Wolcott, J. Zhang, W.C. Hiscox, X. Zhang, A Novel and Formaldehyde-Free Preparation Method for Lignin Amine and Its Enhancement for Soy Protein Adhesive, *Journal of Polymers and the Environment*, 25 (2016) 599-605.
- [73] S. Pradyawong, G. Qi, N. Li, X.S. Sun, D. Wang, Adhesion properties of soy protein adhesives enhanced by biomass lignin, *International Journal of Adhesion and Adhesives*, 75 (2017) 66-73.
- [74] X. Zhang, Y. Zhu, Y. Yu, J. Song, Improve Performance of Soy Flour-Based Adhesive with a Lignin-Based Resin, *Polymers* 9 (2017) 261.
- [75] X. Zhu, D. Wang, N. Li, X.S. Sun, Bio-Based Wood Adhesive from Camelina Protein (a Biodiesel Residue) and Depolymerized Lignin with Improved Water Resistance, *ACS Omega*, 2 (2017) 7996-8004.
- [76] S. Pradyawong, G. Qi, X.S. Sun, D. Wang, Laccase/TEMPO-modified lignin improved soy-protein-based adhesives: Adhesion performance and properties, *International Journal of Adhesion and Adhesives*, 91 (2019) 116-122.
- [77] X. Wu, S. Staggenborg, J.L. Propheter, W.L. Rooney, J. Yu, D. Wang, Features of sweet sorghum juice and their performance in ethanol fermentation, *Industrial Crops and Products*, 31 (2010) 164-170.
- [78] S.D. Desai, J.V. Patel, V.K. Sinha, Polyurethane adhesive system from biomaterial-based polyol for bonding wood, *International Journal of Adhesion and Adhesives*, 23

(2003) 393-399.

[79] D.G. Lay, P. Cranley, A. Pizzi, Polyurethane adhesives, in: Handbook of adhesive technology, CRC Press, 2017, pp. 321-348.

[80] F. Dodangeh, M.S. Dorraji, M. Rasoulifard, H. Ashjari, Synthesis and characterization of alkoxy silane modified polyurethane wood adhesive based on epoxidized soybean oil polyester polyol, *Composites Part B: Engineering*, 187 (2020) 107857.

[81] H. Li, S. Feng, Z. Yuan, Q. Wei, C.C. Xu, Highly efficient liquefaction of wheat straw for the production of bio-polyols and bio-based polyurethane foams, *Industrial crops and products*, 109 (2017) 426-433.

[82] A. Prociak, M. Kurańska, U. Cabulis, J. Ryszkowska, M. Leszczyńska, K. Uram, M. Kirpluks, Effect of bio-polyols with different chemical structures on foaming of polyurethane systems and foam properties, *Industrial Crops and Products*, 120 (2018) 262-270.

[83] O. Oribayo, X. Feng, G.L. Rempel, Q. Pan, Synthesis of lignin-based polyurethane/graphene oxide foam and its application as an absorbent for oil spill clean-ups and recovery, *Chemical Engineering Journal*, 323 (2017) 191-202.

[84] A.N. Hayati, D.A.C. Evans, B. Laycock, D.J. Martin, P.K. Annamalai, A simple methodology for improving the performance and sustainability of rigid polyurethane foam by incorporating industrial lignin, *Industrial Crops and Products*, 117 (2018) 149-158.

[85] X. Chen, Z. Li, L. Zhang, H. Wang, C. Qiu, X. Fan, S. Sun, Preparation of a novel lignin-based film with high solid content and its physicochemical characteristics, *Industrial Crops and Products*, 164 (2021) 113396.

[86] R.V. Gadhave, P. S. Kasbe, P.A. Mahanwar, P.T. Gadekar, Synthesis and characterization of lignin-polyurethane based wood adhesive, *International Journal of Adhesion and Adhesives*, 95 (2019) 102427.

[87] H. Chen, S.S. Nair, P. Chauhan, N. Yan, Lignin containing cellulose nanofibril application in pMDI wood adhesives for drastically improved gap-filling properties with robust bondline interfaces, *Chemical Engineering Journal*, 360 (2019) 393-401.

[88] W.G. Glasser, V.P. Saraf, W.H. Newman, Hydroxy Propylated Lignin-Isocyanate Combinations as Bonding Agents for Wood and Cellulosic Fibers, *The Journal of Adhesion*, 14 (2006) 233-255.

[89] A.M. Nacas, N.M. Ito, R.R.D. Sousa, M.A. Spinacé, D.J. Dos Santos, Effects of NCO:OH ratio on the mechanical properties and chemical structure of Kraft lignin-based polyurethane adhesive, *The Journal of Adhesion*, 93 (2016) 18-29.

[90] J. Saražin, A. Pizzi, S. Amirou, D. Schmiedl, M. Šernek, Organosolv Lignin for Non-Isocyanate Based Polyurethanes (NIPU) as Wood Adhesive, *Journal of Renewable Materials*, 9 (2021) 881-907.

[91] X. Xi, Z. Wu, A. Pizzi, C. Gerardin, H. Lei, B. Zhang, G. Du, Non-isocyanate polyurethane adhesive from sucrose used for particleboard, *Wood Science and Technology*, 53 (2019) 393-405.

[92] X. Chen, A. Pizzi, H. Essawy, E. Fredon, C. Gerardin, N. Guigo, N. Sbirrazzuoli, Non-Furanic Humins-Based Non-Isocyanate Polyurethane (NIPU) Thermoset Wood

- Adhesives, *Polymers*, 13 (2021) 372.
- [93] X. Xi, A. Pizzi, C. Gerardin, H. Lei, X. Chen, S. Amirou, Preparation and evaluation of glucose based non-isocyanate polyurethane self-blowing rigid foams, *Polymers*, 11 (2019) 1802.
- [94] X. Chen, A. Pizzi, X. Xi, X. Zhou, E. Fredon, C. Gerardin, Soy Protein Isolate Non-Isocyanates Polyurethanes (NIPU) Wood Adhesives, *Journal of Renewable Materials*, 9 (2021) 1045-1057.
- [95] Y. Shirmohammadli, D. Efhamisisi, A. Pizzi, Tannins as a sustainable raw material for green chemistry: A review, *Industrial Crops and Products*, 126 (2018) 316-332.
- [96] M. Thébault, A. Pizzi, H.A. Essawy, A. Barhoum, G. Van Assche, Isocyanate free condensed tannin-based polyurethanes, *European Polymer Journal*, 67 (2015) 513-526.
- [97] M. Thébault, A. Pizzi, S. Dumarçay, P. Gerardin, E. Fredon, L. Delmotte, Polyurethanes from hydrolysable tannins obtained without using isocyanates, *Industrial Crops and Products*, 59 (2014) 329-336.
- [98] Y. Liu, K. Li, Preparation and Characterization of Demethylated Lignin-Polyethylenimine Adhesives, *The Journal of Adhesion*, 82 (2006) 593-605.
- [99] P. Dongre, M. Driscoll, T. Amidon, B. Bujanovic, Lignin-Furfural Based Adhesives, *Energies*, 8 (2015) 7897-7914.
- [100] N. Guigo, A. Mija, L. Vincent, N. Sbirrazzuoli, Eco-friendly composite resins based on renewable biomass resources: Polyfurfuryl alcohol/lignin thermosets, *European Polymer Journal*, 46 (2010) 1016-1023.
- [101] Garro, J. M., M. Fechtal, and B. Riedl. Gallic acid as a model of tannins in condensation with formaldehyde. *Thermochimica acta*, 274 (1996) 149-163.
- [102] S. Spina, X. Zhou, C. Segovia, A. Pizzi, M. Romagnoli, S. Giovando, H. Pasch, K. Rode, L. Delmotte, Phenolic resin adhesives based on chestnut (*Castanea sativa*) hydrolysable tannins, *Journal of Adhesion Science and Technology*, 27 (2013) 2103-2111.
- [103] Pizzi, A. Pine tannin adhesives for particleboard. *Holz als Roh-und Werkstoff* 40 (1982) 293-301.
- [104] H.A.M. Bacelo, S.C.R. Santos, C.M.S. Botelho, Tannin-based biosorbents for environmental applications – A review, *Chemical Engineering Journal*, 303 (2016) 575-587.
- [105] A. Pizzi, Tannin-Based Biofoams-a Review, *Journal of Renewable Materials*, 7 (2019) 477-492.
- [106] A. Arbenz, L. Avérous, Chemical modification of tannins to elaborate aromatic biobased macromolecular architectures, *Green Chemistry*, 17 (2015) 2626-2646.
- [107] L. Guo, T. Qiang, Y. Ma, K. Wang, K. Du, Optimisation of tannin extraction from *Coriaria nepalensis* bark as a renewable resource for use in tanning, *Industrial Crops and Products*, 149 (2020) 112360.
- [108] E. da Silva Araujo, M.S. Lorenço, U.L. Zidanes, T.B. Sousa, G. da Silva Mota, V. de Nazaré de Oliveira Reis, M. Gomes da Silva, F.A. Mori, Quantification of the bark *Myrcia eximia* DC tannins from the Amazon rainforest and its application in the formulation of natural adhesives for wood, *Journal of Cleaner Production*, 280 (2021) 124324.

- [109] B. Ndiwe, A. Pizzi, B. Tibi, R. Danwe, N. Konai, S. Amirou, African tree bark exudate extracts as biohardeners of fully biosourced thermoset tannin adhesives for wood panels, *Industrial crops and products*, 132 (2019) 253-268.
- [110] A. Chowdhury, S. Sarkar, A. Chowdhury, S. Bardhan, P. Mandal, M. Chowdhury, Tea waste management: a case study from West Bengal, India, *Indian Journal of Science and Technology*, 9 (2016) 1-6.
- [111] B. Janissen, T. Huynh, Chemical composition and value-adding applications of coffee industry by-products: A review, *Resources, Conservation and Recycling*, 128 (2018) 110-117.
- [112] J.H. Low, W.A.W.A. Rahman, J. Jamaluddin, The influence of extraction parameters on spent coffee grounds as a renewable tannin resource, *Journal of Cleaner Production*, 101 (2015) 222-228.
- [113] L. Ping, N. Brosse, L. Chrusciel, P. Navarrete, A. Pizzi, Extraction of condensed tannins from grape pomace for use as wood adhesives, *Industrial Crops and Products*, 33 (2011) 253-257.
- [114] L. Ping, A. Pizzi, Z.D. Guo, N. Brosse, Condensed tannins extraction from grape pomace: Characterization and utilization as wood adhesives for wood particleboard, *Industrial Crops and Products*, 34 (2011) 907-914.
- [115] A. Ricci, G.P. Parpinello, A.S. Palma, N. Teslić, C. Brillì, A. Pizzi, A. Versari, Analytical profiling of food-grade extracts from grape (*Vitis vinifera* sp.) seeds and skins, green tea (*Camellia sinensis*) leaves and Limousin oak (*Quercus robur*) heartwood using MALDI-TOF-MS, ICP-MS and spectrophotometric methods, *Journal of Food Composition and Analysis*, 59 (2017) 95-104.
- [116] P. Widsten, C.D. Cruz, G.C. Fletcher, M.A. Pajak, T.K. McGhie, Tannins and extracts of fruit byproducts: antibacterial activity against foodborne bacteria and antioxidant capacity, *Journal of agricultural and food chemistry*, 62 (2014) 11146-11156.
- [117] M. Fraga-Corral, P. Garcia-Oliveira, A.G. Pereira, C. Lourenco-Lopes, C. Jimenez-Lopez, M.A. Prieto, J. Simal-Gandara, Technological Application of Tannin-Based Extracts, *Molecules*, 25 (2020) 614.
- [118] P.L. de Hoyos-Martínez, J. Merle, J. Labidi, F. Charrier – El Bouhtoury, Tannins extraction: A key point for their valorization and cleaner production, *Journal of Cleaner Production*, 206 (2019) 1138-1155.
- [119] G. Vázquez, J. González-Alvarez, S. Freire, F. López-Suevos, G. Antorrena, Characteristics of *Pinus pinaster* bark extracts obtained under various extraction conditions, *Holz als Roh-und werkstoff*, 59 (2001) 451-456.
- [120] S. Bianchi, I. Krosiakova, R. Janzon, I. Mayer, B. Saake, F. Pichelin, Characterization of condensed tannins and carbohydrates in hot water bark extracts of European softwood species, *Phytochemistry*, 120 (2015) 53-61.
- [121] A. Pizzi, *Advanced wood adhesives technology*, CRC Press, 1994.
- [122] V. Sealy-Fisher, A. Pizzi, Increased pine tannins extraction and wood adhesives development by phlobaphenes minimization, *Holz als Roh-und Werkstoff*, 50 (1992) 212-220.
- [123] G. Vázquez, G. Antorrena, J. González, J. Alvarez, Tannin-based adhesives for bonding high-moisture *Eucalyptus* veneers: Influence of tannin extraction and press

- conditions, *Holz als Roh-und Werkstoff*, 54 (1996) 93.
- [124] S. Ben Mahmoud, H. Saad, B. Charrier, A. Pizzi, K. Rode, N. Ayed, F. Charrier-El Bouhtoury, Characterization of sumac (*Rhus tripartitum*) root barks tannin for a potential use in wood adhesives formulation, *Wood Science and Technology*, 49 (2014) 205-221.
- [125] D.E. García, W.G. Glasser, A. Pizzi, S.P. Paczkowski, M.-P. Laborie, Modification of condensed tannins: from polyphenol chemistry to materials engineering, *New Journal of Chemistry*, 40 (2016) 36-49.
- [126] A. Pizzi, Condensed tannins for adhesives, *Industrial & Engineering Chemistry Product Research and Development*, 21 (1982) 359-369.
- [127] N. Meikleham, A. Pizzi, A. Stephanou, Induced accelerated autocondensation of polyflavonoid tannins for phenolic polycondensates. I. ¹³C-NMR, ²⁹Si-NMR, X-ray, and polarimetry studies and mechanism, *Journal of Applied Polymer Science*, 54 (1994) 1827-1845.
- [128] C. Lacoste, M.C. Basso, A. Pizzi, M.P. Laborie, A. Celzard, V. Fierro, Pine tannin-based rigid foams: Mechanical and thermal properties, *Industrial Crops and Products*, 43 (2013) 245-250.
- [129] A. Pizzi, K.L. Mittal, *Handbook of adhesive technology*, CRC press, 2017.
- [130] S. Quideau, D. Deffieux, C. Douat-Casassus, L. Pouysegou, Plant polyphenols: chemical properties, biological activities, and synthesis, *Angew Chem Int Ed Engl*, 50 (2011) 586-621.
- [131] H.-F. Gu, C.-M. Li, Y.-j. Xu, W.-f. Hu, M.-h. Chen, Q.-h. Wan, Structural features and antioxidant activity of tannin from persimmon pulp, *Food Research International*, 41 (2008) 208-217.
- [132] M.I. Arina, Y. Harisun, Effect of extraction temperatures on tannin content and antioxidant activity of *Quercus infectoria* (Manjakani), *Biocatalysis and Agricultural Biotechnology*, 19 (2019) 101104.
- [133] Y. Ji, Q. Xu, L. Jin, Y. Fu, Cellulosic paper with high antioxidative and barrier properties obtained through incorporation of tannin into kraft pulp fibers, *Int J Biol Macromol*, 162 (2020) 678-684.
- [134] X. Chen, J. Li, X. Xi, A. Pizzi, X. Zhou, E. Fredon, G. Du, C. Gerardin, Condensed tannin-glucose-based NIPU bio-foams of improved fire retardancy, *Polymer Degradation and Stability*, 175 (2020) 109121.
- [135] T.-T. Yang, J.-P. Guan, R.-C. Tang, G. Chen, Condensed tannin from *Dioscorea cirrhosa* tuber as an eco-friendly and durable flame retardant for silk textile, *Industrial Crops and Products*, 115 (2018) 16-25.
- [136] P. Pisitsak, J. Hutakamol, R. Thongcharoen, P. Phokaew, K. Kanjanawan, N. Sakseng, Improving the dyeability of cotton with tannin-rich natural dye through pretreatment with whey protein isolate, *Industrial Crops and Products*, 79 (2016) 47-56.
- [137] C. Liu, Y. Zhang, X. Li, J. Luo, Q. Gao, J. Li, "Green" bio-thermoset resins derived from soy protein isolate and condensed tannins, *Industrial Crops and Products*, 108 (2017) 363-370.
- [138] Y. Shang, G. Zhu, D. Yan, Q. Liu, T. Gao, G. Zhou, Tannin cross-linked polyethyleneimine for highly efficient removal of hexavalent chromium, *Journal of the*

- Taiwan Institute of Chemical Engineers, 119 (2021) 52-59.
- [139] K. Li, X. Geng, J. Simonsen, J. Karchesy, Novel wood adhesives from condensed tannins and polyethylenimine, *International Journal of Adhesion and Adhesives*, 24 (2004) 327-333.
- [140] J. Li, W. Zhu, S. Zhang, Q. Gao, C. Xia, W. Zhang, J. Li, Depolymerization and characterization of Acacia mangium tannin for the preparation of mussel-inspired fast-curing tannin-based phenolic resins, *Chemical Engineering Journal*, 370 (2019) 420-431.
- [141] C. Lacoste, M.C. Basso, A. Pizzi, A. Celzard, M.P. Laborie, Natural albumin/tannin cellular foams, *Industrial Crops and Products*, 73 (2015) 41-48.
- [142] S. Ghahri, B. Mohebbi, A. Pizzi, A. Mirshokraie, H.R. Mansouri, Improving Water Resistance of Soy-Based Adhesive by Vegetable Tannin, *Journal of Polymers and the Environment*, 26 (2017) 1881-1890.
- [143] S. Ghahri, X. Chen, A. Pizzi, R. Hajihassani, A.N. Papadopoulos, Natural Tannins as New Cross-Linking Materials for Soy-Based Adhesives, *Polymers*, 13 (2021) 595.
- [144] A. Pizzi, Hardening mechanism of tannin adhesives with hexamine, *Holz als Roh und Werkstoff*, (1994).
- [145] Pichelin, F., C. Kamoun, and A. Pizzi. "Hexamine hardener behaviour: effects on wood glueing, tannin and other wood adhesives." *Holz als Roh-und Werkstoff*, 57 (1999) 305-317.
- [146] C. Kamoun, A. Pizzi, Mechanism of hexamine as a non-aldehyde polycondensation resins hardener. Part 1: Hexamine decomposition and reactive intermediates, *Holzforschung und Holzverwertung*, 52 (2000) 16-19.
- [147] C. Kamoun, A. Pizzi, Mechanism of hexamine as a non-aldehyde polycondensation hardener. Part 2: Recomposition of intermediate reactive compounds, *Holzforschung und Holzverwertung*, 52 (2000) 66-67.
- [148] A. Pizzi, Recent developments in eco-efficient bio-based adhesives for wood bonding: opportunities and issues, *Journal of Adhesion Science and Technology*, 20 (2006) 829-846.
- [149] J. Zhang, X. Xi, J. Liang, A. Pizzi, G. Du, S. Deng, Tannin-based adhesive cross-linked by furfuryl alcohol-glyoxal and epoxy resins, *International Journal of Adhesion and Adhesives*, 94 (2019) 47-52.
- [150] X. Chen, J. Li, A. Pizzi, E. Fredon, C. Gerardin, X. Zhou, G. Du, Tannin-furanic foams modified by soybean protein isolate (SPI) and industrial lignin substituting formaldehyde addition, *Industrial Crops and Products*, 168 (2021) 113607.
- [151] J. Li, J. Liao, H. Essawy, J. Zhang, T. Li, Z. Wu, G. Du, X. Zhou, Preparation and characterization of novel cellular/nonporous foam structures derived from tannin furanic resin, *Industrial Crops and Products*, 162 (2021) 113264.
- [152] X. Zhou, B. Li, Y. Xu, H. Essawy, Z. Wu, G. Du, Tannin-furanic resin foam reinforced with cellulose nanofibers (CNF), *Industrial Crops and Products*, 134 (2019) 107-112.
- [153] A. Nicollin, X. Li, P. Girods, A. Pizzi, Y. Rogaume, Fast Pressing Composite Using Tannin-Furfuryl Alcohol Resin and Vegetal Fibers Reinforcement, *Journal of Renewable Materials*, 1 (2013) 311-316.

- [154] U.H.B. Abdullah, A. Pizzi, Tannin-furfuryl alcohol wood panel adhesives without formaldehyde, *European Journal of Wood and Wood Products*, 71 (2012) 131-132.
- [155] M. Basso, S. Giovando, A. Pizzi, M.-C. Lagel, A. Celzard, Alkaline tannin rigid foams, *Journal of Renewable Materials*, 2 (2014) 182-185.
- [156] S. Ghahri, B. Mohebby, A. Pizzi, A. Mirshokraie, H.R. Mansouri, Improving water resistance of soy-based adhesive by vegetable tannin, *Journal of Polymers and the Environment*, 26 (2018) 1881-1890.
- [157] S. Ghahri, X. Chen, A. Pizzi, R. Hajihassani, A.N. Papadopoulos, Natural tannins as new cross-linking materials for soy-based adhesives, *Polymers*, 13 (2021) 595.
- [158] W. Grigsby, J. Bridson, C. Lomas, J.-A. Elliot, Esterification of Condensed Tannins and Their Impact on the Properties of Poly(Lactic Acid), *Polymers*, 5 (2013) 344-360.
- [159] J. Liao, N. Brosse, A. Pizzi, S. Hoppe, X. Zhou, G. Du, Characterization and 3D printability of poly (lactic acid)/acetylated tannin composites, *Industrial Crops and Products*, 149 (2020) 112320.
- [160] J. Liao, N. Brosse, S. Hoppe, X. Zhou, X. Xi, G. Du, A. Pizzi, Interfacial improvement of poly (lactic acid)/tannin acetate composites via radical initiated polymerization, *Industrial Crops and Products*, 159 (2021) 113068.
- [161] F. Braghiroli, V. Fierro, A. Pizzi, K. Rode, W. Radke, L. Delmotte, J. Parmentier, A. Celzard, Reaction of condensed tannins with ammonia, *Industrial Crops and Products*, 44 (2013) 330-335.
- [162] J. Luo, X. Li, H. Zhang, Q. Gao, J. Li, Properties of a soybean meal-based plywood adhesive modified by a commercial epoxy resin, *International Journal of Adhesion and Adhesives*, 71 (2016) 99-104.
- [163] Z. Wang, Y. Chen, S. Chen, F. Chu, R. Zhang, Y. Wang, D. Fan, Preparation and characterization of a soy protein based bio-adhesive crosslinked by waterborne epoxy resin and polyacrylamide, *RSC advances*, 9 (2019) 35273-35279.
- [164] Z.-h. Gao, Y.-h. Zhang, B. Fang, L.-p. Zhang, J. Shi, The effects of thermal-acid treatment and crosslinking on the water resistance of soybean protein, *Industrial Crops and Products*, 74 (2015) 122-131.
- [165] X. Hao, D.-B. Fan, Preparation and characterization of epoxy-crosslinked soy protein adhesive, *Journal of Adhesion Science and Technology*, 32 (2018) 2682-2692.
- [166] H. Lei, G. Du, Z. Wu, X. Xi, Z. Dong, Cross-linked soy-based wood adhesives for plywood, *International journal of adhesion and adhesives*, 50 (2014) 199-203.
- [167] R.J. Li, J. Gutierrez, Y.-L. Chung, C.W. Frank, S.L. Billington, E.S. Sattely, A lignin-epoxy resin derived from biomass as an alternative to formaldehyde-based wood adhesives, *Green chemistry*, 20 (2018) 1459-1466.
- [168] X. Chen, A. Pizzi, E. Fredon, C. Gerardin, J. Li, X. Zhou, G. Du, Preparation and properties of a novel type of tannin-based wood adhesive, *The Journal of Adhesion*, (2020) 1-18.
- [169] S. Jahanshahi, A. Pizzi, A. Abdulkhani, K. Doosthoseini, A. Shakeri, M.C. Lagel, L. Delmotte, MALDI-TOF, ¹³C NMR and FT-MIR analysis and strength characterization of glycidyl ether tannin epoxy resins, *Industrial Crops and Products*, 83 (2016) 177-185.

- [170] J. Luo, Y. Zhou, Q. Gao, J. Li, N. Yan, From Wastes to Functions: A New Soybean Meal and Bark-Based Adhesive, *ACS Sustainable Chemistry & Engineering*, 8 (2020) 10767-10773.
- [171] N. Khundamri, C. Aouf, H. Fulcrand, E. Dubreucq, V. Tanrattanakul, Bio-based flexible epoxy foam synthesized from epoxidized soybean oil and epoxidized mangosteen tannin, *Industrial Crops and Products*, 128 (2019) 556-565.
- [172] A. Pizzi, D. Roux, The chemistry and development of tannin-based weather- and boil-proof cold-setting and fast-setting adhesives for wood, *Journal of Applied Polymer Science*, 22 (1978) 1945-1954.
- [173] A. Pizzi, H. Scharfetter, The chemistry and development of tannin-based adhesives for exterior plywood, *Journal of applied polymer science*, 22 (1978) 1745-1761.
- [174] A. Pizzi, The chemistry and development of tannin/urea-formaldehyde condensates for exterior wood adhesives, *Journal of Applied polymer science*, 23 (1979) 2777-2792.
- [175] A. Pizzi, Tannin-based adhesives: new theoretical aspects, *International Journal of Adhesion and Adhesives*, 1 (1980) 13-16.
- [176] A. Pizzi, F. Cameron, A new hardener for tannin adhesives for exterior particleboards, *Holz als Roh- und Werkstoff*, 39 (1981) 255-259.
- [177] A. Pizzi, M. Merlin, A new class of tannin adhesives for exterior particleboard, *International journal of adhesion and adhesives*, 1 (1981) 261-264.
- [178] Vázquez, G., et al. Tannin-based adhesives for bonding high-moisture Eucalyptus veneers: Influence of tannin extraction and press conditions. *Holz als Roh- und Werkstoff*, 54 (1996) 93.
- [179] A. Pizzi, A universal formulation for tannin adhesives for exterior particleboard, *Journal of Macromolecular Science—Chemistry*, 16 (1981) 1243-1250.
- [180] A. Pizzi, Pine tannin adhesives for particleboard, *Holz als Roh- und Werkstoff*, 40 (1982) 293-301.
- [181] X. Zhou, A. Pizzi, Pine tannin based adhesive mixes for plywood, *International Wood Products Journal*, 5 (2014) 27-32.
- [182] A. Pizzi, Phenolic and tannin-based adhesive resins by reactions of coordinated metal ligands. I. Phenolic chelates, *Journal of Applied Polymer Science*, 24 (1979) 1247-1255.
- [183] A. Pizzi, Phenolic and tannin-based adhesive resins by reactions of coordinated metal ligands. II. Tannin adhesive preparation, characteristics, and application, *Journal of applied polymer science*, 24 (1979) 1257-1268.
- [184] S. Wang, A. Pizzi, Dependence of tannin/hexamine particleboard performance from pressing conditions, *Holz als Roh- und Werkstoff*, 55 (1997).
- [185] A. Pizzi, P. Stracke, A. Trosa, Industrial tannin/hexamine low-emission exterior particleboards, *Holz als Roh- und Werkstoff*, 55 (1997).
- [186] F. Pichelin, C. Kamoun, A. Pizzi, Hexamine hardener behaviour: effects on wood glueing, tannin and other wood adhesives, *Holz als Roh- und Werkstoff*, 57 (1999) 305-317.
- [187] A. Ballerini, A. Despres, A. Pizzi, Non-toxic, zero emission tannin-glyoxal

- adhesives for wood panels, *Holz als Roh-und Werkstoff*, 63 (2005) 477-478.
- [188] P. Navarrete, A. Pizzi, H. Pasch, K. Rode, L. Delmotte, Characterization of two maritime pine tannins as wood adhesives, *Journal of adhesion science and technology*, 27 (2013) 2462-2479.
- [189] H. Mansouri, P. Navarrete, A. Pizzi, S. Tapin-Lingua, B. Benjelloun-Mlayah, H. Pasch, S. Rigolet, Synthetic-resin-free wood panel adhesives from mixed low molecular mass lignin and tannin, *European Journal of Wood and Wood Products*, 69 (2011) 221-229.
- [190] P. Navarrete, A. Pizzi, S. Tapin-Lingua, B. Benjelloun-Mlayah, H. Pasch, K. Rode, L. Delmotte, S. Rigolet, Low formaldehyde emitting biobased wood adhesives manufactured from mixtures of tannin and glyoxylated lignin, *Journal of Adhesion Science and Technology*, 26 (2012) 1667-1684.
- [191] C. Lacoste, M.C. Basso, A. Pizzi, M.-P. Laborie, D. Garcia, A. Celzard, Bioresourced pine tannin/furanic foams with glyoxal and glutaraldehyde, *Industrial Crops and Products*, 45 (2013) 401-405.
- [192] H. Younesi-Kordkheili, Improving physical and mechanical properties of new lignin-urea-glyoxal resin by nanoclay, *European Journal of Wood and Wood Products*, 75 (2017) 885-891.
- [193] H. Younesi-Kordkheili, S. Kazemi Najafi, R. Behrooz, Influence of nanoclay on urea-glyoxalated lignin-formaldehyde resins for wood adhesive, *The Journal of Adhesion*, 93 (2017) 431-443.
- [194] H. Younesi-Kordkheili, S. Kazemi-Najafi, R.B. Eshkiki, A. Pizzi, Improving urea formaldehyde resin properties by glyoxalated soda bagasse lignin, *European Journal of Wood and Wood Products*, 73 (2015) 77-85.
- [195] S. Sun, Z. Zhao, Influence of acid on the curing process of tannin-sucrose adhesives, *BioResources*, 13 (2018) 7683-7697.
- [196] Z. Zhao, K. Umemura, Investigation of a new natural particleboard adhesive composed of tannin and sucrose, *Journal of Wood Science*, 60 (2014) 269-277.
- [197] Z. Zhao, K. Umemura, Investigation of a new natural particleboard adhesive composed of tannin and sucrose. 2. Effect of pressing temperature and time on board properties, and characterization of adhesive, *Bioresources*, 10 (2015) 2444-2460.
- [198] Z. Zhao, Y. Miao, Z. Yang, H. Wang, R. Sang, Y. Fu, C. Huang, Z. Wu, M. Zhang, S. Sun, Effects of sulfuric acid on the curing behavior and bonding performance of tannin-sucrose adhesive, *Polymers*, 10 (2018) 651.
- [199] P. Nordqvist, F. Khabbaz, E. Malmström, Comparing bond strength and water resistance of alkali-modified soy protein isolate and wheat gluten adhesives, *International Journal of Adhesion and Adhesives*, 30 (2010) 72-79.
- [200] C. Yuan, M. Chen, J. Luo, X. Li, Q. Gao, J. Li, A novel water-based process produces eco-friendly bio-adhesive made from green cross-linked soybean soluble polysaccharide and soy protein, *Carbohydr Polym*, 169 (2017) 417-425.
- [201] B. Zhang, B. Fan, P. Huo, Z.-H. Gao, Improvement of the water resistance of soybean protein-based wood adhesive by a thermo-chemical treatment approach, *International Journal of Adhesion and Adhesives*, 78 (2017) 222-226.
- [202] Y. Zhang, M. Zhang, M. Chen, J. Luo, X. Li, Q. Gao, J. Li, Preparation and

characterization of a soy protein-based high-performance adhesive with a hyperbranched cross-linked structure, *Chemical Engineering Journal*, 354 (2018) 1032-1041.

[203] S. Zhao, Z. Wang, Z. Li, L. Li, J. Li, S. Zhang, Core-Shell Nanohybrid Elastomer Based on Co-Deposition Strategy to Improve Performance of Soy Protein Adhesive, *ACS Appl Mater Interfaces*, 11 (2019) 32414-32422.

[204] W. Gu, F. Li, X. Liu, Q. Gao, S. Gong, J. Li, S.Q. Shi, Borate chemistry inspired by cell walls converts soy protein into high-strength, antibacterial, flame-retardant adhesive, *Green Chemistry*, 22 (2020) 1319-1328.

[205] C. Xu, Y. Xu, M. Chen, Y. Zhang, J. Li, Q. Gao, S.Q. Shi, Soy protein adhesive with bio-based epoxidized daidzein for high strength and mildew resistance, *Chemical Engineering Journal*, 390 (2020) 124622.

[206] Y. Xu, Y. Han, S.Q. Shi, Q. Gao, J. Li, Preparation of a moderate viscosity, high performance and adequately-stabilized soy protein-based adhesive via recombination of protein molecules, *Journal of Cleaner Production*, 255 (2020) 120303.

[207] H. Ye, D. Pan, Z. Tian, Y. Zhang, Z. Yu, J. Mu, Preparation and properties of geopolymer/soy protein isolate composites by in situ organic-inorganic hybridization: A potential green binder for the wood industry, *Journal of Cleaner Production*, 276 (2020) 123363.

[208] E. Averina, J. Konnerth, S. D'Amico, H.W.G. van Herwijnen, Protein adhesives: Alkaline hydrolysis of different crop proteins as modification for improved wood bonding performance, *Industrial Crops and Products*, 161 (2021) 113187.

[209] Y. Xu, Y. Han, M. Chen, J. Luo, S.Q. Shi, J. Li, Q. Gao, Constructing a triple network structure to prepare strong, tough, and mildew resistant soy protein adhesive, *Composites Part B: Engineering*, 211 (2021) 108677.

[210] Y. Zeng, P. Xu, W. Yang, H. Chu, W. Wang, W. Dong, M. Chen, H. Bai, P. Ma, Soy protein-based adhesive with superior bonding strength and water resistance by designing densely crosslinking networks, *European Polymer Journal*, 142 (2021) 110128.

[211] Lagel, Marie-Christine, Antonio Pizzi, and Andreas Redl. Phenol-wheat protein-formaldehyde adhesives for wood-based panels. *PRO LIGNO-Open Access Scientific Journal in the Field of Wood Engineering*, 10 (2014) 3-17.

[212] H. Lei, A. Pizzi, P. Navarrete, S. Rigolet, A. Redl, A. Wagner, Gluten Protein Adhesives for Wood Panels, *Journal of Adhesion Science and Technology*, 24 (2010) 1583-1596.

[213] P. Nordqvist, M. Lawther, E. Malmström, F. Khabbaz, Adhesive properties of wheat gluten after enzymatic hydrolysis or heat treatment – A comparative study, *Industrial Crops and Products*, 38 (2012) 139-145.

[214] P. Nordqvist, D. Thedjil, S. Khosravi, M. Lawther, E. Malmström, F. Khabbaz, Wheat gluten fractions as wood adhesives-glutenins versus gliadins, *Journal of Applied Polymer Science*, 123 (2012) 1530-1538.

[215] S. Amirou, A. Pizzi, X. Xi, Wheat protein hydrolysates-resorcinol-aldehydes as potential cold setting adhesives, *European Journal of Wood and Wood Products*, 77 (2019) 453-463.

- [216] X. Xi, A. Pizzi, C. Gerardin, J. Liao, S. Amirou, S. Abdalla, Glutaraldehyde-wheat gluten protein adhesives for wood bonding, *The Journal of Adhesion*, 97 (2019) 88-100.
- [217] H.N. Cheng, K. Kilgore, C. Ford, C. Fortier, M.K. Dowd, Z. He, Cottonseed protein-based wood adhesive reinforced with nanocellulose, *Journal of Adhesion Science and Technology*, 33 (2019) 1357-1368.
- [218] Z. He, D.C. Chapital, H.N. Cheng, K. Thomas Klasson, O.M. Olanya, J. Uknalis, Application of tung oil to improve adhesion strength and water resistance of cottonseed meal and protein adhesives on maple veneer, *Industrial Crops and Products*, 61 (2014) 398-402.
- [219] H.N. Cheng, C. Ford, M.K. Dowd, Z. He, Use of additives to enhance the properties of cottonseed protein as wood adhesives, *International Journal of Adhesion and Adhesives*, 68 (2016) 156-160.
- [220] S. Pradyawong, J. Li, Z. He, X.S. Sun, D. Wang, H.N. Cheng, K.T. Klasson, Blending cottonseed meal products with different protein contents for cost-effective wood adhesive performances, *Industrial Crops and Products*, 126 (2018) 31-37.
- [221] J. Li, S. Pradyawong, Z. He, X.S. Sun, D. Wang, H.N. Cheng, J. Zhong, Assessment and application of phosphorus/calcium-cottonseed protein adhesive for plywood production, *Journal of Cleaner Production*, 229 (2019) 454-462.
- [222] N. Bandara, J. Wu, Chemically Modified Canola Protein–Nanomaterial Hybrid Adhesive Shows Improved Adhesion and Water Resistance, *ACS Sustainable Chemistry & Engineering*, 6 (2017) 1152-1161.
- [223] B. Zhang, X. Xi, Z. Wu, L. Hong, L. Li, M. Tian, An Eco-Friendly Wood Adhesive from Alfalfa Leaf Protein, *Journal of Renewable Materials*, 8 (2020) 1429.
- [224] J. Li, X. Li, J. Li, Q. Gao, Investigating the use of peanut meal: a potential new resource for wood adhesives, *RSC Advances*, 5 (2015) 80136-80141.
- [225] N. Bandara, J. Wu, Randomly Oriented Strand Board Composites from Nanoengineered Protein-Based Wood Adhesive, *ACS Sustainable Chemistry & Engineering*, 6 (2017) 457-466.
- [226] R. Breyer, J. Rivers, K. Shoemake, J. Thompson, W. Liles, Wood composites bonded with protein-modified urea-formaldehyde resin adhesive, in, *Google Patents*, 2005.
- [227] C.R. Frihart, J.M. Wescott, Improved water resistance of bio-based adhesives for wood bonding, in: *Proceedings of ICECFOP1-1st International Conference on Environmentally-Compatible Forest Products: Fernando Pessoa University, Oporto, Portugal, 22-24 September 2004. Porto, Portugal: Edicoes Universidade Fernando Pessoa, 2004: Pages 293-302, 2004.*
- [228] H. Tian, G. Guo, X. Fu, Y. Yao, L. Yuan, A. Xiang, Fabrication, properties and applications of soy-protein-based materials: A review, *Int J Biol Macromol*, 120 (2018) 475-490.
- [229] D. Vnučec, A. Kutnar, A. Goršek, Soy-based adhesives for wood-bonding – a review, *Journal of Adhesion Science and Technology*, 31 (2016) 910-931.
- [230] D. Fukushima, Recent progress of soybean protein foods: chemistry, technology, and nutrition, *Food Reviews International*, 7 (1991) 323-351.

- [231] T.E. Creighton, *Proteins: structures and molecular properties*, Macmillan, 1993.
- [232] G.A. Petsko, D. Ringe, *From sequence to structure*, *Protein structure and function*, 1 (2004) 49.
- [233] Q. Gao, S.Q. Shi, S. Zhang, J. Li, X. Wang, W. Ding, K. Liang, J. Wang, Soybean meal-based adhesive enhanced by MUF resin, *Journal of Applied Polymer Science*, 125 (2012) 3676-3681.
- [234] Q. Gao, S.Q. Shi, J. Li, K. Liang, X. Zhang, Soybean meal-based wood adhesives enhanced by modified polyacrylic acid solution, *BioResources*, 7 (2012) 0946-0956.
- [235] F. Eslah, M. Jonoobi, M. Faezipour, M. Afsharpour, A.A. Enayati, Preparation and development of a chemically modified bio-adhesive derived from soybean flour protein, *International Journal of Adhesion and Adhesives*, 71 (2016) 48-54.
- [236] Z. Wang, Z. Li, Z. Gu, Y. Hong, L. Cheng, Preparation, characterization and properties of starch-based wood adhesive, *Carbohydrate Polymers*, 88 (2012) 699-706.
- [237] Y. Zhang, L. Ding, J. Gu, H. Tan, L. Zhu, Preparation and properties of a starch-based wood adhesive with high bonding strength and water resistance, *Carbohydr Polym*, 115 (2015) 32-37.
- [238] Liu, Yuan, and Kaichang Li. Chemical modification of soy protein for wood adhesives. *Macromolecular Rapid Communications*, 23 (2002) 739-742.
- [239] H. Liu, C. Li, X.S. Sun, Improved water resistance in undecylenic acid (UA)-modified soy protein isolate (SPI)-based adhesives, *Industrial Crops and Products*, 74 (2015) 577-584.
- [240] Y. Liu, K. Li, Development and characterization of adhesives from soy protein for bonding wood, *International Journal of Adhesion and Adhesives*, 27 (2007) 59-67.
- [241] F. Wang, J. Wang, F. Chu, C. Wang, C. Jin, S. Wang, J. Pang, Combinations of soy protein and polyacrylate emulsions as wood adhesives, *International Journal of Adhesion and Adhesives*, 82 (2018) 160-165.
- [242] Y. Xu, Y. Xu, Y. Han, M. Chen, W. Zhang, Q. Gao, J. Li, The Effect of Enzymolysis on Performance of Soy Protein-Based Adhesive, *Molecules*, 23 (2018) 2752.
- [243] N. Chen, Q. Zeng, Q. Lin, J. Rao, Effect of enzymatic pretreatment on the preparation and properties of soy-based adhesive for plywood, *BioResources*, 10 (2015) 5071-5082.
- [244] P. Zheng, N. Chen, S.M. Mahfuzul Islam, L.-K. Ju, J. Liu, J. Zhou, L. Chen, H. Zeng, Q. Lin, Development of Self-Cross-Linked Soy Adhesive by Enzyme Complex from *Aspergillus niger* for Production of All-Biomass Composite Materials, *ACS Sustainable Chemistry & Engineering*, 7 (2018) 3909-3916.
- [245] J. Luo, C. Li, X. Li, J. Luo, Q. Gao, J. Li, A new soybean meal-based bioadhesive enhanced with 5, 5-dimethyl hydantoin polyepoxide for the improved water resistance of plywood, *RSC Advances*, 5 (2015) 62957-62965.
- [246] J. Luo, J. Luo, Y. Bai, Q. Gao, J. Li, A high performance soy protein-based bio-adhesive enhanced with a melamine/epichlorohydrin prepolymer and its application on plywood, *RSC advances*, 6 (2016) 67669-67676.
- [247] J. Luo, J. Luo, J. Zhang, Y. Bai, Q. Gao, J. Li, L. Li, A new flexible soy-based adhesive enhanced with neopentyl glycol diglycidyl ether: Properties and application,

Polymers, 8 (2016) 346.

[248] J. Li, J. Luo, X. Li, Z. Yi, Q. Gao, J. Li, Soybean meal-based wood adhesive enhanced by ethylene glycol diglycidyl ether and diethylenetriamine, *Industrial Crops and Products*, 74 (2015) 613-618.

[249] C. Li, H. Li, S. Zhang, J. Li, Preparation of reinforced soy protein adhesive using silane coupling agent as an enhancer, *BioResources*, 9 (2014) 5448-5460.

[250] Barzegar, Mahsa, et al. Comparison of canola and soy flour with added isocyanate as wood adhesives. *Journal of the American Oil Chemists' Society*, 97 (2020) 1371-1383.

[251] Z. Gao, W. Wang, Z. Zhao, M. Guo, Novel whey protein-based aqueous polymer-isocyanate adhesive for glulam, *Journal of Applied Polymer Science*, 120 (2011) 220-225.

[252] Y. Zhang, W. Zhu, Y. Lu, Z. Gao, J. Gu, Nano-scale blocking mechanism of MMT and its effects on the properties of polyisocyanate-modified soybean protein adhesive, *Industrial Crops and Products*, 57 (2014) 35-42.

[253] W.G. Hand, W. Robert Ashurst, B. Via, S. Banerjee, Curing behavior of soy flour with phenol-formaldehyde and isocyanate resins, *International Journal of Adhesion and Adhesives*, 87 (2018) 105-108.

[254] M. Zhang, Y. Zhang, M. Chen, Q. Gao, J. Li, A high-performance and low-cost soy flour adhesive with a hydroxymethyl melamine prepolymer, *Polymers*, 10 (2018) 909.

[255] Z. Wu, X. Xi, H. Lei, J. Liang, J. Liao, G. Du, Study on soy-based adhesives enhanced by phenol formaldehyde cross-linker, *Polymers*, 11 (2019) 365.

[256] N. Chen, Q. Lin, J. Rao, Q. Zeng, Water resistances and bonding strengths of soy-based adhesives containing different carbohydrates, *Industrial Crops and Products*, 50 (2013) 44-49.

[257] P. Zheng, Y. Li, F. Li, Y. Ou, Q. Lin, N. Chen, Development of defatted soy flour-based adhesives by acid hydrolysis of carbohydrates, *Polymers*, 9 (2017) 153.

[258] N. Chen, Q. Zeng, Q. Lin, J. Rao, Development of defatted soy flour based bio-adhesives using Viscozyme L, *Industrial Crops and Products*, 76 (2015) 198-203.

[259] D. Liu, H. Chen, P.R. Chang, Q. Wu, K. Li, L. Guan, Biomimetic soy protein nanocomposites with calcium carbonate crystalline arrays for use as wood adhesive, *Bioresour Technol*, 101 (2010) 6235-6241.

[260] Z. Wang, S. Zhao, W. Zhang, C. Qi, S. Zhang, J. Li, Bio-inspired cellulose nanofiber-reinforced soy protein resin adhesives with dopamine-induced codeposition of "water-resistant" interphases, *Applied Surface Science*, 478 (2019) 441-450.

[261] Q. Gao, J. Li, S.Q. Shi, K. Liang, X. Zhang, Soybean meal-based adhesive reinforced with cellulose nano-whiskers, *BioResources*, 7 (2012) 5622-5633.

[262] G. Qi, N. Li, D. Wang, X.S. Sun, Development of high-strength soy protein adhesives modified with sodium montmorillonite clay, *Journal of the American Oil Chemists' Society*, 93 (2016) 1509-1517.

[263] X. Liu, K. Wang, W. Gu, F. Li, J. Li, S. Zhang, Reinforcement of interfacial and bonding strength of soybean meal-based adhesive via kenaf fiber-CaCO₃ anchored N-cyclohexyl-2-benzothiazole sulfenamide, *Composites Part B: Engineering*, 155 (2018)

204-211.

- [264] X. Li, M. Chen, J. Zhang, Q. Gao, S. Zhang, J. Li, Physico-chemical properties of soybean meal-based adhesives reinforced by ethylene glycol diglycidyl ether and modified nanocrystalline cellulose, *Polymers*, 9 (2017) 463.
- [265] A. Sangregorio, N. Guigo, J.C. van der Waal, N. Sbirrazzuoli, Humins from biorefineries as thermo-reactive macromolecular systems, *ChemSusChem*, 11 (2018) 4246-4255.
- [266] A. Sangregorio, Valorisation of biorefinery-derived humins: towards the development of sustainable thermosets and composites, in, *COMUE Université Côte d'Azur (2015-2019)*, 2019.
- [267] I. van Zandvoort, Y. Wang, C.B. Rasrendra, E.R. van Eck, P.C. Bruijninx, H.J. Heeres, B.M. Weckhuysen, Formation, molecular structure, and morphology of humins in biomass conversion: influence of feedstock and processing conditions, *ChemSusChem*, 6 (2013) 1745-1758.
- [268] I. van Zandvoort, E.J. Koers, M. Weingarh, P.C. Bruijninx, M. Baldus, B.M. Weckhuysen, Structural characterization of 13 C-enriched humins and alkali-treated 13 C humins by 2D solid-state NMR, *Green Chemistry*, 17 (2015) 4383-4392.
- [269] T.M.C. Hoang, E. Van Eck, W. Bula, J.G. Gardeniers, L. Lefferts, K. Seshan, Humin based by-products from biomass processing as a potential carbonaceous source for synthesis gas production, *Green chemistry*, 17 (2015) 959-972.
- [270] A. Sangregorio, N. Guigo, E.d. Jong, N. Sbirrazzuoli, Kinetics and chemorheological analysis of cross-linking reactions in humins, *Polymers*, 11 (2019) 1804.
- [271] A. Sangregorio, A. Muralidhara, N. Guigo, L.G. Thygesen, G. Marlair, C. Angelici, E. de Jong, N. Sbirrazzuoli, Humin based resin for wood modification and property improvement, *Green Chemistry*, 22 (2020) 2786-2798.
- [272] A.C. Mija, E. De Jong, J.C. van der Waal, G.P.M. Van Klink, Humins-containing foam, in, *Google Patents*, 2020.
- [273] J. Heltzel, S.K. Patil, C.R. Lund, Humin formation pathways, in: *Reaction pathways and mechanisms in thermocatalytic biomass conversion II*, Springer, 2016, pp. 105-118.
- [274] L. Filiciotto, A.M. Balu, A.A. Romero, E. Rodríguez-Castellón, J.C. van der Waal, R. Luque, Benign-by-design preparation of humin-based iron oxide catalytic nanocomposites, *Green Chemistry*, 19 (2017) 4423-4434.
- [275] L. Cheng, H. Guo, Z. Gu, Z. Li, Y. Hong, Effects of compound emulsifiers on properties of wood adhesive with high starch content, *International Journal of Adhesion and Adhesives*, 72 (2017) 92-97.
- [276] X. Zheng, L. Cheng, Z. Gu, Y. Hong, Z. Li, C. Li, Effects of heat pretreatment of starch on graft copolymerization reaction and performance of resulting starch-based wood adhesive, *Int J Biol Macromol*, 96 (2017) 11-18.
- [277] M. Turunen, L. Alvila, T.T. Pakkanen, J. Rainio, Modification of phenol-formaldehyde resol resins by lignin, starch, and urea, *Journal of Applied Polymer Science*, 88 (2003) 582-588.
- [278] P. Li, Y. Wu, Y. Zhou, Y. Zuo, Preparation and characterization of resorcinol-

- dialdehyde starch-formaldehyde copolycondensation resin adhesive, *International journal of biological macromolecules*, 127 (2019) 12-17.
- [279] P. Sandhya, M. Sreekala, M. Padmanabhan, K. Jesitha, S. Thomas, Effect of starch reduced graphene oxide on thermal and mechanical properties of phenol formaldehyde resin nanocomposites, *Composites Part B: Engineering*, 167 (2019) 83-92.
- [280] Y. Zuo, W. Liu, J. Xiao, X. Zhao, Y. Zhu, Y. Wu, Preparation and characterization of dialdehyde starch by one-step acid hydrolysis and oxidation, *International journal of biological macromolecules*, 103 (2017) 1257-1264.
- [281] X.F. Zhao, L.Q. Peng, H.L. Wang, Y.B. Wang, H. Zhang, Environment-friendly urea-oxidized starch adhesive with zero formaldehyde-emission, *Carbohydr Polym*, 181 (2018) 1112-1118.
- [282] L. Chen, Y. Wang, P. Fei, W. Jin, H. Xiong, Z. Wang, Enhancing the performance of starch-based wood adhesive by silane coupling agent (KH570), *International journal of biological macromolecules*, 104 (2017) 137-144.
- [283] Z. Li, J. Wang, C. Li, Z. Gu, L. Cheng, Y. Hong, Effects of montmorillonite addition on the performance of starch-based wood adhesive, *Carbohydrate polymers*, 115 (2015) 394-400.
- [284] Y. Wang, H. Xiong, Z. Wang, L. Chen, Effects of different durations of acid hydrolysis on the properties of starch-based wood adhesive, *International journal of biological macromolecules*, 103 (2017) 819-828.
- [285] L. Chen, Z. Xiong, H. Xiong, Z. Wang, Z.-u. Din, A. Nawaz, P. Wang, C. Hu, Effects of nano-TiO₂ on bonding performance, structure stability and film-forming properties of starch-g-VAc based wood adhesive, *Carbohydrate polymers*, 200 (2018) 477-486.
- [286] X. Zheng, L. Cheng, Z. Gu, Y. Hong, Z. Li, C. Li, Effects of heat pretreatment of starch on graft copolymerization reaction and performance of resulting starch-based wood adhesive, *International journal of biological macromolecules*, 96 (2017) 11-18.
- [287] A. Moubarik, N. Causse, T. Poumadere, A. Allal, A. Pizzi, F. Charrier, B. Charrier, Shear refinement of formaldehyde-free corn starch and mimosa tannin (*Acacia mearnsii*) wood adhesives, *Journal of adhesion science and technology*, 25 (2011) 1701-1713.
- [288] A. Moubarik, A. Allal, A. Pizzi, F. Charrier, B. Charrier, Characterization of a formaldehyde-free cornstarch-tannin wood adhesive for interior plywood, *European Journal of Wood and Wood Products*, 68 (2010) 427-433.
- [289] A. Moubarik, B. Charrier, A. Allal, F. Charrier, A. Pizzi, Development and optimization of a new formaldehyde-free cornstarch and tannin wood adhesive, *European Journal of Wood and Wood Products*, 68 (2010) 167-177.
- [290] S. Oktay, N. Kızılcın, B. Bengü, Development of bio-based cornstarch-Mimosa tannin-sugar adhesive for interior particleboard production, *Industrial Crops and Products*, 170 (2021) 113689.
- [291] A. Nuryawan, E.M. Alamsyah, A review of isocyanate wood adhesive: a case study in Indonesia, *Applied adhesive bonding in science and technology*, 1 (2018) 13.
- [292] S.-m. Wang, J.-y. Shi, W. Xu, Synthesis and characterization of starch-based aqueous polymer isocyanate wood adhesive, *BioResources*, 10 (2015) 7653-7666.

- [293] W. Jiang, A. Kumar, S. Adamopoulos, Liquefaction of lignocellulosic materials and its applications in wood adhesives—A review, *Industrial Crops and Products*, 124 (2018) 325-342.
- [294] S.I. Tohmura, G.Y. Li, T.F. Qin, Preparation and characterization of wood polyalcohol-based isocyanate adhesives, *Journal of applied polymer science*, 98 (2005) 791-795.
- [295] A. Cornille, R. Auvergne, O. Figovsky, B. Boutevin, S. Caillol, A perspective approach to sustainable routes for non-isocyanate polyurethanes, *European Polymer Journal*, 87 (2017) 535-552.
- [296] M. Ghasemlou, F. Daver, E.P. Ivanova, B. Adhikari, Bio-based routes to synthesize cyclic carbonates and polyamines precursors of non-isocyanate polyurethanes: A review, *European Polymer Journal*, 118 (2019) 668-684.
- [297] F.D. Bobbink, A.P. van Muyden, P.J. Dyson, En route to CO₂-containing renewable materials: catalytic synthesis of polycarbonates and non-isocyanate polyhydroxyurethanes derived from cyclic carbonates, *Chemical Communications*, 55 (2019) 1360-1373.
- [298] S. Jin, K. Li, J. Li, H. Chen, A low-cost, formaldehyde-free and high flame retardancy wood adhesive from inorganic adhesives: Properties and performance, *Polymers*, 9 (2017) 513.
- [299] W. Zhou, Q. Ye, S.Q. Shi, Z. Fang, Q. Gao, J. Li, A strong magnesium oxychloride cement wood adhesive via organic-inorganic hybrid, *Construction and Building Materials*, 297 (2021) 123776.
- [300] T. Chen, Z. Wu, X.A. Wang, W. Wang, D. Huang, Q. Wei, B. Wu, Y. Xie, Hierarchical Lamellar Aluminophosphate Materials with Porosity as Ecofriendly Inorganic Adhesive for Wood-Based Boards, *ACS Sustainable Chemistry & Engineering*, 6 (2018) 6273-6280.
- [301] B. Zhang, Z. Chang, J. Li, X. Li, Y. Kan, Z. Gao, Effect of kaolin content on the performances of kaolin-hybridized soybean meal-based adhesives for wood composites, *Composites Part B: Engineering*, 173 (2019) 106919.
- [302] Y. Lin, X. Li, Q. Huang, Preparation and characterization of expanded perlite/wood-magnesium composites as building insulation materials, *Energy and Buildings*, 231 (2021) 110637.
- [303] B. Pang, X.-F. Cao, S.-N. Sun, X.-L. Wang, J.-L. Wen, S.S. Lam, T.-Q. Yuan, R.-C. Sun, The direct transformation of bioethanol fermentation residues for production of high-quality resins, *Green Chemistry*, 22 (2020) 439-447.
- [304] D.G. Roux, D. Ferreira, H.K. Hundt, E. Malan, Structure, stereochemistry, and reactivity of natural condensed tannins as basis for their extended industrial application, in: *Appl. Polym. Symp*, 1975, pp. 335-353.
- [305] G. Tondi, A. Pizzi, Tannin-based rigid foams: Characterization and modification, *Industrial Crops and Products*, 29 (2009) 356-363.
- [306] G. JJ, Compressive properties and biodegradabilities of polyurethane foams derived from condensed tannin, *Mokuzai Gakkaishi*, 39 (1993) 801-806.
- [307] J.-J. Ge, K. Sakai, Decomposition of polyurethane foams derived from condensed tannin II: Hydrolysis and aminolysis of polyurethane foams, *Journal of wood science*,

44 (1998) 103-105.

[308] J. Ge, X. Shi, M. Cai, R. Wu, M. Wang, A novel biodegradable antimicrobial PU foam from wattle tannin, *Journal of applied polymer science*, 90 (2003) 2756-2763.

[309] N. Meikleham, A. Pizzi, Acid-and alkali-catalyzed tannin-based rigid foams, *Journal of Applied Polymer Science*, 53 (1994) 1547-1556.

[310] G. Tondi, A. Pizzi, E. Masson, A. Celzard, Analysis of gases emitted during carbonization degradation of polyflavonoid tannin/furanic rigid foams, *Polymer Degradation and Stability*, 93 (2008) 1539-1543.

[311] G. Tondi, C.W. Oo, A. Pizzi, A. Trosa, M.F. Thevenon, Metal adsorption of tannin based rigid foams, *Industrial Crops and Products*, 29 (2009) 336-340.

[312] J. Sánchez-Martín, J. Beltrán-Heredia, A. Delgado-Regaña, M.A. Rodríguez-González, F. Rubio-Alonso, Adsorbent tannin foams: New and complementary applications in wastewater treatment, *Chemical Engineering Journal*, 228 (2013) 575-582.

[313] A. Celzard, V. Fierro, G. Amaral-Labat, A. Pizzi, J. Torero, Flammability assessment of tannin-based cellular materials, *Polymer Degradation and Stability*, 96 (2011) 477-482.

[314] G. Tondi, W. Zhao, A. Pizzi, G. Du, V. Fierro, A. Celzard, Tannin-based rigid foams: a survey of chemical and physical properties, *Bioresour Technol*, 100 (2009) 5162-5169.

[315] G. Tondi, S. Blacher, A. Léonard, A. Pizzi, V. Fierro, J. Leban, A. Celzard, X-ray microtomography studies of tannin-derived organic and carbon foams, *Microscopy and Microanalysis*, 15 (2009) 384-394.

[316] W. Zhao, V. Fierro, A. Pizzi, G. Du, A. Celzard, Effect of composition and processing parameters on the characteristics of tannin-based rigid foams. Part II: Physical properties, *Materials Chemistry and Physics*, 123 (2010) 210-217.

[317] W. Zhao, A. Pizzi, V. Fierro, G. Du, A. Celzard, Effect of composition and processing parameters on the characteristics of tannin-based rigid foams. Part I: Cell structure, *Materials Chemistry and Physics*, 122 (2010) 175-182.

[318] X. Li, A. Pizzi, C. Lacoste, V. Fierro, A. Celzard, Physical properties of tannin/furanic resin foamed with different blowing agents, *BioResources*, 8 (2013) 743-752.

[319] M.C. Basso, S. Giovando, A. Pizzi, A. Celzard, V. Fierro, Tannin/furanic foams without blowing agents and formaldehyde, *Industrial Crops and Products*, 49 (2013) 17-22.

[320] C. Lacoste, M.C. Basso, A. Pizzi, M.P. Laborie, D. Garcia, A. Celzard, Bioresourced pine tannin/furanic foams with glyoxal and glutaraldehyde, *Industrial Crops and Products*, 45 (2013) 401-405.

[321] X. Chen, N. Guigo, A. Pizzi, N. Sbirrazzuoli, B. Li, E. Fredon, C. Gerardin, Ambient Temperature Self-Blowing Tannin-Humins Biofoams, *Polymers*, 12 (2020) 2732.

[322] X. Chen, J. Li, A. Pizzi, E. Fredon, C. Gerardin, X. Zhou, G. Du, Tannin-furanic foams modified by soybean protein isolate (SPI) and industrial lignin substituting formaldehyde addition, *Industrial Crops and Products*, 168 (2021) 113607.

- [323] A. Martinez de Yuso, M.C. Lagel, A. Pizzi, V. Fierro, A. Celzard, Structure and properties of rigid foams derived from quebracho tannin, *Materials & Design*, 63 (2014) 208-212.
- [324] C. Lacoste, A. Pizzi, M.C. Basso, M.P. Laborie, A. Celzard, Pinus pinaster tannin/furanic foams: PART I. Formulation, *Industrial Crops and Products*, 52 (2014) 450-456.
- [325] C. Lacoste, A. Pizzi, M.P. Laborie, A. Celzard, Pinus pinaster tannin/furanic foams: Part II. Physical properties, *Industrial Crops and Products*, 61 (2014) 531-536.
- [326] M. Čop, C. Lacoste, M. Conradi, M.-P. Laborie, A. Pizzi, M. Sernek, The effect of the composition of spruce and pine tannin-based foams on their physical, morphological and compression properties, *Industrial Crops and Products*, 74 (2015) 158-164.
- [327] C. Lacoste, M. Čop, K. Kemppainen, S. Giovando, A. Pizzi, M.-P. Laborie, M. Sernek, A. Celzard, Biobased foams from condensed tannin extracts from Norway spruce (*Picea abies*) bark, *Industrial Crops and Products*, 73 (2015) 144-153.
- [328] M. Čop, M.P. Laborie, A. Pizzi, M. Sernek, Curing characterisation of spruce tannin-based foams using the advanced isoconversional method, *Bioresources*, 9 (2014) 4643-4655.
- [329] M. Čop, B. Gospodarič, K. Kemppainen, S. Giovando, M.-P. Laborie, A. Pizzi, M. Sernek, Characterization of the curing process of mixed pine and spruce tannin-based foams by different methods, *European Polymer Journal*, 69 (2015) 29-37.
- [330] C. Lacoste, M.C. Basso, A. Pizzi, A. Celzard, E. Ella Ebang, N. Gallon, B. Charrier, Pine (*P. pinaster*) and quebracho (*S. lorentzii*) tannin-based foams as green acoustic absorbers, *Industrial Crops and Products*, 67 (2015) 70-73.
- [331] X. Li, A. Pizzi, M. Cangemi, V. Fierro, A. Celzard, Flexible natural tannin-based and protein-based biosourced foams, *Industrial Crops and Products*, 37 (2012) 389-393.
- [332] X. Li, H.A. Essawy, A. Pizzi, L. Delmotte, K. Rode, D. Le Nouen, V. Fierro, A. Celzard, Modification of tannin based rigid foams using oligomers of a hyperbranched poly(amine-ester), *Journal of Polymer Research*, 19 (2012) 1-9.
- [333] G. Rangel, H. Chapuis, M.-C. Basso, A. Pizzi, C. Delgado-Sanchez, V. Fierro, A. Celzard, C. Gerardin-Charbonnier, Improving water repellence and friability of tannin-furanic foams by oil-grafted flavonoid tannins, *Bioresources*, 11 (2016) 7754-7768.
- [334] J. Eckardt, J. Neubauer, T. Sepperer, S. Donato, M. Zanetti, N. Cefarin, L. Vaccari, M. Lippert, M. Wind, T. Schnabel, A. Petutschnigg, G. Tondi, Synthesis and Characterization of High-Performing Sulfur-Free Tannin Foams, *Polymers*, 12 (2020) 564.
- [335] X. Wu, W. Yan, Y. Zhou, L. Luo, X. Yu, L. Luo, M. Fan, G. Du, W. Zhao, Thermal, morphological, and mechanical characteristics of sustainable tannin bio-based foams reinforced with wood cellulosic fibers, *Industrial Crops and Products*, 158 (2020) 113029.
- [336] G. Tondi, M. Link, C. Kolbitsch, R. Lesacher, A. Petutschnigg, Pilot plant up-scaling of tannin foams, *Industrial Crops and Products*, 79 (2016) 211-218.
- [337] M.C. Basso, S. Giovando, A. Pizzi, H. Pasch, N. Pretorius, L. Delmotte, A. Celzard, Flexible-elastic copolymerized polyurethane-tannin foams, *Journal of Applied*

- Polymer Science, 131 (2014).
- [338] M. Basso, A. Pizzi, C. Lacoste, L. Delmotte, F. Al-Marzouki, S. Abdalla, A. Celzard, MALDI-TOF and ¹³C NMR Analysis of Tannin–Furanic–Polyurethane Foams Adapted for Industrial Continuous Lines Application, *Polymers*, 6 (2014) 2985-3004.
- [339] D.E. García, W.G. Glasser, A. Pizzi, S. Paczkowski, M.P. Laborie, Hydroxypropyl tannin from *Pinus pinaster* bark as polyol source in urethane chemistry, *European Polymer Journal*, 67 (2015) 152-165.
- [340] A. Arbenz, L. Avérous, Synthesis and characterization of fully biobased aromatic polyols–oxybutylation of condensed tannins towards new macromolecular architectures, *RSC Adv.*, 4 (2014) 61564-61572.
- [341] A. Arbenz, A. Frache, F. Cuttica, L. Avérous, Advanced biobased and rigid foams, based on urethane-modified isocyanurate from oxypropylated gambier tannin polyol, *Polymer Degradation and Stability*, 132 (2016) 62-68.
- [342] I. Hussain, M. Sanglard, J.H. Bridson, K. Parker, Preparation and physicochemical characterisation of polyurethane foams prepared using hydroxybutylated condensed tannins as a polyol source, *Industrial Crops and Products*, 154 (2020) 112636.
- [343] A. Szczurek, V. Fierro, A. Pizzi, M. Stauber, A. Celzard, A new method for preparing tannin-based foams, *Industrial Crops and Products*, 54 (2014) 40-53.
- [344] C. Delgado-Sánchez, F. Santiago-Medina, V. Fierro, A. Pizzi, A. Celzard, Optimisation of “green” tannin-furanic foams for thermal insulation by experimental design, *Materials & Design*, 139 (2018) 7-15.
- [345] F.J. Santiago-Medina, C. Delgado-Sánchez, M.C. Basso, A. Pizzi, V. Fierro, A. Celzard, Mechanically blown wall-projected tannin-based foams, *Industrial Crops and Products*, 113 (2018) 316-323.
- [346] F.J. Santiago-Medina, A. Tenorio-Alfonso, C. Delgado-Sánchez, M.C. Basso, A. Pizzi, A. Celzard, V. Fierro, M.C. Sánchez, J.M. Franco, Projectable tannin foams by mechanical and chemical expansion, *Industrial Crops and Products*, 120 (2018) 90-96.
- [347] A. Celzard, W. Zhao, A. Pizzi, V. Fierro, Mechanical properties of tannin-based rigid foams undergoing compression, *Materials Science and Engineering: A*, 527 (2010) 4438-4446.
- [348] M.C. Basso, A. Pizzi, A. Celzard, Dynamic Foaming Behaviour of Polyurethane vs Tannin/Furanic Foams, *Journal of Renewable Materials*, 1 (2013) 273-278.
- [349] G. Tondi, A. Pizzi, H. Pasch, A. Celzard, Structure degradation, conservation and rearrangement in the carbonisation of polyflavonoid tannin/furanic rigid foams – A MALDI-TOF investigation, *Polymer Degradation and Stability*, 93 (2008) 968-975.
- [350] G. Tondi, V. Fierro, A. Pizzi, A. Celzard, Tannin-based carbon foams, *Carbon*, 47 (2009) 1480-1492.
- [351] G. Tondi, A. Pizzi, L. Delmotte, J. Parmentier, R. Gadiou, Chemical activation of tannin–furanic carbon foams, *Industrial Crops and Products*, 31 (2010) 327-334.
- [352] M.C. Basso, Green, Formaldehyde-Free, Foams For Thermal Insulation, *Advanced Materials Letters*, 2 (2011) 378-382.
- [353] A. Celzard, G. Tondi, D. Lacroix, G. Jeandel, B. Monod, V. Fierro, A. Pizzi, Radiative properties of tannin-based, glasslike, carbon foams, *Carbon*, 50 (2012) 4102-

4113.

- [354] P. Jana, V. Fierro, A. Pizzi, A. Celzard, Thermal conductivity improvement of composite carbon foams based on tannin-based disordered carbon matrix and graphite fillers, *Materials & Design*, 83 (2015) 635-643.
- [355] M. Letellier, J. Macutkevic, A. Paddubskaya, A. Klochkov, P. Kuzhir, J. Banys, V. Fierro, A. Celzard, Microwave Dielectric Properties of Tannin-Based Carbon Foams, *Ferroelectrics*, 479 (2015) 119-126.
- [356] G. Tondi, A. Pizzi, R. Olives, Natural tannin-based rigid foams as insulation for doors and wall panels, *Maderas. Ciencia y tecnología*, 10 (2008) 219-227.
- [357] M. Link, C. Kolbitsch, G. Tondi, M. Ebner, S. Wieland, A. Petutschnigg, Formaldehyde-free tannin based foams and their use as lightweight panels, *BioResources*, 6 (2011) 4218-4228.
- [358] X. Zhou, A. Pizzi, A. Sauget, A. Nicollin, X. Li, A. Celzard, K. Rode, H. Pasch, Lightweight tannin foam/composites sandwich panels and the coldset tannin adhesive to assemble them, *Industrial Crops and Products*, 43 (2013) 255-260.
- [359] J. Sánchez-Martín, J. Beltrán-Heredia, A. Delgado-Regaña, M.A. Rodríguez-González, F. Rubio-Alonso, Optimization of tannin rigid foam as adsorbents for wastewater treatment, *Industrial Crops and Products*, 49 (2013) 507-514.
- [360] B. Hao, F. Wang, H. Huang, Y. Wu, S. Jia, Y. Liao, H. Mao, Tannin foam immobilized with ferric ions for efficient removal of ciprofloxacin at low concentrations, *Journal of Hazardous Materials*, 414 (2021) 125567.
- [361] C. Delgado-Sánchez, M. Letellier, V. Fierro, H. Chapuis, C. Gérardin, A. Pizzi, A. Celzard, Hydrophobisation of tannin-based foams by covalent grafting of silanes, *Industrial Crops and Products*, 92 (2016) 116-126.
- [362] M.C. Basso, A. Pizzi, F. Al-Marzouki, S. Abdalla, Horticultural/hydroponics and floral natural foams from tannins, *Industrial Crops and Products*, 87 (2016) 177-181.
- [363] Z. Marie, V. Nicolas, A. Celzard, V. Fierro, Experimental investigation of the physical foaming of tannin-based thermoset foams, *Industrial Crops and Products*, 138 (2019) 111424.
- [364] Z. Marie, V. Nicolas, A. Celzard, V. Fierro, First approach for modelling the physical foaming of tannin-based thermoset foams, *International Journal of Thermal Sciences*, 149 (2020) 106212.
- [365] V. Nicolas, Z. Marie, A. Mija, A. Celzard, V. Fierro, Estimation of the reaction kinetic parameters of a mimosa tannin-based thermoset resin with a simulation approach, *Industrial Crops and Products*, 161 (2021) 113228.
- [366] C. Kolbitsch, M. Link, A. Petutschnigg, S. Wieland, G. Tondi, Microwave Produced Tannin-furanic Foams, *Journal of Materials Science Research*, 1 (2012) 84.
- [367] G. Tondi, M. Link, C. Kolbitsch, A. Petutschnigg, Infrared-catalyzed synthesis of tannin-furanic foams, *BioResources*, 9 (2014) 984-993.
- [368] X. Li, V.K. Srivastava, A. Pizzi, A. Celzard, J. Leban, Nanotube-reinforced tannin/furanic rigid foams, *Industrial Crops and Products*, 43 (2013) 636-639.
- [369] G. Tondi, M. Johansson, S. Leijonmarck, S. Trey, Tannin based foams modified to be semi-conductive: Synthesis and characterization, *Progress in Organic Coatings*, 78 (2015) 488-493.

[370] A. Reyer, G. Tondi, R.J.F. Berger, A. Petutschnigg, M. Musso, Raman spectroscopic investigation of tannin-furanic rigid foams, *Vibrational Spectroscopy*, 84 (2016) 58-66.

3. PRESENTATION DES PUBLICATIONS

3.1 Adhésifs pour bois thermodurcissables au polyuréthane sans isocyanate à base d'humines non furaniques (NIPU)

Résumé: Des humines commerciales principalement non furaniques ont été utilisées pour préparer des résines de polyuréthane sans isocyanate (NIPU) à base d'humine pour les adhésifs pour panneaux de bois. Des résines NIPU à base d'humine pure et des résines NIPU à base d'humine pure ont été préparées aussi, ces dernières pour améliorer les performances des humines. Les espèces chimiques dans les humines brutes et les espèces chimiques formées dans les résines NIPU ont été identifiées par spectrométrie Matrix Assisted Laser Desorption Ionization Time of Flight spectrométrie de masse (MALDI-ToF) et par spectrométrie Infrarouge à Fourier Transform (FTIR). Humines, acide fulvique et dérivés, acide humique et ses fragments, certains lignanes présents et oligomères furaniques présents ont formé des liaisons NIPU. L'analyse thermomécanique (TMA) a montré que comme avec d'autres résines NIPU à base de biomatériaux, toutes ces résines présentaient également deux pics de température de durcissement, le premier autour de 130°C et le second autour de 220°C. Une diminution du module d'élasticité (MOE) entre les deux a indiqué que la première période de durcissement correspondait à une croissance linéaire des oligomères formant un réseau d'enchevêtrement physique. Cela s'est ensuite démantelé, et le second correspondait à la formation d'un réseau chimique réticulé. Ce deuxième pic était plus évident pour les résines tanin-humine NIPU. Tous les panneaux de particules de laboratoire fabriqués et testés soit liés avec des humines pures, soit avec du tanin-Les adhésifs Humine NIPU-ont bien satisfait aux exigences de résistance d'adhérence interne de la norme pertinente pour les panneaux de qualité intérieure. Les adhésifs au tanin-humine ont nettement mieux performé que celui à l'humine pur.

Mots clés: humines non furaniques; acide humique; acide fulvique; adhésifs pour bois; panneaux de bois; adhésifs thermodurcissables; polyuréthanes; NIPU.

Article

Non-Furanic Humins-Based Non-Isocyanate Polyurethane (NIPU) Thermoset Wood Adhesives

Xinyi Chen ¹, Antonio Pizzi ^{1,*}, Hisham Essawy ^{1,2}, Emmanuel Fredon ¹, Christine Gerardin ³, Nathanael Guigo ⁴ and Nicolas Sbirrazzuoli ⁴

- ¹ LERMAB-ENSTIB, University of Lorraine, 27 rue Philippe Seguin, 88000 Epinal, France; xinyi.chen@univ-lorraine.fr (X.C.); hishamessawy@yahoo.com (H.E.); emmanuel.fredon@univ-lorraine.fr (E.F.)
- ² Department of Polymers and Pigments, National Research Centre, Cairo 12622, Egypt
- ³ LERMAB, Faculté des Sciences, University of Lorraine, Blvd. des Aiguillettes, 54000 Nancy, France; christine.gerardin@univ-lorraine.fr
- ⁴ Department of Chemistry, University of the Cote d'Azur, 06103 Nice, France; Nathanael.GUIGO@univ-cotedazur.fr (N.G.); Nicolas.SBIRRAZZUOLI@univ-cotedazur.fr (N.S.)
- * Correspondence: antonio.pizzi@univ-lorraine.fr

Abstract: Predominantly non-furanic commercial humins were used to prepare humin-based non-isocyanate polyurethane (NIPU) resins for wood panel adhesives. Pure humin-based NIPU resins and tannin–humin NIPU resins were prepared, the latter to upgrade the humins' performance. Species in the raw humins and species formed in the NIPU resins were identified by Matrix Assisted Laser Desorption Ionization Time of Flight (MALDI ToF) spectrometry and Fourier Transform Infrared (FTIR). Humins, fulvic acid and derivatives, humic acid and its fragments, some lignans present and furanic oligomers present formed NIPU linkages. Thermomechanical analysis (TMA) showed that as with other biomaterials-based NIPU resins, all these resins also showed two temperature peaks of curing, the first around 130 °C and the second around 220 °C. A decrease in the Modulus of Elasticity (MOE) between the two indicated that the first curing period corresponded to linear growth of the oligomers forming a physical entanglement network. This then disentangled, and the second corresponded to the formation of a chemical cross-linked network. This second peak was more evident for the tannin–humin NIPU resins. All the laboratory particleboard made and tested either bonded with pure humins or with tannin–humin NIPU adhesives satisfied well the internal bond strength requirements of the relevant standard for interior grade panels. The tannin–humin adhesives performed clearly better than the pure humins one.

Citation: Chen, X.; Pizzi, A.; Essawy, H.; Fredon, E.; Gerardin, C.; Guigo, N.; Sbirrazzuoli, N. Non-Furanic Humins-Based Non-Isocyanate Polyurethane (NIPU) Thermoset Wood Adhesives. *Polymers* **2021**, *13*, 372. <https://doi.org/10.3390/polym13030372>

Academic Editor:
Marek M. Kowalczyk

Received: 4 January 2021
Accepted: 17 January 2021
Published: 25 January 2021

Publisher's Note: MDPI stays neutral with regard to jurisdictional claims in published maps and institutional affiliations.



Copyright: © 2021 by the authors. Licensee MDPI, Basel, Switzerland. This article is an open access article distributed under the terms and conditions of the Creative Commons Attribution (CC BY) license (<http://creativecommons.org/licenses/by/4.0/>).

Keywords: non-furanic humins; furanic humins; humic acid; fulvic acid; wood adhesives; wood panels; thermosetting adhesives; polyurethanes; NIPU

1. Introduction

Recently, furanic humins derived from the acid treatment of pure fructose have been the focus of attention for the preparation of various foams and resins [1–10]. This interest was prompted by a Netherlands company having developed a novel process of industrialization to render commercially available this type of interesting material [11]. Unfortunately, up to today, such a process does not seem as yet to have been commercialized, simply because the production unit appears to be still being built.

However, mixed-furanic but predominantly non-furanic humins are abundantly produced by many factories around the world and on several continents. Such humins are a material obtained from humic substances, particularly rich in humic and fulvic acids.

The organic components of soil can be subdivided into fractions that are soluble, largely humic acids, and insoluble, the humins.

Humins make up about 50% of the organic matter in soil. Humins are also produced during the dehydration of sugars, as occurs during the conversion of lignocellulosic biomass to smaller, higher-value organic compounds such as 5-hydroxymethylfurfural (HMF). These humins can be in the form of either viscous liquids or solids depending on the process conditions used. Such humins have a polymeric furanic-type structure, with hydroxyl, aldehyde and ketone functionalities. However, their structure is dependent on feedstock type (e.g., xylose or glucose) or concentration, reaction time, temperature, catalysts and many other parameters involved in the process [12]. They are used in agriculture to enhance fertilizers' effect and absorption by increasing soil fertility, as foliar fertilizers, in the pharmaceutical-cosmetic field [13], in the preparation of catalytic materials [14] and in material applications. However, depending on their origin they appear to predominantly contain humic acids, fulvic acid and also a minor but still noticeable proportion of furanic materials.

Polyurethanes are ubiquitous and very versatile products used today for a great variety of material applications. They are industrially prepared by the reaction of polyols with isocyanates. Great strides have been successfully made to prepare them from bio-sourced polyols. However, isocyanates are the key material to produce them, but they present the problem to be classed as toxic. It is for such a reason that chemical synthesis routes to prepare non-isocyanate polyurethanes have been developed [15–23]. Polyurethanes are used as wood adhesives in structural glulam and finger-jointing. Polymeric diphenylmethane diisocyanate (p-MDI) is also used for wood panel adhesives. The toxicity of p-MDI has again focused research on its substitution by preparing polyurethanes without isocyanates (NIPU).

Several approaches are used to prepare non-isocyanate polyurethanes, namely by reacting hydroxyl group-carrying materials with one or two cycles organic carbonates or CO₂ and diamines [15–24]. All these are using oil-derived synthetic-based materials to prepare NIPUs. More recently, successful attempts to produce NIPUs from natural materials rich in hydroxyl groups have been reported [25–35]. These have the additional characteristic to have simplified the procedure by using a cheaper aliphatic carbonate by eliminating the reaction of preparing cyclic carbonates [25–35]. Among these, glucose- and sucrose-based NIPUs prepared with dimethyl carbonate and hexamethylene diamine were used to bond wood joint and particleboard with encouraging results [32,33].

Thus, non-isocyanate polyurethanes are an interesting route to pursue, considering mixed predominantly non-furanic humins are rich in a number of hydroxyl groups and amino groups. The work described here is then aimed at preparing an NIPU thermosetting wood panel adhesive based on predominantly non-furanic humins and presenting good bonding characteristics.

2. Materials and Methods

2.1. Materials

Gerhumin® (a registered predominantly non-furanic humins solution) was supplied by L.Gobbi S.r.L. (Campo Ligure, Italy). Gerhumin® is extracted in Germany by E. Gerlach GmbH (Lübbecke, Germany). Gerhumin® solution contains 21% solids, 80% of which are organic materials, and 61% of the total solids are humic substances, with 0.7% organic nitrogen on dry material and C/N ratio of 57.1, and pH 9–10. Commercial Mimosa bark condensed tannin extract was supplied by Silva Chimica (St. Michele Mondovi', Italy). Hexamethylene diamine 98%, and dimethyl carbonate (DMC) were bought from Sigma-Aldrich (Saint Louis, France).

2.2. Preparation of Humins-NIPU Adhesives

Four resins were prepared using Gerhumin®. One was prepared with the humins solution alone. Three of them were prepared using Gerhumin® in combination with mimosa bark tannin extract, this latter used to increase the bonding strength of the humin-based adhesives.

Resin A,

Step 1: 20 g tannin + 15 g Gerhumin® + 5 g H₂O + 13.5 g DMC, at 60 °C for 1.5 h;

Step 2: 38.8 g of diamine, at 90 °C for 2 h.

Resin characteristics: viscosity at 23 °C 1620–1650 mPa.s; solids content 54.5%.

Resin B,

Step 1: 40 g Gerhumin® + 13.5 g DMC, at 60 °C for 1.5 h;

Step 2: 38.8 g of diamine, at 90 °C for 2 h.

After the end of the reaction, to obtain the final solid content of 45%, rotary evaporation under reduced pressure was used.

Resin characteristics: viscosity at 23 °C 520–540 mPa.s; solids content 45%.

Resin C,

Step 1: 20 g tannin + 16.67 g H₂O + 13.5 g DMC, at 60 °C for 1.5 h;

Step 2: 15 g Gerhumin®, 90 °C for 1 h;

Step 3: 38.8 g of diamine, 90 °C for 1 h.

Resin characteristics: viscosity at 23 °C 1050–1120 mPa.s; solids content 52.3%.

Resin D,

Step 1: 20 g tannin + 16.67 g H₂O + 13.5 g DMC, at 60 °C for 1.5 h;

Step 2: 38.8 g of diamine + 15 g Gerhumin®, at 90 °C for 2 h.

Resin characteristics: viscosity at 23 °C 1230–1310 mPa.s; solids content 51.7%.

2.3. ATR-FT-MIR Analysis

All of the samples were analyzed with a Perkin-Elmer Frontier ATR-FT-MIR provided by an ATR Miracle diamond crystal. The powder and liquid samples were laid on the diamond eye (1.8 mm) of the ATR equipment and the contact for the sample was ensured by tightly screwing the clamp device. Each extract was scanned registering the spectrum with 32 scans with a resolution of 4 cm⁻¹ in the wave number range between 600 and 4000 cm⁻¹.

2.4. Matrix-Assisted Laser Desorption Ionization Time-of-Flight (MALDI-ToF) Spectrometry Analysis

The original Gerhumin solution and the four resins prepared were examined by MALDI ToF spectrometry. The samples for analysis were prepared by first dissolving 7.5 mg of sample powder in 1 mL of a 50:50 v/v acetone/water solution. Then 10 mg of this solution was added to 10 µL of a 2,5-dihydroxy benzoic acid (DHB) matrix. The locations dedicated to the samples on the analysis plaque were first covered with 2 µL of a NaCl solution 0.1 M in 2:1 v/v methanol/water, and pre-dried. Then 1.5 µL of the sample solution was placed on its dedicated location and the plaque was dried again. Red phosphorous was to standardize the MALDI equipment. MALDI-ToF spectra were obtained using an Axima-Performance mass spectrometer from Shimadzu Biotech (Kratos Analytical Shimadzu Europe Ltd., Manchester, UK) using a linear polarity-positive tuning mode. The measurements were carried out making 1000 profiles. The spectra were accurate to ±1 Da.

2.5. Thermomechanical Analysis (TMA)

The resins were tested by thermomechanical analysis. Matched wood plies were used to minimize the variation due to the wood substrate used. The samples were prepared by applying each adhesive between two beech wood plies, with dimensions of 21 × 6 × 1.1 mm. These beech-resin-beech sandwiches were tested in non-isothermal mode between 25 and 250 °C at a heating rate of 10 °C/minute with Mettler Toledo 40 TMA equipment (Mettler Toledo, Zurich, Switzerland). They were tested in three-point bending on a span of 18 mm exercising a force cycle of 0.1/0.5 N on the specimens, with each force cycle of 12 s (6 s/6 s). The classical mechanics relationship between force and deflection can be expressed as

$$E = [L^3/(4bh^3)][F/(f_{\text{wood}} - f_{\text{adhesive}})]$$

where L = the length of the sample; b = its width; h = its thickness; F = the force applied; f_{wood} is the deflection of the wood and f_{adhesive} the deflection of the wood adhesive sandwich under test. This equation allows the calculation of the Young's modulus E (modulus of elasticity, MOE) for each case tested. Such a measuring system has been introduced and is used to follow the progressive hardening of the adhesive with the increase of temperature and to indicate comparatively if an adhesive system is faster or slower hardening and if it gives stronger joints than another one.

2.6. Wood Particleboard Preparation and Testing

Duplicate one-layer particleboard panels of 350 × 350 × 14 mm dimensions were prepared by adding 10% of the resin solids mixture on dry wood particles for a percentage wood moisture content of the resinated particles of 13% and pressed at a maximum pressure of 28 kg/cm², followed by a pressure-decreasing pressing cycle at 220 °C for a 10 min pressing cycle. The target density of the panels was 720 kg/m³. The panels, after light surface sanding, were tested for dry internal bond (IB) strength (EN 312) [36].

3. Results and Discussion

The dry internal bond (IB) strength results of the laboratory one-layer wood particleboard panels are shown in Table 1. The results indicate that all four types of NIPU resins satisfied the requirement of the relevant European norm [36] for interior grade particleboard panels. It can be noted that the pure humins NIPU resin presented the lowest IB strength value, although this was still well above the requirements of the standards. The tannin–humins NIPU presented better IB strength although these values were rather different for each resin due to the differences in their preparation procedure. Resin A was prepared by premixing tannin and humins and carbonating their mixture with DMC, then the carbonated mixture was reacted with the diamine.

Resin C and D were prepared using the same material proportions but with a different procedure. Thus, in resin C the tannin alone was first carbonated by reaction with DMC, then reacted with the humins for 1 h, and only after this was the mixture reacted with hexamethylene diamine for 1 h.

In resin D, the tannin alone was first carbonated with DMC, then reacted with the premixed humins and diamine.

The difference in preparation procedure does account for the different bonding performance of the A, C and D adhesives, although these differences are not too big. Thus, in resin A, both tannin and humins were carbonated simultaneously and almost equally, ensuring a greater variety of urethane-like linkages in the resin.

In resin C, the tannin was instead first and predominantly carbonated, with the humins reacting both with the pre-carbonated tannin but also with the DMC still unreacted. This means that in resin C one could expect urethane linkages mainly, but not only, involving the tannin, but with the humin-linked urethanes being possibly in the minority.

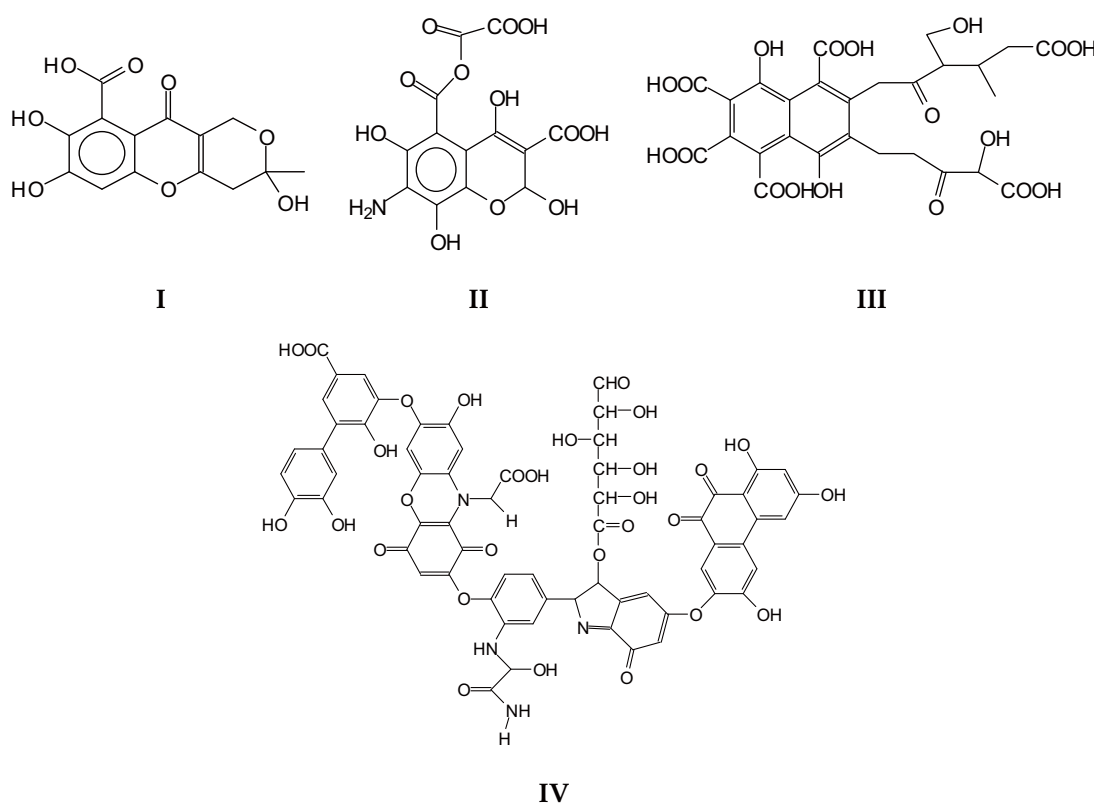
In resin D, the pre-carbonated tannin was instead reacted with the humins + diamine premix, most likely ensuring a more equitable partition of urethane linkages on both tannin and humins.

Table 1. Results of particleboard tests with the experimental non-furanic-based non-isocyanate polyurethane (NIPU) wood adhesives.

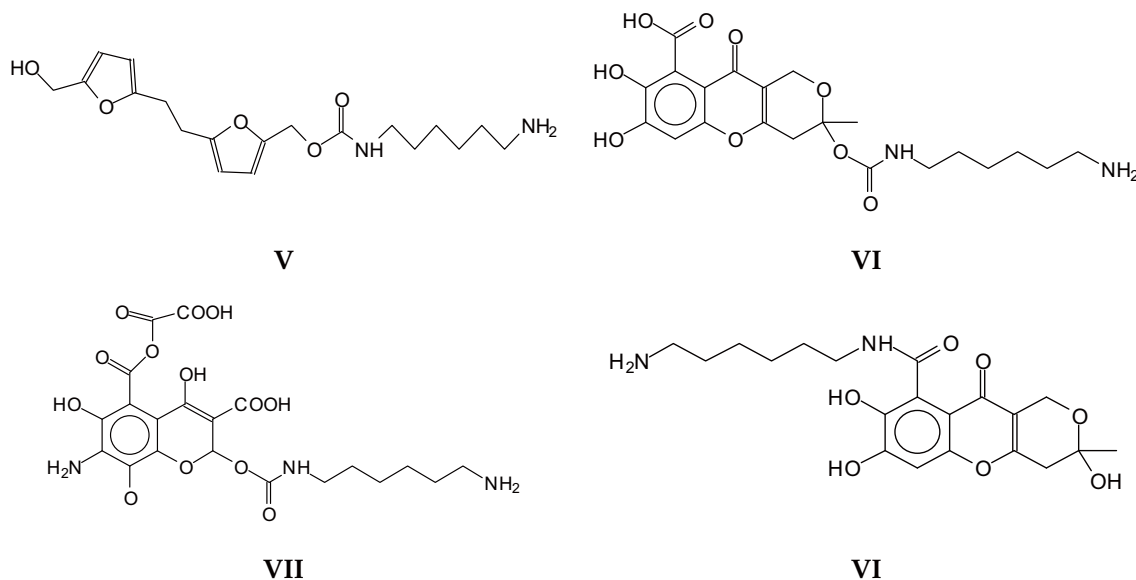
Samples	Density (g/cm ³)	Internal Bond (MPa)	Bending Strength (MPa)	Elastic Modulus (MPa)
A-220 °C	0.77 ± 0.03	0.70 ± 0.08	14.1 ± 1.4	6700.8 ± 523.5
B-220 °C	0.73 ± 0.02	0.44 ± 0.04	6.4 ± 0.4	968.6 ± 34.2
C-220 °C	0.73 ± 0.01	0.65 ± 0.07	12.9 ± 2.0	4081.5 ± 56.0
D-220 °C	0.75 ± 0.03	0.74 ± 0.01	14.4 ± 2.7	4805.2 ± 80.7
EN requirements		≥0.35		

The IB strength results confirm that addition of tannin to yield mixed tannin–humins adhesive resins yield better results than the humins alone. The IB strength results also confirm these differences with resin A and resin D yielding a better IB strength due to the better partition of urethane linkage between tannin and humins, while in resin C a slightly larger part of the humins were either unreacted or not linked.

It is of interest to determine which species were formed for the different resins and what for each of them were the predominant ones. Thus, the structures present in the mix of predominantly non-furanic humins were determined by MALDI ToF (Figure 1). The mix was composed mainly of fulvic acid (I), fulvic acid derivatives (II) and (III), several humic acid fragments (IV) and several other non-furanic structures, and also of some furanic oligomers. Some mono- and di-lignans were also present. The list of the structures present and the relevant MALDI ToF spectra are shown in the Supplementary Materials (Table S1, Figure S1a–g).

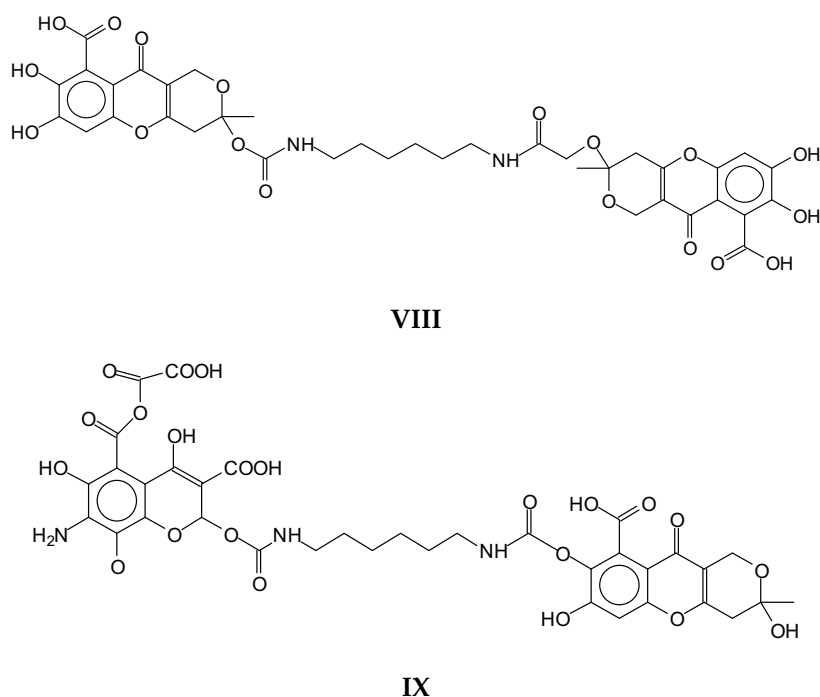


The reaction of the four different formulations of thermosetting NIPU resins confirms the co-reaction of the different components. Thus, for the NIPU resin prepared from non-furanic humins the oligomers formed were urethane-bonded species that had formed by reaction of fulvic acid and derivatives with DMC and diamine, and also furanic species reacted to form NIPUs by reaction with DMC and diamine. These are shown by the following species assigned to the MALDI ToF spectrum peaks at 364 Da (V) furanic, 452 Da (VI) fulvic, non-furanic, with two possible structures at 512 Da (VII) fulvic, non-furanic.

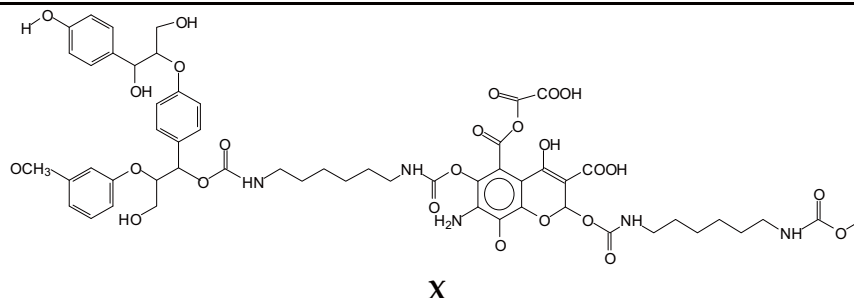


The two possible (VI) structures indicate that the urethane bond can form either on the alcoholic $-OH$ of the fulvic acid structure, or alternatively could form an amide by reaction on the acid moiety of fulvic acid.

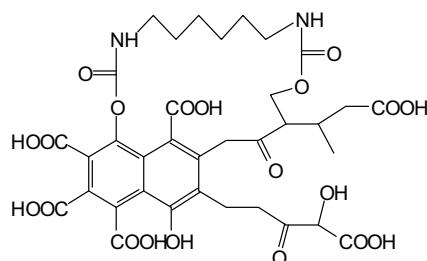
Characteristic dimers and higher oligomers were also found, such as at 796 Da (VIII) non-furanic and with different species linked by the urethane linkages, such as at 847 Da (IX) non-furanics.



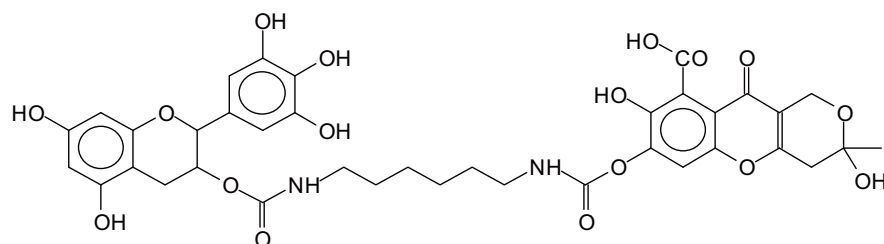
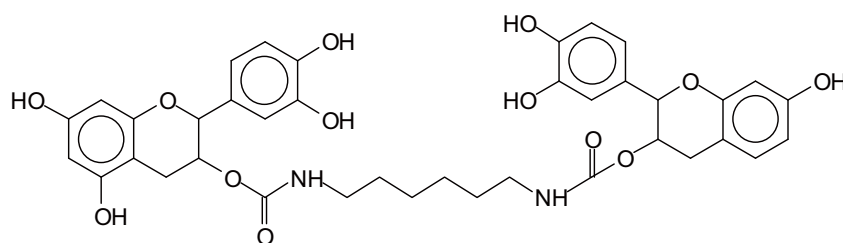
Fulvic acid-derived urethanes linked to lignans present in the predominantly non-furanic humins mix were also identified, such as at 1193 Da (X).



Equally present were some more rare cyclic structures obtained from fulvic acid derivatives where this was possible, such as for the structure at 828 Da (XI).



For the other adhesive resins where mimosa tannin was used as a reaction support for the non-furanic humins mix to prepare the resins, structures involving mixed urethane oligomers involving all the different types of species were identified. Thus urethane linkages between two flavonoids did occur, such as at 732 Da (XII), and between a flavonoid and fulvic acid at 781 Da (XIII), and between flavonoids and humic acid fragments at 1096 Da (XIV).



cm^{-1} assigned to asymmetric and symmetric stretching of alkane chains, and the peaks characteristics of ether groups, present in both the humins and the tannin at 1240 (shoulder), 1029 and 832 cm^{-1} . In the case of the FTIR spectrum of resin B, there was also a small but clear peak at 923 cm^{-1} assigned to the few carboxylic acids present in the humins. The profile of resin C was slightly different from the profile of resin A (and D) with the peaks indicating the formation of urethanes, in particular the peak at 3400 cm^{-1} being of much lower intensity (Figures 2, 4 and 5). In fact, the procedure of preparation of resin C at lower temperature, coupled with the order of addition of the reagents, suggests that the proportion of urethane linkages in this resin was lower than in resins A and D. This is supported also by the lower IB strength of the particleboards bonded with it in Table 1.

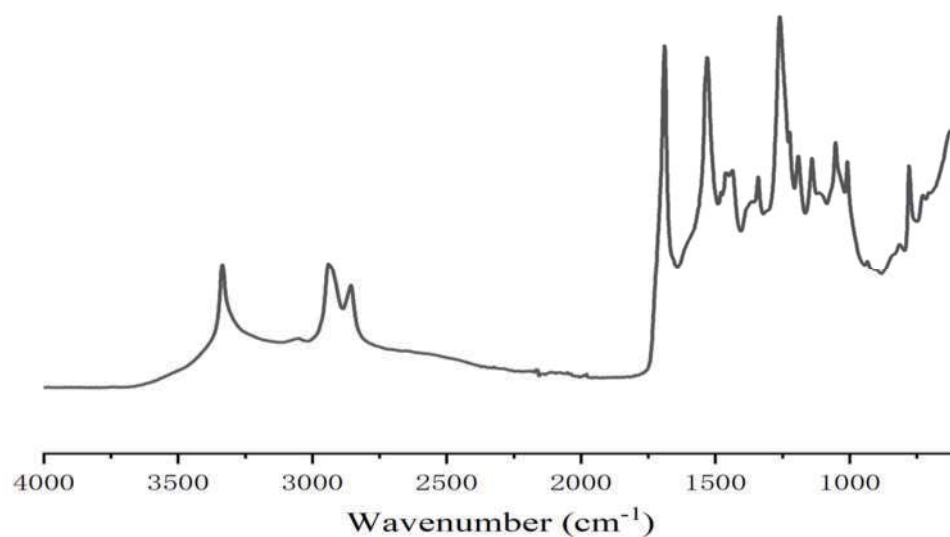


Figure 2. FTIR spectrum of tannin-humin NIPU resin A.

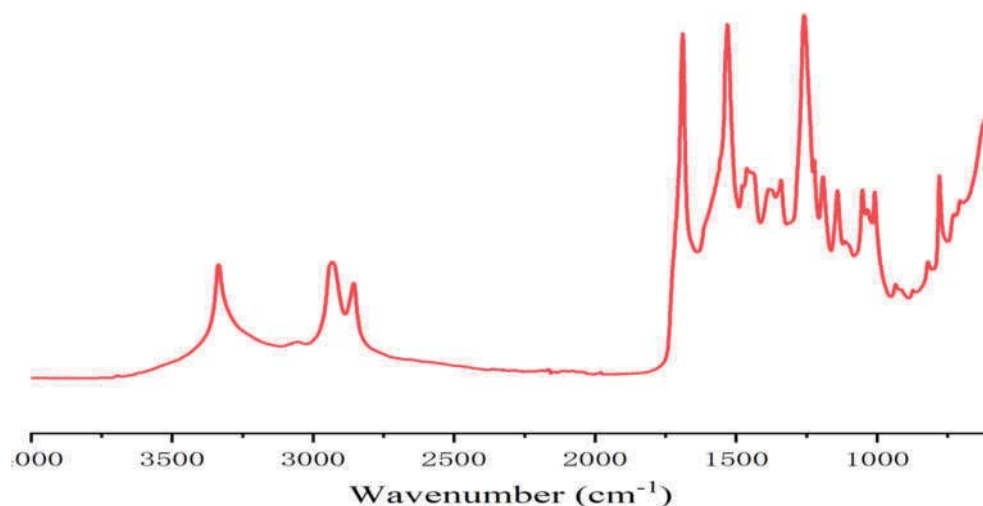


Figure 3. FTIR spectrum of pure humin NIPU resin B.

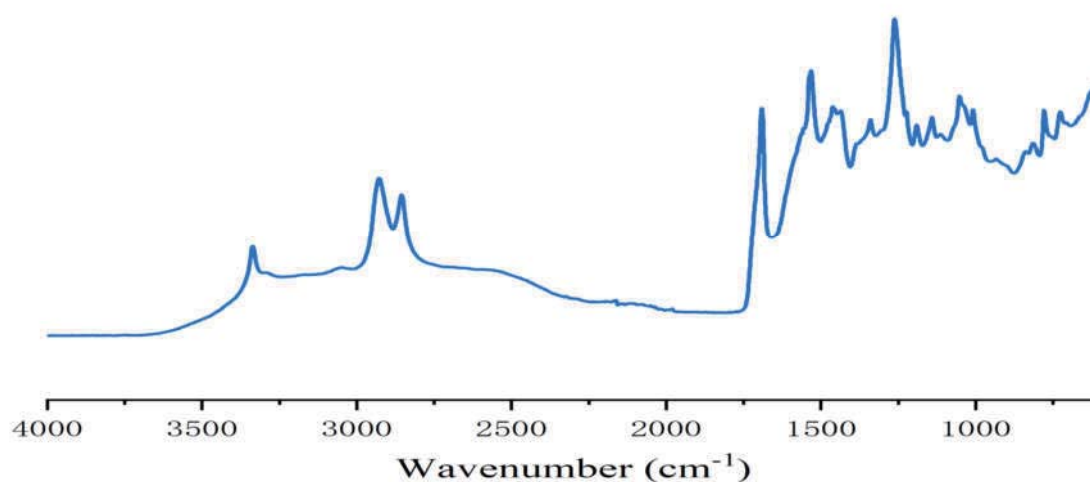


Figure 4. FTIR spectrum of tannin-humin NIPU resin D.

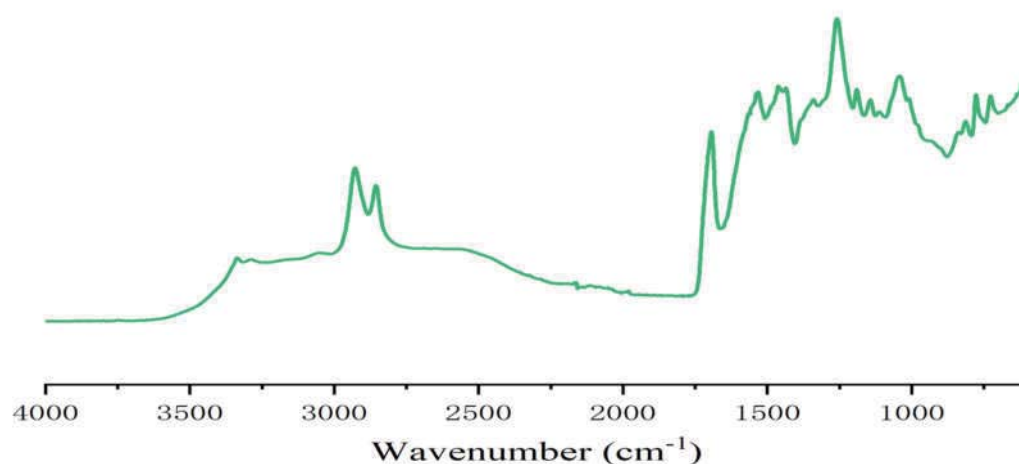


Figure 5. FTIR spectrum of tannin-humin NIPU resin C.

It is of interest to try to understand why resin B, which was a humins-only-based NIPU resin, gave IB strength values that, while passing the requirements of relevant standards, were much lower than the tannin-humin NIPU resins A, C and D. The reasons could be several, such as a higher energy of activation of curing for resin B, a lower reactivity of the resin or a lower level of cross-linking due to a lower proportion of reactive sites on the humins themselves. For this, curing of the resins in a thermomechanical apparatus showed that the increase of the modulus of elasticity (MOE) as a function of the increase in temperature was very different for resins B and A (which had a similar curve to that of resins C and D) (Figure 6). In Figure 6 both resins A and B show two peaks of the MOE value, but while the first peak is of similar intensity, the second one has a much higher MOE value for resin A. Moreover, the first peak has its maximum at 120 °C for resin A and at 135 °C for resin B, while the second peak occurs at the equivalent temperature of 220 °C for both resins.

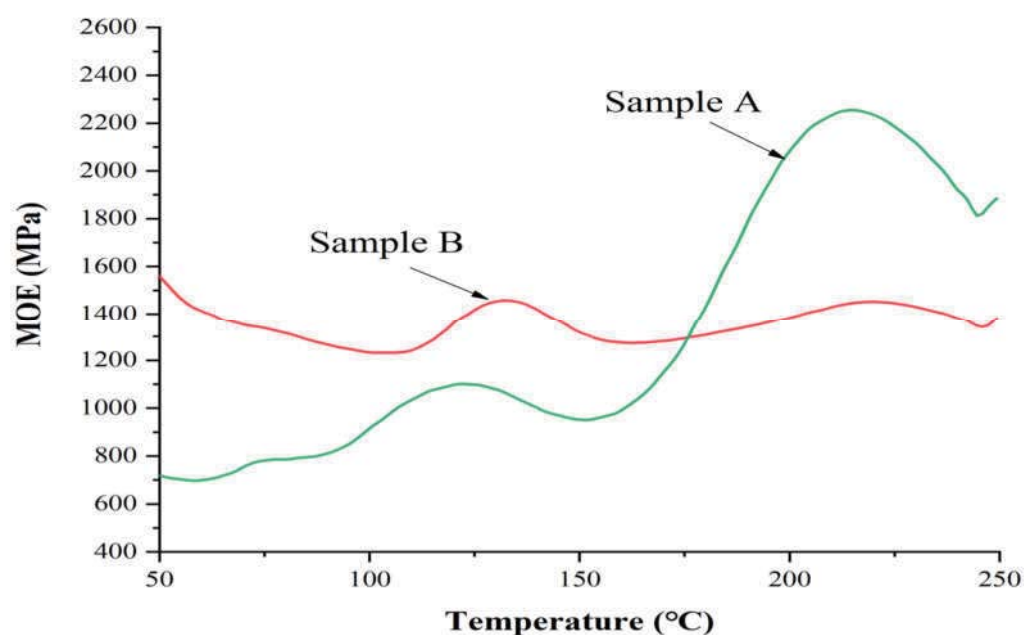


Figure 6. Thermomechanical analysis (TMA) traces for resins A and B.

The two peaks were due to the formation of hardened networks of different nature. The higher temperature of the first peak for resin B indicates that this resin presented possibly a higher energy of activation of curing, possibly coupled with the lower solids content and its lower viscosity. The reason of the much higher modulus of elasticity (MOE) value of the second peak for resin A was due to a far better chemical cross-linking due to the contribution of the very reactive tannin to the network. The differences in the intensity of the second peak for resins A and B cannot be ascribed to differences of the wood substrate, as matched wood samples of even grain from the same piece of veneer were used. Thus, the inference is that the pure humins resin B had a level of ultimate cross-linking much lower due to a lower proportion of reactive sites on the humins themselves, as evidenced looking at the respective structures involved.

The lower temperature peak indicates the formation of an unstable network that is degraded and transformed if the temperature is increased, causing a marked internal re-arrangement. The second peak at higher temperature indicates that curing of the NIPU resin occurred at a high temperature, as already reported in previous literature for similar types of adhesives [32,33]. The increase of Young's modulus has been shown to correlate with the bonding strength of the adhesive [37–42].

It is interesting to speculate as to what was the cause of the marked decrease between the two modulus of elasticity (MOE) peaks in Figure 6. While it could be an unstable structure, a more likely reason could derive from the increase in length of linear oligomers progressively forming a physically entangled network, rather than a chemically cross-linked one. As the temperature increased further, the Brownian movements would make the viscosity of these physically entangled chains markedly decrease and extensively disentangle. The modulus of elasticity (MOE) then started again to increase at the much higher temperature of the second peak once chemical cross-linking finally occurred.

Before the TMA curve of the B resin showed an increase in the modulus value, the overall trend of the modulus value decreased between 50 and 110 °C. This was possibly due to the lower solids content, lower viscosity and higher water allowing the decrease of viscosity due to the increase of temperature to be the effect that predominates on the slow oligomers linear growth. Resin A did not show this trend, its initial viscosity allowing the linear growth of the oligomers to be detected by a slow initial increase of the modulus of elasticity (MOE). Conversely, the adhesive penetrated into the wood, softening or degrading it during heating, thus reducing its strength. It is evident from the TMA traces that the curing temperature leading to

chemical cross-linking was high, starting at 150–160 °C. This means that the hardening temperature to be used for such adhesives is relatively higher than what is common today for equivalent panels bonded with traditional adhesives. After 200 °C, degradation of the wood substrate is known to start [37,40–42], thus for the second peak one needs to consider that wood degradation had already started to occur at the same time, and thus the hardening of the resin was better than what appears from the TMA curves for both resins. The decrease of the curve after the second peak was due to the continuing degradation of the wood substrate.

4. Conclusions

Non-isocyanate polyurethane (NIPU) resins were prepared using commercial humins predominantly composed of fulvic acid and its derivatives, and of humic acid, but also presenting some polyfuranic and lignan structures in their mix. The NIPU resins were prepared by using just the humins or by using a mimosa-condensed tannin–humins mix. FTIR and MALDI ToF spectrometry allowed the identification of the original constituents mix in the humins as well as the NIPU oligomers formed in the reactions used. It appeared that all the different constituents in the humins reacted to form NIPU oligomers. Thus, fulvic acid and its derivatives, humic acid and its fragments, and the furanic and lignan structures present all reacted to form NIPU constituents and contributed to the formation of NIPU resins. Interestingly, humins constituents NIPU oligomers, tannin NIPU oligomers and even several mixed NIPU species derived from the co-reaction of condensed tannin units and humins constituents were also formed. These latter ones showed that in the case of the tannin–humins NIPU both the two biomaterials formed a unitary, all-linked network. TMA was used to assess the resins' curing behavior and showed that two temperatures of curing appeared to occur, the first at around 130 °C and the second around 220 °C. The first appeared to indicate the linear growth of oligomers leading to a physically entangled network which then disentangled and proceeded at the higher temperature to form a chemically cross-linked network. The final cross-linked network appeared to be markedly less cross-linked for the pure humins NIPU resin than for the tannin–humins ones. This was confirmed by the internal bond (IB) strength values of the laboratory wood particleboard bonded with the two types of resin, which was lower for the pure humins NIPU resin than for the tannin–humins ones. Nonetheless, the IB strength values of all the boards bonded with the two types of NIPU resins satisfied the requirements of the European norm for interior grade particleboards.

Supplementary Materials: The following are available online at www.mdpi.com/2073-4360/13/3/372/s1, Table S1 Assignments of oligomer structures present in Gerhumins predominantly non-furanic humins; Table S2. MALDI ToF assignment of oligomers present in tannin–Gerhumins NIPU resin A; Table S3. MALDI ToF assignment of oligomers present in pure Gerhumins NIPU resin B; Table S4. Relative intensity of MALDI peaks for non-furanic humins and tannin–humins NIPU resins; Figure S1a–g: MALDI ToF spectra details of different Da intervals of raw Gerhumins, corresponding to the structures assigned in Table S1; Figure S2a–d: MALDI ToF spectra details of different Da intervals of tannin–Gerhumins NIPU resin A, corresponding to the structures assigned in Table S2; Figure S3a–f: MALDI ToF spectra details of different Da intervals of pure Gerhumins NIPU resin B, corresponding to the structures assigned in Table S3.

Author Contributions: conceptualization, X.C. and A.P.; methodology, X.C., H.E. and A.P.; validation, X.C., A.P., E.F. and C.G.; particleboard preparation X.C. and H.E.; MALDI ToF, FTIR and TMA analysis, X.C.; MALDI ToF, FTIR and TMA interpretation A.P.; investigation, X.C., H.E. and E.F.; resources, A.P.; writing—original draft preparation, A.P.; writing—review and editing, A.P., C.G., N.G. and N.S.; supervision, A.P.; project administration, A.P., E.F. and C.G.; funding acquisition, A.P. All authors have read and agreed to the published version of the manuscript.

Funding: This research received no external funding.

Acknowledgments: The first author thanks the China Scholarship Council for the study bursary granted to him. The LERMAB of the University of Lorraine is supported by a grant overseen by the French National Research Agency (ANR) as part of the Laboratory of Excellence (Labex) ARBRE. Silva Chimica is thanked for supplying the tannin and procuring Gerhumins.

Conflicts of Interest: The authors declare no conflict of interest.

References

1. Sangregorio, A.; Guigo, N.; van der Waal, J.C.; Sbirrazzuoli, N. Humins from Biorefineries as Thermoreactive Macromolecular Systems. *ChemSusChem* **2018**, *11*, 4246–4255.
2. Sangregorio, A. Valorisation of Biorefinery-Derived Humins: Towards the Development of Sustainable Thermosets and Composites. Ph.D. Thesis, Université de la Côte d'Azur, Nice, France, 2019.
3. van Zandvoort, I.; Wang, Y.; Rasrendra, C.B.; van Eck, E.R.H.; Bruijninx, P.C.A.; Heeres, H.J.; Weckhuysen, B.M. Formation, Molecular Structure, and Morphology of Humins in Biomass Conversion: Influence of Feedstock and Processing Conditions. *ChemSusChem* **2013**, *6*, 1745–1758.
4. van Zandvoort, I.; Koers, E.J.; Weingarth, M.; Bruijninx, P.C.A.; Baldus, M.; Weckhuysen, B.M. Structural characterization of ¹³C-enriched humins and alkali-treated ¹³C humins by 2D solid-state NMR. *Green Chem.* **2015**, *17*, 4383–4392.
5. Hoang, T.M.C.; van Eck, E.R.H.; Bula, W.P.; Gardeniers, J.G.E.; Lefferts, L.; Seshan, K. Humin based by-products from biomass processing as a potential carbonaceous source for synthesis gas production. *Green Chem.* **2015**, *17*, 959–972.
6. Sangregorio, A.; Guigo, N.; de Jong, E.; Sbirrazzuoli, N. Kinetics and Chemorheological Analysis of Cross-Linking Reactions in Humins. *Polymers* **2019**, *11*, 1804, doi:10.3390/polym11111804.
7. Sangregorio, A.; Muralidhara, A.; Guigo, N.; Marlair, G.; Angelici, C.; Thygesen, L.G.; de Jong, E.; Sbirrazzuoli, N. Humins based resin for wood modification and properties improvement. *Green Chem.* **2020**, *22*, 2786–2798.
8. Mija, A.C.; de Jong, E.; van der Waal, J.C.; van Klink, G.P.M. Humins-Containing Foam. U.S. Patent No. 10,752,747, 25 August 2020.
9. Licsandru, E.; Mija, A.C. From biorefinery by-product to bioresins. Thermosets based on humins and epoxidized linseed oil. *Cell. Chem. Technol.* **2019**, *53*, 963–969.
10. Chen, X.; Guigo, N.; Pizzi, A.; Sbirrazzuoli, N.; Li, B.; Fredon, E.; Gerardin, C. Ambient Temperature Self-Blowing Tannin-Humins Biofoams. *Polymers* **2020**, *12*, 2732, doi:10.3390/polym12112732.
11. De Jong, E. Avantium, Amsterdam, The Netherlands, Private communication, 2020.
12. Heltzel, J.; Patil, S.K.R.; Lund, C.R.F.; Schlaf, M.; Zhang, Z.C. (Eds.) "Humin Formation Pathways". *Reaction Pathways and Mechanisms in Thermocatalytic Biomass Conversion II: Homogeneously Catalyzed Transformations, Acrylics from Biomass, Theoretical Aspects, Lignin Valorization and Pyrolysis Pathways*, Green Chemistry and Sustainable Technology; Springer: Singapore, 2016, pp. 105–118, doi:10.1007/978-981-287-769-7_5, ISBN 9789812877697.
13. L.Gobbi SRL., Gerhumin. Available online: <https://www.lgobbi.it/en/gerhumin-2/> (accessed on 1 June 2020).
14. Filiciotto, L.; Balu, A.M.; Romero, A.A.; Rodriguez-Castellon, E.; van der Waal, J.C.; Luque, R. Benign-by-design preparation of humin-based iron oxide catalytic nanocomposites. *Green Chem.* **2017**, *19*, 4423–4434.
15. Kathalewar, M.S.; Joshi, P.B.; Sabnis, A.S.; Malshe, V.C. Non-isocyanate polyurethanes: from chemistry to applications. *RSC Adv.* **2013**, *3*, 4110–4129.
16. Poussard, L.; Mariage, J.; Grignard, B.; Detrembleur, C.; Jérôme, C.; Calberg, C.; Heinrichs, B.; De Winter, J.; Gerbaux, P.; Raquez, J.-M.; et al. Non-isocyanate polyurethanes from carbonated soybean oil using monomeric or oligomeric diamines to achieve thermosets or thermoplastics. *Macromolecules* **2016**, *49*, 2162–2171.
17. Ochiai, B.; Utsuno, T. Non-isocyanate synthesis and application of telechelic polyurethanes via polycondensation of diurethanes obtained from ethylene carbonate and diamines. *J. Polym.Sci. Part A Polym. Chem.* **2013**, *51*, 525–533.
18. Figovsky, O.; Shapovalov, L.; Leykin, A.; Birukova, O.; Potashnikova, R. Recent advances in the development of non-isocyanate polyurethanes based on cyclic carbonates. *PU Mag.* **2013**, *10*, 1–9.
19. Rokicki, G.; Parzuchowski, P.G.; Mazurek, M. Non-isocyanate polyurethanes: Synthesis, properties, and applications. *Polym. Advan. Technol.* **2015**, *26*, 707–761.
20. Noreen, A.; Zia, K.; Zuber, M.; Ameer, S.T.; Zahoor, F. Bio-based polyurethane: An efficient and environment friendly coating systems: A review. *Prog. Org. Coat.* **2016**, *91*, 25–32.
21. Birukov, O.; Potashnikova, R.; Leykin, A.; Figovsky, O.; Shapovalov, L. Advantages in chemistry and technology of non-isocyanate polyurethane. *J. Sci. Israel-Technol. Advan.* **2014**, *16*, 3, 92–102.
22. Kathalewar, M.; Sabnis, A.; Waghoo, G. Effect of incorporation of surface treated zinc oxide on non-isocyanate polyurethane based nano-composite coatings. *Prog.Org.Coat.* **2013**, *76*, 1215–1229.
23. Grignard, B.; Thomassin, J.M.; Gennen, S.; Poussard, L.; Bonnaud, L.; Raquez, J.-M.; Dubois, P.; Tran, M.-P.; Park, C.B.; Jerome, C.; et al. CO₂-blown microcellular non-isocyanate polyurethane (NIPU) foams: from bio-and CO₂-sourced monomers to potentially thermal insulating materials. *Green Chem.* **2016**, *18*, 2206–2215.
24. Cornille, A.; Guillet, C.; Benyahya, S.; Negrell, C.; Boutevin, B.; Caillol, S. Room temperature flexible isocyanate-free polyurethane foams. *Eur. Polym. J.* **2016**, *84*, 873–888.
25. Thébault, M.; Pizzi, A.; Dumarcay, S.; Gerardin, P.; Fredon, E.; Delmotte, L. Polyurethanes from hydrolysable tannins obtained without using isocyanates. *Ind. Crop. Prod.* **2014**, *59*, 329–336.
26. Thébault, M.; Pizzi, A.; Essawy, H. A.; Barhoum, A.; Van Assche, G. Isocyanate free condensed tannin-based polyurethanes. *Eur. Polym. J.* **2015**, *67*, 513–526.

27. Thébault, M.; Pizzi, A.; Santiago-Medina, F.J.; Al-Marzouki, F.M.; Abdalla, S. Isocyanate-free polyurethanes by coreaction of condensed tannins with aminated tannins. *J. Renew. Mater.* **2017**, *5*, 1, 21–29.
28. Xi, X.; Pizzi, A.; Gerardin, C.; Du, G. Glucose-biobased Non-Isocyanate Polyurethane Rigid Foams. *J. Renew. Mater.* **2018**, *7*, 301–312.
29. Xi, X.; Pizzi, A.; Gerardin, C.; Lei, H.; Chen, X.; Amirou, S. Preparation and evaluation of Glucose based Non-Isocyanate polyurethane Self-blowing Rigid Foams. *Polymers* **2019**, *11*, 1802.
30. Chen, X.; Li, J.; Xi, X.; Pizzi, A.; Zhou, X.; Fredon, E.; Du, G.; Gerardin, C. Condensed Glucose-Tannin-based NIPU BioFoams of Improved Fire Retardancy. *Polym. Degrad. Stabil.* **2020**, *175*, 109121.
31. Chen, X.; Xi, X.; Pizzi, A.; Fredon, E.; Zhou, X.; Li, J.; Gerardin, C.; Du, G. Preparation and Characterization of Condensed Tannin Non-Isocyanate Polyurethane (NIPU) Rigid Foams by Ambient Temperature Blowing. *Polymers* **2020**, *12*, 750.
32. Xi, X.; Pizzi, A.; Delmotte, L. Isocyanate-Free Polyurethane Coatings and Adhesives from Mono-and Di-Saccharides. *Polymers* **2018**, *10*, 402.
33. Xi, X.; Wu, Z.; Pizzi, A.; Gerardin, C.; Lei, H.; Zhang, B.; Du, G. Non-isocyanate polyurethane adhesive from sucrose used for particleboard. *Wood Sci. Technol.* **2019**, *53*, 393–405.
34. Santiago-Medina, F.J.; Basso, M.C.; Pizzi, A.; Delmotte, L. Polyurethanes from Kraft lignin without using isocyanates. *J. Renew. Mater.* **2018**, *6*, 413–425.
35. Pizzi, A. Tannin-based Biofoams. *J. Renew. Mater.* **2019**, *7*, 477–492.
36. European Norm EN 312-2010. *Particleboards-Specifications*; European Commission, Bruxelles, Belgium, 2010.
37. Pizzi, A.; Garcia, R.; Deglise, X. Thermomechanical analysis of entanglement networks—Correlation of some calculated and experimental parameters. *J. Appl. Polym. Sci.* **1998**, *67*, 1673–1678.
38. Kamoun, C.; Pizzi, A. Particleboard IB forecast by TMA bending in MUF adhesives curing. *Holz Roh Werkst.* **2000**, *58*, 4, 288–289.
39. Lecourt, M.; Humphrey, P.; Pizzi, A. Comparison of TMA and ABES as forecasting systems of wood bonding effectiveness. *Holz Roh Werkst.* **2003**, *61*, 1, 75–76.
40. Garcia, R.; Pizzi, A. Cross-linked and entanglement networks in thermomechanical analysis of polycondensation resins. *J. Appl. Polym. Sci.* **1998**, *70*, 1111–1116.
41. Kamoun, C.; Pizzi, A.; Garcia, R. The effect of humidity on cross-linked and entanglement networking of formaldehyde-based wood adhesives. *Holz Roh Werkst.* **1998**, *56*, 235–243.
42. Pizzi, A.; Lu, X.; Garcia, R. Lignocellulosic substrates influence on TTT and CHT curing diagrams of polycondensation resins. *J. Appl. Polym. Sci.* **1999**, *71*, 915–925.

3.2 Isolat de protéine de soja Non-isocyanates Polyuréthanes (NIPU) Adhésifs pour bois

Résumé: L'isolat de protéine de soja (SPI) a été utilisé pour préparer des adhésifs thermodurcissables à base de polyuréthane sans isocyanate (NIPU) pour panneaux de bois en le faisant réagir avec du carbonate de diméthyle (DMC) et de l'hexaméthylène diamine. Des oligomères linéaires et ramifiés ont été obtenus et identifiés, indiquant comment de telles structures oligomères pourraient se réticuler davantage pour former un réseau durci. Des structures inhabituelles ont été observées, à savoir des liaisons uréthane dérivées de l'acide carbamique couplées à des structures de lactame. Le durcissement de l'adhésif a été suivi d'une analyse thermomécanique (TMA). processus en deux étapes: tout d'abord, à une température plus basse (maximum 130°C), la croissance d'oligomères linéaires s'est produite, formant finalement un réseau physiquement enchevêtré. Celui-ci a semblé s'effondrer et se démêler, provoquant une diminution de la MOE lorsque la température augmente. semble être due aux mouvements browniens de plus en plus marqués des chaînes d'oligomères linéaires avec l'augmentation de la température. s'ensuivent, formant un réseau durci, comme l'a montré l'analyse thermomécanique (TMA) montrant deux pics de MOE distincts, l'un autour de 130°C et l'autre autour de 220°C, avec une diminution très marquée de la MOE entre les 2. Des panneaux de contreplaqué ont été préparés et collés avec l'adhésif pour bois SPI-NIPU et les résultats obtenus sont présentés. L'adhésif a semblé répondre confortablement aux exigences de résistance à sec des normes pertinentes, se révélant adapté aux panneaux de contreplaqué de qualité intérieure. Il n'a pas passer les exigences des tests humides. Cependant, l'ajout de 15% d'éther diglycidyle de glycérol a amélioré les résultats des tests humides mais toujours pas assez pour satisfaire les exigences des normes.

Mots clés: Colles à bois biosourcées; isolat de protéine de soja; les polyuréthanes non isocyanates (NIPU) ; panneaux de bois; MALDI-ToF.

**ARTICLE****Soy Protein Isolate Non-Isocyanates Polyurethanes (NIPU) Wood Adhesives****Xinyi Chen^{1,2}, Antonio Pizzi^{1,*}, Xuedong Xi^{1,2}, Xiaojian Zhou², Emmanuel Fredon¹ and Christine Gerardin³**¹LERMAB, University of Lorraine, Epinal, 88000, France²Yunnan Key Laboratory of Wood Adhesives and Glue Products, Southwest Forestry University, Kunming, 650224, China³LERMAB, University of Lorraine, Nancy, 54000, France

*Corresponding Author: Antonio Pizzi. Email: antonio.pizzi@univ-lorraine.fr

Received: 19 November 2020 Accepted: 11 December 2020

ABSTRACT

Soy-protein isolate (SPI) was used to prepare non-isocyanate polyurethane (NIPU) thermosetting adhesives for wood panels by reacting it with dimethyl carbonate (DMC) and hexamethylene diamine. Both linear as well as branched oligomers were obtained and identified, indicating how such oligomer structures could further cross-link to form a hardened network. Unusual structures were observed, namely carbamic acid-derived urethane linkages coupled with lactam structures. The curing of the adhesive was followed by thermomechanical analysis (TMA). It appeared to follow a two stages process: First, at a lower temperature (maximum 130°C), the growth of linear oligomers occurred, finally forming a physically entangled network. This appeared to collapse and disentangle, causing a decrease of MOE, as the temperature increases. This appears to be due to the ever more marked Brownian movements of the linear oligomer chains with the increase of the temperature. Second, chemical cross-linking of the chains appeared to ensue, forming a hardened network. This was shown by the thermomechanical analysis (TMA) showing two distinct MOE maxima peaks, one around 130°C and the other around 220°C, with a very marked MOE decrease between the two. Plywood panels were prepared and bonded with the SPI-NIPU wood adhesive and the results obtained are presented. The adhesive appeared to pass comfortably the requirements for dry strength of relevant standards, showing to be suitable for interior grade plywood panels. It did not pass the requirements for wet tests. However, addition of 15% of glycerol diglycidyl ether improved the wet tests results but still not enough to satisfy the standards requirements.

KEYWORDS

Bio-based wood adhesives; soy protein isolate; non-isocyanate polyurethanes (NIPU); wood panels; MALDI ToF

1 Introduction

Soy protein has been and is one of the protein of choice to formulate wood adhesives. This is so as it is a renewable raw material of vegetable origin, widely available, and relatively inexpensive [1]. It can be applied (i) in several forms as an additive to traditional synthetic wood adhesives, or (ii) used as a wood adhesive after partial hydrolysis and modifications [2]. Nonetheless, this adhesive material presents a few drawbacks, such as an insufficient water resistance, its improvement being one of the subjects of present research. The approach most generally used to improve this aspect is by adding a chemical cross-linker to



soy protein isolate [3–9]. More recently good results have been obtained by reinforcing soy adhesives with condensed tannins [10–12] as well by preparing wood adhesives from soy flour by generating higher molecular weight, non-volatile non-toxic aldehydes by periodate specific oxidation [13,14].

Polyurethanes are a ubiquitous and widely used material for a number of applications, such as coatings, varnishes, foams and wood adhesives in structural glulam and finger-jointing. Polyurethanes are today prepared using polymeric isocyanate. However, isocyanates are classed as toxic. Polymeric diphenylmethane diisocyanate (p-MDI) is used for wood adhesives. p-MDI is also used as a modifier/crosslinker to improve the performance of protein adhesives [15,16]. The toxicity of p-MDI has focused research on its substitution by preparing polyurethanes without isocyanates (NIPU). Several approaches are used for this, namely by reacting hydroxyl groups-carrying materials with one or two cycles organic carbonates or CO₂ and diamines [17–21]. This research has mainly been directed to the preparation of foams and coatings [22–26]. All these are using oil-derived synthetic-based materials to prepare NIPUs. More recently, successful attempts to produce NIPUs from natural materials rich in hydroxyl groups have been reported [27–37]. These have the additional characteristic to have simplified the procedure by using a cheaper aliphatic carbonate by eliminating the reaction of preparing cyclic carbonates [27–37]. Among these, glucose- and sucrose-based NIPUs prepared with dimethyl carbonate and hexamethylene diamine were used to bond wood joint and particleboard with encouraging results [34,35]. Thus, soy-based non-isocyanate polyurethanes are an interesting route to pursue, considering the amount of hydroxyl groups and amino groups of which SPI's aminoacids are rich, and also considering the possibility of reaction of the numerous amide group of the peptide grouping in the constitutive skeletal chain of proteins. The work described here is then aimed at preparing a NIPU wood adhesive based on soy protein isolate presenting good bonding characteristics.

2 Experimental

2.1 Materials

Soy protein isolate was supplied by Ruikang Biotechnology Co., Ltd. (Dezhou, China). Commercial glycerol diglycidyl ether (GDE, technical grade), hexamethylene diamine 98%, and dimethyl carbonate were bought from Sigma-Aldrich (Saint Louis, France).

2.2 Preparation of SPI-NIPU Adhesive

The SPI-NIPU adhesive was prepared as follows: 80 g SPI is dissolved in 400 g of deionized water under magnetic stirring, then 54 g dimethyl carbonate is added and the mixture heated to 60°C for 120 min. Then 105 g hexamethylenediamine are then added and heated to 90°C for another 2 h, then cooled to room temperature. The mixture can be roto-evaporated under reduced pressure at 55°C to eliminate the excess of water and to obtain a final resin solids content of 45%. with a viscosity of 26.9 ± 1 Pa•s.

2.3 Thermomechanical Analysis (TMA)

The resins were tested by thermomechanical analysis. The samples were prepared by applying each adhesive between two beech wood plies, with dimensions of 21 mm × 6 mm × 1.1 mm. These beech-resin-beech sandwiches were tested in non-isothermal mode between 25°C and 250°C at a heating rate of 10 °C/minute with a Mettler Toledo 40 TMA equipment (Mettler Toledo, Zurich, Switzerland). They were tested in three-point bending on a span of 18 mm exercising a force cycle of 0.1/0.5 N on the specimens, with each force cycle of 12 seconds (6s/6s). The classical mechanics relationship between force and deflection

$$E = [L^3/(4bh^3)][F/(f_{wood} - f_{adhesive})]$$

where L = the length of the sample; b = its width; h = its thickness; F = the force applied f_{wood} the deflection of the wood and f_{adhesive} the deflection of the wood adhesive sandwich under test. This equation allows the calculation of the Young's modulus E for each case tested. Such a measuring system has been introduced and is used to follow the progressive hardening of the adhesive with the increase of temperature and to indicate comparatively if an adhesive system is faster or slower hardening and if it gives stronger joints than another one.

2.4 ATR-FT-MIR Analysis

All of the samples were analyzed with a PerkinElmer Frontier ATR-FT-MIR provided by an ATR Miracle diamond crystal. The powder and liquid samples were laid on the diamond eye (1.8 mm) of the ATR equipment and the contact for the sample was ensured by tightly screwing the clamp device. Each extract was scanned registering the spectrum with 32 scans with a resolution of 4 cm^{-1} in the wave number range between 600 and 4000 cm^{-1} .

2.5 MALDI-ToF Analysis

Samples for matrix assisted laser desorption ionization time-of-flight (MALDI-ToF) analysis were prepared by first dissolving 7.5 mg of sample powder in 1 mL of a 50:50 v/v acetone/water solution. Then 10 mg of this solution was added to 10 μL of a 2,5-dihydroxy benzoic acid (DHB) matrix. The locations dedicated to the samples on the analysis plaque were first covered with 2 μL of a NaCl solution 0.1 M in 2:1 v/v methanol/water, and predried. Then 1.5 μL of the sample solution was placed on its dedicated location and the plaque was dried again. Red phosphorous was to standardize the MALDI equipment. MALDI-ToF spectra were obtained using an Axima-Performance mass spectrometer from Shimadzu Biotech (Kratos Analytical Shimadzu Europe Ltd., Manchester, UK) using a linear polarity-positive tuning mode. The measurements were carried out making 1000 profiles.

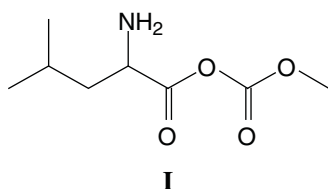
2.6 Three-Layer Plywood Preparation and Testing

The performance of the SPI-NIPU adhesive was tested by preparing laboratory plywood panels and evaluating their shear strength dry, after 24 hours cold water soaking, and after 3 h in water at 63°C . The plywood panels of $400 \text{ mm} \times 200 \text{ mm} \times 5 \text{ mm}$ were prepared for each adhesive using 2 mm poplar (*Populus tremuloides*) veneers. The glue spread used was of 300 g/m^2 double glue line, and hot-pressing time was of 6 minutes at 1.25 MPa pressure at a temperature of 200°C based on the consequence of the TMA trace. After hot pressing the plywood was stored under ambient conditions (20°C and 12% relative humidity) for 48 hours then it was cured and tested the dry shear strength, 24 h cold water soaking strength and for strength after 3 h at 63°C in water according to China National Standard GB/T 14074 (2006) [38], China National Standard GB/T 17657 (1999) [39], and European Norm EN 636:2012 (2012) [40]. To reinforce the SPI-NIPU plywood also panels to which 10% or 15% by weight of a biosourced glycerol diglycidyl ether (GDE) were added to the SPI-NIPU based on solids were also pressed and tested under the same conditions.

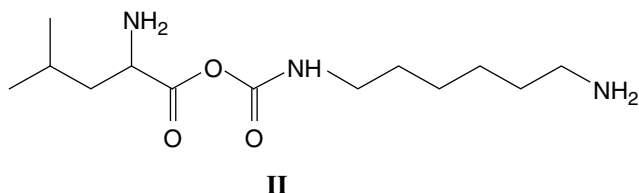
3 Results and Discussion

3.1 MALDI ToF Analysis

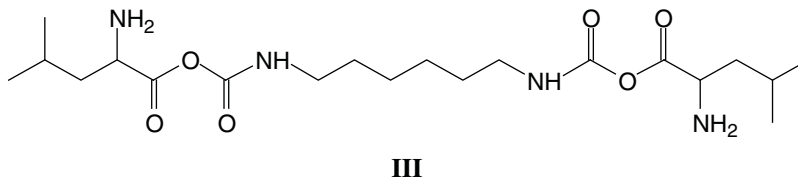
The MALDI ToF analysis shows that SPI-NIPU urethane linkages do form with at least some of the soy protein amino acids. However, the analysis also shows that for SPI it is not a straightforward reaction to NIPUs as described for other bio-sourced materials (Figs. 1a–1d). The assignments for the relevant peaks of the spectra are shown in Tab. 1. Thus, the peaks in Fig. 1a at 189 Da and 215 Da can be assigned to the reaction product of leucine with DMC without and with Na^+ being present, respectively, hence to a structure of type (I):



The same structure is present for 284 Da and 311 Da which can be assigned to triptofan-DMC without or with Na⁺. At 271 Da the structure can be attributed to serine-DMC-hexamethylene diamine + Na⁺. However, at 271 Da and 295 Da the structure that can be deduced is leucine-DMC-hexamethylene diamine without or with Na⁺ of structure (II)

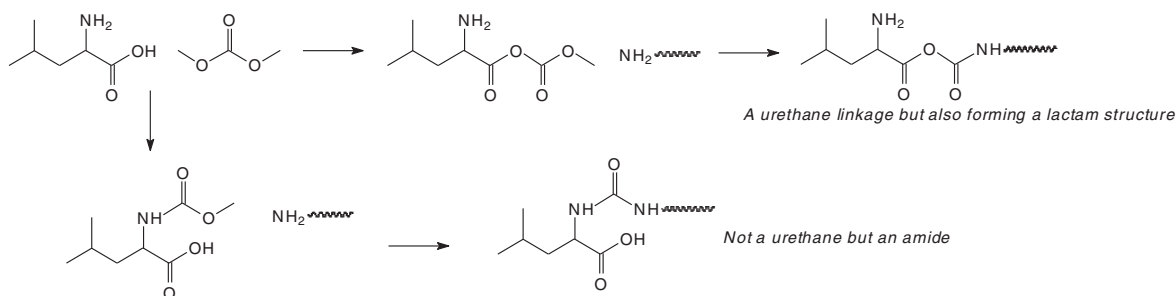


It must be clearly pointed out that while a urethane linkage, namely R-NH-COO-R is formed, the structure so formed is also a lactam, as indicated by the -CO-O-CO- structure. The same type of urethane/lactam linkage is found also at 339 Da and 368 Da these being respectively arginine-DMC-diamine + Na⁺ and tryptophan-DMC-diamine + Na⁺. The small peak at 453 Da indicates the formation of a different oligomer, namely: leucine-DMC-diamine-DMC-leucine + Na⁺, hence a more complex structure of type (III):

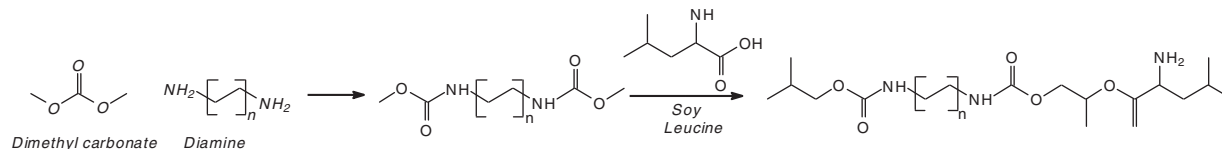


The same type of structure but involving different amino acids is present at 495 Da, 539 Da and 602 Da, these oligomers being respectively leucine-DMC-amine-DMC-arginine + Na⁺, arginine-DMC-amine-DMC-arginine + Na⁺ and tryptophan-DMC-amine-DMC-tryptophan + Na⁺.

It must be pointed out that:

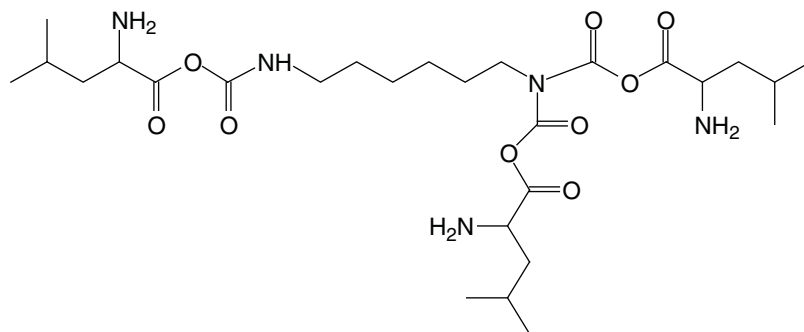


The first one of these reactions can be schematically summarized as



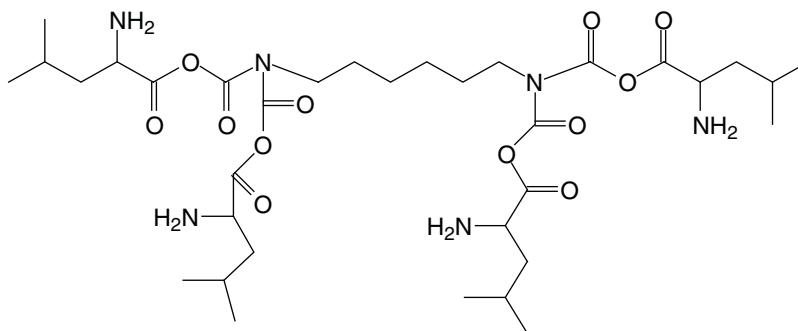
This reaction, as seen, leads to urethanes that eventually share a lactam structure. To avoid the presence of urethane/lactam type structure then a longer carbonate, cyclic or not should be used.

2. That after urethane dimers are formed such as those of the peaks at 453 Da, 495 Da, 539 Da and 602 Da the reaction can further proceed either (i) by reactions forming amides as the NH_2 usable for reaction with DMC do not lead to urethanes, or (ii) by further reaction of the residual NH groups in the urethane linkages with DMC-aminoacid. In effect, there is a peak at 610 Da (with Na^+) assigned to a compound formed in this latter manner by reaction of a third leucine of structure (IV)



IV

And even the peak at 746 Da (without Na^+) of assigned structure (V):

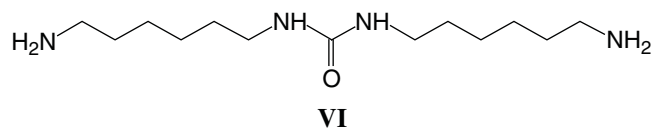


V

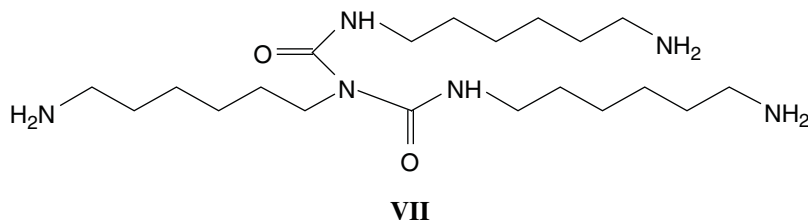
Similar peaks for other soy protein amino acids are also present.

There are then some urethane linkages formed, more than enough to cross-link the protein, even if these are coupled with lactam-like structures. Thus, once the two NH_2 of the diamine are saturated then any further reaction can proceed either (i) through the formation of amides, hence polyamides [41], or (ii) by a chain reaction with any residual -NH- group that is obtained when forming a urethane linkage, or (iii) by using a polyamine rather than a diamine. This means that in any case the hardened network formed is most likely to be cross-linked by a mix of urethane bridges and amides ones.

Parasite side reactions also appear to occur as indicated by the peaks at 256 Da (VI) and 398 Da (VII) assigned to structures derived by the reaction of DMC with the diamine.



And



Although these reactions form also compounds that are platforms for further urethane linkages to be formed either among themselves or with the SPI amino acids.

In summary rather complex tridimensional structures can results from these combinations.

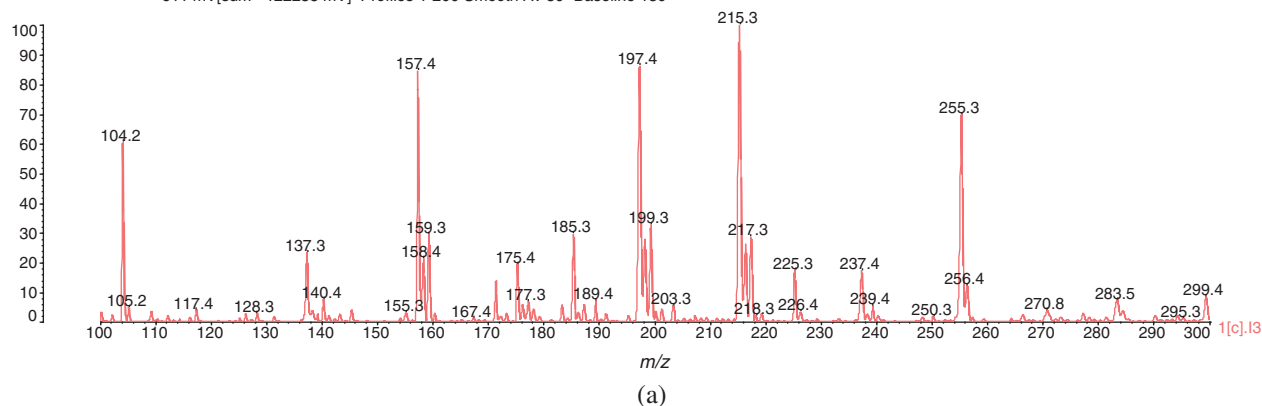
The reaction of formation of soy protein urethanes, when using DMC as the carbonate, leads to urethanes that eventually share a lactam structure. The use of a longer carbonate, preferably cyclic such as propylene carbonate, does not eliminate the presence of such urethane/lactam type structures.

Data: protein nipu0001.l3[c] 4 Nov 2019 15:22 Cal: RED 4 Nov 2019 15:12

Shimadzu Biotech Axima Performance 2.9.3.20110624: Mode Linear, Power: 108, P.Ext. @ 2300 (bin 78)

%Int.

611 mV[sum= 122238 mV] Profiles 1-200 Smooth Av 50 -Baseline 150



Data: protein nipu0001.l3[c] 4 Nov 2019 15:22 Cal: RED 4 Nov 2019 15:12

Shimadzu Biotech Axima Performance 2.9.3.20110624: Mode Linear, Power: 108, P.Ext. @ 2300 (bin 78)

%Int.

308 mV[sum= 61579 mV] Profiles 1-200 Smooth Av 50 -Baseline 150

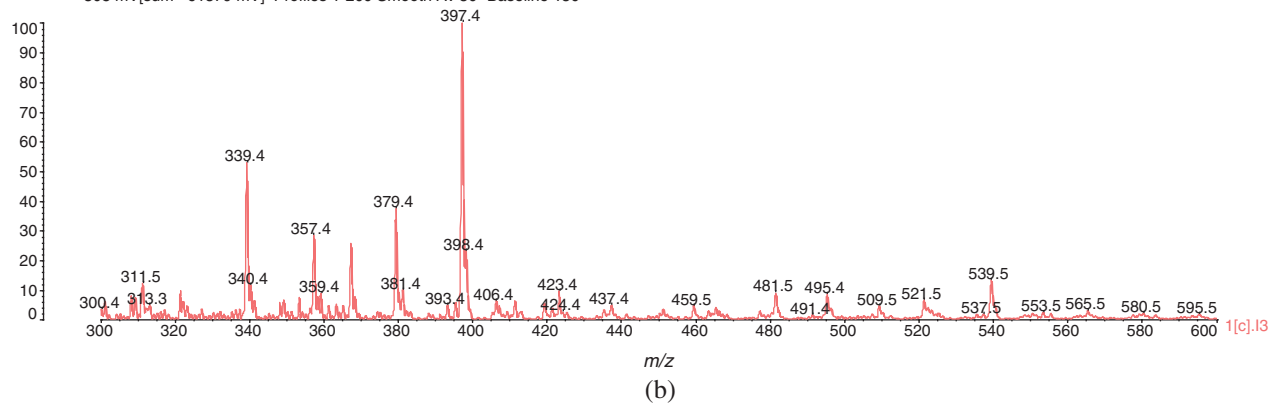


Figure 1: (continued)

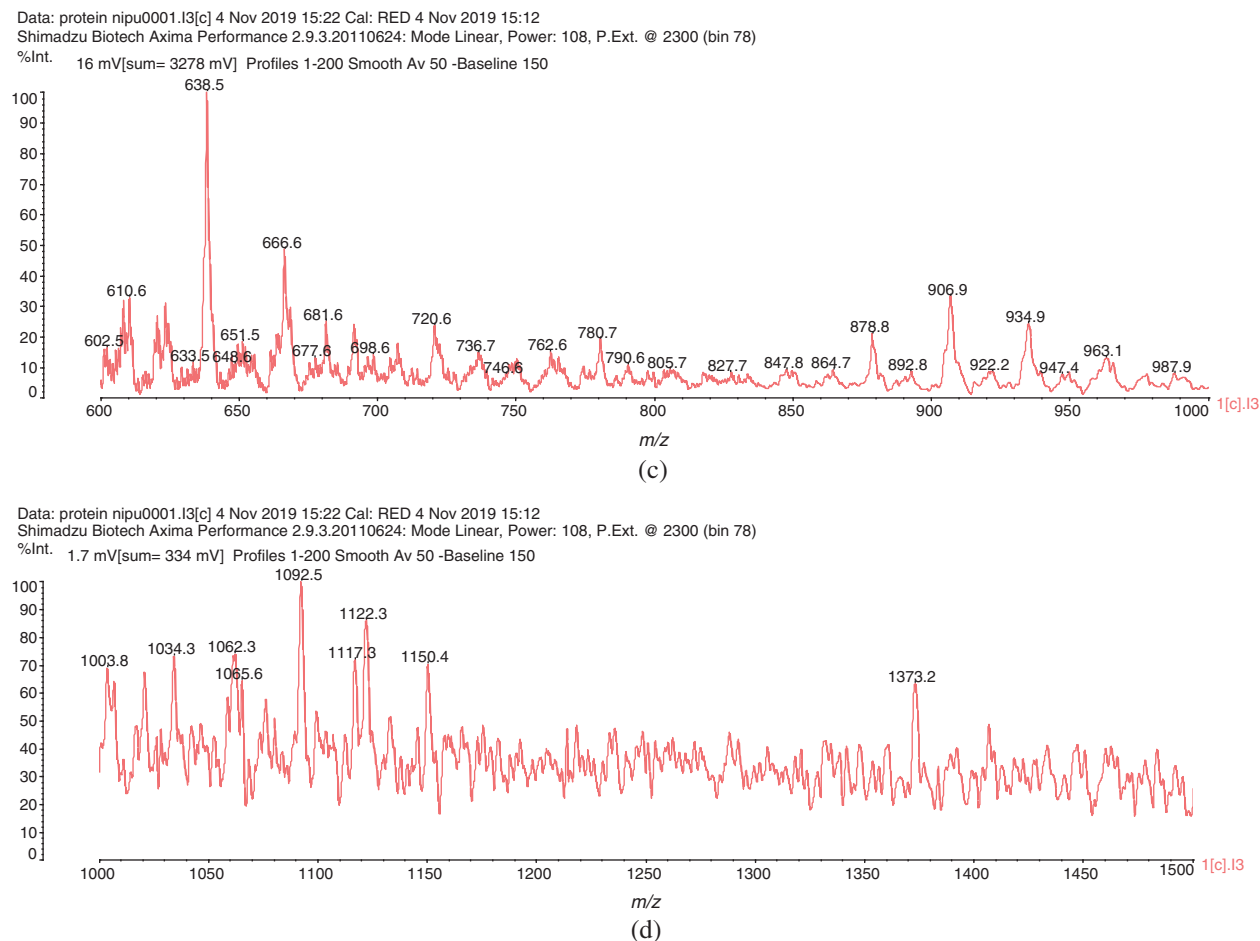


Figure 1: MALDI-ToF spectra of soy protein isolate-based non-isocyanate polyurethane (NIPU) adhesive. (a) 100–300 Da range. (b) 300–600 Da range. (c) 600–1000 Da range. (d) 1000–1500 Da range

The FTIR spectra of SPI and of the SPI-NIPU resin are shown in Fig. 2. The peaks at 1703 cm^{-1} , 1543 cm^{-1} and 1255 cm^{-1} are characteristic of the asymmetric stretching of urethane linkages, with the 1703 cm^{-1} for the SPI NIPU spectrum belonging the C=O of the urethane being quite intense and being absent in the spectrum of SPI alone. This conclusion of the presence of urethane linkages is confirmed by the presence of other peaks. Thus, the appearance of the relatively small peak at 1766 cm^{-1} in the SPI NIPU spectrum is characteristic the R-COO-R of esters derived from the lactam structures, these being esters of the carbamic acid (-NH-COO-) forming the urethanes, confirming the structures assigned by the MALDI-ToF analysis. The big peak at 1639 cm^{-1} is characteristic of amide groups, the peak being quite marked already for SPI alone, thus describing the amide (peptide) linkages holding together the protein skeleton. This same peak becomes even more dominant in the SPI NIPU spectrum where the amides derived from the reactions of the diamine with DMC and the proteins amino acids generate a great number of amides in the urethane structure superposed to the ones already present in the protein skeleton. The presence of the amide groups is supported by the peak at 1370 cm^{-1} (thus of -CO-NH-C-) and the wide peak at 3200 cm^{-1} that mask a number of different group effects. The peak at 1441 cm^{-1} represents the asymmetric stretch of -CH₂- groups of the alkane chains of the diamine included in the finished network. Lastly the peak at $1390\text{--}1400\text{ cm}^{-1}$ belongs to the protonated N-containing groups, such as -NH₃⁺ on the protein aminoacids. The two sharp peaks at 2900 cm^{-1} and 2800 cm^{-1} are assigned to the asymmetric stretching of both the -CH₃ groups of DMC and the asymmetric stretching of the R-CH₂-R

chains from the amine, both before and after reaction. They support such assignments in relation to the peak at 1441 cm^{-1} for the $-\text{CH}_2-$ groups. It must be also pointed out that these peaks are particularly intense as they are the superposition of the asymmetric stretching band of both $-\text{CH}_3$ and $-\text{CH}_2-$ groups.

The thermomechanical analysis traces of SPI-NIPU adhesive is shown in Fig. 3. The curve of the increase of Young's modulus as a function of temperature show two upsurges and two peaks of MOE, namely at 130°C and at 220°C , this latter starting at around 185°C . The curves decrease in MOE value between the two peaks. This means that the peak at 130°C indicates the formation of an unstable network that is degraded and transformed if the temperature is increased causing a marked internal rearrangement. The second peak at higher temperature indicates that curing of the SPI-NIPU resin occurs at a high temperature as already reported in previous literature for similar types of adhesives [34,35]. The increase of Young's modulus has been shown to correlate with the bonding strength of the adhesive [42–48].

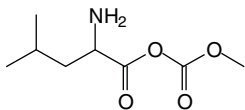
It is interesting to speculate what is the cause of the marked decrease between the two MOE peaks in Fig. 3. While it could be an unstable structure, a more likely reason could derive from the formation of linear polymers arranging themselves in a physically entangled network, rather than a chemically cross-linked one. As the temperature increases further, the Brownian movements would make the viscosity of these physically entangled chains markedly decrease and extensively disentangle, the MOE again starting to increase at the much higher temperature of the second peak once chemical cross-linking does finally occur.

Before the TMA curves show a significant increase in the modulus value, the overall trend of the modulus values in the TMA curves of the NIPU adhesive decreases between 50°C and 75°C . This is mainly due to the decrease in viscosity of the adhesive as the temperature increases, resulting in a lower viscosity and bonding strength. Conversely, the adhesive penetrates into the wood, softening or degrading it during heating thus reducing its strength. It is evident from the TMA trace that the curing temperature to be used for such adhesives is relatively higher than what common to-day for equivalent panels bonded with traditional adhesives. After 200°C degradation of the wood substrate is known to start [45–48], thus the second peak is rather high when considering that wood degradation has already started to occur at the same time. The decrease of the curve afterward is the reflexion of the continuing degradation of the wood substrate.

The results of the 3-ply plywood panels prepared are presented in Tab. 2. These indicate that the SPI NPU adhesive by itself just passes at 0.74 MPa the interior grade limit of the relevant China national standards [38–40] that requires a shear strength equal to, or higher than 0.7 MPa . By adding 10% and 15% biosourced GDE the dry shear strength results improved markedly in both cases passing to 1.34 MPa and 1.73 MPa respectively. This indicates that also the dry strength requirements for interior grade plywood of European Norm EN 636:2012 (2012) are satisfied [40] for interior grade plywood. Such a marked shear strength increase indicates that even the addition of smaller percentages of GDE, around 5% by weight, would be sufficient to comfortably pass the requirements for interior grade plywood panels under industrial conditions. The addition of GDE improves the performance due to additional cross-linking. The 24 hours cold water soaking results and the 3 hours at 63°C tests did not pass the requirements for exterior or semiexterior grade plywood as shown in Tab. 2 which are 0.7 MPa and 1.0 MPa for both the China National Standard and in the European Norm, respectively. This is consistent with the results of the TMA reported in Fig. 3, where it is indicated that these adhesives, in the reaction proportions used in this work, need a higher curing temperature to develop all their strength and achieve good results in the wet-type tests. It means also that such an adhesive under the conditions used is possibly better suited to its use in particleboard where higher pressing temperatures are used. An approach to explore to further decrease the high energy of activation of the curing reaction and thus achieve better wet bonding results would be to use small percentages of ionic liquids as already experienced for other adhesives [49].

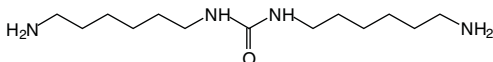
Table 1: Assignment of structures to relevant MALDI-ToF peaks from Figs. 1a–1d

189 Da = reaction product of leucine with DMC, without Na⁺



215 Da = 189 Da + Na⁺

256 Da = Calculated 258 Da, no Na⁺

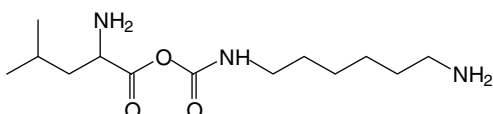


270 Da = tryptofan-DMC

OR

270 = serine-DMC-Amine + Na⁺

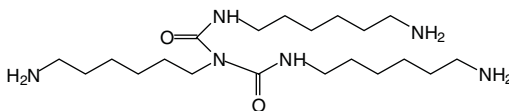
295 Da = leucine-DMC-Hexamethylene diamine + Na⁺



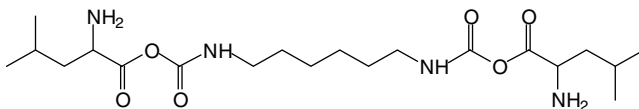
339 Da = the same as 295 Da but with arginine, thus arginine-DMC-amine + Na⁺

368 Da = same as 295 Da but with tryptophan, thus Tryptophan-DMC-Amine + Na⁺

398 Da = Calculated 400 Da, no Na⁺; 423 Da with Na⁺



453 Da = The small peak at 453 Da is leucine-DMC-amine-DMC-leucine + Na⁺

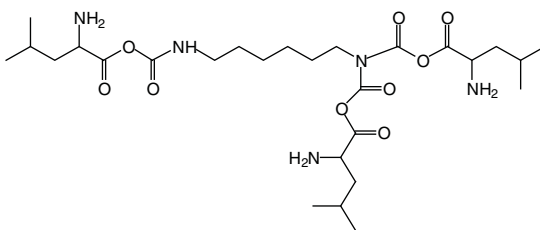


495 Da = leucine-DMC-amine-DMC-arginine + Na⁺

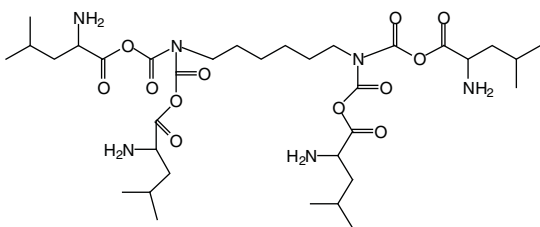
539 Da = arginine-DMC-amine-DMC-arginine + Na⁺

602 Da = tryptophan-DMC-amine-DMC-Tryptophan + Na⁺

610 Da with Na⁺



746 Da, no Na⁺



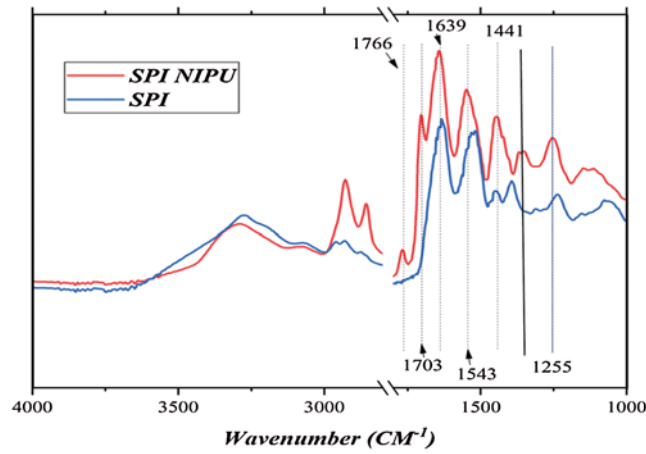


Figure 2: FT-IR spectra of soy protein isolate (SPI) and of soy protein isolate non-isocyanate polyurethane (NIPU) adhesive resin

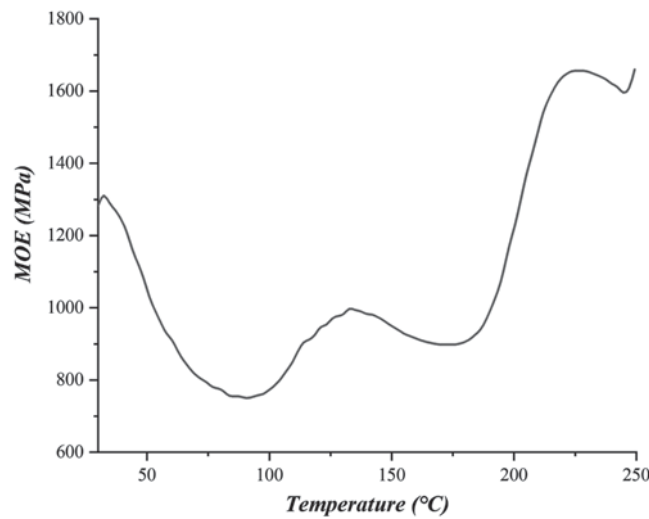


Figure 3: Thermomechanical analysis (TMA) curves of MOE as a function of temperature of joints bonded with soy protein isolate non-isocyanate polyurethane (NIPU) adhesive

Table 2: SPI-NIPU-bonded plywood test results. Percentages wood failure for the dry test are in parenthesis

	Dry	Shear Strength (MPa)	
		63°C for 3h	24 h cold water
SPI-NIPU	0.74	–	–
SPI-NIPU + 10%GDE	1.30 (30)	–	–
SPI-NIPU + 15%GDE	1.73 (90)	0.28	0.34

Note: (-) not tested

4 Conclusions

Soy-protein isolate (SPI) has been used to prepare non-isocyanate polyurethane (NIPU) thermosetting adhesives for wood panels by reacting it with dimethyl carbonate (DMC) and hexamethylene diamine. MALDI-ToF and FTIR spectrometry have shown that urethane linkages are effectively formed in the reaction, in which all three reagents do participate. Some parasite reactions do occur, but these do not appear to detract to the formation of NIPU resins. Both linear as well as branched oligomers were obtained and identified, indicating by their molecular weight growth how such oligomer structures could further cross-link to form a hardened network. While the NIPU oligomers structures identified present the characteristics of urethane linkages derived from the urethane precursor carbamic acid (-NHCOOH-), they also simultaneously present structures characteristic of lactams. This is rather unusual, as they are exclusively due to the use of DMC, the simple organic carbonate used, and will not occur with other types of organic carbonates. Thermomechanical analysis (TMA) monitoring of the curing of the adhesive showed two distinct MOE maxima peaks, one around 130°C and the other around 220°C, with a very marked decrease in MOE between the two. The first peak can be assigned to the growth of linear oligomers forming a physically entangled network. This physically entangled network collapses and disentangles as the temperature increases due to the ever more marked Brownian movements of the linear oligomer chains. The second peak is assigned to the chemical cross-linking of the chains forming a hardened network. Plywood panels were prepared by bonding them with the SPI-NIPU wood adhesive and gave acceptable results for dry strength, with wet strength improving only after addition of 15% of a biosourced glycerol diglycidyl ether.

Funding Statement: The author(s) received no specific funding for this study.

Conflicts of Interest: The authors declare that there are no conflicts of interest regarding the publication of this paper.

References

1. Vnućec, D., Kutnar, A., Goršek, A. (2017). Soy-based adhesives for wood-bonding—A review. *Journal of Adhesion Science and Technology*, 31(8), 910–931. DOI 10.1080/01694243.2016.1237278.
2. Pizzi, A. (2016). Wood products and green chemistry. *Annals of Forest Science*, 73(1), 185–203. DOI 10.1007/s13595-014-0448-3.
3. Zhong, Z., Sun, X. S., Wang, D., Ratto, J. A. (2003). Wet strength and water resistance of modified soy protein adhesives and effects of drying treatment. *Journal of Polymers and the Environment*, 11(4), 137–144. DOI 10.1023/A:1026048213787.
4. Liu, Y., Li, K. (2002). Chemical modification of soy protein for wood adhesives. *Macromolecular Rapid Communications*, 23, 739–742.
5. Sun, X., Bian, K. (1999). Shear strength and water resistance of modified soy protein adhesives. *Journal of the American Oil Chemists' Society*, 76(8), 977–980. DOI 10.1007/s11746-999-0115-2.
6. Hettiarachchy, N. S., Kalapathy, U., Myers, D. J. (1995). Alkali-modified soy protein with improved adhesive and hydrophobic properties. *Journal of the American Oil Chemists' Society*, 72(12), 1461–1464. DOI 10.1007/BF02577838.
7. Lei, H., Du, G., Wu, Z., Xi, X., Dong, Z. (2014). Cross-linked soy-based wood adhesives for plywood. *International Journal of Adhesion and Adhesives*, 50, 199–203. DOI 10.1016/j.ijadhadh.2014.01.026.
8. Eslah, F., Jonoobi, M., Faezipour, M., Asharpour, M., Enayati, A. A. (2016). Preparation and development of a chemically modified bio-adhesive derived from soybean flour protein. *International Journal of Adhesion and Adhesives*, 71, 48–54. DOI 10.1016/j.ijadhadh.2016.08.011.
9. Lin, Q., Chen, N., Bian, L., Fan, M. (2012). Development and mechanism characterization of high performance soy-based bio-adhesives. *International Journal of Adhesion and Adhesives*, 34, 11–16. DOI 10.1016/j.ijadhadh.2012.01.005.

10. Ghahri, S., Pizzi, A., Mohebby, B., Mirshoktaie, A., Mansouri, H. R. et al. (2018). Improving water resistance of soy-based adhesive by vegetable tannin. *Journal of Polymers and the Environment*, 26(5), 1881–1890. DOI 10.1007/s10924-017-1090-6.
11. Ghahri, S., Pizzi, A., Mohebby, B., Mirshoktaie, A., Mansouri, H. R. et al. (2018). Soy-based, tannin-modified plywood adhesives. *Journal of Adhesion*, 94(3), 218–237. DOI 10.1080/00218464.2016.1258310.
12. Ghahri, S., Pizzi, A. (2018). Improving soy-based adhesives for wood particleboard by tannins addition. *Wood Science and Technology*, 52(1), 261–279. DOI 10.1007/s00226-017-0957-y.
13. Frihart, C. R., Lorenz, L. (2019). Specific oxidants improve the wood bonding strength of soy and other plant flours. *Journal of Polymer Science Part A: Polymer Chemistry*, 57(9), 1017–1023. DOI 10.1002/pola.29357.
14. Frihart, C. R., Pizzi, A., Xi, X., Lorenz, L. (2019). Reactions of soy flour and soy protein by non-volatile aldehydes generation by specific oxidation. *Polymers*, 11(9), 1478. DOI 10.3390/polym11091478.
15. Lei, H., Pizzi, A., Navarrete, P., Rigolet, S., Redl, A. et al. (2010). Gluten protein adhesives for wood panels. *Journal of Adhesion Science and Technology*, 24(8–10), 1583–1596. DOI 10.1163/016942410X500963.
16. Wescott, J. M., Traska, A., Frihart, C. R. (2005). Durable soy-based adhesive dispersions. Wood adhesives. San Diego, California, USA. Forest Products Society, Madison, WI, 2005, 263–269.
17. Kathalewar, M. S., Joshi, P. B., Sabnis, A. S., Malshe, V. C. (2013). Non-isocyanate polyurethanes: From chemistry to applications. *RSC Advances*, 3(13), 4110–4129. DOI 10.1039/c2ra21938g.
18. Poussard, L., Mariage, J., Grignard, B., Detrembleur, C., Jérôme, C. et al. (2016). Non-isocyanate polyurethanes from carbonated soybean oil using monomeric or oligomeric diamines to achieve thermosets or thermoplastics. *Macromolecules*, 49(6), 2162–2171. DOI 10.1021/acs.macromol.5b02467.
19. Ochiai, B., Utsuno, T. (2013). Non-isocyanate synthesis and application of telechelic polyurethanes via polycondensation of diurethanes obtained from ethylene carbonate and diamines. *Journal of Polymer Science Part A: Polymer Chemistry*, 51(3), 525–533. DOI 10.1002/pola.26418.
20. Figovsky, O., Shapovalov, L., Leykin, A., Birukova, O., Potashnikova, R. (2013). Recent advances in the development of non-isocyanate polyurethanes based on cyclic carbonates. *PU Magazine*, 10, 1–9.
21. Rokicki, G., Parzuchowski, P. G., Mazurek, M. (2015). Non-isocyanate polyurethanes: Synthesis, properties, and applications. *Polymers for Advanced Technologies*, 26(7), 707–761. DOI 10.1002/pat.3522.
22. Noreen, A., Zia, K. M., Zuber, M., Ameer, S. T., Zahoor, F. (2016). Bio-based polyurethane: An efficient and environment friendly coating systems: A review. *Progress in Organic Coatings*, 91, 25–32. DOI 10.1016/j.porgcoat.2015.11.018.
23. Birukov, O., Potashnikova, R., Leykin, A., Figovsky, O., Shapovalov, L. (2009). Advantages in chemistry and technology of non-isocyanate polyurethane. *Journal of the Scientific Israel-Technological Advances*, 11, 160–167.
24. Kathalewar, M., Sabnis, A., Waghoo, G. (2013). Effect of incorporation of surface treated zinc oxide on non-isocyanate polyurethane based nano-composite coatings. *Progress in Organic Coatings*, 76(9), 1215–1229. DOI 10.1016/j.porgcoat.2013.03.027.
25. Grignard, B., Thomassin, J. M., Gennen, S., Poussard, L., Bonnaud, L. et al. (2016). CO₂-blown microcellular non-isocyanate polyurethane (NIPU) foams: From bio-and CO₂-sourced monomers to potentially thermal insulating materials. *Green Chemistry*, 18(7), 2206–2215. DOI 10.1039/C5GC02723C.
26. Cornille, A., Guillet, C., Benyahya, S., Negrell, C., Boutevin, B. et al. (2016). Room temperature flexible isocyanate-free polyurethane foams. *European Polymer Journal*, 84, 873–888. DOI 10.1016/j.eurpolymj.2016.05.032.
27. Thébault, M., Pizzi, A., Dumarçay, S., Gerardin, P., Fredon, E. et al. (2014). Polyurethanes from hydrolysable tannins obtained without using isocyanates. *Industrial Crops and Products*, 59, 329–336. DOI 10.1016/j.indcrop.2014.05.036.
28. Thébault, M., Pizzi, A., Essawy, H. A., Barhoum, A., Van Assche, G. (2015). Isocyanate free condensed tannin-based polyurethanes. *European Polymer Journal*, 67, 513–526. DOI 10.1016/j.eurpolymj.2014.10.022.
29. Thébault, M., Pizzi, A., Santiago-Medina, F. J., Al-Marzouki, F. M., Abdalla, S. (2017). Isocyanate-free polyurethanes by coreaction of condensed tannins with aminated tannins. *Journal of Renewable Materials*, 5(1), 21–29.

30. Xi, X., Pizzi, A., Gerardin, C., Du, G. (2018). Glucose-biobased non-isocyanate polyurethane rigid foams. *Journal of Renewable Materials*, 7(3), 301–312. DOI 10.32604/jrm.2019.04174.
31. Xi, X., Pizzi, A., Gerardin, C., Lei, H., Chen, X. et al. (2019). Preparation and evaluation of glucose based non-isocyanate polyurethane self-blowing rigid foams. *Polymers*, 11(11), 1802. DOI 10.3390/polym11111802.
32. Chen, X., Li, J., Xi, X., Pizzi, A., Zhou, X. et al. (2020). Condensed tannin-glucose-based NIPU bio-foams of improved fire retardancy. *Polymer Degradation and Stability*, 175, 109121. DOI 10.1016/j.polymdegradstab.2020.109121.
33. Chen, X., Xi, X., Pizzi, A., Fredon, E., Zhou, X. et al. (2020). Preparation and characterization of condensed tannin non-isocyanate polyurethane (NIPU) rigid foams by ambient temperature blowing. *Polymers*, 12(4), 750. DOI 10.3390/polym12040750.
34. Xi, X., Pizzi, A., Delmotte, L. (2018). Isocyanate-free polyurethane coatings and adhesives from mono- and disaccharides. *Polymers*, 10(4), 402. DOI 10.3390/polym10040402.
35. Xi, X., Wu, Z., Pizzi, A., Gerardin, C., Lei, H. et al. (2019). Non-isocyanate polyurethane adhesive from sucrose used for particleboard. *Wood Science and Technology*, 53(2), 393–405. DOI 10.1007/s00226-019-01083-2.
36. Santiago-Medina, F. J., Basso, M. C., Pizzi, A., Delmotte, L. (2018). Polyurethanes from Kraft lignin without using isocyanates. *Journal of Renewable Materials*, 6(4), 413–425. DOI 10.7569/JRM.2017.634172.
37. Pizzi, A. (2019). Tannin-based Biofoams. *Journal of Renewable Materials*, 7(5), 477–492. DOI 10.32604/jrm.2019.06511.
38. China National Standard GB/T 14074 (2006). Testing methods for wood adhesives and their resins.
39. China National Standard GB/T17657-2013 (2013). Test methods for evaluating the properties of wood-based panels and surface decorated wood-based panels.
40. European Norm EN 636: 2012 (2012). Plywood—Specifications, Standardization Committee, European Commission, Bruxelles, Belgium.
41. Xi, X., Pizzi, A., Gerardin, C., Chen, X., Amirou, S. (2020). Soy protein isolate based polyamides as wood adhesives. *Wood Science and Technology*, 54(1), 89–102. DOI 10.1007/s00226-019-01141-9.
42. Pizzi, A., Garcia, R., Deglise, X. (1998). Thermomechanical analysis of entanglement networks - correlation of some calculated and experimental parameters. *Journal of Applied Polymer Science*, 67, 1673–1678.
43. Kamoun, C., Pizzi, A. (2000). Particleboard I.B. forecast by TMA bending in MUF adhesives curing. *Holz als Roh- und Werkstoff*, 58, 4(4), 288–289. DOI 10.1007/s001070050428.
44. Lecourt, M., Humphrey, P., Pizzi, A. (2003). Comparison of TMA and ABES as forecasting systems of wood bonding effectiveness. *Holz als Roh- und Werkstoff*, 61(1), 75–76. DOI 10.1007/s00107-002-0346-5.
45. Pizzi, A., Garcia, R., Deglise, X. (1998). Thermomechanical analysis of entanglement networks—correlation of some calculated and experimental parameters. *Journal of Applied Polymer Science*, 67, 1673–1678.
46. Garcia, R., Pizzi, A. (1998). Cross-linked and entanglement networks in thermomechanical analysis of polycondensation resins. *Journal of Applied Polymer Science*, 70, 1111–1116.
47. Kamoun, C., Pizzi, A., Garcia, R. (1998). The effect of humidity on crosslinked and entanglement networking of formaldehyde-based wood adhesives. *Holz als Roh- und Werkstoff*, 56(4), 235–243. DOI 10.1007/s001070050309.
48. Pizzi, A., Lu, X., Garcia, R. (1999). Lignocellulosic substrates influence on TTT and CHT curing diagrams of polycondensation resins. *Journal of Applied Polymer Science*, 71, 915–925.
49. Younesi-Kordkheili, H., Pizzi, A. (2016). Acid ionic liquids as a new hardener in urea-glyoxal adhesive resins. *Polymers*, 8(3), 57–71. DOI 10.3390/polym8030057.

3.3 Préparation et propriétés d'un nouveau type de colle à bois à base de tanin

Résumé: Un nouvel adhésif pour bois à base de biomasse a été préparé avec de l'extrait de tanin de Mimosa du commerce et de l'éther diglycidyle de glycérol (GDE) par mélange mécanique. Le GDE a servi d'agent de réticulation du tanin sans aucune addition d'aldéhyde, produisant des réseaux tridimensionnels durcis. Différents rapports pondéraux tanin/GDE ont été étudiés par un certain nombre de techniques pour déterminer leur influence sur les propriétés finales. Les résultats ont montré qu'une liaison ester non hydrolysable peut se former entre les groupes époxy du GDE et les groupes hydroxyle du tanin, ce qui est le facteur critique pour la bonne résistance à l'eau obtenue par les colles à bois ainsi préparées. De plus, la résistance au cisaillement sec et humide présente une corrélation positive avec la proportion de GDE ajouté. Même à une proportion relativement faible de GDE (33 % du poids de tanin sec), les résistances au cisaillement à sec et après 24 h à l'eau froide du contreplaqué satisfaisaient aux exigences de la norme pertinente (GB/T 9846-2015, $\geq 0,7$ MPa). La stabilité thermique de la colle à bois à base de tanin ainsi préparée s'est progressivement améliorée avec la proportion croissante de GDE.

Mots clés: Tanin de mimosa; glycérol; l'éther diglycidyle (GDE); adhésif pour bois de biomasse; résistance à l'eau.



Preparation and properties of a novel type of tannin-based wood adhesive

Xinyi Chen^{a,b}, Antonio Pizzi^b, Emmanuel Fredon^b, Christine Gerardin^c, Jinxing Li^a, Xiaojian Zhou^a, and Guanben Du^a

^aKey Laboratory for Forest Resources Conservation and Utilisation in the Southwest Mountains of China, Southwest Forestry University, Kunming, PR China; ^bLERMAB, University of Lorraine, Epinal, France; ^cLERMAB, University of Lorraine, Nancy, France

ABSTRACT

A novel biomass-based wood adhesive was prepared with commercial Mimosa tannin extract and glycerol diglycidyl ether (GDE) by convenient mechanical mixing. GDE served as the crosslinker of the tannin without any aldehyde addition yielding hardened three-dimensional networks. Different weight ratios of tannin/GDE were investigated by a number of techniques to determine their influence on final properties. The results showed that a non-hydrolysable ester bonds can be formed between the epoxy groups of GDE and hydroxyl groups of tannin, this being the critical factor for the good water resistance obtained by the wood adhesives prepared. Moreover, the dry and wet shear strength exhibit positive correlation with the proportion of GDE added. Even at a relatively small proportion of GDE (33% of the weight of dry tannin), the dry and 24 h cold water shear strengths of the bonded plywood satisfied the requirements of relevant standard (GB/T 9846–2015, ≥ 0.7 MPa). The thermal stability of the tannin-based wood adhesive so prepared progressively improved with the increasing proportion of GDE.

ARTICLE HISTORY

Received 15 October 2020
Accepted 9 December 2020

KEYWORDS

Mimosa tannin; glycerol diglycidyl ether (GDE); biomass wood adhesive; water resistance

1. Introduction

The topic of environmental and eco-friendly wood adhesive is now one of the hottest subject and an unavoidable one in the wood industry.^[1] Nowadays, formaldehyde-based wood adhesives are so widely applied due to their low cost, short curing time and strong adhesion.^[2,3] Formaldehyde-based adhesives are account for almost 90% of totally wood adhesives industry.^[3] Nevertheless, traditional synthetic wood adhesives present two main drawbacks, these being their toxic starting materials (i.e. formaldehyde and phenol) and formaldehyde-emission during their use and for long time afterward. Therefore, these drawbacks have created a demand for adhesives prepared from non-toxic and inexpensive materials to replace them.

CONTACT Antonio Pizzi ✉ antonio.pizzi@univ-lorraine.fr 📧 LERMAB, University of Lorraine, Epinal, France; Xiaojian Zhou ✉ xiaojianzhou1982@163.com 📧 Key Laboratory for Forest Resources Conservation and Utilisation in the Southwest Mountains of China, Southwest Forestry University, Kunming, PR China.

© 2020 Taylor & Francis Group, LLC

Now, for a number of years, some biomass resources, including lignin,^[4–7] tannin,^[8–10] protein,^[11–13] non-food starch^[14,15] and agricultural or forest residues,^[16–18] have attracted the attention of researchers to prepare some high-performance wood adhesives. Among these, condensed tannins have been considered to have some interesting features to prepare wood adhesive.^[19] Initially, condensed tannins phenolic nature led to their use to prepare adhesives similar to phenol-formaldehyde (PF) wood adhesive.^[8–10,19,20] It is encouraging that tannin-formaldehyde wood adhesives have been successful commercially for many years.^[19] However, formaldehyde, was still an essential component, even though formaldehyde-emission has been improved by some extent.^[21] Therefore, low or no aldehyde tannin adhesives have been developed by a number of approaches. Hexamethylenetetramine (hexamine),^[22,23] glyoxal,^[24] furfuryl alcohol,^[25] polymeric diphenylmethane diisocyanate (*p*-MDI),^[23,26] poly-ethylenimine (PEI),^[27] as well as carbohydrates-generated non-toxic and non-volatile aldehydes by specific oxidation,^[28] were used to react with different condensed tannins to produce tannin-based wood adhesive without any kinds of volatile and toxic aldehydes. Certainly, some tannin wood adhesives were obtained though biomass resources (starch) mixing with condensed tannin, and alternative aldehydes acting as cross-linkers, leading to low formaldehyde emission.^[13,29–31] Apparently, these improved adhesive formulations reduced effectively the toxic raw-materials consumption and formaldehyde-emission, as well as increasing biomass content.

Herein, a novel, high-bonding performance tannin-based wood adhesive has been synthesized by manual or mechanical mixing without any pre-treatments. The cross-linker used is a commercial product, namely glycerol diglycidyl ether (GDE). Three tannin-based adhesives with different weight ratios of tannin/GDE were studied, from a high 1/1 tannin/GDE ratio to lower GDE proportions. Their properties were studied, including shear strength, hydrolysis residual rate, physico-chemical features and thermal stability. Furthermore, the reaction mechanism of tannin and GDE was confirmed by FT-IR, MALDI-ToF and solid status ¹³C NMR.

2. Materials and methods

2.1. Preparation of tannin-based wood adhesives

The series Mimosa tannin-based wood adhesives were obtained by mixing tannin and GDE directly at room temperature without any pre-synthesis. Briefly, taking a certain amount of Mimosa tannin (*Acacia mearnsii* de Wildt) extract, supplied by Silva Chimica, St. Michele Mondovi, Italy) and then put them into a 100 mL plastic bottle. Thereafter, some amount of distilled water (Laboratory homemade) was added, stirring sufficiently by hand till a homogeneous tannin/water mixture was obtained. After that, setting a weight of glycerol diglycidyl ether (GDE, technical grade, obtained from

Table 1. The formulation of Tannin/GDE Wood Adhesives.

Names	Mimosa Tannin (g)	GDE (g)	Distilled water (g)
Tannin/GDE-1/1	6.6	6.6	6.6
Tannin/GDE-2/1	8.8	4.4	6.6
Tannin/GDE-3/1	9.9	3.3	6.6

Sigma-Aldrich) was added to the tannin/water mixture up to when a homogeneous tannin/GDE/water mixture was obtained by manual stirring. In this work, the ratio of tannin and GDE was variable, and the detailed formulations are shown in Table 1.

2.2. Manufacture of three-layer plywood samples and measurement of shear strength

Three-layer plywood was prepared by using tannin/GDE wood adhesives to bond 2 mm thick poplar veneers. About 320 g/m² of the obtained wood adhesives was applied to the double faces of the veneer. The hot-press gluing condition are 1.25 MPa at a temperature of 160 °C for 6 min. The plywood samples were standby at room condition for at least 24 h before cutting. The plywood was then cut into 100×25×5 mm samples for measuring the dry and wet shear strengths. For wet shear strength testing, the plywood samples were soaked into cold tap water for 24 h and hot water (63 ± 3) °C for 3 h before measuring, according to the Chinese National Standard (GB/T 17657–2013). Six repeated samples were measured for the mean values and standard deviations.

2.3. Measurement of some basic properties of tannin/GDE wood adhesives

2.3.1. pH, viscosity and solid content testing

The pH values of the series of tannin/GDE wood adhesives were measured by using PHS-3C vale meter; The viscosity of those adhesives was tested with Brookfield DV-II+ Viscometer, utilizing spindle No. 4 with 30 rpm at room condition; small amount of wood adhesive samples (~3 g, recorded as W₁) were put in the oven and heated (105 ± 2) °C till the weight difference between two adjacent times is less than 0.02 g, recorded as W₂. The non-volatile resin solid content was calculated by the following formula:

$$\text{Solid content} = W_2/W_1 \times 100 \% \quad (1)$$

2.3.2. Hydrolysis residual rate calculating

Taking some liquid wood adhesive and put them into oven (103 ± 2) °C till the constant weight was obtained, recorded as M₁. And then put those dried adhesive samples into the hot water at 60 °C for 6 h. After that taking the

immersed samples and putting them into oven again at 105 °C till the weight difference between two adjacent times is less than 0.02 g, recorded as M_2 . The residual rate was calculated by the following formula:

$$\text{Hydrolysis residual rate} = M_2/M_1 \times 100 \% \quad (2)$$

Five repeated measurement were carried out, which were calculated for the mean value and standard deviations.

2.3.3. Thermomechanical analysis (TMA)

The relationship between modulus of elasticity (MOE) and temperature was recorded and calculated by the inner-software procedure of TMA equipment (Mettler Toledo, Zurich, Switzerland), which using three-point bending testing condition. Two pieces of beech wood, with the size of $17 \times 5 \times 1.1 \text{ mm}^3$ (Length \times width \times thickness), were assembled with 30 mg tannin/GDE wood adhesives to form a beech-resin-beech sandwiches structure. And then put the testing sample on the testing scaffolding. The testing was carried out between the perform temperature 30 and 250 °C with non-isothermal mode. The heating rate is 10 °C/min with a constant value. Each sample specimens were exercised a 0.1/0.5 N force cycle, which was lasted 12 seconds (6s/6s) per cycle, on an 18 mm span.

2.3.4. Thermogravimetric analysis (TGA)

The thermal stability of tannin/GDE was investigated by the TGA 5500 analysis (Mettler Toledo, Guyancourt, France). About 5–8 mg dried sample powder was put on a platinum pan, and then heating the sample to the desire temperature at a heating rate of 10 °C/min, under a nitrogen atmosphere with the flow of 50 mL/min. The testing temperature was range from 25 to 790 °C.

2.4. The reaction mechanism between tannin and GDE

2.4.1. Fourier transform infrared spectroscopy (FT-IR)

The tannin or tannin/GDE samples were cured (120 ± 2) °C for 2 h, and then got the powder by mortar. The FT-IR was done on a PerkinElmer Frontier ATR-FTMIR equipment. The sample powder was placed on the specifically dedicated testing site. And then tightly screwing the clamp device, ensuring the samples were contacted with transparent glass of the bottle of diamond crystal close-knit. The scan results of each sample were recorded with 32 scans between the wave range of 600 and 4000 cm^{-1} , with the scan resolution of 4 cm^{-1} .

2.4.2. Matrix-assisted laser desorption ionization time-of-flight (MALDI-ToF)

The samples for matrix-assisted laser desorption ionization time-of-flight (MALDI-ToF) analysis were homogeneous covered on the locations dedicated

analysis plaque before testing. Briefly, about 5 mg of samples were dissolved into 1 ml water/acetone mixture solution of 50:50 v/v firstly. And then, taking 10 mg of the above solution, letting them mixed with 10 μ l of a 2,5-dihydroxy benzoic acid (DHB) matrix to form a homogenous mixture and standby. Before covering with samples, the corresponding of locations dedicated analysis plaque were needed to cover with 2 μ l NaCl solution, which is the 0.1 M in 2:1 v/v methanol/water solution, and pre-dried. Finally, taking 1 μ l sample solution and then covered on the corresponding of locations dedicated analysis plaque and dried.

Red phosphorous was act as reference sample to standardize the device before testing each time. The MALDI-ToF spectra were obtained by using the Axima-Performance mass spectrometer from Shimadzu Biotech (Kratos Analytical Shimadzu Europe Ltd., Manchester, UK). The testing was carried out with a linear polarity-positive tuning mode. The measurements were taken by making 1000 profiles per sample with two shots accumulated per profile. The accuracy of the spectrum is ± 1 Da.

2.4.3. Cross polarization-magic angle spinning (CP-MAS ^{13}C NMR)

To investigate the chemical structure of tannin/GDE sample, CP-MAS ^{13}C NMR equipment was utilized. The spectra result was got by the AVANCE II 400 MHz spectrometer (Brüker, Billerica, MA, USA), which using 4 mm probe at a 12-kHz sample spin. The pulse duration time was 4.1 μ s at 90°, and the contact time is 2 ms with a pulse interval of 4 s. The tetramethyl silane (TMS) was served as control reference simple to determine the chemical shifts. The accuracy of the spectrum is ± 1 ppm.

3. Results and discussion

3.1. The basic characterizations of tannin/GDE wood adhesive

A novel mimosa tannin-based high-performance wood adhesive was obtained by mixing tannin with glycerol diglyceryl ether (GDE) at room temperature in distilled water. GDE was chosen as crosslinker due not only to its lower toxicity than other epoxies^[30–33] but also to improve the bond strength of the plywood so obtained. The most effective functional approach which originates from using GDE is that non-hydrolysable ether bonds can be formed with the tannin during the wood panels hot-pressing.^[3] A foreseeable reaction and structure between tannin and GDE is shown in Figure 1. These ethers are obtained by the reaction of the tannin -OHs with the epoxy groups of GDE by water elimination, meanwhile, they could simultaneously enhance the stability of the cured resins by limiting resin degradation.^[3] Therefore, tannin/GDE wood adhesives show a good bonding performance and water resistance. Table 2 shows the basic characterizations of tannin/GDE wood adhesives. The pH values are all

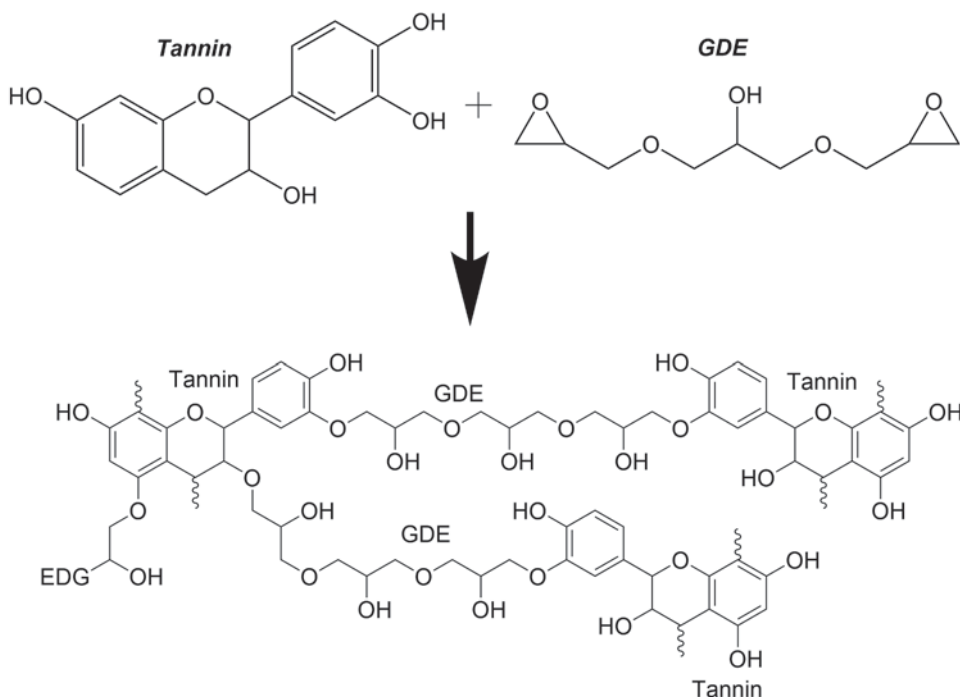


Figure 1. A foreseeable reaction and structure between tannin and GDE.

Table 2. The basic characterizations of tannin/GDE Wood Adhesives.

Adhesive types	pH	Solid content (%)	Viscosity (mPa·s)
Tannin/GDE -1/1	5.47	65.3	3100 ± 156
Tannin/GDE -2/1	5.27	64.97	5600 ± 192
Tannin/GDE -3/1	5.01	63.5	6480 ± 135

around 5 and 5.5. There does not appear to be any major difference in solids content, all being in the 63.5%-65.3% range. The viscosity of these adhesives, however, is significantly different, a higher viscosity being obtained for the higher proportions of tannin. The tannin: GDE weight ratios from 1:1, 2:1 and 3:1, present viscosities of 3100 ± 156, 5600 ± 192 and 6480 ± 135 mPa·s, respectively. This indicates that GDE can effectively dilute the concentration of tannin/water solution so as to obtain a relatively lower viscosity than when the ratio of tannin/GDE is 1:1.

3.2. Performance analysis of tannin/GDE wood adhesive

3.2.1. Thermomechanical analysis (TMA)

The thermomechanical analysis curves have shown in Figure 2, which show the variation of Young's modulus E (MOE) as a function of curing temperature.^[7,23] A higher MOE is obtained by increasing the proportion of GDE, with the highest

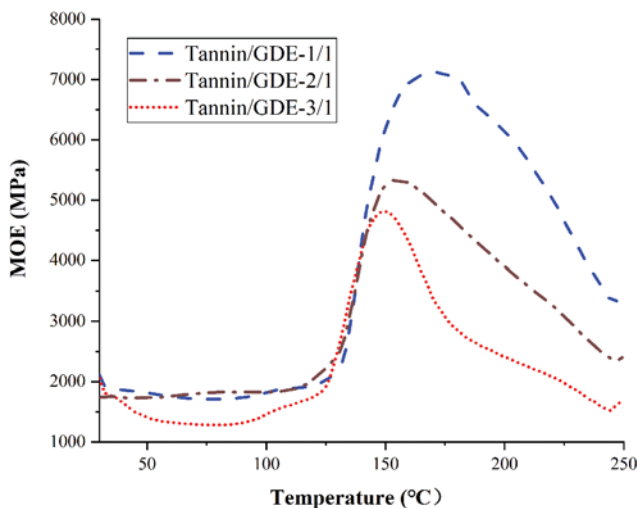


Figure 2. Thermomechanical analysis (TMA) curves of Tannin/GDE adhesives with different proportion.

MOE being almost 7100 MPa when the ratio of tannin/GDE is 1:1, with the MOE becoming 5300 and 4800 MPa for tannin/GDE-2/1 and tannin/GDE-3/1, respectively. This infers that tannin/GDE-1/1 gives the best bonding performance and this decreases for decreasing GDE proportions. Existing literature confirms this.^[7,23,32,33] The shear strength of bonded specimens with tannin/GDE adhesives also confirms this trend. Even though these wood adhesives start curing at the same initial temperature, around 125 °C, the highest MOE occurs at different temperatures for the different cases. Thus, for tannin/GDE-1/1, tannin/GDE-2/1 and tannin/GDE-3/1, the obtained maximum elastic modulus temperature is 170, 154 and 149 °C, respectively. It is most likely that more non-hydrolysable ether bonds could be formed during hot-pressing GDE increases. Therefore, more energy (a higher temperature) is needed during hot pressing to obtain a higher MOE and to form non-hydrolysable ether bonds. Figure 2 shows the MOE value sequence relationships clearly, i.e. tannin/GDE-1/1, tannin/GDE-2/1 and tannin/GDE-3/1. It can be speculated that the tannin/GDE adhesive has a higher thermal stability with higher proportion of GDE.^[33] This kind of result can be deduced from the results of the thermogravimetric analysis.

3.2.2. Thermogravimetric analysis (TGA)

To investigate the thermal stability of fully cured series Tannin/GDE wood adhesives, thermogravimetric analysis (TGA) was carried out. The corresponding results curves of each samples and their first derivatives (DTG) are shown in Figure 3. There appears to be a three-stages thermal degradation process, thus, in the 50–150°C, 150–400°C and 400–600°C. DTG curves show three peaks as well, corresponding to the three thermal degradation stages. For

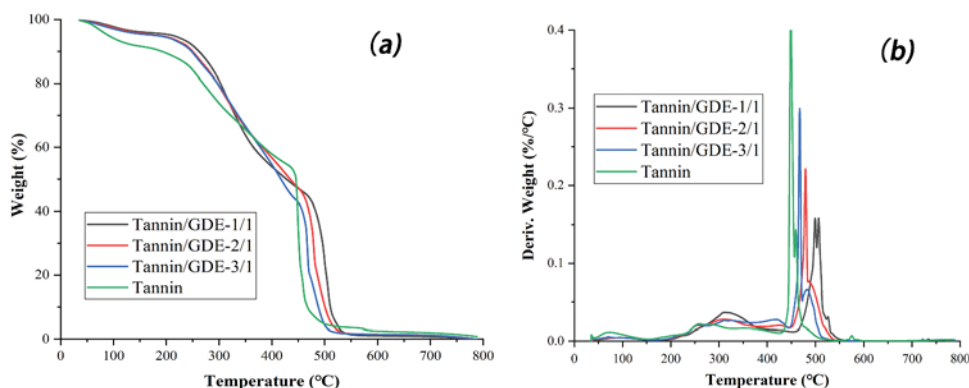


Figure 3. TGA (a) and DTG (b) curves of Tannin/GDE adhesives with different proportion (under air atmosphere).

the first one, in the low-temperature range, this weight loss was attributed to the residual water evaporation and some small molecular impurities degradation.^[34,35] The second stage occurs in the 150–400 °C range, a small peak appearing in this temperature range, which corresponds to some unreacted GDE.^[3] This is confirmed by the peak increasing at the higher proportions of GDE. Finally, the third degradation stage showing a large weight loss can occur in the 400–600°C range, is due to the degradation of the cured adhesive skeleton. Some more stable chemical bonds, such as C-C and C-O, are cleaved within this temperature range.^[34–36] Remarkably, with the increasing GDE addition, the degradation temperature shifts to a higher value, while the weight loss rate shifts to a lower value. FT-IR analysis shows a new bond structure being obtained during the curing process. Thus, a new structure appears to be formed during the curing process, this contributing to improve thermal stability of the wood adhesive.

3.2.3. Hydrolysis residual rate analysis

The hydrolysis residual rate is a parameter commonly used as an indicator to assess the hydrolytic stability of a cured wood adhesive.^[20] It can be calculated by using the weight difference between the original weight of an adhesive and its non-hydrolyzable portion after a specific hydrolysis treatment.^[11–13] The results for the tannin/GDE wood adhesives are shown in Table 3. As the proportion of tannin increases, the residual rate shows a decreasing trend, the lowest rate being 90.05 ± 0.037 for tannin/GDE-3/1. This indicates that the tannin/GDE-3/1 adhesive has the lowest proportion of non-hydrolysable material, thus poorer crosslinking. The residual rate increases with the decreasing amount of tannin, increased of 4% to 94.41 ± 0.031 for the tannin/GDE 2:1. This is so because of more non-hydrolysable ether bonds being formed. Same trend for the tannin/GDE-1/1 improved 6% to 96.29 ± 0.023 . These results are consistent with other research work using

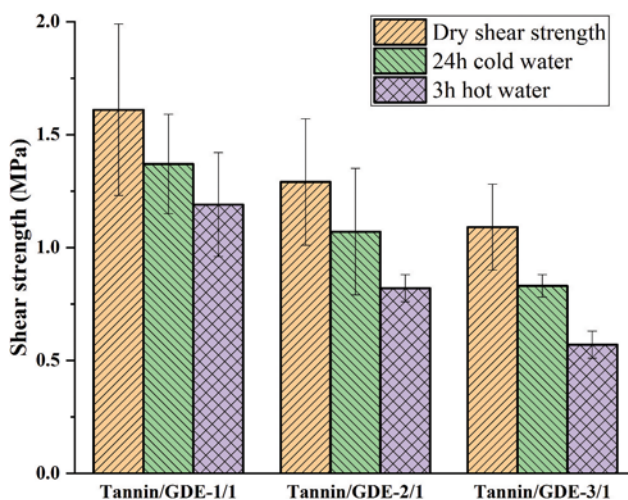
Table 3. Residual rate of tannin/GDE Wood Adhesives.

Adhesive types	Tannin/GDE-1/1	Tannin/GDE-2/1	Tannin/GDE-3/1
Residual rate (%)	96.29 ± 0.023	94.41 ± 0.031	90.05 ± 0.037

epoxy resin to improve bonding performance.^[37,38] In addition, better bonding strength can be obtained by increasing GDE but unfortunately to the expense of decreasing the proportion of biomaterials.

3.3. The bonding performance of tannin/GDE wood adhesives

To determine the bonding performance of the tannin/GDE wood adhesive, the dry, 24 h cold water and 3 h hot water shear strengths of the plywood bonded with them were measured. The results are shown in Figure 4. It can be seen that except for the 3 h hot water treatment wet shear strength of the tannin/GDE-3/1 adhesive, all shear strength values meet the interior-use plywood requirements of China national standard (GB/T 9846–2015, ≥ 0.7 MPa). All tannin/GDE resins show an outstanding bonding performance for the dry and 24 h cold water shear strength. As expected, the shear strength of the tannin/GDE adhesives increases by increasing the amount of GDE. For the tannin/GDE-1/1 adhesive shows the highest shear strength, namely 1.61 MPa for dry strength (over 95% wood failure), 1.37 MPa for 24 h cold water wet strength (over 95% wood failure) and 1.19 MPa for 3 h hot water shear strength (about 85% wood failure), respectively. The causes of this results are more non-hydrolysable ether bonds have formed with the high amount of GDE. This conclusion is in line with the results for the residual rate. The GDE, most probably, acts in two ways: The first and most probable one is that the epoxy

**Figure 4.** The bonding performance of Tannin/GDE adhesives with different proportion.

groups of GDE can react with -OH groups of tannin, resulting in tannin/GDE derived macromolecules forming the 3-D crosslinked network. The second one is that epoxy groups of GDE could also react with the -OH groups of the wood panels surface, but this is the less likely possibility. Hence, the poorer trend for shear strength of tannin/GDE-2/1 and tannin/GDE-3/1 compared to the tannin/GDE-1/1 adhesive. As shown in Figure 4, the shear strength of tannin/GDE-2/1 adhesive is 1.29 MPa for dry strength (over 95% wood failure), 1.07 MPa for 24 h cold water wet strength (about 85% wood failure) and 0.82 MPa for 3 h hot water wet strength (about 50% wood failure), respectively. While the dry shear strength and 24 h cold water shear strength is 1.09 MPa (about 80% wood failure) and 0.83 MPa (about 35% wood failure) for the tannin/GDE-3/1 adhesive, these too having reached the relevant requirements. These trends are also confirmed by the results of the TMA analysis and of the residual rate. More water resistance compounds have formed during the plywood hot-pressing with high amount of GDE to yield a better wet shear strength.

3.4. The reaction mechanism between tannin and GDE

3.4.1. Fourier transform infrared (FT-IR) spectra analysis

For investigating the functional groups changing after cured adhesives, the Fourier Transform Infrared (FT-IR) analysis was used to study the variation of functional groups after adhesives curing. The resulting spectra are shown in Figure 5. Raw tannin was used as control (black spectrum). The spectra of the tannin/GDE adhesives present a similar chemical structure than raw tannin. An intense broad absorption band (region I in Figure 5(a)) between 3200 and 3500 cm^{-1} is associated with -OH group of aromatic and aliphatic stretching vibration.^[34,39,40] Although here also have some difference

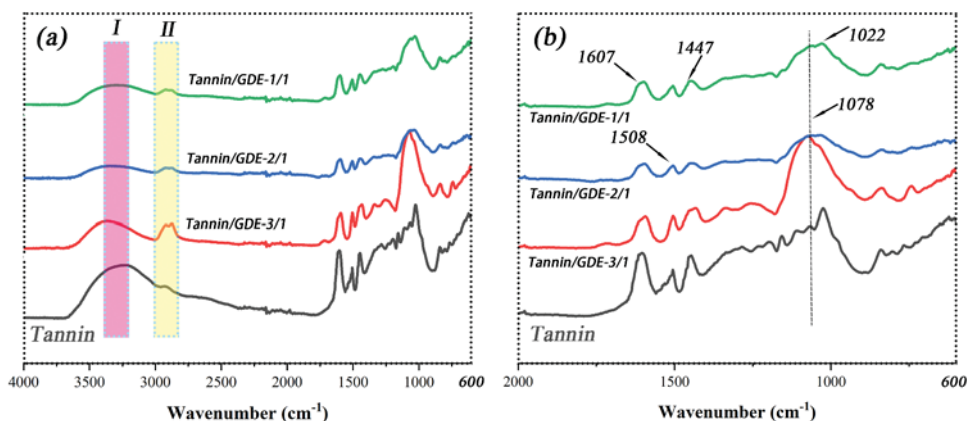


Figure 5. FT-IR spectra comparison of raw tannin and tannin/GDE wood adhesives. (a) The wavenumber is from 600–4000 cm^{-1} ; (b) The wavenumber is from 600–2000 cm^{-1} .

between all four samples, it is still unidentifiable if some change occurs in the number of -OH during the reaction between tannin and GDE. This is so because a new -OH group will be generated by the opening of epoxide ring when GDE reacts with the -OH group of tannin, leaving the same the apparent number of -OH groups. Some characteristic peaks can be seen in the Figure 5(b), 1607, 1508 and 1447 cm^{-1} are related to stretching vibration peaks of aromatic ring of the tannin structure.^[20,41,42] The peak at 1022 cm^{-1} represents the C-O bond stretching vibration, which probably originates from aliphatic C-OH.^[20]

Some apparent changes can be noticed. In Figure 5(a), 2933 and 2860 cm^{-1} in the region II of the four samples, which are attributed to the C-H bond vibration of $-\text{CH}_2-$ or/and $-\text{CH}_3$.^[7,34] Especially in the tannin/GDE wood adhesive samples, the ratio of peaks in the contoured region II are clearly greater than in the raw tannin case. These $-\text{CH}_2-$ groups are mainly coming from the GDE and some carbohydrate impurities of the tannin extract. According to some literatures, the peak of 910 cm^{-1} should be attributed to oxirane rings if it cannot fully reaction with tannin.^[43] Nevertheless, this peak had disappeared after reaction with tannin. Therefore, one can consider that the epoxide groups of GDE have fully reacted with the tannin. Moreover, further evidence can be found in Figure 5(b) black-dotted line, i.e. the peak of 1078 cm^{-1} is attributed to an ether $-\text{C}-\text{O}-$ bond,^[3] obtained by the GDE reaction with the tannin. A small peak at 1078 cm^{-1} can also be seen in the raw tannin, this being attributed to the tannin heterocycle ring. This peak has increased clearly after reaction with GDE. Therefore, these results can suggest that GDE has indeed reacted with the tannin.

3.4.2. MALDI-ToF analysis

MALDI-ToF mass spectrometry is now used to determine the tannin oligomers formed and their distribution.^[36,44,45] As we all known, there are four typical oligomers, which are shown in Figure 6, i.e. Fisetinidin (272.3 + 2 H = 274.3 Da), Robinetinidin (288.3 + 2 H = 290.3 Da), Catechin (288.3 + 2 H = 290.3 Da) and Delphinidin (304.3 + 2 H = 306.3 Da), respectively, are the basic structure units of mimosa tannin-based GDE wood adhesive. Therefore, some foreseeable reaction structures can be speculated according to those monomer structural units. And the MALDI-ToF spectrum of tannin/GDE-1/1 has been done and is shown in Figure 7.

From Figure 7, some regular peak-to-peak gaps can be observed, giving a sequence of peaks such as 273.9 Da, 544.4 Da and 819.4 Da; 560.5 Da and 831.0 Da; 1049.8 Da and 1320.9 Da; 1561.4 (1535.4 + 23) Da and 1806.8. A 272.3–274.3 Da \pm 2 Da (with or without Na^+) repeating unit is then present indicating that fisetinidin (Fi) units are present in the sample.^[45,46]

Identically, a series of peaks, including 576.4 Da, 892.1 (866.7 + 23) Da, 1155 Da and 1443.3 Da; 784.7 Da, 1097.9 (1073 + 23) Da, 1631.2 Da and

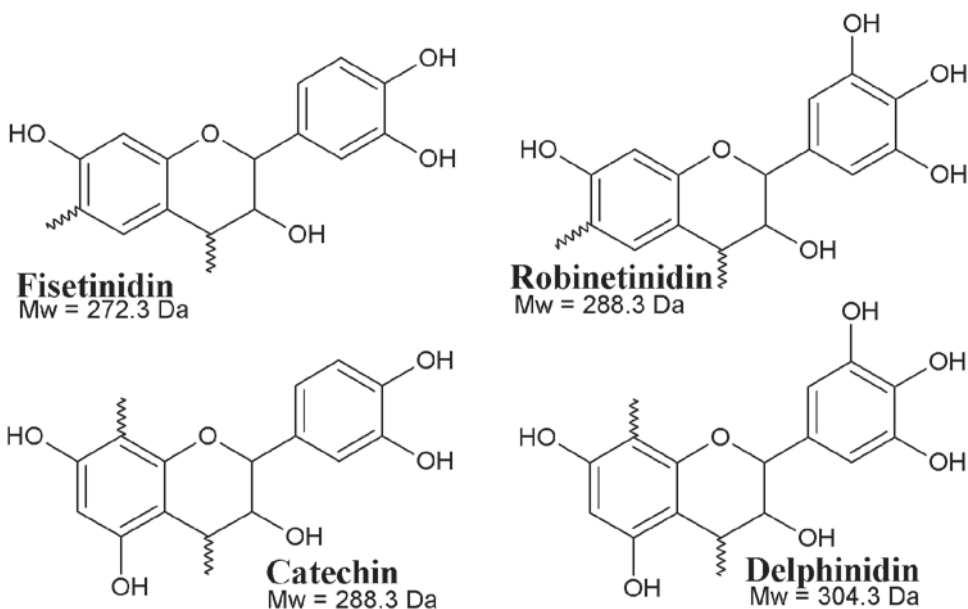


Figure 6. The four basic type structures of mimosa tannin.

1639.0 Da, were separated by a 288.3–290.3 Da \pm 2 Da repeating units. Thus, robinetinidin (Ro) or catechin (Ca) repeating units, or both, are present.^[10,46]

For the same reason, the presence of delphinidin (De) units at 304.3--306.3 Da \pm 2 Da can be deduced from the series of peaks, such as 305.1 Da, 608.5 Da, 939.3 (914.5 + 23) Da and 1222.1/1220.0 Da; 803.3 Da, 1101.7 Da and 1429.6 (1409.2 + 23) Da.^[45,46]

Moreover, because of reaction of tannin with GDE, it can more complex oligomers are also obtained. And the complex obtained-structure always derived from the tannin basic units linked by GDE. Evidence of these can be seen in Figure 7. For instance, the peak at 768.9 Da probable is that GDE act as crosslinker to linked two tannin oligomers:

Or three kinds of tannin oligomers are linked by the GDE molecules, such as the peak 1278.5 Da:

Furthermore, some large crosslinked molecules can be obtained due to the presence of the GDE crosslinker, such as the peak at 1561 Da:

and of a more complex structure, as the peak at 2172.5 Da:

Hence, it can be deduced that GDE has reacted with the tannin during the curing process. The abovementioned peaks and structures are only a few representative formulas among the all peaks of MALDI-ToF spectrum, the more some foreseeable tannin or GDE derived products where been speculated and listed in Table S1.

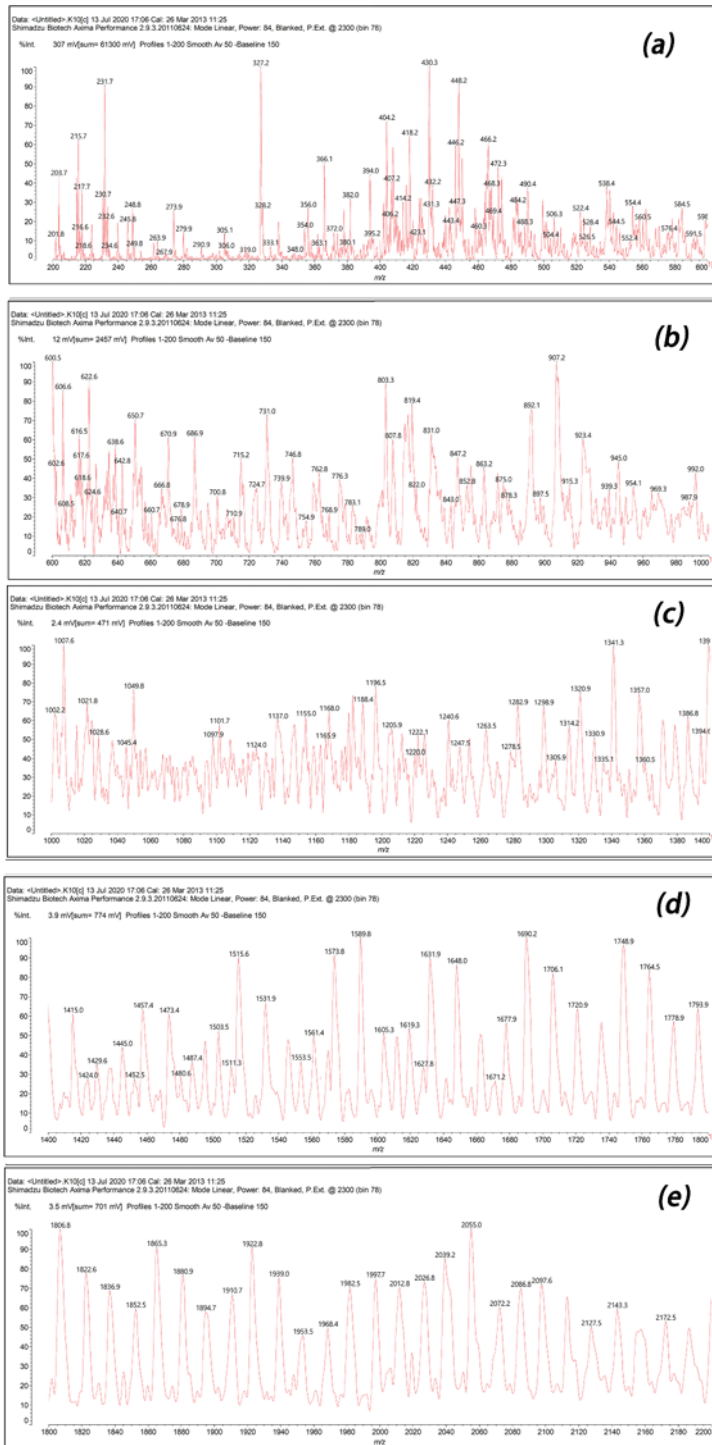


Figure 7. The MALDI-TOF spectra of tannin/GDE wood adhesive (tannin/GDE-1/1), (a) 200–600 Da, (b) 600–1000 Da, (c) 1000–1400 Da, (d) 1400–1800 Da and (e) 1800–2200 Da.

3.4.3. CP-MAS ^{13}C NMR analysis

CP-MAS ^{13}C NMR was used to investigate the tannin/GDE-1/1. The spectrum obtained is shown in Figure 8. The relatively broad and intense peak at 69.04 ppm is possibly a composite peak. It is composed of the alcohol -OHs of the carbohydrates oligomers still present in the tannin extract.^[47] This broad peak is superimposed on and composed too of the 72 ppm signal being the alcoholic -OH on the tannin heterocycle ring at C_3 .^[47,48] Secondly, it is superimposed on the products from the tannin C_3 -OH reacted with GDE, and possibly of the tannin extract carbohydrate residues with the GDE too, so that structures such as $-\text{O}-\text{CH}_2-\text{CH}_2\text{OH}-\text{CH}_2-\text{R}$ can be obtained, which should have a shift of 70.7 ppm.^[44] Therefore, the centre of this composite peak at 69.04 ppm can indicate that the reaction has occurred between tannin extract components and GDE and that their reaction site is on the tannin C_3 position, but opens the possibility that the tannin extract carbohydrate residues have also reacted with GDE. In addition, the peak at 40.8 ppm is related to the $-\text{CH}_2$ -bridges, involving the GDE or the derived products of GDE. Furthermore, a small shoulder peak at 154.45 ppm, which possible belongs to the C_5 or C_7 of A-aromatic ring.^[44,47,48] The peak at 150.14 ppm is possibly the structure obtained from the GDE reacted with tannin at the site C_5 ,^[44] while the peak at 133.42 ppm is the $\text{C}1'$ of flavonoid units.^[47] However, compared with the peak 69.04 ppm, it can be speculated that GDE mostly can react with tannin at its C_3 site with the clear possibility that it has reacted also with the tannin extract carbohydrates. The peak at 40.6 ppm indicates the presence of a certain extent rearrangement of the tannin to catechic acid, an unwanted rearrangement that cannot be completely avoided.^[49,50] The peak characteristic of epoxy groups should appear at 46.4 ppm, but this kind of peak cannot be detected which indicates that the GDE has fully reacted with the tannin extract.

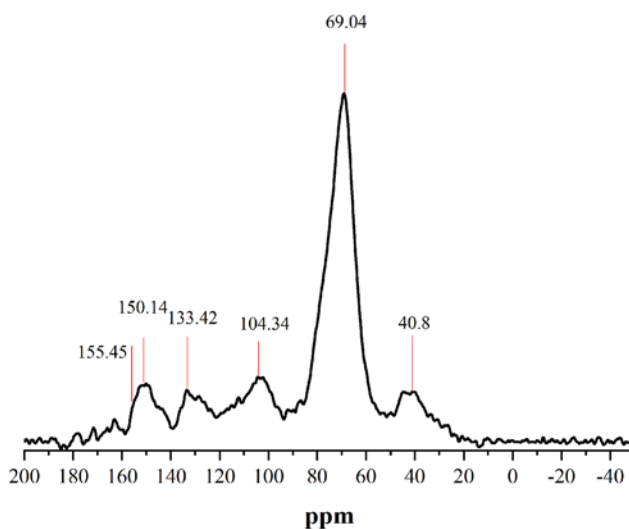


Figure 8. Solid state ^{13}C NMR spectrum of tannin/GDE-1/1 sample.

4. Conclusions

A series of tannin-based wood adhesives were prepared via mixing commercial Mimosa tannin and GDE directly without any pre-treatment. In addition, this series of adhesives present a good bonding performance and water resistance due to the present of non-hydrolysable ether bonds which are formed by reaction of tannin and GDE. The tannin/GDE-1/1 adhesive shows the highest shear strength, namely 1.61 MPa for dry strength, 1.37 MPa for 24 h cold water wet strength and 1.19 MPa for 3 h hot water shear strength, respectively. Moreover, the residual rate can be improved by the GDE addition and present a positive correlation trend. With the increasing of GDE addition, its residual rate passed from 90.05 for tannin/GDE-3/1 to 96.29 for tannin/GDE-1/1, hence it was improved by over 6%. Furthermore, the thermal stability has improved and exhibits the same trend as the residue rate. From the results obtained by FT-IR, MALDI-ToF and ^{13}C NMR, the typical reaction between tannin and GDE has occurred between the epoxy groups of GDE with -OH groups of the tannin extract, resulting in non-hydrolysable ether bonds. Furthermore, these ether bonds are most likely sited at the C_3 of the flavonoid units heterocyclic ring, of the carbohydrate oligomer residues in the tannin extract, and C_5 or C_7 site of A-ring, according to the ^{13}C NMR results.

Funding

This work was supported by the National Natural Science Foundation of China (NSFC 31971595), Yunnan provincial youth and middle-age reserve talents of academic and technical leaders (2019HB026), Scholarship from China Scholarship Council (CSC), Yunnan Provincial Key Laboratory of Wood Adhesives and Glued Products and The LERMAB is supported by a grant of the French Agence Nationale de la Recherche (ANR) as part of the laboratory of excellence (LABEX) ARBRE.

ORCID

Antonio Pizzi  <http://orcid.org/0000-0002-9749-7185>

References

- [1] Wilson, J. B.; Life-cycle Inventory of Medium Density Fiberboard in Terms of Resources, Emissions, Energy and Carbon. *Wood Fiber Sci.* 2010, 42(CORRIM Special Issue), 107–124.
- [2] Salthammer, T.; Mentese, S.; Marutzky, R. Formaldehyde in the Indoor Environment. *Chem. Rev.* 2010, 110(4), 2536–2572. DOI: 10.1021/cr800399g.
- [3] Li, R. J.; Gutierrez, J.; Chung, Y. L.; Frank, C. W.; Billington, S. L.; Sattely, E. S. A Lignin-epoxy Resin Derived from Biomass as an Alternative to Formaldehyde-based Wood Adhesives. *Green Chem.* 2018, 20(7), 1459–1466. DOI: 10.1039/c7gc03026f.

- [4] Aziz, N. A.; Latip, A. F. A.; Peng, L. C.; Abd Latif, N. H.; Brosse, N.; Hashim, R.; Hussin, M. H. Reinforced Lignin-phenol-glyoxal (LPG) Wood Adhesives from Coconut Husk. *Int. J. Biol. Macromol.* 2019, *141*, 185–196. DOI: 10.1016/j.ijbiomac.2019.08.255.
- [5] Chen, H.; Nair, S. S.; Chauhan, P.; Yan, N. Lignin Containing Cellulose Nanofibril Application in pMDI Wood Adhesives for Drastically Improved Gap-filling Properties with Robust Bondline Interfaces. *Chem. Eng. J.* 2019, *360*, 393–401. DOI: 10.1016/j.cej.2018.11.222.
- [6] Hussin, M. H.; Aziz, A. A.; Iqbal, A.; Ibrahim, M. N. M.; Abd Latif, N. H. Development and Characterization Novel Bio-adhesive for Wood Using Kenaf Core (Hibiscus Cannabinus) Lignin and Glyoxal. *Int. J. Biol. Macromol.* 2019, *122*, 713–722. DOI: 10.1016/j.ijbiomac.2018.11.009.
- [7] Chen, X.; Xi, X.; Pizzi, A.; Fredon, E.; Du, G.; Gerardin, C.; Amirou, S. Oxidized Demethylated Lignin as a Bio-based Adhesive for Wood Bonding. *J. Adhes.* 2020, 1–18. DOI: 10.1080/00218464.2019.1710830.
- [8] Hoong, Y. B.; Paridah, M. T.; Luqman, C. A.; Koh, M. P.; Loh, Y. F. Fortification of Sulfited Tannin from the Bark of Acacia Mangium with Phenol-formaldehyde for Use as Plywood Adhesive. *Ind. Crops Prod.* 2009, *30*(3), 416–421. DOI: 10.1016/j.indcrop.2009.07.012.
- [9] Moubarik, A.; Pizzi, A.; Allal, A.; Charrier, F.; Charrier, B. Cornstarch and Tannin in Phenol-formaldehyde Resins for Plywood Production. *Ind. Crops Prod.* 2009, *30*(2), 188–193. DOI: 10.1016/j.indcrop.2009.03.005.
- [10] Li, J.; Zhu, W.; Zhang, S.; Gao, Q.; Xia, C.; Zhang, W.; Li, J. Depolymerization and Characterization of Acacia Mangium Tannin for the Preparation of Mussel-inspired Fast-curing Tannin-based Phenolic Resins. *Chem. Eng. J.* 2019, *370*, 420–431. DOI: 10.1016/j.cej.2019.03.211.
- [11] Yue, L.; Shi, R.; Yi, Z.; Shi, S. Q.; Gao, Q.; Li, J. A High-performance Soybean Meal-based Plywood Adhesive Prepared via an Ultrasonic Process and Using Significantly Lower Amounts of Chemical Additives. *J. Cleaner Prod.* 2020, *274*, 123017. DOI: 10.1016/j.jclepro.2020.123017.
- [12] Xu, Y.; Xu, Y.; Zhu, W.; Zhang, W.; Gao, Q.; Li, J. Improve the Performance of Soy Protein-based Adhesives by a Polyurethane Elastomer. *Polymers.* 2018, *10*(9), 1016. DOI: 10.3390/polym10091016.
- [13] Chen, M.; Luo, J.; Shi, R.; Zhang, J.; Gao, Q.; Li, J. Improved Adhesion Performance of Soy Protein-based Adhesives with a Larch Tannin-based Resin. *Polymers.* 2017, *9*(9), 408. DOI: 10.3390/polym9090408.
- [14] Wang, Z.; Zhu, H.; Huang, J.; Ge, Z.; Guo, J.; Feng, X.; Xu, Q. Improvement of the Bonding Properties of Cassava Starch-based Wood Adhesives by Using Different Types of Acrylic Ester. *Int. J. Biol. Macromol.* 2019, *126*, 603–611. DOI: 10.1016/j.ijbiomac.2018.12.113.
- [15] Li, P.; Wu, Y.; Zhou, Y.; Zuo, Y. Preparation and Characterization of Resorcinol-dialdehyde Starch-formaldehyde Copolycondensation Resin Adhesive. *Int. J. Biol. Macromol.* 2019, *127*, 12–17. DOI: 10.1016/j.ijbiomac.2018.12.249.
- [16] Jiang, W.; Kumar, A.; Adamopoulos, S. Liquefaction of Lignocellulosic Materials and Its Applications in Wood adhesives-A Review. *Ind. Crops Prod.* 2018, *124*, 325–342. DOI: 10.1016/j.indcrop.2018.07.053.
- [17] Alma, M. H.; Basturk, M. A. Liquefaction of Grapevine Cane (*Vitis Vinisera* L.) Waste and Its Application to Phenol-formaldehyde Type Adhesive. *Ind. Crops Prod.* 2006, *24* (2), 171–176. DOI: 10.1016/j.indcrop.2006.03.010.
- [18] Alma, M. H.; Baştürk, M. A.; Shiraiishi, N. Cocondensation of NaOH-catalyzed Liquefied Wood Wastes, Phenol, and Formaldehyde for the Production of Resol-type Adhesives. *Ind. Eng. Chem. Res.* 2001, *40*(22), 5036–5039. DOI: 10.1021/ie000858x.

- [19] Shirmohammadli, Y.; Efhamisisi, D.; Pizzi, A. Tannins as A Sustainable Raw Material for Green Chemistry: A Review. *Ind. Crops Prod.* 2018, *126*, 316–332. DOI: 10.1016/j.indcrop.2018.10.034.
- [20] Liu, J.; Wang, L.; Li, J.; Li, C.; Zhang, S.; Gao, Q.; Zhang, W.; Li, J. Degradation Mechanism of Acacia Mangium Tannin in NaOH/urea Aqueous Solution and Application of Degradation Products in Phenolic Adhesives. *Int. J. Adhes. Adhes.* 2020, *98*, 102556. DOI: 10.1016/j.ijadhadh.2020.102556.
- [21] Pizzi, A.; Recent Developments in Eco-efficient Bio-based Adhesives for Wood Bonding: Opportunities and Issues. *J. Adhes. Sci. Technol.* 2006, *20*(8), 829–846. DOI: 10.1163/156856106777638635.
- [22] Kamoun, C.; Pizzi, A. Mechanism of Hexamine as a Non-aldehyde Polycondensation Resins Hardener. Part 1: Hexamine Decomposition and Reactive Intermediates. *Holzforchung und Holzverwertung.* 2000, *52*(1), 16–19.
- [23] Efhamisisi, D.; Thevenon, M. F.; Hamzeh, Y.; Karimi, A. N.; Pizzi, A.; Pourtahmasi, K. Induced Tannin Adhesive by Boric Acid Addition and Its Effect on Bonding Quality and Biological Performance of Poplar Plywood. *ACS Sustainable Chem. Eng.* 2016, *4*(5), 2734–2740. DOI: 10.1021/acssuschemeng.6b00230.
- [24] Ballerini, A.; Despres, A.; Pizzi, A. Non-toxic, Zero Emission Tannin-glyoxal Adhesives for Wood Panels. *Holz als Roh-und Werkstoff.* 2005, *63*(6), 477–478. DOI: 10.1007/s00107-005-0048-x.
- [25] Zhang, J.; Xi, X.; Liang, J.; Pizzi, A.; Du, G.; Deng, S. Tannin-based Adhesive Cross-linked by Furfuryl Alcohol-glyoxal and Epoxy Resins. *Int. J. Adhes. Adhes.* 2019, *94*, 47–52. DOI: 10.1016/j.ijadhadh.2019.04.012.
- [26] Zhou, X.; Pizzi, A. Pine Tannin Based Adhesive Mixes for Plywood. *Int. Wood Prod. J.* 2014, *5*(1), 27–32. DOI: 10.1179/204264531Y.0000000043.
- [27] Faris, A. H.; Rahim, A. A.; Ibrahim, M. N. M.; Alkurdi, A. M.; Shah, I. Combination of Lignin Polyol-tannin Adhesives and Polyethylenimine for the Preparation of Green Water-resistant Adhesives. *J. Appl. Polym. Sci.* 2016, *133*(20), 43437. DOI: 10.1002/app.43437.
- [28] Xi, X.; Pizzi, A.; Frihart, C.; Lorenz, L.; Gerardin, C. Tannin Plywood Bioadhesives with Non-volatile Aldehydes Generation by Specific Oxidation of Mono-and Disaccharides. *Int. J. Adhes. Adhes.* 2020, *98*, 102499. DOI: 10.1016/j.ijadhadh.2019.102499.
- [29] Navarrete, P.; Pizzi, A.; Tapin-Lingua, S.; Benjelloun-Mlayah, B.; Pasch, H.; Rode, K.; Delmotte, L.; Rigolet, S. Low Formaldehyde Emitting Biobased Wood Adhesives Manufactured from Mixtures of Tannin and Glyoxylated Lignin. *J. Adhes. Sci. Technol.* 2012, *26*(10–11), 1667–1684. DOI: 10.1163/156856111X618489.
- [30] Ping, L.; Gambier, F.; Pizzi, A.; Guo, Z. D.; Brosse, N. Wood Adhesives from Agricultural By-products: Lignins and Tannins for the Elaboration of Particleboards. *Cellulose Chem. Technol.* 2012, *46*(7–8), 457–462.
- [31] Ghahri, S.; Pizzi, A.; Mohebby, B.; Mirshokraie, A.; Mansouri, H. R. Soy-based, Tannin-modified Plywood Adhesives. *J. Adhes.* 2018, *94*(3), 218–237. DOI: 10.1080/00218464.2016.1258310.
- [32] Laigle, Y.; Kamoun, C.; Pizzi, A. Particleboard IB Forcast by TMA Bending in UF Adhesives Curing. *Eur. J. Wood Wood Prod.* 1998, *56*(3), 154. DOI: 10.1007/s001070050288.
- [33] Xi, X.; Liao, J.; Pizzi, A.; Gerardin, C.; Amirou, S.; Delmotte, L. 5-Hydroxymethyl Furfural Modified Melamine Glyoxal Resin. *J. Adhes.* 2019, 1–19. DOI: 10.1080/00218464.2018.1561291.
- [34] Chen, X.; Li, J.; Xi, X.; Pizzi, A.; Zhou, X.; Fredon, E.; Du, G.; Gerardin, C. Condensed Tannin-glucose-based NIPU Bio-foams of Improved Fire Retardancy. *Polym. Degrad. Stab.* 2020, *175*, 109121. DOI: 10.1016/j.polyimdegradstab.2020.109121.

- [35] Luo, J.; Zhou, Y.; Gao, Q.; Li, J.; Yan, N. From Wastes to Functions: A New Soybean Meal and Bark-based Adhesive. *ACS Sustainable Chem. Eng.* 2020, 8(29), 10767–10773. DOI: 10.1021/acssuschemeng.0c02413.
- [36] Chen, X.; Xi, X.; Pizzi, A.; Fredon, E.; Zhou, X.; Li, J.; Gerardin, C.; Du, G. Preparation and Characterization of Condensed Tannin Non-Isocyanate Polyurethane (NIPU) Rigid Foams by Ambient Temperature Blowing. *Polymers.* 2020, 12(4), 750. DOI: 10.3390/polym12040750.
- [37] Li, J.; Luo, J.; Li, X.; Yi, Z.; Gao, Q.; Li, J. Soybean Meal-based Wood Adhesive Enhanced by Ethylene Glycol Diglycidyl Ether and Diethylenetriamine. *Ind. Crops Prod.* 2015, 74, 613–618. DOI: 10.1016/j.indcrop.2015.05.066.
- [38] Luo, J.; Li, C.; Li, X.; Luo, J.; Gao, Q.; Li, J. A New Soybean Meal-based Bioadhesive Enhanced with 5, 5-dimethyl Hydantoin Polyepoxide for the Improved Water Resistance of Plywood. *RSC Adv.* 2015, 5(77), 62957–62965. DOI: 10.1039/C5RA05037E.
- [39] Ferdosian, F.; Yuan, Z.; Anderson, M.; Xu, C. C. Synthesis and Characterization of Hydrolysis Lignin-based Epoxy Resins. *Ind. Crops Prod.* 2016, 91, 295–301. DOI: 10.1016/j.indcrop.2016.07.020.
- [40] Younesi-Kordkheili, H.; Pizzi, A. Improving the Properties of Urea-lignin-glyoxal Resin as a Wood Adhesive by Small Addition of Epoxy. *Int. J. Adhes. Adhes.* 2020, 102, 102681. DOI: 10.1016/j.ijadhadh.2020.102681.
- [41] Xin, J.; Li, M.; Li, R.; Wolcott, M. P.; Zhang, J. Green Epoxy Resin System Based on Lignin and Tung Oil and Its Application in Epoxy Asphalt. *ACS Sustainable Chem. Eng.* 2016, 4, 2754–2761. DOI: 10.1021/acssuschemeng.6b00256.
- [42] Jahanshahi, S.; Pizzi, A.; Abdulkhani, A.; Shakeri, A. Analysis and Testing of Bisphenol A-Free Bio-based Tannin Epoxy-acrylic Adhesives. *Polymers.* 2016, 8(4), 143. DOI: 10.3390/polym8040143.
- [43] Zhang, S.; Liu, T.; Hao, C.; Wang, L.; Han, J.; Liu, H.; Zhang, J. Preparation of a Lignin-based Vitrimer Material and Its Potential Use for Recoverable Adhesives. *Green Chem.* 2018, 20(13), 2995–3000. DOI: 10.1039/c8gc01299g.
- [44] Jahanshahi, S.; Pizzi, A.; Abdulkhani, A.; Doosthoseini, K.; Shakeri, A.; Lagel, M. C.; Delmotte, L. MALDI-ToF, ¹³C NMR and FT-MIR Analysis and Strength Characterization of Glycidyl Ether Tannin Epoxy Resins. *Ind. Crops Prod.* 2016, 83, 177–185. DOI: 10.1016/j.indcrop.2015.11.067.
- [45] Pasch, H.; Pizzi, A.; Rode, K. MALDI-ToF Mass Spectrometry of Polyflavonoid Tannins. *Polymer.* 2001, 42(18), 7531–7539. DOI: 10.1016/S0032-3861(01)00216-6.
- [46] Abdalla, S.; Pizzi, A.; Ayed, N.; Charrier, F.; Bahabri, F.; Ganash, A. MALDI-ToF and ¹³C NMR Analysis of Tunisian Zizyphus Jujuba Root Bark Tannins. *Ind. Crops Prod.* 2014, 59, 277–281. DOI: 10.1016/j.indcrop.2014.05.035.
- [47] Pizzi, A., *Advanced Wood Adhesives Technology*; CRC Press: New York, 1994.
- [48] Nicollin, A.; Zhou, X.; Pizzi, A.; Grigsby, W.; Rode, K.; Delmotte, L. MALDI-TOF and ¹³C NMR Analysis of a Renewable Resource additive-Thermoplastic Acetylated Tannins. *Ind. Crops Prod.* 2013, 49, 851–857. DOI: 10.1016/j.indcrop.2013.06.013.
- [49] Pizzi, A.; Stephanou, A. A Comparative ¹³C NMR Study of Polyflavonoid Tannin Extracts for Phenolic Polycondensates. *J. Appl. Polym. Sci.* 1993, 50(12), 2105–2113. DOI: 10.1002/app.1993.070501209.
- [50] Navarrete, P.; Pizzi, A.; Bertaud, F.; Rigolet, S. Condensed Tannin Reactivity Inhibition by Internal Rearrangements: Detection by CP-MAS ¹³C NMR. *Maderas: Ciencia y tecnología.* 2011, 13(1), 59–68. DOI: 10.4067/S0718-221X2011000100006.

3.4 Les tanins naturels comme nouveaux matériaux de réticulation pour les adhésifs à base de soja

Résumé: Les problèmes de santé humaine et les émissions de formaldéhyde des composites à base de bois sont quelques-uns des inconvénients majeurs des adhésifs synthétiques traditionnels tels que les résines urée-formaldéhyde. Il y a eu de nombreuses tentatives pour réduire les émissions de formaldéhyde et remplacer les résines urée-formaldéhyde par des adhésifs biosourcés pour les composites à base de bois. En raison d'une certaine faiblesse des adhésifs à base de soja, des produits chimiques ont été utilisés comme modificateurs. Des adhésifs modifiés à base de soja sans aucun formaldéhyde ont été utilisés avec succès pour préparer des panneaux de bois. Pour y parvenir, différents produits chimiques de réticulation synthétiques tels que les résines phénol formaldéhyde et la polyamidoamine-épichlorhydrine ont été utilisés. Cependant, en réalité, ce dont nous avons besoin, ce sont des adhésifs totalement verts qui utilisent des matériaux naturels. Dans nos travaux de recherche précédents, l'utilisation de tanins en combinaison avec des adhésifs à base de soja pour fabriquer des composites de bois a été étudiée. Ainsi, dans ce travail de recherche, la faisabilité d'utiliser trois types de tanins naturels (tanins de quebracho, de mimosa et de châtaignier) comme matériaux de réticulation pour la colle de soja a été étudiée. La formation de liaisons chimiques et les comportements d'adhésion des adhésifs de soja modifiés au tanin ont également été étudiés par spectrométrie de masse à temps de vol avec désorption/ionisation laser assistée par matrice (MALDI-ToF-MS) et analyse thermomécanique (TMA). Les résultats ont montré qu'à température ambiante, des liaisons ioniques et covalentes se sont formées entre les flavonoïdes du tanin et les acides aminés; cependant, à température plus élevée, les liaisons covalentes sont largement prédominantes. Sur la base des résultats obtenus à partir de l'analyse thermomécanique, le module d'élasticité (MOE) de l'adhésif de soja est augmenté en ajoutant des tanins à sa formulation. De plus, la formation de liaison chimique a été prouvée par MALDI-ToF-MS.

Mots clés: Tanin; protéine de soja; matériau de réticulation; colle à bois; composites à base de bois.

Article

Natural Tannins as New Cross-Linking Materials for Soy-Based Adhesives

Saman Ghahri ^{1,*} , Xinyi Chen ², Antonio Pizzi ² , Reza Hajihassani ¹  and Antonios N. Papadopoulos ^{3,*} 

¹ Wood and Forest Products Research Division, Research Institute of Forests and Rangelands, Agricultural Research, Education and Extension Organization (AREEO), Tehran 19395-1113, Iran; reza.hajihassani@gmail.com

² LERMAB, University of Lorraine, 88000 Epinal, France; xinyi.chen@univ-lorraine.fr (X.C.); antonio.pizzi@univ-lorraine.fr (A.P.)

³ Laboratory of Wood Chemistry and Technology, Department of Forestry and Natural Environment, International Hellenic University, GR-661 00 Drama, Greece

* Correspondence: sghahri@gmail.com (S.G.); antpap@for.ihu.gr (A.N.P.)

Abstract: Human health problems and formaldehyde emission from wood-based composites are some of the major drawbacks of the traditional synthetic adhesives such as urea formaldehyde resins. There have been many attempts to decrease formaldehyde emission and replace urea formaldehyde resins with bio-based adhesives for wood-based composites. Because of some weakness in soy-based adhesive, chemicals have been used as modifiers. Modified soy-based adhesives without any formaldehyde have been successfully used to prepare wood panels. To achieve this, different synthetic cross-linking chemicals such as phenol formaldehyde resins and polyamidoamine-epichlorohydrin were used. However, in reality, what we need are totally green adhesives that use natural materials. In our previous research work, the use of tannins in combination with soy-based adhesives to make wood composites was investigated. Thus, in this research work, the feasibility of using three types of natural tannins (quebracho, mimosa and chestnut tannins) as cross-linking materials for soy adhesive was studied. The chemical bond formation and adhesion behaviors of tannin-modified soy adhesives were also investigated by Matrix-Assisted Laser Desorption/Ionization Time-of-Flight Mass Spectrometry (MALDI-ToF-MS) and thermo-mechanical analysis (TMA). The results showed that at ambient temperature, both ionic and covalent bonds formed between tannin constituents and amino acids; however, at higher temperature, covalent bonds are largely predominate. Based on the results obtained from the thermo-mechanical analysis, the modulus of elasticity (MOE) of soy adhesive is increased by adding tannins to its formulation. In addition, the chemical bond formation was proved by MALDI-ToF-MS.

Keywords: tannin; soy protein; cross-linking material; wood adhesive; wood based composites



Citation: Ghahri, S.; Chen, X.; Pizzi, A.; Hajihassani, R.; Papadopoulos, A.N. Natural Tannins as New Cross-Linking Materials for Soy-Based Adhesives. *Polymers* **2021**, *13*, 595. <https://doi.org/10.3390/polym13040595>

Academic Editor: Fernão D. Magalhães

Received: 2 February 2021

Accepted: 15 February 2021

Published: 16 February 2021

Publisher's Note: MDPI stays neutral with regard to jurisdictional claims in published maps and institutional affiliations.



Copyright: © 2021 by the authors. Licensee MDPI, Basel, Switzerland. This article is an open access article distributed under the terms and conditions of the Creative Commons Attribution (CC BY) license (<https://creativecommons.org/licenses/by/4.0/>).

1. Introduction

Soybeans are an ideal raw material for making wood adhesives because they are abundant, renewable, environmentally friendly and readily available [1]. Soy-based wood adhesives have many advantages such as low cost, easy handling and low pressing temperature [1]. Recently, researchers have done a considerable amount of work using different methods and adding different chemicals to soybean flour and soybean protein cross-linking as bio-based wood adhesive for wood-based composites [2–6].

Despite the great potential of soybeans—in the form of soy flour (SF) and isolated soy protein (ISP)—as non-formaldehyde adhesives for wood gluing, a major drawback is their low water resistance [7]. Some researchers have already focused themselves on improving the moisture resistance of these adhesives [8,9]. Several chemical modification strategies involving introduction of phenolic, thiol, maleyl, amine and hydroxyl groups into soy proteins have been attempted to improve the adhesive properties of ISP with

limited success [10–15]. A number of cross-linking agents were also used to increase the water resistance of soy adhesives. To this purpose, several additives like polyamidoamine-epichlorohydrin (PAE), sodium dodecyl sulfate (SDS) and other synthetic materials like phenol formaldehyde (PF) resins have been used [16,17]. The main issue in using synthetic cross-linking materials for soy adhesive is their lower environmental friendliness and their dependence on fossil resources. Therefore, chemicals not depending on oil are needed to improve soybean flour while maintaining its acceptable adhesion properties. Consequently, there is great interest in substituting synthetic chemicals for soy adhesives modification to obtain high-performance bio-based adhesives.

Tannins are natural products obtained from plants and are very widespread in nature [18]. Tannins are, after lignins, a major source of polyphenolic components all over the world [19], but they have a considerably greater extraction potential than lignins. Vegetable tannins have been used to tan leather either alone or accompanied by other tanning agents for several thousand years. They are natural products obtained from plants and are very diffuse in the whole plant kingdom [18].

The term natural vegetable tannin is used loosely to define two broad classes of chemical compounds of mainly phenolic nature, namely, condensed or polyflavonoid tannins and hydrolysable tannins [18]. Industrial polyflavonoid tannin extracts are mostly composed of flavon-3-ols repeating units, and two types of phenolic rings having different reactivities with formaldehyde are present on each flavon-3-ol repeating unit, namely A-rings and B-rings, with each repeating unit being linked 4,6 or 4,8 with the units, which precede and follow it [20]. Previous research works showed that the addition of tannin to the materials based on the blends of collagen and chitosan leads to modification of several properties, such as water swelling and mechanical performance [21].

Both condensed polyflavonoid tannins and hydrolysable tannins have already been successfully used as wood composite adhesives [22–31].

Synthesized tannin resin from larch tannin extract with 60.1 wt% has already been successfully used as a modifier of ISP adhesive. The results obtained showed higher crosslinking density and better plywood water uptake resistance and shear strength as well [32]. Moreover, the results of cured ISP-condensed tannin bio-adhesive showed a high cross-linking density, which was attributed to two factors: first, that the imine group ($H_2C=N-CH_2+$) generated by hexamine decomposition reacted with the nucleophilic site of the tannin's A-ring to form an amino methylene bridge [33]. The bridge had the ability to bond with other condensed tannins oligomers and finally increase the crosslinking density of the resultant adhesive. Secondly, the orthoquinone obtained via pyrocatechol oxidation on the tannin's B-ring led to covalent interaction and cross-linking reaction with ISP molecules, which further increased the cross-linking density of the resultant adhesive [34].

Because of the tannin's phenolic nature, due to their similarity to phenol in PF resins, tannins are a good choice for soy adhesive modification. In previous research, tannin-modified soy-based adhesives were successfully used for wood-based composites, and satisfactory results were achieved [35–37].

The problem of synthetic adhesives is outlined in the introduction. They are petroleum derived; hence, they are a finite source, and they use and emit formaldehyde, now classified as toxic and carcinogenic. Adhesives based on other aldehydes are slower reacting, thus the work outlined here is aimed at offering a totally bio-sourced environment adhesive for bonding wood panels.

The aim of this research work is to apply different net natural tannins (hydrolysable and condensed tannin) as cross-linking agents of soy adhesives (isolated soy protein and soy flour) and to show the great potential of tannins (quebracho, mimosa and chestnut tannins) as cross-linkers for soy adhesives which used for wood composite bonding.

2. Materials and Methods

Defatted soy flour (SF) with 47 wt% protein content was purchased from BEHPAK Co. (Iran), and isolated soy protein (ISP) with 90 wt% protein content used in this study

was donated by ADM Co. (USA). The three tannins used were mimosa bark tannin (*Acacia mearnsii*, formerly *mollissima*, de Wildt) extract, chestnut wood tannin (*Castanea sativa*) and quebracho wood tannin (*Schinopsis balansae*) extract (produced by SILVA Chimica, S. Michele Mondovi, Italy). The other chemicals were supplied by ACROS Organics.

2.1. Adhesive Formulation

Adhesive formulations were described in previous research work [34]. Different amounts of SF and ISP (7.35 g) were added to distilled water (29.4 g) and mixed with a mechanical stirrer (700 rpm speed) at room temperature (21 ± 2 °C) to produce soy slurry with 20 wt% solid content. The tannin solution (5, 10 and 15 wt% based on soy dry weight) was then added to the soy slurry and stirred for 30 min. The tannin solutions in water were prepared at 45 wt% concentration. In addition, 6.5 wt% hexamethylenetetramine (hexamine) was used as a hardener; the percentage was based on the dry weight of tannins. Hexamine was added to the adhesives as a 40% aqueous solution. Finally, in the last stage of the adhesive's preparation, the hardener was added and the pH adjusted to 7 with a 50 wt% NaOH water solution. ISP adhesive was prepared according to the same procedure.

2.2. Matrix-Assisted Laser Desorption/Ionization Time-of-Flight (MALDI-ToF) Mass Spectrometry

Mimosa tannin extract was reacted at ambient temperature and at 80 °C for 1 h with soy protein isolates (ISP). Test procedure was performed according to the method as previously described by Chen et al. [37]. Samples for MALDI-ToF analysis were prepared by first dissolving 7.5 mg of sample powder in 1 mL of a 50:50 *v/v* acetone/water solution. Then 10 mg of this solution was added to 10 μ L of a 2,5-dihydroxy benzoic acid (DHB) matrix. The locations dedicated to the samples on the analysis plaque were first covered with 2 μ L of a NaCl solution 0.1 M in 2:1 *v/v* methanol/water, and pre-dried. Then 1.5 μ L of the sample solution was placed on its dedicated location and the plaque was dried again. Red phosphorous was used to standardize the MALDI equipment. MALDI-ToF spectra were obtained using an Axima-Performance mass spectrometer from Shimadzu Biotech (Kratos Analytical Shimadzu Europe Ltd., Manchester, UK) using a linear polarity-positive tuning mode [37].

2.3. FTIR Analysis

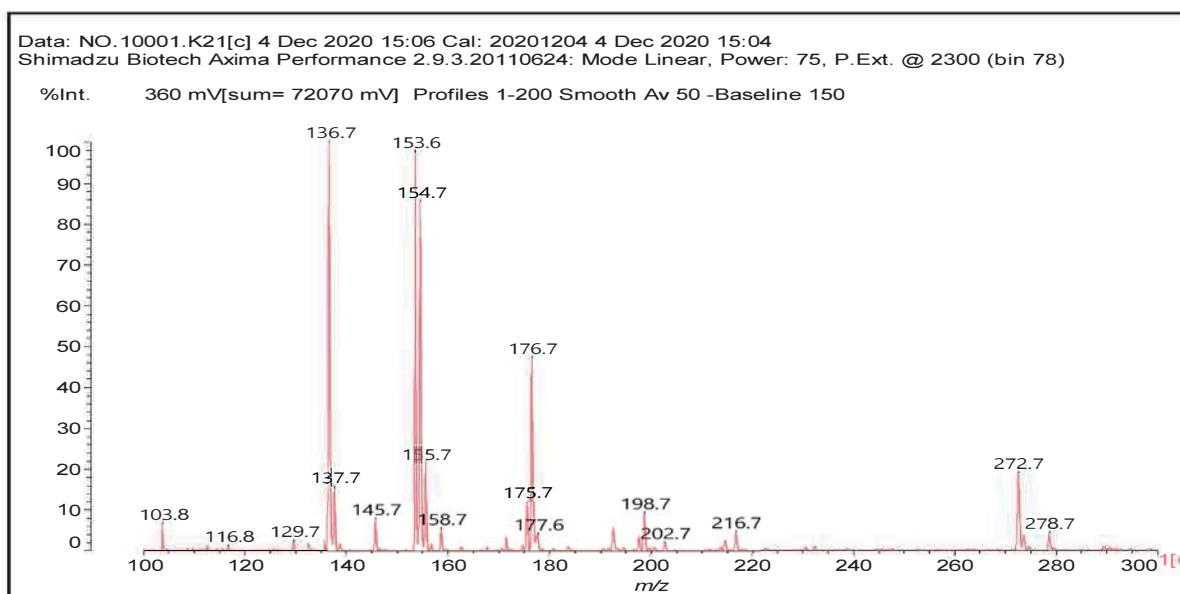
Fourier transform infrared (FTIR) analysis of the reacted product of tannin + ISP reacted at 80 °C for 1 h. The addition of an acid catalyst (pTSA) was carried out using a Shimadzu IR Affinity-1 (Shimadzu Europe Ltd., Manchester, UK) spectrophotometer. A blank sample tablet of potassium bromide, ACS reagent from ACROS Organics (Geel, Belgium), was prepared for the reference spectra. Similar tablets were prepared by mixing potassium bromide with 5% by weight of the sample powders. The spectra were plotted in percentage transmittance by combining 32 scans with a resolution of 2.0 cm^{-1} in the 400–4000 cm^{-1} range.

2.4. Thermomechanical Analysis

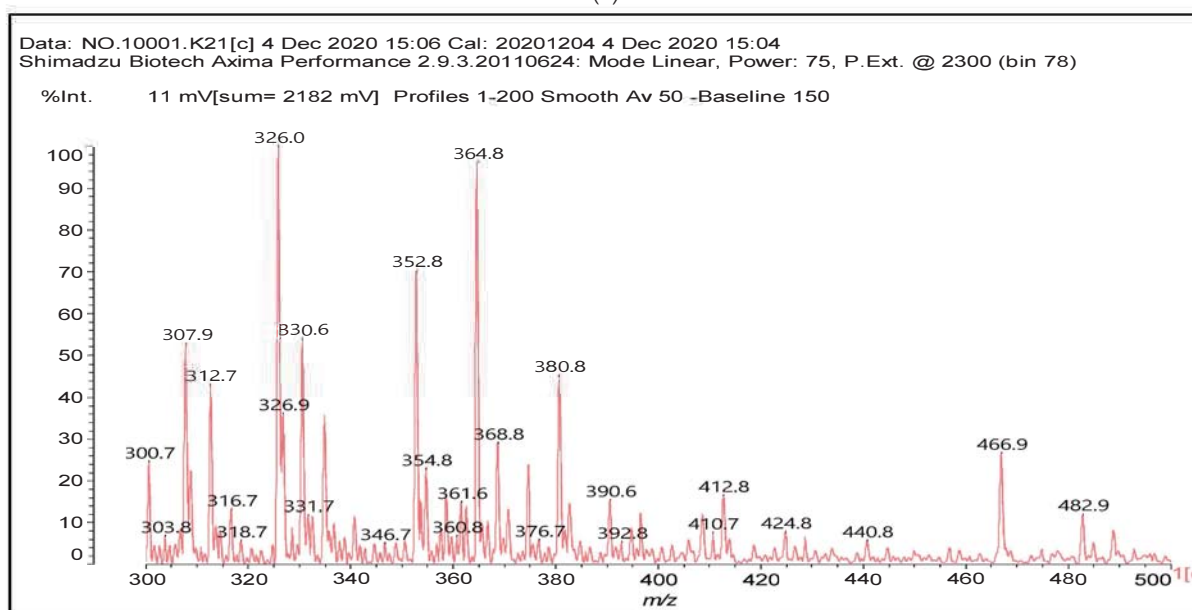
The adhesives were tested dynamically by thermo-mechanical analysis (TMA) on a Mettler 40 apparatus. Different samples of two beech wood plies, each 0.5 mm thick, bonded with each adhesive system, for sample dimensions of 17 mm \times 5 mm \times 1 mm, were tested in non-isothermal mode between 25 °C and 250 °C at a heating rate of 10 °C/min in three-point bending. A force varying continuously between 0.1 N, 0.5 N, and back to 0.1 N was applied on the specimens with each force cycle of 12 s (6 s/6 s). The classical mechanics relation between force and deflection $E = [L^3/(4bh^3)][\Delta F/(\Delta f)]$ (where L is the sample length, b and h are the sample width and thickness, ΔF is the variation of the force applied, and Δf is the deflection obtained) allows the calculation of the modulus of elasticity (MOE) E for each case tested. Different formulations of adhesives were tested by TMA [35].

3. Results and Discussion

The main components found in the different tannin extracts used coincided with what was obtained by previous work by MALDI-ToF analysis [20,38,39]. Figure 1 shows the MALDI-ToF spectra for ISP modified by tannin extracts. The results indicate that new compounds have formed by reactions of different hydrolysable and condensed polyflavonoid tannin extracts with soy protein amino acids. The effect is particularly evident when the reaction is done at 80 °C with a condensed tannin where the predominant linkages are covalent while the ionic linkages present for reactions at ambient temperature have disappeared. The interaction between tannin constituents and amino acids occurs by reaction of the carboxyl group (-COOH) of gallic acid of chestnut tannin with amino groups of amino acids side chains. Quebracho and mimosa tannins react with amino acid functional groups and with the hydroxyl groups (-OH) on phenolic rings.

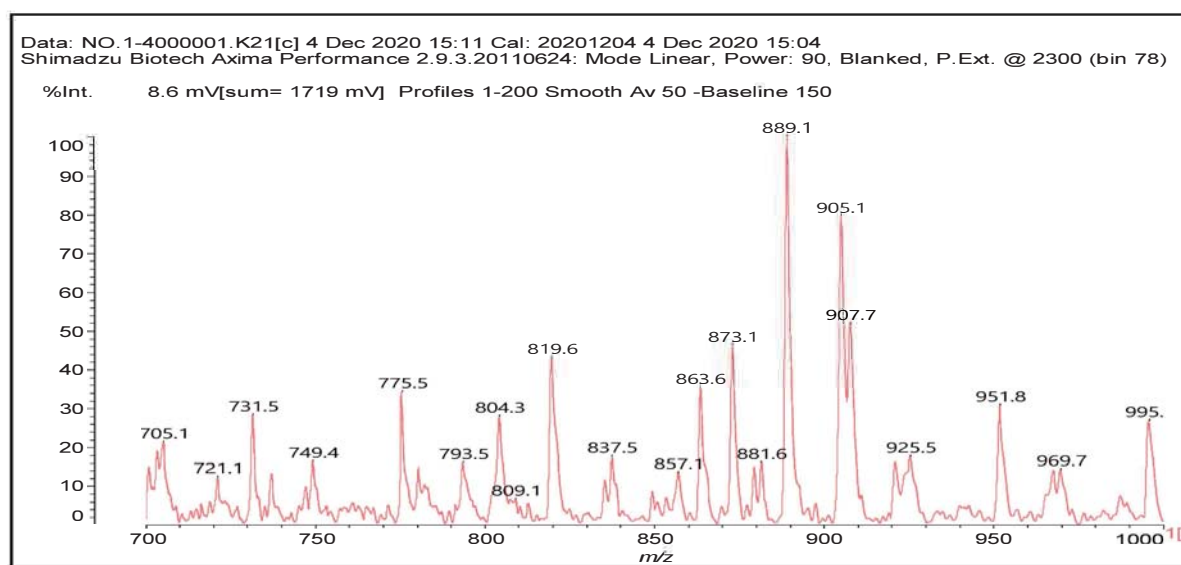


(a)

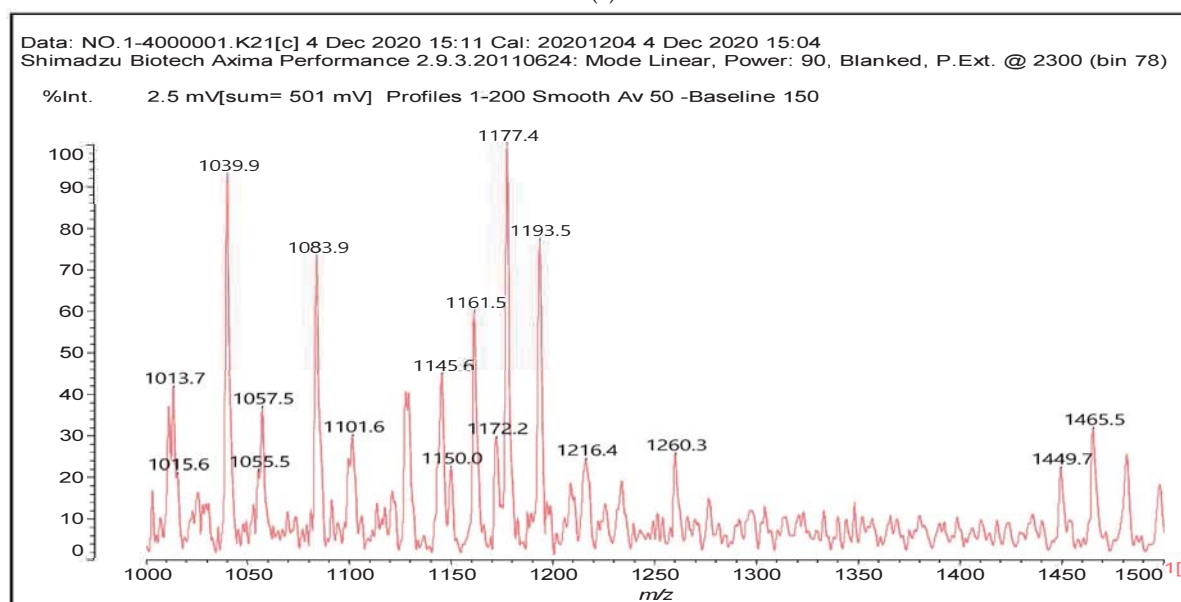


(b)

Figure 1. Cont.



(c)



(d)

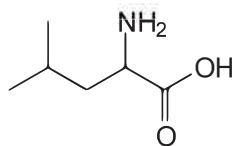
Figure 1. MALDI-ToF spectra of tannin-ISP adhesive. (a) 100–300 Da range. (b) 300–500 Da range. (c) 700–1000 Da range. (d) 1000–1500 Da range.

There are a number of compounds formed and detected by the MALDI-ToF analysis of tannin and ISP, as depicted in Figure 1. The MALDI-ToF spectra clearly show that amino acids are linked to flavonoid monomers and dimers. In addition, the results reveal soy protein polymer chains up to four amino acids linked to flavonoid monomers or dimers, and flavonoid dimers linked to two peptidic chains as well. Regarding covalent bonds, their formation is favored at high temperature. There are two main reactions occurring: one is the amination of the tannin, and this can happen with any amino group of an amino acid. The MALDI analysis indicates that many amino acids when alone react with tannin flavonoid monomers through their amino group. However, when the same amino group is linked as it is in the peptide chain of the protein, the only free amino groups that can react in this way are those of the side chain of arginine because they are not involved in the peptidic bond of the skeletal chain of the protein. The reactions of amines with tannins are well documented, it is facile, both using ammonia or primary amines and demonstrated with other techniques other than MALDI [40,41].

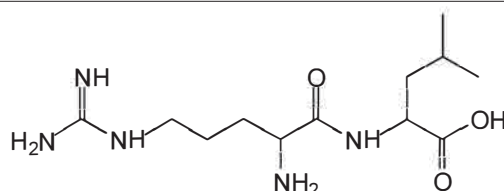
In the case of arginine, its side chain $-NH_2$ groups can substitute the $-OH$ of the flavonoids [40]. The reaction of the carboxylic acid groups of the side chains of aspartic and glutamic acid to form an ester is favored with the alcoholic $-OH$ group on the C3 of the heterocyclic ring of the flavonoids. This is logical because, as the phenolic hydroxyl groups have more acidic character, they will be much less likely to react with the carboxylic acid groups of the side chains of aspartic and glutamic acids. Reaction with the phenolic hydroxyl groups, however, cannot be excluded, but the MALDI technique cannot ascertain it. It is also evident that this esterification reaction can really occur at the elevated temperatures experienced by the adhesive during adhesive hot pressing.

The MALDI-ToF analysis shows the peaks corresponding to the molecular weight of the amino acids and tannin extracts and molecular weight of new compounds resulting from bonds between them (with and without Na^+) in Figure 1. In addition, the assignments for the peaks of the MALDI spectra are shown in Table 1. It must be stressed that the reaction products between single amino acids and a flavonoid monomer or dimer does not count for the cross-linking of the soy adhesive by the tannin because the reaction in these cases appears not to be able to occur on the $-NH-$ or $-COOH$ that are in the skeletal chain of the protein as these are blocked as they participate to the peptidic bond. Thus, the structures that do not count for cross-linking are of the type such as for the 390 Da peak, and many others (Table 1) that correspond to an open fisetinidin structure linked to leucine (without Na^+)(I). This clearly shows covalent bond formation between a tannin extracts monoflavonoid(fisetinidin) with an amino acid $-NH_2$ group substitution of the $-OH$ of the flavonoids as follows:

Table 1. Assignment of structures to relevant MALDI-ToF peaks from Figure 1a to Figure 1d.



131 Da = Leucine, no Na^+



146 Da = glutamic acid, no Na^+

154 Da = Leucine with Na^+

155–156 Da = aspartic acid with Na^+

175.7 Da = no Na^+ , arginine, calculated 174.5 Da

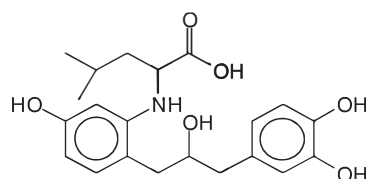
202.7 Da = with Na^+ , Tyrosine, calculated 201.8 Da,

OR no Na^+ , Tryptophan, calc. 204 Da

273 Da Fisetinidin, no Na^+

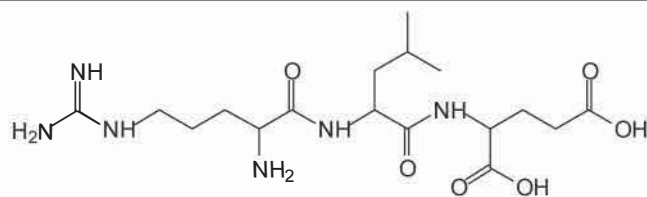
326 Da delphinidin + Na^+

308 Da = arginine-leucine with Na^+ (calculate 310 Da)

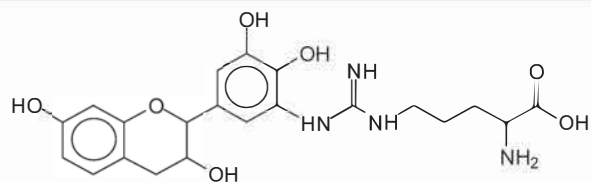


390 Da = Open fisetinidin-leucine no Na^+ (calculated 389.5 Da),

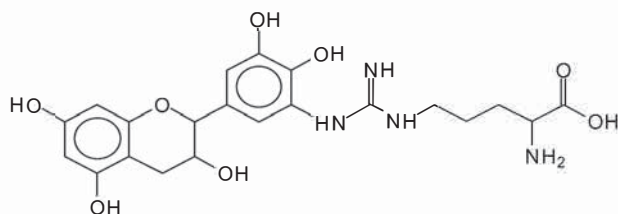
Table 1. Cont.



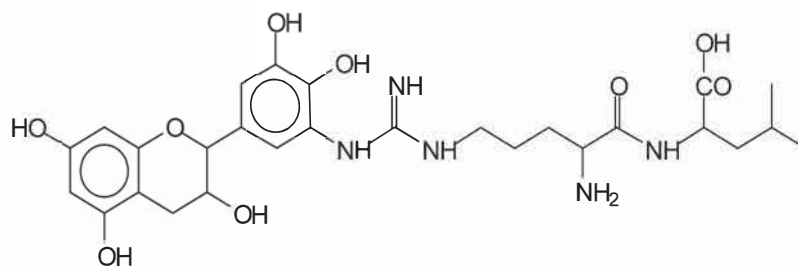
439 Da = aspartic-leucine arginine with Na⁺



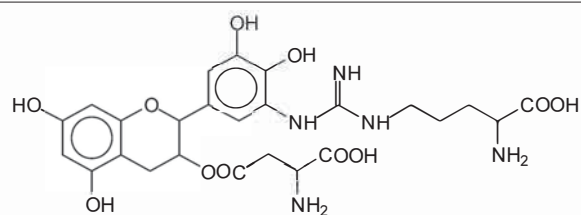
467 Da = robinetinidin-arginine with Na⁺, Calculated 469 Da



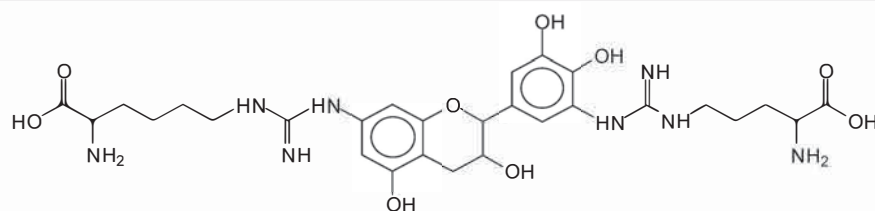
483 Da = delphinidin-arginine with Na⁺ (calculated 485 Da)



575 Da = leucine-delphinidin-arginine, no Na⁺, Calculated 575 Da

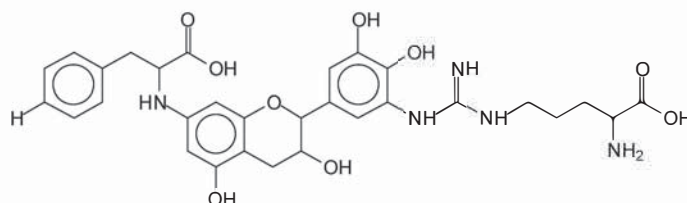


601 Da = aspartic acid-delphinidin-arginine, with Na⁺, calculated 601 Da.

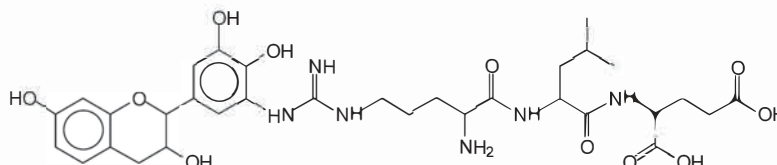


632 Da = arginine-delphinidin-arginine no Na⁺, calculated 632 Da

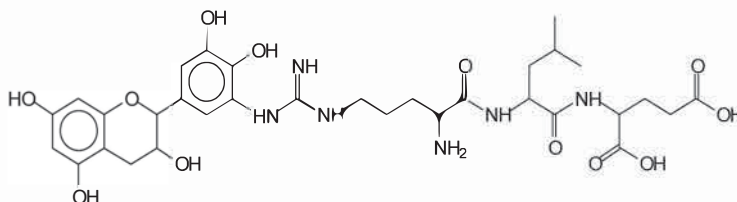
Table 1. Cont.



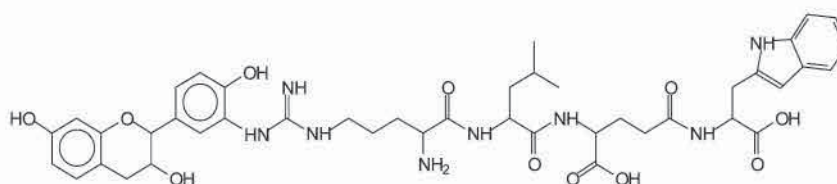
632 Da = Delphinidin-Arginine-Phenylalanine- with Na^+ , calculated



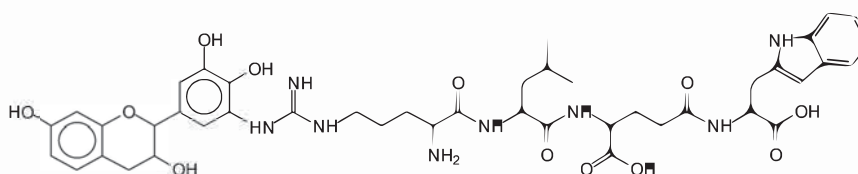
688.8 Da = no Na^+ , calculated 688.7 Da., robinetinidin-arginin-leucin-aspartic acid. Thus, the flavonoid attached to a peptide chain fragment.



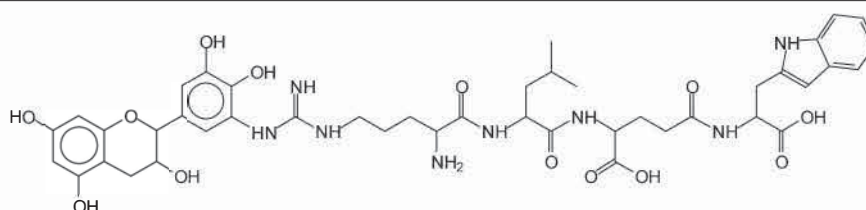
705 Da = no Na^+ , calculated 704.7 Da, delphinidin-arginine-leucin-aspartic acid. Thus, the flavonoid attached to a peptide chain fragment, with Na^+ , calculated 728.5.



857 Da = no Na^+ , calculated 858 Da, fisetinidin-arginine-leucin-aspartic acid-tryptophan. Thus, the flavonoid attached to a peptide chain fragment.



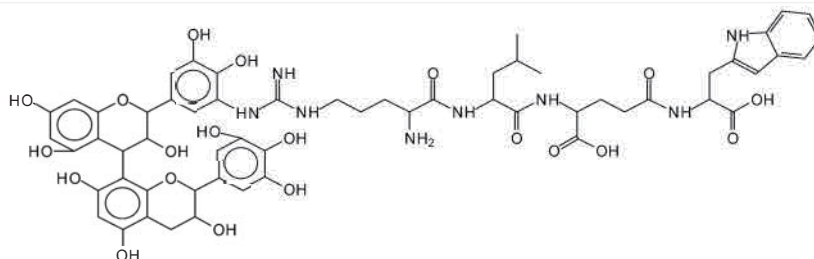
873 Da = no Na^+ , calculated 874 Da, robinetinidin-arginine-leucin-aspartic acid-tryptophan. Thus, the flavonoid attached to a peptide chain fragment.



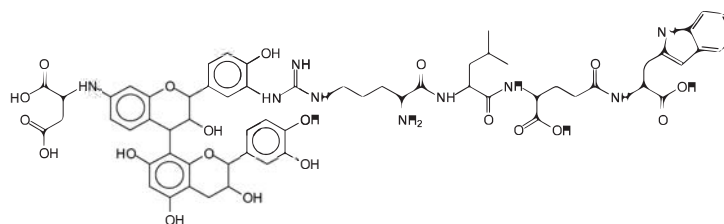
889 Da = no Na^+ , calculated 890 Da, delphinidin-arginine-leucin-aspartic acid-tryptophan. Thus, the flavonoid attached to a peptide chain fragment.

1128 Da = no Na^+ , calculated 1129 Da, fisetinidin dimer-arginine-leucin-aspartic acid-tryptophan. Thus, the flavonoid dimer attached to a peptide chain fragment.

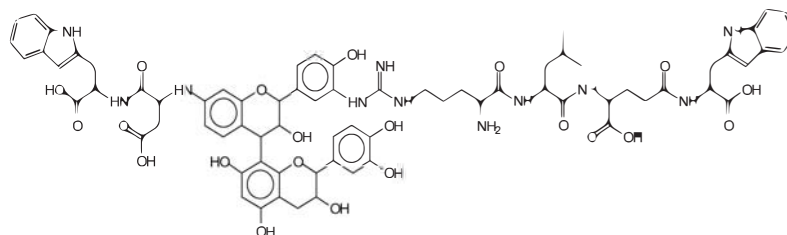
Table 1. Cont.



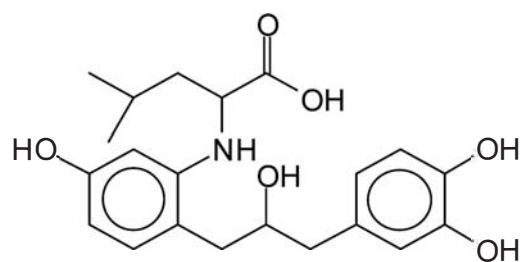
1194 Da = no Na⁺, calculated 1194 Da, delphinidindimer-arginine-leucin-asparticacid-tryptophan. Thus, the flavonoid dimer attached to a peptide chain fragment.



1260 Da = no Na⁺, calculated 1261 Da, aspartic acid-catechin-fisetinidin-arginine-leucin-aspartic acid-tryptophan. Thus, the flavonoid dimer attached to a peptide chain fragment + cross-linked with another amino acid.

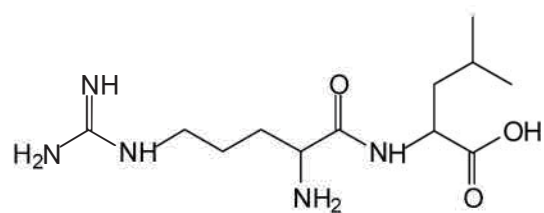


1449 Da = no Na⁺, calculated 1449 Da, Tryptophan-aspartic acid-catechin-fisetinidin-arginine-leucin-aspartic acid-tryptophan. Thus, the flavonoid dimer linked to two peptide chain fragments = cross-link protein tannin proved.



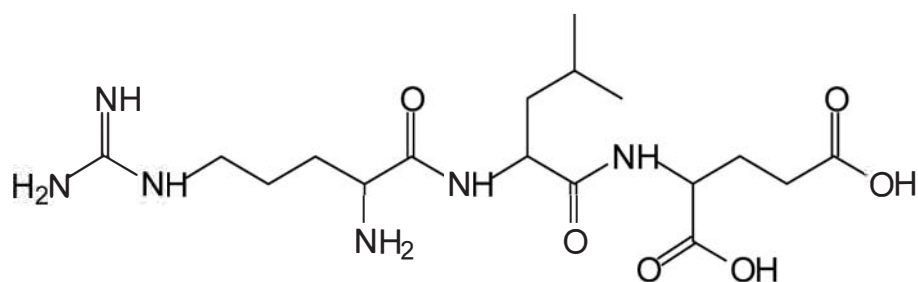
(I).

Equally, there are many peaks of single amino acids or peptide fragments that have not reacted with the flavonoids of the tannin. In addition, other peaks correspond to the several amino acids and tannin extract monomers and oligomers of different molecular weight such as asthose at 131 Da, 146 Da, 154 Da, 156 Da, 175.7 Da, 202.7 Da, 204 Da, 273 Da, 326 Da. In addition, peptide two amino acids dimers such as arginine-leucine with Na⁺(II) were assigned in Table 1 from Figure 1a,b.



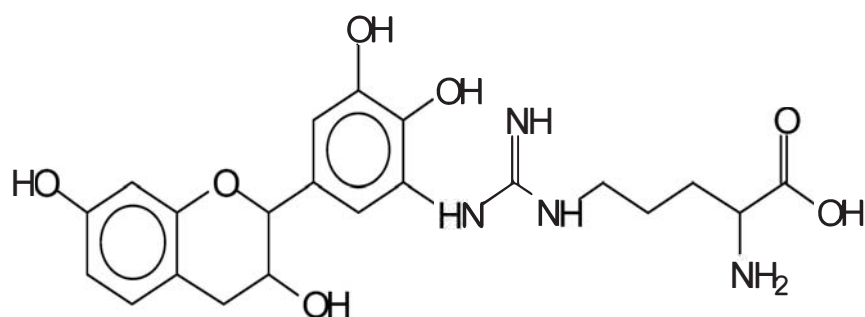
(II).

In the same type of peptide fragments the peak at 439 Da (III) assigned to the trimer of aspartic, leucine and arginine (with Na⁺) from the soy protein polymer chain (Table 1, Figure 1b) and others.



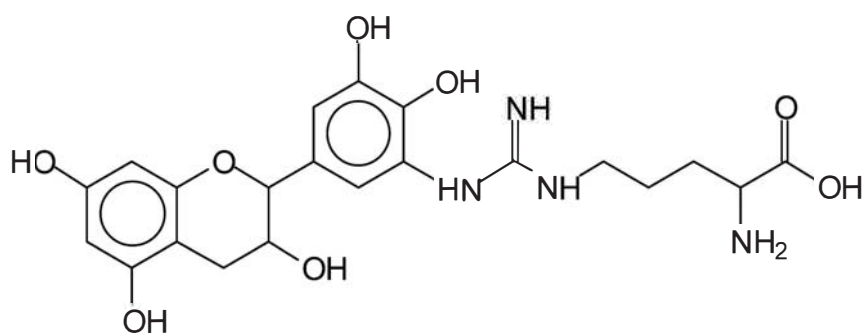
(III).

The type of linkages that will count for cross-linking the main body of the protein are, for example, the link represented by the peak at 467 Da (IV) assigned to a flavonoid robinetinidin linked to an arginine (with Na⁺) (Table 1, Figure 1b).



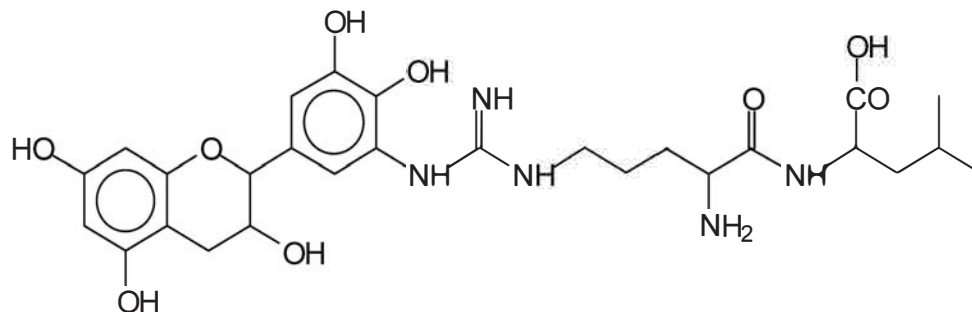
(IV).

Similarly, the 483 Da (V) peak assigned to a delphinidin-arginine dimer (with Na⁺).



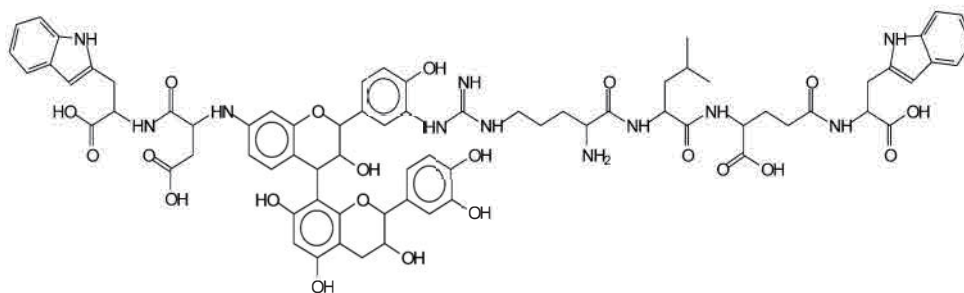
(V).

There are also several peaks in which a flavonoid is linked to a peptidic fragment containing arginine such as the peak at 575 Da, a leucine-delphinidin-arginine oligomer, no Na⁺ (VI).



(VI).

This shows that tannin flavonoid units are indeed linked and cross-link through the amino acids side chains of the main skeletal peptidic chain of the protein. There are many peaks and structures confirming this, such as the peaks at 601 Da, 632 Da, 688 Da, 705 Da, 857 Da, 873 Da, 889 Da, 1146 Da, 1161 Da, 1177 Da, 1194 Da, 1260 Da and 1449 Da (Table 1). For example, the species at 1449 Da (VII) indicates clearly that covalent cross-linking of the protein with a condensed tannin is indeed possible.



(VII).

Several bands are observed in the FTIR spectrum in Figure 2. Some are as follows: cm^{-1} ; 1735 cm^{-1} (shoulder, C=O esters), 1711 cm^{-1} (shoulder, C=O acid in C-C-COOH) 1680 cm^{-1} (C=O amide and C=O in -COOH of acid), 1625 cm^{-1} (primary amine asymmetric stretch R-CH₂-NH₂), 1530 cm^{-1} (amide), 1480 cm^{-1} (amide), 1333 cm^{-1} and 1292 cm^{-1} (secondary amine, R-NH-R), 1165 cm^{-1} , 1150 cm^{-1} , 1030 cm^{-1} (primary amine asymmetric stretch R-CH₂-NH₂), 1000 cm^{-1} , $850 + 700 \text{ cm}^{-1}$ (primary amine).

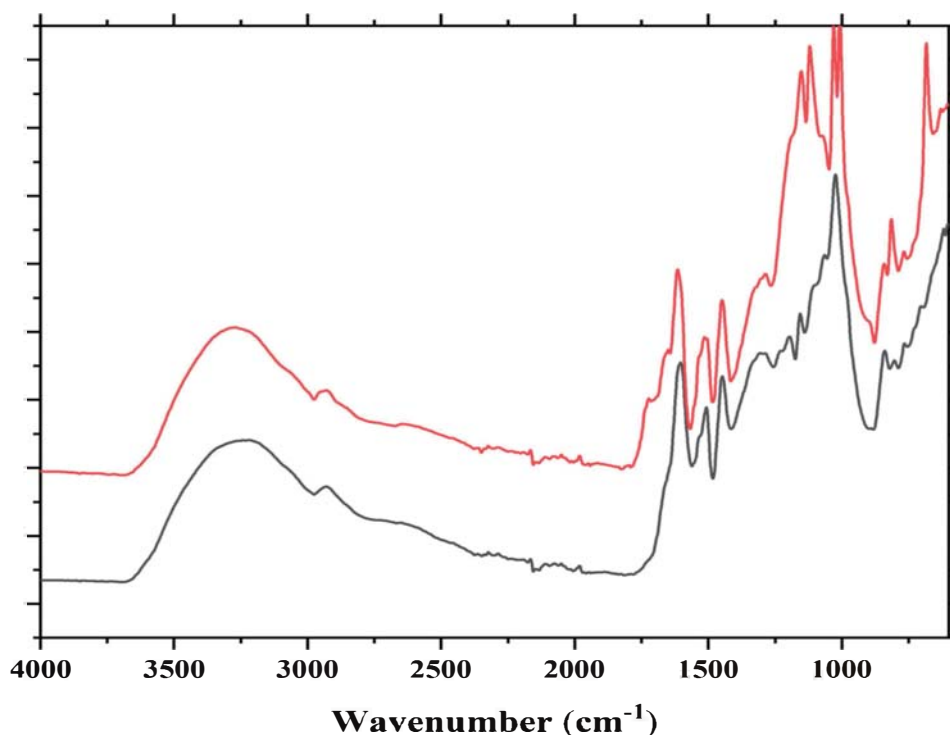
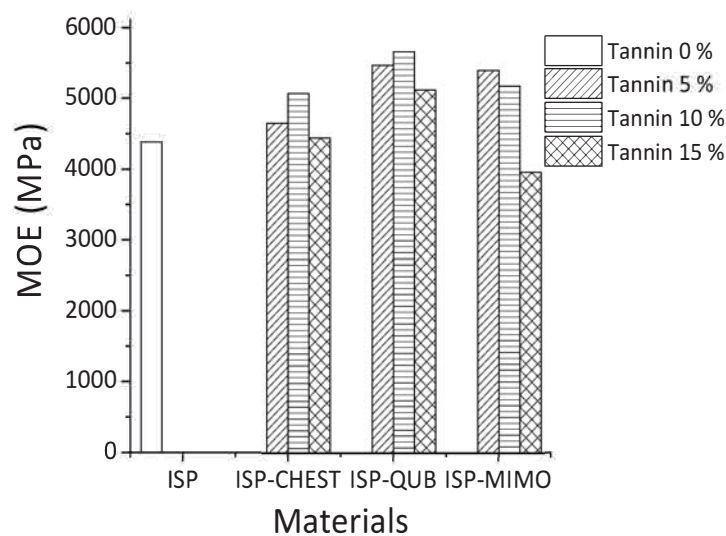


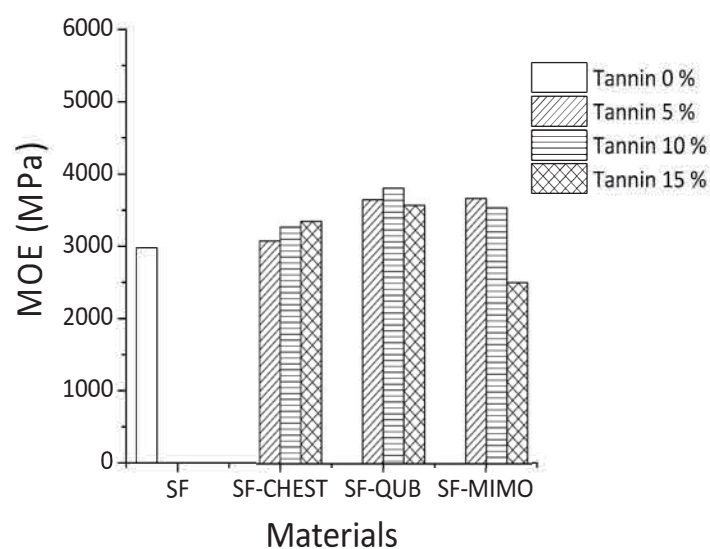
Figure 2. FTIR of reaction product mixture of condensed tannin with ISP at 80 °C without catalyst (lower spectrum) and with catalyst (higher spectrum) both at 80 °C.

In the FTIR, there are indications that support what was found by MALDI ToF analysis, namely that reactions occur through the primary amines in ISP by forming secondary amines, this being indicated by the two characteristic bands at 1333 and 1292 cm^{-1} . That esterification of the tannin hydroxyls by the protein side chain acids does also occur is demonstrated by the 1735 cm^{-1} shoulder. These bands appear to support the MALDI results that the reaction of the protein with the flavonoid units of the tannin can occur both through the amino group of a protein side chain or by esterification with the acid group of a side chain of the protein.

The TMA results for different tannin-modified soy adhesives are shown in Figure 3. The influence of different constituents of chestnut tannin extract (Chest), quebracho (Qub) and mimosa (Mimo) tannins on the modulus of elasticity (MOE) of SF and ISP adhesives as a function of temperature is depicted in Figure 3a,b. When comparing the MOE content of different adhesive formulations, it is clear that the maximum MOE values of resins prepared with ISP are higher than those obtained with SF adhesive. The proportion of tannins added varied from 5% to 10% to 15% by weight. All the adhesives tested, show an increase in the maximum MOE value with increasing proportions of both hydrolysable and condensed. The highest MOE for both tannin-modified ISP and SF adhesives were obtained by the addition of 10% wt quebracho tannins (5660 MPa for ISP and 3799 MPa for SF), 5% wt mimosa tannin (5397 MPa for ISP and 3655 MPa for SF) and 10% wt to 15% wt chestnut tannin for ISP (5069 MPa) and SF (3341 MPa).



(a)



(b)

Figure 3. Effect of different tannins extracts on MOE of ISP (a) and SF (b).

Based on the results obtained from MALDI-TOF mass spectrometry, covalent and ionic bonds can form between soy amino acids and tannins (Figure 3). For these reasons, the MOE of tannin-modified soy flour adhesive is increased. In previous studies on tannin and protein interactions, different bonds such as hydrogen, covalent, ionic and hydrophobic bonding between tannin and protein were reported [21,42,43], and the reaction between tannins and amines has been recently studied and codified in depth [44]. Condensed polyflavonoid quebracho and mimosa tannins when compared to hydrolysable chestnut tannin showed better reaction with soy protein. This happened because of the higher reactivity of aromatic -OH groups in condensed tannins than the aromatic and aliphatic -OH groups in hydrolysable tannins. Between two industrial polyflavonoids, quebracho appears to react well with soy protein. Compared to the more branched structure of mimosa tannin oligomers, quebracho tannin oligomers are predominantly linear and the inter flavonoid link in quebracho tannin structure is more easily hydrolysable. These structural

differences also contribute to the significant differences in reaction of two condensed tannins with soy (SF and ISP) in slurry systems.

4. Conclusions

Three types of natural tannins—chestnut tannin extracts, quebracho and mimosa condensed polyflavonoid tannins—were used as cross-linking agents for SF and ISP adhesives for wood bonding. MALDI-ToF mass spectrometry clearly shows that ionic and covalent bonding between amino acids and tannin constituents are formed at ambient temperature and that covalent bonds do predominate at elevated temperature as present in the hot-pressing of wood panels. They are the bonds exclusively between the $-NH_2$ and $-COOH$ groups of side chains of amino acids in the peptide chain that participate in the tannin/protein cross-linking; thus, the amino acids arginine, aspartic acid and glutamic acid are the only ones able to participate. The TMA results also indicate a higher MOE and better adhesion properties of soy adhesives by adding tannins to their formulation. The quebracho tannin showed higher MOE for both SF and ISP adhesives. Higher MOE was an evidence to confirm bond formation determined by MALDI-ToF. The results obtained from this research clearly show the potential of tannins as cross-linkers for soy-based adhesives to produce totally green adhesives for wood bonding.

Author Contributions: Methodology, S.G. and A.P.; validation, S.G., A.P., A.N.P., X.C., R.H.; investigation, S.G. and A.P., and X.C.; writing—original draft preparation, S.G., A.P., and A.N.P. All authors have read and agreed to the published version of the manuscript.

Funding: This research received no external funding.

Institutional Review Board Statement: Not applicable.

Informed Consent Statement: Not applicable.

Data Availability Statement: The data presented in this study are available on request from the corresponding author.

Conflicts of Interest: The authors declare no conflict of interest.

References

1. Liu, K. *Soybeans: Chemistry, Technology and Utilization*; Springer US: New York, NY, USA, 1997.
2. Vnučec, D.; Goršek, A.; Kutnar, A.; Mikuljan, M. Thermal modification of soy proteins in the vacuum chamber and wood adhesion. *Wood. Sci. Technol.* **2015**, *49*, 225–239. [[CrossRef](#)]
3. Chen, N.; Lin, Q.; Zheng, P.; Rao, J.; Zeng, Q.; Sun, J. Sustainable bio-based adhesive derived from defatted soy flour and epichlorohydrin. *Wood. Sci. Technol.* **2019**, *53*, 801–817. [[CrossRef](#)]
4. Liang, J.; Wu, Z.; Xi, X.; Lei, H.; Zhang, B.; Du, G. Investigation of the reaction between a soy-based protein model compound and formaldehyde. *Wood. Sci. Technol.* **2019**, *53*, 1061–1077. [[CrossRef](#)]
5. Taghiyari, H.R.; Hosseini, B.; Ghahri, S.; Ghofrani, M.; Papadopoulos, A.N. Formaldehyde emission in micron-sized wollastonite-treated plywood bonded with soy flour and urea-formaldehyde resin. *Appl. Sci.* **2020**, *10*, 6709. [[CrossRef](#)]
6. Pizzi, A.; Papadopoulos, A.N.; Policardi, F. Wood composites and their polymer binders. *Polymers* **2020**, *12*, 1115. [[CrossRef](#)]
7. Li, Y.; Chen, F.; Zhang, L.; Yao, Y. Effect of surface changes of soy protein materials on water resistance. *Mater. Lett.* **2015**, *149*, 120–122. [[CrossRef](#)]
8. Hettiarachchy, N.S.; Kalapathy, U.; Myers, D.J. Alkali-modified soy protein with improved adhesive and hydrophobic properties. *J. Am. Oil. Chem. Soc.* **1995**, *72*, 1461–1464. [[CrossRef](#)]
9. Zhu, D.; Damodaran, S. Chemical phosphorylation improves the moisture resistance of soy flour-based wood adhesive. *J. Appl. Polym. Sci.* **2014**. [[CrossRef](#)]
10. Liu, Y.; Li, K. Chemical modification of soy protein for wood adhesives. *Macromol. Rapid. Commun.* **2002**, *23*, 730–742. [[CrossRef](#)]
11. Liu, Y.; Li, K. Modification of soy protein for wood adhesives using mussel protein as a model: The influence of a mercapto group. *Macromol. Rapid. Commun.* **2004**, *25*, 1835–1838. [[CrossRef](#)]
12. Liu, Y.; Li, K. Development and characterization of adhesives from soy protein for bonding wood. *Int. J. Adhes. Adhes.* **2007**, *27*, 59–67. [[CrossRef](#)]
13. Huang, J.; Li, K. A new soy flour-based adhesive for making interior type II plywood. *J. Am. Oil. Chem. Soc.* **2008**, *85*, 63–70. [[CrossRef](#)]
14. Jang, Y.; Huang, J.; Li, K. A new formaldehyde-free wood adhesive from renewable materials. *Int. J. Adhes. Adhes.* **2011**, *31*, 754–759. [[CrossRef](#)]

15. Damodaran, S.; Zhu, D. A formaldehyde-free water-resistant soy flour-based adhesive for plywood. *J. Am. Oil. Chem. Soc.* **2016**, *93*, 1311–1318. [[CrossRef](#)]
16. Wescott, J.M.; Frihart, C.R.; Traska, A.E. High-soy-containing water-durable adhesives. *J. Adhesion. Sci. Technol.* **2006**, *20*, 859–873. [[CrossRef](#)]
17. Rassam, G. Use of Soy/PF resin for old corrugated container (OCC)-wood composites. *Mater. Lett.* **2008**, *62*, 3236–3239. [[CrossRef](#)]
18. Pizzi, A.; Pasch, H.; Rode, K.; Giovando, S. Polymer structure of commercial hydrolyzable tannins by matrix-assisted laser desorption/ionization-time-of-flight mass spectrometry. *J. Appl. Polym. Sci.* **2009**, *113*, 3847–3859. [[CrossRef](#)]
19. Laurichesse, S.; Avérous, L. Chemical modification of lignins: Towards biobased polymers. *Prog. Polym. Sci.* **2014**, *39*, 1266–1290. [[CrossRef](#)]
20. Pasch, H.; Pizzi, A.; Rode, K. MALDI-TOF mass spectrometry of Polyflavonoid tannins. *Polymer* **2001**, *42*, 7532–7539. [[CrossRef](#)]
21. Sionkowska, A.; Kaczmarek, B.; Lewandowska, K. Modification of collagen and chitosan mixtures by the addition of tannic acid. *Mol. Liq.* **2014**, *199*, 318–323. [[CrossRef](#)]
22. Pizzi, A. Tannin-Based Adhesives. In *Wood Adhesives Chemistry and Technology*; Dehkker, M., Ed.; CRC Press: New York, NY, USA, 1983.
23. Pizzi, A. Polyflavonoid Tannins Self-Condensation Adhesives for Wood Particleboard. *J. Adhes.* **2009**, *85*, 57–68. [[CrossRef](#)]
24. Schwarzkopf, M.; Huang, J.; Li, K. A Formaldehyde-Free Soy-Based Adhesive for Making Oriented Strandboard. *J. Adhes.* **2010**, *86*, 352–364. [[CrossRef](#)]
25. Zhou, X.; Segovia, C.; Abdullah, U.H.; Pizzi, A.; Du, G. A novel fiber-veneer-laminated composite based on tannin resin. *J. Adhes.* **2016**, *93*, 461–467. [[CrossRef](#)]
26. Spina, S.; Zhou, X.; Segovia, C.; Pizzi, A.; Romagnoli, M.; Giovando, S.; Pasch, H.; Rode, K.; Delmotte, L. Phenolic resin adhesives based on chestnut (*Castanea sativa*) hydrolysable tannins. *J. Adhe. Sci. Tech.* **2013**, *27*, 2103–2111. [[CrossRef](#)]
27. Santos, J.; Antorrena, G.; Freire, M.S.; Pizzi, A.; González-Álvarez, J. Environmentally friendly wood adhesives based on chestnut (*Castanea sativa*) shell tannins. *Holz. Als. Roh- und. Werkstoff.* **2016**. [[CrossRef](#)]
28. Chen, X.; Pizzi, A.; Gerardin, C.; Li, J.; Zhou, X.; Du, G. Preparation and properties of a novel type of tannin-based wood adhesive. *J. Adhes.* **2020**. [[CrossRef](#)]
29. Mousavi, S.Y.; Huang, J.; Li, K. Further investigation of poly (glycidyl methacrylate-co-styrene) as a curing agent for soy-based wood adhesives. *J. Adhes.* **2020**, *96*, 1258–1269. [[CrossRef](#)]
30. Zuber, S.H.; Hashikin, N.A.A.; Mohd Yusof, M.F.; Hashim, R. Lignin and soy flour as adhesive materials in the fabrication of *Rhizophora* spp. particleboard for medical physics applications. *J. Adhes.* **2020**. [[CrossRef](#)]
31. Ghahri, S.; Bari, E.; Pizzi, A. The Challenge of Environment-Friendly Adhesives for Bio-Composites. In *Eco-Friendly Adhesives for Wood and Natural Fiber Composites*; Springer: Singapore, 2021.
32. Chen, M.; Luo, J.; Shi, R.; Zhang, J.; Qiang Gao, Q.; Li, J. Improved Adhesion Performance of Soy Protein-Based Adhesives with a Larch Tannin-Based Resin. *Polymers* **2017**, *9*, 408. [[CrossRef](#)]
33. Kamoun, C.; Pizzi, A. Mechanism of hexamine as a non-aldehyde polycondensation hardener, Part 1, Hexamine decomposition and reactive intermediates. *Holzforsch. Holzverwert.* **2000**, *52*, 16–19.
34. Liu, C.; Zhang, Y.; Li, X.; Luo, J.; Gao, Q.; Li, J. A high-performance bio-adhesive derived from soy protein isolate and condensed tannins. *RSC Adv.* **2017**, *7*, 21226–21233. [[CrossRef](#)]
35. Ghahri, S.; Pizzi, A.; Mohebbi, B.; Mirshokraie, A.; Mansouri, H.M. Soy-Based, Tannin-Modified Plywood Adhesives. *J. Adhes.* **2018**, *94*, 218–237. [[CrossRef](#)]
36. Ghahri, S.; Pizzi, A. Improving Soy-Based Adhesives for Wood Particleboard by Tannins Addition. *Wood. Sci. Technol.* **2018**, *52*, 261–279. [[CrossRef](#)]
37. Ghahri, S.; Mohebbi, B.; Pizzi, A.; Mirshokraie, A.; Mansouri, H.M. Improving Water Resistance of Soy-Based Adhesive by Vegetable Tannin. *J. Polym. Environ.* **2018**, *26*, 1881–1890. [[CrossRef](#)]
38. Chen, X.; Pizzi, A.; Xi, X.; Zhou, X.; Fredon, E.; Gerardin, C. Soy Protein Isolate Non-Isocyanates Polyurethanes (NIPU) Wood Adhesives. *J. Renew. Mater.* **2021**. [[CrossRef](#)]
39. Pasch, H.; Pizzi, A. Considerations on the macromolecular structure of chestnut ellagitannins by matrix-assisted laser desorption/ionization-time-of-flight mass spectrometry. *J. Appl. Polym. Sci.* **2002**, *85*, 429–437. [[CrossRef](#)]
40. Braghiroli, F.; Fierro, V.; Pizzi, A.; Rode, K.; Radke, W.; Delmotte, L.; Parmentier, J.; Celzard, A. Reaction of condensed tannins with ammonia. *Ind. Crops Prod.* **2013**, *44*, 330–335. [[CrossRef](#)]
41. Thebault, M.; Pizzi, A.; Santiago-Medina, F.J.; Al-Marzouki, F.M.; Abdalla, S. Isocyanate-Free Polyurethanes by Coreaction of Condensed Tannins with Aminated Tannins. *J. Renewable. Mat.* **2017**, *5*, 21–29. [[CrossRef](#)]
42. Rawel, H.M.; Czajka, D.; Rohn, S.; Kroll, J. Interactions of Different Phenolic Acids and Flavonoids with Soy Proteins. *Int. J. Biol. Macromolec.* **2002**, *30*, 137–150. [[CrossRef](#)]
43. Charlton, A.J.; Baxter, N.J.; Lokmankhan, M.; Moir, A.J.; Haslam, E.; Davies, A.P.; Williamson, M.P. Polyphenol/Peptide Binding and Precipitation. *Agric. Food. Chem.* **2002**, *50*, 1593–1601. [[CrossRef](#)]
44. Santiago-Medina, F.J.; Pizzi, A.; Basso, M.C.; Delmotte, L.; Celzard, A. Polycondensation resins by flavonoid tannins reaction with amines. *Polymers* **2017**, *9*, 37. [[CrossRef](#)] [[PubMed](#)]

3.5 Lignine déméthylée oxydée comme adhésif biosourcé pour le collage du bois

Résumé: La lignine a été modifiée avec succès pour préparer une colle à bois biosourcée en seulement deux étapes de synthèse : la déméthylation et l'oxydation au périodate. La spectroscopie infrarouge à transformée de Fourier (FT-IR), la spectrométrie de masse à temps de vol d'ionisation par désorption laser assistée par matrice (MALDI-TOF) et l'analyse thermomécanique (TMA) ont été combinées pour caractériser les adhésifs biosourcés obtenus. De plus, les performances d'adhérence de l'adhésif à base de lignine biologique ont été mesurées en testant la résistance à la traction et au cisaillement des joints collés. Les résultats montrent que la lignine déméthylée donne au joint de bois une résistance au cisaillement à sec acceptable, mais pas de résistance au cisaillement humide. Ainsi, l'oxydant peroxyde de sodium (NaIO_4) a été utilisé pour améliorer les performances de collage des adhésifs à base de lignine. La formulation optimale pour les adhésifs à base de lignine déméthylée oxydée s'est avérée être l'ajout de 20 % de NaIO_4 . L'adhésif présentant des aldéhydes dérivé de l'oxydation spécifique de la lignine, à haute teneur en biomasse, et sa préparation est un produit pratique et peu coûteux et peut être appliqué au collage du bois.

Mots clés: Lignine déméthylée; oxydation; bois biosourcé adhésif; collage du bois.



Oxidized demethylated lignin as a bio-based adhesive for wood bonding

Xinyi Chen^{a,b}, Xuedong Xi^a, Antonio Pizzi ^a, Emmanuel Fredon^a, Guanben Du^b, Christine Gerardin^c, and Siham Amirou^a

^aLERMAB, University of Lorraine, Epinal, France; ^bYunnan Provincial Key Laboratory of Wood Adhesives and Glued Products, Southwest Forestry University, Kunming, Yunnan province, China; ^cLERMAB, University of Lorraine, Nancy, France

ABSTRACT

Lignin was successfully modified to prepare a bio-based wood adhesive by just two synthesis steps: demethylation and periodate oxidation. Fourier Transform Infrared Spectroscopy (FT-IR), Matrix Assisted Laser Desorption Ionization Time of Flight (MALDI-TOF) Mass Spectrometry and Thermomechanical Analysis (TMA) were combined to characterize the bio-based adhesives obtained. Furthermore, the adhesion performance of the bio-based lignin adhesive was measured by testing the tensile shear strength of the bonded joints. The results show that demethylated lignin gives to the wood joint acceptable dry shear strength, but no wet shear strength. Thus, sodium peroxide (NaO₄) oxidant was used to improve the bonding performance of lignin-based adhesives. The optimal formulation for oxidized demethylated lignin adhesives was found to be by 20% addition of NaO₄. The adhesive presented is a lignin-derived non-aldehyde addition, high biomass content, and its preparation is convenient, low-cost product and can be applied to wood bonding.

ARTICLE HISTORY

Received 28 October 2019
Accepted 28 December 2019

KEYWORDS

Demethylated lignin;
oxidation; bio-based wood
adhesive; wood bonding

1. Introduction

Duo to the increasing concern about the depletion of fossil fuels and the increasing awareness of environmental problems, a considerable number of research works have focused on the use of biomass materials.^[1] Thus, lignin being the second most abundant natural organic polymer after cellulose, it has attracted increasing attention from researchers.^[2] As a suitable starting material for some valuable small molecular weight aromatic compounds or polymer products, its structural, chemical and physical properties have been analyzed by using various technological methods.^[3–5] There are three different main types of phenyl-propane monomers units, these being *p-coumaryl alcohol*(H), *coniferyl alcohol*(G), and *sinapyl alcohol*(S).^[6–10] However, because of complex

CONTACT Antonio Pizzi  antonio.pizzi@univ-lorraine.fr  LERMAB, University of Lorraine, 27 rue Philippe Seguin, BP 1041, Epinal88051, France

Color versions of one or more of the figures in the article can be found online at www.tandfonline.com/gadh.

 Supplemental data for this paper can be accessed on the publisher's website.

© 2020 Taylor & Francis Group, LLC

structures, broad chemical differences, and low reactivity, lignin-based commodity materials haven't been commercialized widely, despite their high availability.^[11] Therefore, most lignin resources are generally used as an industrial energy source.^[12,13] Fortunately, in the literature are reported modified lignin uses varying from the synthesis of polymer products for adhesives^[14-17], resins^[18,19] and plastics^[20,21], as well as modifications to try to modify and commercialize such modified lignins.

Many kinds of lignin modification methods, such as demethylation^[11,19,22,23], hydroxy-methylation^[6,24] and phenolation^[25-27], oxidation^[28], etc., have been reported which can be effective to improve the reactivity of lignin. Among these, demethylation appears to be an effective and prospective method^[22,23] as under mild reaction conditions some aromatic methoxy groups are converted to phenolic hydroxyl groups. As a consequence, the proportion of reactive sites will increase as a greater proportion of catechol moieties is present in lignin, and its reactivity improved.^[11,19]

In recent years, many efficient demethylation methods have been reported, such as, under acid conditions, by using hydrogen iodide^[29], hydrogen chloride^[30], and other diverse hydrolysis reactions, and fungal (*white rot fungi or brown rot fungi*)^[31] and bacteria (*Pseudomonas or Sphingomonas*) based methods.^[32] All of these have been used to convert the aromatic methoxy groups to phenolic hydroxyl groups. Nevertheless, some drawbacks have been cited, including environmental issue (like the acid condition), high temperature (up to 225°C)^[11], long processing time (almost 6 h)^[22,31], and high pressure.^[23] Therefore, another more suitable approaches should be selected to replace such extreme reaction conditions. Some studies indicated that a kind of traditional papermaking method was commonly used to treat raw lignin in the demethylation process where a nucleophile substitution reaction occurs between hydroxyl and sulfite ions with lignin being converted to form sulfite pulp.^[11] Furthermore, the aryl methyl ethers of aromatic compounds are cleaved by nucleophilic substitution reactions with sulfite ions, resulting in a decrease of the methoxy group content and in reactivity increases of modified lignin. The demethylation route of lignin is shown in Figure 1. Because lignin after demethylation has more phenolic hydroxyl groups, demethylation-treated lignin has been considered as the starting material to react with formaldehyde and for preparing phenol-formaldehyde (PF) resin.^[11,17] However, such preparation systems still involve formaldehyde and thus more environment friendly approaches to prepare eco-friendly wood adhesives have become a focus of interest.

Oxidation is a commonly used method in starch-based wood adhesives production.^[33] Recently, the specific oxidation of plant flours has attracted the attention of some researchers as regards their effectiveness for adhesives application.^[34,35] Periodate is a specific oxidant cleaving carbon to carbon bonds presenting vicinal aliphatic hydroxyl groups to form aldehydes and

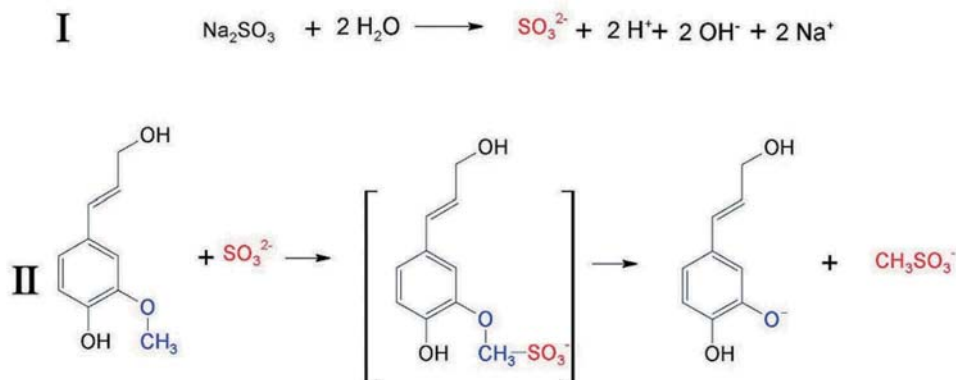


Figure 1. The reaction of lignin demethylation.

dialdehydes.^[34–38] Often the structural units within lignin presents on their aliphatic part both hydroxyl groups vicinal to the β -O-4 bonds to another lignin unit. The β -O-4 linkage is easily cleaved by an oxidant so that aldehydes and possibly also dialdehydes are generated. In addition, the greater proportion of aromatic hydroxyl groups have generated by demethylation thereby increasing aromatic ring reactivity. Hence, the aldehydes generated by periodate oxidation are likely to react with hydroxyl-activated reactive phenolic sites contributing to form a stronger hardened network. Such an adhesive could be classified as a biobased product.

This work is then aimed to prepare a novel lignin-derived, high biomass content wood adhesive with no exterior-added aldehydes by two steps: demethylation and oxidation, and to test its bonding performance as a wood adhesive. Demethylated lignin was synthesized under a moderate condition by using sodium sulfite as a catalyst to be then directly mixed sodium periodate (NaIO_4) at atmospheric pressure. The lignin-based adhesives so obtained were characterized by thermomechanical analysis (TMA), Fourier transform infrared (FT-IR) spectroscopy and Matrix Assisted Laser Desorption Ionisation Time of Flight (MALDI-TOF) mass spectrometry as well as testing them for wood bonding.

2. Experimental

2.1. Materials

The ingredients of the adhesives including commercial corn lignin were supplied by Jinan yanghai environmental protection materials co. LTD, Jinan, Shandong province, China. Sodium periodate (NaIO_4 , 99%), Sodium sulfite (Na_2SO_3 , 97%), sodium hydroxide (NaOH , 99%) were supplied by Sigma-Aldrich. All chemical reagents were analytical grade, without further purification. Deionized water (DI) was produced in the laboratory.

Rotary-cut poplar (*Populus deltoides*) 2 mm thick air-dried veneers, of $45 \times 45 \text{ cm}^2$ nominal dimensions were selected to prepare the bonded wood samples.

2.2. Preparation process

2.1.1. Preparation of demethylated lignin

The demethylated lignin was obtained as follows. Briefly, 16 g corn lignin and 24 g deionized water were added into a 250 mL three-neck round bottomed flask with magnetic stirring. After the lignin is dispersed in water, NaOH (33% concentration) was used to adjust the pH to 8.0–8.5. 1 g sodium sulfite was then added into the mixture. At the same time, the water bath was heated to 90°C and the mixture was kept at reflux for 2 h to obtain the solution of demethylated lignin (DL). The demethylated lignin-based solutions were prepared according to this method in all subsequent steps.

2.1.2. Preparation of demethylated lignin-based wood adhesives

A series of wood adhesives were prepared by as follows: lignin (L) or demethylated lignin (DL) was blended with a certain amount of NaIO_4 . The weight of NaIO_4 was based on the lignin dry weight, from 0–30%, and then the preparation of the adhesives so obtained was recorded as L (0% addition of NaIO_4), L-10 (10% addition of NaIO_4), DL, DL-5, DL-10, DL-15, DL-20, DL-25, DL-30, respectively. When all parts of the adhesives were ready, they were mixed together rapidly under manual stirring for 1–2 minutes. After testing, the viscosity of the lignin-based adhesives was between 225–245 mPa·s, and their solid content was between 32.5%–38.3%.

2.1.3. Preparation and testing of wood specimens with bio-based wood adhesives

Two-layers (Figure 2a) wood specimens were prepared for shear strength testing as already reported previously.^[39] The final sample size (L × W × H) of each specimen was $100 \times 25 \times 3 \text{ mm}^3$, and its adhesive area is $25 \times 25 \text{ mm}^2$. The wood bonding samples were prepared according to the following steps. First, the wood adhesives were obtained by treating lignin with different ratio of NaIO_4 (from 0%–30%), based on dry lignin weight. Second, rotary-cut poplar veneers (each piece $200 \times 100 \times 2 \text{ mm}^3$) were coated evenly with the glue mix (at a spread of 300 g/m^2). Third, the adjacent veneers were assembled with the wood grain direction parallel. The veneers so assembled were then hot-pressed at 0.75 N/mm^2 and a temperature of 160°C for 4min to form a two-layers wood composite. Three layers wood plywood panels (Figure 2b, the wood grain direction of adjacent veneer was perpendicular to each other) were also prepared using the same

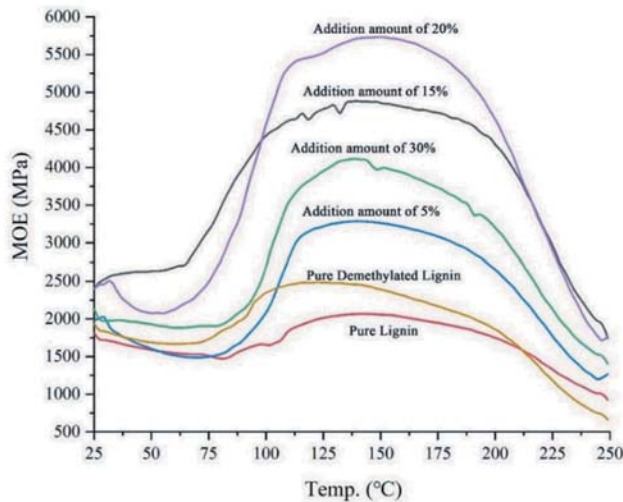


Figure 2. Thermomechanical analysis (TMA) curves of different lignin-based adhesives.

procedure as above by addition of 0 %, 15% and 20% NaIO_4 , respectively. The glue spread used was of 300 g/m^2 double glue line; hot-pressing was carried out at 0.75 N/mm^2 at 160°C for 6 minutes. Finally, each joint was conditioned at ambient temperature and an equilibrium moisture content of 12% for 2 days.

Dry shear strength, 24 h wet shear strength and 2 h boiled water shear strength of all sample were tested according to China National Standard GB/T 14074 (2006)^[40], China National Standard GB/T17657 (1999)^[41] and British Standard BS 1204 (1993).^[42] The tests were carried out by using an Instron 3300 dual column universal testing machine (Instron France, Elancourt, France) at a head rate of 2 mm/min . The standards required minimum average shear strength values for all samples had to be equal to or greater than 0.7 MPa . Each test was replicated six times to obtain the calculated mean values.

2.2. Thermomechanical analysis (TMA)

The lignin-based adhesives were tested by thermomechanical analysis according to a method used previously.^[43,44] The modulus of elasticity (MOE) of the sample resins was measured in three-point bending using TMA equipment (Mettler Toledo, Zurich, Switzerland). The testing samples were prepared by beech-resin-beech sandwiches formed by two small wood plies ($17 \times 5 \times 1.1 \text{ mm}^3$, Longitudinal×Radial×Tangential) joined with 30 mg of the adhesives. TMA analysis was conducted in non-isothermal mode between 25°C to 250°C , at a constant heating rate of 10°C/min , on a span

of 18 mm exercising a force cycle of 0.1/0.5 N on the specimens, with each force cycle of 12 seconds (6s/6s). The Modulus of Elasticity (MOE) of the specimens as a function of time and temperature was recorded for all formulations.

2.3. FT-IR analyses

All the sample extracts were analyzed with a PerkinElmer Frontier ATR-FT-MIR provided with an ATR Miracle diamond crystal. The powder and liquid samples were laid on the diamond eye (1.8 mm) of the ATR equipment and the contact for the sample was ensured by tightly screwing the clamp device. Each extract was scanned registering the spectrum with 32 scans with a resolution of 4 cm^{-1} in the wave number range between 600 and 4000 cm^{-1} .

2.4. MALDI-TOF analysis

Samples for matrix-assisted laser desorption ionization time-of-flight (MALDI-TOF) analysis were prepared by first dissolving 5 mg of sample powder in 1 mL of a 50:50 v/v acetone/water solution. Then, 10 mg of this solution was added to 10 μL of a 2,5-dihydroxy benzoic acid (DHB) matrix. The locations dedicated to the samples on the analysis plaque were first covered with 2 μL of NaCl solution 0.1 M in 2:1 v/v methanol/water and pre-dried. Then, 1 μL of the sample solution was placed on its dedicated location, and the plaque was dried again. Red phosphorous was used to standardize the MALDI equipment.

MALDI-TOF spectra were obtained by means of an Axima Performance mass spectrometer from Shimadzu Biotech (Kratos Analytical Shimadzu Europe Ltd., Manchester, UK) using a linear polarity-positive tuning mode. The measurements were taken by making 1000 profiles per sample with two shots accumulated per profile. The spectrum precision is of +1 Da.

3. Results and discussion

3.1. TMA analysis

The Young's modulus E (MOE) for each case tested can be calculated by using the classical mechanics relation between force and deflection.^[43–45] The TMA curves of all samples are shown in Figure 3. This shows the MOE values of the series of samples bonded with lignin alone and oxidized demethylated lignin-based adhesives by adding different amount of NaIO_4 to the demethylated lignin. Increasing the proportion of NaIO_4 from 0% to 20% causes the MOE to progressively increase and reach the maximum value at 20% NaIO_4 addition. This infers that the best bonding performance is

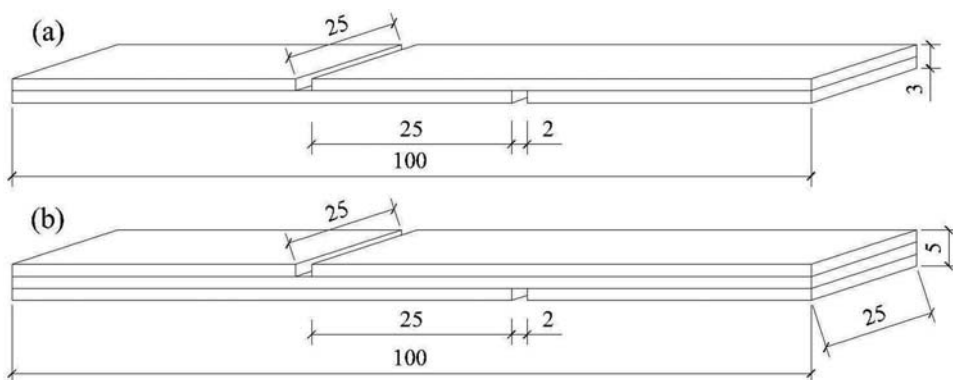


Figure 3. The diagrammatic drawing of wood bonding specimens: (a) for two-layers sample, (b) for three-layers sample.

likely to occur for a 20% NaIO_4 treatment.^[46,47] It is also consistent with the shear strength test results of wood specimens, which shows that 20% addition of NaIO_4 to the lignin adhesives yields the best bonding performance. Furthermore, due to the hypothesis of the generation of aldehyde groups by periodate cleavage of aliphatic carbon-carbon bonds carrying hydroxyl groups, the aldehyde groups so generated can react with the lignin sites to yield increased cross-linking of the final hardened network.^[33,34] These results are supported by the findings of the MALDI-TOF analysis. Nevertheless, an excessive addition of periodate, more than 20%, has an adverse effect on bonding performance due to further conversion of the aldehyde groups into carboxyl groups, consequently decreasing the possibility of cross-linking with the aromatic lignin rings.^[33] As shown in Figure 3, as the proportion of NaIO_4 added increases above 20%, a decreasing trend can be observed for the MOE values measured by TMA.

3.2. FT-IR analysis

Fourier transform Infrared (FT-IR) spectra of the pure lignin (L) and demethylated lignin (DL) samples are shown in Figure 4. The results show that the main functional groups of the demethylated lignin sample are still the same as those of the original lignin. Thus, as for the spectra of all curves in Figure 4, the broad absorption bands at 3362 cm^{-1} , is attributed to the aromatic and aliphatic -OH groups characteristic of the FT-IR spectrum of lignin.^[11,48] Moreover, the absorption bands at 1588 cm^{-1} , 1502 cm^{-1} and 1416 cm^{-1} were assigned to the aromatic ring vibrations of the phenyl-propane skeleton in all samples.^[47,48] The peak at 1331 cm^{-1} and 828 cm^{-1} are assigned to the aromatic C-H in plane deformation vibration of the syringyl moieties of lignin. A peak at 1119 cm^{-1} , is related

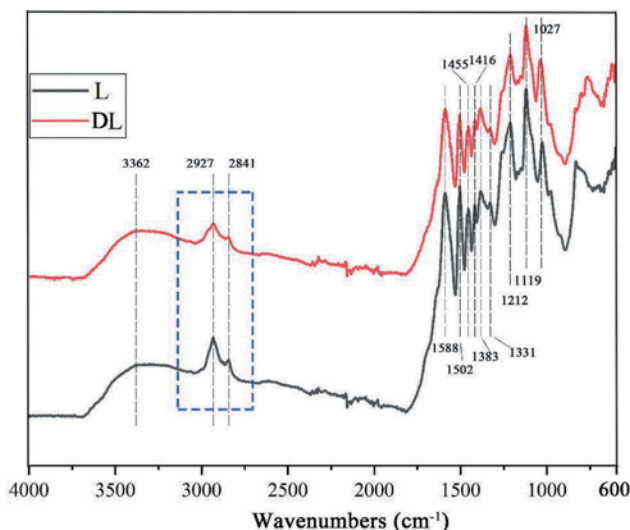


Figure 4. FTIR spectra (4000–600 cm^{-1}) of neat corn lignin (L) and demethylated corn lignin (DL).

to the aromatic C-H in the guaiacyl moiety of lignin.^[49] The band at 2927 cm^{-1} was related to the C-H vibration of $-\text{CH}_2$ and $-\text{CH}_3$ groups. According to the literatures, the peaks at 2841 cm^{-1} and 1455 cm^{-1} can be attributed to the vibration of $-\text{O}-\text{CH}_3$ groups.^[11,49] In Figure 4 it is noticeable, nevertheless, that some differences between pure- and demethylated lignin do occur. For example, in the contoured region the ratio of the aromatic skeletal vibrations at 2841 cm^{-1} and 1455 cm^{-1} in DL were lower than in pure L. This was due to the structure of lignin, as more $-\text{O}-\text{CH}_3$ groups were converted into hydroxyl groups during the demethylation process. It can then be suggested that demethylation occurred successfully.

3.3. MALDI-TOF analysis

MALDI-TOF has already been used to analyze the different oligomers formed by lignin modification.^[50,51] Some larger molecular weight species are noticeable in the MALDI-TOF spectra, these being dimers, trimers or higher oligomers derived from the three typical lignin species (H, G and S) linkages by β -O-4 (approximately 40-60%), α -O-4, β - β , β -5, 5-5'.^[26,52] Therefore, the MALDI-TOF analysis investigates the different oligomers existing in the oxidized demethylated lignin adhesive.

In Figures 6–10 are shown the results of the MALDI-TOF analysis of the different oligomers formed in the preparation of the oxidized demethylated lignin-based adhesives. According previous works, the main foreseeable structure formulas of our lignin-based resins is shown in Table 1. Figure 6 shows the presence of some low molecular weight lignin oligomers as well,

Table 1. Oligomers identified by MALDI-TOF mass spectrometry in the reaction of lignin monomer.

Peak	Chemical Species	
80.6	Glyoxal, with Na ⁺	monomer
175.5	H, with Na ⁺	monomer
196.4	G ₀ , without Na ⁺	monomer
231.5	S, with Na ⁺ or/and H – Glyoxal, with Na ⁺	Monomer/dimer
300.3	G ₀ -Ver or/and H-β1-G ₀ , with Na ⁺	dimer
310.7	H-β1-G, with Na ⁺	dimer
322.3	H-CHO-H, without Na ⁺	Trimer
344.5 and 364.4	G ₀ (-CHO)-G ₀ or S _d – Ver, with or without Na ⁺	dimer
360.4	S ₀ and d (-CHO)-G or/and H- Gly-H, without Na ⁺	Dimer/trimer
408.4	G-β04-S, without Na ⁺ or/and H- Gly-G, with Na ⁺	Dimer/trimer
418.3	H ₀ (-CHO)-H-β1-G or/and G- Gly-G, without Na ⁺	trimer
428.4	G-β04-S, with Na ⁺	dimer
458.4	S ₀ and d (-CHO)- H-β1-G or/and S _d - Gly-G, without Na ⁺ , or/and S _d - Mal -H, with Na ⁺	trimer
462.4	S ₀ and d (-CHO)- H-β1-G ₀ , with Na ⁺ or/and G-β04-S-Glyoxal or/and S _d - Mal -G, without Na ⁺	trimer
484.4	G-β04-S _d - Malonaldehyde, with Na ⁺	trimer
512.4	H- Gly -H-Ver	tetramer
542.4	H ₀ (-CHO)-S _d -β04-G or/and H- Mal -H-Ver or/and G- Gly -H-Ver or/and S-β04-G _d -Ver, without Na ⁺ ,	Trimer/tetramer
572.4 and 592.5	G _d -β04-S ₀ (-CHO)-G, with or without Na ⁺ , G- Mal -H-Ver, without Na ⁺	trimer/tetramer
592.5	S ₀ and d (-CHO)- S ₀ and d (-CHO)-S _d , with Na ⁺	trimer
600.4	G ₀ (-CHO)-H ₀ (-CHO)-H-β1-G, without Na ⁺	tetramer
604.4	G-β04-S ₀ (-CHO)-G, with Na ⁺	trimer
620.5	S ₀ and d (-CHO)-H ₀ (-CHO)-H-β1-G, without Na ⁺	tetramer
658.6	G-β04-G ₀ and d-H-Ver, with Na ⁺	tetramer
684.7	G-β04-S ₀ and d (-CHO)- H-β1-G, with Na ⁺	tetramer
682.6 and 700.5	G-β04-S ₀ (-CHO)- H-β1-G, with Na ⁺ , with or without Na ⁺ , or/and S _d -β04-G ₀ and d-H-Ver, with Na ⁺	tetramer
722.5	G-β04-S ₀ and d (-CHO)-G ₀ (-CHO)-H, without Na ⁺	tetramer
784.5	H ₀ (-CHO)-G-β04-S ₀ and d (-CHO)- H-β1-G _d , without Na ⁺	tetramer
812.6	G-β04-G ₀ and d-H-Ver-Ver, without Na ⁺	pentamer
949.1	G _d -β04-S ₀ and d (-CHO)-G ₀ (-CHO)-G _d -β04-S, without Na ⁺	multimer
949.1	G ₀ and d (-CHO)-G-β04-S ₀ and d (-CHO)-H-β1-G _d -H ₀ (-CHO) or/and G-β04-G ₀ and d-H ₀ -H-Ver-Ver, without Na ⁺	multimer
952.5	G-β04-S ₀ and d (-CHO)-H-β1-G _d -G-ββ	multimer

Note: G₀(-CHO) = Oxidized Monomer G; S₀(-CHO) = Oxidized Monomer S; H₀(-CHO) = Oxidized Monomer H; G_d = demethylated Monomer G; S_d (-CHO) = demethylated Monomer S; H_d(-CHO) = demethylated Monomer H; G₀ and d(-CHO) = Oxidized Demethylated Monomer G; S₀ and d = Oxidized Demethylated Monomer S; H₀ and d = Oxidized Demethylated Monomer H; Ver = veratraldehyde; Gly = glyoxal; Mal = malonaldehyde.

such as 196.4 (demethylated monomer S) and 231.5(monomer S) Da, generated by the partial depolymerization of lignin. And the same results appear in Figure S1 (180.7 Da, monomer G) and Figure S4 (197.7 Da, demethylated monomer S and 255.6 Da, monomer S). These are consistent with lignin depolymerized monomers or demethylated lignin mentioned in previous studies.^[2,10,50,51] In the MALDI-TOF spectrum of lignin (Figure S1) and demethylated lignin (Figure 6 and Figure S4), evidence of demethylation has been found, such as the peak at 210.5 Da (Figure S1) being monomer S, the peak at 197.7 Da (Figure S4) and 196.4 Da (Figure 6) being demethylated structures of monomer S. The 410.2 Da peak in Figure S2 is G- β -O-4-S, while the peaks corresponding to demethylated G- β -O-4-S, are at 412.9 Da (Figure S5) and 418.3 Da (Figure 7). All these attest that the lignin has been demethylated, and the results are confirmed by FTIR as well.

Thus, the evidence above indicates that the ether bond of the β -O-4 linkage too was cleaved easily by the periodate, even with this reaction conducted under mild conditions (cf. Figure 5).^[29,52] This is one of the reasons for lignin being depolymerized under the experimental conditions used. As a consequence of the cleavage of the β -O-4 aryl ether, the aliphatic phenolic -OH content increased.^[53] There are two possible reactions in the conversion of aliphatic hydroxyl groups to aldehyde groups processes. One

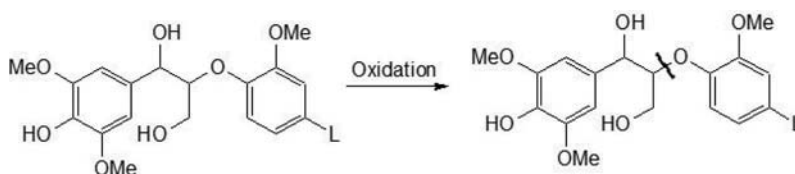


Figure 5. The ether bond of β -O-4 linkage in lignin.

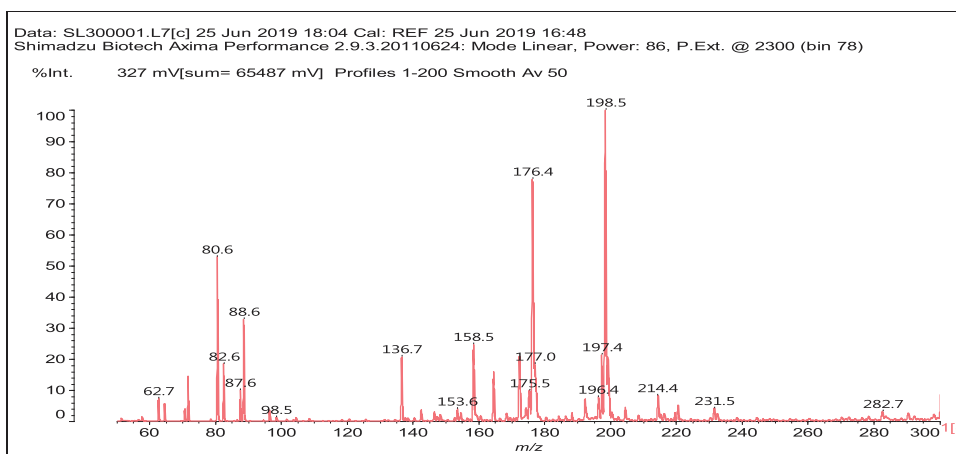


Figure 6. MALDI-TOF spectrum of oxidized demethylated of lignin resin: 20 – 300 Da.

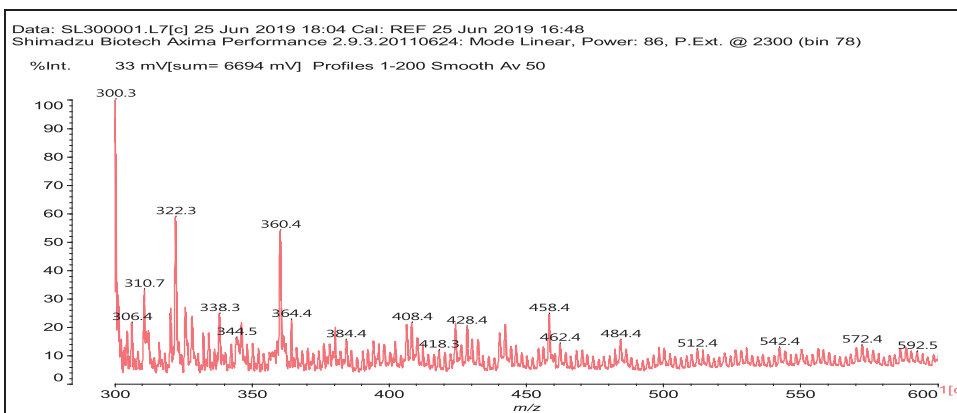


Figure 7. MALDI-TOF spectrum of oxidized demethylated of lignin resin: 300 – 600 Da.

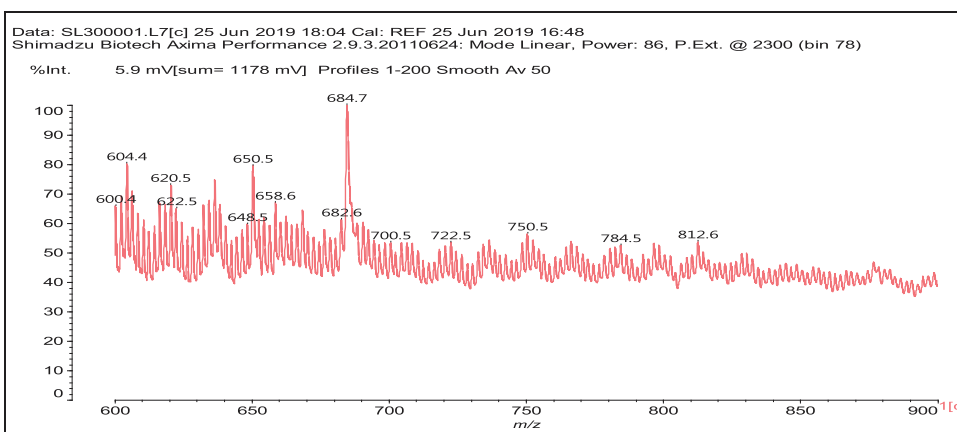


Figure 8. MALDI-TOF spectrum of oxidized demethylated of corn lignin resin: 600 – 900 Da.

concerns the conversion of some lignin aliphatic hydroxyls to aldehyde groups according to the proportion of NaIO_4 addition.^[35] Subsequently, the aldehyde groups can link with demethylated lignin monomers to form larger oligomers and networks. Due to the demethylation more reactive sites have been generated. Nevertheless, an excessive amount of NaIO_4 can also produce some negative effects. Thus, it can convert aldehyde groups to carboxyl groups thereby losing the possibility of reacting them with lignin. The other effect that could occur is that the lignin aromatic rings could be cleaved by the periodate at the carbon-carbon bonds carrying vicinal phenolic hydroxyls, resulting in the formation of small molecular weight aldehydes, such as veratraldehyde (Ver), glyoxal (Gly), malonaldehyde (Mal) and others. This explanation however might be incorrect as the evidence of small molecular weight aldehydes gathered by the MALDI-TOF spectra can have a different origin. This is the case of glyoxal ($58 \text{ Da} + 23 \text{ Da Na}^+ = 81 \text{ Da}$)

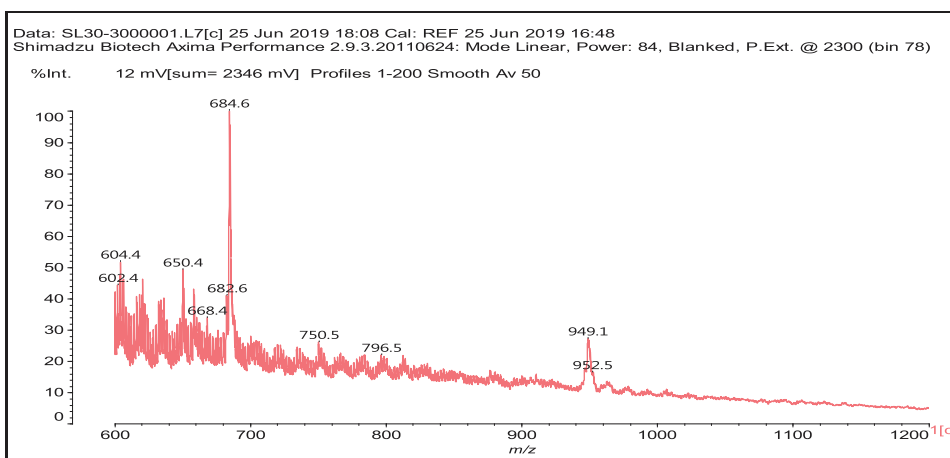


Figure 9. MALDI-TOF spectrum of oxidized demethylated of corn lignin resin: 600 – 1200 Da.

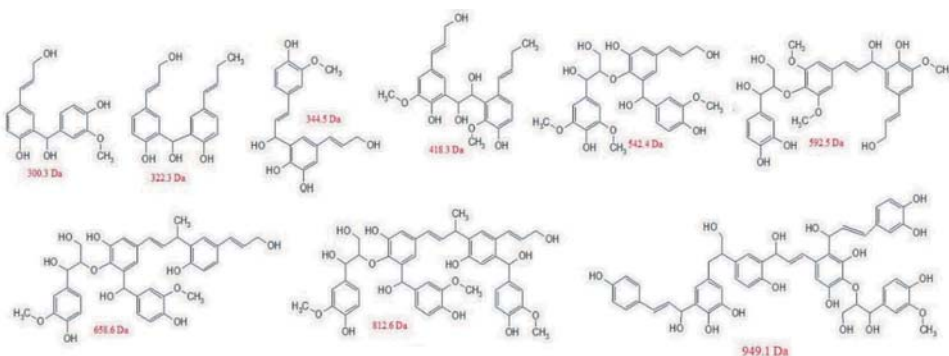


Figure 10. Examples of condensed structures and their peaks in Da as identified by MALDI-TOF (Table 1).

generated by the cleavage of the β -O-4 linkage and the aliphatic $-\text{CH}_2\text{-OH}$ terminal group of a lignin unit. It's interesting that some other small molecular weight aldehydes were observed in Figure 6, such as the peaks at 136.7 Da and 153.6 Da. These aldehydes are most likely to have been involved in reactions to produce some dimer, trimer or higher oligomers. Figures 7–9 show the species obtained by condensation of lignin monomers to dimers, trimers or higher oligomers linked by oxidation-generated aldehyde groups. For instance, some condensed structure can be foreseeable from MALDI-TOF spectra, as shown in Figure 10. It is precisely because of the extensive crosslinking forming a complex hardened network that the bonding performance of bio-based lignin adhesives is improved.

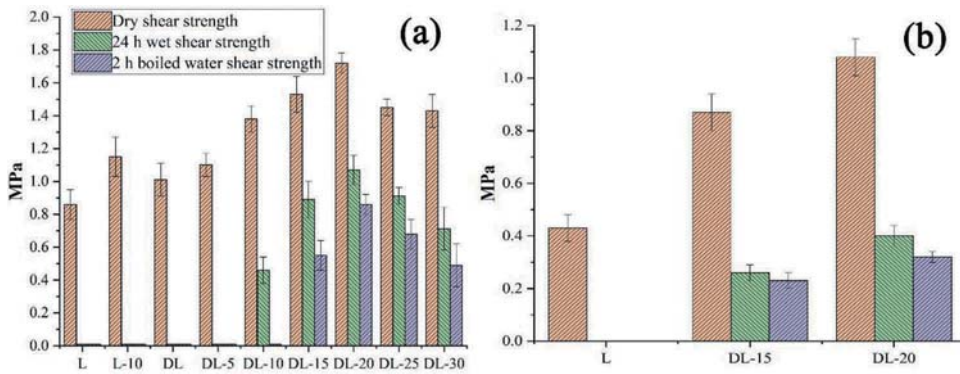


Figure 11. Bonding strength of different lignin/demethylated lignin-based adhesives: (a) for 2-layers; (b) for 3-layers.

4. Bonding performance tests of bio-based lignin adhesives

The bonding strength results, including dry, 24 h cold water and 2 h boiled water wet shear strength, of wood specimens bonded with lignin-based adhesives are shown in Figure 11. For the pure lignin-based adhesives, the dry bond strength of two-layers wood bonding samples passed from 0.86 MPa to 1.15 MPa, when adding 10% of NaIO_4 as shown in Figure 11a. Demethylated lignin is more reactive.^[11,24] Moreover, it is obvious that the dry shear strength of wood specimens bonded with pure lignin-based adhesives is significantly lower than that of the samples bonded demethylated lignin-based adhesives. Furthermore, the wet shear strength (24 h cold water and 2 h boiled water) of samples bonded with pure lignin-based adhesives have not been acquired, while the 24 h cold water shear strength has been obtained when using demethylated lignin-based adhesives.

Figure 11a indicates as well that, the shear strength presents a tendency to increase first and then decrease with the increasing proportion of NaIO_4 . When the minimum additive of NaIO_4 was 10%, starting to obtain the wet shear strength of wood bonding samples after 24 h cold water immersion. Subsequently, the 2 h boiled water wet shear strength can be acquired when NaIO_4 addition proportion reached at 15%. As shown in Figure 11a, the results show that the shear strength reaches its highest value for 20% addition of NaIO_4 , namely 1.72 MPa for dry strength, 0.72 MPa for 24 h cold water wet strength and 0.55 MPa for 2 h boiled water wet strength, respectively. The causes of this is the higher number of aldehydes generated capable of reacting with the higher number of free aromatic sites on demethylated lignin. Moreover, by adding the periodate to the lignin and then applying this adhesive at ambient temperature on the wood, when the wood is in the hot press then even the cellulose and hemicelluloses of the wood substrate/surface

can to a small extent oxidize forming dialdehydes.^[35] Under these conditions, the dialdehydes so formed will promote wood bonding. Nevertheless, the shear strength will gradually decrease when the amount of NaIO_4 added is greater than 20% (i.e. 25% and 30%), as shown in Figure 11a. This is due to the excess of NaIO_4 oxidant converting the aldehyde groups originally formed into unreactive carboxyl groups.^[33,34] The shear strength results of three-layers lignin-based plywood samples are shown in Figure 11b. Apparently, the maximum shear strength appears again at 20% addition of NaIO_4 , 1.08 MPa for dry strength, 0.41 MPa for 24 h cold water wet strength and 0.31 MPa for 2 h boiled water wet strength, respectively. This trend is similar to that for the two-layers bonded samples shown in Figure 11a. In summary, these results show that the bond strength can be increased by adding in moderation the specific oxidant NaIO_4 when using demethylated lignin as a wood adhesive. The wet shear strength of oxidized demethylated lignin-based adhesives, nevertheless, is inferior to the requirements of the China national standard^[54] (GB/T 9846–2015, ≥ 0.7 MPa). Therefore, some further modifications will need to be implemented in further research work to reach the relative standard requirements for this aspect.

5. Conclusion

In summary, a convenient two-steps method: demethylation and oxidation, to prepare bio-based oxidation demethylated lignin adhesive has been demonstrated. The process of demethylation can improve the reactivity of lignin because of some methoxy groups being converted to phenolic hydroxyl groups by a nucleophilic substitution reaction so that more reactive sites on lignin can be generated. A specific oxidant (NaIO_4) was brought into the reaction system to improve the adhesion performance of demethylated lignin wood adhesives. It is precisely because of its specific oxidation that aldehyde groups were generated capable of reacting with demethylated lignin. This results in a more cross-linked hardened network, yielding a better bond strength and a certain level of water resistance. The adhesion strengths of bonded wood specimens reach a maximum value when the amount of NaIO_4 is 20%. It is thus shown that the kind of adhesive presented is a lignin adhesive without exterior aldehydes been added but with lignin-generated aldehydes by periodate treatment, presenting a high biomass content, of rather convenient preparation, low-cost and applicable to wood bonding.

Acknowledgements

This work is supported by the scholarship from China Scholarship Council (CSC), Yunnan Provincial Key Laboratory of Wood Adhesives and Glued Products. The LERMAB is

supported by a grant of the French Agence Nationale de la Recherche (ANR) as part of the laboratory of excellence (LABEX) ARBRE.

ORCID

Antonio Pizzi  <http://orcid.org/0000-0002-9749-7185>

References

- [1] Long, J.; Xu, Y.; Wang, T.; Yuan, Z.; Shu, R.; Zhang, Q.; Ma, L. Efficient Base-catalyzed Decomposition and in Situ Hydrogenolysis Process for Lignin Depolymerization and Char Elimination. *Appl. Energy*. 2015, 141, 70–79. DOI: 10.1016/j.apenergy.2014.12.025.
- [2] Gao, W.; Inwood, J. P.; Fatehi, P. Sulfonation of Hydroxymethylated Lignin and Its Application. *J. Bioresources Bioprod.* 2019, 4(2), 80–88. DOI: 10.21967/jbb.v4i2.228.
- [3] Rahimi, A.; Ulbrich, A.; Coon, J. J.; Stahl, S. S. Formic-acid-induced Depolymerization of Oxidized Lignin to Aromatics. *Nature*. 2014, 515(7526), 249–252. DOI: 10.1038/nature13867.
- [4] Zhao, S.; Huang, X.; Whelton, A. J.; Abu-Omar, M. M. Formaldehyde-Free Method for Incorporating Lignin into Epoxy Thermosets. *ACS Sustainable Chem. Eng.* 2018, 6(8), 10628–10636. DOI: 10.1021/acssuschemeng.8b01962.
- [5] Zhao, S.; Abu-Omar, M. M. Synthesis of Renewable Thermoset Polymers through Successive Lignin Modification Using Lignin-Derived Phenols. *ACS Sustainable Chem. Eng.* 2017, 5(6), 5059–5066. DOI: 10.1021/acssuschemeng.7b00440.
- [6] Upton, B. M.; Kasko, A. M. Strategies for the Conversion of Lignin to High-Value Polymeric Materials: Review and Perspective. *Chem. Rev.* 2016, 116(4), 2275–2306. DOI: 10.1021/acs.chemrev.5b00345.
- [7] Nanayakkara, S.; Patti, A. F.; Saito, K. Chemical Depolymerization of Lignin Involving the Redistribution Mechanism with Phenols and Repolymerization of Depolymerized Products. *Green Chem.* 2014, 16(4), 1897–1903. DOI: 10.1039/C3GC41708E.
- [8] Lahive, C. W.; Deuss, P. J.; Lancefield, C. S.; Sun, Z.; Cordes, D. B.; Young, C. M.; Tran, F.; Slawin, A. M. Z.; de Vries, J. G.; Kamer, P. C. J.; et al. Advanced Model Compounds for Understanding Acid-Catalyzed Lignin Depolymerization: Identification of Renewable Aromatics and a Lignin-Derived Solvent. *J. Am. Chem. Soc.* 2016, 138(28), 8900–8911. DOI: 10.1021/jacs.6b04144.
- [9] Kruger, J. S.; Cleveland, N. S.; Zhang, S.; Katahira, R.; Black, B. A.; Chupka, G. M.; Lammens, T.; Hamilton, P. G.; Bidy, M. J.; Beckham, G. T. Lignin Depolymerization with Nitrate-Intercalated Hydrotalcite Catalysts. *ACS Catal.* 2016, 6(2), 1316–1328. DOI: 10.1021/acscatal.5b02062.
- [10] Deepa, A. K.; Dhepe, P. L. Lignin Depolymerization into Aromatic Monomers over Solid Acid Catalysts. *ACS Catal.* 2015, 5(1), 365–379. DOI: 10.1021/cs501371q.
- [11] Li, J.; Zhang, J.; Zhang, S.; Gao, Q.; Li, J.; Zhang, W. Fast Curing Bio-Based Phenolic Resins via Lignin Demethylated under Mild Reaction Condition. *Polymers*. 2017, 9(9), 428. DOI: 10.3390/polym9090428.
- [12] Shuai, L.; Amiri, M. T.; Questell-Santiago, Y. M.; Héroguel, F.; Li, Y.; Kim, H.; Meilan, R.; Chapple, C.; Ralph, J.; Luterbacher, J. S. Formaldehyde Stabilization Facilitates Lignin Monomer Production during Biomass Depolymerization. *Science*. 2016, 354(6310), 329. DOI: 10.1126/science.aaf7810.

- [13] Yan, L.; Cui, Y.; Gou, G.; Wang, Q.; Jiang, M.; Zhang, S.; Hui, D.; Gou, J.; Zhou, Z. Liquefaction of Lignin in Hot-compressed Water to Phenolic Feedstock for the Synthesis of Phenol-formaldehyde Resins. *Compos. B Eng.* 2017, 112, 8–14. DOI: 10.1016/j.compositesb.2016.10.094.
- [14] Pizzi, A.; Salvadó, J. Lignin-based Wood Panel Adhesives without Formaldehyde. *Holz Als Roh- Und Werkstoff.* 2007, 65(1), 65–70. DOI: 10.1007/s00107-006-0130-z.
- [15] Geng, X.; Li, K. Investigation of Wood Adhesives from Kraft Lignin and Polyethylenimine. *J. Adhes. Sci. Technol.* 2006, 20(8), 847–858. DOI: 10.1163/156856106777638699.
- [16] Pizzi, A.; Recent Developments in Eco-efficient Bio-based Adhesives for Wood Bonding: Opportunities and Issues. *J. Adhes. Sci. Technol.* 2006, 20(8), 829–846. DOI: 10.1163/156856106777638635.
- [17] Wang, S.; Yu, Y.; Di, M. Green Modification of Corn Stalk Lignin and Preparation of Environmentally Friendly Lignin-Based Wood Adhesive. *Polymers.* 2018, 10(6), 631. DOI: 10.3390/polym10060631.
- [18] Zhang, Y.; Pang, H.; Wei, D.; Li, J.; Li, S.; Lin, X.; Wang, F.; Liao, B. Preparation and Characterization of Chemical Grouting Derived from Lignin Epoxy Resin. *Eur. Polym. J.* 2019, 118, 290–305. DOI: 10.1016/j.eurpolymj.2019.05.003.
- [19] Wang, F.; Kuai, J.; Pan, H.; Wang, N.; Zhu, X. Study on the Demethylation of Enzymatic Hydrolysis Lignin and the Properties of Lignin–Epoxy Resin Blends. *Wood Sci. Technol.* 2018, 52(5), 1343–1357. DOI: 10.1007/s00226-018-1024-z.
- [20] Stücker, A.; Schütt, F.; Saake, B.; Lehnen, R. Lignins from Enzymatic Hydrolysis and Alkaline Extraction of Steam Refined Poplar Wood: Utilization in Lignin-phenol-formaldehyde Resins. *Ind. Crops Prod.* 2016, 85, 300–308. DOI: 10.1016/j.indcrop.2016.02.062.
- [21] Pinheiro, F. G. C.; Soares, A. K. L.; Santaella, S. T.; LMAe., S.; Canuto, K. M.; Cáceres, C. A.; MdF., R.; JPDa., F.; Leitão, R. C. Optimization of the Acetosolv Extraction of Lignin from Sugarcane Bagasse for Phenolic Resin Production. *Ind. Crops Prod.* 2017, 96, 80–90. DOI: 10.1016/j.indcrop.2016.11.029.
- [22] Zhou, H.; Qiu, X.; Yang, D.; Laccase, X. S. Xylanase Incubation Enhanced the Sulfomethylation Reactivity of Alkali Lignin. *ACS Sustainable Chem. Eng.* 2016, 4(3), 1248–1254. DOI: 10.1021/acssuschemeng.5b01291.
- [23] Song, Y.; Wang, Z.; Yan, N.; Zhang, R.; Li, J. Demethylation of Wheat Straw Alkali Lignin for Application in Phenol Formaldehyde Adhesives. *Polymers.* 2016, 8(6), 209. DOI: 10.3390/polym8060209.
- [24] Naseem, A.; Tabasum, S.; Zia, K. M.; Zuber, M.; Ali, M.; Noreen, A. Lignin-derivatives Based Polymers, Blends and Composites: A Review. *Int. J. Biol. Macromol.* 2016, 93(Pt A), 296–313. DOI: 10.1016/j.ijbiomac.2016.08.030.
- [25] Podschun, J.; Stücker, A.; Buchholz, R. I.; Heitmann, M.; Schreiber, A.; Saake, B.; Lehnen, R. Phenolated Lignins as Reactive Precursors in Wood Veneer and Particleboard Adhesion. *Ind. Eng. Chem. Res.* 2016, 55(18), 5231–5237. DOI: 10.1021/acs.iecr.6b00594.
- [26] Zhao, M.; Jing, J.; Zhu, Y.; Yang, X.; Wang, X.; Wang, Z. Preparation and Performance of Lignin–Phenol–Formaldehyde Adhesives. *Int. J. Adhes. Adhes.* 2016, 64, 163–167. DOI: 10.1016/j.ijadhadh.2015.10.010.
- [27] Stewart, D.; Lignin as a Base Material for Materials Applications: Chemistry, Application and Economics. *Ind. Crops Prod.* 2008, 27(2), 202–207. DOI: 10.1016/j.indcrop.2007.07.008.

- [28] Gonçalves, A. R.; Benar, P. Hydroxymethylation and Oxidation of Organosolv Lignins and Utilization of the Products. *Bioresour. Technol.* 2001, 79(2), 103–111. DOI: 10.1016/S0960-8524(01)00056-6.
- [29] Akim, L. G.; Shevchenko, S. M.; Zarubin, M. Y. ¹³C NMR Studies on Lignins Depolymerized with Dry Hydrogen Iodide. *Wood Sci. Technol.* 1993, 27(4), 241–248. DOI: 10.1007/BF00195299.
- [30] Chung, H.; Washburn, N. R. Improved Lignin Polyurethane Properties with Lewis Acid Treatment. *ACS Appl. Mater. Interfaces.* 2012, 4(6), 2840–2846. DOI: 10.1021/am300425x.
- [31] Zou, L.; Ross, B. M.; Hutchison, L. J.; Christopher, L. P.; Dekker, R. F. H.; Malek, L. Fungal Demethylation of Kraft Lignin. *Enzyme Microb. Technol.* 2015, 73, 44–50. DOI: 10.1016/j.enzmictec.2015.04.001.
- [32] Riley, R.; Salamov, A. A.; Brown, D. W.; Nagy, L. G.; Floudas, D.; Held, B. W.; Levasseur, A.; Lombard, V.; Morin, E.; Otilar, R., et al. Extensive Sampling of Basidiomycete Genomes Demonstrates Inadequacy of the White-rot/brown-rot Paradigm for Wood Decay Fungi. *Proc. National Academy Sci.* 2014, 111(27), 9923–9928. DOI: 10.1073/pnas.1400592111.
- [33] Zhang, Y.; Ding, L.; Gu, J.; Tan, H.; Zhu, L. Preparation and Properties of a Starch-based Wood Adhesive with High Bonding Strength and Water Resistance. *Carbohydr. Polym.* 2015, 115, 32–37. DOI: 10.1016/j.carbpol.2014.08.063.
- [34] Frihart, C. R.; Lorenz, L. F. Specific Oxidants Improve the Wood Bonding Strength of Soy and Other Plant Flours. *J. Polym. Sci. A Polym. Chem.* 2019, 57(9), 1017–1023. DOI: 10.1002/pola.29357.
- [35] Frihart, C. R.; Pizzi, A.; Xi, X.; Lorenz, L. Reactions of Soy Flour and Soy Protein by Non-volatile Aldehydes Generation by Specific Oxidation. *Polymers.* 2019, 11(9), 1478. DOI: 10.3390/polym11091478.
- [36] Liu, P.; Mai, C.; Zhang, K. Formation of Uniform Multi-Stimuli-Responsive and Multiblock Hydrogels from Dialdehyde Cellulose. *ACS Sustainable Chem. Eng.* 2017, 5(6), 5313–5319. DOI: 10.1021/acssuschemeng.7b00646.
- [37] Kim, U. J.; Kuga, S.; Wada, M.; Okano, T.; Kondo, T. Periodate Oxidation of Crystalline Cellulose. *Biomacromolecules.* 2000, 1(3), 488–492. DOI: 10.1021/bm0000337.
- [38] Liu, P.; Pang, B.; Tian, L.; Schafer, T.; Gutmann, T.; Liu, H.; Volkert, C. A.; Buntkowsky, G.; Efficient, Z. K. Self-Terminating Isolation of Cellulose Nanocrystals through Periodate Oxidation in Pickering Emulsions. *Chem. Sus. Chem.* 2018, 11(20), 3581–3585. DOI: 10.1002/cssc.201801678.
- [39] Xi, X.; Pizzi, A.; Delmotte, L. Isocyanate-free Polyurethane Coatings and Adhesives from Mono- and Di-saccharides. *Polymers.* 2018, 10(4), 402. DOI: 10.3390/polym10040402.
- [40] China National Standard GB/T 14074. *Testing Methods for Wood Adhesives and Their Resins*, 2006. Beijing: Peoples Republic of China.
- [41] China National Standard GB/T17657. *Test Methods for Evaluating the Properties of Wood-based Panels and Surface Decorated Wood-based Panels*, 1999. Beijing: Peoples Republic of China.
- [42] Synthetic Resin Adhesives (Phenolic and Aminoplastic) for Wood. *Specification for Close-Contact Adhesives; British Standard BS 1204*; BSI: London, UK, 1993.
- [43] Lei, H.; Pizzi, A.; Du, G. Coreacting PMUF/isocyanate Resins for Wood Panel Adhesives. *Holz Als Roh- Und Werkstoff.* 2006, 64(2), 117–120. DOI: 10.1007/s00107-005-0044-1.
- [44] Thébault, M.; Pizzi, A.; Dumarçay, S.; Gerardin, P.; Fredon, E.; Delmotte, L. Polyurethanes from Hydrolysable Tannins Obtained without Using Isocyanates. *Ind. Crops Prod.* 2014, 59, 329–336. DOI: 10.1016/j.indcrop.2014.05.036.

- [45] Ghahri, S.; Pizzi, A.; Mohebbi, B.; Mirshokraie, A.; Mansouri, H. R. Soy-based, Tannin-modified Plywood Adhesives. *J. Adhes.* 2016, 94(3), 218–237. DOI: 10.1080/00218464.2016.1258310.
- [46] Laigle, Y.; Kamoun, C.; Pizzi, A. Particleboard IB Forecast by TMA Bending in UF Adhesives Curing. *Eur. J. Wood Wood Prod.* 1998, 56(3), 154. DOI: 10.1007/s001070050288.
- [47] Lecourt, M.; Humphrey, P.; Pizzi, A. Comparison of TMA and ABES as Forecasting Systems of Wood Bonding Effectiveness. *Eur. J. Wood Wood Prod.* 2003, 61(1), 75–76. DOI: 10.1007/s00107-002-0346-5.
- [48] Li, J.; Wang, W.; Zhang, S.; Gao, Q.; Zhang, W.; Li, J. Preparation and Characterization of Lignin Demethylated at Atmospheric Pressure and Its Application in Fast Curing Biobased Phenolic Resins. *RSC Adv.* 2016, 6(71), 67435–67443. DOI: 10.1039/c6ra11966b.
- [49] Tejado, A.; Pena, C.; Labidi, J.; Echeverria, J. M.; Mondragon, I. Physico-chemical Characterization of Lignins from Different Sources for Use in Phenol-formaldehyde Resin Synthesis. *Bioresour. Technol.* 2007, 98(8), 1655–1663. DOI: 10.1016/j.biortech.2006.05.042.
- [50] Navarrete, P.; Pizzi, A.; Pasch, H.; Delmotte, L. Study on Lignin- Glyoxal Reaction by MALDI-TOF and CP-MAS 13C-NMR. *J. Adhes. Sci. Technol.* 2012, 26(8–9), 1069–1082. DOI: 10.1163/016942410X550030.
- [51] Santiago-Medina, F. J.; Pizzi, A.; Basso, M. C.; Delmotte, L.; Abdalla, S. Polycondensation Resins by Lignin Reaction with (Poly) Amines. *J. Renewable Mater.* 2017, 5(5), 388–399. DOI: 10.7569/jrm.2017.634142.
- [52] Mottweiler, J.; Rinesch, T.; Besson, C.; Buendia, J.; Bolm, C. Iron-catalysed Oxidative Cleavage of Lignin and β -O-4 Lignin Model Compounds with Peroxides in DMSO. *Green Chem.* 2015, 17(11), 5001–5008. DOI: 10.1039/C5GC01306B.
- [53] Qu, Y.; Luo, H.; Li, H.; Xu, J. Comparison on Structural Modification of Industrial Lignin by Wet Ball Milling and Ionic Liquid Pretreatment. *Biotechnol. Rep.* 2015, 6, 1–7. DOI: 10.1016/j.btre.2014.12.011.
- [54] China National Standard GB/T 9846. *Plywood for General Use*, 2015. Beijing: Peoples Republic of China.

3.6 Panneau de particules bio-adhésif par lignine glyoxalée et amidon dialdéhyde oxydé réticulé par l'urée

Résumé: Un nouveau système adhésif bio-sourcé est présenté à base d'urée réticulant de un mélange de lignine glyoxalée et de amidon dialdéhyde obtenu par oxydation au peroxyde d'hydrogène de l'amidon. Les espèces moléculaires formées et le mécanisme des réactions impliquées ont été identifiés par FT-IR et spectrométrie de masse MALDI-ToF. L'urée semble réagir à la fois avec la lignine glyoxalée et l'amidon dialdéhyde. Les adhésifs basés sur cette réaction ont été testés en laboratoire sur panneaux de particules, par calorimétrie différentielle à balayage (DSC) et analyse thermomécanique (TMA). Les résultats obtenus pour la force de liaison interne (IB) avec ce système adhésif sont acceptables pour la production de panneaux de particules selon la norme européenne pertinente. Une réticulation chimique supplémentaire par l'utilisation de 5% sur les solides de résine d'éther glycidyle de glycérol partiellement bio-sourcé (GDE) améliore la force de liaison des résines ainsi formées grâce à une réaction de réticulation supplémentaire dont les principaux sites ont également été déterminés.

Mots clés: Nouveaux adhésifs pour bois; panneaux de particules; lignine glyoxalée; amidon dialdéhyde; urée.

Particleboard bio-adhesive by glyoxalated lignin and oxidized dialdehyde starch crosslinked by urea

Xinyi Chen^{1,2}, Antonio Pizzi^{1*}, Bengang Zhang¹, Xiaojian Zhou², Emmanuel Fredon¹, Christine Gerardin³, Guanben Du²

¹LERMAB, University of Lorraine, 27 rue Philippe Seguin, 88000 Epinal, France

²Key Laboratory for Forest Resources Conservation and Utilisation in the Southwest Mountains of China, Southwest Forestry University, Kunming 650224, PR China

³LERMAB, Faculté des Sciences, University of Lorraine, Blvd. des Aiguillettes, 54000 Nancy, France

* Corresponding Author: Antonio PIZZI. E-mail address: antonio.pizzi@univ-lorraine.fr;

Abstract

A new bio-sourced adhesive system is presented based on urea crosslinked glyoxalated lignin and dialdehyde starch obtained by hydrogen peroxide oxidation of starch. The molecular species formed and the reactions mechanism involved were identified by FTIR, ¹³C NMR, and MALDI-ToF mass spectrometry. Urea appears to react with both, glyoxalated lignin and dialdehyde starch. The adhesives based on this reaction were tested by means of laboratory particleboards, differential scanning calorimetry (DSC), and thermomechanical analysis (TMA). The results obtained for internal bond (IB) strength with this adhesive system are acceptable for producing particleboard according to the relevant European standards. Additional, chemical crosslinking by using 5% on resin solids of partially bio-sourced glycerol glycidyl ether (GDE) improves the bonding strength of the resins so formed; the main crosslinking sites were also determined.

Keywords: Novel wood adhesives; particleboard; glyoxalated lignin; dialdehyde starch; urea

1 **Introduction**

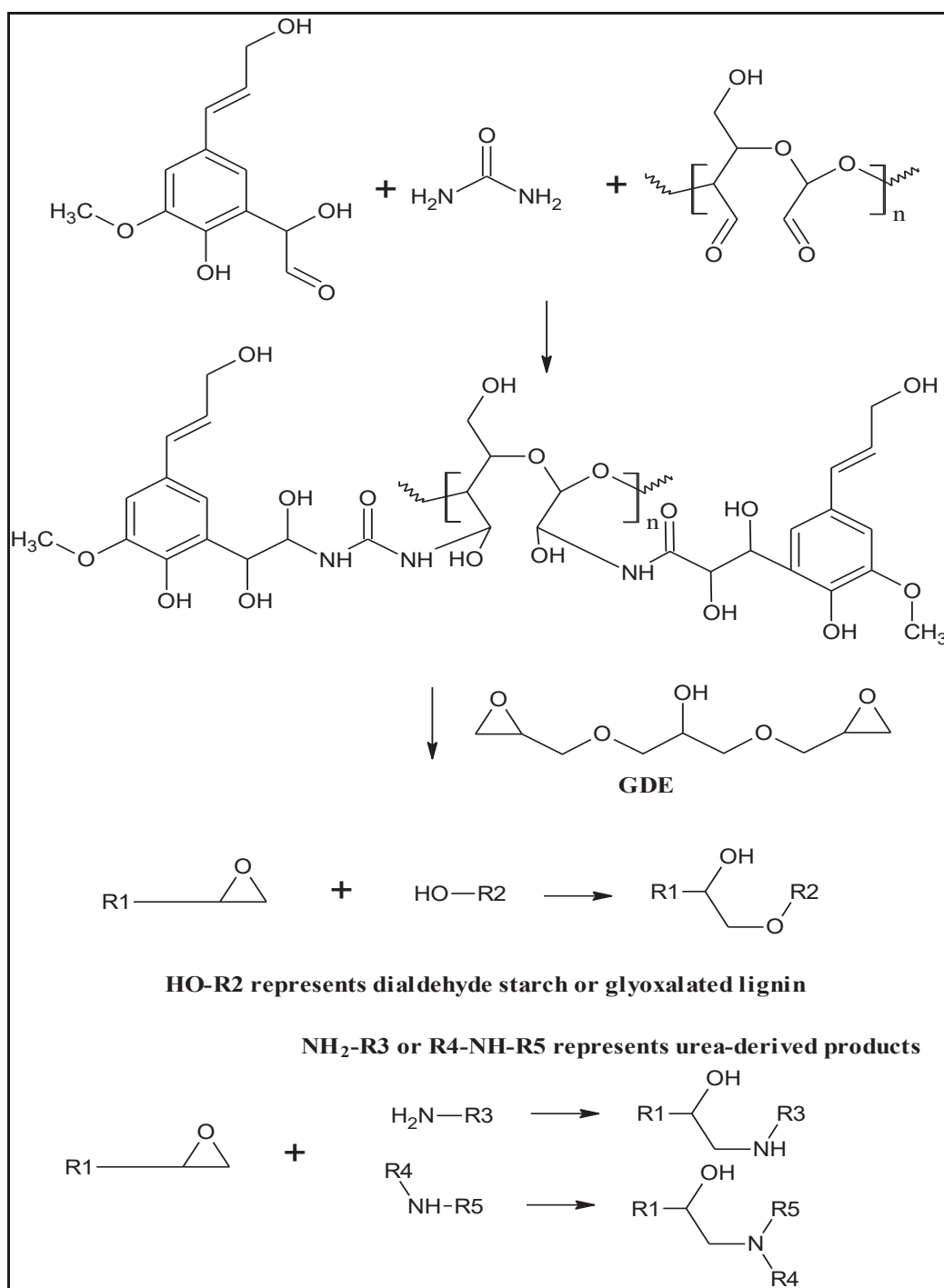
2 Formaldehyde-based synthesized resins still dominate wood adhesives industry markets,
3 despite some unacceptable issues including environment and human health risks (Jahanshaei et
4 al. 2012; Kim et al. 2011; Tabarsa et al. 2011; Younesi-Kordkheili and Pizzi 2017; Younesi-
5 Kordkheili and Pizzi 2018), because of the excellent bonding performance and ever-growing
6 demand from companies. In addition, the petroleum-based starting materials, especially phenol,
7 motivate the researchers to focus on searching for sustainable alternative approaches (Li et al.
8 2019; Ndiwe et al. 2019), for example adhesives based on natural resources (Ndiwe et al. 2019).
9 Thus, the research interest in such new adhesives for wood panels has been and is still increasing
10 now for several years. Such focused research interest is due to a number of factors: (i) the real
11 or perceived future scarcity of oil feedstock and concurrent expected price increases and lower
12 availability of oil-derived synthetic adhesives, (ii) the increased environmental concern of both
13 governments and the population, and (iii) the tighter standard regulations that have been placed
14 progressively in place over the last decades.

15 These concerns have caused considerable research to be pursued on the use of several renewable
16 raw materials for the formulation and preparation of bio-adhesives for wood panels, such as
17 tannins, lignin, chitosan, carbohydrates, humins, furanics, plant and animal proteins, etc. (Arias
18 et al. 2021; Li et al. 2019). Moreover, each of these materials has resulted in a variety of very
19 different formulations, ranging from rather traditional to very unusual approaches. These are
20 far too many to be all mentioned here. It is sufficient to say that on some of the more studied
21 materials such as tannins, lignin, soybean protein, humins, etc., these vary from rather
22 traditional reactions with formaldehyde to alternative aldehydes (Ballerini et al. 2005), almost
23 revolutionary non-isocyanate bio-polyurethanes (Chen et al. 2021a; Chen et al. 2021b; Saražin
24 et al. 2021), or even bio-sourced polyamides (Xi et al. 2019). These novel wood adhesive
25 preparation pathways, compared with typical isocyanate-based polyurethane systems, avoid not
26 only high-price isocyanate and fossil-based polyols, but also rigorous production conditions,
27 using only bio-sourced dimethyl carbonate and hexamethylenediamine under low-temperature
28 (90°C) and atmospheric pressure. It was deemed as a potential strategy for bio-sourced non-
29 isocyanate polyurethane production.

30 Lignin is an important natural polyphenol component in wood, and has been studied extensively
31 to fulfil the above targets for the renewable wood adhesives preparation for replacing fossil-

32 based phenol, and expecting to realize industrialization early (Arias et al. 2021). The
33 complicated macromolecular structure of lignin results in low reactivity; the direct utilization
34 of native lignin to replace phenol not only does not show an acceptable performance but could
35 also reduce the bonding strength of wood panels (Li et al. 2018a). Hence it remains a hot-point
36 for researchers, how to improve the reactivity of native lignin with a proper method so that it
37 can show an efficient function in wood adhesives. Glyoxalated lignin was considered as a
38 relative eco-friendly approach to enhance the reactivity of lignin; this has been studied in the
39 past several years, and, as expected, has already brought some unanticipated success
40 (Mansouri et al. 2011; Younesi-Kordkheili 2017; Younesi-Kordkheili and Pizzi 2020).
41 Nevertheless, the wood panels bonded by urea-lignin-glyoxal (ULG) resins still show lower
42 mechanical strength and thermal properties; thus, some additives including nano-clay, epoxy,
43 and hexamethylene-tetramine have been utilized in combination with ULG for wood panel
44 production.

45 The work presented here is based on a new and rather unusual concept. As regards biomaterials,
46 glyoxalated lignin has been developed for wood adhesives in several formulations (Mansouri
47 et al. 2007; Navarrete et al. 2010). Equally, the specific oxidation by small amounts of sodium
48 periodate of carbohydrates (Bobbitt 1956; Frihart et al. 2019), such as mono- and disaccharides
49 (Bobbitt 1956; Xi et al. 2020), cellulose and hemicelluloses (Codou et al. 2015; Guigo et al.
50 2014), has been described for its use in connection with panel adhesive formulations.
51 Nonetheless, hydrogen peroxide is also known to cause the formation of aldehyde groups by
52 cleavage of C-C bonds carrying vicinal -OH groups (Park 2020; Lubis 2020; Wing and Willett
53 1997; Yu et al. 2017). The approach described here then proposes to use these two materials,
54 namely glyoxalated lignin and hydrogen peroxide treated starch as the two biomaterials to be
55 crosslinked, with the crosslinker being a third low-cost material, namely just urea. Additionally,
56 commercial glycerol diglycidyl ether (GDE) was utilized as enhancer. The reaction schematic
57 describing the approach is shown in Scheme 1.



58

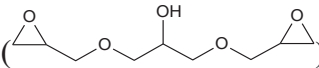
59 Scheme 1 Reaction schematic between glyoxalated lignin and di-aldehyde starch crosslinked by urea and
60 GDE. Additionally possible crosslinking reactions with GDE are shown.

61 The idea for such an unusual formulation approach came from the presentations by Park and
62 Lubis (Park 2020; Lubis 2020) where H₂O₂ oxidized starch was used to link PMDI (polymeric
63 methylene diisocyanate) to urea- formaldehyde resins. This was a very interesting approach and
64 made us have the idea to use urea, without any formaldehyde, to link glyoxalated lignin through
65 urea and oxidized starch. There are several differences to the original presentations of Lubis

66 (2020) and Park (2020): there is no formaldehyde and there is no isocyanate, and finally the
67 formulation is predominantly based on bio-sourced materials. This article describes the results
68 obtained from this approach.

69 **Experimental**

70 **Materials**

71 The commercial lignin used was a desulfurized softwood kraft lignin, namely Biochoice kraft
72 lignin supplied by Domtar Inc. (Montreal, QC, Canada) from their Plymouth, North Carolina
73 mill (Plymouth, NC, USA). Urea (powder, $(\text{NH}_2)_2\text{C}=\text{O}$, 60.06 g/mol, BioReagent, $\geq 98\%$),
74 sodium hydroxide (NaOH, 40.00 g/mol, ACS reagent, $\geq 97.0\%$, pellets), glycerol diglycidyl
75 ether (GDE, $\text{C}_9\text{H}_{16}\text{O}_5$ () $\text{C}_9\text{H}_{16}\text{O}_5$), 204.22 g/mol, technical grade, $\geq 98\%$), and
76 glyoxal (58.04 g/mol, $(\text{CHO})_2$, 40 wt% aqueous solution) were purchased from Sigma-Aldrich
77 (Saint Louis, France). Dialdehyde starch (powder) was purchased from Tai'an City Jinshan
78 Modified Starch Co., Ltd (Shandong, China). All raw materials needed no further pre-treatment
79 prior to their use in this experiment.

80 **Preparation of glyoxalated lignin**

81 Glyoxalated lignin was prepared according to a previously reported method (Navarrete et al.
82 2012a; Navarrete et al. 2012b). Briefly, 250 g lignin powder was slowly added to 350 g
83 deionized water while vigorously stirring with a mechanical overhead stirrer. Simultaneously,
84 about 90 g NaOH (33 % aqueous solution) was introduced slowly to ensure that the lignin and
85 water mixed well and to keep the pH of lignin/water solution at 12-12.5. After this, the solution
86 was moved to a 1 L round-bottom flask, and the reaction temperature increased to $60 \pm 3^\circ\text{C}$ for
87 30 min. Afterwards, 130 g NaOH (33 % water solution) and 149.8 g glyoxal solution were
88 added into the lignin solution alternately at an interval of 30 min, while keeping the reaction
89 pH of the mixture at 12-12.5 and the reaction temperature at $60 \pm 3^\circ\text{C}$ for 3 h. The reaction
90 mixture was then cooled down to room temperature and the pH kept at 12-12.5 for storing. The
91 solid content of the glyoxalated lignin solution thus obtained was around 31 %.

92 **Preparation of adhesives with glyoxalated lignin, urea, and dialdehyde starch**

93 The resultant adhesives for particleboard bonding were prepared by a relatively convenient
94 method. In detail, 6.7 g glyoxalated lignin was placed into a 50 mL plastic bottle. Thereafter, 2
95 g of urea powder was added, by stirring immediately until a homogenous mixture was obtained
96 (about 5-10 min). Then, 2 g of dialdehyde starch powder was added into the above mixture by
97 vigorously stirring with a magnet rotor for 90-120 min at room temperature. Generally, the
98 glyoxalated lignin-urea-dialdehyde starch wood adhesive was labelled as GL-U-Ds.

99 Glycerol diglycidyl ether (GDE) served as an enhancer for the wood adhesive presented here
100 and has been broadly viewed as a partially bio-sourced crosslinker, knowing its high reactivity
101 towards several groups and the fact that there is no known toxicity to animals (ChemADVISOR
102 1995; Derelanko and Auletta 2014; Li et al., 2018b). Bio-based glycerol is one of the dominant
103 feedstocks for GDE production. Therefore, GDE was selected as a modifier to improve the
104 bonding performance of particleboards bonded by GL-U-Ds. Consequently, 5 % of liquid GDE
105 was utilized based on the dry weight of GL-U-Ds. The GDE modified adhesive formulation
106 was labelled as GL-U-Ds-E. The modified adhesive (i.e., GL-U-Ds-E) was prepared within 20-
107 30 minutes prior to particleboard pressing.

108 **Basic properties of glyoxalated lignin-urea-dialdehyde starch wood adhesives (pH,**
109 **viscosity, solid content, and hydrolysis residual rate)**

110 The pH value was measured by using a PHS-3C vale pH meter (Labo-Hub, Shangai, China).
111 The viscosity of the adhesives was tested by a Brookfield DVII+ Viscometer (ES, Garches,
112 France) with spindle No. 4 at 20 rpm and at room temperature. The solid content of the
113 adhesives was measured according to the China National Standard GB/T 14074-2017. The solid
114 content (S) was calculated by the initial weight (M_1) and dried constant weight (M_2 , treated at
115 $120\pm 2^\circ\text{C}$) of adhesives, according to the following formula:

116
$$S = \frac{M_2}{M_1} \times 100\% \quad (1)$$

117 For the determination of the hydrolysis residual rate (H), a certain amount of resin was placed
118 into an oven ($135\pm 2^\circ\text{C}$) for 3 h and then ground into powder (around 200 mesh). Thereafter,
119 the powder samples (W_1) were wrapped by a filter paper and immersed in $60\pm 2^\circ\text{C}$ hot water
120 for 6 h. The treated resin samples were dried at $120\pm 2^\circ\text{C}$ for 3 h, obtaining the non-hydrolyzed
121 weights (W_2). Finally, H was calculated with the following formula:

122
$$H = \frac{W_2}{W_1} \times 100\% \quad (2)$$

123 At least three test replicates were performed for each sample.

124 **Thermomechanical analysis (TMA)**

125 30 mg of wood adhesive was applied to two beech wood veneers of 17×5×1.1 (length × width
126 × thickness) mm³ dimensions and then stacked to form a two-ply sandwich. The relationship of
127 modulus of elasticity (MOE) and temperature was measured by thermomechanical (TMA)
128 equipment (Mettler Toledo 40, Zurich, Switzerland) in three-point bending according to a
129 procedure already reported (Garcia and Pizzi 1998). The heating rate was 10°C/min in a testing
130 range of 30-250°C under a nitrogen protecting atmosphere (50 mL/min).

131 **Differential scanning calorimetry (DSC)**

132 The prepared liquid wood adhesive samples were firstly placed into a refrigerator at -80 °C for
133 12 h. Then, the freeze-dried samples were obtained by using vacuum freeze-drier (TENLIN,
134 FD-1A-80, Jiangsu Tianling Instrument Co., LTD, Jiangsu, China) for 48 h. The curing
135 behavior of the GL-U-Ds and GL-U-Ds-E adhesives was investigated by using a DSC analyzer
136 (Model DSC 204 F1, Netzsch, Germany). The temperature range was 30 - 250 °C (heating rate
137 of 10°C/min) under a protection environment with a 50 mL/min flow of N₂.

138 **Fourier transform infrared spectroscopy (FTIR)**

139 The sample powders were prepared by oven drying the liquid adhesives at 120±2 °C for 2 h
140 and following manual grinding. The infrared spectra of the resins were monitored with a
141 PerkinElmer Frontier FTIR (Perkin Elmer France, Villebonne-sur-Yvette, France). The scan
142 results of each sample were recorded with 32 scans between the wave range of 600 and 4000
143 cm⁻¹, with a scan resolution of 4 cm⁻¹.

144 **Matrix assisted laser desorption ionization time-of-flight (MALDI-ToF) mass
145 spectrometry**

146 The MALDI-TOF spectra were obtained by using an Axima-Performance mass spectrometer
147 from Shimadzu Biotech (Kratos Analytical Shimadzu Europe Ltd., Manchester, UK). 7.5 mg
148 of dried sample powders (which were obtained from the liquid adhesives by oven drying at 120

149 ± 2 °C for 2 h and manual grinding) were first dissolved in a 1 ml water/acetone mixture (50:50
150 v/v) to obtain a sample pre-treatment solution. 1.5 μL of NaCl solution (0.1 M in 2:1 v/v
151 methanol/water) was placed to cover the corresponding spots on the sample holder plaque
152 dedicated to the analysis. Red phosphorous was used as reference sample to standardize the
153 instrument prior to each test. The analysis plaque covered with NaCl solution and red
154 phosphorous was pre-dried well. Then, 1.5 μL of the sample in acetone-water solution was
155 placed into a centrifuge tube. 1.5 μL of 2,5-dihydroxy benzoic acid (DHB) matrix was then
156 placed into the centrifuge tube containing the samples and mixed well. Then, 1.5 μL of the
157 sample/DHB mixture was applied on the sample holder plaque of the instrument, which was
158 pre-covered with the dried NaCl solution. The test was carried out in a linear polarity-positive
159 tuning mode. The measurements were taken by making 1000 profiles per sample with two runs
160 cumulated per profile in the range of 50 to 3000 Da. The accuracy of the spectrum was ± 1 Da.

161 **^{13}C nuclear magnetic resonance (^{13}C NMR)**

162 To investigate the chemical structure of GL-U-Ds and GL-U-Ds-E adhesives, solid state ^{13}C
163 NMR equipment was utilized. The spectra result was obtained by the AVANCE II 400 MHz
164 spectrometer (Brüker, Billerica, MA, USA), using 4 mm probe at a 12-kHz sample spin. The
165 pulse duration time was 4.1 μs at 90° , and the contact time 2 ms with a pulse interval of 4 s.
166 Tetramethyl silane (TMS) served as control reference sample to determine the chemical shifts.
167 The accuracy of the spectrum is ± 1 ppm. The sample powders for measuring were obtained
168 from the liquid adhesives by oven drying at 120 ± 2 °C for 2 h and then manual grinding.

169 **Preparation and testing of particleboard**

170 Six identical monolayer particleboards for each adhesive with dimension of $350 \times 350 \times$
171 12 mm^3 were prepared at three target density values (650, 700, and 800 kg/m^3 , respectively).
172 The solid adhesive loading was set to 10 % based on dry particles. The panels were pressed in
173 a Joos laboratory particleboard press (Joos, Pfalzgrafenweiler, Germany) using a three-stage
174 hot-pressing cycle with the specific pressures of 2.8 MPa, 1.2 MPa, and 0.58 MPa for a total of
175 10 min (3 min; 4 min; and 3 min for each stage, respectively) at 220 °C press temperature,
176 meaning a specific press time of approx. 50 s/mm. The calculation of the hot-press time starts
177 when the pressure reaches the set value. All particleboards were stored under ambient
178 conditions (around 20°C, 65%) for at least two days prior to cutting and testing.

179 The particleboards were first cut into $310 \times 50 \text{ mm}^2$ for modulus of rupture (MOR) and
180 elasticity modulus (MOE) measurement. Then, the tested panels were cut into the size of 50
181 $\text{mm} \times 50 \text{ mm}$ for dry internal bond (IB) strength testing, density, density profile, water
182 absorption, and thickness swelling. At least 6 repeated measurements were performed for each
183 testing according to EN 312 (2010). The density profile of the laboratory particleboards was
184 measured by using an X-ray microdensitometer DAX 6000 (Grecon, Alfeld, Germany).

185 **Results and discussion**

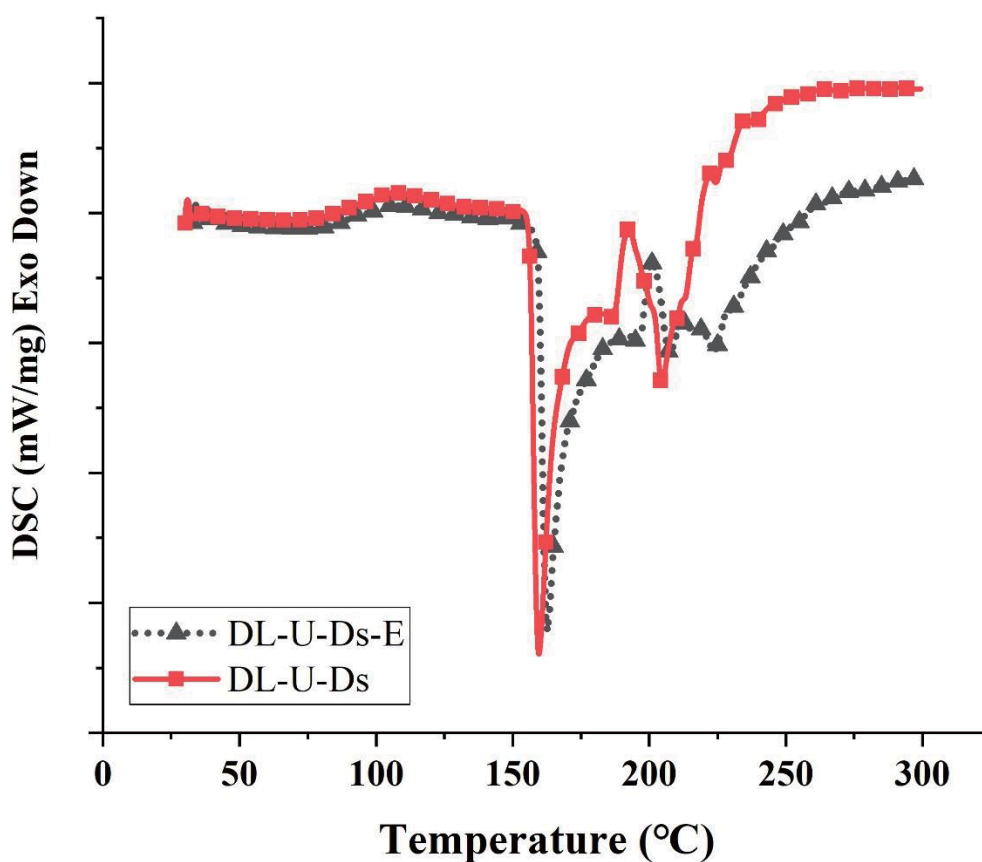
186 **Adhesive analysis**

187 The adhesive characteristics for the formulations were investigated and described in this part.
188 The pH values of the adhesives were around 10. The viscosity of the resin can influence their
189 distribution on the surface of particles, which can directly affect the particleboard properties.
190 The GL-U-Ds adhesive exhibits a viscosity around 100-120 $\text{mPa}\cdot\text{s}$ while it was increased to
191 235-260 $\text{mPa}\cdot\text{s}$ due to the GDE introduced. This increase is caused by a certain crosslinking by
192 adding GDE, which can react with the urea connected glyoxalated lignin or dialdehyde starch
193 in the solution (mainly free amino groups); this extends or branches such polymers, leading to
194 an enlarged molecular structure and, hence, limiting their mobility in the liquid adhesive system.
195 The solid content of GL-U-Ds adhesive is around 50.8-51.9 %, but an increased solid content
196 of 52.3-53.6 % was obtained for GL-U-Ds-E adhesive. The oven-dried sample powders
197 obtained at 135 °C were utilized to investigate the non-hydrolyzed residue ratio of GL-U-Ds
198 and GL-U-Ds-E samples. Around 19.8-20.2 % of non-hydrolyzed residue ratio of GL-U-Ds
199 was obtained, which was related to the lower crosslinking degree, or even not completely cured
200 condition, and about 50.1-52.4 % for GL-U-Ds-E. Therefore, GDE modified sample can endow
201 a more stable structure than GL-U-Ds adhesive under hot water treatment. A three-dimensional
202 structure can be formed by GDE connecting the linear structure products in the GL-U-Ds
203 adhesive. Furthermore, some free oligomers which did not take part in the formation of GL-U-
204 Ds were fixed. The colors of the hydrolyzed solutions of GL-U-Ds (dark) and GL-U-Ds-E (light)
205 samples as shown in Fig. S1 in ESM support this conclusion.

206 **Thermal properties analysis**

207 **Differential scanning calorimetry (DSC) analysis**

208 The curing behavior of freeze-dried GL-U-Ds and GL-U-Ds-E samples was measured by DSC,
209 and the obtained curves are shown in Fig. 1. The samples with/without GDE addition presented
210 a typical exothermic cure behavior like most thermoset resins (Pradyawong et al. 2018;
211 Younesi-Kordkheili and Pizzi 2020). However, it is different to other reports that epoxy resin
212 can reduce the curing temperature of the adhesives (Younesi-Kordkheili and Pizzi 2020); the
213 GL-U-Ds-E sample exhibits a slightly higher curing temperature (162.7°C) than GL-U-Ds
214 (159.5°C). This result is further supported by TMA. Compared with the significantly increased
215 bonding performance by GDE addition, this slightly increased curing temperature is acceptable.
216 A small endothermic peak at around 100 °C can be seen in both, which is attributed to the
217 evaporation of residual water after freeze-drying, and moreover, coupled with the probable
218 water produced from condensation reaction. A big exothermic peak at around 160 °C is
219 assigned to the curing reaction of the wood adhesives. The delayed exothermic peak in GL-U-
220 Ds-E sample is probably related to the additional crosslinking formed by the reaction of GDE
221 with other components of the resin, especially OH- groups of starch and lignin and secondary
222 amino groups of the urea.



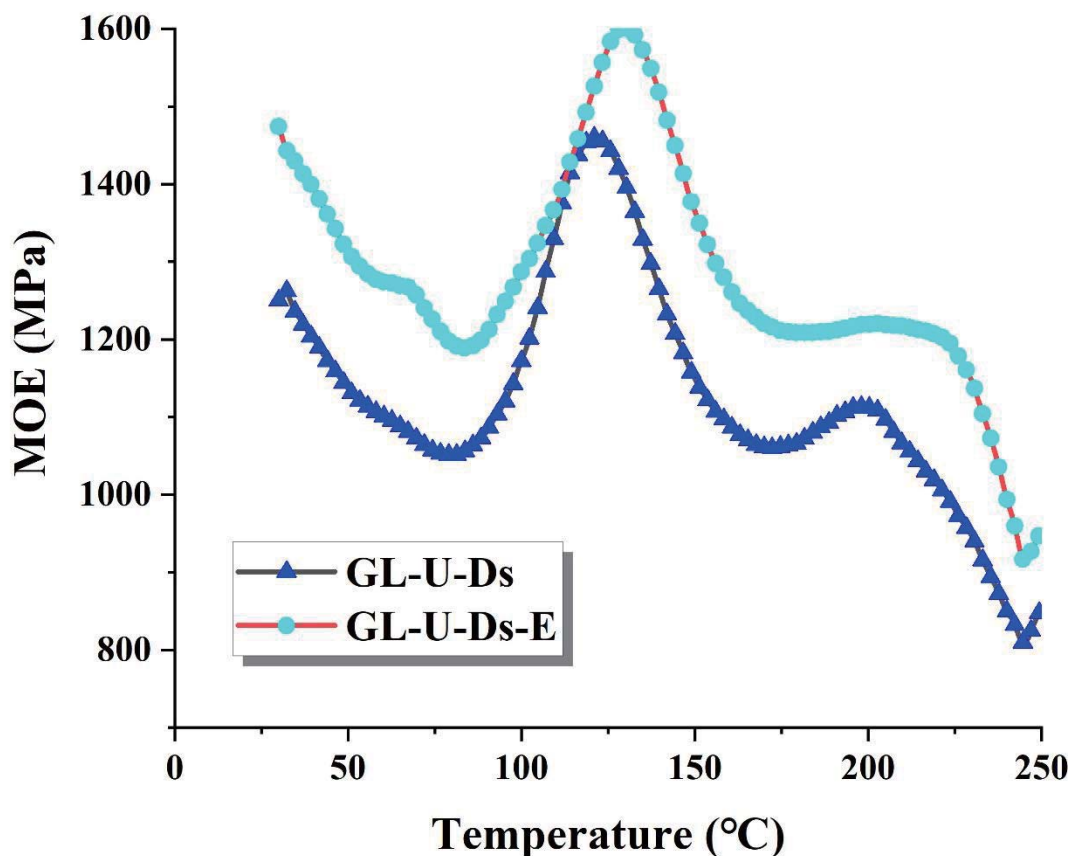
223

224

Fig.1 DSC curves of GL-U-Ds and GL-U-Ds-E samples.

225 **Thermomechanical analysis (TMA)**

226 Finally, it is interesting to deduce from the results of the thermomechanical analysis what occurs
227 kinetically for the two types of adhesives during the increase in temperature. In Fig. 2, the two
228 curves show two equally intense peaks of MOE with the maxima at 125 and 130 °C for the GL-
229 U-Ds and GL-U-Ds-E adhesives, respectively. The maximum for the GL-U-Ds adhesive is at a
230 slightly lower temperature but presents a lower maximum MOE value (1430 MPa) than the GL-
231 U-Ds-E adhesive (1600 MPa). The combination of the slightly higher peak temperature but
232 higher MOE for the GL-U-Ds-E is due to the additional cross-linking, stabilizing the
233 crosslinked network engendered by reaction of the GDE with the other components of the resin,
234 with the additional reactions needing slightly higher reaction energy. This phenomenon is
235 similar to the DSC measurement result. The MALDI structures IV-a and IV-b described follow
236 showing structures where the glycerol glycidyl ether has reacted either with two starch
237 oligomers, or linking a starch monomer and a modified lignin. Both curves then decrease, as at
238 the temperature higher than 200 °C, the reduction of the MOE of both samples due to the start
239 of the softening of the wood substrate (above the glass transition temperature of lignin and
240 hemicellulose) and of the adhesive. Nonetheless it must be noted that the decrease in MOE of
241 the GL-U-Ds-E adhesive starts at a higher temperature; the higher strength of its better
242 crosslinked network counterbalancing somewhat the loss of MOE due to wood substrate
243 softening. The GL-U-Ds-E adhesive still maintains a higher MOE value than the GL-U-Ds
244 although they underwent the high temperature thermal softening. It is attributed to a better
245 thermal stability of GDE-modified sample. As shown in Fig. S2 in ESM, a better thermal
246 stability for GDE modified sample (GL-U-Ds-E) was verified by thermogravimetric analysis
247 (TGA) investigation. The pyrolysis char residues are 20.7% and 26.5% for GL-U-Ds and GL-
248 U-Ds-E samples at 790 °C, respectively.



249

250

Fig.2 TMA curves of GL-U-Ds and GL-U-Ds-E samples.

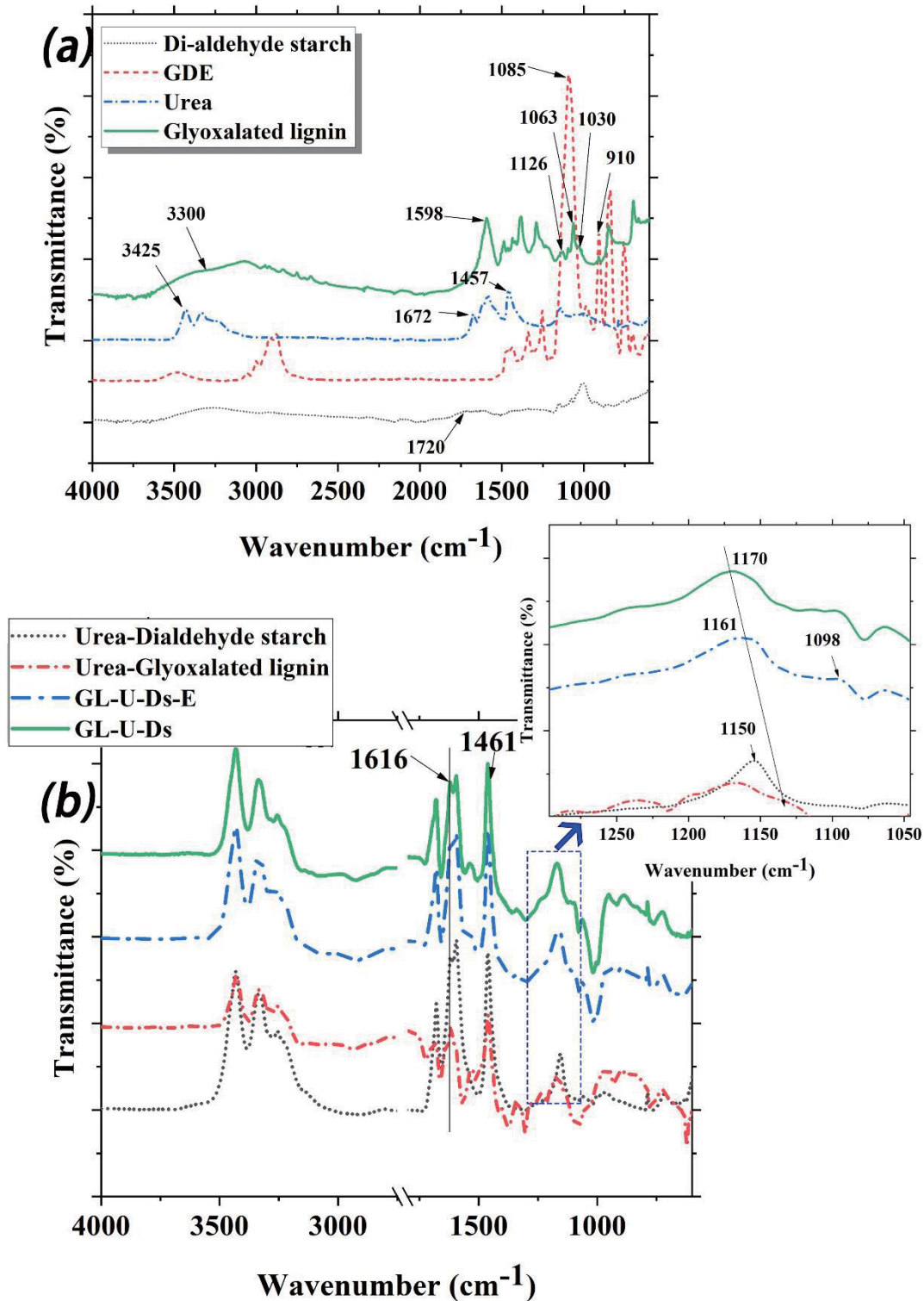
251 Reaction mechanism of wood adhesives

252 Fourier transform infrared spectroscopy (FTIR) analysis

253 To investigate the crosslinking reaction in the presented adhesives system, FTIR analyses were
 254 performed and their spectra are illustrated in Fig. 3. Figure 3 (a) presents the spectra of the
 255 various raw materials of the adhesives used in this work. Some characteristic bonds belong to
 256 neat urea, such as the N-H stretching at 3425 cm^{-1} , the C=O stretching at 1672 cm^{-1} , and the
 257 C-N stretching at 1457 cm^{-1} , respectively (Carcamo-Martinez et al. 2021; Chan-Chan et al.
 258 2017). For the dialdehyde starch, the typical -C=O bond was detected at 1720 cm^{-1} , attributed
 259 to the aldehyde groups of dialdehyde starch (Zuo et al. 2017). The typical characteristic peak
 260 for epoxy groups in GDE at 910 cm^{-1} was confirmed, and the peak at around 1085 cm^{-1} was
 261 identified to be ether bonds (Chen et al. 2020; Li et al. 2018b; Younesi-Kordkheili and Pizzi
 262 2020). The characteristic bands of syringyl unit (S) and guaiacyl unit (G) can be seen in two
 263 small peaks in Fig. 3(a) at 1126 cm^{-1} and 1030 cm^{-1} , respectively. The peak at around 1598
 264 cm^{-1} is related to the p-hydroxyphenyl unit (H) (Gao et al. 2021). In addition, a clearly sharp

265 peak at 1063 cm^{-1} was assigned to the C-O deformation, which probably belongs to secondary
266 alcohols and aliphatic ethers and out-of-plane stretching of phenols (Chaleawlert-umpon and
267 Liedel 2017). This phenomenon was possibly attributed to the introduction of -OH containing
268 aliphatic side chains, which can be observed from the broad stretching vibration around 3300
269 cm^{-1} .

270 Figure 3(b) presents the spectra of some reaction products, such as from the reaction of urea
271 and dialdehyde starch or of urea and glyoxalated lignin, and two wood adhesive samples (GL-
272 U-Ds and GL-U-Ds-E), respectively. The sharp peaks at 1150 cm^{-1} and 1461 cm^{-1} were
273 confirmed as the deformation vibration band of -C-N- and the stretching vibration bond of -N-
274 H-, respectively. The peak at 1616 cm^{-1} was assigned to the carbonyl group stretching of urea
275 (-NH-C=O) which can verify the reaction between urea and dialdehyde starch (Oktay et al.
276 2021). Moreover, those characteristic bonds also remained in the adhesive samples. For the
277 reaction of urea and glyoxalated lignin, the new structure based on -CHOH-NH- was confirmed
278 by the spectrum at the peaks 1164 cm^{-1} and 1461 cm^{-1} based on the deformation vibration band
279 of -C-N- and the stretching vibration bond of -N-H-, respectively. The introduction of GDE did
280 not change the main structure of the adhesive sample (GL-U-Ds) when comparing with GL-U-
281 Ds-E. The absorption peak at around 910 cm^{-1} belongs to the epoxide groups (Chen et al., 2020;
282 Li et al. 2018b; Younesi-Kordkheili and Pizzi 2020). However, the epoxide groups at the peak
283 910 cm^{-1} finally vanished in the spectrum of Fig. 3(b), which infers the consumption of the
284 epoxy groups by the various crosslinking reactions, such as between GDE and either imino
285 groups of the urea-derived products or even between GDE and hydroxyl groups (Younesi-
286 Kordkheili and Pizzi 2020). Compared with the adhesive sample GL-U-Ds, a mild change can
287 be observed in the curves of GL-U-Ds-E after addition of GDE, which is probably due to GDE
288 grafting on the main chains of GL-U-Ds by the reaction of the epoxy group with the imino
289 groups on the urea-derived products. The GDE modification does not change the backbone
290 structure of GL-U-Ds adhesive. It can be speculated that GDE enhanced three-dimensional
291 structures in GL-U-Ds-E, which were formed based on the main chains of GL-U-Ds. The peak
292 of the sample GL-U-Ds at 1170 cm^{-1} (deformation vibration band of -C-N-) moved to 1161 cm^{-1}
293 $^{-1}$ in the GL-U-Ds-E and became broader. This is probably attributed to the reaction of the -NH₂
294 groups and imino groups of urea derived products and GDE. Additionally, some ether bonds
295 appeared at around 1100 cm^{-1} due to the crosslinking between hydroxyl groups and epoxide
296 groups, which will also enhance the bonding performance of the adhesives (Chen et al. 2020;
297 Li et al. 2018b).



298

299 **Fig. 3.** FTIR spectra of the experimental raw materials and adhesives.300 **MALDI-ToF analysis**

301 For a better understanding of the reactions at molecular level, the original products (dialdehyde
 302 starch and glyoxalated lignin) and the adhesive sample powders (GL-U-Ds and GL-U-Ds-E)
 303 obtained under 120 °C for 2 h were examined by MALDI-ToF spectrometry. The relevant

304 MALDI-ToF spectra of the GL-U-Ds-E products are shown in Figs.4a-e, and some possible
305 crosslinking structures are listed in Table 1. The totality of the other relevant MALDI-ToF
306 spectra of glyoxalated lignin, of the dialdehyde starch and of GL-U-Ds as well as the table of
307 all the reaction products obtained that could be identified are reported in the Supplementary
308 Material (Table S1, Figs S3a-d; S4a-g; S5a-d). It is interesting to see which moieties have
309 formed. Although various crosslinking reactions occur in the adhesives during the oven-drying
310 process, some possible reaction products can be inferred by MALDI-ToF, FTIR, and ^{13}C NMR
311 spectrometry. Fragments of lignin monomers, lignin monomers and glyoxalated lignin
312 monomers and dimers, and dialdehyde starch monomers, dimers and trimers have been
313 identified. The more complicated reactions were classified as the following:

314 (I) Compounds formed by reaction of dialdehyde starch with urea are observed, from the
315 simpler ones to more complex ones such as I-a: a dialdehyde starch monomer reacted with two
316 urea molecular, I-b: one urea bridging a dialdehyde starch monomer and a dimer, and I-c: a
317 dialdehyde starch dimer and a trimer reacted with two urea monomers.

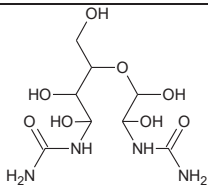
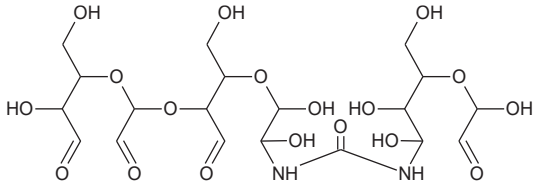
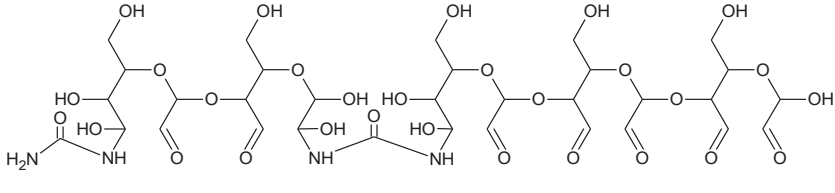
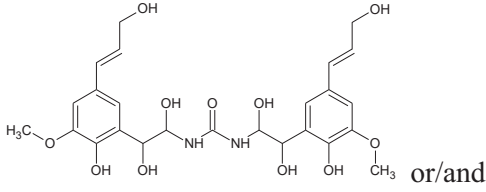
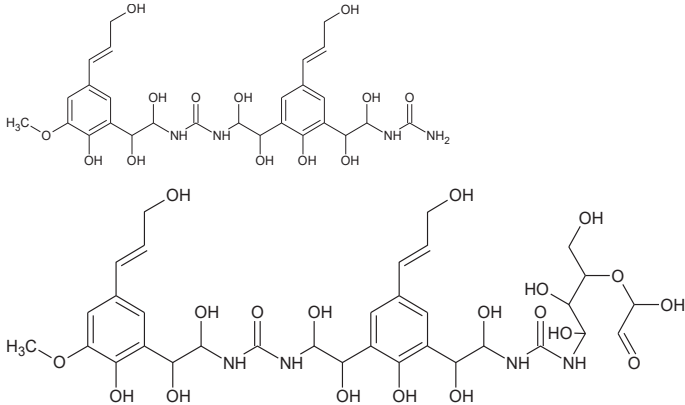
318 (II) Equally, the glyoxalated lignin monomers can be linked by the bridge of free aldehyde
319 groups and urea so that some oligomers can be observed, as shown in Table 1 (II-a).
320 Additionally, compounds formed by urea bridging dialdehyde starch monomer and glyoxalated
321 lignin unit (II-b) can also be detected. Of even greater interest are compounds in which the
322 glyoxalated lignin units are linked through urea bridges to dialdehyde starch oligomers (II-c,
323 trimer and tetramer).

324 (III) The epoxide groups of GDE exhibit a high reactivity to $-\text{NH}_2$ of urea. For example, GDE
325 as monomer reacted with urea-derived monomers, as described in Table 1 (III-a). Equally, the
326 GDE can also serve as the link bridge to connect the two free $-\text{NH}_2$ groups of glyoxalated lignin
327 monomer and dialdehyde starch (III-b).

328 (IV) It also is of interest, with which components GDE reacts. The non-hydrolyzed ether bonds
329 can be formed by the $-\text{OH}$ groups of the biomass and epoxide groups of GDE, which was also
330 verified for lignin and tannin (Chen et al. 2020; Li et al. 2018b). A few compounds identified
331 show that the alcoholic character $-\text{OHs}$ of dialdehyde starch and lignin monomer appear to be
332 the crosslinking sites, such as shown for IV-a and IV-b in Table 1.

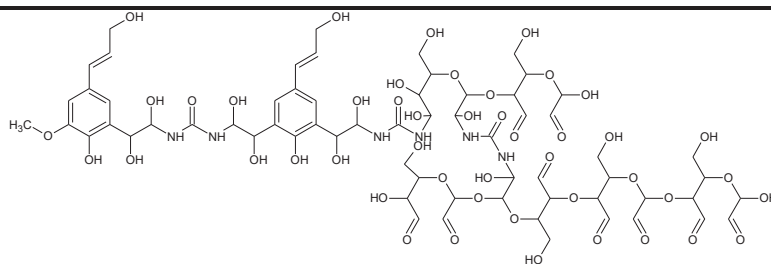
333 Therefore, similar to the abovementioned reactions in the adhesive, a more complicated three-
 334 dimensional crosslink structure can be formed, as shown in Table 1 (V). The existence of GDE
 335 promoted the degree of crosslinking between all raw materials, forming non-hydrolyzed ether
 336 bonds, which enhances the properties of the adhesive, especially its water resistance. This result
 337 can be proven by the measurement of the warm water hydrolyzed residues and the color changes
 338 of the samples treated with water, which is shown in Fig. S1 in ESM.

339 Table 1 Possible crosslinking structures detected in GL-U-Ds-E

Types	Peaks	Moiety
I-a	300.8 (Fig. 4a)	
I-b	577.7 (Fig. 4b)	
I-c	978.7 (Fig. 4c)	
II-a	536.9 or/and 625.4 (Fig. 4b)	
II-b	801.2 (Fig. 4c)	

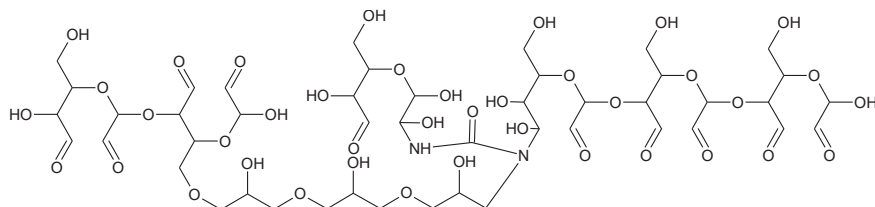
II-c 1704

(Fig.
4e)



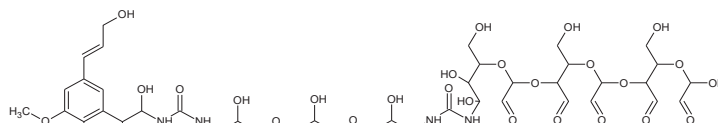
III-a 1302.9

(Fig.
4d)



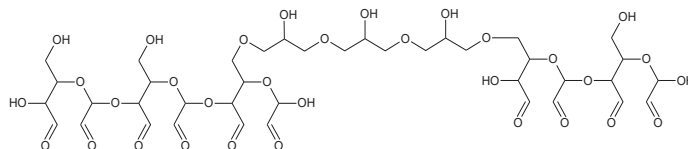
III-b 1084.4

(Fig.
4c)



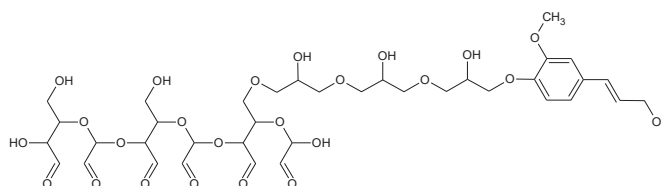
IV-a 1039.6

(Fig.
4c)



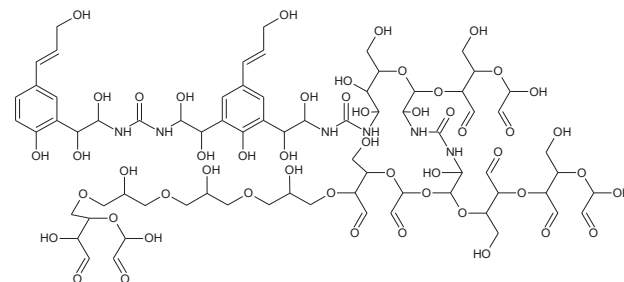
IV-b 907.3

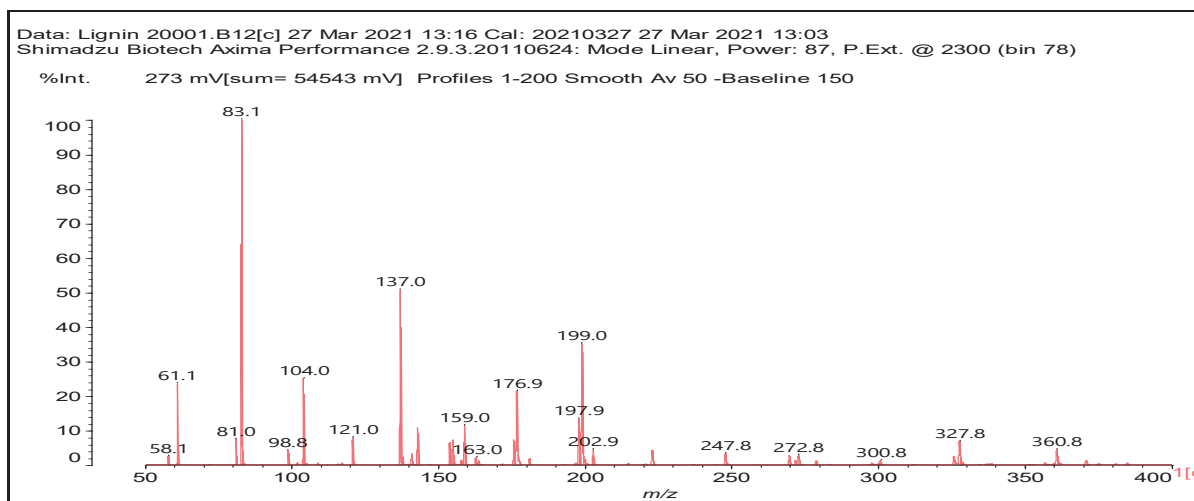
(Fig.
4c)



V 1871.8

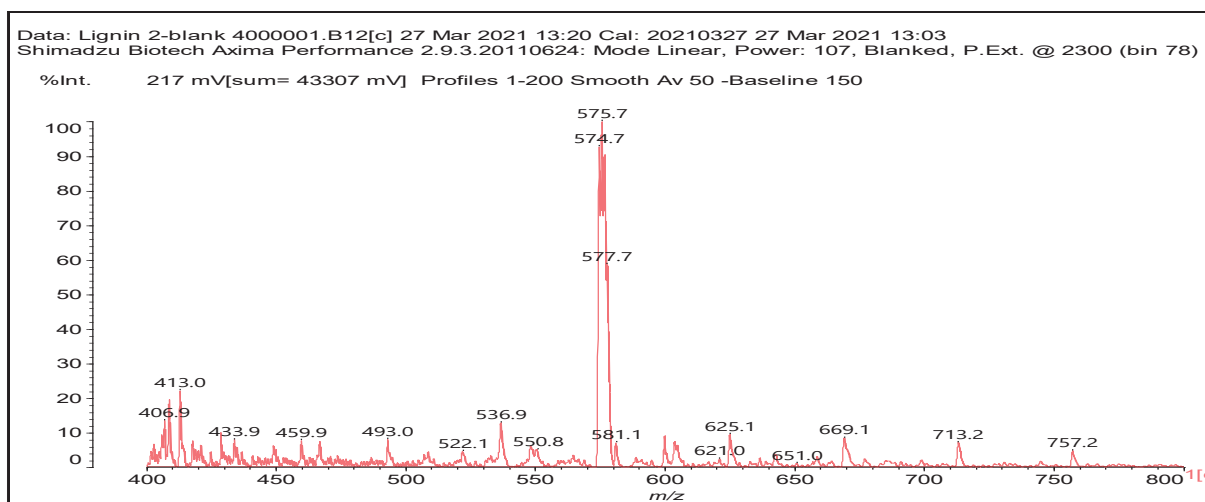
(Fig.
4e)





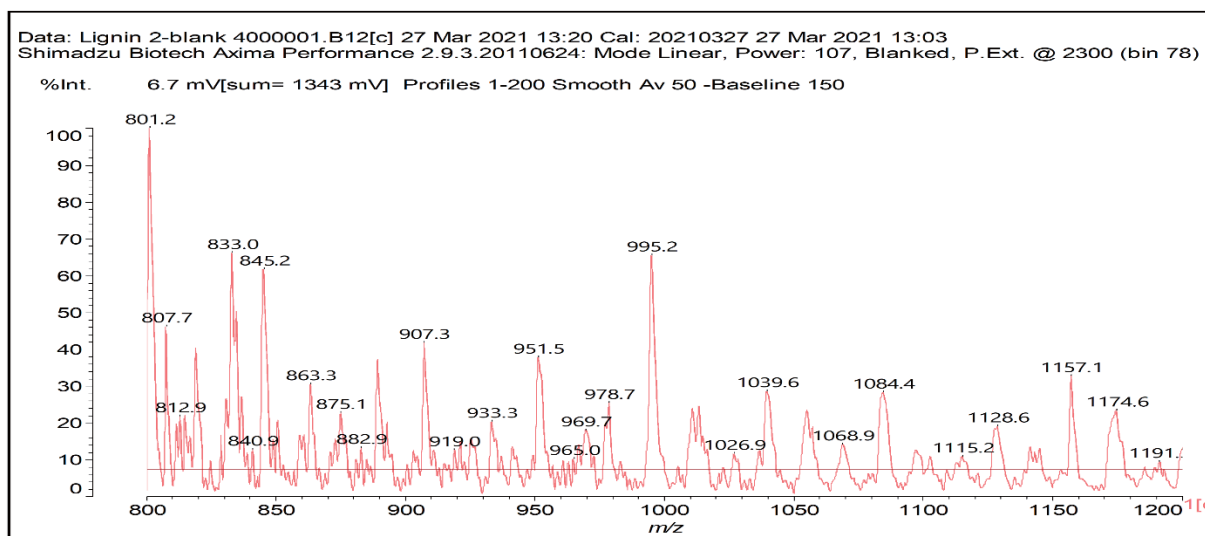
341

342 **Fig. 4a**



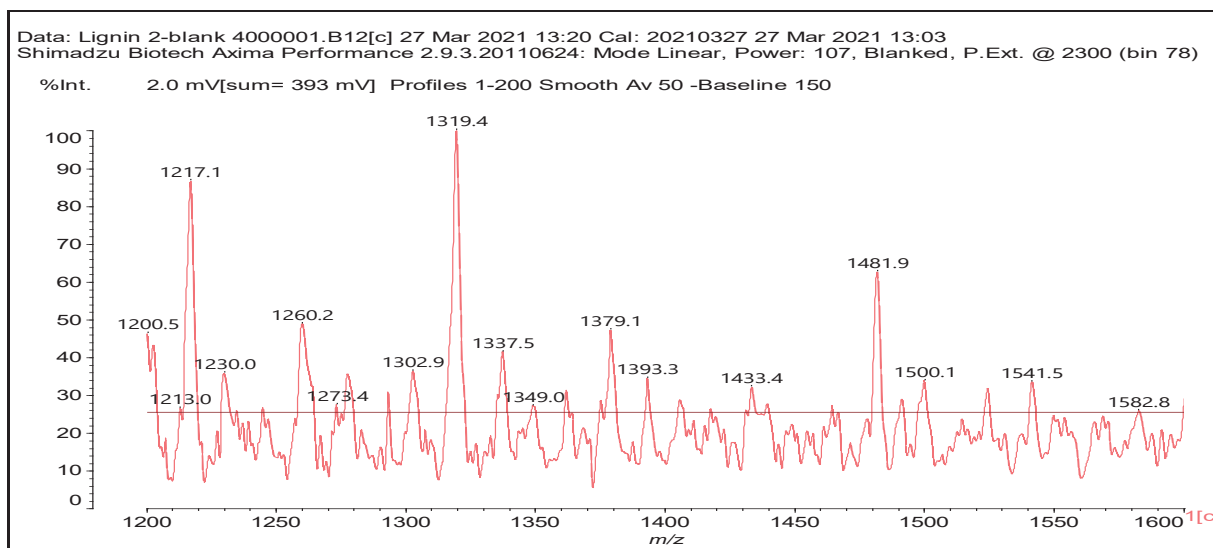
343

344 **Fig. 4b**

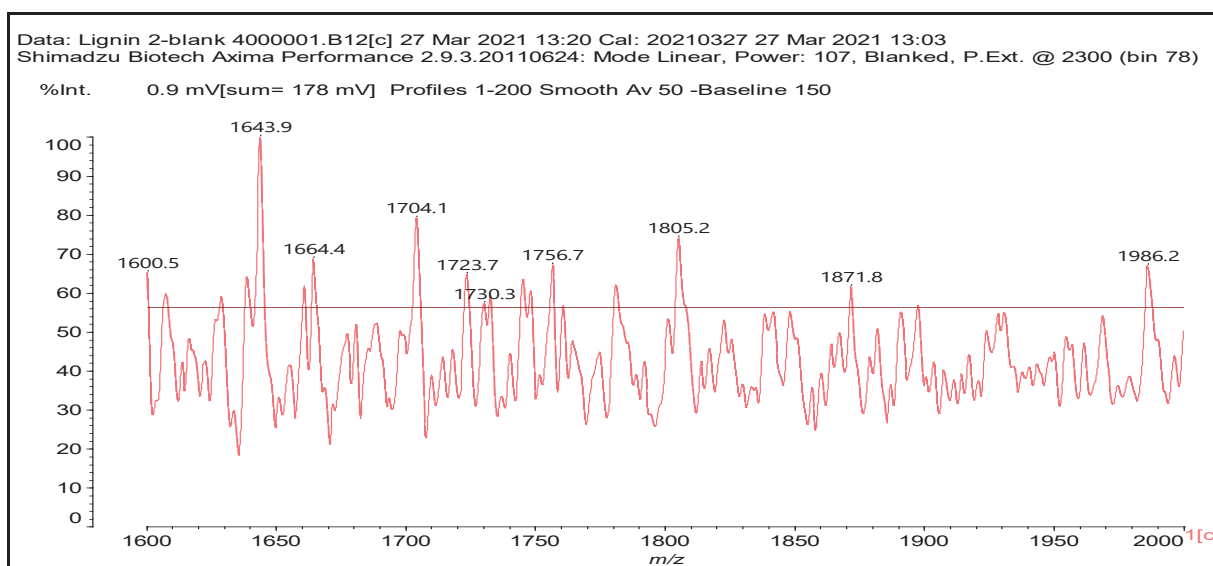


345

346 **Fig. 4c**



347

348 **Fig. 4d**

349

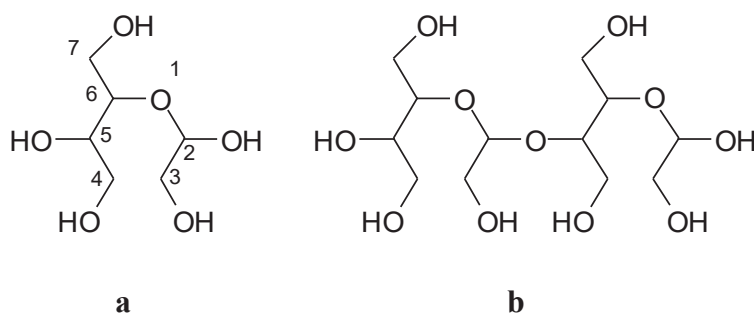
350 **Fig. 4e**

351 **Fig. 4** MALDI-ToF spectra of oven-dried GL-U-Ds-E at 120 °C for 2 h: (a) 50 Da to 400 Da
352 range; (b) 400 Da to 800 Da range; (c) 800 Da to 1200 Da range; (d) 1200 Da to 1600 Da range;
353 (e) 1600 Da to 2000 Da range.

354 **¹³C NMR analysis**

355 Figure 5 displays the ¹³C NMR spectra of glyoxalated lignin, dialdehyde starch (commercially
356 available), GL-U-Ds, and GL-U-Ds-E. The spectrum of dialdehyde starch shows the following
357 peaks that can be related to the different atoms of the molecule. First of all, the absence of peaks

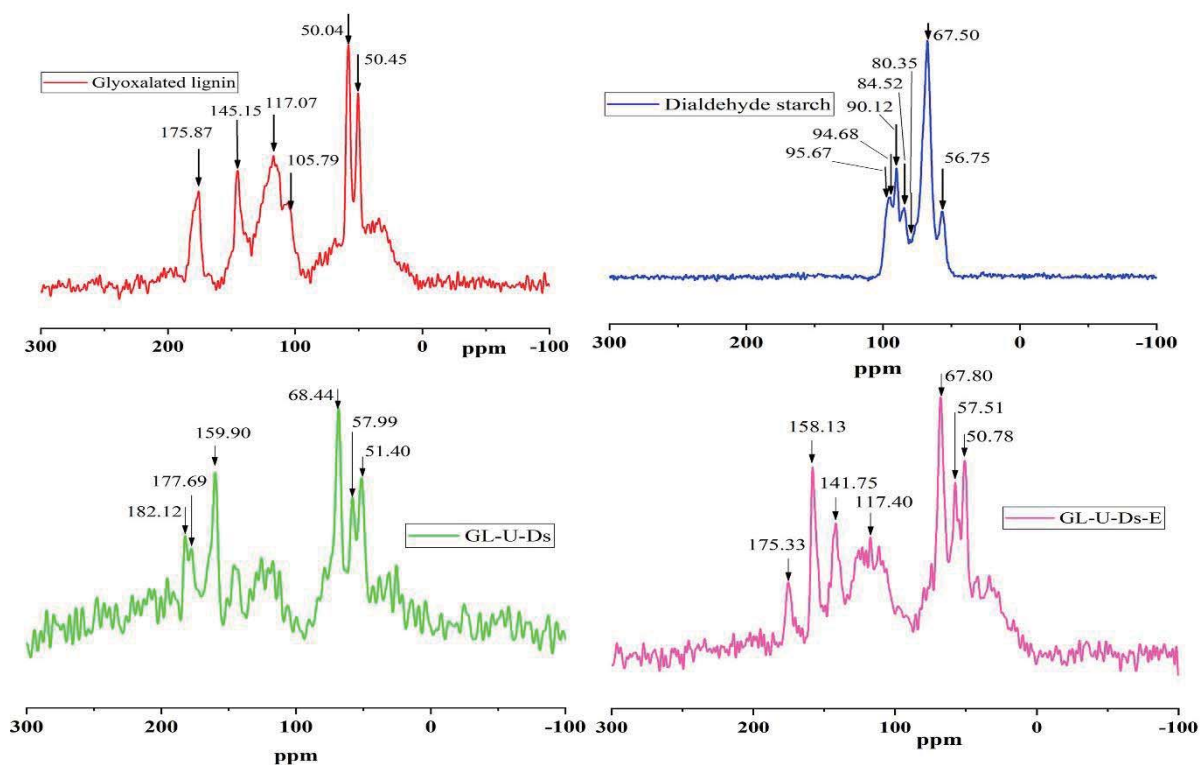
358 between 190 and 200 ppm indicates that the aldehydes generated are in solution not in the -
 359 CHO form but in the form of hemiacetals, characteristics of aldehydes in water (Despres et al.
 360 2007). This is confirmed by the peaks at 80 and 84 ppm. The assignments are 56.7 ppm (C7),
 361 67.5 ppm (C3, C4), thus the hidden aldehyde groups, the 90 ppm (C2 not reacted, just left as
 362 C-OH), 94 and 95 ppm (C2, and C5 reacted attached to other starch units, thus C-O-C), such as
 363 typical formula (a) and (bII) of dialdehyde starch.



366 In the spectrum of glyoxalated lignin, the two peaks at 50 ppm are -CH₃ signals of different
 367 kind, in a different environment. The peak at 145 ppm is (Ar)C-OCH₃, thus of the aromatic
 368 carbon attached to a methoxy group. The presence of the peak at 129-130 ppm as a shoulder of
 369 the peak at 117 ppm indicates that the ortho site of the aromatic nuclei of lignin has reacted
 370 with glyoxal. The peak at 105 ppm is the peak of the carbon of the glyoxal in hemiacetal form
 371 that remains still unreacted.

372 The most indicative spectrum is the one of the original GL-U-Ds, thus of the product obtained
 373 by the reaction of glyoxalated lignin with urea and dialdehyde starch. There are several clear
 374 indications that the three materials have co-reacted. The 159.9 ppm peak of the C=O of urea,
 375 this generally occurs at 164-165 ppm and shifted to 159.9 ppm indicates that the urea is at
 376 minimum disubstituted and possibly even tri-substituted (Despres et al. 2007), thus has reacted.
 377 The shift of the 67.5 ppm peak to 68.4 ppm of the C3 and C4, thus of the generated aldehydes
 378 of the dialdehyde starch, and moreover its marked decrease in relation to the 57 and 51 ppm
 379 peaks indicates that the dialdehyde starch in the spectrum of GL-U-Ds has reacted as well. This
 380 coupled with the considerable decrease, almost disappearance of the C2 and C5 signals at 95
 381 and 95 ppm and of the free C2 at 90 ppm indicates that the dialdehyde starch has been involved
 382 in major reactions. Equally, the shift of the glyoxalated lignin from 175.8 ppm to 177.7 ppm,
 383 coupled with the increase of the 182.1 ppm peak from a small shoulder in the GL-U-Ds
 384 spectrum to be higher than the 177.7 ppm peak, contributes to the indication that the glyoxalated
 385 lignin has participated in the reaction with urea and dialdehyde starch. The complete

386 disappearance of the free glyoxal hemiacetal at 80 and 84 ppm confirms that no free aldehyde
387 groups seem anymore to be present in the GL-U-Ds spectrum, thus indicating that all the three
388 species have co-reacted. The spectrum of GL-U-Ds-E shows in principle a similar peak
389 information to the GL-U-Ds; this means that the main chain structure of GL-U-Ds did not
390 change when introducing GDE into the chemical system.



391
392 Fig. 5. ^{13}C NMR spectra of dialdehyde starch, oven-dried samples including glyoxalated lignin,
393 GL-U-Ds, and GL-U-Ds-E.

394 Physical properties of the laboratory particleboards

395 Table 2 shows the mechanical properties of laboratory particleboards (PB) manufactured in this
396 research. The IB strength of the base formulation of the GL-U-Ds adhesive satisfies the
397 requirement of EN 312-2010 for 12 mm boards of the board type P2 only for the board with the
398 highest density of 800 kg/m^3 . At the two lower densities under the given production conditions,
399 especially the amount of adhesive added, IB does not satisfy the requirement of the standard,
400 also considering the requested statistical security of the results. Conversely, at 800 kg/m^3 IB
401 increases considerably indicating that such an adhesive formulation can possibly be adapted for
402 the bonding of PB with a higher density for potential construction or building applications
403 (Khedari et al., 2004; Nakanishi et al., 2018; Uemura Silva et al., 2021).

404 The low IB at the usually given densities for particleboards of such thickness as used here
405 indicates that a further crosslinking agent will be needed. The too low IBs at 700 kg/m^3 or lower
406 densities are likely due to the formation of mainly linear macromolecular starch and lignin-
407 derived products with only a low level of chemical crosslinking by urea and with the majority
408 of hydrophilic groups still existing even after the reaction with urea. Therefore, such limited
409 crosslinking by urea could not provide enough cohesive bond strength. Thus, GDE as additional
410 crosslinker was used to enhance the mechanical properties of the PB, (i) by increasing the
411 degree of crosslinking by reaction of the hydrophilic groups (-OH, -NH₂, and -NH-) with GDE,
412 promoting more stable three-dimensional structures based on the low crosslinked and mainly
413 linear products in GL-U-Ds, in order to obtain an enhanced cohesive bond strength; (ii) by
414 fixing the free oligomers in GL-U-Ds and make them participate in the crosslinking network
415 forming. This result was supported by the water hydrolysis residue testing, as shown in Figure
416 S1 in ESM. Partially bio-sourced glycerol diglycidyl ether (GDE) was used as additional
417 crosslinker, to increase tridimensional networking of the adhesive (Chrysanthos et al. 2011;
418 Younesi-Kordkheili and Pizzi 2020). The proportion used was only 5% by weight of liquid
419 GDE based on the total resin solids load of the adhesive. This amount is based on former results
420 that 5% of epoxy resin can improve the adhesive performance significantly (Younesi-
421 Kordkheili and Pizzi 2020). As expected, its addition yielded improved IBs, as shown in Table
422 2. Nevertheless, the lowest density (650 kg/m^3) did not fulfill the requirements of EN 312; the
423 particleboard with density of 700 kg/m^3 can reach 0.48 MPa and satisfy the standard
424 requirements.

425 The IBs are conform to the density profiles of the panels at the three densities (as shown in Fig.
426 6), where the inner core density of the panels is 580 kg/m^3 , 650 kg/m^3 and 800 kg/m^3 for the
427 boards having total densities of 650, 700 and 800 kg/m^3 , respectively. The low-density boards
428 show a typical U-shaped density profile, with higher densities in the outer zones, despite the
429 fact that one-layer boards have been produced (Wong et al. 1999). With increased particleboard
430 densities, the densities in the board center will go up, then finally, the core density to be equal
431 to or even higher than the density in the outer layer. This indicates that the inherent IB weakness
432 of the 650 kg/m^3 boards is mainly due to the very low density of the inner core, and the high
433 IBs of the 800 kg/m^3 boards are due to the very high contribution of the density of their inner
434 core. The stronger bonding, mainly by hydrogen bonds and other secondary forces, between
435 adhesives and wood substrate was formed due to the more tightly packed wood particles at high
436 pressure caused by high-density condition (Cheng et al. 2004; Sulaiman et al. 2018). In addition,

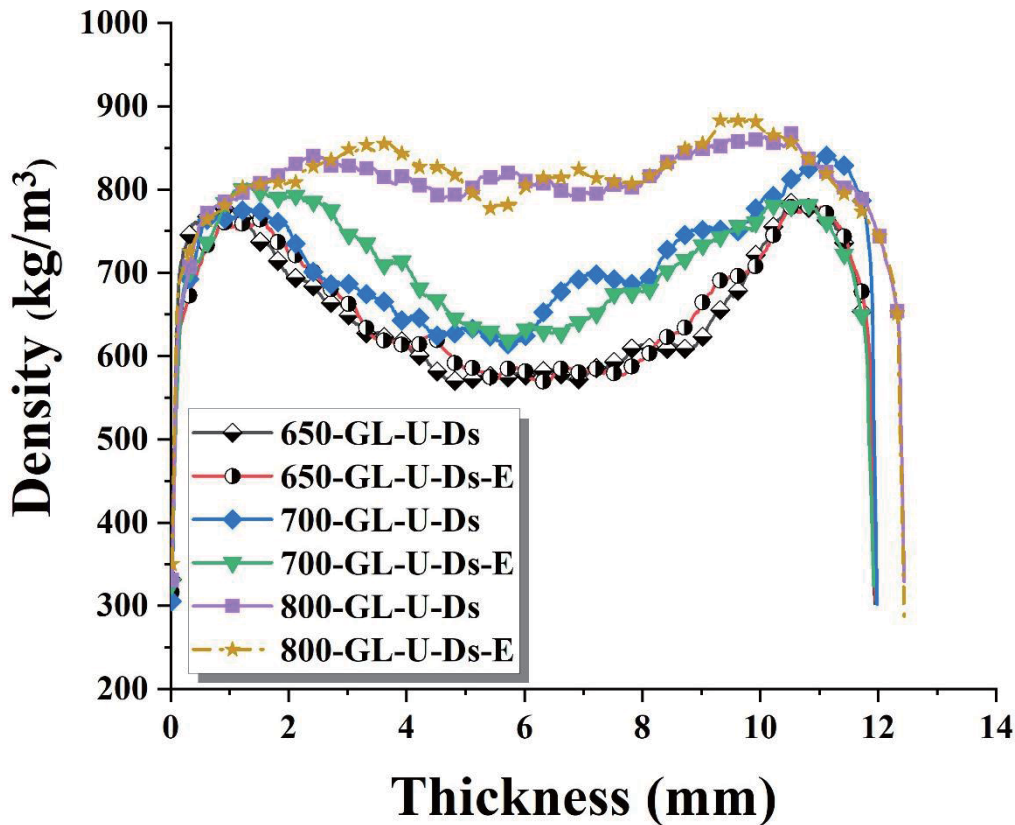
437 it confirms that the improvement of the IB of boards with the same densities is really due to the
 438 increased cohesive strength with a high crosslinking degree of the adhesive itself by comparing
 439 the same adhesive without GDE addition.

440 Table 2. Results of laboratory particleboards prepared with the two experimental adhesives

Adhesives	Density (kg/m ³)	Thickness (mm) ^b	IB (MPa)	MOR (MPa)	MOE (MPa)
GL-U-Ds	650 (650) ^a	11.9±0.2	0.22±0.05	6.5±0.3	986±9
	700 (710)	11.9±0.1	0.36±0.07	8.0±0.3	1337±13
	800 (790)	12.0±0.2	0.6±0.05	13.4±0.4	2216±19
GL-U-Ds-E	650 (660)	11.9±0.1	0.35±0.07	8.7±0.8	1488±11
	700 (720)	11.8±0.1	0.48±0.06	10.3±0.2	2085±20
	800 (800)	12.1±0.1	0.81±0.09	15.4±0.6	2912±22
P2 (EN312, 2010)			≥0.40	>11	>1800

^a represents the densities obtained by experiments

^b represents the thickness of laboratory particleboards after storage at room condition for at least 2 days.



441

442 **Fig. 6** Density profile of lab particleboards bonded with the experimental adhesives at 650,
 443 700 and 800 kg/m³ panel density.

444 Table 3 shows the results thickness swelling and water absorption of the laboratory monolayer
 445 particleboards after 2 and 24 hours of immersion in cold water. The results indicate that the
 446 addition of 5% glycerol glycidyl ether can reduce thickness swelling and water absorption
 447 remarkably. Notwithstanding that the laboratory boards are monolayer of core wood chips, even
 448 introducing more compact surfaces by making three layer particleboards would result in too
 449 high a thickness swelling. This indicated that higher proportion of glycerol glycidyl ether (GDE)
 450 would be necessary to bring thickness swelling to an acceptable level. The sensitivity to water
 451 is due to the presence of the dialdehyde starch, and swelling is decreased on addition of GDE
 452 as the residual alcoholic -OHs of the starch can be consumed as shown by the MALDI-ToF
 453 analysis and a certain crosslinking can be achieved.

454 **Table 3.** Results of 2 h and 24 h thickness swelling and water absorption of monolayer
 455 particleboard bonded with experimental adhesives

Adhesives	Density (kg/m ³)	2h thickness swelling (%)	2 h water absorption (%)	24 h thickness swelling (%)	24 h water absorption (%)
	650 (650) ^a	≥100	112±3	≥100	116±3
GL-U-Ds	700 (710)	≥100	97±4	≥100	102±2
	800 (790)	≥100	104±5	≥100	108±6
	650 (660)	37±2	91±4	48±1	95±7
GL-U-Ds-E	700 (720)	24±3	66±5	38±2	77±6
	800 (800)	48±4	74±5	63±1	87±3

()^a represents the densities obtained by experiments

456 Conclusion

457 The work presented here shows that reaction of glyoxalated lignin and dialdehyde starch by
458 crosslinking with urea is possible and yields results that are acceptable for bonding
459 particleboards. The main results obtained are:

460 (1) Urea can serve as a bridge or even as a crosslinker to connect glyoxalated lignin and
461 dialdehyde starch; this was verified by FTIR, ¹³C NMR, and MALDI-ToF analysis.

462 (2) The GL-U-Ds adhesive can be used to prepare wood particleboards; however, acceptable
463 mechanical properties were obtained only at high density (800 kg/m³). Therefore, additional
464 crosslinking is needed to improve the board quality.

465 (3) The thermal behavior of GL-U-Ds and GL-U-Ds-E adhesives was investigated by DSC and
466 TMA. However, it was shown that GL-U-Ds-E showed a slightly delayed curing temperature
467 in DSC. GDE as crosslinker can significantly influence the cure behavior of GL-U-Ds, resulting
468 in a better thermal stability, which was proven by TGA analysis.

469 (4) FTIR, ¹³C NMR, and MALDI-ToF were utilized to analyze the reactions of GDE with
470 residual hydroxyl groups of the dialdehyde starch and, possibly, with aliphatic and/or aromatic
471 hydroxyl groups of the glyoxalated lignin. In addition, the reaction of urea-derived products
472 and GDE was confirmed as well.

473 (5) Additional chemical crosslinking by the use of 5% on resin solids of partial bio-sourced
474 GDE improves the cohesive bonding strength of the resins. Improved mechanical properties
475 and water retardancy of laboratory particleboards were obtained.

476 Acknowledgements

477 This work was in part supported by the National Natural Science Foundation of China (NSFC
478 31971595), Scholarship from China Scholarship Council (CSC) and by the LERMAB,
479 University of Lorraine. The LERMAB of the University of Lorraine is supported by a grant
480 overseen by the French National Research Agency (ANR) as part of the Laboratory of
481 Excellence (Labex) ARBRE. Special thanks to Mr. Haizhu Wu and Mrs. Yuhong Rong for their
482 help in the DSC testing and the sample freeze-drying.

483 **Conflict of interest statement:** The authors declare no conflict of interest

484 References

- 485 Arias, A., González-Rodríguez, S., Barros, M. V., Salvador, R., de Francisco, A. C., Piekarski, C. M.,
486 Moreira, M. T. (2021). Recent developments in bio-based adhesives from renewable natural resources.
487 *J Clean Prod* 314:127892. <https://doi.org/10.1016/j.jclepro.2021.127892>.
- 488 Park, B., 2020. A Cross-Linker for UF and Hybrid Oxidized Starch/UF Resins, Proceedings,
489 International Virtual-Conference on Bio-Based Adhesives for Wood, The Korean Society of Wood
490 Science and Technology, Republic of Korea.
- 491 Ballerini, A., Despres, A., & Pizzi, A. (2005). Non-toxic, zero emission tannin-glyoxal adhesives for
492 wood panels. *Holz Roh- Werkst*, 63:477-478. <https://doi.org/10.1007/s00107-005-0048-x>.
- 493 Bobbitt, J. M. (1956). *Periodate oxidation of carbohydrates*. *Advances in carbohydrate chemistry* 11:1-
494 41. [https://doi.org/10.1016/S0096-5332\(08\)60115-0](https://doi.org/10.1016/S0096-5332(08)60115-0).
- 495 Cárcamo-Martínez, Á., Mallon, B., Anjani, Q. K., Domínguez-Robles, J., Utomo, E., Vora, L. K.,
496 Larrañeta, E., Donnelly, R. F. (2021). Enhancing intradermal delivery of tofacitinib citrate: Comparison
497 between powder-loaded hollow microneedle arrays and dissolving microneedle arrays. *Int J Pharm*
498 593:120152. <https://doi.org/10.1016/j.ijpharm.2020.120152>.
- 499 Chaleawert-umpon, S., & Liedel, C. (2017). More sustainable energy storage: lignin based electrodes
500 with glyoxal crosslinking. *J Mater Chem A* 5:24344-24352. <https://doi.org/10.1039/C7TA07686J>.
- 501 Chan-Chan, L.H., González-García, G., Vargas-Coronado, R.F., Cervantes-Uc, J.M., Hernández-
502 Sánchez, F., Marcos-Fernandez, A., Cauich-Rodríguez, J.V. (2017). Characterization of model
503 compounds and poly(amide-urea) urethanes based on amino acids by FTIR, NMR and other analytical
504 techniques. *Eur Polym J* 92:27-39. <https://doi.org/10.1016/j.eurpolymj.2017.04.014>.
- 505 ChemADVISOR, I. (1995). *Regulated Chemicals Directory 1995*. Springer Netherlands.
- 506 Chen, X., Pizzi, A., Essawy, H., Fredon, E., Gerardin, C., Guigo, N., Sbirrazzuoli, N. (2021a). Non-
507 Furanic Humins-Based Non-Isocyanate Polyurethane (NIPU) Thermoset Wood Adhesives. *Polymers*
508 13:372. <https://doi.org/10.3390/polym13030372>.
- 509 Chen, X., Pizzi, A., Fredon, E., Gerardin, C., Li, J., Zhou, X., Du, G. (2020). Preparation and properties
510 of a novel type of tannin-based wood adhesive. *J Adhes*: 1-18.
511 <https://doi.org/10.1080/00218464.2020.1863215>.

- 512 Chen, X., Pizzi, A., Xi, X., Zhou, X., Fredon, E., Gerardin, C. (2021b). Soy Protein Isolate Non-
513 Isocyanates Polyurethanes (NIPU) Wood Adhesives. *J Renew Mater* 9:1045-1057.
514 <https://doi.org/10.32604/jrm.2021.015066>.
- 515 Cheng, E., Sun, X., Karr, G.S. (2004). Adhesive properties of modified soybean flour in wheat straw
516 particleboard. *Compos Part A Appl Sci Manuf* 35:297-302.
517 <https://doi.org/10.1016/j.compositesa.2003.09.008>.
- 518 Chrysanthos, M., Galy, J., Pascault, J. P. (2011). Preparation and properties of bio-based epoxy networks
519 derived from isosorbide diglycidyl ether. *Polymer* 52:3611-3620.
520 <https://doi.org/10.1016/j.polymer.2011.06.001>.
- 521 Codou, A., Guigo, N., Heux, L., Sbirrazzuoli, N. (2015). Partial periodate oxidation and thermal cross-
522 linking for the processing of thermoset all-cellulose composites. *Compos Sci Technol* 117:54-61.
523 <https://doi.org/10.1016/j.compscitech.2015.05.022>.
- 524 Derelanko, M.J., Auletta, C.S. (2014). Handbook of toxicology. CRC press, Boca Raton.
- 525 Despres, A., Pizzi, A., Pasch, H., Kandelbauer, A. (2007). Comparative ¹³C NMR and MALDI-TOF of
526 species variation and structure maintenance during MUF resins preparation. *J Appl Polym Sci* 106:1106-
527 1128. <https://doi-org.bases-doc.univ-lorraine.fr/10.1002/app.26573>.
- 528 EN 312. Wood-based panels; Particleboards-Specifications. European Committee for Standardisation.
529 2010.
- 530 Frihart, C.R., Pizzi, A., Xi, X., Lorenz, L.F. (2019). Reactions of Soy Flour and Soy Protein by Non-
531 Volatile Aldehydes Generation by Specific Oxidation. *Polymers* 11:1478.
532 <https://doi.org/10.3390/polym11091478>.
- 533 Gao, C., Li, M., Zhu, C., Hu, Y., Shen, T., Li, M., Ji, X., Lyu, G., Zhuang, W. (2021). One-pot
534 depolymerization, demethylation and phenolation of lignin catalyzed by HBr under microwave
535 irradiation for phenolic foam preparation. *Compos B Eng* 205: 108530.
536 <https://doi.org/10.1016/j.compositesb.2020.108530>.
- 537 Garcia, R., Pizzi, A. (1998). Crosslinked and entanglement networks in thermomechanical analysis of
538 polycondensation resins. *J Appl Polym Sci* 70:1111-1119. [https://doi.org/10.1002/\(SICI\)1097-4628\(19981107\)70:6<1111::AID-APP7>3.0.CO;2-R](https://doi.org/10.1002/(SICI)1097-4628(19981107)70:6<1111::AID-APP7>3.0.CO;2-R).
- 539 Guigo, N., Mazeau, K., Putaux, J.-L., Heux, L. (2014). Surface modification of cellulose microfibrils
541 by periodate oxidation and subsequent reductive amination with benzylamine: a topochemical study.
542 *Cellulose* 21:4119-4133. <https://doi.org/10.1007/s10570-014-0459-0>.
- 543 Jahanshaei, S., Tabarsa, T., Asghari, J. (2012). Eco-friendly tannin-phenol formaldehyde resin for
544 producing wood composites. *Pigment Resin Technol* 41:296-301.
545 <https://doi.org/10.1108/03699421211264857>.
- 546 Khedari, J., Nankongnab, N., Hirunlabh, J., Teekasap, S. (2004). New low-cost insulation particleboards
547 from mixture of durian peel and coconut coir. *Build Environ* 39:59-65.
548 <https://doi.org/10.1016/j.buildenv.2003.08.001>.
- 549 Kim, K. H., Jahan, S. A., Lee, J. T. (2011). Exposure to formaldehyde and its potential human health
550 hazards. *J Environ Heal* 29:277-299. <https://doi.org/10.1080/10590501.2011.629972>.
- 551 Li, J., Zhang, J., Zhang, S., Gao, Q., Li, J., Zhang, W. (2018a). Alkali lignin depolymerization under
552 eco-friendly and cost-effective NaOH/urea aqueous solution for fast curing bio-based phenolic resin.
553 *Ind Crop Prod* 120:25-33. <https://doi.org/10.1016/j.indcrop.2018.04.027>.
- 554 Li, J., Zhu, W., Zhang, S., Gao, Q., Xia, C., Zhang, W., Li, J. (2019). Depolymerization and
555 characterization of Acacia mangium tannin for the preparation of mussel-inspired fast-curing tannin-
556 based phenolic resins. *Chem Eng J* 370:420-431. <https://doi.org/10.1016/j.cej.2019.03.211>.
- 557 Li, R.J., Gutierrez, J., Chung, Y.-L., Frank, C.W., Billington, S.L., Sattely, E.S. (2018b). A lignin-epoxy
558 resin derived from biomass as an alternative to formaldehyde-based wood adhesives. *Green Chem*
559 20:1459-1466. <https://doi.org/10.1039/C7GC03026F>.
- 560 Lubis, M. A. R., (2020). Tunable Oxidized Starch Adhesives with Blocked-pMDI for Medium Density
561 Fiberboard and Its Recycling, Proceedings, International Virtual-Conference on Bio-Based Adhesives
562 for Wood, The Korean Society of Wood Science and Technology, Republic of Korea.
- 563 Mansouri, H., Navarrete, P., Pizzi, A., Tapin-Lingua, S., Benjelloun-Mlayah, B., Pasch, H., Rigolet, S.
564 (2011). Synthetic-resin-free wood panel adhesives from mixed low molecular mass lignin and tannin.
565 *Eur J Wood Prod* 69:221-229. <https://doi.org/10.1007/s00107-010-0423-0>.

- 566 Mansouri, N.E.E., Pizzi, A., Salvado, J. (2007). Lignin-based polycondensation resins for wood
567 adhesives. *J Appl Polym Sci* 103:1690-1699. <https://doi.org/10.1002/app.25098>.
- 568 Nakanishi, E.Y., Cabral, M.R., Gonçalves, P.d.S., Santos, V.d., Savastano Junior, H. (2018).
569 Formaldehyde-free particleboards using natural latex as the polymeric binder. *J Clean Prod* 195:1259-
570 1269. <https://doi.org/10.1016/j.jclepro.2018.06.019>.
- 571 Navarrete, P., Mansouri, H., Pizzi, A., Tapin-Lingua, S., Benjelloun-Mlayah, B., Rigolet, S. (2010).
572 Synthetic-resin-free wood panel adhesives from low molecular mass lignin and tannin. *J Adhes Sci*
573 *Technol* 24:1597-1610. <https://doi.org/10.1163/016942410X500972>.
- 574 Navarrete, P., Pizzi, A., Pasch, H., Delmotte, L. (2012a). Study on Lignin-Glyoxal Reaction by MALDI-
575 TOF and CP-MAS ¹³C-NMR. *J Adhes Sci Technol* 26:1069-1082.
576 <https://doi.org/10.1163/016942410X550030>.
- 577 Navarrete, P., Pizzi, A., Tapin-Lingua, S., Benjelloun-Mlayah, B., Pasch, H., Rode, K., Delmotte, L.,
578 Rigolet, S. (2012b). Low Formaldehyde Emitting Biobased Wood Adhesives Manufactured from
579 Mixtures of Tannin and Glyoxylated Lignin. *J Adhes Sci Technol* 26:1667-1684.
580 <https://doi.org/10.1163/156856111X618489>.
- 581 Ndiwe, B., Pizzi, A., Tibi, B., Danwe, R., Konai, N., Amirou, S. (2019). African tree bark exudate
582 extracts as biohardeners of fully biosourced thermoset tannin adhesives for wood panels. *Ind Crop Prod*
583 132:253-268. <https://doi.org/10.1016/j.indcrop.2019.02.023>.
- 584 Oktay, S., Kızılcın, N., Bengü, B. (2021). Oxidized cornstarch-Urea wood adhesive for interior
585 particleboard production. *Int J Adhesion Adhes* 110:102947.
586 <https://doi.org/10.1016/j.ijadhadh.2021.102947>.
- 587 Pradyawong, S., Li, J., He, Z., Sun, X.S., Wang, D., Cheng, H.N., Klasson, K.T. (2018). Blending
588 cottonseed meal products with different protein contents for cost-effective wood adhesive performances.
589 *Ind Crop Prod* 126:31-37. <https://doi.org/10.1016/j.indcrop.2018.09.052>.
- 590 Saražin, J., Pizzi, A., Amirou, S., Schmiedl, D., Šernek, M. (2021). Organosolv Lignin for Non-
591 Isocyanate Based Polyurethanes (NIPU) as Wood Adhesive. *J Renew Mater* 9:881-907.
592 <https://doi.org/10.32604/jrm.2021.015047>.
- 593 Sulaiman, N.S., Hashim, R., Sulaiman, O., Nasir, M., Amini, M.H.M., Hiziroglu, S. (2018). Partial
594 replacement of urea-formaldehyde with modified oil palm starch based adhesive to fabricate
595 particleboard. *Int J Adhesion Adhes* 84:1-8. <https://doi.org/10.1016/j.ijadhadh.2018.02.002>.
- 596 Tabarsa, T., Jahanshahi, S., Ashori, A. (2011). Mechanical and physical properties of wheat straw boards
597 bonded with a tannin modified phenol-formaldehyde adhesive. *Compos B Eng* 42:176-180.
598 <https://doi.org/10.1016/j.compositesb.2010.09.012>.
- 599 Uemura Silva, V., Nascimento, M.F., Resende Oliveira, P., Panzera, T.H., Rezende, M.O., Silva, D.A.L.,
600 Borges de Moura Aquino, V., Rocco Lahr, F.A., Christoforo, A.L. (2021). Circular vs. linear economy
601 of building materials: A case study for particleboards made of recycled wood and biopolymer vs.
602 conventional particleboards. *Constr Build Mater* 285:122906.
603 <https://doi.org/10.1016/j.conbuildmat.2021.122906>.
- 604 Wing, R., Willett, J. (1997). Water soluble oxidized starches by peroxide reactive extrusion. *Ind Crop*
605 *Prod* 7:45-52. [https://doi.org/10.1016/S0926-6690\(97\)00069-1](https://doi.org/10.1016/S0926-6690(97)00069-1).
- 606 Wong, E.-D., Zhang, M., Wang, Q., Kawai, S. (1999). Formation of the density profile and its effects
607 on the properties of particleboard. *Wood Sci Technol* 33, 327-340.
608 <https://doi.org/10.1007/s002260050119>.
- 609 Xi, X., Pizzi, A., Frihart, C.R., Lorenz, L., Gerardin, C. (2020). Tannin plywood bioadhesives with non-
610 volatile aldehydes generation by specific oxidation of mono- and disaccharides. *Int J Adhesion Adhes*
611 98:102499. <https://doi.org/10.1016/j.ijadhadh.2019.102499>.
- 612 Xi, X., Pizzi, A., Gerardin, C., Lei, H., Chen, X., Amirou, S. (2019). Preparation and evaluation of
613 glucose based non-isocyanate polyurethane self-blowing rigid foams. *Polymers* 11:1802.
614 <https://doi.org/10.3390/polym11111802>.
- 615 Younesi-Kordkheili, H. (2017). Improving physical and mechanical properties of new lignin- urea-
616 glyoxal resin by nanoclay. *Eur J Wood Prod* 75:885-891. <https://doi.org/10.1007/s00107-016-1153-8>.
- 617 Younesi-Kordkheili, H., Pizzi, A. (2017). Ionic liquids as enhancers of urea-glyoxal panel adhesives as
618 substitutes for urea-formaldehyde resins. *Eur J Wood Prod* 75:481-483.
619 <https://doi.org/10.1007/s00107-016-1116-0>.

- 620 Younesi-Kordkheili, H., Pizzi, A. (2018). Properties of plywood panels bonded with ionic liquid-
 621 modified lignin-phenol-formaldehyde resin. *J Adhes* 94:143-154.
 622 <https://doi.org/10.1080/00218464.2016.1263945>.
- 623 Younesi-Kordkheili, H., Pizzi, A. (2020). Improving the properties of urea-lignin-glyoxal resin as a
 624 wood adhesive by small addition of epoxy. *Int J Adhesion Adhes* 102:102681.
 625 <https://doi.org/10.1016/j.ijadhadh.2020.102681>.
- 626 Yu, Y., Wang, Y.N., Ding, W., Zhou, J., Shi, B. (2017). Preparation of highly-oxidized starch using
 627 hydrogen peroxide and its application as a novel ligand for zirconium tanning of leather. *Carbohydr*
 628 *Polym* 174:823-829. <https://doi.org/10.1016/j.carbpol.2017.06.114>.
- 629 Zuo, Y., Liu, W., Xiao, J., Zhao, X., Zhu, Y., Wu, Y. (2017). Preparation and characterization of
 630 dialdehyde starch by one-step acid hydrolysis and oxidation. *Int J Biol Macromol* 103:1257-1264.
 631 <https://doi.org/10.1016/j.ijbiomac.2017.05.188>.

3.7 Adhésifs pour bois en polyuréthane sans isocyanate à base de tanin (NIPU) à température de durcissement inférieure : préparation et évaluation des propriétés

Résumé: L'éther diglycidyle de glycérol bio-sourcé (GDE) a été utilisé dans des proportions appropriées comme activateur pour diminuer la température de durcissement, pour améliorer les performances de collage, tout en réduisant l'émission de substances nocives (hexaméthylènediamine) dans le processus de préparation des adhésifs NIPU à base de tanin. Le mécanisme d'amélioration suggéré a été étudié par spectrométrie de masse à temps de vol de désorption/ionisation laser assistée par matrice (MALDI-ToF) et spectroscopie infrarouge à transformée de Fourier (FT-IR). Les groupes époxy du GDE se réticulent facilement avec des molécules contenant des amino groupes favorisant les réactions se produisant et entraînant une température de durcissement plus basse. De plus, la réaction d'estérification entre le groupe hydroxyle C3 de l'hétérocycle du tanin flavonoïde et les groupes époxy du GDE s'est également produite. La température de durcissement réduite, la morphologie de la surface de fracture améliorée et la stabilité thermique améliorée ont été démontrées par analyse thermomécanique (TMA), microscopie électronique à balayage (MEB) et analyse thermogravimétrique (TGA), respectivement. Les performances de liaison ont été considérablement améliorées, satisfaisant les exigences du standard pour le contreplaqué de qualité intérieure ($\geq 0,7$ MPa), même si sous une température de durcissement relativement inférieure par rapport aux adhésifs NIPU au tanin non modifié. Par conséquent, cette stratégie de modification a amélioré les propriétés de collage, réduit la consommation d'énergie de préparation et diminué les substances nocives libérées, ce qui est conforme aux exigences d'un processus de production plus propre.

Mots clés: Colles à bois; contreplaqué; tanin de mimosa; éther diglycidyle de glycérol; NIPU; MALDI-ToF.



Contents lists available at ScienceDirect

International Journal of Adhesion and Adhesives

journal homepage: www.elsevier.com/locate/ijadhadh

Low curing temperature tannin-based non-isocyanate polyurethane (NIPU) wood adhesives: Preparation and properties evaluation

Xinyi Chen^{a,b}, Antonio Pizzi^{b,*}, Emmanuel Fredon^b, Christine Gerardin^c, Xiaojian Zhou^{a,**}, Bengang Zhang^d, Guanben Du^a

^a Key Laboratory for Forest Resources Conservation and Utilisation in the Southwest Mountains of China (Southwest Forestry University), Ministry of Education, Kunming, 650224, PR China

^b LERMAB, University of Lorraine, 27 Rue Philippe Seguin, BP 1041, 88051, Epinal, France

^c LERMAB, University of Lorraine, Boulevard Does Aiguillettes, 54000, Nancy, France

^d LERMAB, University of Lorraine, 7 Rue Fusillés de La Résistance, 88000, Epinal, France

ARTICLE INFO

Keywords:

Wood adhesives
Plywood
Mimosa tannin
Glycerol diglycidyl ether
NIPU
MALDI-TOF

ABSTRACT

Bio-sourced glycerol diglycidyl ether (GDE) has been used in appropriate proportions as an enhancer to decrease the curing temperature, and improve the bonding performance, while reducing the emission of harmful substances, such as hexamethylenediamine, in the preparation process of tannin-based NIPU adhesives. The route of suggested enhancement was investigated by matrix-assisted laser desorption/ionization time-of-flight (MALDI-TOF) mass spectrometry and Fourier transform infrared spectroscopy (FT-IR). The epoxy groups of GDE easily cross-link with molecules containing amino groups, promoting the reactions proceeding and resulting in a lower curing temperature. In parallel, the esterification reaction between the C3 hydroxyl groups of the flavonoid tannin heterocyclic ring and the epoxy groups of GDE occurred as well. The reduced curing temperature, improved fracture surface morphology, and enhanced thermal stability were demonstrated by thermomechanical analysis (TMA), scanning electron microscopy (SEM), and thermogravimetric analysis (TGA), respectively. The bonding performance was significantly enhanced, satisfying the standard requirements for interior grade plywood (≥ 0.7 MPa), even though under a relatively lower curing temperature compared to unmodified tannin NIPU adhesives. Therefore, this modification strategy enhanced the bonding properties, reduced the energy consumption during preparation, and decreased release of harmful substances, which is in line with the requirements for a cleaner production process.

1. Introduction

Commercial polyurethane (PU) adhesives are extensively used in the wood industry because of their excellent performance characteristics, such as strong adhesion, good stability and non-toxic emission when compared to traditional formaldehyde-based wood adhesives [1–5]. In classical commercially available PUs synthesis systems, polyols, and isocyanates, both petrochemical feedstocks, are the two main components of these PU systems [6,7]. However, they present two major drawbacks, namely the depletion of a limited non-renewable petroleum-based resource, high-price, and the toxicity of the isocyanate.

The demand for materials safety and environment friendliness led first to substitute bio-based polyols partially or completely for fossil-

based ones to manufacture “bio-based” PU products. For instance, polyols based on lignocellulosic biomass [8–11], vegetable oils [12–16], and other types of renewable materials [1,17,18] have been proposed. These “bio-based” PU resins have been commonly used for many products in a variety of application fields. It is worth noting that this strategy has contributed to some extent to the acceptance of partially bio-based PUs by the chemical industry. Nevertheless, isocyanate is still the inevitable constituent in these “bio-polyols” strategy, with its foreseeable, unavoidable risks [3,14].

In the last few years, routes to non-isocyanate polyurethane (NIPU) preparation have been deemed as the ones with the greatest potential and most competitive for industrial application when compared to traditional isocyanate-based PUs [19–21]. Typically, five-membered

* Corresponding author.

** Corresponding author.

E-mail addresses: antonio.pizzi@univ-lorraine.fr (A. Pizzi), xiaojianzhou1982@163.com (X. Zhou).

<https://doi.org/10.1016/j.ijadhadh.2021.103001>

Received 2 March 2021; Accepted 27 September 2021

Available online 29 September 2021

0143-7496/© 2021 Elsevier Ltd. All rights reserved.

cyclic carbonate groups have been reacted with diamines to obtain urethane linkages [19,22]. Biomass containing epoxy groups or epoxidized biomass has been usually used to prepare five-membered cyclic carbonates. These epoxy groups are then converted by using CO₂, always under a high-pressure condition, with catalyst and long reaction times [19,23]. As a consequence of this disadvantage, an appreciable amount of research has focused on how to prepare cyclic carbonates under milder reaction conditions, even at atmospheric pressure [24]. Although high pressure was so avoided, this preparation process still, however, requires long reaction times, and the use of a catalyst. Apparently, all these preparation methods need strict reaction equipments and present a very high time cost.

In our previous work the main aim was to continue developing a novel NIPU preparation route with widely available simple aliphatic carbonates obtained under atmospheric pressure, with low time-cost and without a need for a catalyst, along with the elimination of the intermediate cyclization reaction. Moreover, this route was developed from a variety of bio-sourced materials [22,25–33]. Tannin was the first material to be involved in the synthesis of tannin-based NIPU resins for wood coating and bio-based tannin foams [25–28]. However, tannin-based NIPUs have never been used as wood panel adhesives. Thereafter, carbohydrates (mainly glucose and sucrose) were used as well as biosourced feedstocks to prepare NIPU resins, for wood adhesives, coatings, and foams [22,29–32]. However, the curing temperature of sugar-based NIPU wood adhesive, at over 200°C, was acceptable for some wood panel types such as particleboards but limited somewhat their application for other panel types [30]. Hence, to render bio-based NIPU systems more acceptable for industrial applications, in particular as wood adhesives, it is still of special interest to decrease their curing temperature. Besides, the free excess of hexamethylenediamine (HMDA) can be in part released during the high temperature panel hot pressing (over 200°C) in the surface layers, as this temperature is above its volatilization point. This consequently may be an environmental hazard and harmful. However, it does not volatilize from the board core where the temperature reaches a maximum of 115°C.

Commercial GDE resin was particularly selected as an enhancer to decrease the curing temperature of tannin-based NIPU wood adhesives and improve their properties because of its bio-sourced nature [34–36]. Meanwhile, the panel surfaces excess of free HMDA was eliminated during the preparation process because of its high reactivity with epoxy groups, thus reducing the adhesives potential environmental impact. For this, the enhanced reaction mechanism in the presence of GDE needs to be explained. Thus, to further determine the role of GDE as part of the adhesive, the hydrolysis rate, and physico-chemical features of the wood adhesives with and without GDE have to be studied as well. Moreover, the extent of crosslinking and thermal stability was investigated.

2. Materials and methods

2.1. Materials

Commercial mimosa tannin extract (*Acacia mearnsii*, De Wild) was supplied by Silva Chimica (St. Michele Mondovi, Italy). Commercial products, including glycerol diglycidyl ether (GDE, technical grade), dimethyl carbonate (DMC, anhydrous, ≥99%), hexamethylenediamine (HMDA, technical grade, 70% aqueous solution), were obtained from Sigma-Aldrich. All other raw materials employed in the experiments were directly used without any pre-treatment.

2.2. Preparation of tannin non-isocyanate polyurethane (NIPU) adhesive

Tannin-based NIPU adhesive was prepared according to our previous fabrication procedure [27,28]. Briefly, 16.67 g distilled water was charged into a three-neck round flask fitted with magnetic bar and thermometer while placed in a water bath. Then, 20 g mimosa tannin was added and mixing was run sufficiently till a homogenous mixture

was obtained. Thereafter, 13.5 g DMC was added into the flask and the mixture was heated to 50°C and maintained at this temperature for 1 h. Finally, 38.8 g of HMDA was inserted into the reaction mixture and stirring was continued for 2 h more. The as-obtained resin was cooled down to room temperature and coded as raw tannin NIPU (marked as adhesive 1).

For the GDE-modified adhesive, different amounts of GDE (9%, 18%, 27%, 39%, and 45%, depending on the solid content of raw tannin NIPU adhesives, respectively) were added into the raw tannin NIPU adhesive, and denoted methodically as adhesive 2 to adhesive 6, respectively.

2.3. Characterization of tannin adhesive series

2.3.1. pH, viscosity, and solid content of tannin adhesive series

The pH values were measured using a pH meter (PHS-3C vale meter) while the viscosity of the tannin NIPU wood adhesives were evaluated by utilizing Viscometer (Brookfield DV-II+), spindle No. 4 with 100 rpm at ambient temperature. The solid content (S) was calculated by recording the initial weight (M₁) and constant weight of a heat-treated sample for 2 h (M₂, at 103 ± 2 °C) of adhesives, according to the formula presented in Eq. (1):

$$S = \frac{M_2}{M_1} \times 100\% \quad (1)$$

Five replicates were tested for each sample in order to calculate the mean values and standard deviations.

2.3.2. Residual weight after hydrolysis

The wood adhesive in liquid form was transferred into an oven at 200°C till a constant weight was reached (W₁). Next, the cured adhesive samples were immersed in hot water at 60°C for 6 h. The residual (non-hydrolyzed) weight (W₂) was obtained after oven drying at 103 ± 2 °C. The residual weight (H) was calculated following the formula in Eq. (2):

$$H = \frac{W_2}{W_1} \times 100\% \quad (2)$$

Five repeated experiments were performed for calculation of the mean and standard deviation.

2.3.3. Matrix assisted laser desorption ionization time-of-flight (MALDI-TOF)

The MALDI-TOF investigation was performed by following a reported procedure [33,37] using an Axima-Performance mass spectrometer from Shimadzu Biotech (Kratos Analytical Shimadzu Europe Ltd., Manchester, UK). The accuracy of the spectrum is ±1 Da.

2.3.4. Fourier transform infrared spectroscopy (FT-IR)

The infrared spectroscopy was performed on a PerkinElmer Frontier ATR-FTMIR. The spectra of the samples were recorded for 32 scans between the range of 600 and 4000 cm⁻¹, with a scan resolution of 4 cm⁻¹.

2.3.5. Thermomechanical analysis (TMA) of the samples

30 mg of the prepared adhesive was applied to two beech wood chips, with dimensions of 17 × 5 × 1.1 (Length × Width × Thickness) mm³ and then stacked to two-ply samples. The relationship of modulus of elasticity (MOE) and temperature was recorded by TMA (Mettler Toledo 40, Zurich, Switzerland) following the method of three-point bending. A heating rate of 10 °C/min was applied in the range 30–250°C, while the relevant curves of modulus of elasticity (MOE) against temperature were registered.

2.3.6. Morphological investigation using scanning electron microscopy (SEM)

For investigating the surface morphology of the cured wood adhesives, scanning electron microscopy (SEM, Hitachi TM-3000, Milexia,

Paris, France) was used at an acceleration voltage of 15 kV. The sample surfaces were coated by a thin gold layer to increase the conductivity of the samples before testing.

2.3.7. Thermogravimetric analysis (TGA)

The thermal stability of tannin-based adhesives was investigated by TGA 5500 analyzer (Mettler Toledo, Guyancourt, France). 5–8 mg of dried powder was put into a platinum pan, and heating was started on the sample to the desired temperature at a heating rate of 10 °C/min, under nitrogen atmosphere with a flow rate of 50 mL/min in the temperature range from 50 to 700 °C.

2.4. Preparation of three-ply plywood with as-obtained wood adhesives

Three layers of wood veneer (rotary-cut populus deltoides poplar, 2 mm thick, air-dried), were loaded with the as-obtained wood adhesives (about 380 g/m² for double face) and stacked into three-ply samples. The hot-pressing was conducted under a constant pressure of 1.25 MPa for 6 min and 9 min at 185 °C, respectively. Finally, the produced three-ply plywood samples were left at ambient conditions for a minimum of 24 h before testing.

The plywood was then cut into 100 × 25 × 5 mm³ specimens for evaluation of the dry and wet shear strength. The pre-treatment for wet shear strength (hot water) measurements was carried out according to the Chinese National Standard (GB/T 17657–2013). Five repeated trials were performed for each group.

3. Results and discussion

3.1. Characteristics of tannin-based wood adhesives

Some basic characteristics, including pH, viscosity, solids content, and residual weight of the hydrolyzed control as well as the GDE-modified tannin NIPU wood adhesives are shown in Table 1. The pH was found to be within 10 and 11 and could be maintained or even slightly decreased with increasing the proportion of GDE added. This probably can be attributed to the dilution effect due to GDE which acted as diluent, as well as the consumption of amino groups of the diamine by their rapid reaction with the epoxy groups. Nevertheless, this slight change in pH was not of any influence on the bonding strength of these adhesives. This point is of interest as adhesives non-tolerant to any changes in pH can significantly be affected in terms of their curing behavior and bonding performance [38,39].

The viscosity of the tannin-based adhesive was increased distinctly with GDE addition as observed in Table 1, from 140 mPa s for the unmodified tannin NIPU adhesive (adhesive 1), to 1380 mPa s for adhesive 6. An exotherm was observed during the adhesive preparation, and the more GDE was added, the stronger was the exothermicity, especially for

Table 1
Basic characteristics of the series of tannin-based NIPU wood adhesives developed.

Adhesive	GDE (%)	pH	Solid content (%)	Viscosity (mPa.s)	Residual (%)
1	0	11.1	54.38 ± 0.37	140 ± 13	86.72 ± 1.81
2	9	10.9	60.47 ± 0.45	210 ± 22	89.88 ± 1.22
3	18	10.6	62.68 ± 0.55	420 ± 18	90.19 ± 0.96
4	27	10.4	66.2 ± 0.29	750 ± 39	92.26 ± 1.12
5	39	10.2	69.06 ± 0.39	940 ± 59	94.32 ± 0.98
6	45	10.2	72.02 ± 0.48	1380 ± 55	95.54 ± 0.98

GDE addition above 27 %. Therefore, it can be speculated that this exothermal response and the energy it generates at room temperature contributes to lowering the curing temperature needed in the hot press. Thus, the reaction advances much faster and polymeric chains get longer. This results in chain lengthening and then chain entanglement as the distance between the chains becomes shorter. This development maximizes the secondary forces between the chains such as hydrogen bonds, which leads finally to increases in viscosity. At higher GDE addition, such as for adhesive 5 and adhesive 6, the spontaneous heating of the system due to the exotherm reaction starts 15 min after GDE is added to the control tannin NIPU resin and the viscosity of the resin increases markedly in only 30 min until final curing. This behavior is of ultimate concern as regards to the negative effect on the adhesive storing or glue spreading, resulting in a reduced bonding performance and shortened pot life. However, this drawback can be overcome if the addition of GDE is done very shortly before application to the wood substrate. This means that this adhesive system can then be used as a 2-component adhesive.

The solids content of adhesive 1 was determined as 54.38%, and increased appreciably up to 72.02 % for adhesive 6, presenting a clear correlation with the addition of GDE. This is mainly attributed to the retaining of HMDA as part of the hardened adhesive when GDE is used, especially because it is not easily evaporated. Otherwise, the free excess of HMDA in the panels surfaces normally evaporates during the high temperature hot-pressing.

The residual weight after exposure to hydrolytic conditions shows an increasing trend with the increase of the GDE addition, from 86.72 % for adhesive 1 to 95.45 % for adhesive 6. This simply implies that the higher proportion of GDE leads to a higher degree of crosslinking as compared to the control tannin NIPU resin. Specifically, a non-hydrolyzable ether bond can build up between tannin and GDE, which impacts positively on the hydrolytic stability [40].

3.2. Suggested reaction mechanism

3.2.1. MALDI-TOF analysis

The MALDI-TOF analysis gives an insight on the type of species formed by the reaction of the tannin with dimethyl carbonate (DMC), hexamethylenediamine and the glycerol diglycidyl ether (GDE) (Fig. 1 a-d). Combinations of species are formed, from which some are contributing to cross-linking reactions of the adhesive system. Thus, the 218.7 Da species (I) is formed by the reaction of one diamine with two DMC molecules as identified in Table 2. This type of species also participates eventually in the cross-linking of tannin-based NIPU, by presenting the capacity to react with two flavonoid monomers or oligomers. That this is indeed the case is shown by species of structure (II) assigned to the peak at 774.0 Da with Na⁺.

The peak at 774.0 Da (with Na⁺) can also be assigned to the reaction product of GDE with two fisetinidin monomers leading to structure (III) and indicating that cross-linking occurs through not only the formation of urethane linkages, but also the active participation of GDE in network formation. The reaction of tannins with diglycidyl ether has already been reported [32,37]. The two structures are equally probable as the mono protonated version of (II) has a calculated value of 773 Da, while the calculated value of structure (III) comes to 774 Da by bearing deprotonation in mind. Thus, both structures are likely and the possibility should be considered of the two being present together.

Several flavonoid species are detected in the MALDI-TOF spectra, such as those assigned at 289.7 Da (Catechin and/or Robinetinidin) and 325.7–326.7 Da (Gallocatechin). Several different flavonoid monomers being linked to DMC and diamine by a urethane bond can be noticed such as the structures assigned to the peaks at 440.6 Da and 469.6 Da (Table S1).

Structures formed by the reaction of a flavonoid monomer with the GDE are also noted, which are represented by the peaks at 516–517 Da, 533 Da (Table S1) as well as mixed structures, where a flavonoid

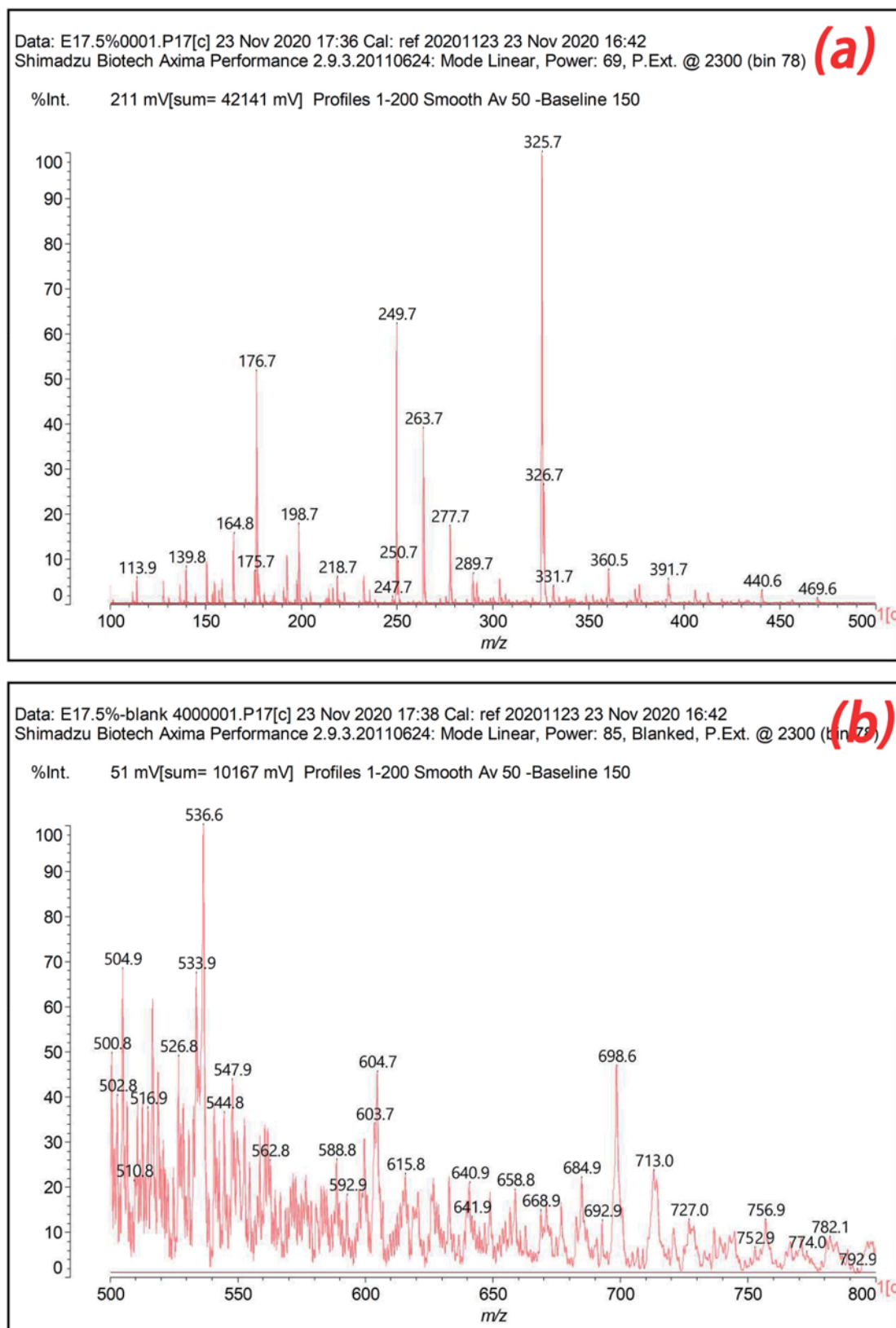


Fig. 1. MALDI-TOF spectrum of GDE-modified adhesive 4: (a) 100–500 Da; (b) 500–800 Da; (c) 800–1400 Da; (d) 1400–2000 Da.

monomer has reacted with GDE as well as with DMC and the diamine, as confirmed from the assignment to species (IV) of the peak at 713.0 Da.

From 1000 Da and up, the predominant peaks reveal chemical

species in which the flavonoids have reacted with GDE, DMC and the diamine, indicating the steps of the progress of cross-linking of the adhesive system. These species cross-link three flavonoid monomers such

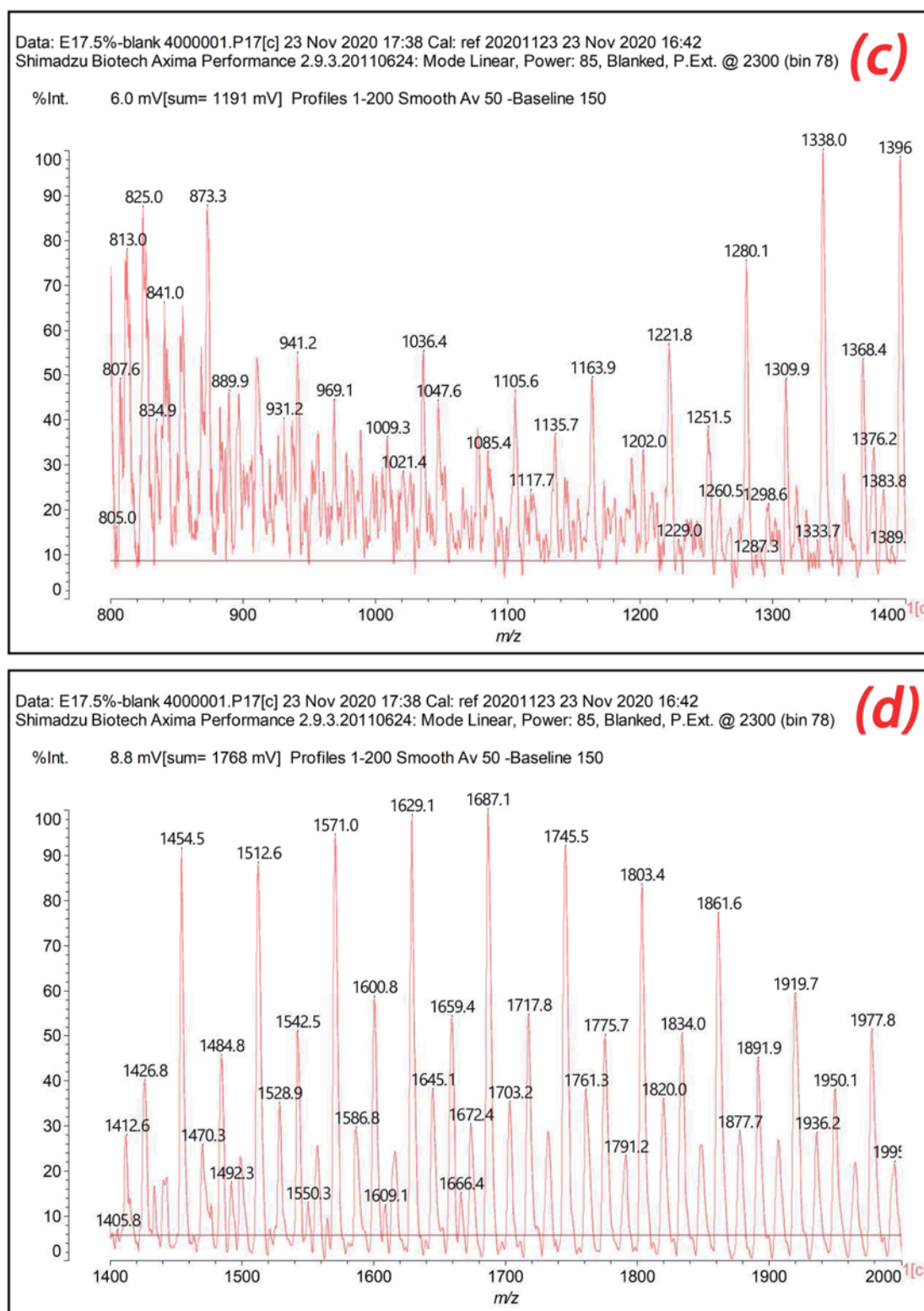


Fig. 1. (continued).

as structure (V) at 1009.3 Da without Na^+ , as well as the flavonoid oligomers of the tannin, such as the structures assigned to the peaks at 1280 Da, 1298.6 Da, 1396 Da, 1405.8 Da, 1412.6 Da, and 1672.4 Da (Table 2). For instance, the peak at 1672.4 Da, assigned to structure (VI), starts to show quite clearly the progress of cross-linking in the mixed adhesive system once it is heated in a hot press.

It must be pointed out that all the structures in Table S1

(Supplementary Material), in which flavonoid monomers or dimers are linked such as those at 774 Da, 1009 Da, 1280.1 Da, 1297 Da, 1396 Da, 1405 Da, 1412 Da, and 1674 Da can be equally linked through DMC-diamine urethane linkages as well as through the additional reaction with GDE, or both. Thus, for example the structure at 1280.1 Da in Table 2, can also be interpreted as presenting flavonoid dimers and monomers linked at the same time through DMC-diamine formed

Table 2
Some oligomeric structures predictably obtained.

Types	Oligomers
I	
II	
III	
IV	
V	
VI	
VII	
VIII	

polyurethane linkages as well as bridges obtained by reaction with GDE, such as structure (VII) as both assignments present the same molecular weight.

One further consideration that cannot be resolved with the data available is with which -OH groups of the flavonoids the two types of bridging do occur, whether with the phenolic hydroxyls of either the A

or B rings of flavonoids or through their alcoholic -OH on the C3 of the heterocycle ring.

The possibility that the urethane copolymers undergo further cross-linking via reaction with the glycerol glycidyl ether justifies how such additional cross-linking improves the mechanical performance of the panels bonded with the proposed NIPU system. Table 2 illustrates

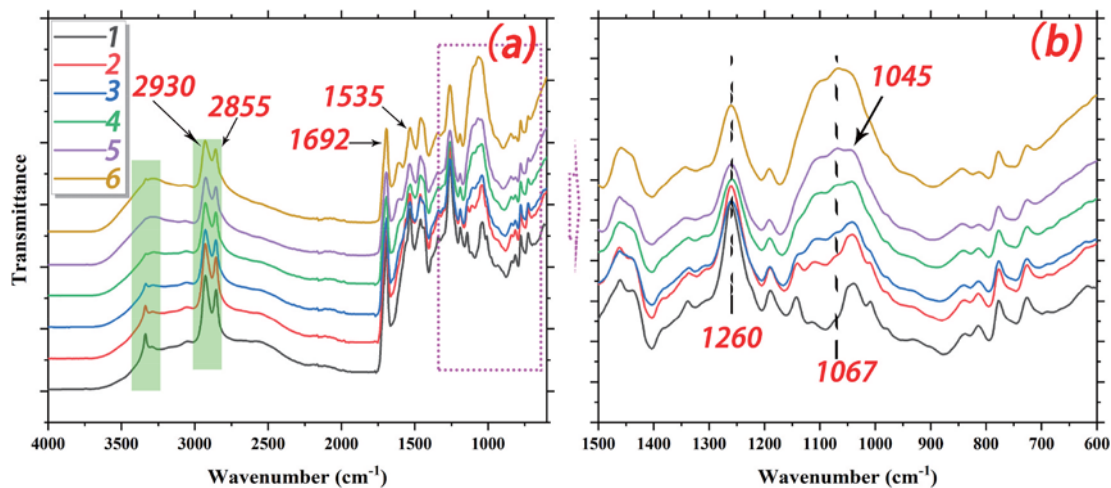


Fig. 2. FT-IR spectra of the tannin-based adhesives: (a) 600-4000 cm^{-1} ; (b) 600-1500 cm^{-1} .

species such as structure (VIII), which is assigned to the peak at 1036.4 Da (without Na^+) revealing its formation as a result of the high reactivity of tannin-based NIPU molecules.

3.2.2. Analysis using fourier transform infrared (FT-IR) spectroscopy

Fourier transform infrared (FT-IR) spectroscopy was used to study the variation of functional groups before and after reaction, and the resultant spectra are displayed in Fig. 2. A sharp peak at 3335 cm^{-1} can be seen clearly in the control tannin-NIPU adhesive (Fig. 2 (a)), which is attributed to the -NH/-OH groups stretching vibrations [26]. This peak acquired gradually intensifying broadness with the GDE addition because of the opened oxirane rings, causing emergence of more hydroxyl groups (-OH). The peaks at 2930 cm^{-1} and 2855 cm^{-1} (Fig. 2 a) are related to the symmetric and asymmetric stretching vibrations of -CH_2 and -CH_3 , respectively, which are related to the presence of HMDA and GDE [41]. A strong peak at 1692 cm^{-1} was observed in all adhesive samples, due to the C=O double bond of the NIPU amides [25,26]. Moreover, the urethane characteristic band is represented by the C-N stretching at 1535 cm^{-1} [25–28]. These results corroborate that the main skeleton is typical of a PU even with the insertion of tiny doses of GDE.

However, emergence of new peaks can be observed after the incorporation of GDE compared with control tannin NIPU adhesive (adhesive 1, Fig. 2 b). For instance, a new broad peak at 1067 cm^{-1} in the GDE-modified adhesives which was invisible in the unmodified one, is assigned to the formed aliphatic ethers (C-O-C) as a result of the reaction between tannin and GDE [42,43]. This conclusion is supported by the peak related to the heterocyclic ether of the flavonoid C-ring at 1250 cm^{-1} , which disappeared in the tannin NIPUs in the Fig. 2 (b). The disappearance of the ether peak of the flavonoid heterocycle indicates that the heterocycle ring has been opened and the flavonoid units, which

have reacted, are in their open form. In addition, amine representative peaks observed at 1260 cm^{-1} and 1045 cm^{-1} , respectively, progressively decrease in intensity, which ensures that the epoxy groups of GDE have consumed a certain proportion of amino groups [25,44]. Moreover, the related peaks to epoxy ether bonds, namely at 752 cm^{-1} and 831 cm^{-1} were no longer observable in all GDE-modified adhesives (from adhesive 2 to adhesive 6), which proves the full involvement of GDE in the reaction.

3.3. Thermomechanical analysis (TMA)

The starting curing behaviors of condensed tannin-based NIPU adhesives with different GDE addition were studied by TMA. The relevant curves of MOE as a function of temperature are exhibited in Fig. 3. Two peaks are clearly apparent in all adhesives, same as with previously biomass NIPU adhesives reported in the literature [32,33,45]. The first peak occupies the $75\text{--}125^\circ\text{C}$ range while the other one develops above 150°C . Therefore, after an initial MOE decrease due to the lower viscosity when the temperature starts increasing, the modulus of elasticity (MOE) gradually increases as a consequence of the formation of linear oligomers forming just a physically entangled network. After that, the MOE decreases due to the partial disentangling of the linear oligomers formed due to the increase in chain mobility as the temperature increases. Finally, the real chemical cross-linking does start and the MOE gradually increases to a peak indicating the formation of a chemically cross-linked network. The chemical cross-linking which finally occurs when the temperature is high enough, shows an improved modulus of elasticity (MOE).

Furthermore, adhesive 1 started curing at a rather high temperature, approximately 205°C , this result is similar to results obtained with other biomass based NIPU wood adhesives [22,30,32,45]. The maximum MOE

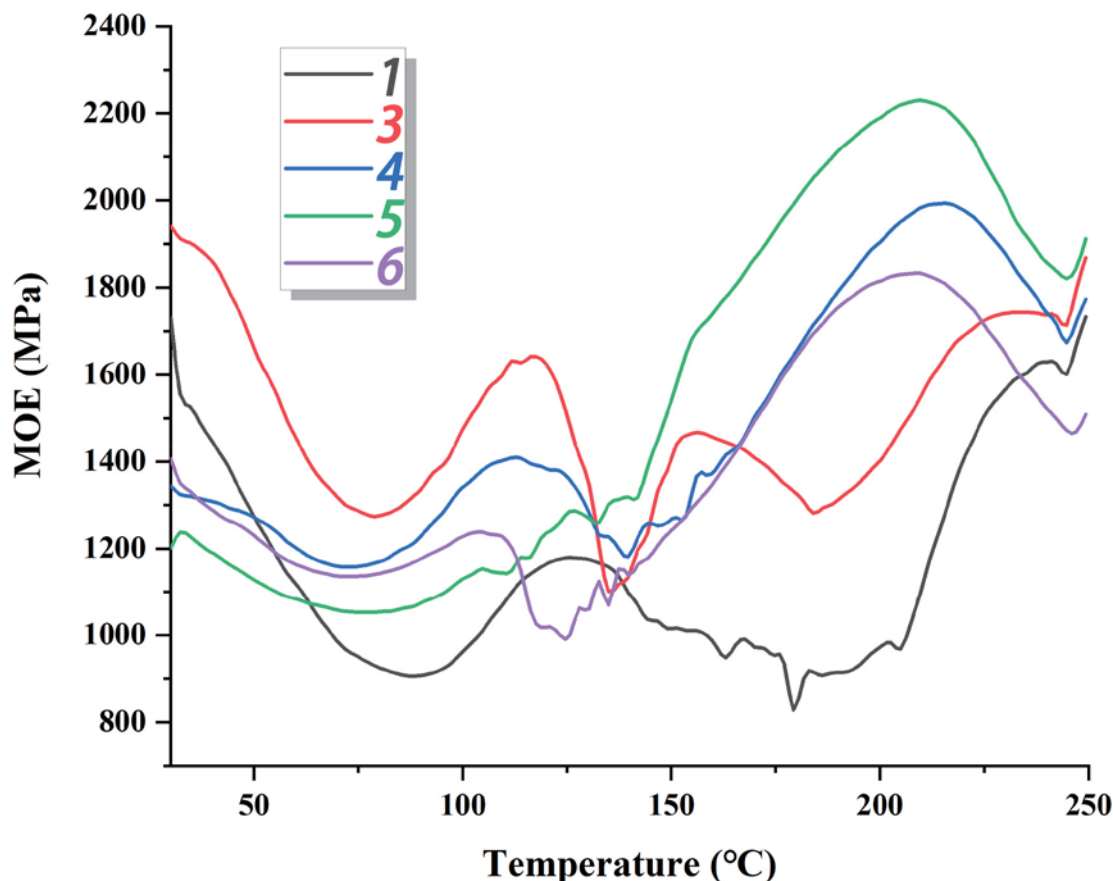


Fig. 3. Thermomechanical analysis (TMA) curves for the tannin-based NIPU adhesives.

was reached at 230°C. However, this rather high temperature limits somewhat the expansion of NIPU adhesives for industrial applications such as particleboard. Thus, it is necessary to minimize this drawback and to try to decrease the curing temperature of NIPU adhesives. By introducing glycerol diglycidyl ether (GDE) as a reaction enhancer, the starting cure temperature of the adhesive can be decreased. This trend can be seen in Fig. 3. The starting cure temperature for adhesive 3 occurs at 185°C with improvement of the maximum MOE, which is reached at 225°C. Thus, it can be noticed that the modified adhesives show a better bonding performance with respect to the neat tannin-based NIPU adhesive [22,30]. Moreover, the starting cure temperature of the resultant adhesives decreases even further with increasing GDE levels, finally tending towards the 145°C–155°C range. Interestingly, the maximum MOE values for adhesives 4 and 5 are considerably higher than the others. When the addition is over 45% (adhesive 6), the starting cure temperature drop becomes progressively far too small to be of interest. It encounters also an excessively fast increase in viscosity at ambient temperature. A too high GDE addition would also have a negative effect on the adhesive spreading on veneer surfaces. The lower MOE value in

such a case (as shown in Fig. 3) is strong evidence for this assumption.

3.4. Thermogravimetric (TG) analysis

The thermal decomposition behavior of a series of tannin-based NIPU adhesives was studied by thermogravimetric analysis, and the corresponding thermograms as well as relevant DTG are collected in Fig. 4. A multi-stage response was encountered for the decomposition behavior as can be seen in all curves. The first stage shows a small weight loss within the temperature interval 50–120°C, which belongs to the evaporation of adsorbed water from the adhesives. The temperature range 125–275°C is assigned to the initial degradation of the samples, typically from some small molecular weight substances (saccharide impurities) and unstable chemical linkages such as ether bonds [44]. In addition, the release of excess HDMA can also cause weight loss in this stage because its boiling point is around 190°C. It is interesting to note that the weight loss of this stage decreased markedly and the corresponding peaks were shifted to a higher temperature as GDE addition was progressively increased. This is simply attributed to the significant

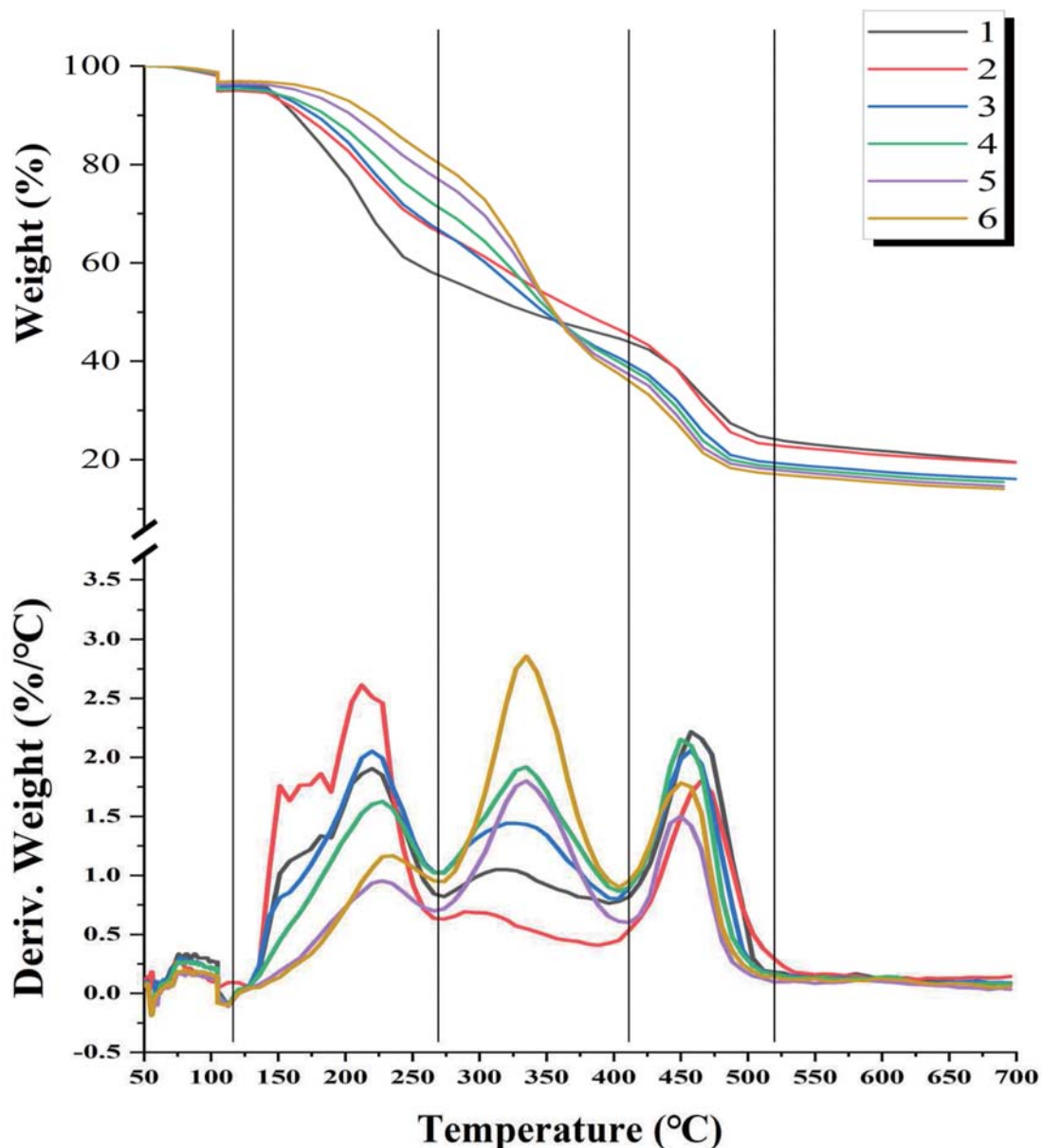


Fig. 4. Thermogravimetric (TG) and differential thermogravimetric (DTG) curves of tannin-based NIPU adhesives.

reduction of free HDMA, caused by its high reaction potential with GDE, thereby higher count of more chemically stable larger oligomers are formed. The third stage of weight loss appeared within the 275–425°C range due to the decomposition of the urethane groups [27]. This is the main degradation step, in which the major part of weight loss takes place in this stage with increasing GDE addition. Conversely, the unmodified/low GDE loaded adhesives showed a relatively smaller weight loss in this stage. This trend indicates that a large number of C–N crosslinks other than the urethane groups exist in the products, possibly formed by the reaction of epoxy groups with $-NH_2$, of even more free HDMA. Therefore, from the second and third degradation stages shown in Fig. 4, we can deduce that the main weight loss peaks were shifted to a higher temperature as the amount of GDE added increases. Accordingly, a lower proportion of free HDMA is present and consequently released during the wood panels hot-pressing, thus reducing the environmental

risks. The last weight loss stage occurs in the 425–525°C temperature range, which is attributed to covalent C–C bonds breaking. Some pyrolysis residual products coming from the previous few stages can also undergo further decomposition [27,46].

3.5. Scanning electron microscopy (SEM) analysis

To further investigate the crosslinking of the series of tannin-based adhesives prepared, their fracture surface morphology was observed by scanning electron microscopy (SEM) and the results are presented in Fig. 5. A homogenous, robust fracture surface reflecting the strength of crosslinking can be seen with the unmodified adhesives (Fig. 5 (Nr.1)). No serious defects on the fracture surface of adhesive 1 were observed. This finding demonstrates that the crosslinking reaction can occur during hot-pressing, resulting in a good bonding performance even

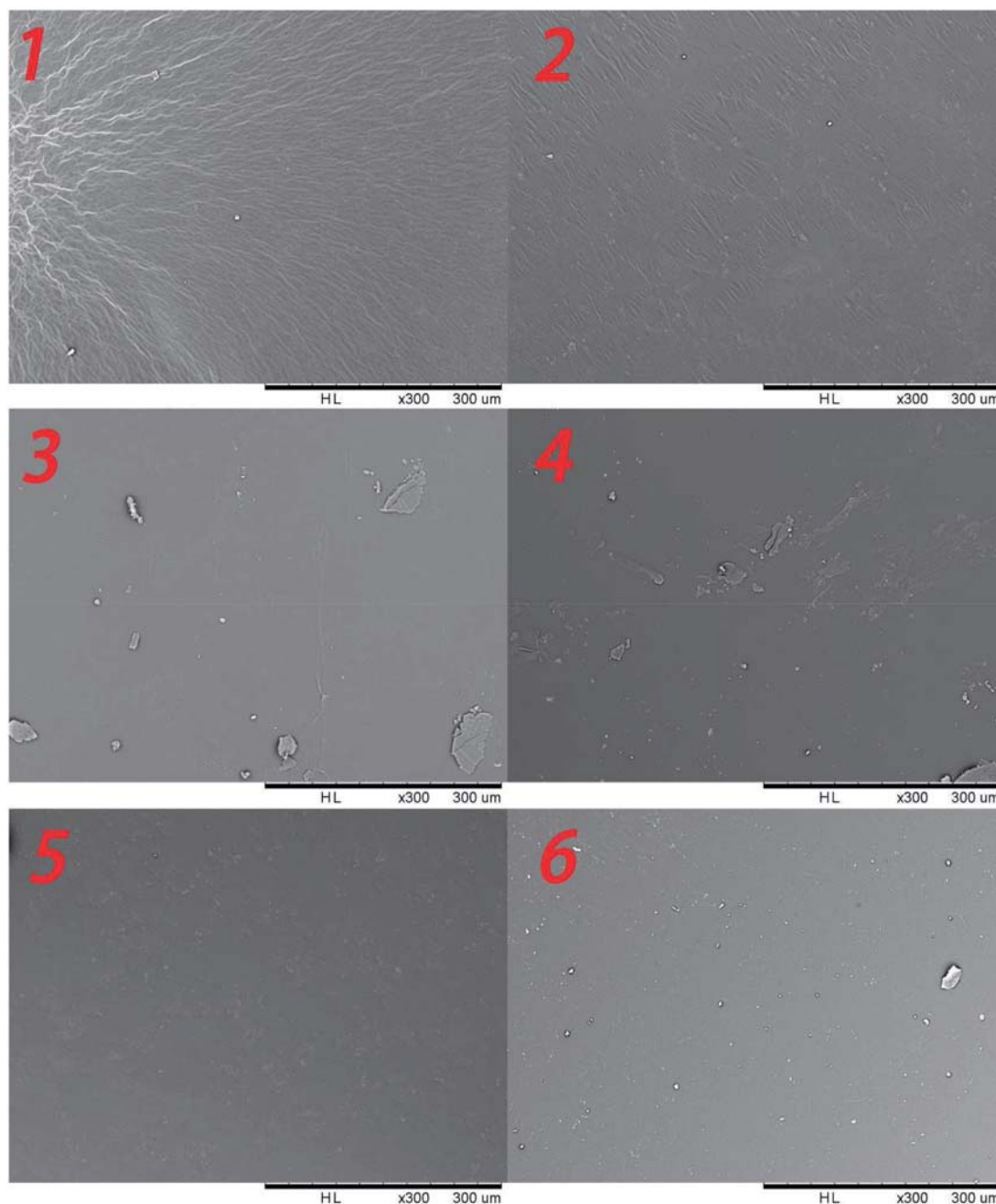


Fig. 5. Fracture surface micrographs of the tannin-based adhesives.

when the joints are exposed to hot/boiling water pre-treatment [22]. However, uneven wrinkles still can be observed, which can be explained by the chains of the crosslinking network being too closely packed so that there is not enough space available for stretching. The GDE addition appears to have served as a “bridge” to increase the chain length and stretching space of the final products, so as to obtain more unfolded chains and a toughened cross-linked network structure. From images 2–6 in Fig. 5, the morphology of the fracture surface of the adhesives

showed a smoother surface as the level of GDE increases. For example, no wrinkles could be identified in the fracture surface of joints glued with adhesives 5 and 6, indicating that a uniform and stable cross-linked network can be formed in the presence of GDE as a modifier for the adhesive formulation compared to the unmodified basic tannin NIPU formulation.

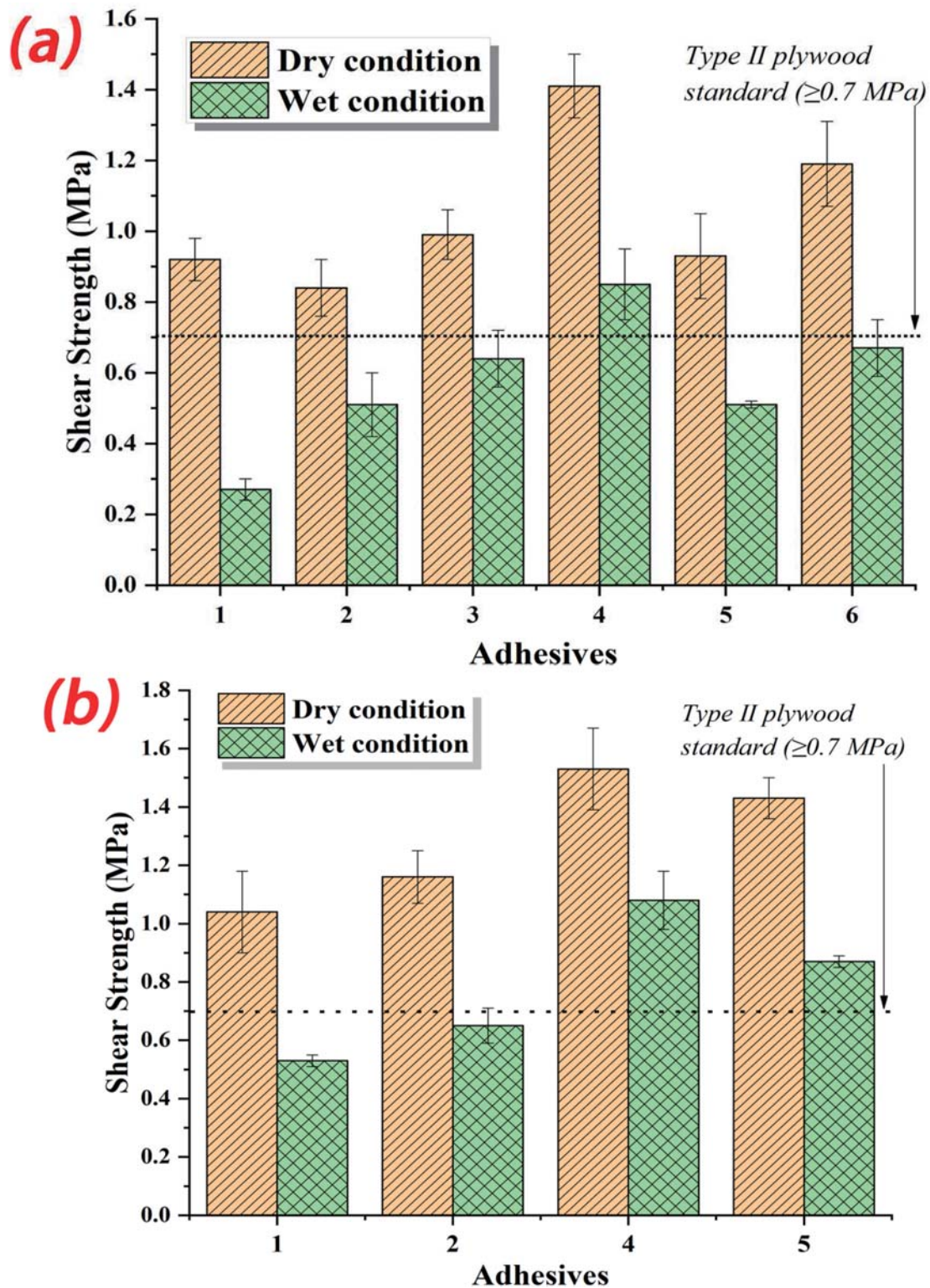


Fig. 6. Shear strength values of plywood bonded with the series of tannin-based adhesives. (a) hot press for 6 min; (b) hot press for 9 min.

3.6. Evaluation of bonding strength

The dry and wet (3 h soaking in hot water, tested wet) shear strengths of 3-ply plywood bonded with the different tannin-based NIPU adhesives were evaluated and the corresponding results are shown in Fig. 6 for two different hot-pressing times for the specimens. The bonded plywood with the unmodified tannin NIPU adhesive (Nr.1) showed a dry shear strength of 0.92 MPa, which satisfies the relevant standard requirement (≥ 0.7 MPa). Nevertheless, its wet shear strength only reached 0.27 MPa, far from the plywood requirements for interior use. This was attributed to the mass loss resulting from HMDA evaporation and/or incomplete curing during hot-pressing. It is well known that most of the biomass materials (glucose, non-furanic humins, and lignin) based NIPU adhesives need higher curing temperatures or longer curing times for a satisfactory bonding performance to be obtained [42]. Thus, unstable chemical bonds and free unlinked molecules in the network respond to the hydrolytic conditions in different ways such as cleavage of the bonds and dissolution in water, resulting in the appearance of some defects in the original adhesive layer. The residual weights after hydrolysis (shown in Table 1) support this explanation. The bonding performance can hold different degrees of improvement with the GDE introduction and reach maximum strength values of 1.41 MPa (dry) and 0.85 MPa (wet) for plywood bonded with adhesive 4. In addition, their corresponding wood failures are attained at 65 % and 25 %, respectively. These results indicate that the GDE addition enhanced the bonding performance, principally due to GDE preventing weight loss, and parallel formation of stable, robust chemical structures (non-hydrolyzed ether bonds) [40,42]. The high reactivity between epoxy groups and amino groups promoted the adhesive to start curing and crosslinking more actively in shorter time [47]. High GDE addition can improve the cross-linking between the different components present, but the high reactivity has to some extent a negative effect on the preparation of plywood. It was noticed that the shear strength of plywood based on adhesives 5 and 6 was lower as compared to that of adhesive 4. This is due to the high reactivity of epoxy and amino groups, which induces the rapid increase of viscosity of the adhesive, rendering it more difficult for the adhesive to spread and grip efficiently the wood surface.

Similarly, Fig. 6 (b) shows the comparable shear strength values obtained with a hot-pressing time of 9 min. The plywood bonded by adhesive 1 presented the lowest strength value, 1.04 MPa and 0.57 MPa for the dry and wet conditions, respectively, but still higher than the plywood pressed for 6 min. The shear strength was enhanced as the GDE addition increased further, and progressively met the plywood requirements for indoor use. The plywood specimen bonded with adhesive 4 showed the best bonding performance, 1.53 MPa and 1.03 MPa for the dry and wet conditions, respectively, along with 80% and 35 % wood failure, respectively. Therefore, a longer press time can enhance the bonding performance but will consume a higher energy.

4. Conclusions

Commercial glycerol diglycidyl ether (GDE) was evaluated as an enhancer for tannin-based NIPU wood adhesives and it can be concluded from the results that the crosslinking reactions between GDE epoxy groups and amino groups containing derived-products of NIPU proceeded smoothly, which proves the role of GDE to promote the curing at a reduced curing temperature and advancement of crosslinking. The improvement extended to a higher viscosity, solids content, and residual weight after exposure to hydrolytic conditions. The enhancement imposed on the crosslinking network as a result of much stronger bonds formation was also translated into higher thermal stability, which was also supported by a favorable morphology of the fracture surface. Most important, plywood bonded with the unmodified adhesive could not attain good wet shear strength, however, the GDE-modified adhesive presented a relevantly higher wet shear strength than the unmodified

adhesive due to its more cross-linked cured network especially at a longer hot press time.

Acknowledgements

This work was supported by the Key Program of Applied and Basic Research in Yunnan Province (Grant No. 202101AS070008), the National Natural Science Foundation of China (NSFC 31971595), Yunnan provincial youth and middle-age reserve talents of academic and technical leaders (2019HB026), Scholarship from China Scholarship Council, Yunnan Provincial Key Laboratory of Wood Adhesives and Glued Products.

The LERMAB, where this work was actually conceived and conducted, is supported by a grant of the French Agence Nationale de la Recherche (ANR) as part of the laboratory of excellence (LABEX) ARBRE.

Appendix A. Supplementary data

Supplementary data to this article can be found online at <https://doi.org/10.1016/j.ijadhadh.2021.103001>.

References

- [1] Cui S, Liu Z, Li Y. Bio-polyols synthesized from crude glycerol and applications on polyurethane wood adhesives. *Ind Crop Prod* 2017;108:798–805. <https://doi.org/10.1016/j.indcrop.2017.07.043>.
- [2] Cui S, Luo X, Li Y. Synthesis and properties of polyurethane wood adhesives derived from crude glycerol-based polyols. *Int J Adhesion Adhes* 2017;79:67–72. <https://doi.org/10.1016/j.ijadhadh.2017.04.008>.
- [3] Dodangeh F, Seyed Dorraji MS, Rasoulifard MH, Ashjari HR. Synthesis and characterization of alkoxy silane modified polyurethane wood adhesive based on epoxidized soybean oil polyester polyol. *Compos B Eng* 2020;187:107857. <https://doi.org/10.1016/j.compositesb.2020.107857>.
- [4] Jasiūnas L, Peck G, Bridziuvienė D, Miknius L. Mechanical, thermal properties and stability of high renewable content liquefied residual biomass derived bio-polyurethane wood adhesives. *Int J Adhesion Adhes* 2020;101:102618. <https://doi.org/10.1016/j.ijadhadh.2020.102618>.
- [5] Gadhave RV, Kasbe PS, Mahanwar PA, Gadekar PT. Synthesis and characterization of lignin-polyurethane based wood adhesive. *Int J Adhesion Adhes* 2019;95:102427. <https://doi.org/10.1016/j.ijadhadh.2019.102427>.
- [6] Ghosh S, Ganguly S, Remanan S, Mondal S, Jana S, Maji PK, et al. Ultra-light weight, water durable and flexible highly electrical conductive polyurethane foam for superior electromagnetic interference shielding materials. *J Mater Sci Mater Electron* 2018;29:10177–89. <https://doi.org/10.1007/s10854-018-9068-2>.
- [7] Fan X, Tan BH, Li Z, Loh XJ. Control of PLA stereoisomers-based polyurethane elastomers as highly efficient shape memory materials. *ACS Sustainable Chem Eng* 2017;5:1217–27. <https://doi.org/10.1021/acscuschemeng.6b02652>.
- [8] Li H, Xu CC, Yuan Z, Wei Q. Synthesis of bio-based polyurethane foams with liquefied wheat straw: process optimization. *Biomass Bioenergy* 2018;111:134–40. <https://doi.org/10.1016/j.biombioe.2018.02.011>.
- [9] de Haro JC, Allegretti C, Smit AT, Turri S, D'Arrigo P, Griffini G. Biobased polyurethane coatings with high biomass content: tailored properties by lignin selection. *ACS Sustainable Chem Eng* 2019;7:11700–11. <https://doi.org/10.1021/acscuschemeng.9b01873>.
- [10] Li H, Feng S, Yuan Z, Wei Q, Xu CC. Highly efficient liquefaction of wheat straw for the production of bio-polyols and bio-based polyurethane foams. *Ind Crop Prod* 2017;109:426–33. <https://doi.org/10.1016/j.indcrop.2017.08.060>.
- [11] Zhang J, Hori N, Takemura A. Optimization of agricultural wastes liquefaction process and preparing bio-based polyurethane foams by the obtained polyols. *Ind Crop Prod* 2019;138:111455. <https://doi.org/10.1016/j.indcrop.2019.06.018>.
- [12] Pillai PK, Li S, Bouzidi L, Narine SS. Metathesized palm oil & novel polyol derivatives: structure, chemical composition and physical properties. *Ind Crop Prod* 2016;84:205–23. <https://doi.org/10.1016/j.indcrop.2016.02.008>.
- [13] Liu J, Yang Y, Gao B, Li YC, Xie J. Bio-based elastic polyurethane for controlled-release urea fertilizer: fabrication, properties, swelling and nitrogen release characteristics. *J Clean Prod* 2019;209:528–37. <https://doi.org/10.1016/j.jclepro.2018.10.263>.
- [14] Borowicz M, Paciorek-Sadowska J, Isbrandt M. Synthesis and application of new bio-polyols based on mustard oil for the production of selected polyurethane materials. *Ind Crop Prod* 2020;155:112831. <https://doi.org/10.1016/j.indcrop.2020.112831>.
- [15] Liu H, Li C, Sun XS. Soy-oil-based waterborne polyurethane improved wet strength of soy protein adhesives on wood. *Int J Adhesion Adhes* 2017;73:66–74. <https://doi.org/10.1016/j.ijadhadh.2016.09.006>.
- [16] Patil CK, Rajput SD, Marathe RJ, Kulkarni RD, Phadnis H, Sohn D, et al. Synthesis of bio-based polyurethane coatings from vegetable oil and dicarboxylic acids. *Prog Org Coat* 2017;106:87–95. <https://doi.org/10.1016/j.porgcoat.2016.11.024>.

- [17] Peyrton J, Chambaretaud C, Sarbu A, Averous L. Biobased Polyurethane foams based on new polyols architectures from microalgae oil. *ACS Sustainable Chem Eng* 2020;8:12187–96. <https://doi.org/10.1021/acssuschemeng.0c03758>.
- [18] Si W-J, Yang L, Weng Y-X, Zhu J, Zeng J-B. Poly (lactic acid)/biobased polyurethane blends with balanced mechanical strength and toughness. *Polym Test* 2018;69:9–15. <https://doi.org/10.1016/j.polymertesting.2018.05.004>.
- [19] Grignard B, Thomassin J-M, Gennen S, Poussard L, Bonnaud L, Raquez J-M, et al. CO₂-blown microcellular non-isocyanate polyurethane (NIPU) foams: from bio- and CO₂-sourced monomers to potentially thermal insulating materials. *Green Chem* 2016;18:2206–15. <https://doi.org/10.1039/C5GC02723C>.
- [20] Blattmann H, Mülhaupt R. Multifunctional POSS cyclic carbonates and non-isocyanate polyhydroxyurethane hybrid materials. *Macromolecules* 2016;49:742–51. <https://doi.org/10.1021/acs.macromol.5b02560>.
- [21] Ghasemlou M, Daver F, Ivanova EP, Adhikari B. Synthesis of green hybrid materials using starch and non-isocyanate polyurethanes. *Carbohydr Polym* 2020;229:115535. <https://doi.org/10.1016/j.carbpol.2019.115535>.
- [22] Xi X, Pizzi A, Delmotte L. Isocyanate-free polyurethane coatings and adhesives from mono- and di-saccharides. *Polymers* 2018;10:402. <https://doi.org/10.3390/polym10040402>.
- [23] Samanta S, Selvakumar S, Bahr J, Wickramaratne DS, Sibi M, Chisholm BJ. Synthesis and characterization of polyurethane networks derived from soybean-oil-based cyclic carbonates and bioderivable diamines. *ACS Sustainable Chem Eng* 2016;4:6551–61. <https://doi.org/10.1021/acssuschemeng.6b01409>.
- [24] Wang C, Wu Z, Tang L, Qu J. Synthesis and properties of cyclic carbonates and non-isocyanate polyurethanes under atmospheric pressure. *Prog Org Coating* 2019;127:359–65. <https://doi.org/10.1016/j.porgcoat.2018.11.040>.
- [25] Thébault M, Pizzi A, Essawy HA, Barhoum A, Van Assche G. Isocyanate free condensed tannin-based polyurethanes. *Eur Polym J* 2015;67:513–26. <https://doi.org/10.1016/j.eurpolymj.2014.10.022>.
- [26] Thébault M, Pizzi A, Dumarçay S, Gerardin P, Fredon E, Delmotte L. Polyurethanes from hydrolysable tannins obtained without using isocyanates. *Ind Crop Prod* 2014;59:329–36. <https://doi.org/10.1016/j.indcrop.2014.05.036>.
- [27] Chen X, Li J, Xi X, Pizzi A, Zhou X, Fredon E, et al. Condensed tannin-glucose-based NIPU bio-foams of improved fire retardancy. *Polym Degrad Stabil* 2020;175:109121. <https://doi.org/10.1016/j.polydegradstab.2020.109121>.
- [28] Chen X, Xi X, Pizzi A, Fredon E, Zhou X, Li J, et al. Preparation and characterization of condensed tannin non-isocyanate polyurethane (NIPU) rigid foams by ambient temperature blowing. *Polymers* 2020;12:750. <https://doi.org/10.3390/polym12040750>.
- [29] Xi X, Pizzi A, Gerardin C, Lei H, Chen X, Amirou S. Preparation and evaluation of glucose based non-isocyanate polyurethane self-blowing rigid foams. *Polymers* 2019;11:1802. <https://doi.org/10.3390/polym11111802>.
- [30] Xi X, Wu Z, Pizzi A, Gerardin C, Lei H, Zhang B, et al. Non-isocyanate polyurethane adhesive from sucrose used for particleboard. *Wood Sci Technol* 2019;53:393–405. <https://doi.org/10.1007/s00226-019-01083-2>.
- [31] Xi X, Pizzi A, Gerardin C, Du G. Glucose-biobased non-isocyanate polyurethane rigid foams. *J Renew Mater* 2019;7:301–12. <https://doi.org/10.32604/jrm.2019.04174>.
- [32] Chen X, Pizzi A, Xi X, Zhou X, Fredon E, Gerardin C. Soy protein isolate non-isocyanates polyurethanes (NIPU) wood adhesives. *J Renew Mater* 2021;9:1045–57. <https://doi.org/10.32604/jrm.2021.015066>.
- [33] Chen X, Pizzi A, Essawy H, Fredon E, Gerardin C, Guigo N, et al. Non-furanic humins-based non-isocyanate polyurethane (NIPU) thermoset wood adhesives. *Polymers* 2021;13:372. <https://doi.org/10.3390/polym13030372>.
- [34] Sutter M, Silva ED, Duguet N, Raoul Y, Métay E, Lemaire M. Glycerol ether synthesis: a bench test for green chemistry concepts and technologies. *Chem Rev* 2015;115:8609–51. <https://doi.org/10.1021/cr5004002>.
- [35] Pizzi A, Meikleham N. Induced accelerated autocondensation of polyflavonoid tannins for phenolic polycondensates. III. CP-MAS ¹³C-NMR of different tannins and models. *J Appl Polym Sci* 1995;55:1265–9. <https://doi.org/10.1002/app.1995.070550812>.
- [36] Jean-Pierre Habas V.L., Amelia Ulloa, HabasOlivia Giani, US20150011680A1, 2012.
- [37] Jahanshahi S, Pizzi A, Abdulkhani A, Doosthoseini K, Shakeri A, Lagel M, et al. MALDI-TOF, ¹³C NMR and FT-MIR analysis and strength characterization of glycidyl ether tannin epoxy resins. *Ind Crop Prod* 2016;83:177–85. <https://doi.org/10.1016/j.indcrop.2015.11.067>.
- [38] Abdullah UHB, Pizzi A. Tannin-furfuryl alcohol wood panel adhesives without formaldehyde. *Eur J Wood Prod* 2013;71:131–2. <https://doi.org/10.1007/s00107-012-0629-4>.
- [39] Pizzi A, Stephanou A. Phenol-formaldehyde wood adhesives under very alkaline conditions. Part I: behaviour and proposed mechanism. *Holzforschung* 1994;48:35–40. <https://doi.org/10.1515/hfsg.1994.48.1.35>.
- [40] Li RJ, Gutierrez J, Chung Y-L, Frank CW, Billington SL, Sattely ES. A lignin-epoxy resin derived from biomass as an alternative to formaldehyde-based wood adhesives. *Green Chem* 2018;20:1459–66. <https://doi.org/10.1039/C7GC03026F>.
- [41] Li H, Li C, Gao Q, Zhang S, Li J. Properties of soybean-flour-based adhesives enhanced by attapulgit and glycerol polyglycidyl ether. *Ind Crop Prod* 2014;59:35–40. <https://doi.org/10.1016/j.indcrop.2014.04.041>.
- [42] Chen X, Pizzi A, Fredon E, Gerardin C, Li J, Zhou X, et al. Preparation and properties of a novel type of tannin-based wood adhesive. *J Adhes* 2020;1–18. <https://doi.org/10.1080/00218464.2020.1863215>.
- [43] Montané X, Dinu R, Mija A. Synthesis of resins using epoxies and humins as building blocks: a mechanistic study based on in-situ FT-IR and NMR spectroscopies. *Molecules* 2019;24:4110. <https://doi.org/10.3390/molecules24224110>.
- [44] Xu Y, Han Y, Shi SQ, Gao Q, Li J. Preparation of a moderate viscosity, high performance and adequately-stabilized soy protein-based adhesive via recombination of protein molecules. *J Clean Prod* 2020;255:120303. <https://doi.org/10.1016/j.jclepro.2020.120303>.
- [45] Saražin J, Pizzi A, Amirou S, Schmiel D, Šernek M. Organosolv lignin for non-isocyanate based polyurethanes (NIPU) as wood adhesive. *J Renew Mater* 2021;9:881–907. <https://doi.org/10.32604/jrm.2021.015047>.
- [46] Santos OSH, Coelho da Silva M, Silva VR, Mussel WN, Yoshida MI. Polyurethane foam impregnated with lignin as a filler for the removal of crude oil from contaminated water. *J Hazard Mater* 2017;324:406–13. <https://doi.org/10.1016/j.jhazmat.2016.11.004>.
- [47] Li J, Luo J, Li X, Yi Z, Gao Q, Li J. Soybean meal-based wood adhesive enhanced by ethylene glycol diglycidyl ether and diethylenetriamine. *Ind Crop Prod* 2015;74:613–8. <https://doi.org/10.1016/j.indcrop.2015.05.066>.

3.8 Bio-mousses NIPU condensées à base et tanin-glucose de résistance au feu améliorée

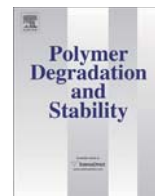
Résumé: Des mousses polyuréthanes non isocyanates auto-gonflantes à base de glucose ont été préparées dans nos travaux précédents. Ils ont montré d'excellentes propriétés comparables aux mousses commerciales en utilisant simplement une procédure de préparation simple. Ces mousses présentent néanmoins un inconvénient critique qui est leur inflammabilité. Dans la recherche présentée ici, un composé phénolique naturel, le tanin condensé, a été testé comme retardateur de flamme pour améliorer la résistance au feu des mousses NIPU à base de glucose. Un certain nombre de mousses NIPU à base de glucose à substitution tanin (tanin de mimosa remplaçant le glucose à 0%, 25% et 50%, respectivement) ont été préparées et caractérisées par microscopie électronique à balayage (MEB), spectroscopie infrarouge à transformée de Fourier (FT-IR), Analyse thermogravimétrique (TG), expérience d'allumage et indice limite d'oxygène (LOI). D'autres propriétés physiques et mécaniques, telles que les processus de moussage, la densité, la résistance à la compression, etc. ont également été étudiées. Les résultats ont indiqué que les mousses NIPU à base de glucose modifié par des tanins (T/G (1/3)-Fs et (T/G (1/1)-Fs)) présentent une taille de cellule moyenne plus petite, une résistance à la compression améliorée et une densité plus élevée que (T/G (0/4)-Fs). L'analyse FT-IR a montré que des liaisons uréthane se sont formées, la structure chimique de la mousse NIPU à base de glucose étant néanmoins conservée même si le glucose était partiellement remplacé par le tanin condensé. L'analyse thermogravimétrique a montré que la présence de tanin condensé diminuait légèrement la stabilité thermique des composites de mousse tanin-glucose NIPU. En outre, des expériences d'allumage ont également été réalisées dans lesquelles les mousses NIPU à base de glucose avec un tanin condensé ont montré un temps de combustion plus long que pur (T/G (0/4)-Fs). Enfin, les valeurs limites de l'indice d'oxygène (LOI) de 17,5% à 25,5%, montrent une valeur plus élevée avec l'augmentation de la substitution des tanins condensés.

Mots clés: Tanin condensé Mousse de biomasse Résistance au feu NIPU à base de glucose Résistance à la compression



Contents lists available at ScienceDirect

Polymer Degradation and Stability

journal homepage: www.elsevier.com/locate/polydegstab

Condensed tannin-glucose-based NIPU bio-foams of improved fire retardancy



Xinyi Chen ^{a,1}, Jinxing Li ^{b,1}, Xuedong Xi ^a, Antonio Pizzi ^{a,*}, Xiaojian Zhou ^b, Emmanuel Fredon ^a, Guanben Du ^b, Christine Gerardin ^c

^a LERMAB, University of Lorraine, 27 Rue Philippe Seguin, BP 1041, 88051, Epinal, France

^b Yunnan Provincial Key Laboratory of Wood Adhesives and Glued Products, Southwest Forestry University, Kunming, Yunnan province, China

^c LERMAB, University of Lorraine, Boulevard Does Aiguillettes, 54000, Nancy, France

ARTICLE INFO

Article history:

Received 22 January 2020

Received in revised form

21 February 2020

Accepted 28 February 2020

Available online 1 March 2020

Keywords:

Condensed tannin

Biomass foam

Fire resistance

Glucose-based NIPU

Compressive strength

ABSTRACT

Glucose-based self-blowing non-isocyanate polyurethanes foams were prepared in our previous work. They showed excellent properties comparable to commercial foams by just using a simple preparation procedure. These foams, nevertheless, present a critical drawback that is their flammability. In the research presented here a natural phenolic compound, condensed tannin, was tested as a flame-retardant to improve the fire resistance of glucose-based NIPU foams. A number of tannin-substituted glucose-based NIPU foams (mimosa tannin replacing glucose at 0%, 25% and 50%, respectively) were prepared and characterized by scanning electron microscopy (SEM), Fourier transform infrared spectroscopy (FT-IR), Thermogravimetric analysis (TG), ignition experiment and limiting oxygen index (LOI). Other physical and mechanical properties, such as foaming processes, density, compression strength, etc. were also investigated. The results indicated that the tannin-modified glucose-based NIPU foams (T/G (1/3)-Fs and (T/G (1/1)-Fs)) exhibit smaller mean cell size, improved compression strength and higher density than (T/G (0/4)-Fs). The FT-IR analysis showed that urethane linkages were formed, the chemical structure of glucose-based NIPU foam being nonetheless preserved even if the glucose was partially replaced by the condensed tannin. Thermogravimetric analysis showed that the presence of condensed tannin decreased the thermal stability of the tannin-glucose NIPU foam composites slightly. In addition, ignition experiments were also carried out in which the glucose-based NIPU foams with a condensed tannin showed longer burning time than neat (T/G (0/4)-Fs). Finally, limiting oxygen index (LOI) values from 17.5% to 25.5%, show a higher value with the increasing condensed tannin substitution.

© 2020 Elsevier Ltd. All rights reserved.

1. Introduction

Polyurethane foams (PUs), being light-weight, and presenting excellent insulating property, as well as superior mechanical properties, have been extensively utilized in buildings as thermal and acoustic insulation materials [1–3]. However, PUs exhibit substantial drawbacks, including toxic and expensive raw materials, flammability and dripping after combustion, even though they are widely utilized [4].

Demands for safer, non-toxic and inexpensive materials have driven researchers to explore new technologies and starting

materials. Lignin [5–7], tannin [8–10], sugar [11,12], forestry and agriculture waste [6,13,14] and other natural hydroxy-carrying compounds, are typical biomass resources that as partial or complete replacement of petroleum-based polyhydric alcohols have been tried to prepare PUs. It is the most commonly utilized strategy and this kind of foams is known, incorrectly, as “bio-foams”. Besides, another one is that non-isocyanate strategies for PU foams have been reported in the literature [15,16]. For example, such a latter approach used easily available, cost-effective materials and methods, such as the aminolysis of five-membered cyclic carbonates, to replace isocyanate when making PUs [4,17–22]. Unfortunately, some shortcomings were still discovered, including harsh reaction conditions and environment (high temperature, catalyst) [23], high toxic reagent (epichlorohydrin) [22] and high pressure [18,20].

We had initially sought a more environment friendly

* Corresponding author.

E-mail address: antonio.pizzi@univ-lorraine.fr (A. Pizzi).

¹ These authors contributed equally to this work.

preparation strategy recently. Fortunately, a bio-mass resource-based (mimosa tannin, a condensed tannin), low temperature (around 90 °C) and atmospheric pressure synthesis route was found [24,25]. Meanwhile, the glucose-based NIPUs so prepared have been used for wood coatings and wood bonding as well as to prepare foams [11,12,26]. The open cell foams obtained by high-temperature induced foaming has excellent properties, and its cellular structure is recovered after the pressure on it is released, even if the cell walls were flattened by compression.

Nevertheless, in common with traditional PUs, the all glucose-based NIPU foams, regardless if obtained at high temperature or room temperature, are flammable [12,26]. This limits their applications as fire resistance materials. Therefore, to improve their fire resistance still remained the key aim of the research work presented here. The literature reports that numerous types of flame retarding additive can improve the fire resistance of materials effectively, for instance, halogenated compounds [27], phosphorus-containing compounds [28,29] and nano-additives [30–34]. They either trigger a flame retarding barrier, or play a role as a layer blocking flammable gases, or both [35]. However, they will release toxic halogen- or phosphorus-containing gases which can threaten the environment during burning and the foam properties will deteriorate because of the high content of additives.

Nowadays, some researchers have turned their attention to bio-based flame retardants, such as tannin [36,37], caseins [38], phytic acid [39] and banana pseudo-stem sap liquid [40]. Tannins became the first candidate bio resourced material, which can be obtain from the bark, seeds and other parts of plentiful species of trees [41–43]. Moreover, they have many special properties such as antibacterial and antioxidant [44,45], precipitate proteins [46], reductants and stabilizers [47]. It was reported that tannins can act as a natural fire resistance to aid tree survival [48]. This is mainly attributed to their similar reactivity to phenol, phenoxy radicals could quench the oxygen free radicals when the polymer is decomposed during heating [35]. In addition, tannins have high char production efficiency when burning (55% char for condensed tannin and 28% char for tannic acid) [37,49,50], resulting in a protective layer, which is made of char and can block heat, oxygen, and flammable gases [51]. At the same time, due to their effect, the tannins can increase the foam mechanical properties while acting as a fire retardant [35].

Thus, the work presented here is focused on condensed tannin as a natural fire retardant to improve the flame resistance of glucose-based non-isocyanate polyurethane foams. The resins and foams prepared were obtained at ambient pressure, at different ratios of glucose and tannin. The morphology and performance of glucose/tannin foams were investigated by SEM, FT-IR and TG and other techniques. The fire resistance of all foams was determined by means of direct ignition and limiting the oxygen index (LOI) measurement.

2. Materials and methods

2.1. Materials

Mimosa tannin extract is a commercial product, namely mimosa tannin extracted from the bark of *Acacia mearnsii* (De Wild), supplied by Silva Chimica (St. Michele Mondovi, Italy). Glutaraldehyde (C₅H₈O₂, 50% water solution) was obtained from Acros Organics, France; Glucose (99.99%, anhydrous), Hexamethylenediamine (HDMA, 98%), Dimethyl carbonate (DMC, 99%, anhydrous), Hexamethylenetetramine (99%, ACS reagent), Citric acid (99.5%, ACS reagent), were supplied by Sigma-Aldrich (Saint Louis, France). All these chemical reagents did not need any further purification before use. Deionized water (DI) was produced in the laboratory.

2.2. Preparation process

2.2.1. Preparation of the glucose or glucose-tannin-based non-isocyanate polyurethanes (NIPUs)

The neat glucose or glucose-tannin-based NIPUs were prepared according to a procedure already reported [52]. Three kinds of NIPUs mixtures for foaming preparing were prepared in this work. Glucose or glucose/tannin mixture and deionized water were placed into three-necked flask with condensing reflux, magnetic stirring and thermometer. And then, dimethyl carbonate (DMC) was added into the mixture and stirred thoroughly, mixed evenly, and heated to 65 °C and remained for 1 h. Subsequently, 70% solution (in water) of hexamethylenediamine was added into the mixture under mechanical stirring, while the mixture was heated to 90 °C and remained for 2 h. Finally, the glucose or glucose-tannin-based NIPUs were obtained and cooled down to room temperature, standby application. The proportions of materials used are shown in Table 1.

2.3. Foam preparation

All foam samples were prepared according to our previous work already reported [12]. 10 g of G-NIPUs or T/G-NIPUs and 1 g hexamethylenetetramine were added into a 100 mL plastic beaker and then stirred at for 1 min. 8 g of the complex acid blowing agent (citric acid: glutaraldehyde = 3:1) was added and then the mixtures were stirred at room temperature for 10–15 s. The as-obtained flexible foams were placed at in ambient environment until the foam structure trend to stable. According to the species of T/G (0/4)-NIPUs, T/G (1/3)-NIPUs and T/G (1/1)-NIPUs as utilized in the experiments, the obtained flexible foams were recorded as T/G (0/4)-Fs, T/G (0/4)-Fs and T/G (0/4)-Fs, respectively. Subsequently, all flexible foam samples were put into the oven overnight at 70–80 °C and were taken out from the plastic beakers. The final cured foam samples were placed at ambient temperature (25 °C and 12% relative humidity) for 2 days prior to characterization.

2.4. Measurements

2.4.1. Behavior of foaming process

The behavior of the foaming process was investigated in terms of previous reported [53]. The rising time (the time from pouring the complex acid blowing agent into the NIPUs until full expansion of the resulting foam) and tack free time (the time from pouring the complex acid blowing agent into the NIPUs until the skin of the foam was no longer sticky) were two critical parameters of foaming process. A thermometer was fixed and deposited into inner of T/G-NIPUs to measure the foaming temperature changes in the foaming process. The rising time, tack free time and foaming temperature were accurate recorded and monitored, respectively. Each foaming process replicate was tested five times and average value was taken.

2.5. Fourier transform infrared (FT-IR) spectroscopy

The functional groups of all foam samples were analyzed with a PerkinElmer Frontier ATR-FT-MIR provided by an ATR Miracle

Table 1
The formulation of glucose or glucose-tannin-based NIPUs.

Samples	Tannin (g)	Glucose (g)	DMC (g)	HDMA (g)	Water (g)
T/G (0/4)-NIPUs	0	40	27	77.6	33.34
T/G (1/3)-NIPUs	10	30	27	77.6	33.34
T/G (1/1)-NIPUs	20	20	27	77.6	33.34

diamond crystal. The sample powders were laid on the diamond eye (1.8 mm) of the ATR equipment and the contact for the sample was ensured by tightly screwing the clamp device. Each sample was scanned registering the spectrum with 32 scans with a resolution of 4 cm^{-1} in the wave number range between 600 and 4000 cm^{-1} .

2.6. Scanning electron microscopy (SEM) observation

To investigate the cell microstructure and morphology of glucose or tannin-glucose-based NIPUs foams, the scanning electron microscopy (Gemini SEM 300, Germany) was used with an acceleration voltage of 10 kV. The cell morphologies were statistically analyzed depend on the SEM images by Nano Measurer 1.2 [54]. The cell size distributions of all foams were calculated. The abovementioned parameters were calculated by averaging several tens of individual cells for each sample.

2.7. Apparent density

The apparent densities were obtained as the ratio of weight to cubic specimen volume, according to ASTM D1622-08. The size of the samples was $30\text{ mm} \times 30\text{ mm} \times 30\text{ mm}$. The average of five samples was determined.

2.8. TG analysis

The thermal stability of the foams was measured by using a TGA5500 analyzer (TA instruments, USA). Sample powder amounting to 5–8 mg was transferred to a platinum pan, with the temperature ranging from $25\text{ }^{\circ}\text{C}$ to $790\text{ }^{\circ}\text{C}$ at a heating rate of $10\text{ }^{\circ}\text{C}\cdot\text{min}^{-1}$ in a nitrogen atmosphere.

2.9. Compression strength

The compression strength of the foams in the direction parallel to that of the foam rise were determined under ambient conditions by using a universal testing machine (Instron 3300, Elancourt, France). The size of the samples was $25\text{ mm} \times 25\text{ mm} \times 25\text{ mm}$, and the crosshead rate was fixed at 2.0 mm min^{-1} for each sample. At least three samples were tested to determine the average value.

2.10. Direct ignition test

The direct ignition test was carried out according to a method already described in the literature [12]. Foam samples were made to specification size, $30\text{ mm} \times 30\text{ mm} \times 30\text{ mm}$, and then were exposed facially to a stainless-steel frame preheated on a Bunsen burner (around $1000\text{ }^{\circ}\text{C}$). Making sure the samples were located in the outer flame area of the Bunsen burner. The burning time was calculated starting by the samples were placed on the burner, till the flame of sample was considered as extinguished. Subsequently, the sample chars were weighted and noted as quality of residue. All tests were carried out in a closed environment to minimize the influence of other factors. Each foam type was tested three times.

2.10.1. Limiting oxygen index (LOI)

The limiting oxygen index (LOI) was measured according to a method reported in the literature [53] using an HC-2 oxygen index meter (Jiangning Analysis Instrument Company, China). All samples were prepared to specification size of $80\text{ mm} \times 10\text{ mm} \times 10\text{ mm}$. The LOI values used were the averages for the five samples.

3. Results and discussion

3.1. Preparation of tannin-glucose-based NIPUs foams (T/G (0/4)-Fs, T/G (1/3)-Fs and T/G (1/1)-Fs)

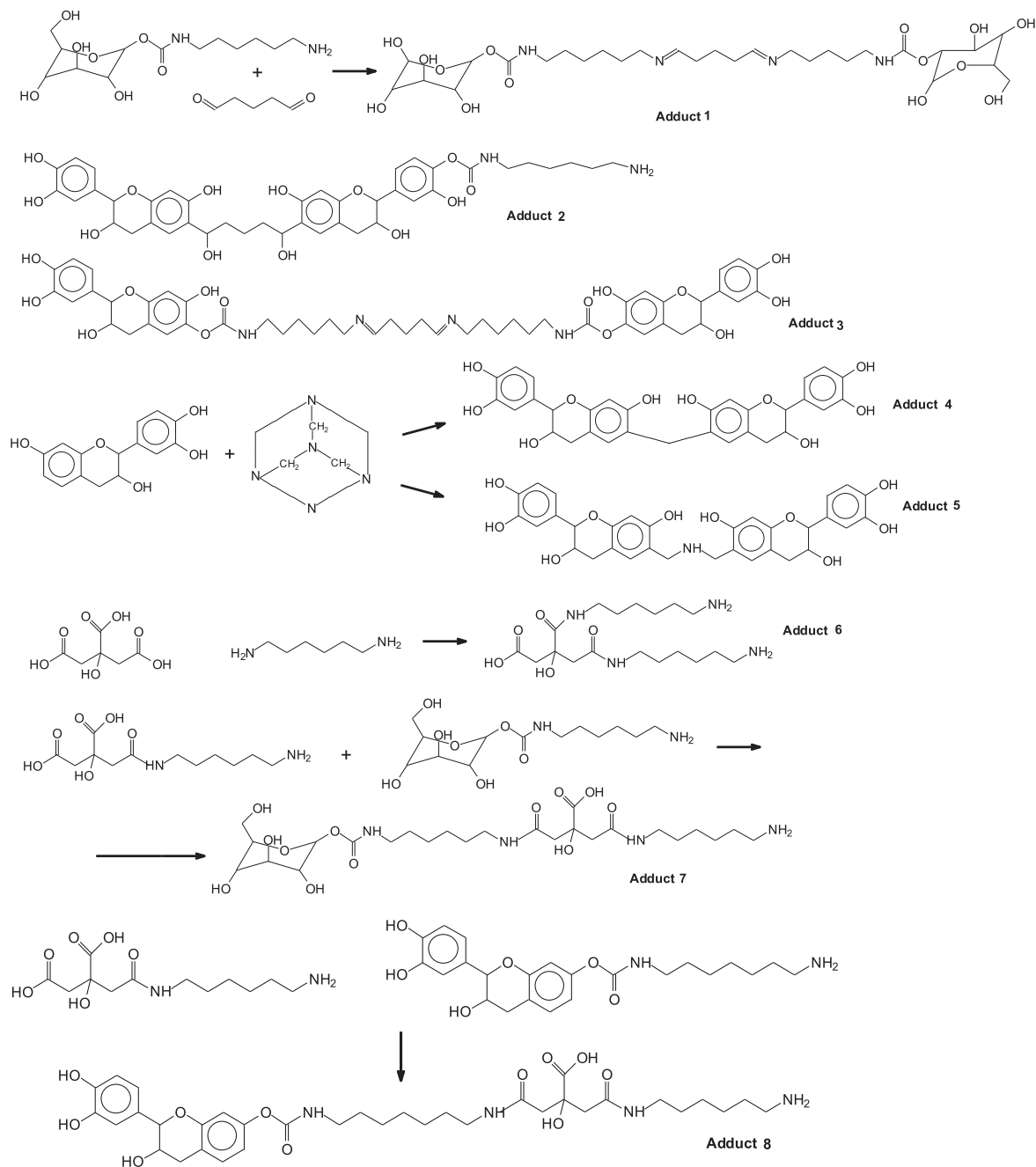
The tannin-glucose-based NIPUs foams (T/G (0/4)-Fs, T/G (1/3)-Fs and T/G (1/1)-Fs) were prepared with ease at ambient temperature. The main foreseeable adducts formed by multiple reactions eventually leading to structural networks in the foam are shown in Scheme 1. The foaming process can be divided into two main processes: the first one is the foaming process. The energy in this stage was produced from the rather violent reaction with citric acid and $-\text{NH}_2$ groups (obtaining the adducts 6, 7 and 8), which provides the self-blowing energy at room temperature [12]. The second one is the network crosslinking. Hexamethylenetetramine and glutaraldehyde act as crosslinkers to ensure that the liquid foam formed does not collapse and be maintained (obtaining the adducts 1, 2, 3, 4 and 5). And then, these adducts can further crosslink to form large molecules, which can intertwine with each other. Ultimately, this effect causes the sharp increase of the viscosity of the mixture and then its gelling, resulting in a three-dimensional network (cf. Scheme 2). In fact, these two processes occur almost simultaneously. The reason for this analysis is to better understand the whole foaming process.

3.2. Apparent density

The prepared liquid flexible foams so prepared need to be hardened by heating, which was necessary to obtain and measure stable physical properties. Consequently, tannin-glucose-based foams (T/G (0/4)-Fs, T/G (1/3)-Fs and T/G (1/1)-Fs) with stable properties were prepared and shown in Fig. 1. Some subtle differences between these three foam types can be seen, such as apparent color, foam cell status and cells size. The foam structures will be discussed in the following section, by comparing the scanning electron microscopy (SEM) observation. All foams, once the tannin was introduced, showed a black/red surface color. The reason of this is the reddening of mimosa tannin under acid conditions. Moreover, the apparent densities of the foams (cf. Table 2) increased as a function of the increase in the proportion of tannin. Thus, 50% tannin substitution yielded foams (T/G (1/1)-Fs) with the higher density, approximately 0.25 g cm^{-3} , while the T/G (0/4)-Fs without tannin presented the lower density, around 0.15 g cm^{-3} . This increase in foam density is ascribed to the more rapid gelling with tannin and glutaraldehyde resulting in a higher cross-linking level much earlier in the foaming process. Moreover, hexamethylenetetramine can provide further cross-linking with tannin when the soft foams are heat-hardened. Thus, it appears that the extent of cross-linking progressively increases with the addition of tannin.

3.3. Fourier transform infrared (FT-IR) spectroscopy

Fourier Transform Infrared (FT-IR) spectra of all foams are shown in Fig. 2, to investigate the functional groups changes occurring in these foam preparations. The results indicate that T/G (0/4)-Fs, T/G (1/3)-Fs and T/G (1/1)-Fs presents similar chemical structures, however, and quite distinct from neat tannin (red curve) and glucose (black curve). The main absorption peaks on the spectra were identified by arrows and imaginary segmented lines. In view of Fig. 2, an intense broad absorption band between 3500 and 3100 cm^{-1} is characteristic of the $-\text{OH}$ groups [16,55]. This broad peak is clearly apparent in the FT-IR spectra of neat tannin and glucose as well. The 3337 cm^{-1} $-\text{N}-\text{H}$ stretching peak is attributed to secondary amides, and concerns two kinds of reaction products obtained (one of them being urethane groups) [24]. Furthermore, there are two clear absorption peaks at 2930 cm^{-1} and 2856 cm^{-1} , especially in the NIPU

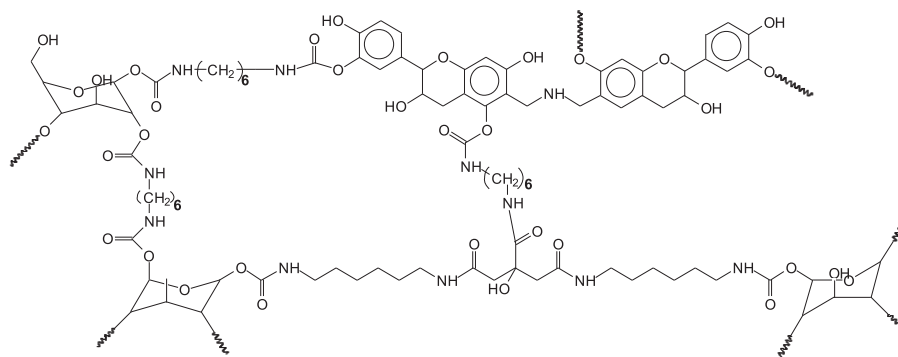


Scheme 1. The main foreseeable adducts formed by multiple reactions eventually leading to structural networks in the foam.

foams, which are attributed to the C–H stretching vibration of $-\text{CH}_2$ and $-\text{CH}_3$ [16,52]. As shown in Fig. 2 (b), there is some strong evidence for the formation of carbamate bonds. Of these the 1702 cm^{-1} band was attributed to the C=O from urethane groups and the 1645 cm^{-1} band to the C=O from ester groups [16,52]. Moreover, the 1536 cm^{-1} band is also characteristic of the urethane group confirming the formation of carbamate structures [16]. In the FT-IR spectrum of neat tannin and glucose, nevertheless, these kinds of absorption peaks have not been detected. Such evidence shows that glucose-based NIPU foams are obtained by the non-isocyanate approach taken under atmospheric pressure and low temperature. Therefore, even if glucose was only partially replaced by condensed tannin, the chemical structure of glucose-based NIPUs foams does not appear to be affected.

3.4. SEM analysis

SEM was used to investigate the foams morphology at different replacement levels of condensed tannin. The SEM images of the T/G (0/4)-Fs, T/G (1/3)-Fs and T/G (1/1)-Fs are shown in Fig. 3. From this it appears that all foams present a regular cells morphology. A considerable number of open pores are observed in Fig. 3 (a), (d) and (g), attributed to water evaporation in the precursor resins during foaming and drying. Furthermore, some ruptures or debris also can be observed in all foams, these being ascribed to the cutting process in preparing the samples [54]. Comparing Fig. 3(b) and (e), (h), thicker cell walls were obtained with increasing the presence of condensed tannin. This phenomenon belongs to the thickening function of tannin-derived products on glucose-based



Scheme 2. A schematic example of some of the mixed linkages present in a possible network structure of tannin/glucose foam.

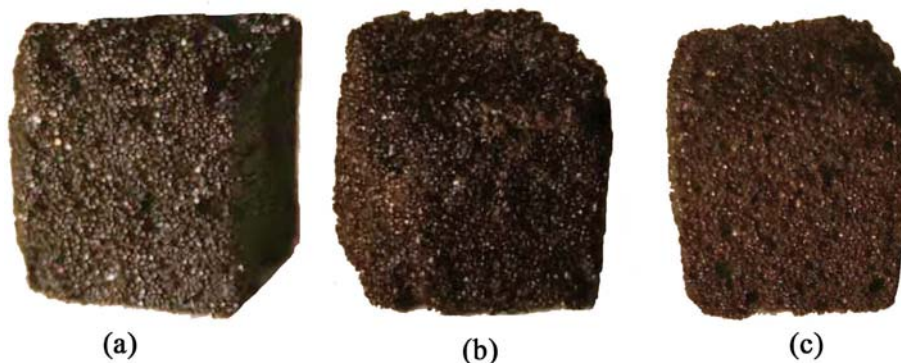


Fig. 1. Digital images of three kinds of target foam samples. (a) T/G (0/4)-Fs; (b) T/G (1/3)-Fs; (c) T/G (1/1)-Fs.

Table 2

Apparent density mean cell size and specific compressive strength of T/G (0/4)-Fs, T/G (1/3)-Fs and T/G (1/1)-Fs.

Samples	Apparent density (g cm^{-3})	Mean cell size (μm)	Specific compressive strength (kPa/kg m^{-3})
T/G (0/4)-Fs	0.15 ± 0.02	252.18 ± 41.55	1.22 ± 0.19
T/G (1/3)-Fs	0.19 ± 0.02	246.23 ± 49.19	1.27 ± 0.23
T/G (1/1)-Fs	0.25 ± 0.03	243.08 ± 50.40	1.51 ± 0.20

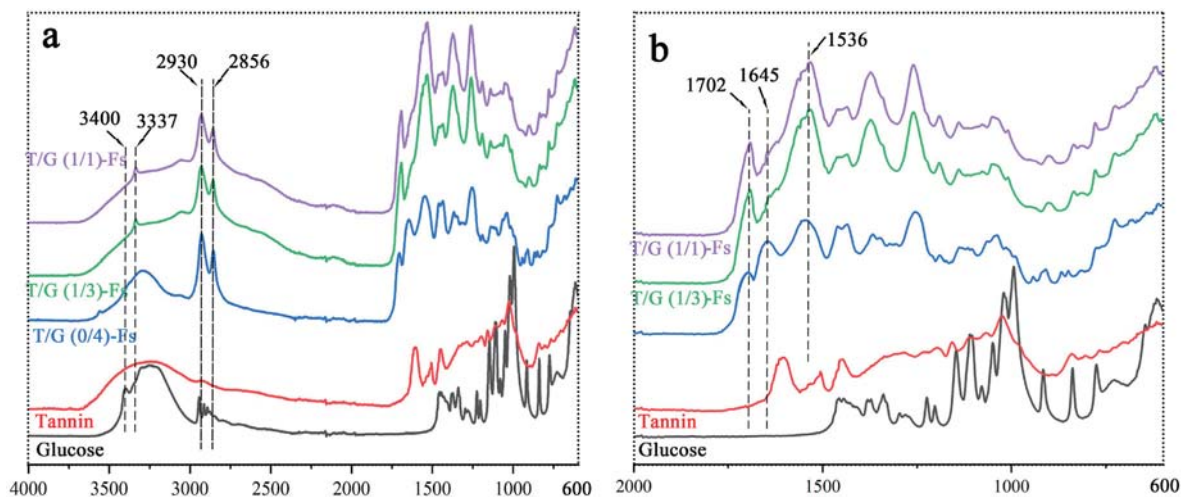


Fig. 2. FT-IR spectra of neat tannin, glucose, glucose based NIPUs foam and tannin/glucose based NIPUs foam. (a) the wavenumber from 600 to 4000 cm^{-1} ; (b) the wavenumber from 600 to 2000 cm^{-1} .

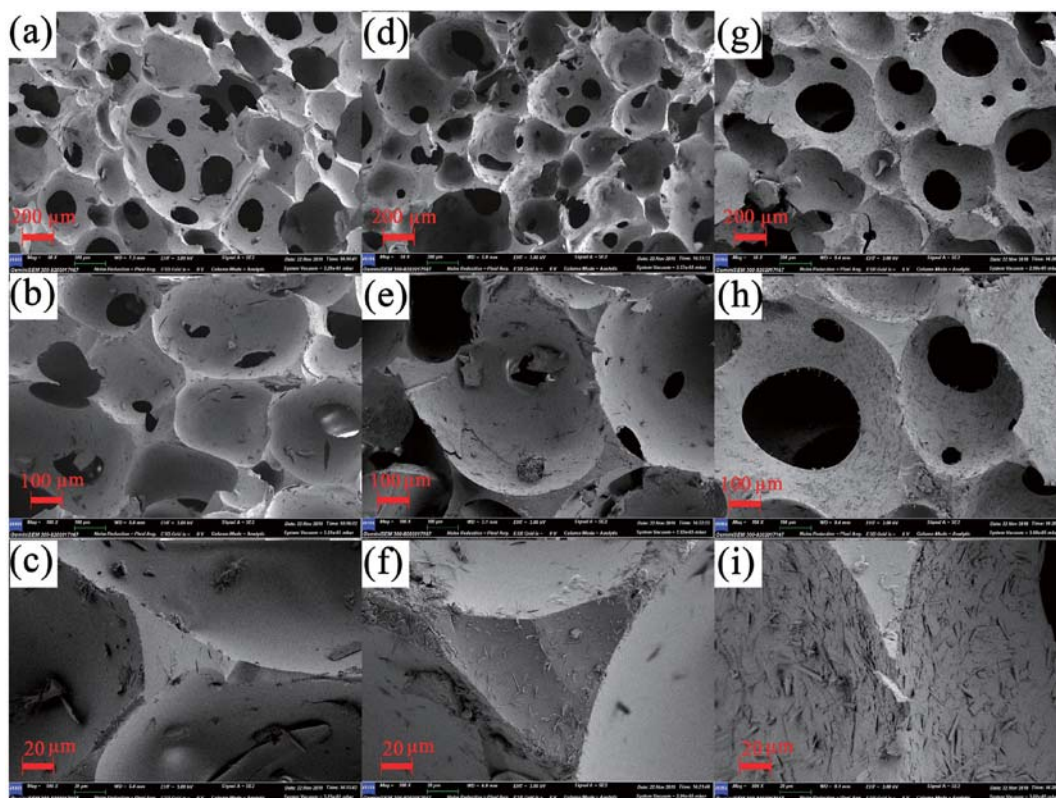


Fig. 3. SEM images of the T/G (0/4)-Fs (a–c), T/G (1/3)-Fs (d–f) and T/G (1/1)-Fs (g–i).

NIPU foam. Furthermore, in Fig. 3(f), (i), some fibrous polymers can also be clearly seen, interspersed in the cell wall or attached to their surfaces. These fibrous polymers as filler interspersed in glucose-based NIPU foam, resulted not only in an expansion effect that thickened the cell wall, but in the progressive increases of compression strength. As well as the number of fibrous polymers and cell walls thickness progressively increases by tannin addition the compression strength also progressively increases. Just because of this reason, the condensed modified foams obtained a smaller mean cell size (cf. Table 2).

According to literatures [55], condensed tannins have higher temperature (above 500 °C) carbonization efficiency under an atmospheric environment. Therefore, in view of Fig. 3(f), (i), the tannin-derived fibrous polymers inserted into, or covering the cell walls can be transformed into char or a char covering layer after high temperature decomposition. This is mainly attributed to their similar reactivity to phenol, phenoxy radicals being able to quench the oxygen free radicals when the polymer is decomposed during heating [35]. Therefore, the char so formed can either retard or even prevent effectively the combustion process of the foams. Conversely, without any tannin addition a smooth fracture surface and inner surface of T/G (0/4)-Fs can be seen in Fig. 3(c). Precisely due to this surface smoothness of T/G (0/4)-Fs, glucose-derived products alone do not have high carbonization efficiency so that they can only provide a limited protection during ignition and LOI testing. Hence, the interspersed and attached tannin-derived polymers in T/G (1/3)-Fs and T/G (1/1)-Fs cell wall can form a protecting char layer when these foams are exposed to high temperatures condition. These can well explain why in ignition experiments only a much smaller flame can be seen and a higher LOI was obtained for T/G (1/3)-Fs and T/G (1/1)-Fs foams, compared to T/G (0/4)-Fs.

3.5. Thermogravimetric analysis (TGA)

Thermogravimetric analysis (TGA) has been routinely used to evaluate the thermal stability of various foams [54–57]. Thus, the TGA (a) and DTG (b) curves of T/G (0/4)-Fs, T/G (1/3)-Fs and T/G (1/1)-Fs under N_2 atmosphere are shown in Fig. 4. The corresponding specific degradation temperatures and char yields at 790 °C are listed in Table 3. The T_{max} value reported in Table 3 is the maximum temperature shown by DTG curves peaks at different pyrolysis stages. It can be observed that all foam samples present a similar pyrolysis behavior, with two-stage decomposition which are typical of the pyrolysis of polyurethane foams [58]. The first mass loss stage occurs within the temperature range of 150 °C–300 °C, which belongs to the decomposition reaction of the bond cleavage of urethane [56]. The second mass loss stage occurs between 380 °C and 600 °C, this been attributed to the breaking of C–C bonds and the further decomposition of pyrolysis residual products from the first stage [55,56]. It is still worth noting that the DTG curve views a small peak at low temperature between 50 °C and 100 °C, which may be ascribed to decompose of excess acid and hexamethylenetetramine, as well as volatilize of absorbed water.

In Fig. 4, some significant differences can be observed when increasing the condensed tannin content, resulting in a slight decrease of the pyrolysis temperature of the foams. Nevertheless, the percentage value of the final residual mass at 790 °C indicates that all foam samples have a similar percentage mass loss, their residual mass being around 14–15% under a N_2 atmosphere. Between T/G (0/4)-Fs, T/G (1/3)-Fs and T/G (1/1)-Fs, a noticeable change can be seen, which is a shift of the decomposition temperature to lower temperatures, from 225 °C (first stage) 462 °C (second stage) decrease to 210 °C (first stage) and 441 °C (second stage) and 208 °C (first stage) 435 °C (second stage), respectively

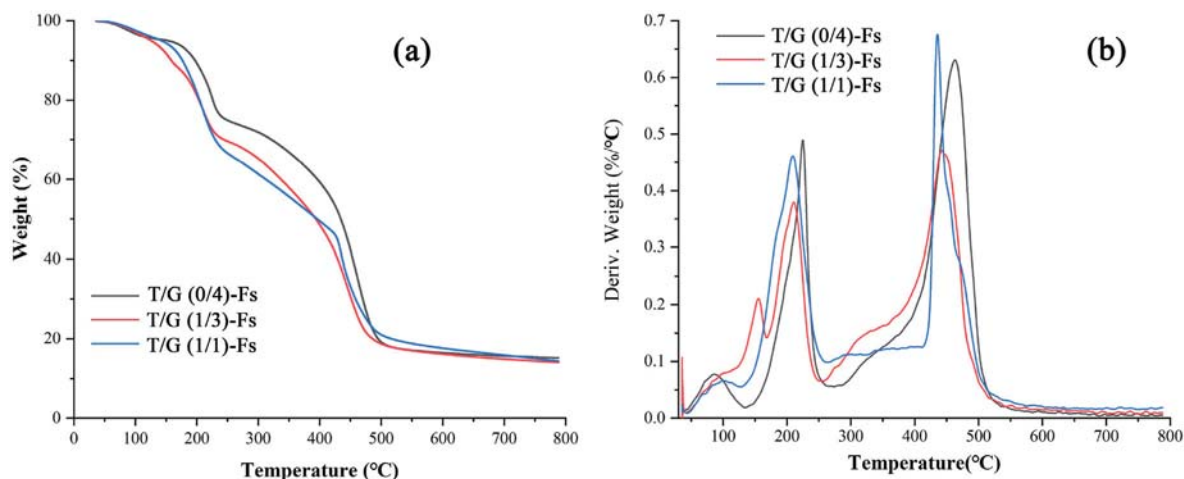


Fig. 4. TGA (a) and DTG (b) curves of T/G (0/4)-Fs, T/G (1/3)-Fs and T/G (1/1)-Fs (under N_2 atmosphere).

Table 3

DTG data of T/G (0/4)-Fs, T/G (1/3)-Fs and T/G (1/1)-Fs (under N_2 atmosphere).

Samples	T_{max} ($^{\circ}C$)		Residual mass at 790 $^{\circ}C$ (%)
	Step I	Step II	
T/G (0/4)-Fs	225	462	15.1
T/G (1/3)-Fs	210	441	14.4
T/G (1/1)-Fs	208	435	14.2

(cf. Table 3). This is likely to be the initial thermal depolymerization of mimosa tannin extract at lower temperature, this occurring around 146 $^{\circ}C$ and the partial breakage of the intermolecular bonds of condensed tannin at around 450 $^{\circ}C$ [55]. This phenomenon was similar with others described in the literature [54,55]. Therefore, condensed tannin addition reduced thermal stability of NIPU foams under a N_2 atmosphere.

3.6. Compressive mechanical properties

Compression experiments were conducted to determine the effect of different tannin substitution on the compressive mechanical properties of glucose-based NIPU foams. The compressive stress-strain curves of T/G (0/4)-Fs, T/G (1/3)-Fs and T/G (1/1)-Fs samples are shown in Fig. 5. The three-section curve is composed of three stages, namely the elastic behavior of the foam's cell wall bending(I), cell collapse(II) and densification(III) [59]. As shown in Fig. 5, T/G (1/1)-Fs shows the highest compression strength and then T/G (1/3)-Fs and T/G (0/4)-Fs samples. The reason one for this is that the T/G (1/1)-Fs sample shows greater density than T/G (1/3)-Fs and T/G (0/4)-Fs samples, as the foams density is directly proportional to compression strength. This result echo those of many other studies, i.e. higher density leads in general to higher strength [8,53]. In addition, the second reason is attributed to thicker cell walls of tannin modified foams (T/G (1/3)-Fs and T/G (1/1)-Fs), resulting to obtain a better compression loading distribution over the cell walls and thus an improved compression resistance [54]. Thicker cell walls originate from the tannin-derived products, which are interspersed within the foam cell walls and which tend to thicken the cell walls by their expanding action. This conclusion is supported by the results in Fig. 3. Interestingly, there may still be another possible explanation for the higher compression properties. The inserted tannin-derived products may have served as a framework to improve the compression resistance as well.

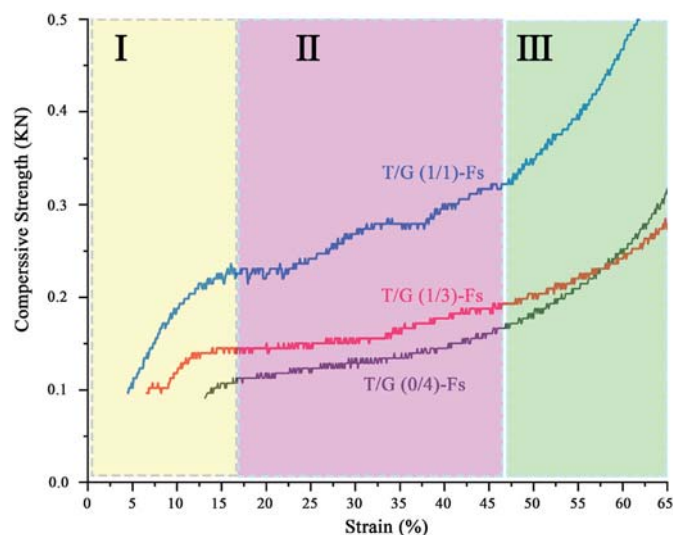


Fig. 5. Compressive stress-strain curves of T/G (0/4)-Fs, T/G (1/3)-Fs and T/G (1/1)-Fs.

According to the relevant literatures [54] and the tests described here, lower density foam samples have thinner cell walls, thereby they can only provide a rather limited contribution to compression resistance [60]. Thus, to investigate whether any upgrading in mechanical properties is only attributed to the increasing density of materials, the specific compressive strength of all foams was measured depending on the literature [53]. The specific compressive strength of all foam samples is shown in Table 2, which indicated that the specific strength exhibits the increasing trend with the increasing of condensed tannin addition. For T/G (0/4)-Fs, T/G (1/3)-Fs and T/G (1/1)-Fs samples, the corresponding of specific compressive strength is 1.22 $kPa/kg\ m^{-3}$, 1.27 $kPa/kg\ m^{-3}$ and 1.51 $kPa/kg\ m^{-3}$, respectively. The results showed the improvement of mechanical properties of tannin modified-foams that this progress of strength is not exclusively attributed to the density alone, but related to the contribution of the cell wall [53]. This conclusion also justifies the above-mentioned analysis. Therefore, taking into account Table 3 and Fig. 5, the results further indicate that the compression strength of these foams is improved by adding increasing proportions of condensed tannin.

3.7. Ignition experiment of T/G (0/4)-Fs, T/G (1/3)-Fs and T/G (1/1)-Fs samples

Although there are some limitations in the fire resistance evaluation of the ignition experiments reported here, they can indicate to a certain extent the combustion resistance of the material. Therefore, we designed this test to investigate the flammability of T/G (0/4)-Fs, T/G (1/3)-Fs and T/G (1/1)-Fs ignition combustion experiments were conducted on the foam samples directly. The digital photos of ignition experiments and the results are shown in Fig. 6 and Table 4, respectively. The burning time increased with the increase of tannin addition, from 175s for T/G (0/4)-Fs to 245s for T/G (1/3)-Fs, and then 372s for T/G (1/1)-Fs. The burning time of T/G (1/1)-Fs was more than twice longer of T/G (0/4)-Fs. This conclusion being also related to the density of the foams [12]. Furthermore, the residual weight of the foam samples after burning was also evaluated. The same trend as the burning time was observed, with the T/G (1/1)-Fs foam sample presenting the higher residual weight at 15.52%. This is attributed to the higher char rate of condensed tannin when heating. Therefore, condensed tannin modified foams obtained longer burning time and higher residual mass.

As shown in Fig. 6, T/G (0/4)-Fs and T/G (1/3)-Fs shows a high flammability and a very intense flame was observed in just a very short time (30s), when the foams are either devoid of tannin or have a lower tannin content. Simultaneous, in this case a large number of black fumes (dotted blue frame) was released while the

foam was burning. T/G (0/4)-Fs (Fig. 6 (b)) and T/G (1/3)-Fs (Fig. 6 (a)) samples do not show major differences in combustion flame. This is similar to traditional isocyanate-based polyurethane foams, indicating that these two foams are a highly flammable. However, the final burning product of T/G (1/3)-Fs samples can be maintained approximately in its original shape, compared to the completely irregular residue shape of T/G (0/4)-Fs. In addition, the combustion behavior of T/G (1/1)-Fs, shows a delicate small flame of which can be seen at the beginning of the burning experiment, are shown in Fig. 6(c). The intense flame and black fumes of T/G (0/4)-Fs and T/G (1/3)-Fs cannot be seen, from the beginning to the end of the experiment. Furthermore, the final product after burning keeps the original shape as well. These combustion phenomena show that while T/G (0/4)-Fs or T/G (1/3)-Fs and T/G (1/1)-Fs are all combustible, nevertheless, the ignitability is markedly lower when condensed tannin addition reached a certain proportion. All this suggests that condensed tannin have a certain inhibitory effect on the combustion behavior of T/G-Fs foam.

Table 4
The results of the ignition experiments.

Samples	Burning time (s)	Residue (g)	Residual (%)
T/G (0/4)-Fs	175 ± 11	0.13 ± 0.02	9.87 ± 0.13
T/G (1/3)-Fs	245 ± 10	0.15 ± 0.02	12.54 ± 0.09
T/G (1/1)-Fs	372 ± 18	0.34 ± 0.03	15.52 ± 0.15

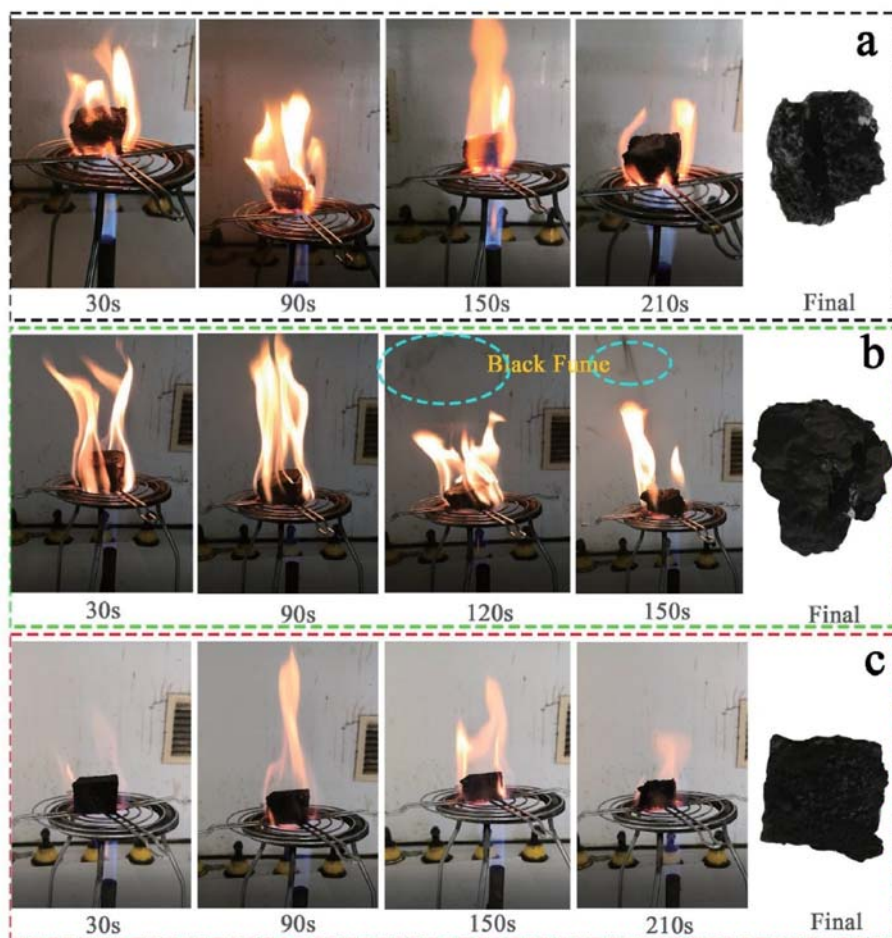


Fig. 6. The digital photos of ignition experiments: (a) T/G (1/3)-Fs; (b) T/G (0/4)-Fs; (c) T/G (1/1)-Fs.

3.8. Limiting oxygen index (LOI)

The limiting oxygen index (LOI) reflects the minimum oxygen concentration while the polymer is burning in the mixed oxygen and nitrogen atmosphere to evaluate effectively the flame retardancy in polymers [54]. A material can be defined as flame-retardant when its LOI value is greater than 27%. Conversely, it can be defined as inflammable when its LOI value is less than 22% [61]. The LOI values of each foam samples were then evaluated and the results obtained are shown in Fig. 7. The LOI values of neat glucose-based NIPU foam (T/G (0/4)-Fs) are around 17.5%, indicating that this kind of foam belong to the class of inflammable materials, needing additional flame retardants to improve its fire resistance if we want to expend its application field [12]. As expected, the condensed tannin-glucose NIPU foams, T/G (1/3)-Fs and T/G (1/1)-Fs, presented improved LOI values of 20.0% and 25.5%, respectively. The cause of this improved results is probably attributed to the presence of the condensed tannin, which have a considerable proportion of aromatic rings. Therefore, the condensed tannin-glucose NIPU foams are more easily carbonized when the carbon atoms reach a high proportion level [35, 54, 62]. In addition, from the structure of all foams, due to the enlarged cells (lower density) and a greater number of perforations of G-Fs (as shown in Fig. 3(a), (d) and (g)), the oxygen can enter to the inner parts of the foam, thereby increasing the oxygen concentration and thus rendering the foam more inflammable [54]. Combined with the SEM images, the tannin-derived fibrous polymers either interspersed in the cell walls of T/G (1/3)-Fs and T/G (1/1)-Fs or covering them may well be the one of critical factors of the improved fire resistance of these foams. Exactly as explained above, these tannin-derived fibrous polymers can then be easily converted into a char layer to improve the fire resistance of tannin-glucose-based NIPU foams. The ignition experiment results of all foam samples does also support such a conclusion. Therefore, the addition of condensed tannin can improve the LOI values of T/G (0/4)-Fs.

4. Conclusions

Condensed tannin as a natural flame retardant to modify the fire resistance of glucose-based NIPU foam was investigated. It is concluded that the presence of mimosa tannin substituting

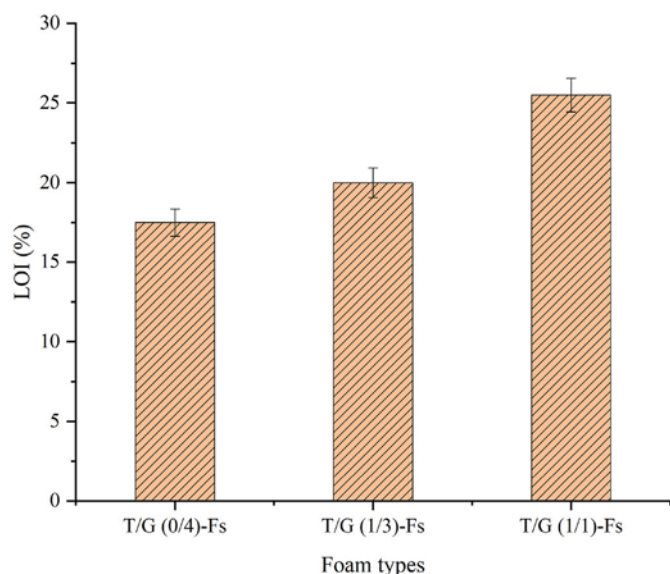


Fig. 7. LOI of T/G (0/4)-Fs, T/G (1/3)-Fs and T/G (1/1)-Fs.

different proportions of glucose in the NIPU foam can improve the ignitability of glucose-based NIPU foams. FT-IR results indicated that urethane linkages were formed in all foam formulations. The three kind of foams exhibited similar regular cell morphology, i.e. plenty of open pores can be seen clearly, but the T/G (1/3)-Fs and T/G (1/1)-Fs foams had smaller mean cell sizes than the T/G (0/4)-Fs. The compressive mechanical properties were all enhanced on account of the different amount replacement of glucose by condensed tannin. The thermal stability of T/G (1/3)-Fs and T/G (1/1)-Fs with added condensed tannin decreased then T/G (0/4)-Fs. However, the ignition experiment shows that with an increasing proportion of condensed tannin, the burning time lengthened, from 175s for T/G (0/4)-Fs to 372s for T/G (1/1)-Fs, respectively. The LOI values were determined to investigate the fire resistance of glucose-based NIPU foams, indicating that T/G (1/1)-Fs obtained the highest LOI value (25.5%, still belonging to the combustible grade, but not to the inflammable range) due to its highest condensed tannin content. Conversely, the LOI values of neat glucose-based NIPU foams (T/G (0/4)-Fs) are around 17.5%, belonging to inflammable grade. It can be seen from this, that condensed tannin can improve the fire resistance of T/G (0/4)-Fs, and yield better mechanical properties. This low-cost and highly effective biobased self-blowing glucose-/tannin-based foam presents a definite potential for practical application.

Declaration of competing interest

The authors declare that they have no known competing financial interests or personal relationships that could have appeared to influence the work reported in this paper.

CRediT authorship contribution statement

Xinyi Chen: Data curation, Formal analysis, Investigation, Methodology, Software, Visualization, Writing - original draft. **Jinxing Li:** Formal analysis, Investigation. **Xuedong Xi:** Investigation, Methodology. **Antonio Pizzi:** Conceptualization, Formal analysis, Funding acquisition, Project administration, Resources, Supervision, Validation, Writing - review & editing. **Xiaojian Zhou:** Formal analysis, Resources, Supervision. **Emmanuel Fredon:** Resources, Supervision, Validation. **Guanben Du:** Funding acquisition. **Christine Gerardin:** Funding acquisition, Validation.

Acknowledgement

This work was supported by the Yunnan Provincial Natural Science Foundation (2017FB060), National Natural Science Foundation of China (NSFC 31760187), Scholarship from China Scholarship Council (CSC), Yunnan Provincial Key Laboratory of Wood Adhesives and Glued Products and The LERMAB is supported by a grant of the French Agence Nationale de la Recherche (ANR) as part of the laboratory of excellence (LABEX) ARBRE.

References

- [1] L. Qian, L. Li, Y. Chen, B. Xu, Y. Qiu, Quickly self-extinguishing flame retardant behavior of rigid polyurethane foams linked with phosphaphenanthrene groups, *Compos. B Eng.* 175 (2019) 107186, <https://doi.org/10.1016/j.compositesb.2019.107186>.
- [2] P. Nuño, F.G. Bulnes, J.C. Granda, F.J. Suárez, D.F. García, A scalable WebRTC platform based on open technologies, in: 2018 International Conference on Computer, Information and Telecommunication Systems (CITS), 2018, pp. 1–5, <https://doi.org/10.1109/CITS.2018.8440161>.
- [3] N. Gama, L.C. Costa, V. Amaral, A. Ferreira, A. Barros-Timmons, Insights into the physical properties of biobased polyurethane/expanded graphite composite foams, *Compos. Sci. Technol.* 138 (2017) 24–31, <https://doi.org/10.1016/j.compscitech.2016.11.007>.
- [4] M. Bourguignon, J.-M. Thomassin, B. Grignard, C. Jerome, C. Detrembleur, Fast

- and facile one-pot one-step preparation of nonisocyanate polyurethane hydrogels in water at room temperature, *ACS Sustain. Chem. Eng.* 14 (7) (2019) 12601–12610, <https://doi.org/10.1021/acssuschemeng.9b02624>.
- [5] Y.-Y. Wang, C.E. Wyman, C.M. Cai, A.J. Ragauskas, Lignin-based polyurethanes from unmodified kraft lignin fractionated by sequential precipitation, *ACS Appl. Polym. Mater.* 1 (7) (2019) 1672–1679, <https://doi.org/10.1021/acscapm.9b00228>.
- [6] M. Wadekar, W. Eevers, R. Vendamme, Influencing the properties of Lignin PU films by changing copolymer chain length, lignin content and NCO/OH mol ratio, *Ind. Crop. Prod.* 141 (2019) 111165, <https://doi.org/10.1016/j.indcrop.2019.111655>.
- [7] S. Gómez-Fernández, M. Günther, B. Schartel, M.A. Corcuera, A. Eceiza, Impact of the combined use of layered double hydroxides, lignin and phosphorous polyol on the fire behavior of flexible polyurethane foams, *Ind. Crop. Prod.* 125 (2018) 346–359, <https://doi.org/10.1016/j.indcrop.2018.09.018>.
- [8] G. Tondi, W. Zhao, A. Pizzi, G. Du, V. Fierro, A. Celzard, Tannin-based rigid foams: a survey of chemical and physical properties, *Bioresour. Technol.* 100 (21) (2009) 5162–5169, <https://doi.org/10.1016/j.biortech.2009.05.055>.
- [9] M.C. Basso, S. Giovando, A. Pizzi, H. Pasch, N. Pretorius, L. Delmotte, A. Celzard, Flexible-elastic copolymerized polyurethane-tannin foams, *J. Appl. Polym. Sci.* 131 (13) (2014) 40499, <https://doi.org/10.1002/app.40499>.
- [10] N. Khundamri, C. Aouf, H. Fulcrand, E. Dubreucq, V. Tanrattanakul, Bio-based flexible epoxy foam synthesized from epoxidized soybean oil and epoxidized mangosteen tannin, *Ind. Crop. Prod.* 128 (2019) 556–565, <https://doi.org/10.1016/j.indcrop.2018.11.062>.
- [11] X. Xi, Z. Wu, A. Pizzi, C. Gerardin, H. Lei, B. Zhang, G. Du, Non-isocyanate polyurethane adhesive from sucrose used for particleboard, *Wood Sci. Technol.* 53 (2) (2019) 393–405, <https://doi.org/10.1007/s00226-019-01083-2>.
- [12] X. Xi, A. Pizzi, C. Gerardin, H. Lei, X. Chen, S. Amirou, Preparation and evaluation of glucose based non-isocyanate polyurethane self-blowing rigid foams, *Polymers* 11 (11) (2019) 1802, <https://doi.org/10.3390/polym11111802>.
- [13] H. Wang, H.-Z. Chen, A novel method of utilizing the biomass resource: rapid liquefaction of wheat straw and preparation of biodegradable polyurethane foam (PUF), *J. Chin. Inst. Chem. Eng.* 38 (2) (2007) 95–102, <https://doi.org/10.1016/j.jcice.2006.10.004>.
- [14] R.G. dos Santos, R. Carvalho, E.R. Silva, J.C. Bordado, A.C. Cardoso, M. do Rosário Costa, M.M. Mateus, Natural polymeric water-based adhesive from cork liquefaction, *Ind. Crop. Prod.* 84 (2016) 314–319, <https://doi.org/10.1016/j.indcrop.2016.02.020>.
- [15] E. Vanbiervliet, S. Fouquay, G. Michaud, F. Simon, J.-F. Carpentier, S.M. Guillaume, Non-isocyanate polythiourethanes (NIPTUs) from cyclo-dithiocarbonate telechelic polyethers, *Macromolecules* 52 (15) (2019) 5838–5849, <https://doi.org/10.1021/acs.macromol.9b00695>.
- [16] X. He, X. Xu, Q. Wan, G. Bo, Y. Yan, Solvent- and catalyst-free synthesis, hybridization and characterization of bio-based nonisocyanate polyurethane (NIPU), *Polymers* 11 (6) (2019) 1026, <https://doi.org/10.3390/polym11061026>.
- [17] P.K. Dannecker, M.A.R. Meier, Facile and sustainable synthesis of erythritol bis(carbonate), a valuable monomer for non-isocyanate polyurethanes (NIPUs), *Sci. Rep.* 9 (1) (2019) 1–6, <https://doi.org/10.1038/s41598-019-46314-5>.
- [18] A. Lee, Y. Deng, Green polyurethane from lignin and soybean oil through non-isocyanate reactions, *Eur. Polym. J.* 63 (2015) 67–73, <https://doi.org/10.1016/j.eurpolymj.2014.11.023>.
- [19] A. Cornille, G. Michaud, F. Simon, S. Fouquay, R. Auvergne, B. Boutevin, S. Caillol, Promising mechanical and adhesive properties of isocyanate-free poly(hydroxyurethane), *Eur. Polym. J.* 84 (2016) 404–420, <https://doi.org/10.1016/j.eurpolymj.2016.09.048>.
- [20] N. Esmaili, M. Vafayan, A. Salimi, M.J. Zohuriaan-Mehr, Kinetics of curing and thermo-degradation, antioxidant activity, and cell viability of a tannic acid based epoxy resin: from natural waste to value-added biomaterial, *Thermochim. Acta* 655 (2017) 21–33, <https://doi.org/10.1016/j.tca.2017.06.005>.
- [21] M. Tryznowski, A. Swiderska, T. Gojofit, Z. Żoiek-Tryznowska, Wood adhesive application of poly(hydroxyurethane)s synthesized with a dimethyl succinate-based amide backbone, *RSC Adv.* 7 (48) (2017) 30385–30391, <https://doi.org/10.1039/C7RA05455F>.
- [22] N. Esmaili, M.J. Zohuriaan-Mehr, A. Salimi, M. Vafayan, W. Meyer, Tannic acid derived non-isocyanate polyurethane networks: synthesis, curing kinetics, antioxidant activity and cell viability, *Thermochim. Acta* 664 (2018) 64–72, <https://doi.org/10.1016/j.tca.2018.04.013>.
- [23] G. Liu, G. Wu, S. Huo, C. Jin, Z. Kong, Synthesis and properties of non-isocyanate polyurethane coatings derived from cyclic carbonate-functionalized polysiloxanes, *Prog. Org. Coating* 112 (2017) 169–175, <https://doi.org/10.1016/j.porgcoat.2017.07.013>.
- [24] M. Thébault, A. Pizzi, H.A. Essawy, A. Barhoum, G. Van Assche, Isocyanate free condensed tannin-based polyurethanes, *Eur. Polym. J.* 67 (2015) 513–526, <https://doi.org/10.1016/j.eurpolymj.2014.10.022>.
- [25] M. Thébault, A. Pizzi, F.J. Santiago-Medina, F.M. Al-Marzouki, S. Abdalla, Isocyanate-free polyurethanes by coreaction of condensed tannins with aminated tannins, *J. Renew. Mater.* 5 (1) (2017) 21–29, <https://doi.org/10.7569/JRM.2016.634116>.
- [26] X. Xi, A. Pizzi, C. Gerardin, G. Du, Glucose-bio-based non-isocyanate polyurethane rigid foams, *J. Renew. Mater.* 7 (3) (2019) 301–312, <https://doi.org/10.32604/jrm.2019.04174>.
- [27] D. Lenoir, K. Kampke-Thiel, Gordon L. Fire and polymers II, in: Formation of Polybrominated Dibenzodioxins and Dibenzofurans in Laboratory Combustion Processes of Brominated Flame Retardants, vol. 599, American Chemical Society, Washington, DC, 1995, pp. 377–392, <https://doi.org/10.1021/bk-1995-0599.ch025> (Chapter 25).
- [28] B. Schartel, A. Balabanovich, U. Braun, U. Knoll, J. Artner, M. Ciesielski, M. Döring, R. Perez, J.K.W. Sandler, V. Altstadt, T. Hoffmann, D. Pospiech, Pyrolysis of epoxy resins and fire behavior of epoxy resin composites flame-retarded with 9, 10-dihydro-9-oxa-10-phosphaphenanthrene-10-oxide additives, *J. Appl. Polym. Sci.* 104 (4) (2007) 2260–2269, <https://doi.org/10.1002/app.25660>.
- [29] W. Zhang, X. Li, R. Yang, Pyrolysis and fire behaviour of epoxy resin composites based on a phosphorus-containing polyhedral oligomeric silsesquioxane (DOPO-POSS), *Polym. Degrad. Stabil.* 96 (10) (2011) 1821–1832, <https://doi.org/10.1016/j.polymdegradstab.2011.07.014>.
- [30] M. Hussain, R.J. Varley, Z. Mathys, Y.B. Cheng, G.P. Simon, Effect of organo-phosphorus and nano-clay materials on the thermal and fire performance of epoxy resins, *J. Appl. Polym. Sci.* 91 (2) (2004) 1233–1253, <https://doi.org/10.1002/app.13267>.
- [31] S.K. Lee, B.C. Bai, J.S. Im, S.J. In, Y.-S. Lee, Flame retardant epoxy complex produced by addition of montmorillonite and carbon nanotube, *J. Ind. Eng. Chem.* 16 (6) (2010) 891–895, <https://doi.org/10.1016/j.jiec.2010.09.014>.
- [32] C.M. Becker, A.D. Gabbardo, F. Wypych, S.C. Amico, Mechanical and flame-retardant properties of epoxy/Mg-Al LDH composites, *Compos. Appl. Sci. Manuf.* 42 (2) (2011) 196–202, <https://doi.org/10.1016/j.compositesa.2010.11.005>.
- [33] M.-J. Kim, I.-Y. Jeon, J.-M. Seo, L. Dai, J.-B. Baek, Graphene phosphonic acid as an efficient flame retardant, *ACS Nano* 8 (3) (2014) 2820–2825, <https://doi.org/10.1021/nn4066395>.
- [34] J. Gu, C. Liang, X. Zhao, B. Gan, H. Qiu, Y. Guo, X. Yang, Q. Zhang, D.-Y. Wang, Highly thermally conductive flame-retardant epoxy nanocomposites with reduced ignitability and excellent electrical conductivities, *Compos. Sci. Technol.* 139 (2017) 83–89, <https://doi.org/10.1016/j.compscitech.2016.12.015>.
- [35] Y.-O. Kim, J. Cho, H. Yeo, B.W. Lee, B.J. Moon, Y.-M. Ha, Y.R. Jo, Y.C. Jung, Flame retardant epoxy derived from tannic acid as bio-based hardener, *ACS Sustain. Chem. Eng.* 7 (4) (2019) 3858–3865, <https://doi.org/10.1021/acssuschemeng.8b04851>.
- [36] MRd Silveira, R.S. Peres, V.F. Moritz, C.A. Ferreira, Intumescent coatings based on tannins for fire protection, *Mater. Res.* 22 (2) (2019), 0433, <https://doi.org/10.1590/1980-5373-mr-2018-0433>.
- [37] S. Nam, B.D. Condon, Z. Xia, R. Nagarajan, D.J. Hinchliffe, C.A. Madison, Intumescent flame-retardant cotton produced by tannic acid and sodium hydroxide, *J. Anal. Appl. Pyrol.* 126 (2017) 239–246, <https://doi.org/10.1016/j.jaap.2017.06.003>.
- [38] F. Carosio, A. Di Blasio, F. Cuttica, J. Alongi, G. Malucelli, Flame retardancy of polyester and polyester-cotton blends treated with caseins, *Ind. Eng. Chem. Res.* 53 (10) (2014) 3917–3923, <https://doi.org/10.1021/ie404089t>.
- [39] G. Laufer, C. Kirkland, A.B. Morgan, J.C. Grunlan, Intumescent multilayer nanocoating, made with renewable polyelectrolytes, for flame-retardant cotton, *Biomacromolecules* 13 (9) (2012) 2843–2848, <https://doi.org/10.1021/bm300873b>.
- [40] S. Basak, K.K. Samanta, S. Saxena, S. Chattopadhyay, R. Narkar, R. Mahangade, G.B. Hadge, Flame resistant cellulosic substrate using banana pseudostem sap, *Pol. J. Chem. Technol.* 17 (1) (2015) 123–133, <https://doi.org/10.1515/pjct-2015-0018>.
- [41] M.N. Belgacem, A. Gandini, *Monomers, Polymers and Composites from Renewable Resources*, Elsevier, Netherland, 2008, pp. 179–200 (Chapter 8).
- [42] M.N. Belgacem, A. Gandini, *Monomers, Polymers and Composites from Renewable Resources*, Elsevier, Netherland, 2008, pp. 225–272 (Chapter 10-11).
- [43] A. Arbenz, L. Avérous, Chemical modification of tannins to elaborate aromatic bio-based macromolecular architectures, *Green Chem.* 17 (5) (2015) 2626–2646, <https://doi.org/10.1039/C5GC00282F>.
- [44] M. Ma, S. Dong, M. Hussain, W. Zhou, Effects of addition of condensed tannin on the structure and properties of silk fibroin film, *Polym. Int.* 66 (1) (2017) 151–159, <https://doi.org/10.1002/pi.5272>.
- [45] S.P. Ekambaram, S.S. Perumal, A. Balakrishnan, Scope of hydrolysable tannins as possible antimicrobial agent, *Phytother. Res.* 30 (7) (2016) 1035–1045, <https://doi.org/10.1002/ptr.5616>.
- [46] B. Adamczyk, J.-P. Salminen, A. Smolander, V. Kitunen, Precipitation of proteins by tannins: effects of concentration, protein/tannin ratio and pH, *Int. J. Food Sci. Technol.* 47 (4) (2012) 875–878, <https://doi.org/10.1111/j.1365-2621.2011.02911.x>.
- [47] R. Majumdar, B.G. Bag, P. Ghosh, Mimusops elengi bark extract mediated green synthesis of gold nanoparticles and study of its catalytic activity, *Appl. Nanosci.* 6 (4) (2016) 521–528, <https://doi.org/10.1007/s13204-015-0454-2>.
- [48] H. Tributsch, S. Fiechter, The material strategy of fire-resistant tree barks, *High Perform. Struct. Mater.* IV 97 (2008) 43–52.
- [49] G. Tondi, S. Wieland, T. Wimmer, M.F. Thévenon, A. Pizzi, A. Petutschnigg, Tannin-boron preservatives for wood buildings: mechanical and fire properties, *Eur. J. Wood Wood Prod.* 70 (5) (2012) 689–696.
- [50] M.A. Pantoja-Castro, H. González-Rodríguez, Study by infrared spectroscopy and thermogravimetric analysis of tannins and tannic acid, *Rev. Latinoam. Quim.* 39 (3) (2011) 107–112.
- [51] Z. Xia, A. Singh, W. Kiratitanavit, R. Mosurkal, J. Kumar, R. Nagarajan,

- Unraveling the Mechanism of Thermal and Thermo-Oxidative Degradation of Tannic Acid, vol. 605, 2015, pp. 77–85, <https://doi.org/10.1016/j.tca.2015.02.016>.
- [52] X. Xi, A. Pizzi, L. Delmotte, Isocyanate-free polyurethane coatings and Adhesives from mono- and di-saccharides, *Polymers* 10 (4) (2018) 402, <https://doi.org/10.3390/polym10040402>.
- [53] X. Zhou, B. Li, Y. Xu, H. Essawy, Z. Wu, G. Du, Tannin-furanic resin foam reinforced with cellulose nanofibers (CNF), *Ind. Crop. Prod.* 134 (2019) 107–112, <https://doi.org/10.1016/j.indcrop.2019.03.052>.
- [54] J. Li, A. Zhang, S. Zhang, Q. Gao, W. Zhang, J. Li, Larch tannin-based rigid phenolic foam with high compressive strength, low friability, and low thermal conductivity reinforced by cork powder, *Compos. B Eng.* 156 (2019) 368–377, <https://doi.org/10.1016/j.compositesb.2018.09.005>.
- [55] A. Zhang, J. Li, S. Zhang, Y. Mu, W. Zhang, J. Li, Characterization and acid-catalysed depolymerization of condensed tannins derived from larch bark, *RSC Adv.* 7 (56) (2017) 35135–35146, <https://doi.org/10.1039/C7RA03410E>.
- [56] O.S. Santos, M. Coelho da Silva, V.R. Silva, W.N. Mussel, M.I. Yoshida, Polyurethane foam impregnated with lignin as a filler for the removal of crude oil from contaminated water, *J. Hazard Mater.* 324 (2017) 406–413, <https://doi.org/10.1016/j.jhazmat.2016.11.004>.
- [57] S. Ranote, D. Kumar, S. Kumari, R. Kumar, G.S. Chauhan, V. Joshi, Green synthesis of Moringa oleifera gum-based bifunctional polyurethane foam braced with ash for rapid and efficient dye removal, *Chem. Eng. J.* 361 (2019) 1586–1596, <https://doi.org/10.1016/j.cej.2018.10.194>.
- [58] Z.-J. Cao, W. Liao, S.-X. Wang, H.-B. Zhao, Y.-Z. Wang, Polyurethane foams with functionalized graphene towards high fire-resistance, low smoke release, superior thermal insulation, *Chem. Eng. J.* 361 (2019) 1245–1254, <https://doi.org/10.1016/j.cej.2018.12.176>.
- [59] J. Merle, M. Birot, H. Deleuze, C. Mitterer, H. Carré, F.C.-E. Bouhtoury, New biobased foams from wood byproducts, *Mater. Des.* 91 (2016) 186–192, <https://doi.org/10.1016/j.matdes.2015.11.076>.
- [60] G. Tondi, A. Pizzi, Tannin-based rigid foams: characterization and modification, *Ind. Crop. Prod.* 29 (2–3) (2009) 356–363, <https://doi.org/10.1016/j.indcrop.2008.07.003>.
- [61] J. Liu, R.-Q. Chen, Y.-Z. Xu, C.-P. Wang, F.-X. Chu, Resorcinol in high solid phenol-formaldehyde resins for foams production, *J. Appl. Polym. Sci.* 134 (22) (2017) 44881, <https://doi.org/10.1002/app.44881>.
- [62] B. Li, S. Feng, H. Niasar, Y. Zhang, Z. Yuan, J. Schmidt, et al., Preparation and characterization of bark-derived phenol formaldehyde foams, *RSC Adv.* 6 (47) (2016) 40975–40981, <https://doi.org/10.1039/C6RA05392K>.

3.9 Préparation et caractérisation des mousses rigides de polyuréthane non isocyanate condensé (NIPU) par soufflage à température ambiante

Résumé: Une mousse rigide de polyuréthane sans isocyanate (NIPU) à base de tanin de mimosa auto-soufflant à température ambiante a été produite, sur la base d'une formulation de résine de polyuréthane sans isocyanate (NIPU) à base de tanin. Un mélange d'acide citrique et de glutaraldéhyde a servi d'agent gonflant utilisé pour fournir de l'énergie moussante et réticuler les produits dérivés du tanin pour synthétiser les mousses NIPU. Des séries de mousses NIPU à base de tanin contenant une quantité différente d'acide citrique et de glutaraldéhyde ont été préparées. Le mécanisme de réaction des mousses NIPU à base de tanin a été étudié par Fourier Transform InfraRed (FT-IR), spectrométrie de masse à désorption laser assistée par matrice (MALDI-TOF) et par résonance magnétique nucléaire ^{13}C (RMN ^{13}C). Les résultats ont indiqué que des liaisons uréthane se sont formées. La morphologie des mousses NIPU à base de tanin, y compris les propriétés physiques et mécaniques, a été caractérisée par compression mécanique, par microscopie électronique à balayage (MEB) et analyse thermogravimétrique (TGA). Toutes les mousses préparées présentent une morphologie à cellules ouvertes similaire. Néanmoins, le nombre de pores de la paroi cellulaire diminuait avec des additions croissantes de glutaraldéhyde, tandis que des cellules plus larges étaient obtenues avec des additions croissantes d'acide citrique. Les propriétés mécaniques de compression se sont améliorées avec le niveau plus élevé de réticulation due à la quantité plus élevée de glutaraldéhyde. De plus, les résultats de la TGA ont montré que les mousses NIPU à base de tanin préparées avaient une stabilité thermique similaire, bien que l'une d'entre elles (T-Fs-7) ait présenté la production de charbon et de matière résiduelle les plus élevées, approchant 18,7 % à 790°C.

Mots clés: tanin mimosa; mousse rigide NIPU; auto-soufflant; MALDI-TOF; RMN ^{13}C ; FTIR

Article

Preparation and Characterization of Condensed Tannin Non-Isocyanate Polyurethane (NIPU) Rigid Foams by Ambient Temperature Blowing

Xinyi Chen ¹, Xuedong Xi ¹, Antonio Pizzi ^{1,*} , Emmanuel Fredon ¹, Xiaojian Zhou ², Jinxing Li ², Christine Gerardin ³ and Guanben Du ²

¹ LERMAB, University of Lorraine, 27 rue Philippe Seguin, 88000 Epinal, France; xinyi.chen@univ-lorraine.fr (X.C.); xuedong.xi@univ-lorraine.fr (X.X.); emmanuel.fredon@univ-lorraine.fr (E.F.)

² Yunnan Key Laboratory of Wood Adhesives and Glue Products, Southwest Forestry University, Kunming 650224, China; xiaojianzhou1982@163.com (X.Z.); Jinxingli126@hotmail.com (J.L.); guanben@swfu.edu.cn (G.D.)

³ LERMAB, University of Lorraine, Boulevard des Aiguillettes, 54000 Nancy, France; christine.gerardin@univ-lorraine.fr

* Correspondence: antonio.pizzi@univ-lorraine.fr; Tel.: +33-623126940

Received: 6 March 2020; Accepted: 27 March 2020; Published: 30 March 2020



Abstract: Ambient temperature self-blowing mimosa tannin-based non-isocyanate polyurethane (NIPU) rigid foam was produced, based on a formulation of tannin-based non-isocyanate polyurethane (NIPU) resin. A citric acid and glutaraldehyde mixture served as a blowing agent used to provide foaming energy and cross-link the tannin-derived products to synthesize the NIPU foams. Series of tannin-based NIPU foams containing a different amount of citric acid and glutaraldehyde were prepared. The reaction mechanism of tannin-based NIPU foams were investigated by Fourier Transform InfraRed (FT-IR), Matrix Assisted Laser Desorption Ionization (MALDI-TOF) mass spectrometry, and ¹³C Nuclear Magnetic Resonance (¹³C NMR). The results indicated that urethane linkages were formed. The Tannin-based NIPU foams morphology including physical and mechanical properties were characterized by mechanical compression, by scanning electron microscopy (SEM), and thermogravimetric analysis (TGA). All the foams prepared showed a similar open-cell morphology. Nevertheless, the number of cell-wall pores decreased with increasing additions of glutaraldehyde, while bigger foam cells were obtained with increasing additions of citric acid. The compressive mechanical properties improved with the higher level of crosslinking at the higher amount of glutaraldehyde. Moreover, the TGA results showed that the tannin-based NIPU foams prepared had similar thermal stability, although one of them (T-Fs-7) presented the highest char production and residual matter, approaching 18.7% at 790 °C.

Keywords: mimosa tannin; rigid NIPU foam; self-blowing; MALDI-TOF; ¹³C NMR; FTIR

1. Introduction

Tannin, because of their distinct chemical properties, are classified into hydrolysable tannins and condensed or polyflavonoid tannins [1]. They are natural phenolic compounds, fairly ubiquitous in the vegetable world and commonly utilized as a starting materials in many fields, such as medicine [2,3], wastewater treatment [4–6], activated carbon [7,8], wood adhesives [9–12], fire resistance [13,14], coatings [15–17], etc. Among these applications, their use to prepare biobased foams for thermal and acoustic insulation and other applications has already attracted attention, especially in the case of condensed tannin [18–20]. Condensed tannins are mostly composed of polyhydroxy-flavan-3-ol

oligomers, flavan-3,4-diols, and other flavonoid analogs linked by carbon-carbon bonds between flavonoid monomer units [1,21].

Several preparation approaches have been reported to produce tannin-based foams. The most used approach is by preparing tannin-furanic foams, obtained by the acid condensation of tannins and furfuryl alcohol [18,22–26], with foam expansion driven by a blowing agent activated by the temperature increase caused by the acid self-condensation of furfuryl alcohol. In such an approach, three-dimensional stabilization is achieved by adding a cross-linker, initially an aldehyde or other compounds [27–29]. Subsequently, to develop another kind of tannin-based foam or gel, other materials were utilized, such as amines [6,30], soy flour [27], lignin [20,28], polymeric diphenyl methane isocyanate (p-MDI) [30], etc. Using these raw materials mixed with different tannins did yield some tannin-based foam with better properties. In these methods, however, some of the chemicals added are either non-environmentally-friendly (volatile foaming agent) or have high prices. Therefore, mechanically blown tannin foam types were prepared as a novel preparation method [21,31,32]. This concept was inspired from the preparation of meringue from egg whites, tannin, or tannin-furan resin that were mixed with other ingredients, and then a large amount of air was introduced into the mixture by vigorous mechanical stirring, forming a liquid foam with a fast expansion speed [32]. Blowing agents were not needed in this approach, but the foams obtained had higher density and higher compressive strength than standard chemical foaming tannin-furan foams.

All the approaches described led to phenolic-type tannin or tannin-furanic foams. However, the greatest interest is still in polyurethane foams, in their preparation from mainly bio-based materials, and especially for non-isocyanate polyurethane foams (NIPU). Bio-based NIPU foams have already been prepared from a variety of other approaches and renewable raw materials [33–48]. Hence, based on the previous preparation methods and formulations, making use of some novel approaches and formulations to produce tannin-based foams did become one of the main targets of this research work. Moreover, while tannin-based NIPU resins have already been prepared for coatings or wood adhesives applications [49–51], tannin-based NIPU foams have never been reported. It is for these reasons that the present work deals with the preparation of self-blowing condensed tannin NIPU foams, the study of their morphology, their synthesis mechanism, their thermal stability, and their mechanical compression properties.

2. Materials and Methods

2.1. Materials

Commercial mimosa tannin (*Acacia mearnsii*, De Wild) bark extract was obtained from Silva Chimica (St. Michele Mondovi, Italy). A 50% water solution of glutaraldehyde was obtained from Acros Organics (Geel, Belgium). Hexamethylenediamine (HDMA, 98%), Dimethyl carbonate (DMC, 99%, anhydrous), Hexamethylenetetramine (Hexamine, 99%, ACS reagent), and Citric acid (99.5%, ACS reagent) were supplied by Sigma-Aldrich (Saint Louis, France). All chemical reagents did not need purification before use.

2.2. Preparation of the Tannin-Based NIPU Resins

The method of tannin-based NIPU resin synthesis has been reported previously [52]. First, 40 g mimosa tannin was placed into a three-necked flask with condensing reflux condenser, a magnetic stirrer, and a thermometer. Then, 33.34 g of deionized water was added and stirred thoroughly. Second, 27 g of dimethyl carbonate (DMC) was added into the mixture, then mixed evenly, and heated to 65 °C, which keeps it at this temperature for 60 min. Third, 77.6 g of hexamethylene diamine (HDMA) (70% water solution) was added to the mixture, under continuous mechanical stirring, and heated to 90 °C, keeping it at this temperature for 120 min. Lastly, the resin obtained was collected and cooled down to room temperature, and ready for application.

2.3. Rigid Tannin-Based NIPU Foam Preparation

Foam formulations were prepared using the amounts of reagents listed in Table 1. The foams were obtained by mixing two compounds. The first one is a homogeneous acid mixture, the composition of which consists of citric acid (50% in water solution) and glutaraldehyde (50% in water solution). The second compound is a homogeneous tannin NIPU resin, composed of the mimosa tannin-based resin and hexamine. Briefly, different dosages of tannin-based resins (as referred) and hexamine were added into plastic cups, and stirred rapidly, which resulted in homogeneous tannin resins ready for application. The mixture of citric acid and glutaraldehyde was weighed and put into a foaming module, and, then, the tannin-based resin and hexamine mix was added immediately, while stirring manually for an optimal predetermined period of 10–15 s. Subsequently, the foams were left to grow at ambient temperature (25 °C). When the self-blowing step was finished, a homogeneous dark and red liquid self-supporting foam was obtained. Thus, it was by necessity cured at 70–80 °C overnight to obtain the final rigid foam. Lastly, the hardened foam samples were conditioned for a minimum of two days at 25 °C and 12% relative humidity before being characterized.

Table 1. The formulation compounds of tannin-based NIPU foams.

Foams	Resins (g)	Hexamine (g)	Citric Acid (g)	Glutaraldehyde (g)
T-Fs-2	10	2	6	2
T-Fs-5	10	0	6	2
T-Fs-7	10	2	6	4
T-Fs-9	10	2	4	0
T-Fs-11	10	2	8	2
T-Fs-13	10	2	9	3

2.4. Apparent Density

According to the standard method of ASTM D1622-08, all testing foam samples were prepared to a size of 30 mm × 30 mm × 30 mm. The ratio of weight to cubic volume of the specimen volume was defined as density. Five sample repeats were tested for each foam.

2.5. Scanning Electron Microscopy (SEM) Analysis

Scanning electron microscopy (SEM, Hitachi TM-3000)(Milexia, Paris, France) was used to analyze the microstructure and morphology of the foams obtained. All samples were made into 0.5 cm² (cross section). Then, a thin layer of gold-palladium was sputtered on the surface of the foams so that a better definition is obtained.

2.6. Fourier Transform Infrared (FT-IR) Spectroscopy

PerkinElmer Frontier ATR-FT-MIR (PerkinElmer, Villebon-sur-Yvette, France) was used to investigate the functional groups of all foams. The sample powder was placed in a 1.8-mm diamond eye of the Attenuated Total Reflection Fourier Transform InfraRed (ATR-FT-MIR) equipment. In addition, 32 scans at a resolution of 4 cm⁻¹ were done for each sample between 600 and 4000 cm⁻¹.

2.7. MALDI-TOF

A total of 5 mg of sample powder were dissolved in 1 mL of a 50:50 *v/v* acetone/water solution. Then, 10 µL of a 2,5-dihydroxy benzoic acid (DHB) matrix was added to 10 mg of the sample solution. Furthermore, 2 µL of an NaCl solution 0.1 M in 2:1 *v/v* methanol/water were applied and pre-dried on the sample support plaque, which is followed by the addition of 1 µL of the sample solution. The plaque was then dried again. The standardization of the MALDI spectrometer was done with red phosphorous. The spectrometer used was an Axima-Performance from Shimadzu Biotech (Kratos Analytical Shimadzu Europe Ltd., Manchester, UK). The tuning mode was linear

polarity-positive. A total of 1000 transients for each sample were done with two shots accumulated per profile. The spectrum precision is of ± 1 Da.

2.8. Solid State CP MAS ^{13}C NMR

Solid state Cross Polarisation-Magic Angle Spinning CP MAS ^{13}C NMR was used to analyze the cured foam powder. The spectrometer used was an AVANCE II 400 MHz spectrometer (Bruker, Billerica, MA, USA). Furthermore, 100.6 MHz was the frequency used at a 12-kHz sample spin, and the recycling delay was 1 s, depending on the ^1H spin lattice relaxation times (t_1) estimated with the inversion-recovery pulse sequence, and a contact time of 1 ms. The decoupling field was 78 kHz with 15,000 being the number of transients. Tetramethylsilane (TMS) was used as the shift control. The spectra precision was of ± 1 ppm. Spinning side bands suppression was used.

2.9. Compression Resistance

The samples were cut into a uniform size of 25 mm \times 25 mm \times 25 mm. A universal testing machine (Instron 3300, Elancourt, France) was used to test the compression strength of the foams. The direction of load was parallel to that of the foam rise under ambient conditions. The crosshead rate was fixed at 2.0 mm \cdot min $^{-1}$. At least three sample repeats were tested for each foam.

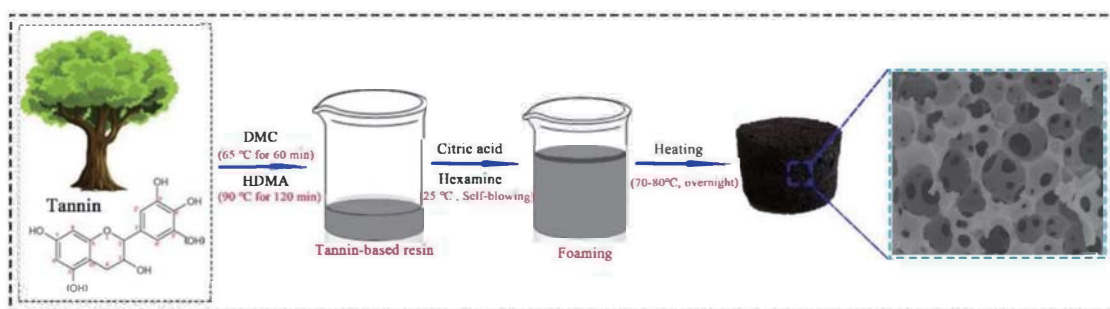
2.10. Thermogravimetric Analysis (TGA)

A TGA5500 analyzer (Mettler Toledo, Guyancourt, France) was used to measure the foam's thermal stability. Anywhere from 5 to 8 mg sample powder was placed on the platinum pan, and then heated with the sample at a temperature rate of 10 $^\circ\text{C}\cdot$ min $^{-1}$, under a nitrogen atmosphere (50 mL/min). The temperature range used was 25 $^\circ\text{C}$ to 790 $^\circ\text{C}$.

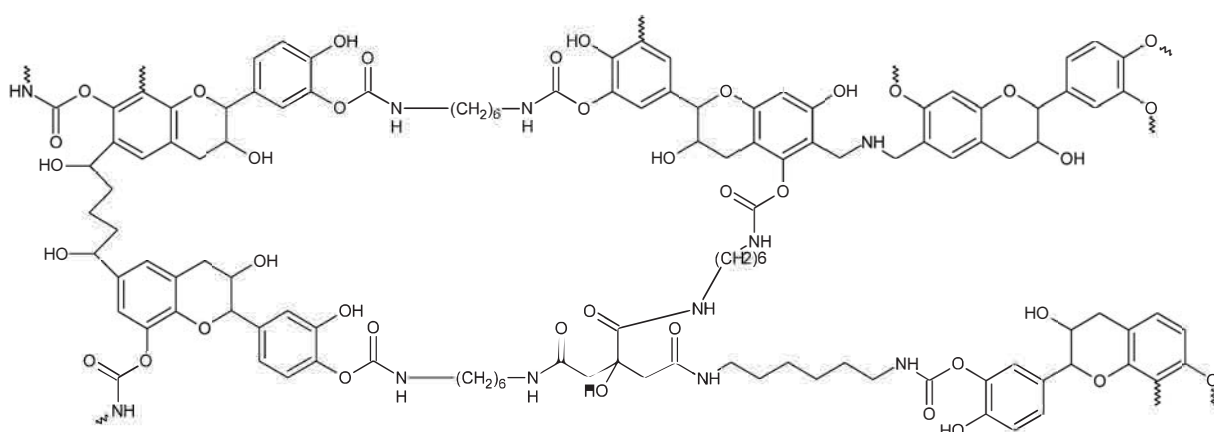
3. Results and Discussion

3.1. Preparation of Tannin-Based NIPU Foams

The tannin-based NIPU foams were prepared by a self-blowing approach. Because foaming and cross-linking occur almost simultaneously, they could not be strictly separated into two processes occurring independently. However, to investigate the process, the process can be assumed as two main separate steps: one is the foaming and the other one is the cross-linking. The whole preparation process of a tannin-based NIPU foam is shown in Scheme 1. The self-blowing energy for foaming (cf. Scheme 1) comes from the reaction of citric acid and the amino groups of both the hexamine and possibly with some still free amino groups of the tannin NIPU resin, resulting in the volume expansion of the liquid foams [53]. Glutaraldehyde functions as cross-linker, ensuring that the liquid foams system does not collapse and maintains itself self-supporting. Again, glutaraldehyde cross-links by reacting with the amino groups and with the reactive aromatic ring sites of the tannins [53], which contributes to form the three-dimensional structure of the tannin-based NIPU foam. Furthermore, hexamine participates to cross-linking by forming bridges between tannin molecules during the periods of foaming and heating. It must be noted that the liquid foams could not be maintained without collapsing when not adding the cross-linkers, i.e., hexamine or glutaraldehyde. This conclusion was confirmed in preparation experiments (cf. Table 2, where for T-Fs-5 and T-Fs-9, no foam samples were obtained). Therefore, the cross-linking process is a critical step for maintaining the three-dimensional structure of the liquid tannin-based NIPU foams obtained. Ultimately, this double effect causes the volume expansion, the sharp increase of the viscosity of the mixture, and then its gelling, which results in a three-dimensional network. A schematic example of some of the mixed linkages present in a possible network structure of tannin foams is shown in Scheme 2.



Scheme 1. The whole preparation process of a tannin-based NIPU foam.



Scheme 2. A schematic example of some of the mixed linkages present in a possible network structure of tannin-based NIPU foam.

Table 2. Apparent density, compressive strength, and specific compressive strength of tannin-based NIPU foams.

Foams	Apparent Density (g/cm ³)	Compressive Strength (KN)	Specific Compressive Strength (kPa/kg·m ⁻³)
T-Fs-2	0.15 ± 0.02	0.15 ± 0.02	1.62 ± 0.33
T-Fs-5	-	-	-
T-Fs-7	0.26 ± 0.04	0.57 ± 0.03	3.47 ± 0.38
T-Fs-9	-	-	-
T-Fs-11	0.12 ± 0.03	0.13 ± 0.01	1.63 ± 0.24
T-Fs-13	0.22 ± 0.02	0.32 ± 0.03	2.31 ± 0.18

3.2. Apparent Density

The self-blowing process can provide a flexible liquid foam with a three-dimensional network, which needs to be hardened by heating so that the necessary strength for measuring can be obtained. As shown in Figure 1, tannin-based NIPU foams with stable properties were prepared. The black foam with slightly red coloring is due to the presence of tannin [54]. The apparent densities of the foams are shown in Table 2. The foams apparent densities increase with the increasing proportion of glutaraldehyde. The maximum foams apparent density approximates 0.26 g·cm⁻³ for the addition of 4 g of glutaraldehyde. The reason for such an increase is the high reactivity of glutaraldehyde, which bridges two tannin oligomers with each other or with amino groups. It causes a rapid gel, which results in a higher cross-linking level much earlier in the foaming process. Furthermore, the relationship of citric acid with the foams' apparent density was also investigated. Table 2 shows that the addition of citric acid can slightly affect the foams' apparent density. Comparing T-Fs-2 with T-Fs-11 shows that the foam apparent density decreases slightly with the increasing amount of citric acid, from 0.15 g·cm⁻³

to $0.12 \text{ g}\cdot\text{cm}^{-3}$. This is attributed to the foaming energy originating from the reaction of citric acid with the $-\text{NH}_2$ groups [53]. Thus, a larger expansion volume can be obtained by increasing the amount of citric acid to obtain a smaller apparent density.



Figure 1. Digital photo of tannin-based NIPU foam.

3.3. Scanning Electron Microscopy (SEM) Analysis

Scanning electron microscopy (SEM) observation was utilized to investigate the morphology and microscopic structure of different foam formulations. The SEM images of foam samples are shown in Figure 2. It shows that all these foams present an open-cell structure. A considerable number of open pores are observed in the SEM images, which are attributed to water evaporation in the precursor resins during foaming and drying. Furthermore, some ruptures or debris and incomplete cellular structures can be seen in all foam samples, with these being due to the cutting process for preparing the samples [54].

Comparing Figure 2a (2 g glutaraldehyde) and Figure 2b (4 g glutaraldehyde), although they present a similar morphology and microscopic structure, less perforations are clearly apparent in T-Fs-7. The most likely explanation of this is that the high reactivity of glutaraldehyde with the tannin in the NIPU resin promotes the formation of higher molecular weight macromolecules, which causes a more rapid and more marked increase in the viscosity of the foaming system. Consequently, this weakens the pore-creating effect of water evaporation during foaming and drying. This effect can still be clearly observed even at a high amount of citric acid. Figure 2d also shows fewer cell perforations than in Figure 2a. Equally, as the volume expansion of the liquid foam is hindered by the high viscosity, this eventually results in a high-density foam. This conclusion is confirmed by the results in Table 2.

Thus, it appears that the dual function of citric acid is to effectively influence both foam morphology and its microscopic structure. This can be seen when a larger proportion of citric acid was used, as shown in Figure 2c (8 g of citric acid) and Figure 2d (9 g of citric acid). The reason for this might be that more citric acid can react with amino groups to provide more energy for foaming, which leads to a better volume expansion of the liquid foam [53]. Simultaneously, this resulted in a smaller foam density, as shown in Table 2. Thus, citric acid not only appears to provide more energy for foaming but also appears to contribute to strengthen and stabilize the three-dimensional foam structure.

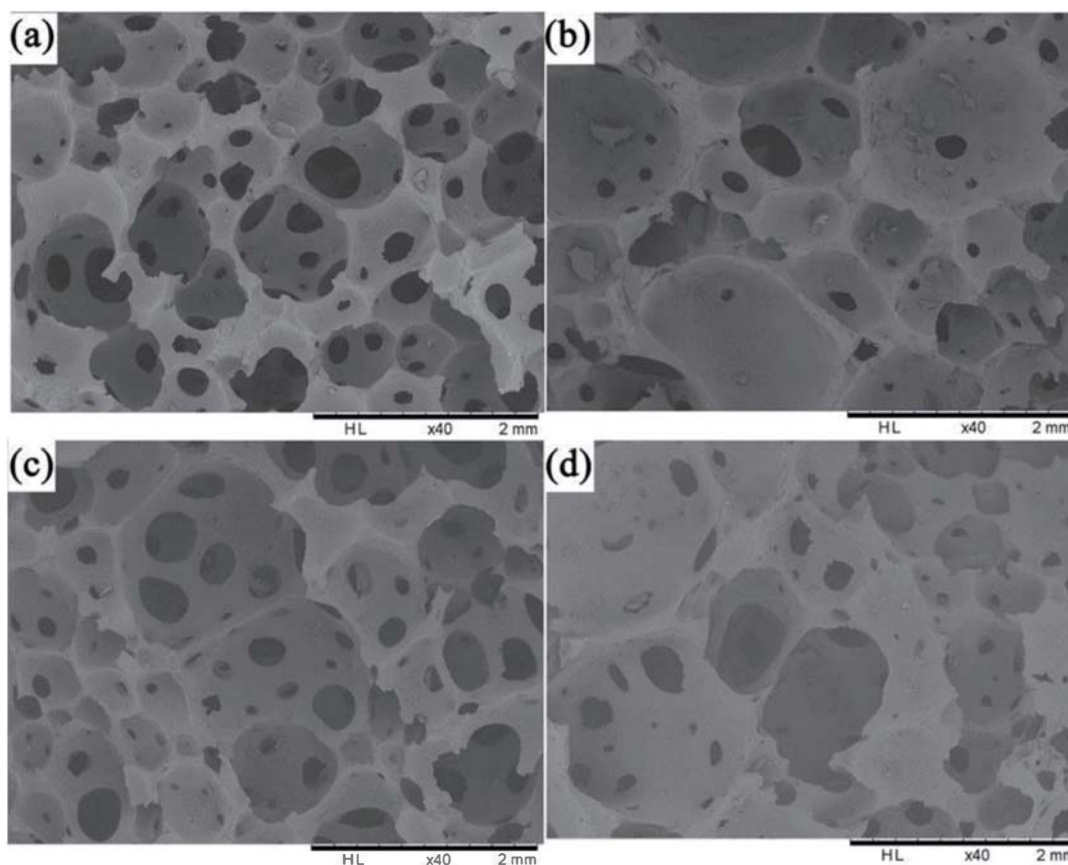


Figure 2. SEM images of tannin-based NIPU foams. (a) T-Fs-2, (b) T-Fs-7, (c) T-Fs-11, and (d) T-Fs-13.

3.4. The Reaction Mechanism of Tannin-Based NIPU Foams

3.4.1. Fourier Transform Infrared (FT-IR) Spectroscopy

Fourier transform infrared (FT-IR) spectra of neat mimosa tannin and, of the NIPU foams, are shown in Figure 3, to investigate the functional groups changes occurring in these foam preparations. The results indicate that some significant variation can be found between mimosa tannin and the NIPU foams obtained from it. The FT-IR spectra curves of all foam samples present similarities with each other. The infrared absorption spectrum of the mimosa tannin and of the NIPU foams show an intense band between 3500 and 3100 cm^{-1} attributed to the $-\text{OH}$ stretching vibration [55,56]. Moreover, a band at 3337 cm^{-1} in all NIPU foams spectra is assigned to $-\text{N}-\text{H}$ stretching of the NIPU urethane linkages derived from the reaction of the tannin with DMC and HDMA [50]. Citric acid reacts with $-\text{NH}_2$ groups to produce amides as well. There are two bands at 2934 cm^{-1} and 2860 cm^{-1} , relative to the $\text{C}-\text{H}$ stretching vibration of $-\text{CH}_2$ and $-\text{CH}_3$ [56,57]. These two bands are not detected in mimosa tannin, which indicates some functional groups have been changed during the preparation of the tannin-based resin and the foaming. Furthermore, present in the foams but not in the tannin, are the band at 1693 cm^{-1} assigned to a $\text{C}=\text{O}$ and that confirms its assignment and the assignment of the 3337 cm^{-1} bands to belong to a urethane linkage [52]. Moreover, the final confirmation of the urethane linkage is the presence of its other characteristic band at 1533 cm^{-1} (cf. Scheme 1 adducts 1). In addition, the band at 1261 cm^{-1} is representative of amines $\text{C}-\text{N}$ elongation [50].

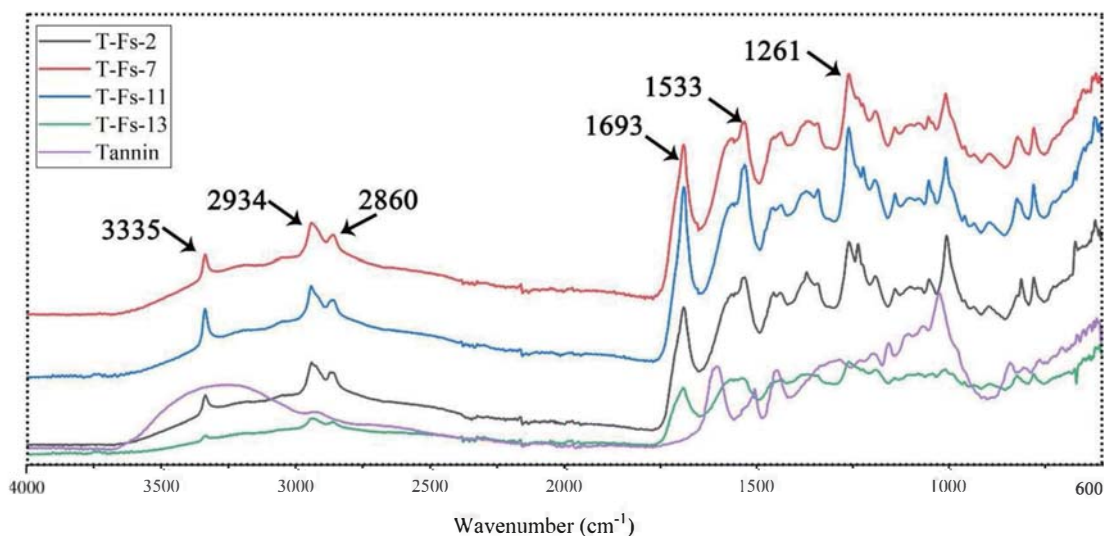


Figure 3. FT-IR spectra of tannin-based NIPU foams.

3.4.2. MALDI-TOF Analysis

To determine the distribution of condensed tannin oligomers and its derived condensation products, MALDI-TOF mass spectrometry has been used. The basic flavonoid units composing the tannin used are shown in Figure 4. The MALDI-TOF spectra of tannin-based NIPU foam T-Fs-7 is shown in Figure 5. Furthermore, some foreseeable species in the preparation of the co-reaction of tannin-based biomass foam are shown in Table 3. In general, as shown in Figure 4, four types of flavonoid units are involved in the formation of condensed tannin-derived oligomers, i.e., Fisetinidin, Robinetinidin, Catechin, and Delphinidin, respectively [24,50,58]. The tannin-derived products will originate from the combination of these units with each other and with other reagents. In view of Figure 5a, unreacted flavonoid oligomers (+23 Da from Na⁺) of condensed tannin monomers can be seen, i.e., 298–299 Da, 311–312 Da, and 326.2 Da.

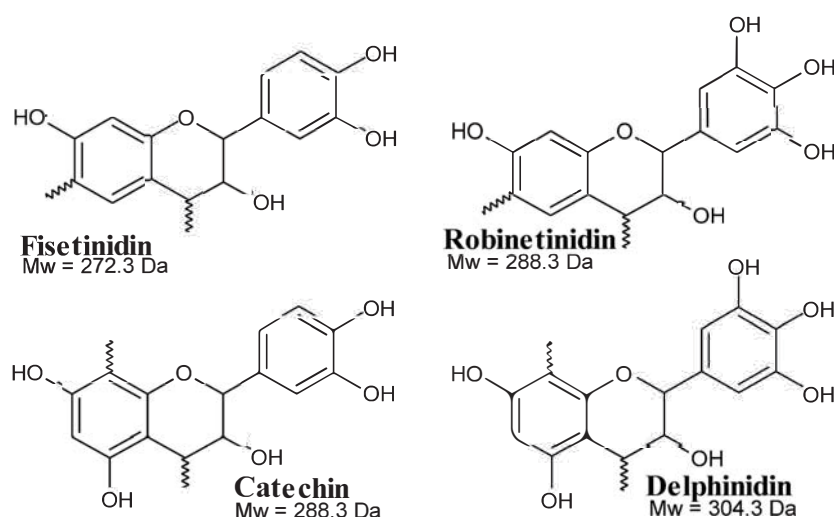
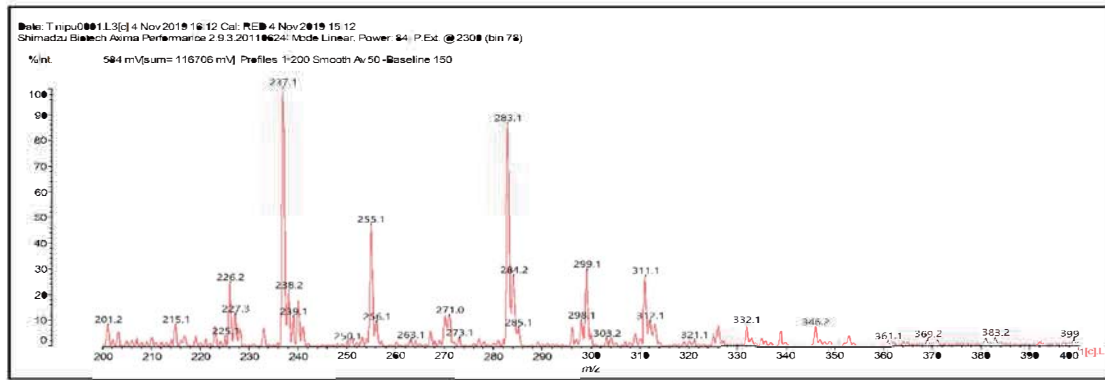
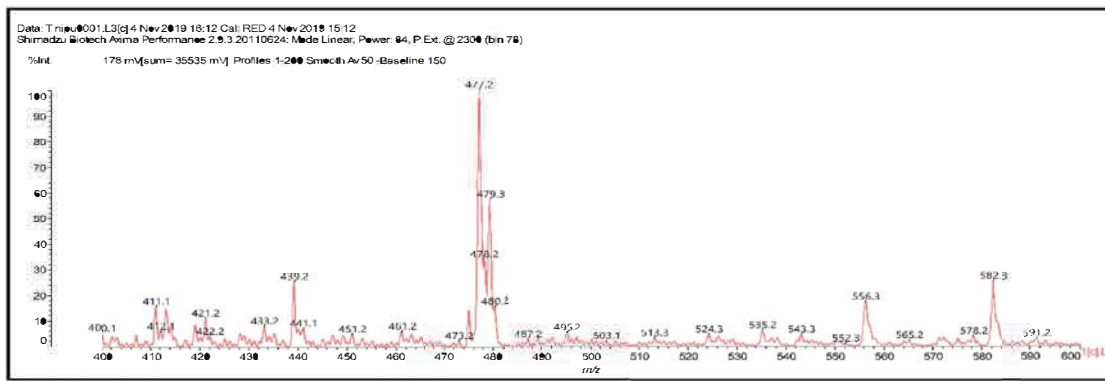


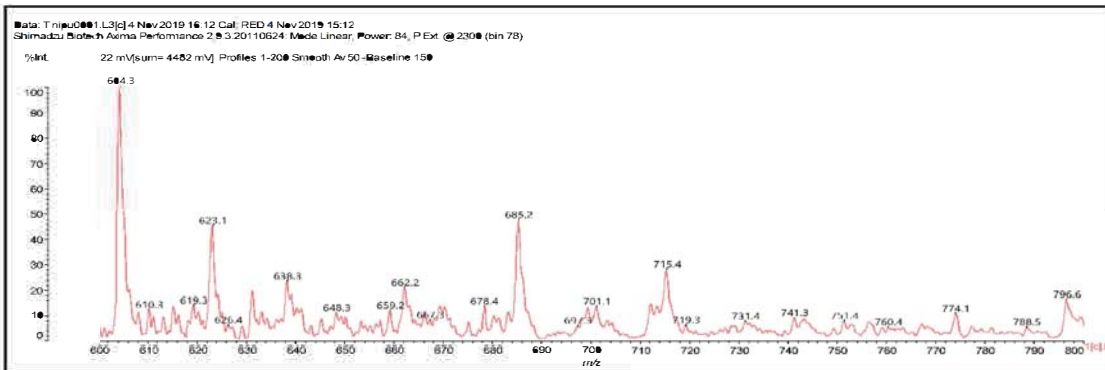
Figure 4. The four main structures of flavonoid units of the condensed tannin used.



(a)

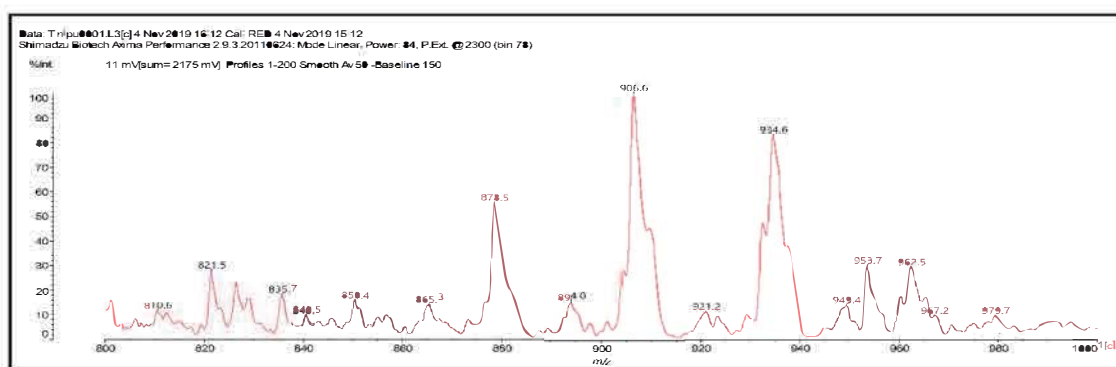


(b)



(c)

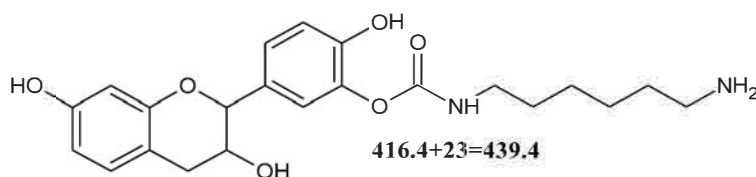
Figure 5. Cont.



(d)

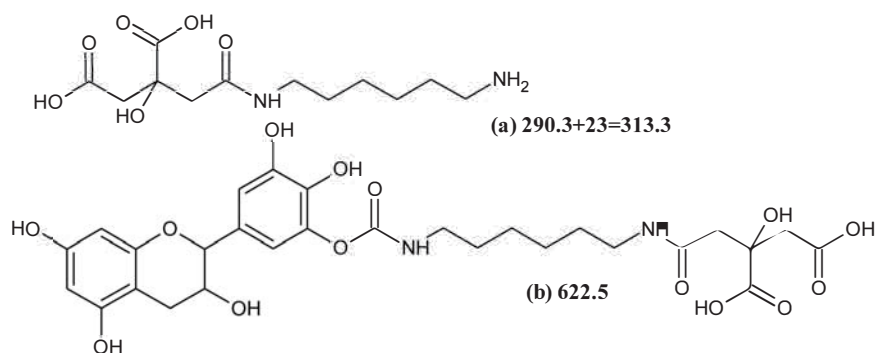
Figure 5. MALDI-TOF spectra of tannin-based NIPU foam (T-Fs-3), (a) 200–400 Da range, (b) 400–600 Da range, (c) 600–800 Da range, and (d) 800–1000 Da range.

Furthermore, some peaks in Figure 5 show that the tannin-derived NIPUs are obtained during the tannin-based NIPU resin preparation [49,51]. Thus, the peaks at 433.2 Da, 439.2 Da, 451.8 Da, and 556.3 Da shown in Figure 5b, are assigned tannin-based NIPU oligomers (cf. Scheme 3) and all have already been reported [49–51]. This kind of tannin-derived oligomers (Tannin-based non-isocyanate polyurethanes, recorded as tannin-based NIPU) can be recognized by the urethane bonds (–NH–CO–O–), which support and confirm the FT-IR and solid state ^{13}C NMR findings. Higher NIPU tannin oligomers can also be formed.



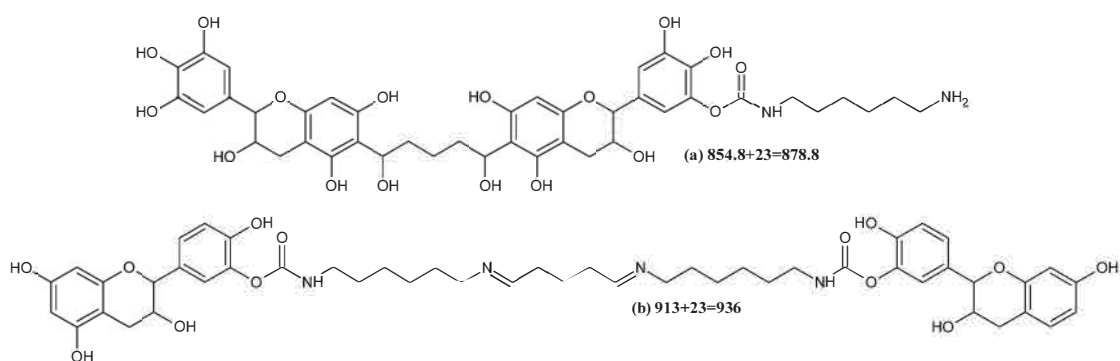
Scheme 3. One of the possible structures of the urethane between a flavonoid unit, DMC, and HDMA.

On account of the high reactivity between citric acid and $-\text{NH}_2$ groups (HDMA or tannins-based NIPU), the possible reaction products can be detected. This series of reactions is also the source of energy for foam volume expansion [53]. These peaks are such as 313.1 Da in Figure 5a, 411.1 Da in Figure 5b, 604.3 Da, 615.4 Da, 619.5 Da, and 741.5 Da in Figure 5c, and 828.6 Da, 865.2 Da, 878.6 Da, 906.6 Da, 921.5 Da, 954.5 Da, and 963.4 Da in Figure 5d. Among all these, they are reaction combination products based on citric acid (cf. Scheme 4). Ultimately, an amide bond (–NH–CO–) can be formed with citric acid in these derived products. Moreover, there are two types of these products derived from the reactions of citric acid, according to whether they do or do not include tannin-based NIPU, i.e., urethane bonds (–NH–CO–O–). Examples of these two types are shown in Scheme 4.



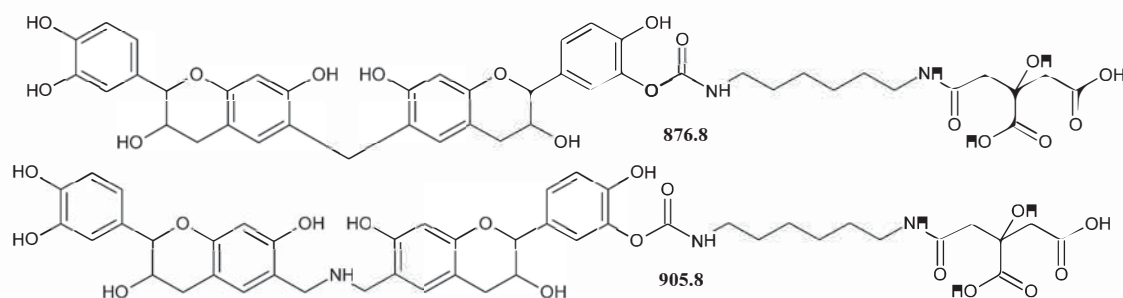
Scheme 4. Two kinds of citric acid derived products: (a) $-NH-CO-$ bond containing molecules and (b) both $-NH-CO-$ and $-NH-CO-O-$ bonds containing molecules.

Glutaraldehyde forms bridges and crosslinks connecting two or more oligomers to yield larger molecular weight products [53]. Glutaraldehyde can react with ease with tannin-derived NIPUs and other $-NH_2$ groups. The foreseeable cross-linked oligomers are shown in Scheme 5. Thus, glutaraldehyde either links directly with the aromatic rings of tannin units or with the compounds presenting $-NH_2$ groups. Examples of the cases as shown in Scheme 5 are represented by the peaks at 649.3 Da, 662.2 Da, 683.4 Da, 699.4 Da, and 715.4 Da in Figure 5c, 821.5 Da, 830.1 Da, 878.6 Da, 894.4 (921.5) Da, 934.9 Da, and 951 Da in Figure 5d. Even a new cross-link $-C=N-$ bond can occur in these products.



Scheme 5. Examples of two kinds of glutaraldehyde derived products: (a) glutaraldehyde bridging directly two aromatic tannin rings, and (b) glutaraldehyde bridging oligomers presenting $-NH_2$ groups.

Hexamethylenetetramine (hexamine) has been commonly used as a hardener of tannin-based wood adhesives and foams, as already reported [59,60]. Without doubt, it can also play a positive role in crosslinking and curing the liquid foams. Moreover, while tannins and hexamine have a complex polymerization reaction mechanism, two types of linkages can still be distinguished [61–63], namely two kinds of methylene-based reactive fragments derived from hexamine can serve as cross-linkers: $-CH_2-NH-CH_2-$ and $N-(CH_2)_3-$. Typical tannin-hexamine structures are shown in Scheme 6. From Figure 5, the MALDI-TOF spectra indicate some evidence of this, including the peaks at 578.3 Da, 582.4 Da, 591.2 Da in Figure 5b, 604.3 Da, 611.3 Da, 615.4 Da, 619.5 Da, 623.2 Da, 631.3 Da, 638.4 Da, 768.7 Da, and 796.5 Da in Figure 5c, and 878.6 Da, 906.6 Da, 954.5 Da, and 963.4 Da in Figure 5d. They are assigned to some tannin-hexamine reaction products.



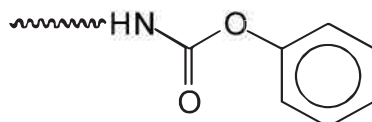
Scheme 6. Example of foreseeable structures of tannin-hexamine reaction products.

Table 3. MALDI-TOF interpretation of species obtained in the co-reaction of a tannin-based NIPU foam (Fisetinidin—Fi; Robinetinidin—Ro; Delphinidin—De). Note: the MW of Catechin and Robinetinidin are the same. Whenever Ro is indicated, it could well be Catechin. Since the relative abundance of Robinetinidin is much higher in mimosa tannin, Ro is always indicated in this table.

Peak (Da)	Experimental Peak (Da)	Species
299.1	274.2	Fi
311.1	290.2 + 23 = 313.2	Ro with Na ⁺
313.1	290.3 + 23 = 313.3	Citric acid-HDMA
326.2	306.2 + 23 = 329.2	De with Na ⁺
433.2	432.4	Ro-DMC-HDMA
411.1	388.5 + 23 = 411.5	Citric acid-(HDMA) ₂ with Na ⁺
439.3	416.4 + 23 = 439.4	Fi-DMC-HDMA with Na ⁺
451.2	448.4	De-DMC-HDMA
556.3	558.6	Fi-(DMC) ₂ -2HDMA
578.3	576.5	Fi-CH ₂ -Ro
582.4	560.5 + 23 = 583.5	Fi-CH ₂ -Fi with Na ⁺
591.3	592.5	Ro-CH ₂ -Ro
604.3	606.5 and/or 605.5	Ro-DMC-HDMA-Citric and/or Ro-CH ₂ NHCH ₂ -Fi
615.4	590.6 + 23 = 613.6 and/or 590.5 + 23 = 612.5 and/or 592.5 + 23 = 615.5	De-(DMC) ₂ -(HDMA) ₂ and/or Fi-DMC-HDMA-Citric and/or Ro-CH ₂ -Ro with Na ⁺
611.3	589.5 + 23 = 612.5	Fi-CH ₂ NHCH ₂ -Fi with Na ⁺
619.5	621.5 and/or 622.5	De-DMC-HDMA-Citric and/or Ro-CH ₂ NHCH ₂ -Ro
623.2	624.5	De-CH ₂ -De
631.3	608.5 + 23 = 631.5	Ro-CH ₂ -De with Na ⁺
638.4	637.5	Ro-CH ₂ NHCH ₂ -De
649.3	648.6	Fi-CH(-OH)-(CH ₂) ₃ -CH(-OH)-Fi
662.2	664.6	Ro-CH(-OH)-(CH ₂) ₃ -CH(-OH)-Fi
683.4	680.6	Ro-CH(-OH)-(CH ₂) ₃ -CH(-OH)-Ro
699.4	696.6	De-CH(-OH)-(CH ₂) ₃ -CH(-OH)-Ro
715.4	712.6	De-CH(-OH)-(CH ₂) ₃ -CH(-OH)-De
741.5	720.7 + 23 = 743.7	De-DMC-(HDMA) ₂ -Citric with Na ⁺
768.7	747.7 + 23 = 770.7	Fi-CH ₂ NHCH ₂ -Ro-DMC-HDMA with Na ⁺
796.5	795.7	De-CH ₂ NHCH ₂ -Ro-DMC-HDMA
828.6	830.9	Fi-(DMC) ₂ -(HDMA) ₃ -Citric
821.6	822.8	Ro-CH(-OH)(CH ₂) ₃ CH(-OH)-Ro-DMC-HDMA
830.1	806.8 + 23 = 829.8	Fi-CH(-OH)(CH ₂) ₃ CH(-OH)-Ro-DMC-HDMA with Na ⁺
865.2	862.9	De-(DMC) ₂ -(HDMA) ₃ -Citric
878.6	854.8 + 23 = 877.8 and/or 876.8	De-CH(-OH)(CH ₂) ₃ CH(-OH)-De-DMC-HDMA with Na ⁺ , and/or Fi-CH ₂ -Fi-DMC-HDMA-Citric
894.4 (921.5)	897 and/or 897 + 23 = 920	Fi-DMC-HDMA-CH(-OH)(CH ₂) ₃ CH(-OH)-Fi without and/or with Na ⁺ (920 Da)
906.6	905.8	Fi-CH ₂ NHCH ₂ -Fi-DMC-HDMA-Citric and/or Ro-CH ₂ NHCH ₂ -Ro-CH ₂ -Fi
921.5	921.8	Ro-CH ₂ NHCH ₂ -Fi-DMC-HDMA-Citric and/or Ro-CH ₂ NHCH ₂ -Ro-CH ₂ -Ro and/or De-CH ₂ NHCH ₂ -Ro-CH ₂ -Fi
934.9	913 + 23 = 936	Ro-DMC-HDMA-CH(-OH)(CH ₂) ₃ CH(-OH)-Fi-DMC-HDMA with Na ⁺
951	829 + 23 = 952	Ro-DMC-HDMA-CH(-OH)(CH ₂) ₃ CH(-OH)-Ro-DMC-HDMA with Na ⁺
954.5	953.8	De-CH ₂ NHCH ₂ -Ro-DMC-HDMA-Citric
963.4	937.8 + 23 = 960.8	Ro-CH ₂ NHCH ₂ -Ro-DMC-HDMA-Citric with Na ⁺

3.4.3. Solid State CP MAS ^{13}C NMR Analysis

Solid state Cross Polarization Magic Angle Spinning (CP MAS) ^{13}C NMR is a useful technique to investigate the composition of the foams prepared [24,64,65]. The ^{13}C NMR spectrum of a tannin-based NIPU foam (T-Fs-7) is shown in Figure 6. Several peaks can be observed. First of all, the peaks belonging to the tannins are relatively small. One can, thus, distinguish the shoulder at 157 ppm of the tannin C5 and C7, the wide peak at 153–155 ppm both belonging to the C9 of flavonoid units, and possibly the C=O of a urethane linkage does contribute [24]. The small peak/shoulder at 150 ppm more clearly belongs to a urethane linkage. This belonging to the aromatic ring carbon linked to a urethane linkage is of the type shown below.



This supports the indication that urethane linkages on the aromatic tannin rings have formed and subsist in the final foam network. The peak at 48 ppm is assigned to the $-\text{CH}_2-$ of glutaraldehyde next to an unreacted aldehyde group. An overlapping peak does appear at 40 ppm and presents two little peaks that can be seen in this position. The peak at 40 ppm and the shoulder at 38 ppm belong to the $-\text{CH}_2-$ next to the aldehyde group that has reacted with the tannin aromatic ring site. The other one possible explanation is that it belongs to $-\text{CH}_2-$ on the unreacted heterocycle C4 site of the flavonoid [64]. This is, however, unlikely, considering the intensity of the signal in relation to the low intensity of all the other signals of the flavonoid carbons. The more likely explanation is that it is likely to belong to the inner $-\text{CH}_2-$ groups of glutaraldehyde or citric acid.

The huge and broad peak at 24 ppm is assigned to the sum of $-\text{CH}_2-$ groups of hexamethylenediamine and the remaining ones of glutaraldehyde. The peak at 69 ppm is assigned to the C–OH generated by the reaction of aldehyde groups of glutaraldehyde with an aromatic ring site of the tannin and masks the C3 signal of flavonoid units. The peak at 173 ppm and the shoulder at 175 ppm belong to the C=O groups of citric acid under two different environments. One is unreacted, and the other reacted to form a $-\text{CO}-\text{NH}-$ bond derived from the reaction of the acid with compounds carrying $-\text{NH}_2$ groups. The wide series of peaks at 197–203 ppm are assigned to the $-\text{CHO}$ group of glutaraldehyde. Regarding the flavonoid units, the peak at 143–145 ppm belongs to the C3', C4', and C5' of the flavonoid B-ring, the peak at 130–131 ppm to the C1', the small peak at 120 ppm to the C6', and the peaks at 110 ppm and 115 ppm to the two types of interflavonoid oligomer bond C4, C8 and C4, C6. The small peak at 82 ppm belongs to the flavonoid C2. The marked peaks at 59 ppm belongs to the carbohydrates that are present in the industrial tannin extract used.

Thus, it is confirmed that the condensed tannin-based NIPU has been synthesized by combining the tannin with DMC and HDMA in the tannin-based resin preparation stage. A clear and marked shoulder peak at 173.7 ppm is that of the $-\text{CO}-\text{NH}-$ bond, which exist in plenty of compounds in the foam rooted from the reaction citric acid with $-\text{NH}_2$ containing molecules. The more likely explanation is that it is likely to belong to the inner $-\text{CH}_2-$ groups of glutaraldehyde or citric acid.

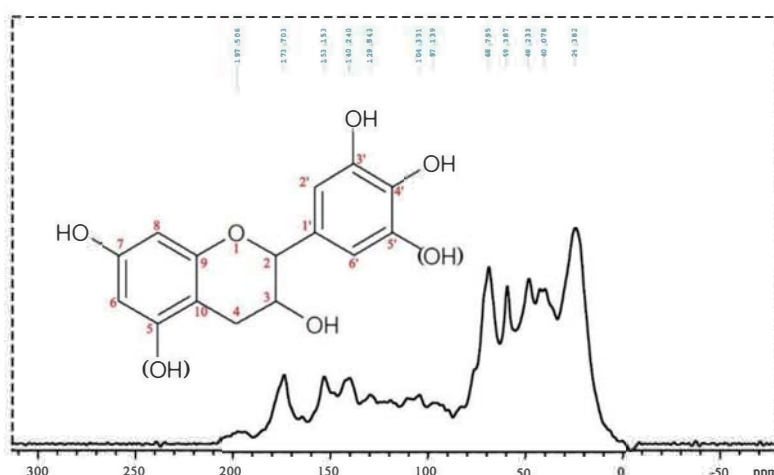


Figure 6. Solid state ^{13}C NMR spectrum of tannin-based NIPU foam (T-Fs-7).

3.5. Compression Mechanical Properties

The compression stress-strain curves of T-Fs-2, T-Fs-7, T-Fs-11, and T-Fs-13 samples are shown in Figure 7. Intuitively, T-Fs-7 exhibits the highest compression strength, for 0.57 kN, and then T-Fs-13 for 0.32 kN, T-Fs-2 for 0.15 kN, and T-Fs-11 for 0.12 kN, respectively. The reason for this is attributed to the apparent density of the foams with this being directly proportional to compression strength [53]. This conclusion is in line with previous works indicating that higher density leads to higher strength [18,53,66]. In addition, lower density foams have a thinner cell wall [18,54]. Theoretically, thinner cell walls can only provide a rather limited contribution to compression resistance. Thus, eliminating the influence of the foam's density, the specific compression strength was evaluated according to the literature [66]. The results of specific compression strength for all foam samples are shown in Table 2. For T-Fs-2, T-Fs-7, T-Fs-11, and T-Fs-13 samples, the corresponding specific compressive strengths are $1.62 \text{ kPa/kg}\cdot\text{m}^{-3}$, $3.47 \text{ kPa/kg}\cdot\text{m}^{-3}$, $1.63 \text{ kPa/kg}\cdot\text{m}^{-3}$, and $2.31 \text{ kPa/kg}\cdot\text{m}^{-3}$, respectively. Their trend is clearly in line with the apparent foam's densities. The conclusion of this is that the strength trend is not only exclusively attributed to the foam density alone, but also related to the contribution of the cell wall. Furthermore, another possible explanation is the dependence on the number of cell wall perforations, which can break the structural integrity of the cell. Therefore, this contributes to the decrease of compression strength. This conclusion is also supported by the combination of Figure 2 and Table 2. In brief, the improvement of mechanical properties of tannin-based biomass foams is a result of a multi-factor synergy.

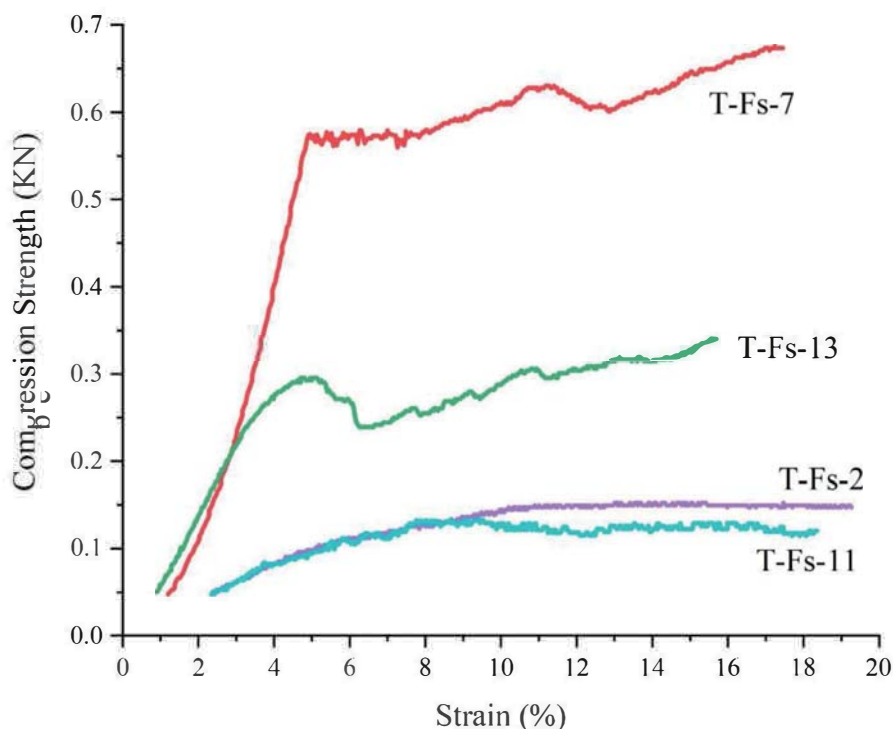


Figure 7. Compressive stress-strain curves of T-Fs-2, T-Fs-7, T-Fs-11, and T-Fs-13.

3.6. Thermogravimetric Analysis (TGA)

To evaluate the thermal stability of tannin-based biomass foams, the thermogravimetric analysis (TGA) curves of T-Fs-2, T-Fs-7, T-Fs-11, and T-Fs-13 are shown in Figure 8. The corresponding specific degradation temperatures and char yields at 790 °C are listed in Table 4. The T_{max} value reported in Table 4 is the maximum temperature shown by DTG curve peaks at different pyrolysis stages. A three-stage similar pyrolysis behavior of tannin-based NIPU foams are observed in Figure 8. The initial weight loss occurs within the temperature range of 30 to 150 °C with this being related to the decomposition of the excess acid and hexamine and the release of the volatilized absorbed water [54]. In this step, 3.3% of weight loss occurred for T-Fs-2 and T-Fs-7 while 3.6% of weight loss occurred for T-Fs-11 and T-Fs-13. The second weight loss range is between 150 °C and 250 °C, showing 18.3% of weight loss for T-Fs-2, 19.2% of weight loss for T-Fs-7, 19.3% of weight loss for T-Fs-11, and 18.1% of weight loss for T-Fs-13. The weight loss in this range is related to decomposition reactions by bond cleavage of urethane and tannin intermolecular bonds (onset temperature of mimosa tannin was 146 °C) [55,67]. The third weight loss occurs in the 350 °C and 550 °C range. This is the stage where the largest weight mass loss occurs, which is larger than 40%. Thus, in this temperature range, 44.1% of weight loss for T-Fs-2, 41.2% of weight loss for T-Fs-7, 43.7% of weight loss for T-Fs-11, and 42.9% of weight loss for T-Fs-13 take place. This step may be caused by breaking C–C bonds and the decomposition of pyrolysis residual products from the first two stages [55,67]. These results show that the tannin-based NIPU foams present similar pyrolysis temperature weight losses (within 8 °C). Nevertheless, a slight difference in the residual mass at 790 °C of the tannin-based NIPU foams occurs, according to a predictable trend. The residual masses of 16.5% for T-Fs-2 and T-Fs-11, 17.3% for T-Fs-13, and 18.7% for T-Fs-13 show an increasing relation with the higher proportion of glutaraldehyde addition. This is due to a better cross-linked three-dimensional foam system due to the increasing addition of glutaraldehyde.

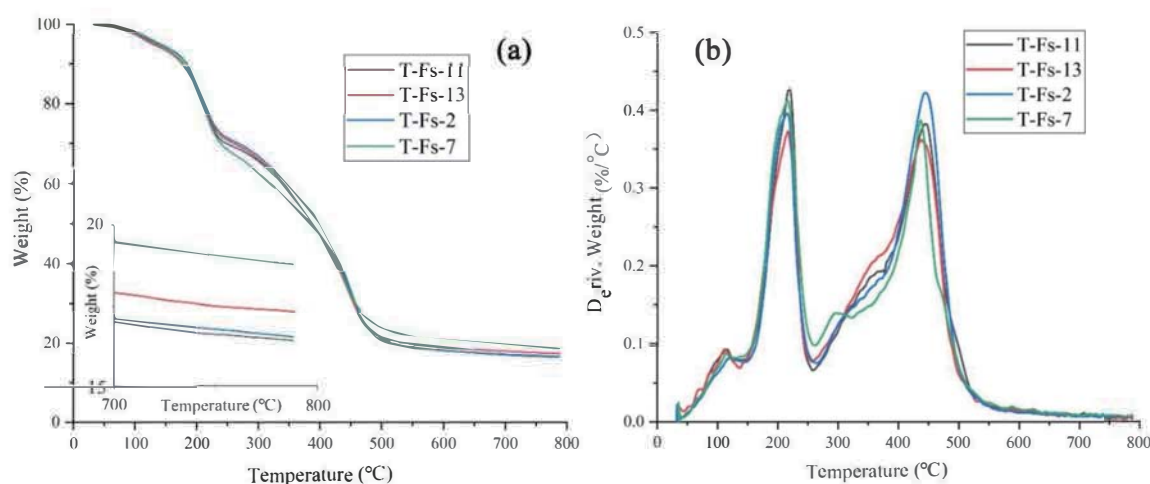


Figure 8. TGA (a) and Derivative Thermogravimetry (DTG) (b) curves of T-Fs-2, T-Fs-7, T-Fs-11, and T-Fs-13 (under N₂ atmosphere).

Table 4. TGA data of T-Fs-2, T-Fs-7, T-Fs-11, and T-Fs-13 (under nitrogen atmosphere).

Samples	T_{max} (°C)			Residual Mass at 790 °C (%)
	Step I	Step II	Step III	
T-Fs-2	119.2	214.8	444.8	16.5
T-Fs-7	115.1	215.4	436.2	18.7
T-Fs-11	114.8	218.6	445.4	16.4
T-Fs-13	112.2	216.1	437.1	17.3

4. Conclusions

The work presented in this case reports a novel mimosa tannin-based NIPU rigid foam using ambient temperature self-expansion to cause the foaming. An acid mixture blowing agent, including citric acid and glutaraldehyde, was used to provide the foaming energy and cross-link the tannin-derived products to produce self-supporting tannin-based NIPU foams without needing any volatile blowing agents. Four types of tannin-based foams were prepared by using different proportions of citric acid and glutaraldehyde. FT-IR, MALDI-TOF, and ¹³C NMR contributed to the analysis of the reaction mechanism and products formed indicating, among others, that urethane linkages were formed. Furthermore, SEM images exhibit similar open-cell morphology. The number of cell-wall pores decreased with increasing additions of glutaraldehyde, while bigger foam cells were obtained with the increasing addition of citric acid. The compressive mechanical properties were enhanced by the improved level of cross-linking between tannin NIPU molecules at higher amounts of glutaraldehyde. Thermogravimetric analysis (TGA) results showed that T-Fs-7 presented the highest char production, approaching a residual 18.7% at 790 °C under nitrogen atmosphere.

Author Contributions: X.C. designed and performed the experiments, and analysed part of the data. A.P. conceived the project, supervised the work, and interpreted the NMR. G.D. supervised part of the work; J.L. analyzed part of the data. X.C., X.X., X.Z., and J.L. assisted in part of the experiments and testing. X.C. and A.P. wrote the paper. A.P., E.F., and C.G. revised and proofed the manuscript. All authors have read and agreed to the published version of the manuscript.

Acknowledgments: The Yunnan Provincial Natural Science Foundation (2017FB060), National Natural Science Foundation of China (NSFC 31760187), Scholarship from China Scholarship Council (CSC), Yunnan Provincial Key Laboratory of Wood Adhesives and Glued Products and The LERMAB supported this work. A grant of the French Agence Nationale de la Recherche (ANR) as part of the laboratory of excellence (LABEX) ARBRE also supported this work.

Conflicts of Interest: The authors declare no conflict of interest.

References

1. Pizzi, A. Tannin-based biofoams-A review. *J. Renew. Mater.* **2019**, *7*, 474–489. [[CrossRef](#)]
2. Guo, J.; Sun, W.; Kim, J.P.; Lu, X.; Li, Q.; Lin, M.; Mrowczynski, O.; Rizk, E.B.; Cheng, J.; Qian, G.; et al. Development of tannin-inspired antimicrobial bioadhesives. *Acta Biomater.* **2018**, *72*, 35–44. [[CrossRef](#)] [[PubMed](#)]
3. Shin, M.; Kim, K.; Shim, W.; Yang, J.W.; Lee, H. Tannic acid as a degradable mucoadhesive compound. *ACS Biomater. Sci. Eng.* **2016**, *2*, 687–696. [[CrossRef](#)]
4. Bacelo, H.A.; Santos, S.C.; Botelho, C.M. Tannin-based biosorbents for environmental applications-a review. *Chem. Eng. J.* **2016**, *303*, 575–587. [[CrossRef](#)]
5. Sánchez-Martín, J.; Beltrán-Heredia, J.; Gibello-Pérez, P. Adsorbent biopolymers from tannin extracts for water treatment. *Chem. Eng. J.* **2011**, *168*, 1241–1247. [[CrossRef](#)]
6. Morisada, S.; Rin, T.; Ogata, T.; Kim, Y.H.; Nakano, Y. Adsorption removal of boron in aqueous solutions by amine-modified tannin gel. *Water Res.* **2011**, *45*, 4028–4034. [[CrossRef](#)] [[PubMed](#)]
7. Braghiroli, F.L.; Fierro, V.; Izquierdo, M.T.; Parmentier, J.; Pizzi, A.; Celzard, A. Nitrogen-doped carbon materials produced from hydrothermally treated tannin. *Carbon* **2012**, *50*, 5411–5420. [[CrossRef](#)]
8. Selmi, T.; Sanchez-Sanchez, A.; Gadonneix, P.; Jagiello, J.; Seffen, M.; Sammouda, H.; Celzard, A.; Fierro, V. Tetracycline removal with activated carbons produced by hydrothermal carbonisation of Agave americana fibres and mimosa tannin. *Ind. Crop. Prod.* **2018**, *115*, 146–157. [[CrossRef](#)]
9. Liu, C.; Zhang, Y.; Li, X.; Luo, J.; Gao, Q.; Li, J. A high-performance bio-adhesive derived from soy protein isolate and condensed tannins. *Rsc Adv.* **2017**, *7*, 21226–21233. [[CrossRef](#)]
10. Xi, X.; Pizzi, A.; Frihart, C.R.; Lorenz, L.; Gerardin, C. Tannin plywood bioadhesives with non-volatile aldehydes generation by specific oxidation of mono-and disaccharides. *Int. J. Adhes. Adhes.* **2019**, *98*, 102499. [[CrossRef](#)]
11. Ping, L.; Brosse, N.; Chrusciel, L.; Navarrete, P.; Pizzi, A. Extraction of condensed tannins from grape pomace for use as wood adhesives. *Ind. Crop. Prod.* **2011**, *33*, 253–257. [[CrossRef](#)]
12. Li, J.; Zhu, W.; Zhang, S.; Gao, Q.; Xia, C.; Zhang, W.; Li, J. Depolymerization and characterization of Acacia mangium tannin for the preparation of mussel-inspired fast-curing tannin-based phenolic resins. *Chem. Eng. J.* **2019**, *370*, 420–431. [[CrossRef](#)]
13. Xia, Z.; Kiratitanavit, W.; Facendola, P.; Thota, S.; Yu, S.; Kumar, J.; Mosurkal, R.; Nagarajan, R. Fire resistant polyphenols based on chemical modification of bio-derived tannic acid. *Polym. Degrad. Stab.* **2018**, *153*, 227–243. [[CrossRef](#)]
14. Laoutid, F.; Karaseva, V.; Costes, L.; Brohez, S.; Mincheva, R.; Dubois, P. Novel bio-based flame retardant systems derived from tannic acid. *J. Renew. Mater.* **2018**, *6*, 559–572. [[CrossRef](#)]
15. Nardeli, J.V.; Fugivara, C.S.; Pinto, E.R.P.; Polito, W.L.; Messaddeq, Y.; José Lima Ribeiro, S.; Benedetti, A.V. Preparation of Polyurethane Monolithic Resins and Modification with a Condensed Tannin-Yielding Self-Healing Property. *Polymers* **2019**, *11*, 1890. [[CrossRef](#)] [[PubMed](#)]
16. Nardeli, J.V.; Fugivara, C.S.; Taryba, M.; Montemor, M.F.; Ribeiro, S.J.; Benedetti, A.V. Novel healing coatings based on natural-derived polyurethane modified with tannins for corrosion protection of AA2024-T3. *Corros. Sci.* **2020**, *162*, 108213. [[CrossRef](#)]
17. Nardeli, J.V.; Fugivara, C.S.; Taryba, M.; Pinto, E.R.; Montemor, M.F.; Benedetti, A.V. Tannin: A natural corrosion inhibitor for aluminum alloys. *Prog. Org. Coat.* **2019**, *135*, 368–381. [[CrossRef](#)]
18. Tondi, G.; Zhao, W.; Pizzi, A.; Du, G.; Fierro, V.; Celzard, A. Tannin-based rigid foams: A survey of chemical and physical properties. *Bioresour. Technol.* **2009**, *100*, 5162–5169. [[CrossRef](#)]
19. Li, X.; Pizzi, A.; Cangemi, M.; Fierro, V.; Celzard, A. Flexible natural tannin-based and protein-based biosourced foams. *Ind. Crop. Prod.* **2012**, *37*, 389–393. [[CrossRef](#)]
20. Grishechko, L.I.; Amaral-Labat, G.; Szczurek, A.; Fierro, V.; Kuznetsov, B.N.; Pizzi, A.; Celzard, A. New tannin-lignin aerogels. *Ind. Crop. Prod.* **2013**, *41*, 347–355. [[CrossRef](#)]
21. Santiago-Medina, F.J.; Tenorio-Alfonso, A.; Delgado-Sánchez, C.; Basso, M.C.; Pizzi, A.; Celzard, A.; Fierro, V.; Sánchez, M.C.; Franco, J.M. Projectable tannin foams by mechanical and chemical expansion. *Ind. Crop. Prod.* **2018**, *120*, 90–96. [[CrossRef](#)]

22. Zhao, W.; Pizzi, A.; Fierro, V.; Du, G.; Celzard, A. Effect of composition and processing parameters on the characteristics of tannin-based rigid foams. *Part I Cell Struct. Mater. Chem. Phys.* **2010**, *122*, 175–182. [[CrossRef](#)]
23. Lacoste, C.; Basso, M.C.; Pizzi, A.; Laborie, M.P.; Garcia, D.; Celzard, A. Bioresourced pine tannin/furanic foams with glyoxal and glutaraldehyde. *Ind. Crop. Prod.* **2013**, *45*, 401–405. [[CrossRef](#)]
24. Basso, M.C.; Pizzi, A.; Lacoste, C.; Delmotte, L.; Al-Marzouki, F.M.; Abdalla, S.; Celzard, A. MALDI-TOF and ¹³C NMR analysis of tannin-furanic-polyurethane foams adapted for industrial continuous lines application. *Polymers* **2014**, *6*, 2985–3004. [[CrossRef](#)]
25. Lacoste, C.; Pizzi, A.; Basso, M.C.; Laborie, M.P.; Celzard, A. Pinus pinaster tannin/furanic foams: PART I. Formulation. *Ind. Crop. Prod.* **2014**, *52*, 450–456. [[CrossRef](#)]
26. Lacoste, C.; Basso, M.C.; Pizzi, A.; Celzard, A.; Ebang, E.E.; Gallon, N.; Charrier, B. Pine (*P. pinaster*) and quebracho (*S. lorentzii*) tannin-based foams as green acoustic absorbers. *Ind. Crop. Prod.* **2015**, *67*, 70–73. [[CrossRef](#)]
27. Amaral-Labat, G.; Grischechko, L.; Szczurek, A.; Fierro, V.; Pizzi, A.; Kuznetsov, B.; Celzard, A. Highly mesoporous organic aerogels derived from soy and tannin. *Green Chem.* **2012**, *14*, 3099–3106. [[CrossRef](#)]
28. Merle, J.; Birot, M.; Deleuze, H.; Mitterer, C.; Carré, H.; Charrier-El Bouhtoury, F. New biobased foams from wood byproducts. *Mater. Des.* **2016**, *91*, 186–192. [[CrossRef](#)]
29. Basso, M.C.; Giovando, S.; Pizzi, A.; Pasch, H.; Pretorius, N.; Delmotte, L.; Celzard, A. Flexible-elastic copolymerized polyurethane-tannin foams. *J. Appl. Polym. Sci.* **2014**, *131*, 40499. [[CrossRef](#)]
30. Li, X.; Essawy, H.A.; Pizzi, A.; Delmotte, L.; Rode, K.; Le Nouen, D.; Fierro, V.; Celzard, A. Modification of tannin based rigid foams using oligomers of a hyperbranched poly (amine-ester). *J. Polym. Res.* **2012**, *19*, 21. [[CrossRef](#)]
31. Santiago-Medina, F.J.; Delgado-Sánchez, C.; Basso, M.C.; Pizzi, A.; Fierro, V.; Celzard, A. Mechanically blown wall-projected tannin-based foams. *Ind. Crop. Prod.* **2018**, *113*, 316–323. [[CrossRef](#)]
32. Szczurek, A.; Fierro, V.; Pizzi, A.; Stauber, M.; Celzard, A. A new method for preparing tannin-based foams. *Ind. Crop. Prod.* **2014**, *54*, 40–53. [[CrossRef](#)]
33. Kihara, N.; Endo, T. Synthesis and properties of poly (hydroxyurethane)s. *J. Polym. Sci. Part A Polym. Chem.* **1993**, *31*, 2765–2773. [[CrossRef](#)]
34. Kihara, N.; Kushida, Y.; Endo, T. Optically active poly (hydroxyurethane)s derived from cyclic carbonate and L-lysine derivatives. *J. Polym. Sci. Part A Polym. Chem.* **1996**, *34*, 2173–2179. [[CrossRef](#)]
35. Kim, M.R.; Kim, H.S.; Ha, C.S.; Park, D.W.; Lee, J.K. Syntheses and thermal properties of poly (hydroxy) urethanes by polyaddition reaction of bis (cyclic carbonate) and diamines. *J. Appl. Polym. Sci.* **2001**, *81*, 2735–2743. [[CrossRef](#)]
36. Tomita, H.; Sanda, F.; Endo, T. Model reaction for the synthesis of polyhydroxyurethanes from cyclic carbonates with amines: Substituent effect on the reactivity and selectivity of ring-opening direction in the reaction of five-membered cyclic carbonates with amine. *J. Polym. Sci. Part A Polym. Chem.* **2001**, *39*, 3678–3685. [[CrossRef](#)]
37. Rokicki, G.; Piotrowska, A. A new route to polyurethanes from ethylene carbonate, diamines and diols. *Polymer* **2002**, *43*, 2927–2935. [[CrossRef](#)]
38. Ubaghs, L.; Fricke, N.; Keul, H.; Höcker, H. Polyurethanes with pendant hydroxyl groups: Synthesis and characterization. *Macromol. Rapid Commun.* **2004**, *25*, 517–521. [[CrossRef](#)]
39. Ochiai, B.; Inoue, S.; Endo, T. Salt effect on polyaddition of bifunctional cyclic carbonate and diamine. *J. Polym. Sci. Part A Polym. Chem.* **2005**, *43*, 6282–6286. [[CrossRef](#)]
40. Birukov, O.; Potashnikova, R.; Leykin, A.; Figovsky, O.; Shapovalov, L. Advantages in chemistry and technology of non-isocyanate polyurethane. *J. Sci. Isr. Technol. Adv.* **2014**, *11*, 160–167.
41. Boyer, A.; Cloutet, E.; Tassaing, T.; Gadenne, B.; Alfos, C.; Cramail, H. Solubility in CO₂ and carbonation studies of epoxidized fatty acid diesters: towards novel precursors for polyurethane synthesis. *Green Chem.* **2010**, *12*, 2205–2213. [[CrossRef](#)]
42. Besse, V.; Auvergne, R.; Carlotti, S.; Boutevin, G.; Otazaghine, B.; Caillol, S.; Pascault, J.-P.; Boutevin, B. Synthesis of isosorbide based polyurethanes: An isocyanate free method. *React. Funct. Polym.* **2013**, *73*, 588–594. [[CrossRef](#)]

43. Fleischer, M.; Blattmann, H.; Mülhaupt, R. Glycerol-, pentaerythritol-and trimethylolpropane-based polyurethanes and their cellulose carbonate composites prepared via the non-isocyanate route with catalytic carbon dioxide fixation. *Green Chem.* **2013**, *15*, 934–942. [[CrossRef](#)]
44. Nohra, B.; Candy, L.; Blanco, J.F.; Guerin, C.; Raoul, Y.; Mouloungui, Z. From petrochemical polyurethanes to biobased polyhydroxyurethanes. *Macromolecules* **2013**, *46*, 3771–3792. [[CrossRef](#)]
45. Annunziata, L.; Diallo, A.K.; Fouquay, S.; Michaud, G.; Simon, F.; Brusson, J.M.; Carpentier, J.F.; Guillaume, S.M. α , ω -Di (glycerol carbonate) telechelic polyesters and polyolefins as precursors to polyhydroxyurethanes: An isocyanate-free approach. *Green Chem.* **2014**, *16*, 1947–1956. [[CrossRef](#)]
46. Blattmann, H.; Fleischer, M.; Bähr, M.; Mülhaupt, R. Isocyanate-and phosgene-free routes to polyfunctional cyclic carbonates and green polyurethanes by fixation of carbon dioxide. *Macromol. Rapid Commun.* **2014**, *35*, 1238–1254. [[CrossRef](#)]
47. Camara, F.; Benyahya, S.; Besse, V.; Boutevin, G.; Auvergne, R.; Boutevin, B.; Caillol, S. Reactivity of secondary amines for the synthesis of non-isocyanate polyurethanes. *Eur. Polym. J.* **2014**, *55*, 17–26. [[CrossRef](#)]
48. Comille, A.; Auvergne, R.; Figovsky, O.; Boutevin, B.; Caillol, S. A perspective approach to sustainable routes for non-isocyanate polyurethanes. *Eur. Polym. J.* **2017**, *87*, 535–552. [[CrossRef](#)]
49. Thébault, M.; Pizzi, A.; Dumarçay, S.; Gerardin, P.; Fredon, E.; Delmotte, L. Polyurethanes from hydrolysable tannins obtained without using isocyanates. *Ind. Crop. Prod.* **2014**, *59*, 329–336. [[CrossRef](#)]
50. Thébault, M.; Pizzi, A.; Essawy, H.A.; Barhoum, A.; Van Assche, G. Isocyanate free condensed tannin-based polyurethanes. *Eur. Polym. J.* **2015**, *67*, 513–526. [[CrossRef](#)]
51. Thébault, M.; Pizzi, A.; Santiago-Medina, F.J.; Al-Marzouki, F.M.; Abdalla, S. Isocyanate-free polyurethanes by coreaction of condensed tannins with aminated tannins. *J. Renew. Mater.* **2017**, *5*, 21–29. [[CrossRef](#)]
52. Xi, X.; Pizzi, A.; Delmotte, L. Isocyanate-free polyurethane coatings and adhesives from mono- and di-saccharides. *Polymers* **2018**, *10*, 402. [[CrossRef](#)] [[PubMed](#)]
53. Xi, X.; Pizzi, A.; Gerardin, C.; Lei, H.; Chen, X.; Amirou, S. Preparation and Evaluation of Glucose Based Non-Isocyanate Polyurethane Self-Blowing Rigid Foams. *Polymers* **2019**, *11*, 1802. [[CrossRef](#)] [[PubMed](#)]
54. Li, J.; Zhang, A.; Zhang, S.; Gao, Q.; Zhang, W.; Li, J. Larch tannin-based rigid phenolic foam with high compressive strength, low friability, and low thermal conductivity reinforced by cork powder. *Compos. Part B Eng.* **2019**, *156*, 368–377. [[CrossRef](#)]
55. Santos, O.S.H.; da Silva, M.C.; Silva, V.R.; Mussel, W.N.; Yoshida, M.I. Polyurethane foam impregnated with lignin as a filler for the removal of crude oil from contaminated water. *J. Hazard. Mater.* **2017**, *324*, 406–413. [[CrossRef](#)] [[PubMed](#)]
56. Li, X.; Qi, Y.; Yue, G.; Wu, Q.; Li, Y.; Zhang, M.; Guo, X.; Li, X.; Ma, L.; Li, S. Solvent- and catalyst-free synthesis of an azine-linked covalent organic framework and the induced tautomerization in the adsorption of U(VI) and Hg(II). *Green Chem.* **2019**, *21*, 649–657. [[CrossRef](#)]
57. Zhou, F.; Zhang, T.; Zou, B.; Hu, W.; Wang, B.; Zhan, J.; Ma, C.; Hu, Y. Synthesis of a novel liquid phosphorus-containing flame retardant for flexible polyurethane foam: Combustion behaviors and thermal properties. *Polym. Degrad. Stab.* **2020**, *171*, 109029. [[CrossRef](#)]
58. Lacoste, C.; Čop, M.; Kempainen, K.; Giovando, S.; Pizzi, A.; Laborie, M.P.; Sernek, M.; Celzard, A. Biobased foams from condensed tannin extracts from Norway spruce (*Picea abies*) bark. *Ind. Crop. Prod.* **2015**, *73*, 144–153. [[CrossRef](#)]
59. Pizzi, A.; Tekely, P. Mechanism of polyphenolic tannin resin hardening by hexamethylenetetramine: CP-MAS ^{13}C -NMR. *J. Appl. Polym. Sci.* **1995**, *56*, 1645–1650. [[CrossRef](#)]
60. Pichelin, F.; Kamoun, C.; Pizzi, A. Hexamine hardener behaviour: effects on wood glueing, tannin and other wood adhesives. *Holz Als Roh-Und Werkst.* **1999**, *57*, 305–317. [[CrossRef](#)]
61. Kamoun, C.; Pizzi, A. Mechanism of hexamine as a non-aldehyde polycondensation resins hardener. Part 1: Hexamine decomposition and reactive intermediates. *Holzforsch. Holzverwert.* **2000**, *52*, 16–19.
62. Kamoun, C.; Pizzi, A. Mechanism of hexamine as a non-aldehyde polycondensation hardener. Part 2: Recomposition of intermediate reactive compounds. *Holzforsch. Holzverwert.* **2000**, *52*, 66–67.
63. Kamoun, C.; Pizzi, A.; Zanetti, M. Upgrading of MUF resins by buffering additives-Part 1: Hexamine sulphate effect and its limits. *J. Appl. Polym. Sci.* **2003**, *90*, 203–214. [[CrossRef](#)]
64. Tondi, G. Tannin-based copolymer resins: Synthesis and characterization by solid state ^{13}C NMR and FT-IR spectroscopy. *Polymers* **2017**, *9*, 223. [[CrossRef](#)]

65. Basso, M.C.; Pizzi, A.; Maris, J.P.; Delmotte, L.; Colin, B.; Rogaume, Y. MALDI-TOF, ¹³C NMR and FTIR analysis of the cross-linking reaction of condensed tannins by triethyl phosphate. *Ind. Crop. Prod.* **2017**, *95*, 621–631. [[CrossRef](#)]
66. Zhou, X.; Li, B.; Xu, Y.; Essawy, H.; Wu, Z.; Du, G. Tannin-furanic resin foam reinforced with cellulose nanofibers (CNF). *Ind. Crop. Prod.* **2019**, *134*, 107–112. [[CrossRef](#)]
67. Zhang, A.; Li, J.; Zhang, S.; Mu, Y.; Zhang, W.; Li, J. Characterization and acid-catalysed depolymerization of condensed tannins derived from larch bark. *Rsc. Adv.* **2017**, *7*, 35135–35146. [[CrossRef](#)]



© 2020 by the authors. Licensee MDPI, Basel, Switzerland. This article is an open access article distributed under the terms and conditions of the Creative Commons Attribution (CC BY) license (<http://creativecommons.org/licenses/by/4.0/>).

3.10 Biomousses Tannin-Humins auto-gonflantes à température ambiante

Résumé: Des mousses tanins-furaniques auto-soufflantes à température ambiante ont été préparées en substituant une grande partie, voire une majorité, d'alcool furfurylique par des humines, un matériau polyfurannique issu du traitement acide à haute température du fructose. Les mousses à cellules fermées ont été préparées et durcies à température ambiante, tandis que les mousses à cellules interconnectées ont été préparées et durcies à 80°C, ceci étant dû à l'évaporation plus vigoureuse du solvant. Ces mousses semblent présenter des caractéristiques similaires à celles d'autres mousses tanins-furaniques à base uniquement d'alcool furfurylique. Une série de structures oligomères tanin-humines-alcool furfurylique ont été définies, indiquant que les trois réactifs co-réagissent. Les humines de poids moléculaire encore plus élevé semblent bien réagir avec les tanins condensés, et même à température ambiante, mais ils réagissent plus lentement que l'alcool furfurylique. Cela est dû à leur poids moléculaire moyen élevé et à leur viscosité élevée, ce qui fait que leur réaction avec d'autres espèces chimiques est contrôlée par diffusion. Ainsi, de petites augmentations de solvant ont conduit à des mousses avec moins de fissures et de structures ouvertes. Il a montré que l'alcool furfurylique semble également avoir un rôle en tant que solvant des humines, et pas seulement en tant que co-réactif et générateur de chaleur d'auto-polymérisation pour l'expansion et le durcissement de la mousse. La contrainte-déformation pour les différentes mousses a montré une résistance à la compression plus élevée à la fois pour la mousse avec la plus faible et la plus forte proportion d'humines, donc dans les proportions dominantes d'alcool furfurylique ou d'humines. Ainsi, en raison de leur réactivité plus lente lorsque leur proportion augmente jusqu'à un certain niveau critique, ils sont plus nombreux à participer proportionnellement au temps d'expansion/durcissement de la mousse à la réaction.

Mots clés: humines; mousses; tanins; mousses tanniques-furaniques; température ambiante; auto-soufflant; spectrométrie de temps de vol à ionisation par désorption laser assistée par matrice (MALDI ToF).

Article

Ambient Temperature Self-Blowing Tannin-Humins Biofoams

Xinyi Chen ¹, Nathanael Guigo ², Antonio Pizzi ^{1,*} , Nicolas Sbirrazzuoli ² , Bin Li ², Emmanuel Fredon ¹ and Christine Gerardin ³

¹ LERMAB, University of Lorraine, 27 rue Philippe Seguin, 88000 Epinal, France; xinyi.chen@univ-lorraine.fr (X.C.); emmanuel.fredon@univ-lorraine.fr (E.F.)

² Department of Chemistry, University of the Cote d'Azur, 06103 Nice, France; Nathanael.GUIGO@univ-cotedazur.fr (N.G.); Nicolas.SBIRRAZZUOLI@univ-cotedazur.fr (N.S.); bin.li@univ-cotedazur.fr (B.L.)

³ LERMAB, University of Lorraine, Boulevard des Aiguillettes, 54000 Nancy, France; christine.gerardin@univ-lorraine.fr

* Correspondence: antonio.pizzi@univ-lorraine.fr

Received: 5 November 2020; Accepted: 17 November 2020; Published: 17 November 2020



Abstract: Ambient temperature self-blowing tannin–furanic foams have been prepared by substituting a great part—even a majority—of furfuryl alcohol with humins, a polyfuranic material derived from the acid treatment at high temperature of fructose. Closed-cell foams were prepared at room temperature and curing, while interconnected-cell foams were prepared at 80 °C and curing, this being due to the more vigorous evaporation of the solvent. These foams appear to present similar characteristics as other tannin–furanic foams based only on furfuryl alcohol. A series of tannin–humins–furfuryl alcohol oligomer structures have been defined indicating that all three reagents co-react. Humins appeared to react well with condensed tannins, even higher molecular weight humins species, and even at ambient temperature, but they react slower than furfuryl alcohol. This is due to their high average molecular weight and high viscosity, causing their reaction with other species to be diffusion controlled. Thus, small increases in solvent led to foams with less cracks and open structures. It showed that furfuryl alcohol appears to also have a role as a humins solvent, and not just as a co-reagent and self-polymerization heat generator for foam expansion and hardening. Stress-strain for the different foams showed a higher compressive strength for both the foam with the lowest and the highest proportion of humins, thus in the dominant proportions of either furfuryl alcohol or the humins. Thus, due to their slower reactivity as their proportion increases to a certain critical level, more of them do proportionally participate within the expansion/curing time of the foam to the reaction.

Keywords: humins; foams; tannins; tannin–furanic foams; ambient temperature; self-blowing; matrix assisted laser desorption ionization time-of-flight spectrometry (MALDI ToF)

1. Introduction

Heat insulation capacity, along with light, weight and sound absorption capacity are today sought-after foam characteristics, as foams are widely used in a number of applications where such properties are essential. Totally biosourced foams have recently been the focus of considerable research. A few types of ambient temperature, or even moderate temperature, self-blowing foams derived by mostly biosourced raw materials have been described in the literature. These have been based either on the self-blowing reaction of tannins with furfuryl alcohol, these being the older types [1–6], or on mono- and disaccharides non-isocyanate polyurethanes (NIPU) [7–9], or on tannin-based NIPUs [10], or even on tannin–monosaccharide NIPUs [11], or on mixtures of these strategies of approach.

The emphasis here is on ambient temperature self-blowing, the use of temperature to obtain foams being less attractive for a certain number and types of applications.

Condensed flavonoid tannins are vegetable polyphenolics, widespread in the plants world and commonly used as a raw material in a number of applications. Among these applications, their use to prepare biosourced foams for thermal and acoustic insulation and other applications has already attracted some attention [2,5,6,12]. Condensed tannins are mainly composed of polyhydroxy-flavan-3-ol and flavan-3,4-diol oligomers linked by carbon–carbon bonds between flavonoid monomer units [1]. The most used approach reported to prepare self-blowing tannin-based foams is by the acid condensation of tannins and furfuryl alcohol [1], with foam expansion driven by a blowing agent activated by the temperature increase caused by the acid self-condensation of furfuryl alcohol [1,2,5,6,13–20].

Humins are dark and viscous residual products obtained by the acid treatment of polysaccharides [21,22]. Humins coming from the acid conversion of fructose or glucose do yield polyfuranic materials still carrying furanic alcohol moieties [21–25]. Thus, under very acid conditions, humins can self-crosslink if heated, and the reaction can be accelerated by adding a strong acid initiator, such as p-toluene sulfonic acid (pTSA) [26]. Humins' solution in water can be employed, for instance, to create upon thermal treatment a polyfuranic network within wood cells. This so-called 'humination of wood' is following the same approach as in furfurylation of wood with aqueous furfuryl alcohol (FA) solutions [27]. Pure humins foams have been prepared by applying heat under very acid conditions [28]. However, this approach yields foams of a very limited variety of characteristics. This is due to the limited possibility of formulation of these heterogeneous distribution materials when foamed alone [28]. It is for this reason that some attempts could be made to mix such waste materials with other materials, in order to formulate foams more adaptable to a greater variety of situations. The only previous attempt of this approach was to react epoxidized linseed oil with humins [29]. Such a system was used to prepare thermoset resins and not strictly used to prepare foams. However, it used the addition of a synthetic mercaptan-terminated hardener that, notwithstanding its general use as a rapid curing agent for synthetic epoxy resins at ambient temperatures, caused the epoxidized linseed oil plus humins mix to need to be cured for several hours at 130 °C.

The goal set in this paper was rather restrictive, namely to prepare an ambient temperature self-blowing biobased foam also using the humins. For these reasons, a condensed tannin extract was chosen for such a purpose, as on top of presenting all the needed characteristics also possesses a very advantageous environmental imprint [30,31]. This paper then deals with the preparation and characterization of ambient temperature self-blowing tannin–furanic totally biosourced rigid foams in which humins represent up to the major proportion of their furanic component.

2. Materials and Methods

2.1. Materials

Commercial mimosa tannin (*Acacia mearnsii*, De Wild) bark extract and furfuryl alcohol (FA) were supplied by Silva Chimica (St. Michele Mondovi, Italy). Polyfuranic humins were laboratory prepared by the acid treatment of fructose at the Dept. of Chemistry, Université de la Côte d'Azur, Nice. p-Toluene sulfonic acid (p-TSA) was obtained from Sigma Aldrich (St. Louis, MO, USA). Glyoxal 40% solution (Acros Organics, Geel, Belgium).

2.2. Preparation of Humins

The humins were prepared from the acid-catalyzed dehydration of D-fructose in aqueous media following previous experimental protocols [23–25]. First, a mixture of 1 M aqueous solution of D-fructose (100 mL) and 0.01 M H₂SO₄ was prepared. This mixture was introduced into a 300 mL Teflon lined hydrothermal synthesis autoclave reactor and heated at 150 or 180 °C during 6 h. After reaction a solid residue was isolated by filtration on a 0.2 µm filter and washed several times with about 1 L of deionized water. The solid humins were then dried under vacuum at 80 °C during

16 h and ground into powder. The mass yields (i.e., mass % of humins based on initial fructose basis) was $18 \pm 1\%$ at $150\text{ }^{\circ}\text{C}$ and $30 \pm 2\%$ at $180\text{ }^{\circ}\text{C}$ in good agreement with van Zandvoort et al. [23].

2.3. Preparation of Tannin-Humin Foams

Two different series of tannin–humins foams were prepared.

The initial exploratory series was composed of the following formulations:

- 1 FA + glyoxal control, thus an only furanic foam without tannin [32]
- 2 FA + glyoxal + humins: 2.5 g humins + 9 g FA + 11.4 g glyoxal + 4 g olive powder + 3.6 g p-TSA + 1.5 DE (foaming agent); thus, a mixed furfuryl alcohol-humins. An only furanic foam.
- 3 Tannin + FA + humins (epoxy): 12 g tannin + 5.2 g FA + 4.4 g humins + 6 g p-TSA + 1.5 g DE + 6.6 g water.
- 4 Tannin + FA + humins: 15 g tannin + 5.2g FA + 3.7 g humins + 6 g p-TSA + 1.5 g DE + 3 g water.

Formulations 1 (control) 2 and 3 were self-blown and cured at ambient temperature ($24\text{ }^{\circ}\text{C}$), while formulation 4 was cured at $80\text{ }^{\circ}\text{C}$ to qualitatively observe the difference in morphology between foam 3 and foam 4. Their differences in composition were used to ensure a stronger cell walls for foam 4, as broken cell walls were expected by curing at $80\text{ }^{\circ}\text{C}$.

After these initial formulations the systematic study that followed used the formulations shown in Table 1. All the formulations were self-blown at ambient temperature ($23\text{ }^{\circ}\text{C}$).

Table 1. The formulation of tannin–humins foams.

Samples	Tannin (g)	Humins (g)	FA (g)	Water (g)	p-TSA (g)	DE (g)
F-H2.0-FA6-W1.5		2.0	6.0	1.5		
F-H3.7-FA6-W1.5		3.7	6.0	1.5		
F-H4.5-FA6-W1.5	15.0	4.5	6.0	1.5	6.0	1.5
F-H5.5-FA6-W1.5		5.5	6.0	1.5		
F-H5.9-FA5-W1.5		5.9	5.0	1.5		
F-H3.7-FA6-W2.0		3.7	6.0	2.0		

2.4. MALDI-ToF Analysis

Samples for matrix-assisted laser desorption ionization time-of-flight (MALDI-ToF) analysis were prepared first by dissolving 5 mg of sample powder in 10 mL of a 50:50 *v/v* acetone/water solution. Then 10 mg of this solution was added to 10 μL of a 2,5-dihydroxy benzoic acid (DHB) matrix to obtain a homogeneous solution. The locations dedicated to the samples on the analysis plaque were first covered with 2 μL of a NaCl solution 0.1 M in 2:1 *v/v* methanol/water, and pre-dried. Then, 1 μL of the sample solution was placed on its dedicated location and the plaque was dried again. The reference substance used for the equipment calibration was red phosphorus. MALDI-ToF spectra were obtained using an Axima-Performance mass spectrometer from Shimadzu Biotech (Kratos Analytical Shimadzu Europe Ltd., Manchester, UK) using a linear polarity positive tuning mode. The measurements were carried out making 1000 profiles per sample with two shots accumulated per profile. The spectra precision is of $\pm 1\text{ Da}$.

For the MALDI ToF analysis the foam sample was ground to a very fine powder homogeneously covered on the target point of dedicated analysis plaque through series of steps before testing. The target testing spots were first covered with the 1.5 μL of a 0.1 M NaCl (in a methanol:water mixture (1:1)) and then completely dried. Secondly, 7.5 mg of samples were dissolved into a 1 mL 50:50 *v/v* water/acetone mixture solution. Then, 1.5 μL of this solution was mixed with 1.5 μL of DHB (2,5-dihydroxy benzoic acid) matrix to obtain a homogenous solution. Finally, 1.5 μL of sample-DHB solution were placed on the corresponding testing spots, and dried completely. Before each test, the device was calibrated by using as reference red phosphorous. The measurements were carried out making 1000 profiles per sample with two shots accumulated per profile. The spectra precision is of $\pm 1\text{ Da}$.

2.5. FTIR

Fourier transform infra-red (FTIR) analysis was carried out using a Shimadzu IR Affinity-1 (Shimadzu Europe Ltd., Manchester, UK) spectrophotometer. A blank sample tablet of potassium bromide, ACS reagent from ACROS Organics (Geel, Belgium), was prepared for the reference spectra. Similar tablets were prepared by mixing potassium bromide with 5% by weight of the sample powders. The spectra were plotted in percentage transmittance by combining 32 scans with a resolution of 2.0 cm^{-1} in the $400\text{--}4000\text{ cm}^{-1}$ range.

2.6. Apparent Density

According to the standard method of ASTM D1622-08, all testing foam samples were prepared to a size of $30 \times 30 \times 30\text{ mm}^3$. The ratio of weight to cubic volume of the specimen volume was defined as density. Five sample repeats were tested for each foam.

2.7. Scanning Electron Microscopy (SEM) Analysis

Scanning electron microscopy (SEM, Hitachi TM-3000) (Milexia, Paris, France) was used to analyze the microstructure and morphology of the foams obtained. All samples were made into 0.5 cm^2 (cross section). Then, a thin layer of gold–palladium was sputtered on the surface of the foams so that a better definition could be obtained.

2.8. Compression Strength

The samples were cut into a uniform size of $25 \times 25 \times 25\text{ mm}$. A universal testing machine (Instron 3300, Elancourt, France) was used to test the compression strength of the foams. The direction of load was parallel to that of the foam rise under ambient conditions. The crosshead rate was fixed at $2.0\text{ mm}\cdot\text{min}^{-1}$. At least three sample repeats were tested for each foam.

3. Results and Discussion

Humins are known to have a polyfuranic structure [21–23]. However, they are a mixture of a variety of polyfuranic oligomers rather than possessing a unitary polyfuranic structure. To further clarify the types of oligomers present in the humins used for foam formulation, and to ascertain their suitability for this task, MALDI ToF analysis was carried out. Figures 1–6 report the more significant MALDI ToF spectra (more spectra are presented in the Supplementary Material) and Table 2 reports the assigned structures that could be interpreted from the spectra. From Table 2 it can be noticed that in the mix derived from the hydrolysis of fructose either at 180 or $150\text{ }^\circ\text{C}$ there are a considerable number of small furan-derived monomers, dimers and trimers, of which in particular structures of type I (139 Da Peak), II (203 Da peak) and III (284 Da peak) and their derivatives are examples (Scheme 1)

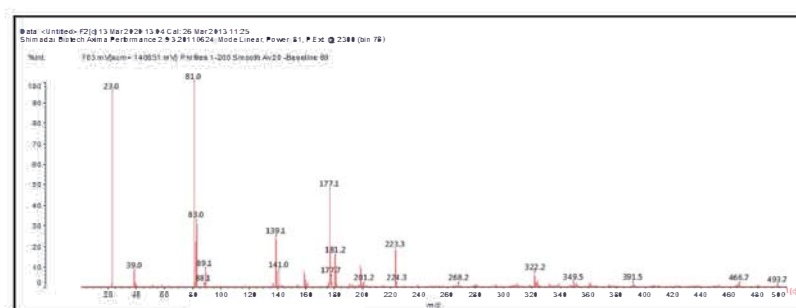


Figure 1. Matrix assisted laser desorption ionization time-of-flight spectrometry (MALDI ToF) spectrum of humins obtained at $180\text{ }^\circ\text{C}$ from fructose, 20–500 Da range.

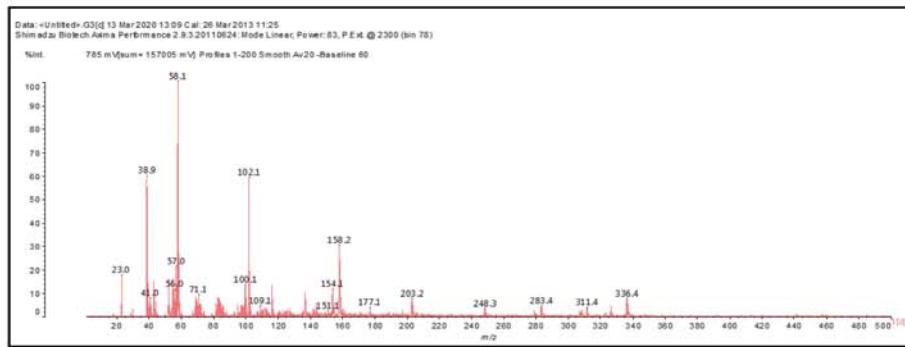


Figure 2. MALDI ToF spectrum of humins obtained at 150 °C from fructose, 20–500 Da range.

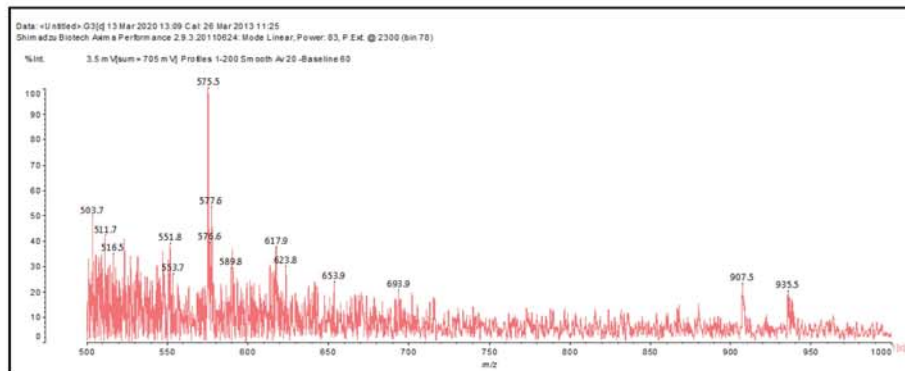


Figure 3. MALDI ToF spectrum of humins obtained at 150 °C from fructose, 500–1000 Da range.

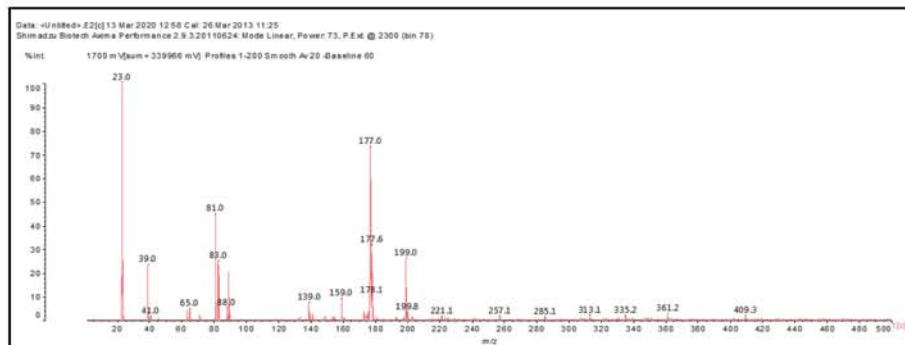


Figure 4. MALDI ToF spectrum of humins obtained at 180 °C from fructose, 20–500 Da range.

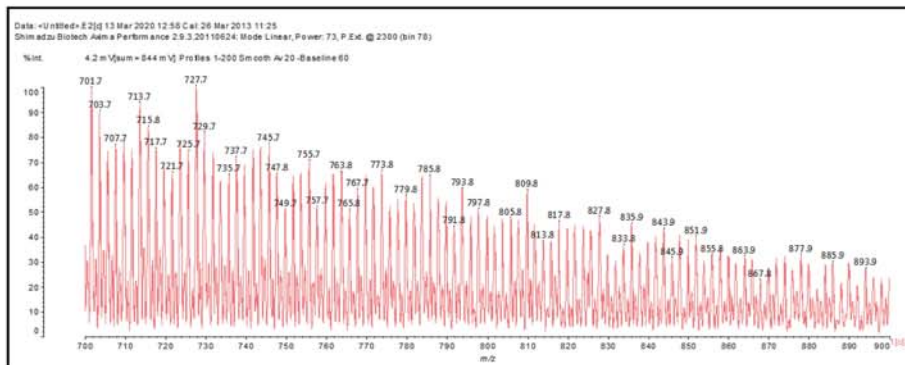


Figure 5. MALDI ToF spectrum of humins obtained at 180 °C from fructose, 700–900 Da range.

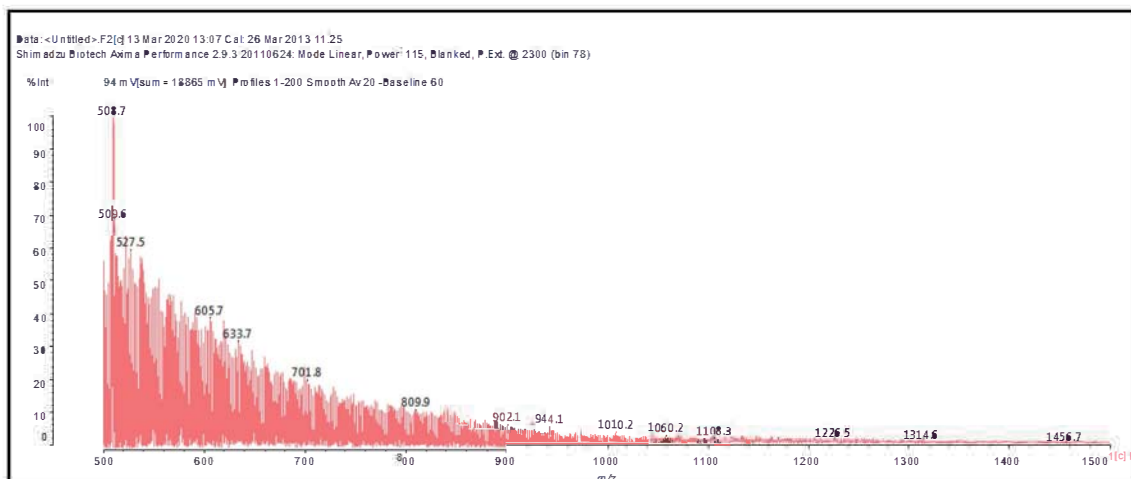
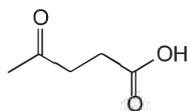


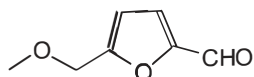
Figure 6. MALDI ToF spectrum of humins obtained at 180 °C from fructose, 500–1500 Da range.

Table 2. Assignment to relevant structures of MALDI ToF peaks of fructose laboratory derived humins.

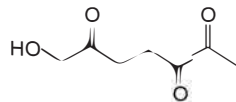
139 Da both theoretical and experimental, no Na⁺



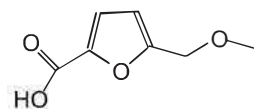
139 Da (calculated 140) no Na⁺



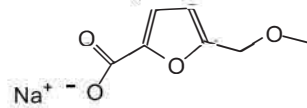
159 Da (calculated 158 Da) no Na⁺



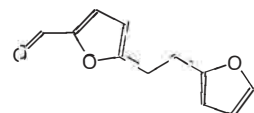
159 Da (calculated 156 Da) no Na⁺



177–179 Da (Calculated 178 Da) with Na⁺



202–203 Da (Calc 203) with Na⁺



203 Da (Calc 203 Da) with Na⁺ [22]

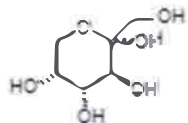
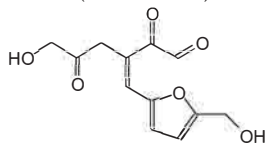
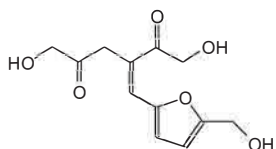


Table 2. Cont.

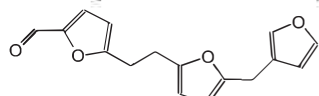
257 Da (calc 252 Da)



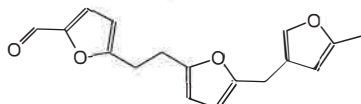
257 Da (Calc 254 Da)



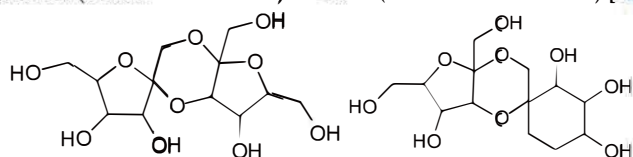
268 Da (Calculated 270 Da) no Na+, (180 °C no oxidation spectrum)



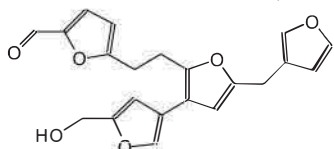
284 Da no Na+ (150 °C and 180° oxidized spectra)



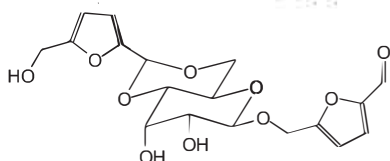
322 Da (Calculated 324 Da) no Na+ (180 °C not oxidized) [22]



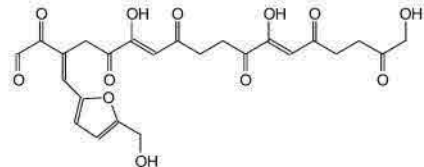
391 Da (Calculated 389 Da) with Na+, (180 °C not oxidized)



392 Da (Calculated 396 Da) (180 °C not oxidized) [22]



506 Da (no Na+) and 526 Da (with Na+) Calc.: 504 Da and 527 Da



623 Da (Calculated 623 Da) with Na+ (150 °C spectrum)

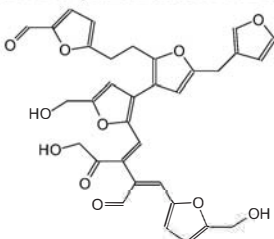
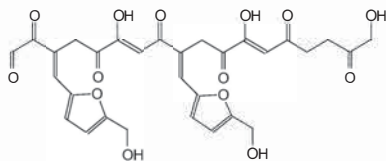
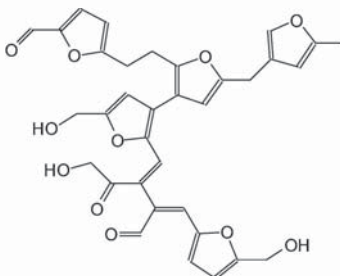


Table 2. Cont.

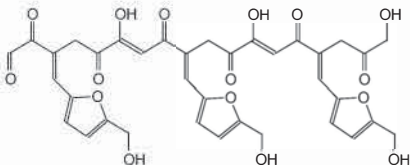
635 Da (with Na⁺)



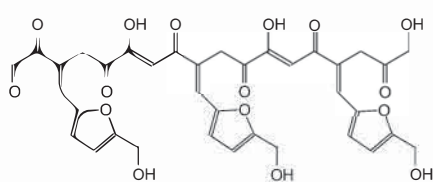
636 Da (Calculated 637 Da) with Na⁺, (180 °C not oxidized spectrum)



720 Da no Na⁺

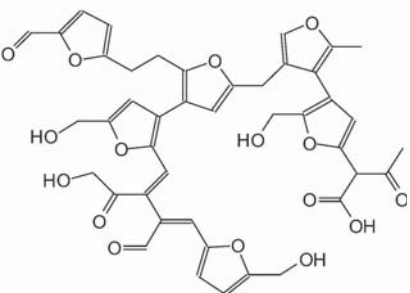


741 Da (calc 743 Da) with Na⁺



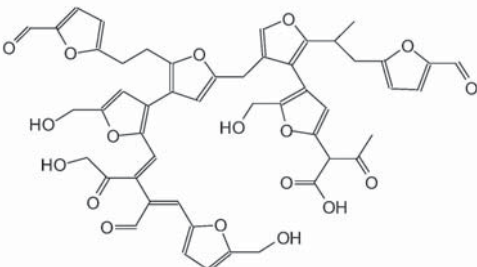
810 Da (Calculated 810 Da) without Na⁺ (180 °C Oxidized, 180 °C not oxidized, 150 °C)

833 Da (Calculated 833 Da) with Na⁺ (180 °C Oxidized, 180 °C not oxidized)



935 Da (Calculated 932 Da) without Na⁺ (180 °C Oxidized, 150 °C)

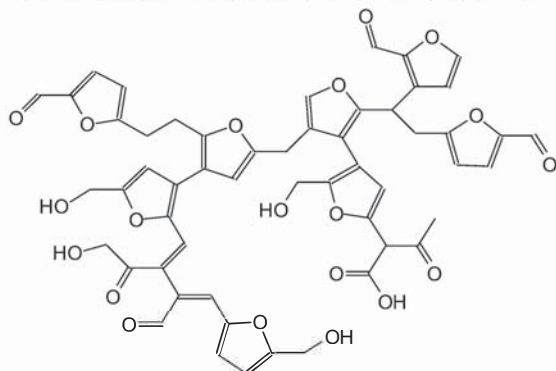
950-952-954 Da (Calculated 955 Da) with Na⁺ (180 °C oxidized and not oxidized)



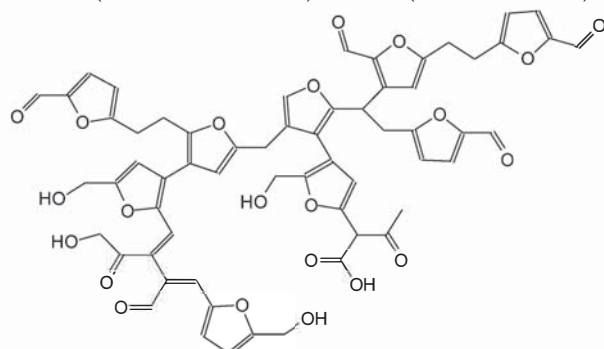
1010 Da (Calculated 1012 Da) no Na⁺ (180 °C not oxidized)

Table 2. Cont.

1033 Da (Calculated 1035 Da) with Na⁺ (180 °C oxidized)

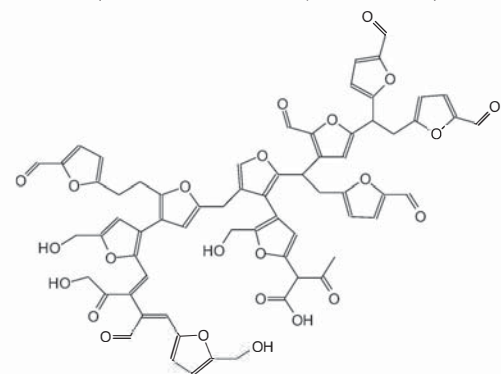


1137 Da (Calculated 1135 Da) no Na⁺ (180 °C oxidized)

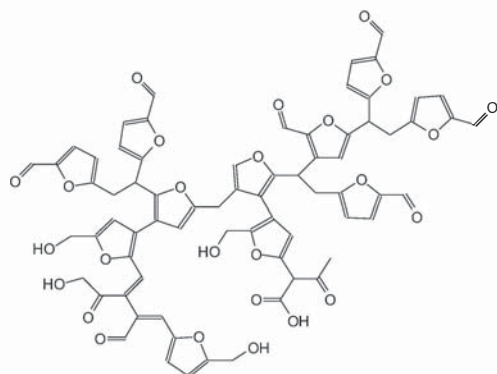


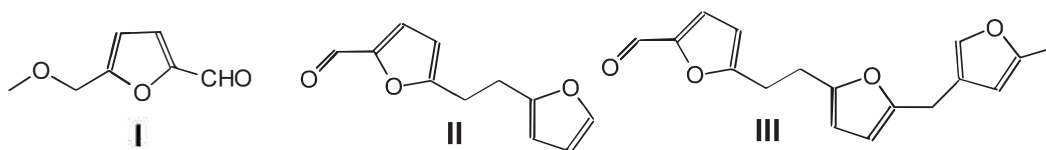
1227 Da (Calculated 1228 Da) no Na⁺ (180 °C not oxidized)

1250 Da (Calculated 1252 Da) with Na⁺ (150 °C)



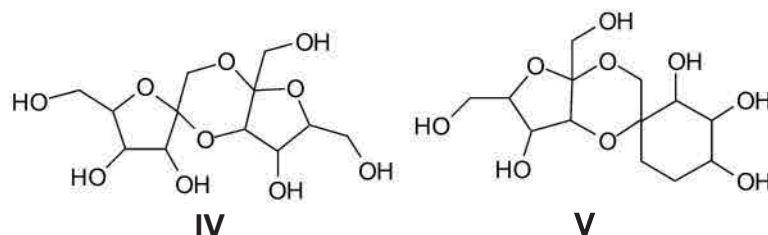
1351 Da With Na⁺





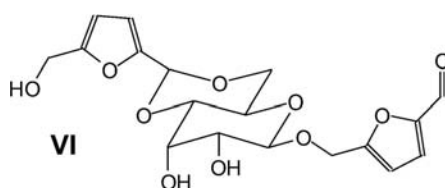
Scheme 1. Small furanic species present in the humins used.

More complex structures such as IV and V, both corresponding to the 322 Da peak, already previously identified [22] have also been confirmed (Scheme 2).



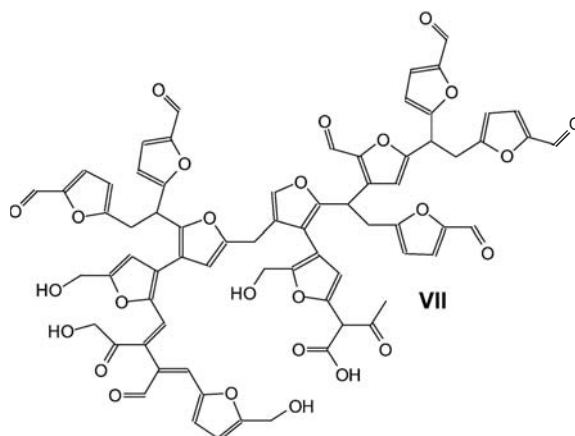
Scheme 2. More complex small structures present in the humins used.

Furanic structures still linked to condensed fructose moieties also appear to be present such as structure VI, assigned to the peak at 392 Da, also already previously identified [22] (Scheme 3).



Scheme 3. Example of furanic structures still linked to condensed fructose moieties present in the humins used.

It is the progression from structures I, II and III that however brings to the more classical representation of the polyfuranic structure of acid-derived fructose humins, this being represented among others by the peaks at 1227, 1250 and 1351 Da (VII), such as in Scheme 4 and higher more complex oligomers. This served to control that the humins prepared presented the polyfuranic structure expected and needed to formulate the tannin–humins foams.



Scheme 4. Example of a type of polyfuranic structure present in the humins used.

Two initial tannin–humins-FA formulations were prepared including two furanic foams controls. The two tannin–humins-FA were expanded and hardened one at ambient temperature (23 °C) and the other at 80 °C to see how preparation temperature influenced the morphology of the finished foams. The differences observed by scanning electron microscopy (SEM) were indeed quite major as can be seen in Figure 7. The foam prepared at ambient temperature presented a closed cells structure while the one prepared at 80 °C clearly presented an interconnected cells structure, with a number of open pores and cell walls breaks. The reason for this difference is due to the more vigorous evaporation of water at 80 °C breaking weaker cell wall sites in the structure. This does not occur at ambient temperature. This means that a foam of this type prepared at ambient temperature, once stabilized, is more suitable for thermal isolation applications, while when prepared at 80 °C it is more suitable for acoustic insulation [12].

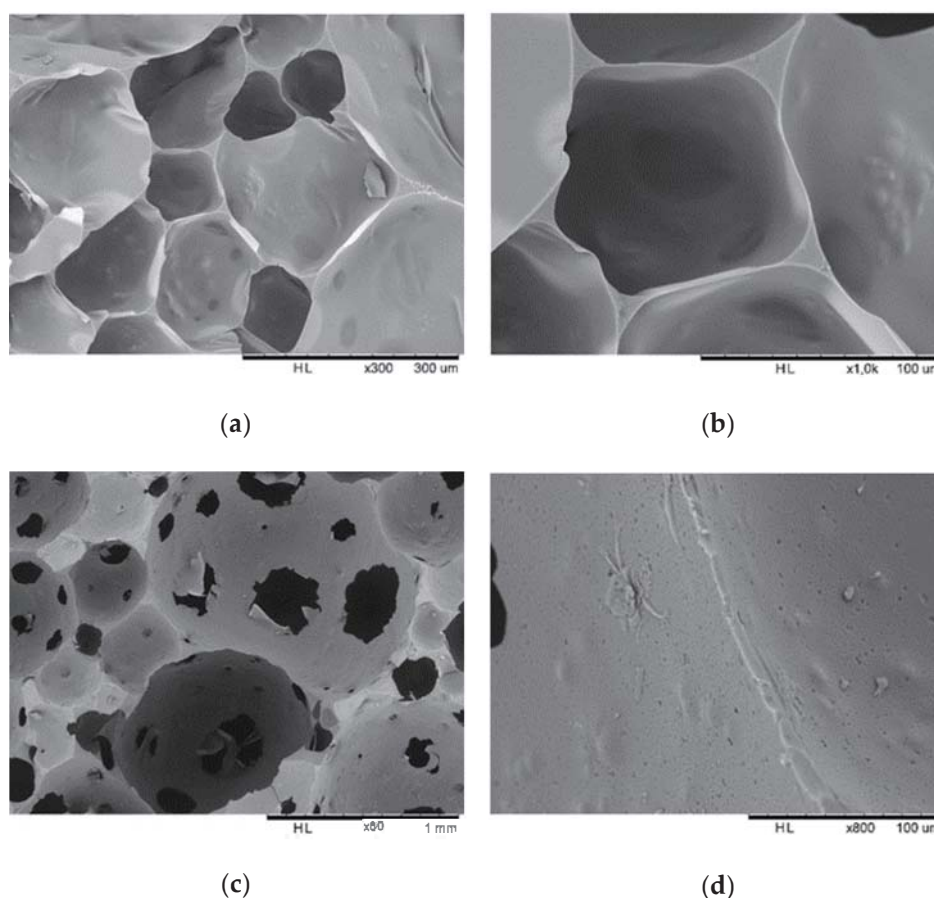


Figure 7. SEM of initial formulation 3 foam with magnitude of (a) 300× and (b) 10,000×, ambient temperature curing. SEM of initial formulation 4 with magnitude of (c) 80× and (d) 800×, 80 °C curing.

The foams in Table 1 were prepared to observe the effect of the differences in formulation on foam characteristics. The influence of small differences in the proportion of the water present and of the relative differences in humins to furfuryl alcohol proportions were studied. The results obtained, shown in Table 3 and Figures 8–11, indicated remarkable differences in behavior or structure and characteristics. SEM observation (Figures 8–10) showed that: (i) a small variation in the proportion of water (Figure 8a,b) does not appear to change much the structure of the foam when cured at ambient temperature; (ii) a decrease in the proportion of furfuryl alcohol, even if not major, appears to cause some cell wall rupture (Figure 9a,b) and a more open cells structure, even if the apparent uniformity of the cell wall still appears rather uniform and strong; (iii) a variation in the relative proportions of humins to furfuryl alcohol shows instead much more apparent structural differences (Figure 10a–d): when the proportion of humins is low and FA is dominant, a closed cell structure predominates

(Figure 10a). This at first transforms itself in a slightly more porous structure at the following two higher levels of humins (Figure 10b,c) proportion to return to a more closed cell structure at the highest relative proportions of humins used (Figure 10d).

Table 3. Apparent density, compressive strength and specific compressive strength of tannin–humins foams.

Samples	Density (g/cm ³)	Compressive Strength (MPa)	Specific Compressive Strength (kPa/kg·m ⁻³)
F-H2.0-FA6-W1.5	0.20	1.59	7.95
F-H3.7-FA6-W1.5	0.16	0.81	5.06
F-H4.5-FA6-W1.5	0.11	0.39	3.54
F-H5.5-FA6-W1.5	0.21	1.38	6.57
F-H5.9-FA5-W1.5	0.24	1.58	6.58
F-H3.7-FA6-W2.0	0.19	1.70	8.94

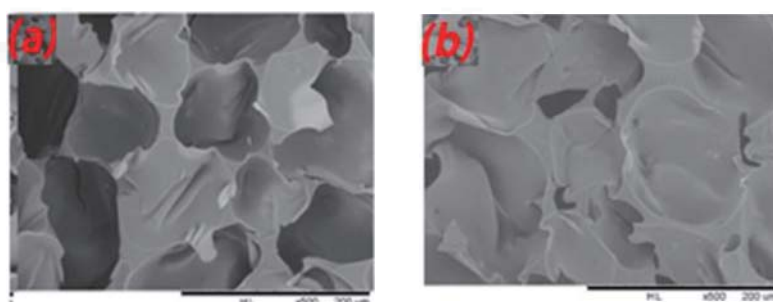


Figure 8. Effect on foam morphology of different proportions of water. (a) F-H3.7-FA6-W2.0; (b) F-H3.7-FA6-W1.5.

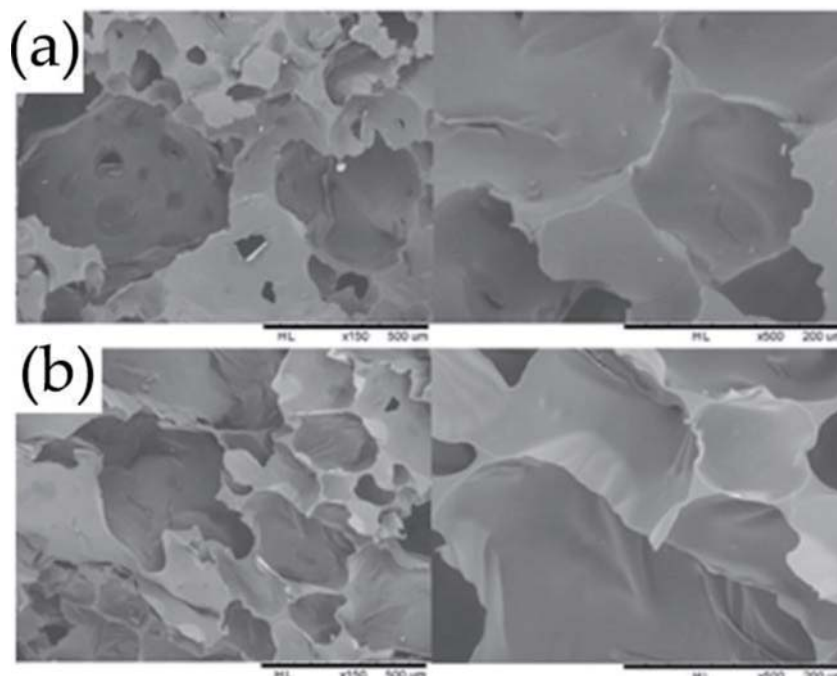


Figure 9. Effect on foam morphology of small difference proportions of furfuryl alcohol (FA): (a) F-H5.9-FA5-W1.5; (b) F-H5.5-FA6-W1.5.

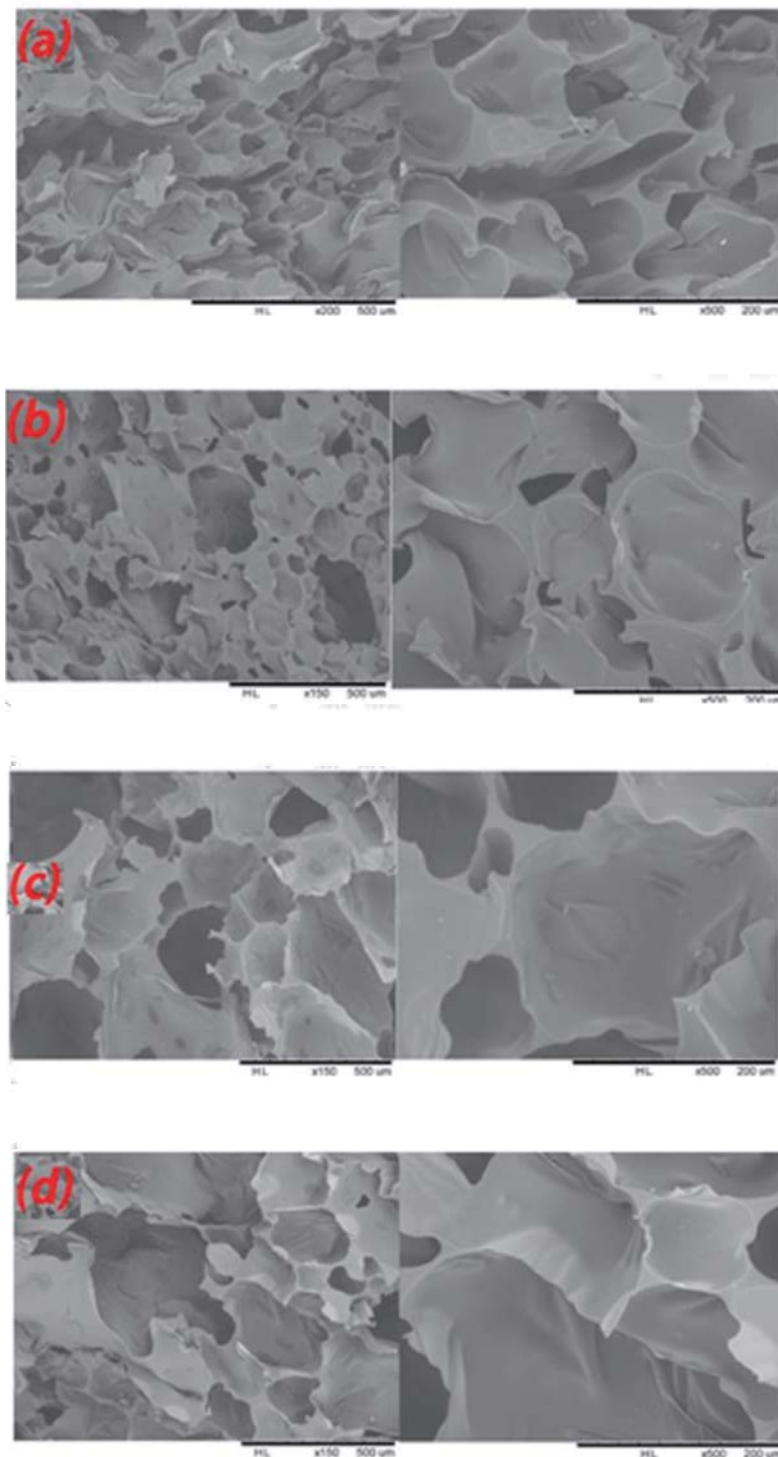


Figure 10. Effect on foam morphology of different proportions of humins. (a) F-H2.0-FA6-W1.5; (b) F-H3.7-FA6-W1.5; (c) F-H4.5-FA6-W1.5; (d) F-H5.9-FA6-W1.5.

These SEM observations explain the results of compression strength observed in Figure 11, and derives from the results shown in Table 3. Thus, in Figure 11 the curves of stress–strain of the different foams indicate higher compression strength as a function of strain for both the foam with the lowest and the highest proportion of humins in relation to furfuryl alcohol, and lower compression strength for the two intermediate humins proportion cases. This indicates that humins appear to be, in general, either less or slower reacting than furfuryl alcohol at ambient temperature by the

time the foam is set, but that as their proportion increases to a certain critical level more of them do proportionally participate within the expansion/curing time of the foam to the reaction to contribute to its strength characteristics. This observation infers that, if moderately higher foaming/curing temperatures are used, humins would most likely participate to a greater measure to the strength of the cell walls, but would also most likely present a predominant interconnected cells structure. These conclusions are confirmed and supported by the results for overall foam density, compression strength and particularly specific compression strength in Table 2, where in effect the overall density at first progressively decreases from the H2.0 to the H3.7 and H4.5 (humins percentage on total furanic material of respectively 25%, 38% and 43%), and then progressively increases passing from the H4.5 to the H5.5 and the H5.9 (humins percentage on total furanic material of respectively 43%, 48% and 54%) all these parameters peaking for the H5.9. The compression strength and specific compression strength do follow the same trend as the density and of the strength/strain curves in Figure 11.

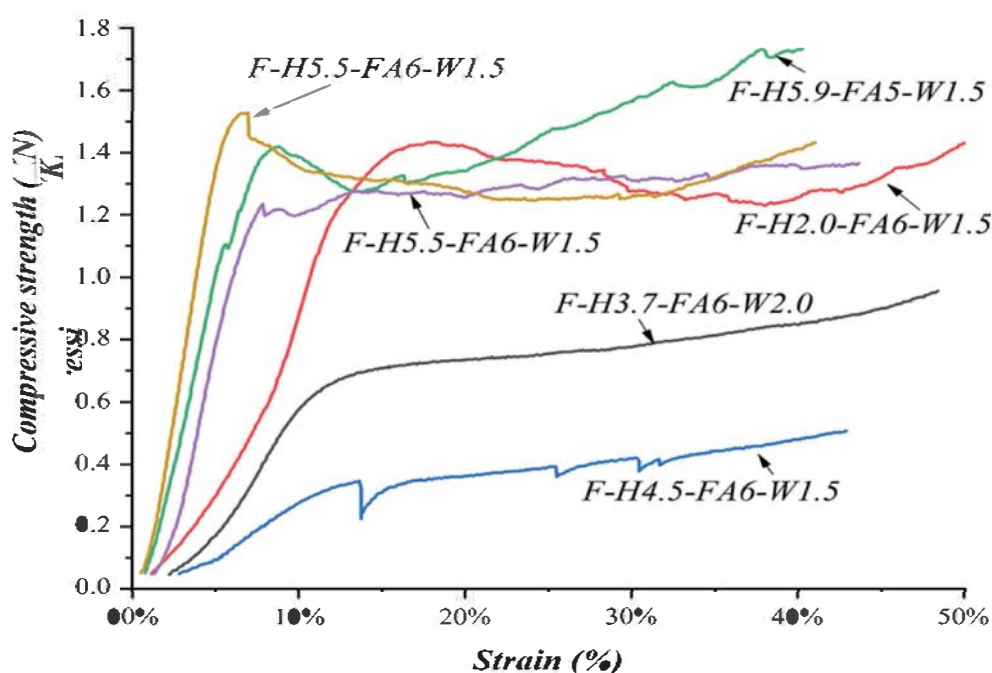


Figure 11. Compression strength as a function of percentage strain for the different tannin–humins foams.

However, it is interesting to observe the effect of a small increase of water on the H3.7 formulation, for which the density increases slightly but leads to an impressive increase in compression strength and more noticeably of specific compression strength. This result, supported by the SEM observations, indicate that the apparent lower reactivity of humins is due, partly or even mainly, to the hindrance to its reaction consequence of its high viscosity. The reaction is then clearly diffusion-controlled, a drawback that can be partially be eliminated or decreased by adding small proportions of a solvent (in this case water). The picture that is then obtained about the use of humins for tannin–humins biofoams is that a higher proportion of humins can be used to replace in the formulation furfuryl alcohol—if small to moderate proportions of a suitable solvent, for example water, are added. An increase in temperature can also help in decreasing the humins viscosity, but while curing the reactivity/mobility problem of the material will also contribute to increase the proportion of open cells in the foam structure. It is interesting too that the compression stress at >1 MPa is rather good, and it is higher than the majority of the expanded polystyrene foams used for isolation, and higher than for the foams of humins alone [28].

An example of the appearance of the foams prepared is shown in Figure 12. The appearance of the initial exploratory foams is also shown in Figure SM3 in the Supplementary Material.



Figure 12. Photographic record of appearance of the experimental tannin–humins foams once cut into cubes.

The FT-IR of the raw humins and of the different humins-FA mixes show some interesting features as well (Figure 13). The raw humins show the peaks at 1038 cm^{-1} and the very broad peak between 3000 and 3600 cm^{-1} of hydrogen bonded alcohol groups. The three peaks at around 1700 cm^{-1} correspond to aldehyde groups under different surrounding conditions, while the 1500 cm^{-1} peak is assigned to alkane groups asymmetric stretching, and the peak at 800 cm^{-1} to alkene groups present in structures as that of the 1351 Da peak in the MALDI ToF spectra. In the experimental humins-FA mixes the peak that appear superimposed to the humins groups are the 1310 cm^{-1} and 1029 cm^{-1} assigned to the stretching of the hydrogen-bonded alcohol function of furfuryl alcohol, which appears just very near to the 1038 cm^{-1} peak of humins, The furanic structures $\text{C}=\text{C}$ groups of both humins and furfuryl alcohol both appear at around 1200 cm^{-1} with two vicinal sharp peaks, the smaller assigned to the humins and the taller and sharper to the furfuryl alcohol.

It is of interest to observe the results of the MALDI ToF spectra of the finished foams, to see if the three main constituents—mainly tannin extract, furfuryl alcohol and humins oligomers—have jointly reacted. The list of the compounds identified for the F-4.5 H + 6 FA+1.5 W in Figure 14a–f is shown in Table 4. Several compounds and oligomers present in the MALDI spectra of the humins alone are also present in the MALDI spectra of the tannin–humins-FA foam, such as the ones at 621 , 635 , 1009 , 1035 , 1136 Da , and others. Additionally, present are the characteristic peaks of unreacted flavonoid monomers and dimers such as 304 and 327 Da , both for a gallo catechin monomer without and with Na^+ , 604 Da for a robinetinidin or catechin dimer with Na^+ , 607 Da for a gallo catechin dimer without Na^+ , 897 Da for a (gallo catechin)₂-robinetinidin trimer without Na^+ , 910 Da for a gallo catechin trimer without Na^+ , etc. However, there are a considerable number of peaks assigned to reaction products of flavonoid monomers and dimers with humins smaller molecular weight species as well as with both humins species and furfuryl alcohol. Some of the more significative ones will be discussed here (Scheme 5).

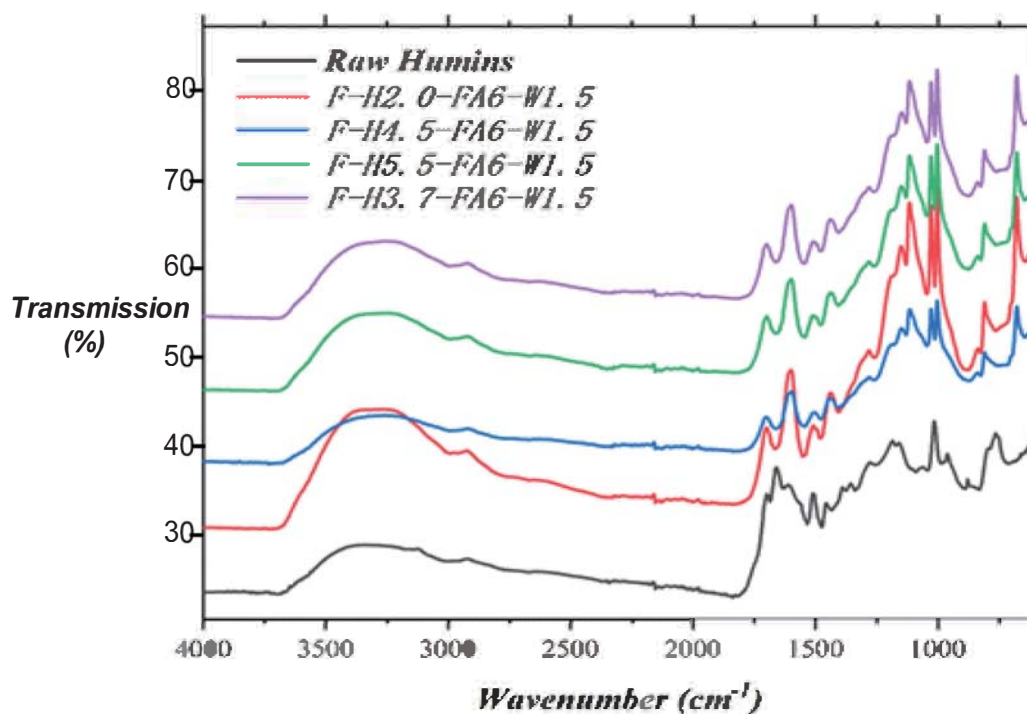
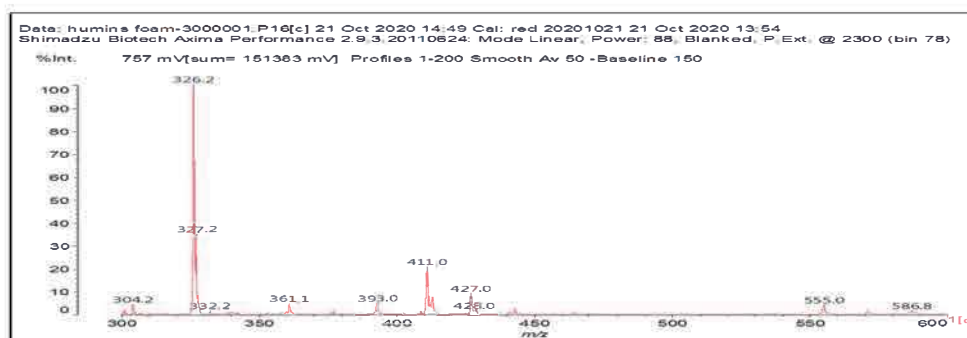
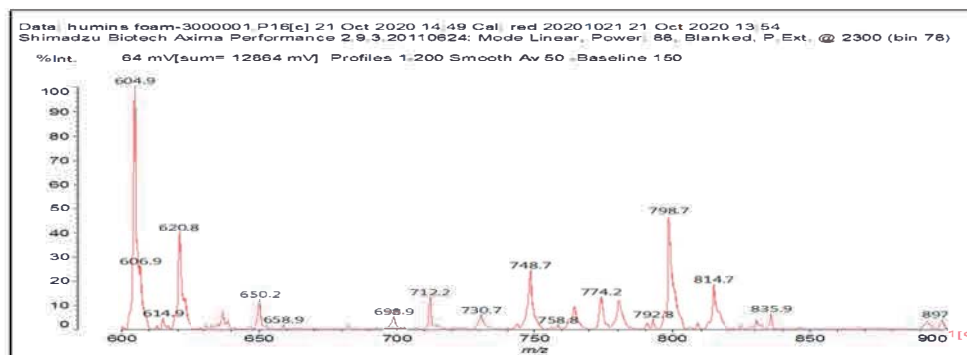


Figure 13. FT-IR of the different mixes of humins (H) and furfuryl alcohol (FA) used for the preparation of the tannin-humins foams.

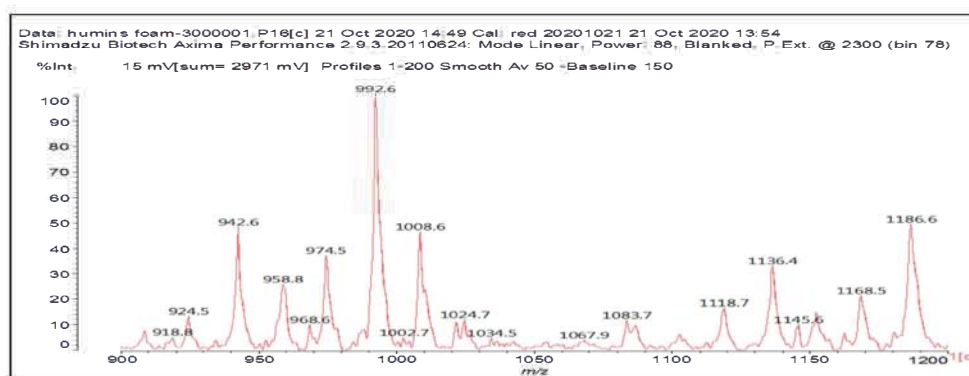


(a)

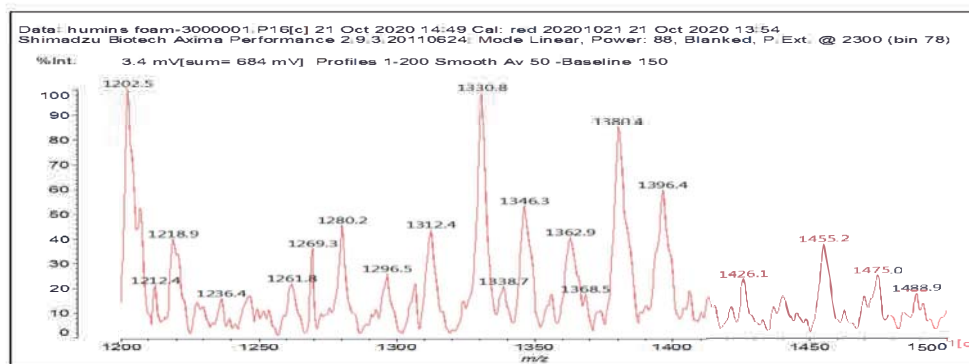


(b)

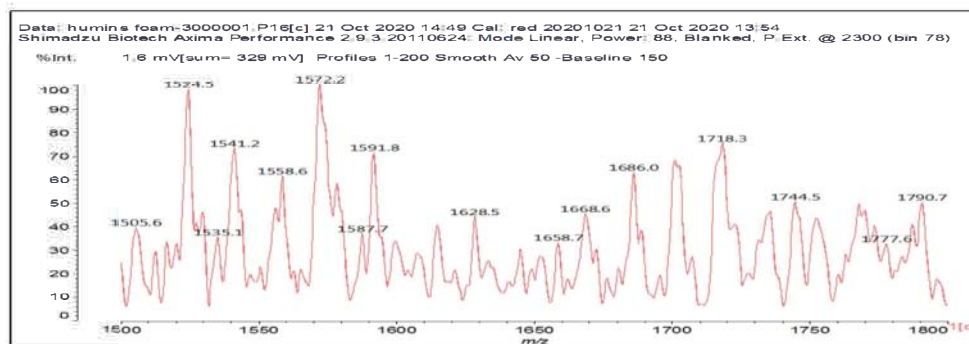
Figure 14. Cont.



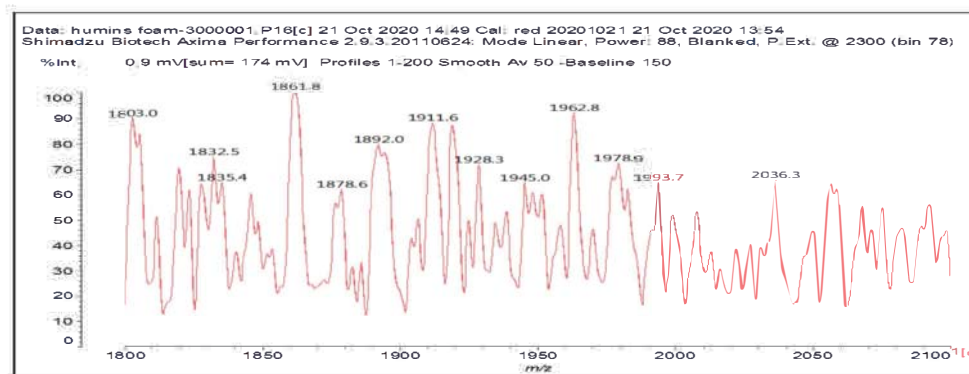
(c)



(d)



(e)



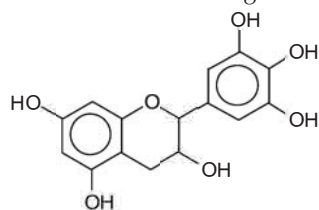
(f)

Figure 14. MALDI ToF spectrum of F-H4.5-FA6-W1.5 foams: (a) 300 to 600 Da range; (b) 600 to 900 Da range; (c) 900 to 1200 Da range; (d) 1200 to 1500 Da range; (e) 1500 to 1800 Da range; (f) 1800 to 2100 Da range.

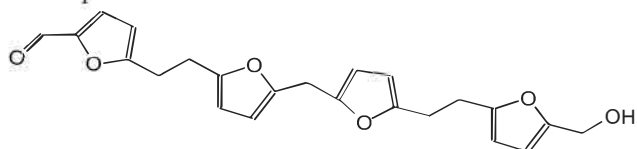
Table 4. MALDI ToF analysis assignments of relevant peaks of foam F-H4.5-FA6-W1.5.

304 Da Flavonoid gallocatechin, no Na+

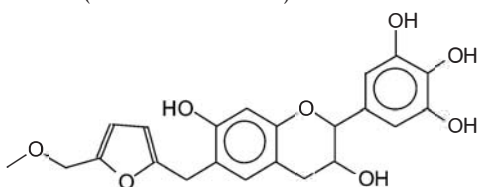
326–327 Da Flavonoid gallocatechin with Na+



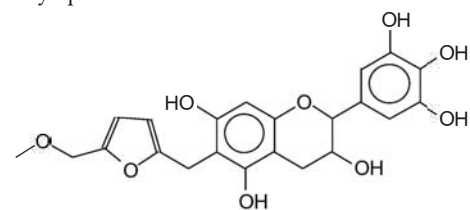
393 Da peak



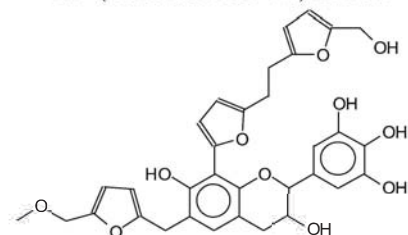
411 Da (Calculated 414 Da) no Na+



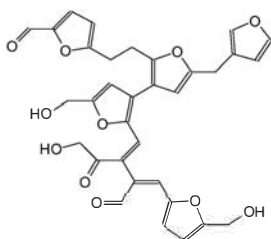
427–428 Da (Calculated 430) no Na+ reaction of a flavonoid with the humins aldehyde at 141 Da in humins only spectrum.



605 Da= (Calculated 605 Da) no Na+



621 Da with Na+



635 Da

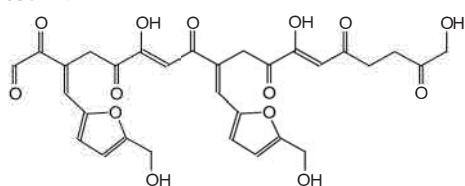
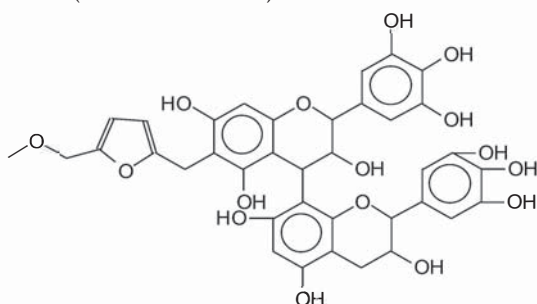


Table 4. Cont.

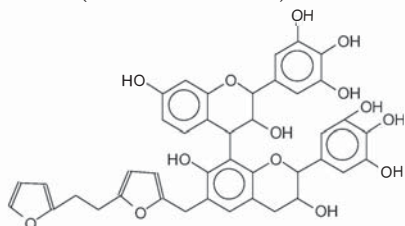
731 Da (calculated 733 Da) without Na+

758 Da (calculated 756 Da) with Na+



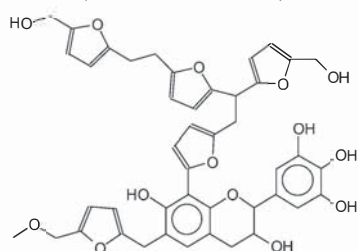
749 Da (Calculated 752 Da) no Na+, and

774 Da (Calculated 775 Da) with Na+



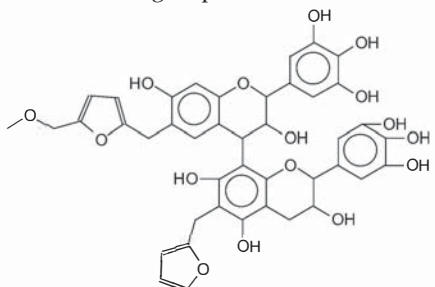
792 Da = 774 Da + 1x-OH (on A-ring of one flavonoid unit)

793 Da (Calculated 794 Da) no Na+ and 815 Da with Na+



783 Da = as 798 Da but based on a fisetinidin + fisetinidin dimer

798.8 Da (Calculated 798.5 Da) no Na+. A delphinidin–robinetinidin dimer reacted with a humins low molecular weight species and with furfuryl alcohol:



815 Da (calculated 915 Da) no Na+, reaction of flavonoid dimer with furfuryl alcohol and a 141 Da humins low molecular weight species

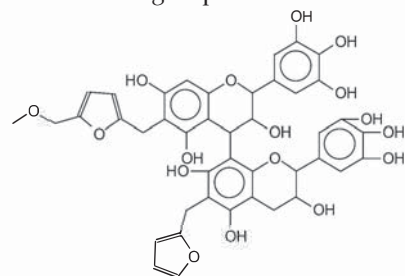
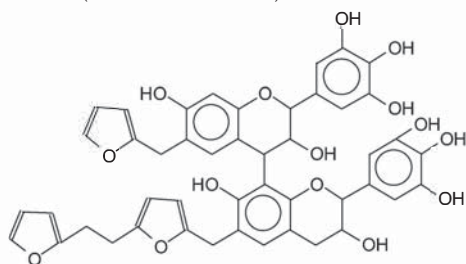
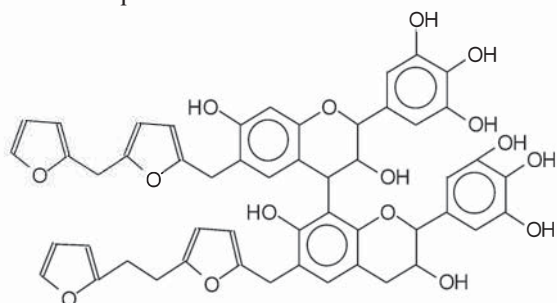


Table 4. Cont.

835 Da (calculated 833 Da) no Na+

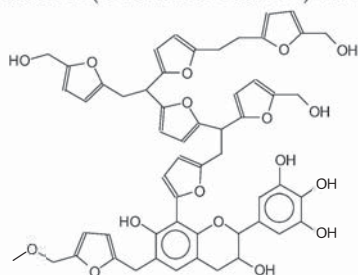


912 Da (Calculated 912) no Na+, small peak, reaction of a flavonoid dimer with polyfurfuryl alcohol and a humins compound



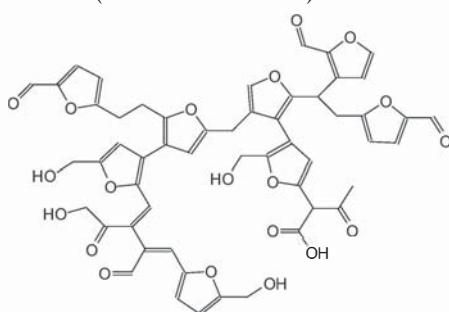
925 Da = (calculated 928 Da) = 912 + 1x-OH, no Na+

1008 Da (Calculated 1007 Da) with Na+.



1009 Da no Na+

1035 Da (Calculated 1035 Da) with Na+ in 180 °C oxidized



1136 Da (Calculated 1135 Da) no Na+ in 180 °C oxidized

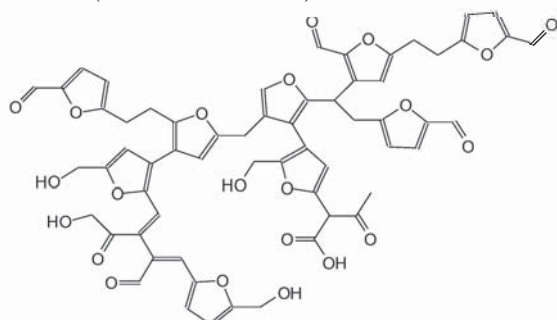
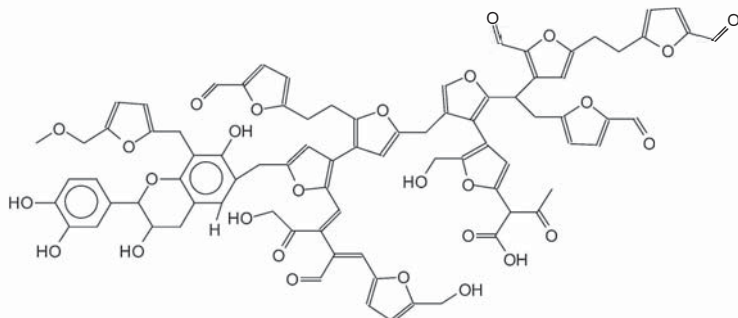
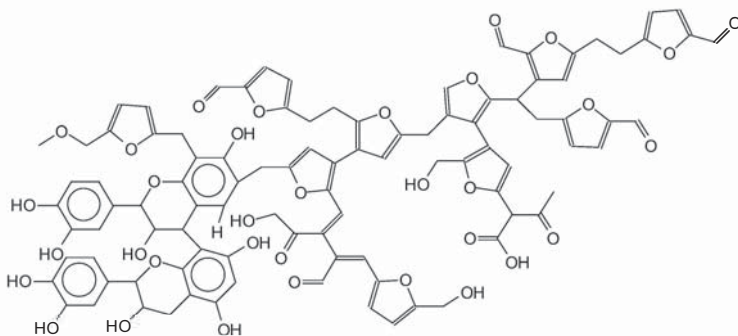


Table 4. Cont.

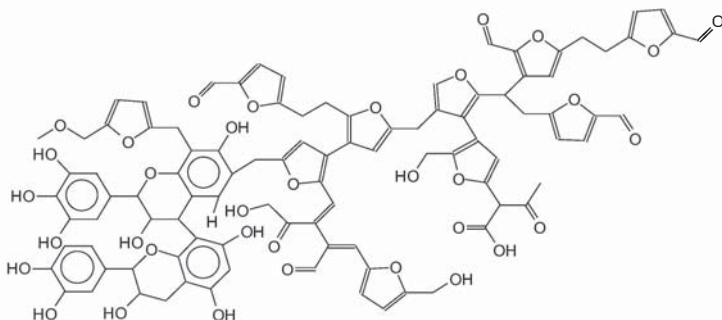
1535–1541 Da (Calc. 1538) with Na+



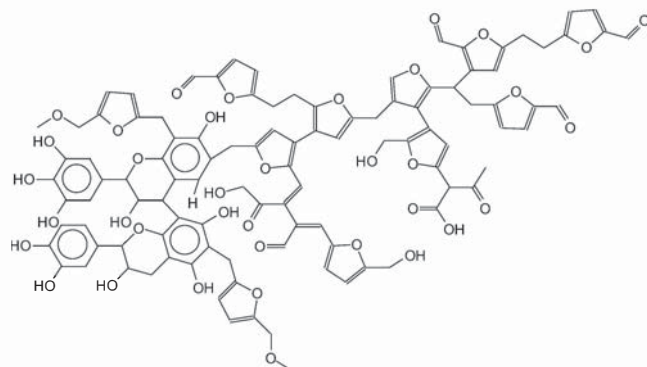
1803 Da (Calculated 1803) no Na+



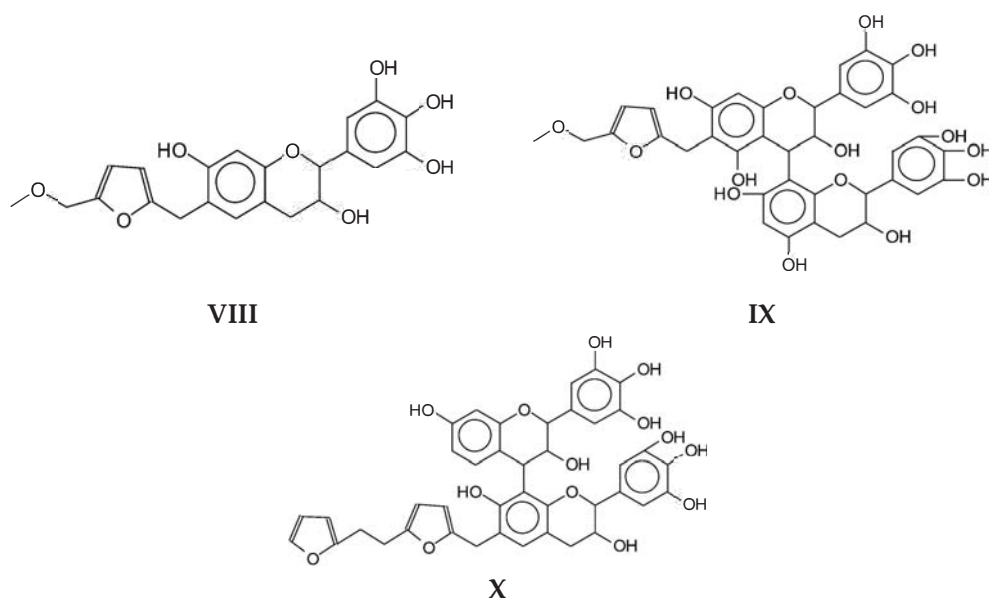
1819 Da (Calculated 1819 Da) no Na+



1945 Da (Calculated 1943) no Na+

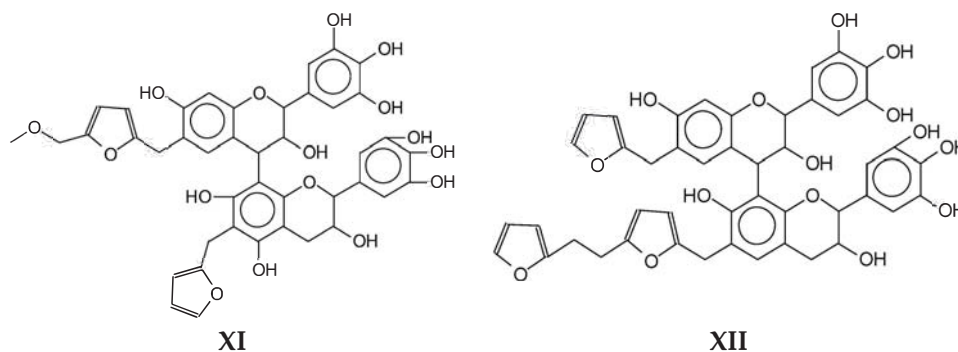


Species of type VIII (411 Da), IX (731 and 758 Da) and X (peaks 749 and 774 Da) are obtained by reaction of humins present species with different flavonoids monomers and dimers from the tannin. The peaks at 411, 427, 731, 749, 758, 774, 792, 912, 925 Da all belong to this category of tannin–humins oligomers.



Scheme 5. Examples of structures produced in the foams coreaction showing that flavonoid monomers and oligomers do react with simple humins structures.

Mixed species showing that both furfuryl alcohol and humins species have also both reacted at the same time with flavonoid structures from the tannin are also present. Examples of these, are the co-reacted tannins-humins-furfuryl alcohol structures as the ones at 798 Da (XI), 815 Da, and 835 Da (XII) (Scheme 6).

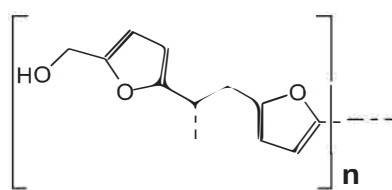


Scheme 6. Examples of structures produced in the foams coreaction showing that flavonoid oligomers do react with both furfuryl alcohol and simple humins structures.

There are at least two series where the successive peaks are all separated by an interval of 193–194 Da. The first of these series of oligomers belongs to the peaks at 411, 605, 799, 992, 1186, 1380, 1574, 1769, 1962 Da. The repeating motive is then a humins one, namely (XIII) (Scheme 7).

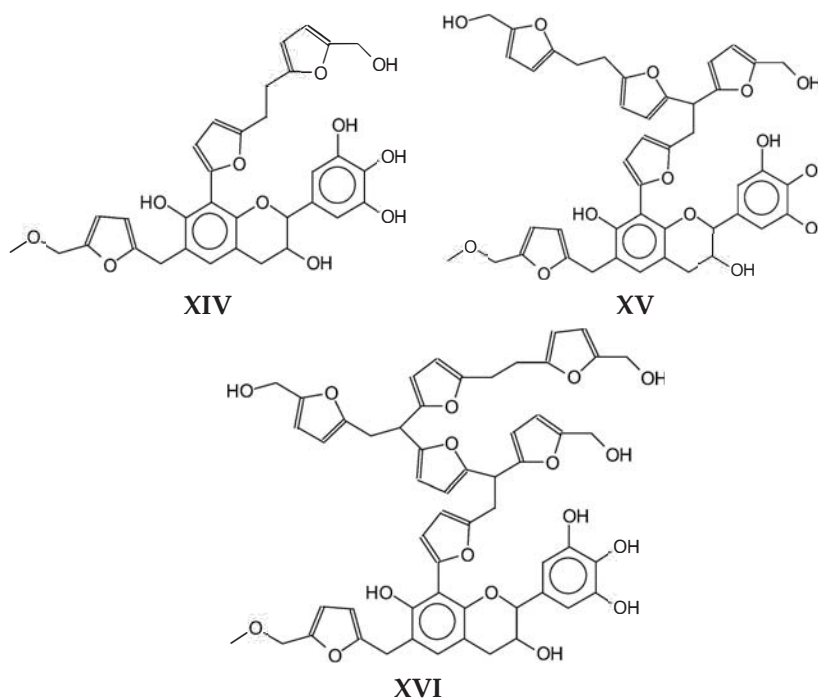
The peak at 411 Da is assigned to structure VIII above. Examples of the structures of some of the ones that follows in the series are 605 Da (XIV) and 798 Da (XV) without Na⁺. The species at 1008 Da (XVI) with Na⁺ is part of the same series. It is clear that this series of oligomers is formed by fragments of increasingly higher molecular weight humins having reacted with flavonoids (Scheme 8).

Equally the series 393, 587, 781, 975, 1169, 1363, 1558 Da are also separated by the same repeating unit above, this being a series of lesser peaks. This series comes exclusively from the reaction of smaller humins molecules to form the complex and sizable polyfuranic structure of the humin polymer. The first term of this series (393 Da, XVII) is shown in Scheme 9.



XIII

Scheme 7. Repeating unit of one of the series of peaks observed.

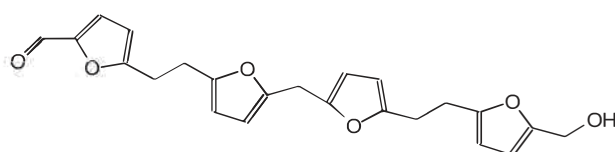


XIV

XV

XVI

Scheme 8. Examples of structures produced in the foams coreaction showing that flavonoid monomers and oligomers do react with complex oligomeric humins structures.



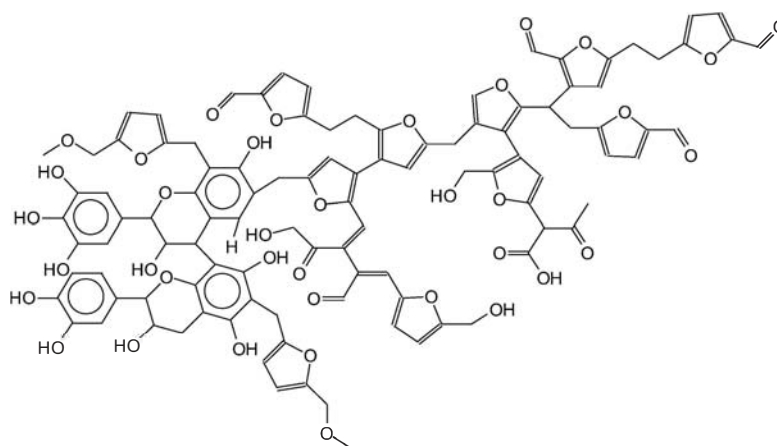
XVII

Scheme 9. Example of reaction of simpler humins structure capable of reacting with itself to form more complex humins networks.

To arrive finally to some of the higher molecular weight structures such as structure XVIII (1945 Da) where a rather sizeable humins oligomer has linked to a flavonoid dimer onto which are already linked some smaller molecular weights humins compounds (Scheme 10).

All the above indicates clearly that there is reaction between the humins oligomers and the tannin flavonoids, and principally that any humins furanic hydroxymethyl and aldehyde group, even on very high molecular weight humins oligomers, can react with the flavonoid tannin sites. The relatively high molecular weight species in the humins mix does then explain why its reaction with the tannin is slower than that of furfuryl alcohol. In the case of humins, as already remarked above, it is their bulky molecular size that determines that their reaction is heavily diffusion controlled, hence slower [33,34].

The reaction of tannin with furfuryl alcohol is particularly well studied and defined [35] and the mixed flavonoid–furfuryl alcohol–humins oligomers attest that all the three species co-react.



Scheme 10. Example of higher molecular weight structure in the foams derived from the reaction of humins higher and lower molecular weight oligomers with flavonoid oligomers of the tannin.

The above considerations explain the not ruptured morphology of the foam caused by even a very small increase in solvent. It indicates that humins foams will react better if their viscosity is lowered, either by moderately increasing their temperature, or by adding relatively low proportions of suitable solvents.

It explains why the use of slightly higher proportions of water have this effect, and why furfuryl alcohol works also as an adequate solvent to mobilize humins. When furfuryl alcohol is used not only as a reagent but also as a humins solvent, what must be considered is the relative balance of the two materials: too low a proportion of furfuryl alcohol will increase the effect of diffusion hindrance to the reaction of the humins decreasing their reaction capability, while too much of the more reactive furfuryl alcohol may limit the role of the humins in the co-reaction.

4. Conclusions

Ambient temperature self-blowing tannin–furanic foams, with both closed and interconnected cells, in which a great part of furfuryl alcohol has been substituted by humins, a polyfuranic material derived from the acid treatment at high temperature of fructose, have been prepared. Ambient temperature foam expansion yielded closed cells foams, while the use of a higher curing temperature (80 °C) yielded open cells foams. It must be pointed out the difference in calling some foams “open-cell” rather than “interconnected cells” foams. This difference is important, as foams having an interconnected cellular structure may combine some of the advantages of closed-cell foams (mechanical performance) and open-cell foams (absorption, acoustic applications).

They appear to present the equivalent characteristics of tannin–furanic foams prepared previously, such as self-extinguishing fire resistance, compression strength but with the advantage of a greater ease of close cells formation. The reaction of condensed tannin, furfuryl alcohol and humins has been shown to occur by the oligomers mix formed, namely tannin–humins, tannin–furfuryl alcohol and in particular tannin–humins–furfuryl alcohol, oligomer types and their structures having been determined. Humins have been shown to react well with condensed tannins, even at ambient temperature, but the reaction is slowed down by their high viscosity in relation to that of tannin with furfuryl alcohol. While even higher molecular weight humins species do appear to react with tannin, their lower rate of reaction is due to their rather high molecular weight, hence their high viscosity, causing the reaction to mainly be diffusion controlled. This feature appears to explain why even small increases in solvent proportions improve the results, and indicates the additional role of furfuryl alcohol as humins solvent

and not just as a co-reagent contributing to both cross-linking and to the heat increase leading to foam expansion and its hardening.

Supplementary Materials: The following are available online at <http://www.mdpi.com/2073-4360/12/11/2732/s1>, Figure SM1. Title: MALDI ToF spectrum of humins obtained at 180 °C oxidized, from fructose, 1000–1500 Da range. Reported to indicate 1137 Da peak. Figure SM2. Title: MALDI ToF spectrum of humins obtained at 150 °C from fructose, 1000–1500 Da range. Reported to indicate 1250 Da peak. Figure SM3. Title: Photograph of cut section of initial tannin-humin foam formulations (a) cured at 80 °C, (b) cured at ambient temperature.

Author Contributions: Conceptualization, X.C. and A.P.; humins preparation B.L., N.G. and N.S.; validation, X.C., A.P., E.F. and C.G.; foams preparation X.C.; MALDI ToF, FTIR, SEM and TMA analysis, X.C.; MALDI ToF, FTIR, SEM and TMA interpretation, A.P.; investigation, X.C., E.F. and N.G.; resources, A.P., N.G. and N.S.; writing—original draft preparation, A.P.; writing—review and editing, A.P., N.G. and N.S.; supervision, A.P.; project administration, A.P., E.F. and C.G.; funding acquisition, A.P. All authors have read and agreed to the published version of the manuscript.

Funding: This research received no external funding.

Acknowledgments: The first author thanks the China Scholarship Council for the study bursary granted to him. The LERMAB of the University of Lorraine is supported by a grant overseen by the French National Research Agency (ANR) as part of the Laboratory of Excellence (Labex) ARBRE.

Conflicts of Interest: The authors declare no conflict of interest.

References

1. Pizzi, A. Tannin-based biofoams—A review. *J. Renew. Mater.* **2019**, *7*, 474–489. [[CrossRef](#)]
2. Meikleham, N.; Pizzi, A. Acid and alkali-setting tannin-based rigid foams. *J. Appl. Polym. Sci.* **1994**, *53*, 1547–1556. [[CrossRef](#)]
3. Tondi, G.; Zhao, W.; Pizzi, A.; Du, G.; Fierro, V.; Celzard, A. Tannin-based rigid foams: A survey of chemical and physical properties. *Bioresour. Technol.* **2009**, *100*, 5162–5169. [[CrossRef](#)] [[PubMed](#)]
4. Li, X.; Pizzi, A.; Cangemi, M.; Fierro, V.; Celzard, A. Flexible natural tannin-based and protein-based biosourced foams. *Ind. Crops Prod.* **2012**, *37*, 389–393. [[CrossRef](#)]
5. Lacoste, C.; Pizzi, A.; Basso, M.C.; Laborie, M.-P.; Celzard, A. Pinus pinaster tannin/furanic foams: Part 2: Physical properties. *Ind. Crops Prod.* **2014**, *61*, 531–536. [[CrossRef](#)]
6. Lacoste, C.; Pizzi, A.; Basso, M.C.; Laborie, M.P.; Celzard, A. Pinus pinaster tannin/furanic foams: Part 1. Formulation. *Ind. Crops Prod.* **2014**, *52*, 450–456. [[CrossRef](#)]
7. Xi, X.; Pizzi, A.; Delmotte, L. Isocyanate-free Polyurethane Coatings and Adhesives from Mono- and Di-Saccharides. *Polymers* **2018**, *10*, 402. [[CrossRef](#)]
8. Xi, X.; Pizzi, A.; Gerardin, C.; GDu, G. Glucose-based Non-Isocyanate Polyurethane Biofoams. *J. Renew. Mater.* **2019**, *7*, 301–312. [[CrossRef](#)]
9. Xi, X.; Pizzi, A.; Gerardin, C.; Lei, H.; Chen, X.; Amirou, S. Preparation and evaluation of Glucose based Non-Isocyanate polyurethane Self-blowing Rigid Foams. *Polymers* **2019**, *11*, 1802. [[CrossRef](#)]
10. Chen, X.; Xi, X.; Pizzi, A.; Fredon, E.; Zhou, X.; Li, J.; Gerardin, C.; Du, G. Preparation and Characterization of Condensed Tannin Non-Isocyanate Polyurethane (NIPU) Rigid Foams by Ambient Temperature Blowing. *Polymers* **2020**, *12*, 750. [[CrossRef](#)]
11. Chen, X.; Li, J.; Xi, X.; Pizzi, A.; Zhou, X.; Fredon, E.; Du, G.; Gerardin, C. Condensed Glucose-Tannin-based NIPU BioFoams of Improved Fire Retardancy. *Polym. Degrad. Stabil.* **2020**, *175*, 109121. [[CrossRef](#)]
12. Lacoste, C.; Basso, M.C.; Pizzi, A.; Celzard, A.; Ella Bang, E.; Gallon, N.; Charrier, B. Pine (*P. pinaster*) and quebracho (*Schinopsis lorentzii*) tannin based foams as green acoustic absorbers. *Ind. Crops Prod.* **2015**, *67*, 70–73. [[CrossRef](#)]
13. Pizzi, A.; Tondi, G.; Pasch, H.; Celzard, A. MALDI-TOF Structure determination of complex thermoset networks—Polyflavonoid tannin-furanic rigid foams. *J. Appl. Polym. Sci.* **2008**, *110*, 1451–1456. [[CrossRef](#)]
14. Tondi, G.; Pizzi, A.; Pasch, H.; Celzard, A. Structure degradation, conservation and rearrangement in the carbonization of polyflavonoid tannin/furanic rigid foams—A MALDI-TOF investigation. *Polym. Degrad. Stabil.* **2008**, *93*, 968–975. [[CrossRef](#)]
15. Tondi, G.; Pizzi, A.; Olives, G.R. Natural tannin-based rigid foams as insulation in wood construction. *Maderas-Cienc. Technol.* **2008**, *10*, 219–227. [[CrossRef](#)]

16. Tondi, G.; Pizzi, A. Tannin based rigid foams: Characterisation and modification. *Ind. Crops Prod.* **2009**, *29*, 356–363. [[CrossRef](#)]
17. Basso, M.C.; Pizzi, A.; Al-Marzouki, F.; Abdalla, S. Horticultural/hydroponics and floral foams from tannins. *Ind. Crops Prod.* **2016**, *87*, 177–181. [[CrossRef](#)]
18. Basso, M.C.; Pizzi, A.; Celzard, A. Influence of formulation on the dynamics of preparation of tannin based foam. *Ind. Crops Prod.* **2013**, *51*, 396–400. [[CrossRef](#)]
19. Basso, M.C.; Pizzi, A.; Celzard, A. Dynamic monitoring of tannin foams preparation: Surfactant effects. *BioResources* **2013**, *8*, 5807–5816. [[CrossRef](#)]
20. Basso, M.C.; Lagel, M.C.; Pizzi, A.; Celzard, A.; Abdalla, S. First tools for tannin-furanic foams design. *BioResources* **2015**, *10*, 5233–5241. [[CrossRef](#)]
21. Sangregorio, A.; Guigo, N.; van der Waal, J.C.; Sbirrazzuoli, N. Humins from Biorefineries as Thermoreactive Macromolecular Systems. *ChemSusChem* **2018**, *11*, 4246–4255. [[CrossRef](#)] [[PubMed](#)]
22. Sangregorio, A. Valorisation of Biorefinery-Derived Humins: Towards the Development of Sustainable Thermosets and Composites. Ph.D. Thesis, Université de la Côte d’Azur, Nice, France, 2019.
23. Van Zandvoort, I.; Wang, Y.; Rasrendra, C.B.; van Eck, E.R.H.; Bruijninx, P.C.A.; Heeres, H.J.; Weckhuysen, B.M. Formation, Molecular Structure, and Morphology of Humins in Biomass Conversion: Influence of Feedstock and Processing Conditions. *ChemSusChem* **2013**, *6*, 1745–1758. [[CrossRef](#)] [[PubMed](#)]
24. Van Zandvoort, I.; Koers, E.J.; Weingarth, M.; Bruijninx, P.C.A.; Baldus, M.; Weckhuysen, B.M. Structural characterization of ¹³C-enriched humins and alkali-treated ¹³C humins by 2D solid-state NMR. *Green Chem.* **2015**, *17*, 4383–4392. [[CrossRef](#)]
25. Hoang, T.M.C.; van Eck, E.R.H.; Bula, W.P.; JGardeniers, J.G.E.; Lefferts, L.; Seshan, K. Humin based by-products from biomass processing as a potential carbonaceous source for synthesis gas production. *Green Chem.* **2015**, *17*, 959–972. [[CrossRef](#)]
26. Sangregorio, A.; Guigo, N.; de Jong, E.; Sbirrazzuoli, N. Kinetics and Chemorheological Analysis of Cross-Linking Reactions in Humins. *Polymers* **2019**, *11*, 1804. [[CrossRef](#)] [[PubMed](#)]
27. Sangregorio, A.; Muralidhara, A.; Guigo, N.; Marlair, G.; Angelici, C.; Thygesen, L.G.; de Jong, E.; Sbirrazzuoli, N. Humins based resin for wood modification and properties improvement. *Green Chem.* **2020**, *22*, 2786–2798. [[CrossRef](#)]
28. Mija, A.C.; de Jong, E.; van der Waal, J.C.; van Klink, G.P.M. Humins-Containing Foam. U.S. Patent No. 10,752,747, 25 August 2020.
29. Licsandru, E.; Mija, A.C. From biorefinery by-product to bioresins. Thermosets based on humins and epoxidized linseed oil. *Cell. Chem. Technol.* **2019**, *53*, 963–969. [[CrossRef](#)]
30. Cornillet, C.; Labat, G.; Gaillard, J.-M. FCBA, Analyse des Cycles de Vie (LCA), Presentation project BEMA, 16 February 2012. In *Restitution du programme Bois Eco Matériaux Aquitaine (BEMA)*; Bois Ecomateriaux Aquitaine: Bordeaux, France, 2012; pp. 73–88.
31. Arias, A.; González-García, S.; Feijoo, G.; Moreira, M.T. Tannin-based bio-adhesives for the wood panel industry as an environmentally friendly alternative to petrochemical resins. *J. Ind. Ecol.* **2020**, in press.
32. Xi, X.; Pizzi, A.; Lei, H.; Du, G.; Zhou, X.; Lin, Y. Characterization and preparation of furanic-glyoxal foams. *Polymers* **2020**, *12*, 692. [[CrossRef](#)]
33. Goodner, M.D.; DeSimone, J.M.; Kiserow, D.J.; Roberts, G.W. An Equilibrium Model for Diffusion-Limited Solid-State Polycondensation. *Ind. Eng. Chem. Res.* **2000**, *39*, 2797–2806. [[CrossRef](#)]
34. Aronhime, M.T.; Gillham, J.K. Time-temperature-transformation (TTT) cure diagram of thermosetting polymeric systems. In *Epoxy Resins and Composites III. Advances in Polymer Science*; Dušek, K., Ed.; Springer: Berlin/Heidelberg, Germany, 1986; Volume 78. [[CrossRef](#)]
35. Abdullah, U.H.B.; Pizzi, A. Tannin-Furfuryl alcohol wood panel adhesives without formaldehyde. *Eur. J. Wood Prod.* **2013**, *71*, 131–132. [[CrossRef](#)]

Publisher’s Note: MDPI stays neutral with regard to jurisdictional claims in published maps and institutional affiliations.



© 2020 by the authors. Licensee MDPI, Basel, Switzerland. This article is an open access article distributed under the terms and conditions of the Creative Commons Attribution (CC BY) license (<http://creativecommons.org/licenses/by/4.0/>).

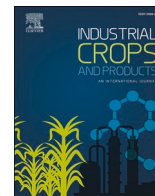
3.11 Mousses tannin-furaniques modifiées par l'isolat de protéine de soja (SPI) et l'addition de formaldéhyde de substitution de lignine industrielle

Résumé: L'isolat de protéine de soja (SPI) a été testé dans cette étude en tant qu'agent de réticulation et substitut de formaldéhyde pour la préparation de mousses polyvalentes durables à haute teneur en biomasse tannin-furanic-SPI (TFS) et lignine-tannin-furanic-SPI (LTFS). De plus, l'ignifugation a été améliorée par la lignine utilisée comme ignifugeant naturel. La spectroscopie infrarouge à transformée de Fourier (FT-IR), couplée à la spectrométrie de masse à temps de vol par désorption/ionisation laser assistée par matrice (MALDI-ToF-MS), a révélé une réaction de réticulation covalente entre le tanin et le SPI. Les mousses TFS et LTFS ont montré par microscopie électronique à balayage (MEB) une structure cellulaire fermée sans pores. L'incorporation de SPI a entraîné des propriétés mécaniques améliorées et des rapports de pulvérisation réduits, une stabilité thermique améliorée et une conductivité thermique accrue (environ 0,042 à 0,044 W/m•K par rapport à la mousse témoin. Ces résultats ont été corroborés par une valeur d'indice limite d'oxygène (LOI) plus élevée, un taux de dégagement de chaleur plus faible et un résidu carbonisé plus élevé, obtenus par LOI et calorimétrie au cône. L'ajout de lignine a encore amélioré les propriétés thermiques et l'ignifugation de Les mousses TFS, bien qu'elles diminuent leurs performances mécaniques. Les mousses TFS et LTFS étaient respectueuses de l'environnement, comme le montrent les mesures de faibles émissions de formaldéhyde. Cette nouvelle mousse TFS durable semble avoir un bon potentiel pour une application industrielle.

Mots clés: Tanin de mimosa; SPI ;Smousse rigide; durableIndice d'oxygène limite (LOI); Retard de flamme.

Contents lists available at [ScienceDirect](https://www.sciencedirect.com)

Industrial Crops & Products

journal homepage: www.elsevier.com/locate/indcrop

Tannin-furanic foams modified by soybean protein isolate (SPI) and industrial lignin substituting formaldehyde addition

Xinyi Chen^{a,b,1}, Jinxing Li^{a,1}, Antonio Pizzi^{b,*}, Emmanuel Fredon^b, Christine Gerardin^c, Xiaojian Zhou^{a,*}, Guanben Du^a

^a Key Laboratory for Forest Resources Conservation and Utilisation in the Southwest Mountains of China (Southwest Forestry University), Ministry of Education, Kunming, 650224, PR China

^b LERMAB, University of Lorraine, 27 Rue Philippe Seguin, BP 1041, 88051, Epinal, France

^c LERMAB, University of Lorraine, BoulevardDoesAiguillettes, 54000, Nancy, France

ARTICLE INFO

Keywords:

Mimosa tannin
SPI
Sustainable rigid foam
Limiting oxygen index (LOI)
Flame retardancy

ABSTRACT

Soybean protein isolate (SPI) was tested in this study as a crosslinker and formaldehyde substitute for preparing high biomass content sustainable rigid tannin-furanic-SPI (TFS) and lignin-tannin-furanic-SPI (LTFS) versatile foams. Additionally, flame retardancy was improved by lignin used as a natural fire-retardant. Fourier-transform infrared spectroscopy (FT-IR), coupled with matrix-assisted laser desorption/ionization time-of-flight mass spectrometry (MALDI-ToF-MS), revealed a covalent cross-linking reaction between tannin and SPI. TFS and LTFS foams showed by scanning electron microscopy (SEM) a closed cell structure without any pores. The incorporation of SPI resulted in enhanced mechanical properties and reduced pulverization ratios, improved thermal stability and increased thermal conductivity (approximately 0.042–0.044 W/m K compared with control foam). Furthermore, the TFS foams exhibited outstanding flame retardancy and suppressed smoke generation while undergoing combustion. These results were supported by a higher limiting oxygen index (LOI) value, a lower heat-release rate, and a higher char residue, obtained by LOI and cone calorimetry. The addition of lignin further enhanced the thermal properties and flame retardancy of TFS foams although it decreased their mechanical performance. The TFS and LTFS foams were environmentally friendly, as shown by the low formaldehyde emission measurements. This novel sustainable TFS foam appears to have a good potential for industrial application.

1. Introduction

Sought-after characteristics, such as flame retardancy, better thermal stability, lightweight, and thermal insulation, are found in phenolic foam (PF). Yet PF has high friability and inferior mechanical properties and is a fossil fuel-based resource, which limits somewhat its large-scale commercial applications (Chen et al., 2020a; Wu et al., 2020). Therefore, foams with improved mechanical properties using natural renewable feedstocks have attracted much attention. Condensed tannin—a vegetal polyphenolic material which is widespread—has been applied in several fields (Chen et al., 2020a; Meikleham and Pizzi, 1994; Pizzi, 2019).

Phenolic tannin-furanic-formaldehyde foams were first reported by Meikleham and Pizzi in 1994 and have since received significant

attention (Meikleham and Pizzi, 1994; Pizzi, 2019). The interest of these foams is not only because they are based on a renewable resource but also because of their self-blowing preparation under ambient/moderate temperature, and their comparable performance with commercial PF foams (Meikleham and Pizzi, 1994; Pizzi, 2019; Tondi and Pizzi, 2009; Tondi et al., 2008a, c; Zhou et al., 2019).

The preparation approaches for these foams are based on a heat-generated expansion initiated by a blowing agent evaporation coupled with an acid-catalysis self-condensation of furfuryl alcohol, without (Basso et al., 2011) or with a cross-linker ensuring the foam structure does not collapse (Celzard et al., 2010; Tondi et al., 2009b; Tondi and Pizzi, 2009; Tondi et al., 2008a, c; Zhou et al., 2019). Various foams have been obtained for different application fields, such as rigid, semi-rigid, and flexible foams via formulation and/or processing

* Corresponding authors.

E-mail addresses: antonio.pizzi@univ-lorraine.fr (A. Pizzi), xiaojianzhou@hotmail.com (X. Zhou).

¹ These authors contributed equally to this work.

<https://doi.org/10.1016/j.indcrop.2021.113607>

Received 25 February 2021; Received in revised form 29 April 2021; Accepted 30 April 2021

Available online 7 May 2021

0926-6690/© 2021 Elsevier B.V. All rights reserved.

adjustment (Basso et al., 2014a, b; Basso et al., 2011; Celzard et al., 2011, 2010; Lacoste et al., 2013; Li et al., 2012c; Meikleham and Pizzi, 1994; Pizzi, 2019; Tondi et al., 2009a, b; Tondi and Pizzi, 2009; Tondi et al., 2008a, c; Zhou et al., 2019). Yet, because of their brittleness they powder easily on frictioning them and present lower mechanical compression properties, these foams have limited commercial application. Their susceptibility to powdering under friction has been solved well (Rangel et al., 2016). However, to reduce the foam brittleness and to enhance other properties (flame retardancy, thermal stability, and thermal insulation) so as to achieve their industrialization, some improved formulations have been developed by introducing organic/inorganic additives, such as polymeric diphenylmethane diisocyanate (p-MDI) (Li et al., 2012a), hyperbranched poly(amino-ester) (Li et al., 2012b), multi-walled carbon nanotubes (Li et al., 2013), disordered carbon matrix and graphite fillers (Jana et al., 2015), cellulose nanofibers (CNF) (Zhou et al., 2019), wood cellulosic fiber (Wu et al., 2020), hydroxy-methylated lignin (Pizzi, 2019) and boric and/or phosphoric acid (Celzard et al., 2011). Formaldehyde-free modifications have been introduced early on to take into account human health and the environment. Thus, formulations with no aldehydes at all (Basso et al., 2013, 2011), or with non-toxic and non-volatile aldehydes such as glyoxal and glutaraldehyde (Lacoste et al., 2013), or fossil-based resources such as PEG-400 and polymeric diphenylmethane diisocyanate (p-MDI) (Li et al., 2012a), and biorefinery byproduct such as polyfuranic humins (Chen et al., 2020a) have been reported as the part of feedstocks that can replace formaldehyde to produce tannin-furanic foams. Mechanical or/and chemical expansion methods have also been utilized to prepare tannin-based rigid foams with lower density, thermal insulation, and robust cell structure (Santiago-Medina et al., 2018a, b; Szczurek et al., 2014).

Plant or animal proteins have also attracted attention for their successful utilization for bio-foams preparation. Albumin was initially used to design and manufacture flexible biofoams (Basso and Pizzi, 2017; Basso et al., 2015; Li et al., 2012c, d) with a series of different natural albumin and albumin/tannin cellular foams following (Basso and Pizzi, 2017; Basso et al., 2015; Lacoste et al., 2015). Biomass foams based on wheat gluten have also been reported (Chiou et al., 2020). However, soy flour and soy protein isolate (SPI) are plant-sourced, renewable, sustainable, and easily obtained from soybean-oil production processing, which is why it has been a commonly applied bioresource for the food industry (Guo et al., 2018; Ma et al., 2020), film preparation (Cao et al., 2007; Gu et al., 2019; Wang et al., 2017), in biomedicine (Zhao et al., 2018), and for wood adhesive applications (Liu et al., 2017; Zhao et al., 2018). SPI was once the main raw material or reinforcement filler for different kinds of foam design (Frihart and Lorenz, 2019; Frihart et al., 2019; Liu et al., 2017, 2015; Wang et al., 2019; Xi et al., 2020; Xiao et al., 2013; Zhao et al., 2019). This encouraged us to design and investigate SPI for tannin-furanic foam preparation because of the reputed reaction crosslinking reaction between tannin and SPI (Ghahri et al., 2018a; Ghahri and Pizzi, 2018; Ghahri et al., 2018b; Liu et al., 2017) as only a small amount of SPI addition can achieve unexpected effectiveness.

Thus, here are presented novel mimosa tannin-furanic-SPI (TFS) and lignin-tannin-furanic-SPI (LTFS) versatile foams. Lignin was selected as the natural flame-retardant to improve the flame retardancy of the resultant TFS foams. The reaction between tannin and SPI was examined. The combined properties of the control, TFS, and LTFS foams, including apparent density, morphology, pulverization ratios, and mechanical properties, were systematically evaluated. Furthermore, the thermal stability, thermal conductivity, and especially fire retardancy of the foams were investigated. The formaldehyde emission of the foams obtained was determined to further demonstrate its environment-friendly characteristics.

2. Materials and methods

2.1. Materials

Commercial mimosa tannin extract (*Acacia mearnsii*, De Wild, its main components as shown in Table S1) was provided by Silva Chimica (St. Michele Mondovi, Italy). Soy protein isolate (SPI) was purchased from Ruikang Biotechnology Co., LTD (Dezhou, China). Lignin was obtained from Anhui BASF Biotechnology Co. LTD (Anhui, China). Furfuryl alcohol (FA, 98 %), Formaldehyde (F, 37 %), p-toluene-4-sulfonic acid (p-TSA, 65 %) and Diethyl ether (DE, 98 %) were purchased from Sigma-Aldrich (Saint Louis, France). All materials and chemicals used the experiments were employed directly without further treatment.

2.2. Preparation of tannin-based foams

This research reported tannin-based foams were prepared according to the formulation showed in Table 1. The control foam was obtained according to reference (Zhou et al., 2019) and the principle originally presented in reference (Meikleham and Pizzi, 1994). In brief, tannin extract was mixed with furfuryl alcohol thoroughly. A certain amount of deionized water (as shown in Table 1) was added into the mixture and stirred intensely for 10 s. A mixture solution containing formaldehyde and p-TSA was added to the tannin and furfuryl alcohol mixture and stirred for 5 s. The blowing agent diethyl ether was added into the mixture and then stirred for 20 s till to obtain a homogenous slurry. The product was placed in an oven for foaming and aging for at 24 h. The resulting black foam was obtained and labeled as the control.

The TFS and LTFS foams were prepared following the control sample processes, as outlined in Table 1. The SPI or lignin/SPI mixture was used to substitute for formaldehyde completely. The SPI addition amount in TFS and LTFS foams depended on the formaldehyde solid content of the control. In parallel, the results of pre-experiments showed that 1–4 g SPI and 0.5–2 g lignin were appropriate. The resultant foams without lignin were labelled as TFS and the foams with lignin were labelled as LTFS. All resulting foams were stored under ambient conditions for at least two days before sample preparation and testing.

2.3. Foam characterization

The apparent densities of the foams prepared were checked according to the ASTM D1622–03 standard (Li et al., 2019). The foam dimensions were 30 × 30 × 30 mm. Five repeated trials were conducted to calculate the mean values and standard deviations.

The foam morphology was observed by scanning electron microscopy (SEM, Hitachi TM-3000, Milieux, Paris, France) under the acceleration voltage of 15 kV. To increase the electric conductivity of samples, a thin gold coating process was conducted before measuring.

Fourier-transform infrared spectroscopy (FT-IR, PerkinElmer Frontier ATR-FTMIR) was utilized to investigate the functional groups during the foam preparation. Each sample were recorded with 32 scans between the wave range of 600 and 4000 cm^{-1} , with a scan resolution of 4 cm^{-1} .

Matrix-assisted laser desorption/ionization time-of-flight mass spectrometry (MALDI-ToF-MS, AXIMA Performance, Shimadzu, Manchester, UK) was adopted to detect products-derived from the reaction between tannin and SPI. The measurements were carried out making 1000 profiles per sample with two shots accumulated per profile. The spectrum precision was of ± 1 Da (Jahanshahi et al., 2016).

The viscosity of foaming resin precursor was tested with a Brookfield DV-II + Viscometer, chose spindle No. 4 at 12 rpm under ambient environmental conditions.

The pulverization ratios were evaluated following the reference (Li et al., 2021). The samples were cut to the uniform size of 50 × 50 × 50 mm. The repeat experiments were performed five times.

The compression strengths were carried out by using the universal

Table 1

Formulation of series of tannin-SPI-based and tannin-SPI-lignin-based foams. Tannin, FA, Water, p-TSA and DE are in the same proportion for all the foams in the Table.

Samples	Tannin (g)	FA (g)	F (g)	SPI (g)	Lignin (g)	Water (g)	p-TSA (g)	DE (g)
Control	30	10.4	7.4			10	12	2.2
TFS1				1				
TFS2				2				
TFS3				3				
TFS4				4				
L0.5TFS3	30	10.4		3	0.5	4	12	2.2
L1TFS3				3	1			
L1.5TFS3				3	1.5			
L2TFS3				3	2			

testing machine (Instron 3300, Elancourt France) with a foam dimension of $30 \times 30 \times 30$ mm (Chen et al., 2020b). Each experiment's average value was from the three repeated measurements.

Thermal conductivity experiments were performed under ambient conditions by using a YBF-2 apparatus (Dahua Ltd., Hangzhou) with the foam slice radius 50 mm and thickness 10 mm, according to the method reported by references (Li et al., 2019; Zhou et al., 2019). Three repeated experiments were conducted, and we report the average and standard deviations.

Thermogravimetry analysis (TGA) was carried out using a TGA5500 analyzer (TA Instruments, USA). The measurements of foams were made between 25°C and 790°C with a heating rate of 10°C/min under nitrogen atmosphere.

Limiting oxygen index (LOI) measurements of samples were conducted based on the China National Standards GB/T 2406.2–2009 utilizing XWR-2046 oxygen index apparatus (Yilu Instrument Co., LTD, Changzhou, China) (Li et al., 2019). The size of samples was $80 \times 10 \times 10$ mm for testing. The average value and standard deviations were obtained from five experiments trials.

A cone calorimeter (CC, FTT, UK) was used to estimate the combustion behavior of the control, TFS and LTFS samples according to ISO 5660 standards (Kong et al., 2018). The size of the samples was $100 \times 100 \times 50$ mm. The testing was carried out under a heat flux of 35 kW/m².

The formaldehyde emission was tested according to China National Standards GB/T 17657–2013. The samples were pre-balanced at 65 % humidity and 20°C at least 7 days before testing. Three repeated trials were conducted.

3. Results and discussions

3.1. The preparation of tannin-furanic-SPI foams

The fabrication of versatile tannin-furanic-SPI foams with high biomass content (~88 %) derived from natural lignocellulosic biomass-derived products (furfuryl alcohol and tannin) and a sustainable soybean derivative (SPI) is schematically illustrated in Fig. 1. This formulation avoided the toxic formaldehyde utilization, improving the

fabrication safety and environmentally friendly nature of the foams with enhanced properties.

There are a number of simultaneous reactions occurring, as described by MALDI-ToF-MS analysis in this work, and they contribute to the expansion of the foams and to their stability of crosslinking. The furfuryl alcohol self-condensation exotherm accelerated the evaporation of the blowing agent, resulting in a volume expansion of the resultant foam. Furfuryl alcohol not only links to the tannin, but also reacts with the amino groups of the amino side-chains of SPI, namely of arginine. The MALDI-ToF-MS analysis confirmed the formation of such covalent bonds. In addition, esterification of the carboxylic acids side-chain of SPI, aspartic and glutamic acid, also probably occurs with the tannin flavonoid units alcoholic C3 hydroxyl groups and possibly also with its phenolic hydroxyl groups. Ionic bonds between the same groups, that are also known to occur at ambient temperature between soy protein and tannin (Ghahri et al., 2018a; Ghahri and Pizzi, 2018; Ghahri et al., 2018b) reduce drastically under the action of a higher temperature. Thus, the three-dimensional structure of the foams was obtained and maintained also by the additional cross-linking engendered by the interaction between tannin and SPI.

The contributing function of the crosslinker in this reaction processing was confirmed. The experimental results showed that the volume expansion reached a maximum and then shrank with the collapse of the cellular structure. As shown in Figure S1, the homogeneous, dark, and rigid control, TFS, and LTFS foams were obtained.

3.2. The suggested reaction mechanism between tannin and SPI

3.2.1. MALDI-ToF-MS analysis

The MALDI-ToF-MS spectra reported in the literature indicate that under the conditions used not only there are the reactions of furfuryl alcohol self-polymerization (Tondi et al., 2008b), furfuryl alcohol with the tannin (Abdullah and Pizzi, 2012; Pizzi et al., 2008), and furfuryl alcohol with the amino groups of the side chains of the protein (Liang et al., 2017), but that there are also reactions that occur between the tannin and SPI without any intervention of other compounds. It is for this reason that a MALDI-ToF-MS analysis of the reaction of tannin with SPI alone under the same conditions used for the foam was carried out,

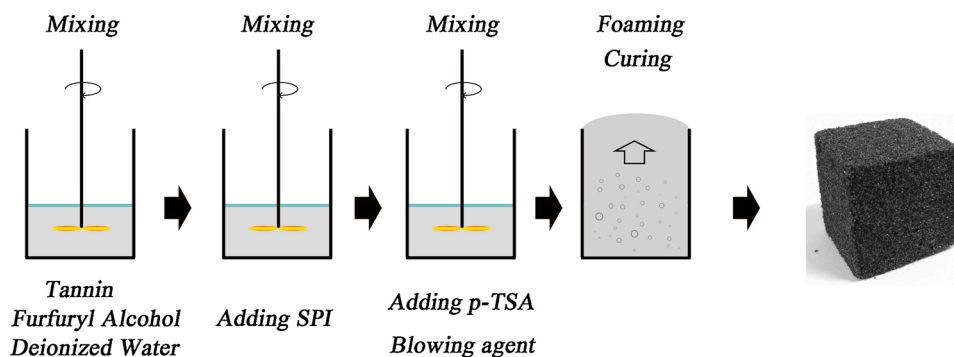


Fig. 1. Schematic illustration of the fabrication of tannin-furanic-SPI foam.

the corresponding spectra being summarized in Fig. 2(a)–(c).

These MALDI-ToF-MS spectra showed that tannin and aminoacids such as arginine presenting amino groups on their side chain do react by substituting some of the hydroxyl groups of the tannin linking it to the protein, as shown in Table 2(a). This amination reaction of tannin is known and used, for instance, with ammonia (Braghieroli et al., 2013; Santiago-Medina et al., 2017; Thébault et al., 2017). Also, esterification reactions of the alcoholic and possibly even of the phenolic –OH groups of the tannin with the carboxylic acid function of the side chain of other amino acids, such as aspartic acid or glutamic acid do occur as shown in Table 2(b) and (c). Thus, mono flavonoids reacted with a single aminoacid, such as fisetinidin-leucine, with the flavonoid in both its normal

and its open form as at 410 Da, and at 390 Da do occur, their corresponding structures being summarized in Table S2.

Although several such compounds are found in the spectra, they do not contribute to the tannin and protein cross-linking because once the amino acid is not free but linked within the skeletal peptide chain of the protein the amino group is changed to an amide, and the –NH– amide group is less likely to react with the tannin (both for its lower reactivity and for the steric hindrance engendered). Thus, the amination of the tannin can occur only through amino acids with amino or imino groups on the side chains of the protein. In soy these are arginine, lysine and proline. The existence of this reaction is then proved by the reaction of tannin monomers and dimers with peptides containing one of these

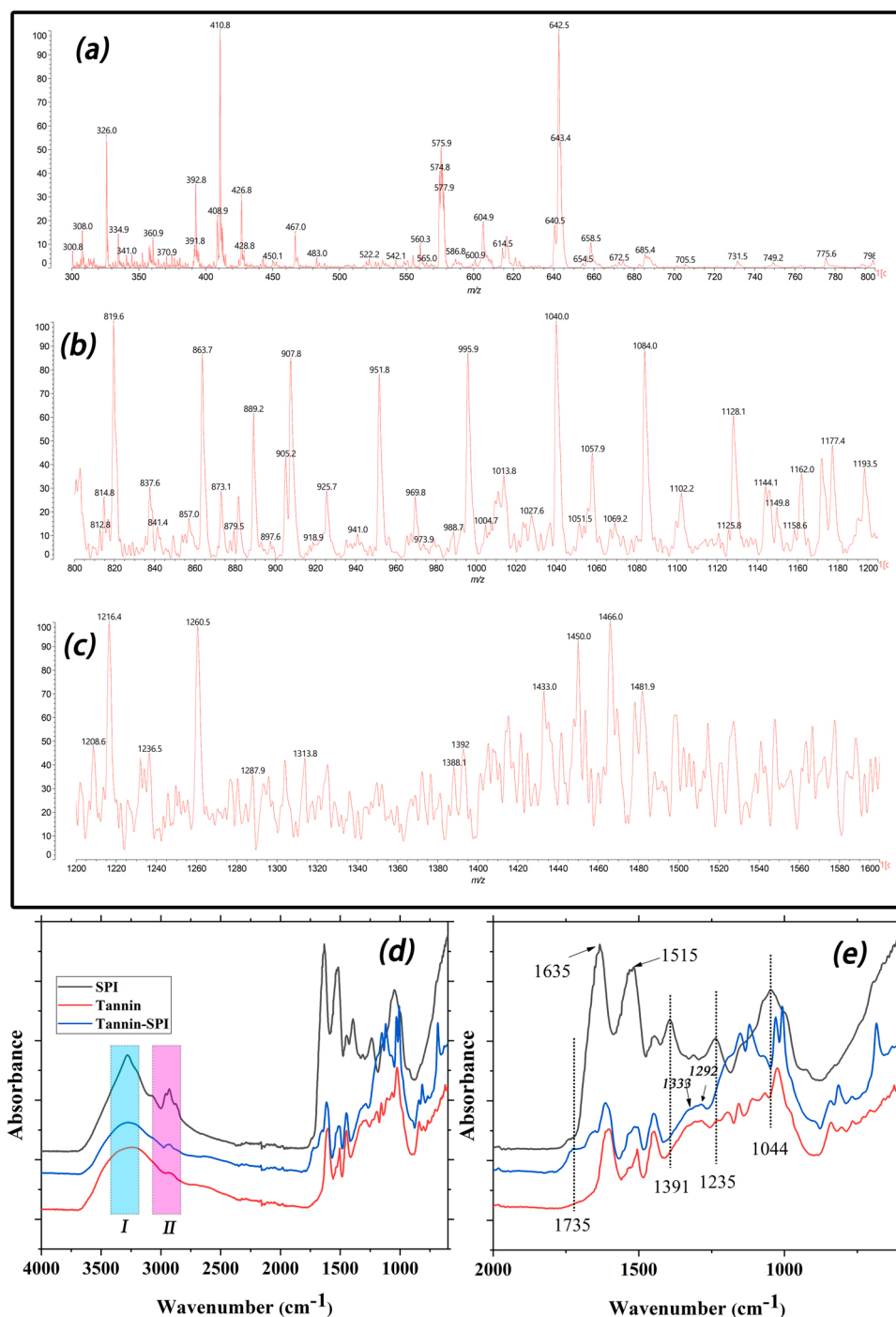
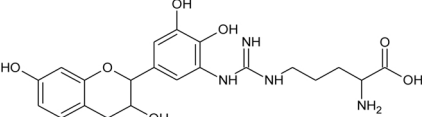
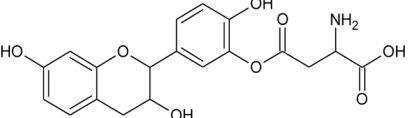
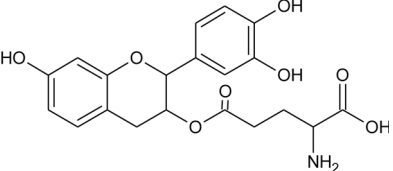
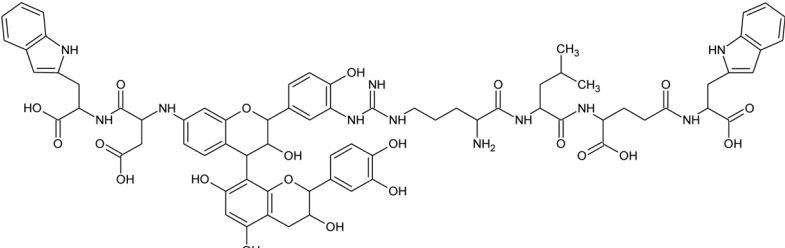
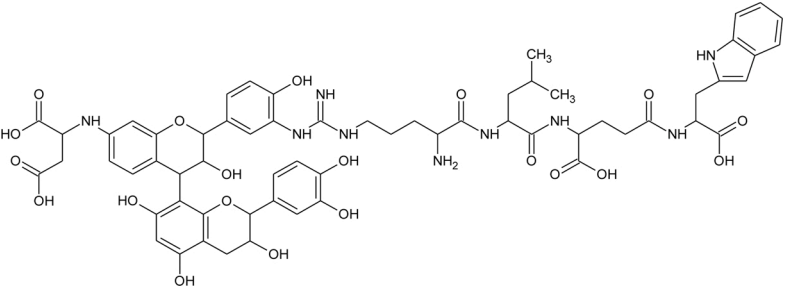
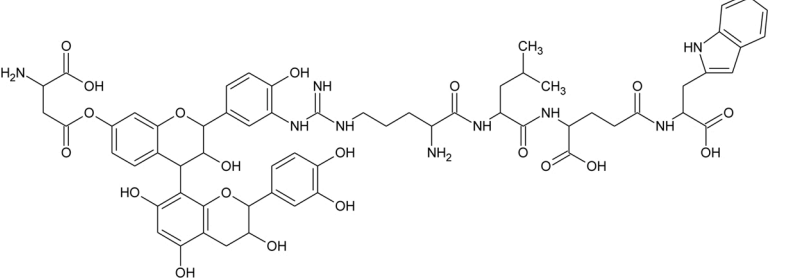


Fig. 2. MALDI-ToF-MS spectrum of the reaction product between Tannin and SPI (a) 300–800 Da; (b) 800–1200 Da; (c) 1200–1600 Da; FT-IR spectrum of pristine SPI, raw tannin, and the reaction product between tannin and SPI (d) 600–4000 cm^{-1} ; (e) 600–2000 cm^{-1} .

Table 2

MALDI ToF structures assignments: (a) Robinetinidin **or** Catechin-Arginine with Na^+ ; (b) Fisetinidin-Aspartic acid without Na^+ ; (c) Fisetinidin-Glutamic acid with Na^+ ; (d) Tryptophan-Aspartic acid-Robinetinidin **or** Catechin-Fisetinidin-Arginine-Leucin-Aspartic acid-Tryptophan without Na^+ ; (e) and (f) Aspartic acid-Robinetinidin **or** Catechin-Fisetinidin-Arginine-Leucin-Aspartic acid-Tryptophan without Na^+ .

Types	Oligomers
(a)	
(b)	
(c)	
(d)	
(e)	
(f)	

three aminoacids, such as the structure represented by the series of peaks at 857 Da, 873.1 Da, 889.2 Da, 1128.1 Da, 1144.1 Da, 1162 Da, 1177.4 Da, 1193.5 Da, 1260.5 Da, 1450 Da, and 1466 Da which are presented in Table S2. The latter one of these, for example, is a catechin-fisetinidin flavonoid dimer linked on one site to a peptide fragment of four amino acids, arginine-leucin-aspartic acid-tryptophan, through the side chain $-\text{NH}_2$ of arginine, but also linked and linked to a second peptide chain fragment formed by tryptophan-aspartic acid in which the free $-\text{NH}_2$ not converted to skeletal amide of one of the two amino acids has reacted with the flavonoid dimer too, thus a structure as of the type in Table 2(d).

To illustrate, as an example, the possibility that the reaction of the

protein with the flavonoid units of the tannin can occur either through the amino group of a protein side chain or by esterification with the acid group of a side chain of the protein, the peak at 1260 Da can be brought as an example (Table 2(e) and (f)).

It must be considered that in the case of the structure assigned to the 1260 Da peak (Table 2(f)), esterification is most likely to occur first at the alcoholic $-\text{OH}$ on the flavonoids C3 before occurring on the more acid phenolic $-\text{OH}$ groups. The assigned compounds to the MALDI-ToF-MS peaks in Table S2 confirm that reactions contributing to cross-linking directly between tannin and soy protein do occur. It confirms also that their interaction is not only based on the classical protein tanning reaction like in leather making thought to be based exclusively on

secondary forces interactions between the two materials (Ghahri et al., 2018a; Ghahri and Pizzi, 2018; Ghahri et al., 2018b). Moreover, depending from the condition of reaction also coupling by ionic bonds between $-\text{NH}_3^+$ of the protein and the phenolic $-\text{O}^-$ of the tannin as shown already for both condensed and hydrolysable tannins (Ghahri et al., 2018a; Ghahri and Pizzi, 2018; Ghahri et al., 2018b).

3.2.2. Fourier transform infrared (FT-IR) spectroscopy

The FT-IR spectra of pristine SPI, raw tannin, and the reaction product of tannin and SPI are shown in Fig. 2. In region I of Fig. 2(d), a broad absorption band approximately 3400 cm^{-1} is related to the characteristic peak of free and bound $-\text{NH}-$ or/and $-\text{OH}$ groups (Liu et al., 2017; Wang et al., 2017). The hydrogen bonds could be formed between $-\text{NH}-$ or/and $-\text{OH}$ groups and the carbonyl groups of protein-peptide linkages (Wang et al., 2017). Furthermore, an adsorption peak at 2925 cm^{-1} (region II) can be seen, which is ascribed to symmetric and asymmetric stretching vibrations in $-\text{CH}_2/-\text{CH}_3$ groups (Chen et al., 2020b). In addition, the SPI characteristic peaks, such as 1635 cm^{-1} , 1515 cm^{-1} , and 1235 cm^{-1} (Fig. 2(e)), which are attributed to $\text{C}=\text{O}$ stretching (amide I), $-\text{NH}-$ deformation (amide II), and $-\text{CN}-$ stretching and $-\text{NH}-$ vibration (amide III), respectively (Wang et al., 2017). The peaks 1391 cm^{-1} ($-\text{COO}-$), 1235 cm^{-1} (amide III), and 1044 cm^{-1} ($-\text{C}-\text{O}-$) of SPI disappeared after reacting with tannin, which is assigned to the reaction between SPI and tannin. Furthermore, in Fig. 2(e), there are indications that reactions occur through the primary amines in SPI by forming secondary amines, this being indicated by the two characteristic peaks at 1333 cm^{-1} and 1292 cm^{-1} . The esterification of the tannin hydroxyls by the protein side-chain acids is demonstrated by the 1735 cm^{-1} shoulder. These bands appear to support the MALDI-ToF-MS results that both the reaction of the protein with the flavonoid units of the tannin can occur either through the amino group of a protein side chain or by esterification with the acid group of a side chain of the protein.

3.3. Physical and mechanical properties

The physical and mechanical properties of TFS and LTFS foams were determined and are summarized in Table 3 and Fig. 3. The control sample showed a lower density, 83.5 kg/m^3 , which is similar to literature-reported values of conventional tannin-furanic-formaldehyde foams (Celzard et al., 2010; Tondi et al., 2009b). The tannin-furanic-formaldehyde foam exhibited high brittleness, and the pulverization ratios was 13.68 %, because of their lower cross-linking

Table 3

The viscosity of foaming resins, density, pulverization ratios and specific compressive strength of control, TFS, and LTFS foams ^a.

Foams	Viscosity (mPa's)	Density (kg/m^3)	Pulverization ratios (%)	Specific compressive strength (kPa/ $\text{kg}\cdot\text{m}^{-3}$)
Control	2200(35)	83.5(2.5)	13.68(1.03)	2.75
TFS1	17,500 (145)	94.4(3.1)	4.83(0.72)	4.34
TFS2	27,650 (221)	98.3(2.6)	4.22(0.49)	4.88
TFS3	35,500 (187)	108.6 (4.8)	3.68(0.21)	5.24
TFS4	48,500 (180)	112.5 (5.5)	2.64(0.38)	6.13
L0.5TFS3	26,250 (195)	96.5(1.8)	10.01(2.15)	1.76
L1TFS3	32,900 (207)	98.6(2.1)	8.55(1.12)	1.93
L1.5TFS3	36,750 (214)	99.6(3.4)	8.24(1.74)	2.31
L2TFS3	40,850 (224)	93.8(2.2)	11.48(2.21)	1.91

^a The values in the parentheses are standard deviations.

densities and/or their incomplete solidification behaviors. Generally, low density tannin-furanic-formaldehyde foams shows a large mass-loss when gently touched or frictioned it (Li et al., 2021) unless some special arrangements are made (Rangel et al., 2016). The densities of TFS foams were higher than the control, around $94.4\text{--}112.5\text{ kg/m}^3$. This result is related to the increased viscosity of the foaming precursor mixture (Table 3). The strong gelation ability of SPI along with the reaction of tannin and SPI can rapidly increase the viscosity of the foaming precursor, even with a small addition of it. Therefore, higher viscosity seems to be a disadvantage for raw materials homogeneous mixing, as well as for bubble formation and volume expansion, resulting in a higher density than the control. This is also found for phenolic foams manufacturing (Jing et al., 2014; Yang et al., 2014, 2013). Additionally, the pulverization ratios (Table 3) of TFS foams had a lower value, only reaching 2.64%–4.83%. This result is probably because of the higher densities of TFS foams, resulting in a lower brittleness than the control sample. Besides, the covalent cross-linking of tannin with SPI contributes to decrease brittleness. With the introduction of lignin, the foam densities decreased slightly ($93.8\text{--}99.6\text{ kg/m}^3$) compared to TFS foams. One reason for this phenomenon is the larger cells of the lignin-modified TFS foams, which can be observed from their morphology. The larger cells obtained were probably due to the cell nucleation being affected by lignin addition during the foam preparation (Dolomanova et al., 2011; Xue et al., 2014). Besides, a small amount of lignin reduced the viscosity of the foaming precursor (Table 3) due to the high dispersion and wettability, resulting in lower densities for LTFS than for TFS foams. Therefore, the pulverization ratios increased, as summarized in Table 3.

Fig. 3(a) shows the morphological characteristics of the control, TFS, and LTFS foams. As expected, a closed cell structure with many "pores", regular cellular structure, and a smooth cellular surface were obtained, as previously reported (Pizzi, 2019; Wu et al., 2020; Zhou et al., 2019). Nevertheless, the TFS and LTFS cellular structures exhibited larger, inhomogeneous, and rough surface performance compared to the control sample. The major reason for this phenomenon is that the homogeneous cellular structure was squeezed in the direction perpendicular to the foam growth because of the slightly shrinkage of foam blocks after the foam reached maximal expansion showing a marked anisotropy. Therefore, some elliptical foam cells can be seen in Fig. 3(a). The cell walls were squeezed and then some wrinkles formed on the surface. For lignin-modified LTFS foams, relatively larger cells were observed than for the control and the TFS samples. This was because the cell nucleation process was influenced by lignin addition (Xue et al., 2014). Therefore, fewer foam nuclei would entrap more blowing gas, leading to a larger cell structure and lower density (Li et al., 2017). As shown in Fig. 3(a) and (b), some clear particles are noticeable on the surface of LTFS foams, but are not visible on the surface of control and TFS foams. The numbers of particles increased with gradually increasing lignin additions. This indicates that lignin can form a protective layer on the surface of the foams as it can be converted to a carbon char layer when in a fire. These particles are one of the factors providing better fire resistance for LTFS than TFS foams.

Fig. 3(c) and (d) show the compressive stress-strain curves and values of control, TFS, and LTFS foams when undergoing a compressive load. The multi-stage deformation observed is consistent with several studies on polymer foams (Chen et al., 2020b, c; Gao et al., 2021; Wu et al., 2020). When comparing TFS and control foams, the compression strength of TFS foams was higher than the control. This can be attributed to the increased density of TFS foams. Moreover, as shown in Table 2, the specific compressive strength increases with the SPI amount. This result indicates that the improved compression strength of TFS foams is not only influenced by the density but also related to the stronger foam cell wall structure resulting from the greater crosslinking between tannin and SPI. Also, the physical entwine between tannin and long chains SPI can promote the improvement of cell wall intensity. The LTFS foams exhibit a lower compression strength than TFS, but similar to that of the control foam. Its less densities are the one of mainly factors for this

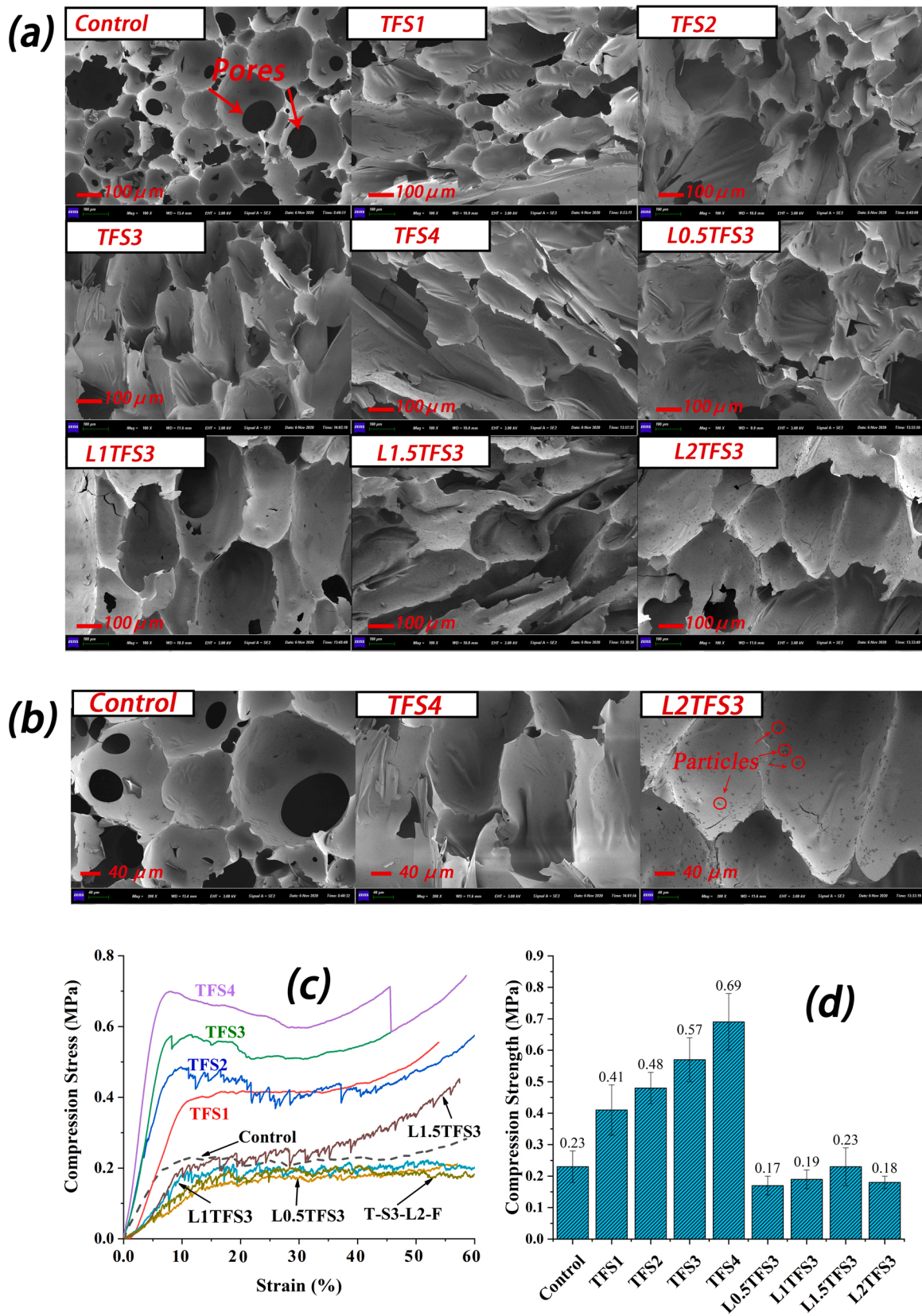


Fig. 3. (a) SEM images ($\times 100$) of control, TFS, and LTFS foams; (b) Magnified SEM images ($\times 200$) of control, TFS, and LTFS foams; (c) The stress-strain curves for compression; (d) Compression strength.

result. Moreover, the compressive strength possesses the same trend in foam densities, which suggests that the foam density is not the only factor for the compression strength. The existence of lignin can influence the crosslinking of tannin and SPI which is likely to decrease the strength of the cell wall. In addition, the larger cell structures for LTFS than TFS foams reduced the supporting capacity within the unit pressure range, which were attribute to the reduced cell struts (Li et al., 2021).

3.4. Evaluation of thermal conductivity and thermal stability

The thermal conductivity of the control, TFS, and LTFS foams were evaluated by the hot plate method and the results are shown in Fig. 4 (a). The control sample displayed the lowest thermal conductivity, only 0.0391 W/m K lower than from other studies of tannin-furanic-formaldehyde foams (Wu et al., 2020; Zhou et al., 2019). The TFS foams had a higher thermal conductivity value, from 0.0431 W/m K for TFS1 to 0.0442 W/m K for TFS4 than the control sample, and increasing trend with the increase of SPI. This result probably is attributed to changes in foams density, in general, the higher density will have a higher thermal conductivity (Pizzi, 2019; Szczurek et al., 2014; Tondi and Pizzi, 2009). In parallel, the non-homogenous cell structures (as shown in SEM results) from TFS foams improved their thermal conductivity. Cell morphology can influence the thermal conductivity of polymer foams which as reported by previous study (Li et al., 2021). Lignin-modified LTFS samples had a lowered thermal conductivity value, from 0.04198 W/m K for L0.5TFS3 to 0.0425 W/m K for L1.5TFS3, lower than TFS foams but higher than the control. One of the most obvious changes in the lignin-modified TFS foams was the lower foam density. Therefore, this change can directly lead to the decreased thermal conductivity of LTFS foams. Moreover, by comparing TFS and control samples, the uneven morphology and structure of the cells of the former is the reason that it can achieve a higher thermal conductivity than the latter even at similar foam density. For TFS and LTFS foams in this study, the thermal conductivity was higher than the control, still presenting a better performance compared to other insulating materials, thus indicating their outstanding thermal insulation properties.

The thermal stability of the control, TFS, and LTFS foams was studied by thermogravimetric analysis under air conditions. The TG and DTG curves were obtained and are shown in Fig. 4(b) and (c), respectively, and the corresponding data are listed in Table 4. For the control sample, the first weight-loss stage appeared at a temperature range of 25–150°C, which is ascribed to the evaporation of the residual blowing agent as well as of absorbed water (Chen et al., 2020b; Li et al., 2019; Wu et al., 2020). The second prominent weight loss (38.14 %, as shown in Table 4) stage occurred between 150–500°C because of the degradation of the polymer chain forming small molecules (Wu et al., 2020). For instance, the basic structure of soy protein cleaves and decomposes from 250–350°C (Liu et al., 2011). The aromatic skeleton of lignin and tannin has better thermal stability, however, thermolysis will occur when the temperature is above 450°C (Chen et al., 2020b; Li et al., 2019; Xue et al., 2014; Zhang et al., 2017). The last one abrupt weight loss (51.33

%, as shown in Table 4) occurred when the temperature was above 500°C from pyrolysis of the residual compounds, such as carbon-based char from the second stage (Chen et al., 2020b). These carbon-based compounds formed and covered on the surface of the polymer, thus isolating it from the air and improving the thermal stability of materials. The complete pyrolysis of the control foam, with ~96 % weight loss, occurred when the temperature increased to 790°C, resulting in thermally-stable char residues (4.59 %, as shown in Table 4).

For the TFS foams, the thermal degradation temperature peaks of the second and third stages were higher than the control, as shown in Table 4. This is related to the stable and compact crosslinked structure between tannin and SPI (Ghahri et al., 2018a; Ghahri and Pizzi, 2018; Ghahri et al., 2018b). The final thermally-stable char residues reached 37.16 % at 4 g SPI addition, but only 5.15 % at 1 g SPI addition, which was still higher than the control. Hence, such high final residues of TFS foams indicated that the SPI substitution for formaldehyde increased char formation and improved thermal stability. As for the lignin addition, from the DTG curves, it can be seen that the initial and second thermal degradation temperature peaks presented a similar trend with the TFS foams. The degradation temperature peak in the third stage appears to have shifted from ~640°C to ~770°C, as shown in Table 4. Therefore, this phenomenon can show that the high carbon content lignin improved the formation of thermally-stable char (carbonization) (Kong et al., 2018). Moreover, its final mass residue has increased by introducing of lignin, approximately 38–43 %. Hence, the thermal stability of TFS foams can further be improved by lignin.

3.5. Evaluation of flame-retardant properties

The flame resistance of the control, TFS, and LTFS samples was evaluated by measuring the limiting oxygen index (LOI) and the results are shown in Fig. 5a. As expected, the LOI of a typical tannin-furanic-formaldehyde foam, i.e., the control sample in this work, is 29.37 %, indicating it is a flame-retardant material (Zhou et al., 2019). The SPI-substituted TFS samples had higher LOI values, from 38.17%–40.37 %, when the SPI replacement addition was from 1 g to 4 g, 29.96–37.45 % higher than the control sample. This effect can be ascribed to the closed-cell morphology structure of TFS and LTFS foams. SEM images (Fig. 3) show that closed-cell structures with many “pores” are in the control sample. The air can then circulate in the foam interior through these opened pores, thereby providing a more suitable environment for combustion (Li et al., 2019). Conversely, the TFS and LTFS foams relatively closed-cell structures block the air exchange between the inside and outside of the foam cells, acting as a flame retardant.

Lignin-modified TFS samples (LTFS) have a higher LOI value than TFS foams (Fig. 5). The LOI value of L0.5TFS3 is 40.5 % which increased to 41.33 % with 1.5 g lignin addition (L1.5TFS3). These results indicated that lignin contributed to the flame-retardant performance of LTFS foams. Its high carbon-containing polyphenol structure contributes to higher char carbon productivity at higher temperatures (Chen et al., 2020b; Wu et al., 2020; Yang et al., 2012). Hence, the char covering

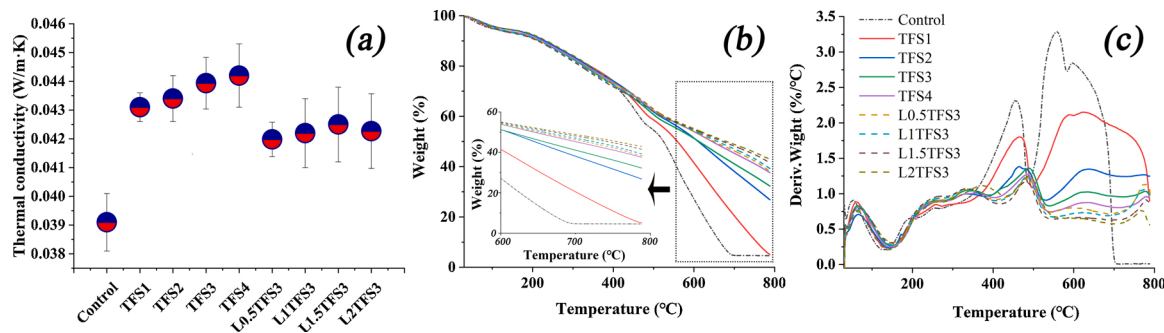


Fig. 4. (a) The thermal conductivity of the control, TFS, and LTFS foams; (b) TG and (c) DTG curves of the control, TFS and LTFS foams.

Table 4

TGA data of the control, TFS and LTFS foams.

Foams	T-max ^a (°C)			Weight loss (%)			Residual mass at 790°C (%)
	Step I	Step II	Step III	Step I	Step II	Step III	
Control	52.28	455.64	558.82	5.94	38.14	51.33	4.59
TFS1	61.24	466.59	624.81	5.80	35.17	53.88	5.15
TFS2	63.73	468.72	634.44	5.19	35.70	32.25	26.84
TFS3	65.45	486.21	639.01	6.35	36.21	25.13	32.28
TFS4	64.78	487.81	639.71	6.10	34.79	21.5	37.61
L0.5TFS3	65.73	484.88	774.73	6.18	34.49	20.80	38.52
L1TFS3	66.39	485.53	773.40	5.96	36.03	18.76	39.25
L1.5TFS3	67.38	482.96	772.53	6.57	36.79	15.10	41.54
L2TFS3	65.59	481.35	779.78	5.24	37.27	14.48	43.01

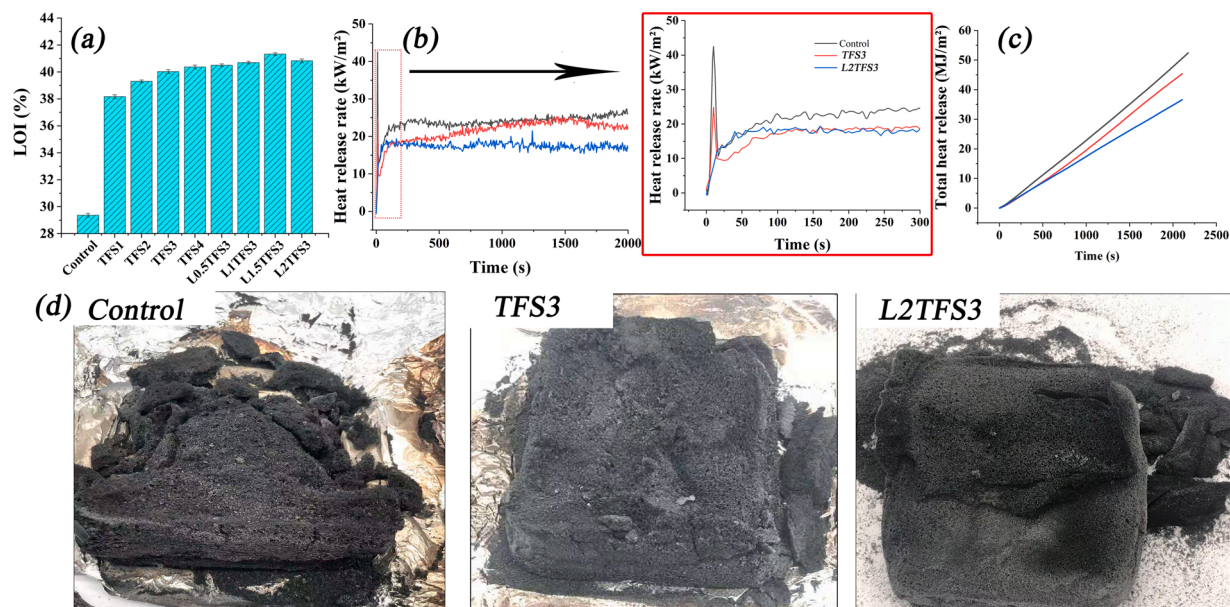
^a Temperature corresponding to the maximum weight loss rate.

Fig. 5. The flammability properties of tannin-furanic-SPI foams. (a) The LOI values of the control, TFS, and LTFS samples; (b) The average heat release rate (HRR); (c) The total heat release (THR) curves of the control, TFS3, and L2TFS3; (d) The corresponding digital photographs of char residues after cone calorimeter measurements.

layer further obstructs contact of the combustion interface with the air, thereby protecting the materials (Yang et al., 2012). However, the LOI value is lower with 2 g lignin (40.83 %). This decreased in the LOI value for L2TFS3 is attributed to the inflammability of lignin when applied in larger amounts.

Cone calorimetry was used to simulate and evaluate the combustion behavior of the control, TFS3, and L1.5TFS3 samples in a real fire scenario under a constant heat flux of 35 kW/m² from a conical heater. The legible peaks of the heat-release rate (PHRR) flaming combustion for the control and TFS3 foams are shown in Fig. 5(b). This peak is attributed to the oxidation reaction of volatile pyrolysis substances in the high-temperature environment (Kong et al., 2018). For TFS, the maximum peak value was significantly lower than the control. In parallel, as shown in Fig. 5(c), the TFS foam had a lower THR value than the control. These results indicate that the TFS foams have better flame-retardancy than the control. A valley characterizes the HRR curves which means the char layer protected the materials as combustion continued. The HRR curves increased, thereafter maintaining a stable level longer than 2000s. No strong flame was observed when the foams were put on the butane torch. These foams are then self-extinguishing after the flame is removed from the sample surface, as shown in Figure S2 and Video S1.

For the L1.5TFS3 sample, the initial peak disappeared and the curve merged in the exothermic phase. Compared to the TFS foam, a lower THR value (Table 5) was obtained which indicated that as the lignin was

introduced, the flame-retardant properties of LTFS improved. This was because of the high char production performance of lignin in the high-temperature environment. It covers the surface of materials and forms a barrier of further contact between air and the combustion interface, enhancing the flame-retardancy of TFS foams.

The values of this peak reached 19.49–42.16 kW/m² (Table 5), lower than most other foams, such as PU foams (Cao et al., 2019; Rao et al., 2018) or wood-based materials (Kong et al., 2018). These results indicated that these foams have lower HRR, better than others that have been developed. Apart from the HRR, the release of smoke (especially CO) also influences the quality of the safety of the material when in a fire (Kong et al., 2018). The control sample exhibited the highest TSP value (Table 5), and after the modification of foam preparation, the novel biomass TFS and LTFS had a lower TSP value. This further indicated that the fire retardancy of TFS and LTFS was better than that of the control sample. The residue trend of all samples can be seen in the TGA results. For Fig. 5(d), the control sample almost lost its original shape, turning to a fragile condition after burning. The TFS3 and L1.5TFS3 preserved their original shapes better, with the latter performing best. This feature is particularly important for materials in a fire.

3.6. Formaldehyde emission

To examine if the foams are environment-friendly, formaldehyde

Table 5Detailed cone calorimetry data of the control, TFS, and LTFS samples ^a.

Foams	PHRR ^b (kW/m ²)	THR ^b (MJ/m ²)	TSP ^b (m ²)	Residue ^b (wt %)	Ref.
Control	42.16 (2.62)	42.65 (2.16)	0.13 (0.02)	26.73(1.55)	
TFS3	25.38 (2.05)	38.65 (1.08)	0.11 (0.01)	32.41(2.34)	★ ^c
L1.5TFS3	19.49 (1.68)	31.57 (1.98)	0.05 (0.01)	41.34(3.66)	
Wood	167.86 (4.06)	68.69 (2.29)	2.18 (0.28)	–	
Wood/PFA	233.21 (34.94)	83.36 (2.65)	5.37 (0.35)	–	(Kong et al., 2018)
Wood/PFA/ ADP	156.61 (4.94)	45.10 (0.16)	0.22 (0.04)	–	
PUF-0	232.7(21)	10.7(2)	5.93 (0.6)	–	
PUF-EG	207.9(23)	10.1(1.7)	5.36 (0.3)	–	(Cao et al., 2019)
PUF-200	103(13)	5.9(1.0)	2.08 (0.2)	–	
Pure FPUF	310(11)	22.5(0.5)	4.51 (0.06)	4.3(0.7)	(Rao et al., 2018)

^a The values in the parentheses are standard deviations.^b PHRR, THR, TSP and residue represented the time to ignition, peak heat release rate, total heat release, total smoke production and residue after tests, respectively.^c ★ represents this work.

emission tests were conducted and the results are listed in Table 6. As expected, the control sample released the most formaldehyde, two times that of TFS3 and L1.5TFS3. This indicates that the final tannin-furanic-formaldehyde foam released free formaldehyde despite this also being released during the foam curing process. Yet, the formaldehyde emission of the control sample was still lower than the relevant standard requirement. The TFS and LTFS foams do not utilize formaldehyde, avoiding the release of free-formaldehyde. Thus, the application of soybean protein resources was expanded in this study as a substitute for a toxic substance. In short, these novel biomass foams have many improved properties suggesting a wide of industrial production and application prospects.

4. Conclusions

High biomass, environment-friendly, and flame retardant TFS foams were developed in this study. Mechanical properties, thermal performance, and flame retardancy were measured by substituting SPI for formaldehyde.

The main results obtained were:

- (1) A strong crosslinking reaction between tannin and SPI, yielding closed cells foam structures, thus enhancing mechanical properties, reducing pulverization ratios, and improving thermal conductivity (approximately 0.042–0.044 W/m K of the modified tannin foams as well as yielding a better thermal stability.
- (2) The increased LOI value, a lower heat-release rate, and increased char residue were obtained. The TFS foams exhibited strong flame retardancy and suppressed smoke generation while undergoing combustion.
- (3) Lignin addition decreased the crosslinking of tannin and SPI, increased foam cell size, thereby altering the mechanical properties of TFS foams. The addition of lignin further improved the thermal stability of TFS foams, along with a lower heat-release rate and lower smoke production. This indicates that LTFS enhanced flame retardancy more than that of TFS.
- (4) The low formaldehyde emission confirms the good environmental performance of these novel biomass foams. Such novel

Table 6Formaldehyde emission of the control, TFS3, and L1.5TFS3 foams ^a.

Samples	Formaldehyde emission (mg/m ³)
Control	0.08 (0.02)
TFS3	0.03(0.01)
L1.5TFS3	0.03(0.01)
GB/T 17657–2013	≤0.124

^a The values in the parentheses are standard deviations.

sustainable TFS foams have thus a good potential for industrial application.

CRedit authorship contribution statement

Xinyi Chen: Conceptualization, Methodology, Software, Data curation, Writing - original draft. **Jinxing Li:** Methodology, Software, Investigation, Writing - original draft. **Antonio Pizzi:** Conceptualization, Data curation, Writing - original draft. **Emmanuel Fredon:** Visualization, Supervision. **Christine Gerardin:** Supervision. **Xiaojian Zhou:** Conceptualization, Data curation, Writing - review & editing, Funding acquisition. **Guanben Du:** Supervision, Writing - review & editing, Funding acquisition.

Declaration of Competing Interest

The authors declare no conflict of interest.

Acknowledgement

This work was supported by National Natural Science Foundation of China (NSFC 31760187, 31971595), Yunnan Provincial Natural Science Foundation (2017FB060), the “Ten-thousand Program”-youth talent support program and Yunnan Provincial Reserve Talents for Middle & Young Academic and Technical Leaders (2019HB026), Scholarship from China Scholarship Council (CSC), Yunnan Provincial Key Laboratory of Wood Adhesives and Glued Products. The LERMAB is supported by a grant of the French Agence Nationale de la Recherche as part of the Laboratory of excellence (LABEX) ARBRE.

Appendix A. Supplementary data

Supplementary material related to this article can be found, in the online version, at doi:<https://doi.org/10.1016/j.indcrop.2021.113607>.

References

- Abdullah, U.H.B., Pizzi, A., 2012. Tannin-furfuryl alcohol wood panel adhesives without formaldehyde. *Eur. J. Wood Wood. Prod.* 71, 131–132. <https://doi.org/10.1007/s00107-012-0629-4>.
- Basso, M.C., Pizzi, A., 2017. New closed-and open-cell, aldehyde-free protein foams. *J. Renewable Mater.* 5, 48–53. <https://doi.org/10.7569/JRM.2016.634124>.
- Basso, M.C., Li, X., Fierro, V., Pizzi, A., Giovando, S., Celzard, A., 2011. Green, formaldehyde-free, foams for thermal insulation. *Adv. Mater. Lett.* 2, 378–382. <https://doi.org/10.5185/amlett.2011.4254>.
- Basso, M.C., Giovando, S., Pizzi, A., Celzard, A., Fierro, V., 2013. Tannin/furanic foams without blowing agents and formaldehyde. *Ind. Crops Prod.* 49, 17–22. <https://doi.org/10.1016/j.indcrop.2013.04.043>.
- Basso, M., Lacoste, C., Pizzi, A., Fredon, E., Delmotte, L., 2014a. Flexible tannin-furanic films and lacquers. *Ind. Crops Prod.* 61, 352–360. <https://doi.org/10.1016/j.indcrop.2014.07.019>.
- Basso, M.C., Giovando, S., Pizzi, A., Pasch, H., Pretorius, N., Delmotte, L., Celzard, A., 2014b. Flexible-elastic copolymerized polyurethane-tannin foams. *J. Appl. Polym. Sci.* 131 <https://doi.org/10.1002/app.40499>.
- Basso, M.C., Pizzi, A., Delmotte, L., 2015. A new approach to environmentally friendly protein plastics and foams. *Bio. Res.* 10, 8014–8024. <https://doi.org/10.15376/biores.10.4.8014-8024>.
- Braghirolli, F., Fierro, V., Pizzi, A., Rode, K., Radke, W., Delmotte, L., Parmentier, J., Celzard, A., 2013. Reaction of condensed tannins with ammonia. *Ind. Crops Prod.* 44, 330–335. <https://doi.org/10.1016/j.indcrop.2012.11.024>.

- Cao, N., Fu, Y., He, J., 2007. Preparation and physical properties of soy protein isolate and gelatin composite films. *Food Hydrocoll.* 21, 1153–1162. <https://doi.org/10.1016/j.foodhyd.2006.09.001>.
- Cao, Z.J., Liao, W., Wang, S.X., Zhao, H.B., Wang, Y.Z., 2019. Polyurethane foams with functionalized graphene towards high fire-resistance, low smoke release, superior thermal insulation. *Chem. Eng. J.* 361, 1245–1254. <https://doi.org/10.1016/j.cej.2018.12.176>.
- Celzard, A., Zhao, W., Pizzi, A., Fierro, V., 2010. Mechanical properties of tannin-based rigid foams undergoing compression. *Mat. Sci. Eng. A-Struct.* 527, 4438–4446. <https://doi.org/10.1016/j.msea.2010.03.091>.
- Celzard, A., Fierro, V., Amaral-Labat, G., Pizzi, A., Torero, J., 2011. Flammability assessment of tannin-based cellular materials. *Polym. Degrad. Stab.* 96, 477–482. <https://doi.org/10.1016/j.polymdegradstab.2011.01.014>.
- Chen, X., Guigo, N., Pizzi, A., Shirazzuoli, N., Li, B., Fredon, E., Gerardin, C., 2020a. Ambient temperature self-blowing tannin-humins biofoams. *Polymers* 12, 2732. <https://doi.org/10.3390/polym12112732>.
- Chen, X., Li, J., Xi, X., Pizzi, A., Zhou, X., Fredon, E., Du, G., Gerardin, C., 2020b. Condensed tannin-glucose-based NIPU bio-foams of improved fire retardancy. *Polym. Degrad. Stab.* 175, 109121. <https://doi.org/10.1016/j.polymdegradstab.2020.109121>.
- Chen, X., Xi, X., Pizzi, A., Fredon, E., Zhou, X., Li, J., Gerardin, C., Du, G., 2020c. Preparation and characterization of condensed tannin non-isocyanate polyurethane (NIPU) rigid foams by ambient temperature blowing. *Polymers* 12, 750. <https://doi.org/10.3390/polym12040750>.
- Chiou, B.-S., Cao, T., Bilbao-Sainz, C., Vega-Galvez, A., Glenn, G., Orts, W., 2020. Properties of gluten foams containing different additives. *Ind. Crops Prod.* 152, 112511. <https://doi.org/10.1016/j.indcrop.2020.112511>.
- Dolomanova, V., Rauhe, J.C.M., Jensen, L.R., Pyrz, R., Timmons, A.B., 2011. Mechanical properties and morphology of nano-reinforced rigid PU foam. *J. Cell. Plast.* 47, 81–93. <https://doi.org/10.1177/0021955X10392200>.
- Frihart, C.R., Lorenz, L.F., 2019. Specific oxidants improve the wood bonding strength of soy and other plant flours. *J. Polym. Sci. Part A: Polym. Chem.* 57, 1017–1023. <https://doi.org/10.1002/pola.29357>.
- Frihart, C.R., Pizzi, A., Xi, X., Lorenz, L.F., 2019. Reactions of Soy flour and Soy protein by non-volatile aldehydes generation by specific oxidation. *Polymers* 11, 1478. <https://doi.org/10.3390/polym11091478>.
- Gao, C., Li, M., Zhu, C., Hu, Y., Shen, T., Li, M., Ji, X., Lyu, G., Zhuang, W., 2021. One-pot depolymerization, demethylation and phenolation of lignin catalyzed by HBr under microwave irradiation for phenolic foam preparation. *Compos. Part B-Eng.* 205, 108530. <https://doi.org/10.1016/j.compositesb.2020.108530>.
- Ghahri, S., Pizzi, A., 2018. Improving soy-based adhesives for wood particleboard with tannins addition. *Wood Sci. Technol.* 52, 261–279. <https://doi.org/10.1007/s00226-017-0957-y>.
- Ghahri, S., Mohebbi, B., Pizzi, A., Mirshokraie, A., Mansouri, H.R., 2018a. Improving water resistance of soy-based adhesive by vegetable tannin. *J. Polym. Environ.* 26, 1881–1890. <https://doi.org/10.1007/s10924-017-1090-6>.
- Ghahri, S., Pizzi, A., Mohebbi, B., Mirshokraie, A., Mansouri, H.R., 2018b. Soy-based, tannin-modified plywood adhesives. *J. Adhes.* 94, 218–237. <https://doi.org/10.1080/00218464.2016.1258310>.
- Gu, W., Liu, X., Li, F., Shi, S.Q., Xia, C., Zhou, W., Zhang, D., Gong, S., Li, J., 2019. Tough, strong, and biodegradable composite film with excellent UV barrier performance comprising soy protein isolate, hyperbranched polyester, and cardanol derivative. *Green Chem.* 21, 3651–3665. <https://doi.org/10.1039/C9GC01081E>.
- Guo, Y., Zhang, X., Hao, W., Xie, Y., Chen, L., Li, Z., Zhu, B., Feng, X., 2018. Nano-bacterial cellulose/soy protein isolate complex gel as fat substitutes in ice cream model. *Carbohydr. Polym.* 198, 620–630. <https://doi.org/10.1016/j.carbpol.2018.06.078>.
- Jahanshahi, S., Pizzi, A., Abdulkhani, A., Doosthoseini, K., Shakeri, A., Lagel, M., Delmotte, L., 2016. MALDI-TOF, ¹³C NMR and FT-MIR analysis and strength characterization of glycidyl ether tannin epoxy resins. *Ind. Crops Prod.* 83, 177–185. <https://doi.org/10.1016/j.indcrop.2015.11.067>.
- Jana, P., Fierro, V., Pizzi, A., Celzard, A., 2015. Thermal conductivity improvement of composite carbon foams based on tannin-based disordered carbon matrix and graphite fillers. *Mater. Des.* 83, 635–643. <https://doi.org/10.1016/j.matdes.2015.06.057>.
- Jing, S., Li, T., Li, X., Xu, Q., Hu, J., Li, R., 2014. Phenolic foams modified by cardanol through bisphenol modification. *J. Appl. Polym. Sci.* 131. <https://doi.org/10.1002/app.39942>.
- Kong, L., Guan, H., Wang, X., 2018. In situ polymerization of furfuryl alcohol with ammonium dihydrogen phosphate in Poplar Wood for improved dimensional stability and flame retardancy. *ACS Sustainable Chem. Eng.* 6, 3349–3357. <https://doi.org/10.1021/acssuschemeng.7b03518>.
- Lacoste, C., Basso, M.C., Pizzi, A., Laborie, M.-P., Garcia, D., Celzard, A., 2013. Bioresourced pine tannin/furanic foams with glyoxal and glutaraldehyde. *Ind. Crops Prod.* 45, 401–405. <https://doi.org/10.1016/j.indcrop.2012.12.032>.
- Lacoste, C., Basso, M., Pizzi, A., Celzard, A., Laborie, M., 2015. Natural albumin/tannin cellular foams. *Ind. Crops Prod.* 73, 41–48. <https://doi.org/10.1016/j.indcrop.2015.03.087>.
- Li, X., Basso, M., Fierro, V., Pizzi, A., Celzard, A., 2012a. Chemical modification of tannin/furanic rigid foams by isocyanates and polyurethanes. *Maderas Cienc. Y Tecnol.* 14, 257–265. <https://doi.org/10.4067/S0718-221X2012005000001>.
- Li, X., Essawy, H., Pizzi, A., Delmotte, L., Rode, K., Le Nouen, D., Fierro, V., Celzard, A., 2012b. Modification of tannin based rigid foams using oligomers of a hyperbranched poly (amine-ester). *J. Polym. Res.* 19, 1–9. <https://doi.org/10.1007/s10965-012-0021-4>.
- Li, X., Pizzi, A., Cangemi, M., Fierro, V., Celzard, A., 2012c. Flexible natural tannin-based and protein-based biosourced foams. *Ind. Crops Prod.* 37, 389–393. <https://doi.org/10.1016/j.indcrop.2011.12.037>.
- Li, X., Pizzi, A., Cangemi, M., Navarrete, P., Segovia, C., Fierro, V., Celzard, A., 2012d. Insulation rigid and elastic foams based on albumin. *Ind. Crops Prod.* 37, 149–154. <https://doi.org/10.1016/j.indcrop.2011.11.030>.
- Li, X., Srivastava, V., Pizzi, A., Celzard, A., Leban, J., 2013. Nanotube-reinforced tannin/furanic rigid foams. *Ind. Crops Prod.* 43, 636–639. <https://doi.org/10.1016/j.indcrop.2012.08.008>.
- Li, B., Wang, Y., Mahmood, N., Yuan, Z., Schmidt, J., Xu, C., 2017. Preparation of bio-based phenol formaldehyde foams using depolymerized hydrolysis lignin. *Ind. Crops Prod.* 97, 409–416. <https://doi.org/10.1016/j.indcrop.2016.12.063>.
- Li, J., Zhang, A., Zhang, S., Gao, Q., Zhang, W., Li, J., 2019. Larch tannin-based rigid phenolic foam with high compressive strength, low friability, and low thermal conductivity reinforced by cork powder. *Compos. Part B Eng.* 156, 368–377. <https://doi.org/10.1016/j.compositesb.2018.09.005>.
- Li, J., Liao, J., Essawy, H., Zhang, J., Li, T., Wu, Z., Du, G., Zhou, X., 2021. Preparation and characterization of novel cellular/nonporous foam structures derived from tannin furanic resin. *Ind. Crops Prod.* 162, 113264. <https://doi.org/10.1016/j.indcrop.2021.113264>.
- Liang, J., Wu, Z., Lei, H., Xi, X., Li, T., Du, G., 2017. The reaction between furfuryl alcohol and model compound of protein. *Polymers* 9, 711. <https://doi.org/10.3390/polym9120711>.
- Liu, B., Jiang, L., Zhang, J., 2011. Extrusion foaming of poly (lactic acid)/Soy protein concentrate blends. *Macromol. Mater. Eng.* 296, 835–842. <https://doi.org/10.1002/mame.201000449>.
- Liu, H., Li, C., Sun, X.S., 2015. Improved water resistance in undecylenic acid (UA)-modified soy protein isolate (SPI)-based adhesives. *Ind. Crops Prod.* 74, 577–584. <https://doi.org/10.1016/j.indcrop.2015.05.043>.
- Liu, C., Zhang, Y., Li, X., Luo, J., Gao, Q., Li, J., 2017. “Green” bio-thermoset resins derived from soy protein isolate and condensed tannins. *Ind. Crops Prod.* 108, 363–370. <https://doi.org/10.1016/j.indcrop.2017.06.057>.
- Ma, X., Chen, W., Yan, T., Wang, D., Hou, F., Miao, S., Liu, D., 2020. Comparison of citrus pectin and apple pectin in conjugation with soy protein isolate (SPI) under controlled dry-heating conditions. *Food Chem.* 309, 125501. <https://doi.org/10.1016/j.foodchem.2019.125501>.
- Meikleham, N., Pizzi, A., 1994. Acid-and alkali-catalyzed tannin-based rigid foams. *J. Appl. Polym. Sci.* 53, 1547–1556. <https://doi.org/10.1002/app.1994.070531117>.
- Pizzi, A., 2019. Tannin-based biofoams-A review. *J. Renewable Mater.* 7, 474–489. <https://doi.org/10.32604/jrm.2019.06511>.
- Pizzi, A., Tondi, G., Pasch, H., Celzard, A., 2008. Matrix-assisted laser desorption/ionization time-of-flight structure determination of complex thermoset networks: polyflavonoid tannin-furanic rigid foams. *J. Appl. Polym. Sci.* 110, 1451–1456. <https://doi.org/10.1002/app.28545>.
- Rangel, G., Chapuis, H., Basso, M.-C., Pizzi, A., Delgado-Sanchez, C., Fierro, V., Celzard, A., Gerardin-Charbonnier, C., 2016. Improving water repellence and friability of tannin-furanic foams by oil-grafted flavonoid tannins. *Bioresources* 11, 7754–7768. <https://doi.org/10.15376/biores.11.3.7754-7768>.
- Rao, W.-H., Zhu, Z.-M., Wang, S.-X., Wang, T., Tan, Y., Liao, W., Zhao, H.-B., Wang, Y.-Z., 2018. A reactive phosphorus-containing polyol incorporated into flexible polyurethane foam: self-extinguishing behavior and mechanism. *Polym. Degrad. Stab.* 153, 192–200. <https://doi.org/10.1016/j.polymdegradstab.2018.04.029>.
- Santiago-Medina, F.-J., Pizzi, A., Basso, M.C., Delmotte, L., Celzard, A., 2017. Polycondensation resins by flavonoid tannins reaction with amines. *Polymers* 9, 37. <https://doi.org/10.3390/polym9020037>.
- Santiago-Medina, F., Delgado-Sánchez, C., Basso, M., Pizzi, A., Fierro, V., Celzard, A., 2018a. Mechanically blown wall-projected tannin-based foams. *Ind. Crops Prod.* 113, 316–323. <https://doi.org/10.1016/j.indcrop.2018.01.049>.
- Santiago-Medina, F., Tenorio-Alfonso, A., Delgado-Sánchez, C., Basso, M., Pizzi, A., Celzard, A., Fierro, V., Sánchez, M., Franco, J., 2018b. Projectable tannin foams by mechanical and chemical expansion. *Ind. Crops Prod.* 120, 90–96. <https://doi.org/10.1016/j.indcrop.2018.04.048>.
- Szczurek, A., Fierro, V., Pizzi, A., Stauber, M., Celzard, A., 2014. A new method for preparing tannin-based foams. *Ind. Crops Prod.* 54, 40–53. <https://doi.org/10.1016/j.indcrop.2014.01.012>.
- Thébault, M., Pizzi, A., Santiago-Medina, F.J., Al-Marzouki, F.M., Abdalla, S., 2017. Isocyanate-free polyurethanes by Coreaction of condensed tannins with aminated tannins. *J. Renewable Mater.* 5, 21–29. <https://doi.org/10.7569/JRM.2016.634116>.
- Tondi, G., Pizzi, A., 2009. Tannin-based rigid foams: characterization and modification. *Ind. Crops Prod.* 29, 356–363. <https://doi.org/10.1016/j.indcrop.2008.07.003>.
- Tondi, G., Pizzi, A., Olives, R., 2008a. Natural tannin-based rigid foams as insulation for doors and wall panels. *Maderas Cienc. Y Tecnol.* 10, 219–227. <https://doi.org/10.4067/S0718-221X2008000300005>.
- Tondi, G., Pizzi, A., Pasch, H., Celzard, A., Rode, K., 2008b. MALDI-ToF investigation of furanic polymer foams before and after carbonization: aromatic rearrangement and surviving furanic structures. *Eur. Polym. J.* 44, 2938–2943. <https://doi.org/10.1016/j.eurpolymj.2008.06.029>.
- Tondi, G., Fierro, V., Pizzi, A., Celzard, A., 2009a. Tannin-based carbon foams. *Carbon* 47, 1480–1492. <https://doi.org/10.1016/j.carbon.2009.01.041>.
- Tondi, G., Oo, C., Pizzi, A., Trosa, A., Thévenon, M.-F., 2009b. Metal adsorption of tannin based rigid foams. *Ind. Crops Prod.* 29, 336–340. <https://doi.org/10.1016/j.indcrop.2008.06.006>.
- Tondi, G., Zhao, W., Pizzi, A., Du, G., Fierro, V., Celzard, A., 2009c. Tannin-based rigid foams: a survey of chemical and physical properties. *Bioresour. Technol.* 100, 5162–5169. <https://doi.org/10.1016/j.biortech.2009.05.055>.

- Wang, Z., Kang, H., Zhang, W., Zhang, S., Li, J., 2017. Improvement of interfacial interactions using natural polyphenol-inspired tannic acid-coated nanoclay enhancement of soy protein isolate biofilms. *Appl. Surf. Sci.* 401, 271–282. <https://doi.org/10.1016/j.apsusc.2017.01.015>.
- Wang, Z., Zhao, S., Zhang, W., Qi, C., Zhang, S., Li, J., 2019. Bio-inspired cellulose nanofiber-reinforced soy protein resin adhesives with dopamine-induced codeposition of “water-resistant” interphases. *Appl. Surf. Sci.* 478, 441–450. <https://doi.org/10.1016/j.apsusc.2019.01.154>.
- Wu, X., Yan, W., Zhou, Y., Luo, L., Yu, X., Luo, L., Fan, M., Du, G., Zhao, W., 2020. Thermal, morphological, and mechanical characteristics of sustainable tannin bio-based foams reinforced with wood cellulosic fibers. *Ind. Crops Prod.* 158, 113029. <https://doi.org/10.1016/j.indcrop.2020.113029>.
- Xi, X., Pizzi, A., Gerardin, C., Chen, X., Amirou, S., 2020. Soy protein isolate-based polyamides as wood adhesives. *Wood Sci. Technol.* 54, 89–102. <https://doi.org/10.1007/s00226-019-01141-9>.
- Xiao, Z., Li, Y., Wu, X., Qi, G., Li, N., Zhang, K., Wang, D., Sun, X.S., 2013. Utilization of sorghum lignin to improve adhesion strength of soy protein adhesives on wood veneer. *Ind. Crops Prod.* 50, 501–509. <https://doi.org/10.1016/j.indcrop.2013.07.057>.
- Xue, B.-L., Wen, J.-L., Sun, R.-C., 2014. Lignin-based rigid polyurethane foam reinforced with pulp Fiber: synthesis and characterization. *ACS Sustainable Chem. Eng.* 2, 1474–1480. <https://doi.org/10.1021/sc5001226>.
- Yang, H., Wang, X., Yuan, H., Song, L., Hu, Y., Yuen, R.K.K., 2012. Fire performance and mechanical properties of phenolic foams modified by phosphorus-containing polyethers. *J. Polym. Res.* 19, 9831. <https://doi.org/10.1007/s10965-012-9831-7>.
- Yang, Z., Yuan, L., Gu, Y., Li, M., Sun, Z., Zhang, Z., 2013. Improvement in mechanical and thermal properties of phenolic foam reinforced with multiwalled carbon nanotubes. *J. Appl. Polym. Sci.* 130, 1479–1488. <https://doi.org/10.1002/app.39326>.
- Yang, C., Zhuang, Z.-H., Yang, Z.-G., 2014. Pulverized polyurethane foam particles reinforced rigid polyurethane foam and phenolic foam. *J. Appl. Polym. Sci.* 131. <https://doi.org/10.1002/app.39734>.
- Zhang, A., Li, J., Zhang, S., Mu, Y., Zhang, W., Li, J., 2017. Characterization and acid-catalysed depolymerization of condensed tannins derived from larch bark. *RSC Adv.* 7, 35135–35146. <https://doi.org/10.1039/C7RA03410E>.
- Zhao, Y., Wang, Z., Zhang, Q., Chen, F., Yue, Z., Zhang, T., Deng, H., Huselstein, C., Anderson, D.P., Chang, P.R., 2018. Accelerated skin wound healing by soy protein isolate-modified hydroxypropyl chitosan composite films. *Int. J. Biol. Macromol.* 118, 1293–1302. <https://doi.org/10.1016/j.ijbiomac.2018.06.195>.
- Zhao, S., Wang, Z., Li, Z., Li, L., Li, J., Zhang, S., 2019. Core-shell nanohybrid elastomer based on co-deposition strategy to improve performance of soy protein adhesive. *ACS Appl. Mater. Interfaces* 11, 32414–32422. <https://doi.org/10.1021/acsami.9b11385>.
- Zhou, X., Li, B., Xu, Y., Essawy, H., Wu, Z., Du, G., 2019. Tannin-furanic resin foam reinforced with cellulose nanofibers (CNF). *Ind. Crops Prod.* 134, 107–112. <https://doi.org/10.1016/j.indcrop.2019.03.052>.

4. CONCLUSIONS GENERALES

Dans cette recherche, les ressources de biomasse, y compris le tanin de mimosa, la lignine, l'isolat de protéine de soja (SPI) et les humines ont été les matières de départ pour produire des adhésifs et des mousses pour bois.

I Préparation de colles pour bois à base du système de résine polyuréthane non isocyanate (NIPU).

Les systèmes d'adhésifs pour bois à base de polyuréthane sans isocyanate (NIPU) présentés dans cette recherche sont basés sur les groupes -OH des ressources de la biomasse réticulés par le carbonate de diméthyle (DMC) et l'hexaméthylènediamine. Les humines commerciales (principalement composées d'acide fulvique et de ses dérivés, et d'acide humique, mais présentant également des structures polyfuraniques et lignanes dans leur mélange), l'isolat de protéine de soja (SPI) et le tanin de mimosa ont été utilisés pour préparer des adhésifs à bois NIPU pour le contreplaqué, ou panneaux de particules. Comme prévu, ces adhésifs présentent d'excellentes performances de liaison à l'exception du SPI qui a besoin d'un réticulant supplémentaire pour améliorer ses propriétés d'adhérence et de cohésion. Comparés aux produits à base de formaldéhyde disponibles dans le commerce, les adhésifs obtenus évitent le formaldéhyde chimique qui présente un risque pour la santé humaine.

Cependant, la voie de préparation des adhésifs pour bois NIPU présente toujours un inconvénient principal, une température de durcissement plus élevée, normalement supérieure à 200 °C, mais elle est acceptée dans la fabrication de panneaux de particules de bois. Par conséquent, l'éther glycidyle de glycérol partiellement biosourcé (GDE) commercial a été utilisé comme produit chimique supplémentaire, lors de la fabrication de contreplaqué, non seulement pour réduire leur température de durcissement, mais également pour améliorer davantage les performances de liaison. De toute évidence, cette stratégie fonctionne très bien, ce qui a été prouvé par nos recherches.

Ainsi, la préparation de la biomasse NIPU pour les colles à bois est une méthode efficace, mais des recherches systématiques supplémentaires sur les aspects suivants

peuvent être envisagées :

(1) *Substitution par l'hexaméthylènediamine (HMDA)*. Si l'hexaméthylène diamine est partiellement biosourcée, les amines sont en général encore nocives pour la santé humaine. Par conséquent, une biomasse contenant des groupes amino devrait être trouvée, qui peut éventuellement être utilisée pour remplacer partiellement ou complètement le HMDA, résultant en un système de résine NIPU encore plus acceptable pour l'environnement, comme une protéine végétale.

(2) *Optimisation des formulations*. La formulation actuelle de NIPU est toujours dans un système en excès de HMDA, résultant de son évaporation en raison de la température de durcissement élevée qui est supérieure au point de volatilisation du HMDA. Par conséquent, il est digne et nécessaire d'obtenir un dosage approprié de HMDA. C'est-à-dire qu'une nouvelle formulation NIPU avec une quantité réduite de HMDA doit être développée tout en ne perdant pas les performances de liaison NIPU.

II Préparation de colles à bois à base de tanin, de protéine de soja et de lignine.

La nature macromoléculaire du tanin, de la protéine de soja et de la lignine a servi de matériaux de départ pour préparer des adhésifs pour bois. Dans la recherche rapportée dans cette thèse, quelques moyens pratiques pour préparer des adhésifs pour bois à base de ces sources de biomasse, y compris (a) du tanin mélangé directement avec du GDE commercial, (b) du tanin mélangé avec de la protéine de soja, (c) une action oxydante spécifique (NaIO_4) directement sur la lignine, et (d) l'urée utilisée comme agent de réticulation de la lignine glyoxalée et de l'amidon dialdéhyde ont été signalés. Parmi ceux-ci, certains peuvent présenter des performances de liaison exceptionnelles (formulation a) ou nécessiter un réticulant supplémentaire pour améliorer encore leurs propriétés (formulation d). Néanmoins, certains d'entre eux présentent également les défauts généraux qui sont normalement montrés par certains adhésifs pour bois de biomasse, tels qu'une résistance à l'eau inférieure (formulations b et c). Mais, quoi qu'il en soit, ils offrent une nouvelle stratégie d'utilisation de la biomasse pour préparer des colles à bois. Cependant, ils fournissent de nouvelles stratégies d'utilisation de la biomasse pour préparer des adhésifs pour bois en vue de

recherches ultérieures.

(1) Adhésifs à base de tanins pour bois, aminés et hautement ramifiés. Ceci est motivé par la formulation tanin-protéine de soja. Un nouveau produit chimique aminé hautement ramifié obtenu à partir de produits dérivés de l'urée peut servir d'agent de réticulation pour réagir avec le tanin, et même avec la lignine.

(2) Dialdéhyde carbohydrates préparés par oxydation spécifique par NaIO_4 . En particulier l'amidon dialdéhyde, ses groupes aldéhyde peuvent réagir avec le tanin ou la lignine et le produit obtenu peut alors être utilisé pour préparer des colles à bois.

III Préparation de mousses à base de tanin à base d'un système de résine NIPU.

La résine NIPU à base de tanin est un précurseur efficace pour la préparation de mousse en raison de sa préparation facile, en utilisant simplement un acide biosourcé pour catalyser leur expansion de volume. Ces mousses présentent l'inconvénient typique de la mousse de polyuréthane, l'inflammabilité, mais cela s'améliore en présence d'un retardateur de flamme naturel, à savoir le tanin. De plus, ces mousses NIPU à base de tanin présentent des structures alvéolaires différentes, à cellules semi-ouvertes leur conférant une résistance mécanique acceptable. Par conséquent, leur ignifugation et leurs propriétés mécaniques acceptables sont l'indice critique pour une application industrielle.

En ce qui concerne une stratégie de développement ultérieure, certaines formulations nouvelles peuvent également être développées :

(1) Modification typique de la formulation de mousses tanin-NIPU. Ce travail porterait principalement sur leur ignifugation améliorée, leur résistance mécanique, leur isolation thermique, etc.

(2) Préparation de mousse souple de tanin-NIPU. Comme la mousse souple PU conventionnelle, la mousse souple tanin-NIPU a également une application potentielle pour le traitement de l'eau en raison de sa stratégie de fabrication respectueuse de l'environnement, le bioplastifiant glycérol pouvant être introduit et remplir cet objectif. Des expériences préliminaires ont déjà été réalisées dans cette ligne.

IV Mousses tanin-furanique avec substitution complète de formaldéhyde

Les mousses tanin-furanique typiques ont été intensément étudiées ces dernières années comme étant d'un intérêt particulier en raison de leur quasi-totalité bio-sourcée, pour leur exceptionnelle résistance au feu, leur résistance chimique et leurs bonnes caractéristiques d'absorption acoustique. Dans cette recherche, deux réticulants biosourcés, l'isolat de protéine de soja (SPI) et les résidus de bioraffinerie humines peuvent remplacer complètement le formaldéhyde ou un autre réticulant à base de pétrole, ainsi qu'une résistance mécanique améliorée pour les nouvelles mousses à base de tanin. De plus, les mousses à base de tanin résultantes non seulement héritent des avantages des mousses tanin-furanique-formaldéhyde typiques, mais obtiennent également des progrès, en particulier leur résistance mécanique et leur ignifugation voire leur aspect d'isolation thermique. Les propriétés intégrées des mousses à base de tanin résultantes, notamment l'ignifugation, l'isolation thermique, la légèreté, le respect de l'environnement et les performances mécaniques acceptables, sont leur supériorité unique pour une application prometteuse sur l'isolation thermique des bâtiments par rapport à certains produits commerciaux.

De plus, la poursuite du développement des mousses tanins-furaniques à l'aide d'un agent de réticulation respectueux de l'environnement est prometteuse pour de futures recherches :

(1) Enquête sur l'agent de réticulation de la biomasse. Un agent de réticulation des ressources de la biomasse, l'amidon dialdéhyde, peut fonctionner pour les formulations à base de tanin-furanique sans formaldéhyde. L'amidon dialdéhyde a été utilisé dans cette thèse pour un autre système polymère. Par conséquent, cela montre une nouvelle direction pour des travaux de recherche ultérieurs sur la préparation de mousses à base de tanin-furanique sans formaldéhyde.

(2) Nouvelle application pour les mousses à base de tanin. Cela pourrait certainement être une direction pour développer de nouvelles applications pour ces matériaux poreux à base de tanin, tels qu'ils agissent comme absorbants pour le traitement des eaux contaminantes, et pour les électrodes.